ISTANBUL TECHNICAL UNIVERSITY ★ EURASIA INSTITUTE OF EARTH SCIENCES

TECTONIC AND MAGMATIC STRUCTURE OF LAKE VAN BASIN AND ITS STRUCTURAL EVOLUTION, EASTERN ANATOLIA ACCRETIONARY COMPLEX (EAAC), E-TURKEY

Ph.D. Thesis by
Mustafa TOKER

Department : Climate and Marine Sciences

Programme : Earth System Sciences

JANUARY 2011

ISTANBUL TECHNICAL UNIVERSITY ★ EURASIA INSTITUTE OF EARTH SCIENCES

TECTONIC AND MAGMATIC STRUCTURE OF LAKE VAN BASIN AND ITS STRUCTURAL EVOLUTION, EASTERN ANATOLIA ACCRETIONARY COMPLEX (EAAC), E-TURKEY

Ph.D. Thesis by
Mustafa TOKER
(601042205)

Date of submission : 15 September 2010
Date of defence examination: 28 January 2011

Supervisor (Chairman) : Prof. Dr. A. M. Celal Şengör (ITU)
Members of the Examining Committee : Prof. Dr. Emin Demirbağ (ITU)
Prof. Dr. Timur Ustaömer (IU)
Prof. Dr. Erdin Bozkurt (METU)
Prof. Dr. Gürol Seyitoğlu (AU)

JANUARY 2011

İSTANBUL TEKNİK ÜNİVERSİTESİ ★ AVRASYA YER BİLİMLERİ ENSTİTÜSÜ

VAN GÖLÜ HAVZASININ TEKTONİK VE MAGMATİK YAPISI VE YAPISAL EVRİMİ, DOĞU ANADOLU YIĞIŞIM KARMAŞIĞI (DOĞU TÜRKİYE)

DOKTORA TEZİ
Mustafa TOKER
(601042205)

Tezin Enstitüye Verildiği Tarih : 15 Eylül 2010
Tezin Savunulduğu Tarih : 28 Ocak 2011

Tez Danışmanı : Prof. Dr. A. M. Celal ŞENGÖR (İTÜ)
Diğer Jüri Üyeleri : Prof. Dr. Emin Demirbağ (İTÜ)
Prof. Dr. Timur Ustaömer (İÜ)
Prof. Dr. Erdin Bozkurt (ODTÜ)
Prof. Dr. Gürol Seyitoğlu (AÜ)

OCAK 2011

In memory of 200th birthday of Charles Darwin…

…Sorrow is knowledge, those that know the most must mourn the deepest, the tree of knowledge is not the tree of life.

Lord Byron

O Mensch! Gib acht!
Was spricht die tiefe Mitternacht?
"Ich schlief, ich schlief -,
Aus tiefem Traum bin ich erwacht: -
Die Welt ist tief,
Und tiefer als der Tag gedacht.
Tief ist ihr Weh -,
Lust - tiefer noch als Herzeleid:
Weh spricht: Vergeh!
Doch alle Lust will Ewigkeit -,
- will tiefe, tiefe Ewigkeit!"

Alle Lust Will Ewigkeit...

Aus: Friedrich Nietzsche (1844-1900): Also sprach Zarathustra (1883-1891)

…The sleep of reason brings forth monsters: El sueño de la razón produce monstruos.

Francisco de Goya (1796)

FOREWORD

I do strongly feel the need to acknowledge, it is to express my deep appreciation and thanks for scientist, philosopher and my supervisor, Prof. Dr. A. M. Celal Şengör that the collaborative, optimistic and philosophical attitude in his profession has always been my inspiration that allowed me accomplishing this PhD study. Therefore I owe my deep gratitude to his philosophy of science and sharing it with me.

My most sincere thanks go to my examining committee Emin Demirbağ and Namık Çağatay, who provided me unique scientific support with endless patients. It is thanks to their efforts and their precision in scientific research that I was able to complete this work. I also sincerely feel the need to acknowledge, it is to emphasize my appreciation for three thesis reviewers, Prof. Dr. Gürol Seyitoğlu (AU), Prof. Dr. Erdin Bozkurt (METU) and Prof. Dr. Timur Ustaömer (IU).

I should not forget to mention the help and guidance of my principal investigator Sebastian Krastel during my field, offshore and laboratory studies and would like to thank him and my special friends, İclal Başak Ağdaş, Tuba Sayi, Zehra Yıldız, Meray Akkor and Selma Baş for their helping lovely hand in the field and laboratory. I also owe thanks to Dr. Fuat Şaroğlu who fished out poorly known paper documents from the dusty shelves of the his library, MTA in Ankara. During this study I had well support and fruitful discussions with many of my colleagues; Caner Imren for GeoChirp data, Sinan Özeren for crustal elasticity, Tuncay Taymaz for seismotectonics, Niyazi Türkelli for crustal tomography and Aysun Güney-Boztepe for seismology.

Special thanks go to İclal Başak Ağdaş and Tuba Sayi. Their precious and lovely friendship and support since we ever met will never be forgotton. I owe special thanks to Nüzhet Dalfes, Aral Okay, Nilgün Okay, Ercan Özcan, Mehmet Karaca, Tayfun Kindap, Atilla Uluğ and Ş. Can Genç for their strong motivation during my study. I am indebted very special thanks to Okan Tüysüz and Emin Demirbağ. They were always an important backer during my entire stage of the PhD, providing great motivation, wisdom and reference. Their friendly inspirations are invaluable and will be always remembered. I can't ignore the great minutes help of Sinan Özeren for extracting my conclusions from crustal deformation and GPS. Special thanks go to Dr. Sebastian Krastel who welcomed me during my stays in Bremen, particularly the great dinner in his house and allowed me to work in the university despite the national holiday of Germany. He has been with me during the review discussion of Lake Van seismic reflection profiles in Thessaloniki (Greece) International Congress, during Special Session of Eastern Anatolia Accretionary Complex, The Carpathian Balkan Geological Association (CBGA-2010 September).

I would like to send many thanks which are due to the scientific crew of our seismic team of Lake Van Star geophysical survey and again I am grateful to Sebastian Krastel for his excellent supports when using the Kingdom-suite software program for his helpful comments as a leader of the geophysical survey. I thank the ICDP scientists in the ICDP-2006, June meeting in Van (Lake Van workshop participants), Dr. T. Litt, Dr. F. Nissen, Dr. R. Oberhänsli, Dr. M. Sturm, Dr. H. U. Schminke, Dr. R. Emmermann, Dr. T. Wöhrl (for ICDP-Training Course, 2007, Germany) and Prof. Dr. Orhan Tatar, Prof. Dr. Durmuş Boztuğ, Prof. Dr. Cahit Helvacı for personal supports and Prof. Dr. A. M. Celal Şengör for many helpful discussions in the field trip and Dr. Sebastian Krastel for processing data and data acquisition. Dr. Fuat

Şaroğlu and Prof. Dr. Boris Natalin are gratefully acknowledged for fruitful discussions and for constructive comments on the Lake Van-Muş basin system and the Eastern Anatolia Accretionary Complex (EAAC). I further acknowledge helpful supports for seismic survey by Prof. Dr. A. Ümit Tolluoğlu and Prof. Dr. Sefer Örçen. They are the first to propose the Lake Van project in 2004 and still frontiers.

This work benefited from a grant from ICDP-2004 PaleoVan project and financially supported by Deutsche Forschungsgemeinschaft (German Money Foundation) by contributions of Van, Yüzüncüyıl Univ. (YYU), Bremen Univ. (BU), Bonn Univ. (BU), Potsdam Univ. (PU), Alfred Wegener Inst. (AWI) and Istanbul Technical University (ITU). I gratefully acknowledge the logistic supports of Van, Yüzüncüyıl Univ. (YYU) and financial support of Germany Money Foundation for multi-channel seismic survey of the Paleo-Van drilling project of the International Continental Drilling Program-2004 (ICDP-2004).

Last but not least, I am grateful to all members of my family; my emotional father Ibrahim, my poetic mother Nimet, my brother and sister Şenol and Şengül, who patiently tolerated all my good and bad times while preparing this thesis with a dramatic memory of my other brothers and sisters, dead at birth. A little sweet-heart angel and autumnal lady, Nergis (Narcissos) Önalgil, with her epic and poetic-medieval heart and ancient-lyric soul has given unspoken, deep inspirations and lovely motivated me during the times of “melancholy” in frozen winter of my thoughts and feelings in seasonal dreams. Finally, I do sincerely wish to send my deepest regards, misses and loves to all the past, unforgetable times during my whole draconian life, those never appear again and those who had been melted and absorbed within my heart…It is the past of individual wisdom, an epic and lyric heart in “philosophem”, “art” and “science” and the face of a poet.

January 2011

Mustafa TOKER

Climate and Marine Sciences

TABLE OF CONTENTS

Page

ABBREVIATIONS

A : Away
BP-M : Bitlis Pötürge-Massive
BT : Basement Thrust
C : Central
ÇBB : Çarpanak Basement Block
CE : Crypto-Explosion
CEMP : Central Europe-Magmatic Province
CLVZ : Crustal Low Velocity Zone
CS : Cryptic Suture
Cssf : Convergent strike slip fault
ÇSZ : Çarpanak Spur Zone
CTB : Central Tatvan Basin
CW : Conjugate Wrenching
D : Dimensional
D : Dome
DDDD : Depressurizing, Dewatering, Destabilization, Degradation
DEM : Digital Elevation Model
Dssf : Divergent strike slip fault
E : East
EAAC : Eastern Anatolia Accretionary Complex
EB : External Basin
EF-CVV : Extensional Fissure-Central Vent Volcano
Es-Tt : Eastern segment-Transtension
ETSE : Eastern Turkey Seismic Experiment
F : Flower structure
FCF-ID : Faulted Clinoform Failures-Internal Destabilization
ffd : fault flank depression
Fig. : Figure
Figs. : Figures
fms : fault margin sag
G : Granite
GPS : Global Positioning System
HAz : Hydrothermal Alteration zone
IB : Internal Basin
ICDP : International Continental Drilling Program
KOERI : Kandilli Observatory and Earthquake Research Institute
LAB : Lithosphere-Asthenosphere Boundary
LR : Lateral Ramp
Ls : Lacustrine shelf
LST : Lowstand System Tract
M : Multiple
Ma : Million ages
MF : Maacama Fault

mf : micro-fractures/faults
MH-SD : Magma Hydrothermal-Sediment Deformations
mNFS : mini Negative Flower Structure
MORB : Mid-Ocean Ridge Basalts
MRSCS : Multiple Rotational Slumping of Clinoform Successions
MS : Muş Suture
MSCS : Multiple Slumping of Clinoform Successions
Mt : Mountains
MTA : Maden Tetkik Arama Enstitüsü
N : North
Nosf : Normal oblique slip fault
OIB : Ocean Island Basalts
P : Profile
P : Pull-apart
PDZ : Principal Displacement Zone
R : Ramp
RF : Rigid Flake
Rosf : Reverse oblique slip fault
Rosf-FR : Reverse oblique slip fault-Fault Reactivation
RS : Ridged Sill
S : Sagging
S : South
S : Surge zone
S_1, S_2, S_3 : $Sill_1$, $Sill_2$, $Sill_3$
SAF : San Andreas Fault
SCS : Slumping of Clinoform Successions
SGF : San Gabriel Fault
SLBB : Sublacustrine Basement Block
SLs : Sublacustrine slope
SMST : Shelf-Margin System Tract
SR : Sedimentary Ridge
SSDS : Soft Sediment Deformation Structures
SSs : Strike Slip sedimentation
T : Toward
T : Transform
Tp : Transpression
TP : Transpression
Tt : Transtension
UCD : Upper Crustal Discontinuity
VE : Vertical Exaggeration
W : West
Ws-Tt : Western segment-Transtension

LIST OF FIGURES

Page

TECTONIC AND MAGMATIC STRUCTURE OF LAKE VAN BASIN, AND ITS STRUCTURAL EVOLUTION, EASTERN ANATOLIA ACCRETIONARY COMPLEX (EAAC), E-TURKEY

SUMMARY

The Eastern Anatolia Accretionary Complex (EAAC), one of the major mountain ranges on Earth, constitutes a unique Geosciences laboratory hosting natural phenomena and processes on virtually all geosciences and sub-disciplines. There are several cross-cutting themes of tremendous scientific interest and practical relevance, such as the subduction-accretion, slab delamination, and crustal consolidation. These interactions over different timescales provide several critical implications for post-collisional crust-forming processes in Turkic-type orogens. Due to the slab break off, EAAC seems to have global impacts of delamination phenomena in Tethyside superorogenic systems and characterizes the most prominent example of hot and small Turkic-type orogens based on delamination event. EAAC as a younger Turkic-type orogeny involves crustal tectonics and magmatism that generate intense intraplate thin-skinned deformation, and extensional alkaline magmatism associated with strike-slip basin formation and orographic sedimentation. Due to its origin related to an active convergent-plate margin that causes thrust imbrication of terrane blocks, weak and irresistant suture complexes bounding major tectonic blocks, this orogeny shows extreme complexity, with strong gradients in tectonic and magmatic structure during post-collisional period.

It becomes clearer that questions on post-collisional evolution of EAAC are answered in tectonic patterns and deformation styles of the accretionary wedge-basins in the Turkic-type orogeny. The peculiar one of these wedge-basins is orogen-parallel Lake Van trough that is the deepest basin of the rotated portions of EAAC and thrust-bounded region. This lake is emplaced at N-end of Bitlis-Pötürge Massive (BP-M) along Muş suture, separating EAAC from BP-M. Lake Van region is a place where no mantle lid exists and hot asthenosphere is doming, therefore, it has dome-shaped structure with the highest elevation (2 km), termed as Lake Van Dome. The domal pattern of the lake, in fact, is a morphological paradigm, well representing the surficial effects of delamination event, crustal consolidation and crust-forming process. Not surprisingly, outline anatomy of Lake Van Dome clearly exhibits an orogenic structure with its formation of the squashy basin and thus, both its morphological and limnological characteristics may imply basement reactivation and orogenic features of the Highlands rifting phenomena in the domal center of accretionary complex.

Compared to other convergent lakes in major mountain ranges, such as Lake Baikal, Lake Van is not well studied, its geophysical characteristics are poorly documented and understood. An overall understanding of this lake as a complex highlands system is still lacking. This lack assumes utmost importance given the fact that Lake Van and surrounding highlands are prone to thinning convergent crust, decompressional melting magmatism and post-collisional opening of sutures, through which

extensional magma propagates. These processes dictate how ascending magmatic materials are transported through the crust toward the surface and react with their surrounding environment within the volcanic or magmatic edifice. A sequential development of these events is focused on understanding the rich dynamics of multiple linked systems with weak basement coupling and with many internal variables that exhibit multiscale interactions beneath the lake. Multi-component approach into basement and basin margin weakening highlights the relative roles of upper crustal tectonics, magmatism and the role of delamination and break off events, just beneath the lake. This generates deep insights into upper crust-driven seismicity and its results in basin response and subsequent impact on anisotropic variability of the convergent crust.

The previous study of this research remarks that the most explosive eruptions and long-term period seismicity are the consequences of gas-rich magmas and large pressure buildups as the magma releases gas during its ascent to shallow sedimentary levels through extensional and transtensional boundary faults in lake margins. Perturbations in the lake, such as magma-hydrothermal activity with the number of earthquakes, are attributed to the formation of fractures in the envelope surrounding a cooling magma body and upward migration of magma, allowing release of magmatic volatiles to the overlying hydrothermal system. Such distinctive characteristics reflect the influence of volcano-magmatic inputs on physical and chemical conditions. These inputs consist of hot gas and liquids that ultimately result from the interactions between groundwater and fluids released by a magma body at depth. Hence, Lake Van constitutes unique windows for better understanding both various extensional aspects of the theory of intraplate deformation based on Turkic-type orogeny and nature and characteristics of intraplate crustal deformation in E-Turkey. Thus, this research deals with some critical aspects of post-orogenic processes and discusses a prominent example of accretionary wedge-basins in the world and its crustal growth through neotectonic history.

The focus and objectives of Lake Van basin research are to provide a better understanding and overview of tectonic and magmatic processes in accretionary orogens and their role in the formation and evolution of the continental crust. Understanding post-collisional dynamics of accretionary wedges beneath Lake Van and their effect on Lake Van basin formation is essentially needed in this study. Particularly, it is aimed to recognize and clarify why accretionary orogens and related wedge basins are subjected to tectonic unstability, basin margin weakening, and basement reactivation, and how kinematic boundary conditions (versus stress) are changed in accretionary wedge-basins, causing thrust-sheet block rotation and producing extensional and strike-slip basin systems. Scientific data material and methodology of research framework is mainly based on seismic data equipment of International Continental Drilling Program (ICDP-seismic survey of PaleoVan Project-2004), multi-channel seismic reflection profiling and high-resolution GeoChirp system. Interpretation techniques of seismic sequence stratigraphy are applied for basin analysis and some specific approaches into basin model assumption are developed and interactively used. An examination and evaluation of multi-channel seismic reflection and high-resolution chirp data also cover the geological consequences of the largely Neogene delamination that characterizes the segments of interest, in response to late stage reorganization of the subduction zone, the delamination and break-off of the subducting slab. Seismic structural interpretation

of these events requires a comprehensive understanding of the entire Turkic-type orogenic system.

In seismic reflection research of Lake Van, the high quality data set is a predictor of tectonic and magmatic response with surprisingly good accuracy. The largely seismic data-based contributions investigate the following special subjects of the preliminary results to exhibit and interpret tectonic and magmatic record of orogeny in Lake Van basin. Seismic structural interpretation of overall deformations observed in and along the lake leads to clear evidences of basement reactivation, inversion tectonics, suture-parallel extension/strike-slip deformation, as well as extensional magmatism, magma-hydrothermal sediment deformations and post-magmatic hydrothermal alterations. Though there are many unanswered questions about all these issues, there are arguably even fewer constraints on the maturation of propagating magmas on extensional fault flanks of the lake. As an example, Lake water-intruding magma exchanges during maturation affect magma composition, permeability, and geophysical properties and are a major influence on lake water chemistry, evident by previous Helium isotope studies. Seismic reflection data evident considerable complications of tectonic and magmatic peculiarities and showed structural expressions of strike-/oblique-slip deformation, suggesting extensional and transtensional tectonic evolution of the lake. Seismic evidences also show that offset on shallow-seated and dipping extensional faults occurs in the lake. However, the controversy persists over the existence and mechanics of offsets on shallow-seated, low-angle extensional detachments. This substantially leads to an overall understanding of structural and sedimentary evolution of Lake Van basin.

Sediments in central Tatvan basin were deposited during the development of an extensional phase that created a half-graben system oriented generally W-E. There is no precise dating on the initial formation of the central graben but regional correlations would suggest that it began during Pliocene times. Central Tatvan basin is controlled by number of marginal strike-slip faults that moves in transtensional and transpressional system. Whole strike-slip fault system is negative flower in S and positive flower structure types in N, and forming highs (horsts) and lows (grabens). This tectonic phase is formed in Quaternary. In Late Quaternary, transpressional tectonics caused central Tatvan basin to shallowing toward N-margin. Thus, transpression at its peak in Quaternary period caused whole sedimentary fill inside the basin lifted, folded and faulted. Seismic structural interpretation showed the presence of reactivation of older structures by Plio-Quaternary extensional and strike-slip period, particularly during Plio-Pleistocene. Based on their faulting and folding timing generation, central Tatvan basin and Lake Van structural evolution into:

An extensional phase, during this phase the most prominent is rifting process that resulted in formation of central half graben, internal subbasins and horst structures as well as reactivaton of older structures. Basin fill during this phase yielded syn-extensional sedimentation. During this phase, rifting cessation and sagging processes during Quaternary that accompanied by generation of the basinal strike-slip fault as well as transtensional faulting in S- and transpressional faulting in N-margins. Structural orientation of the faulting is relatively W-E. During the same stage, release tension has resulted in extensional fractures, fissures, vents, en echelon faulting, half-graben redevelopment and graben-subbasins. The extensional stage that inverted the entire central Tatvan basin resulted in the formation of the strike-slip structures along pre-existing thrust fault. This extension is in accordance to the sinistral and dextral

strike-slip faults along N- and S-margins, particularly, along the greater intraplate Muş suture in S.

Dextral transtension in S-margin along the Muş suture produced a younger pull-apart subbasin bounded by syn-depositional, smaller en echelon faults in SE-delta, while a sinistral transpression produced backthrusts, folds, horsts and external subbasin observed along the N-margin. Structural interpretation and kinematics for the formation of internal subbasins, geometry and kinematic considerations of the right-stepping transtensional shear zone in S-margin, and graben doglegs-shaped subbasins in SE-delta indicate that the extensional stress was oriented predominantly E-W during the extensional-transtensional regime in W-margin and pull-apart formation, "sphenochasm", of the subbasins in W-end of SE-delta. As a result, a divergent strike-slip stress regime dominated the lake as the result of reactivation changes in the basin.

Transtensional regime in S- and W-margins gave rise to a series of extensional graben basin and subbasins followed by a prolonged period of subsidence and sedimentation extending into the Late Quaternary. Since then, the W-E trending strike-slip propagation of the shear zone in S along the Muş suture has reactivated the older intraplate convergence zone between EAAC (East Anatolia Accretionary Complex) and BP-M (Bitlis Pötürge-Massive). Since, beginning in the Late Pliocene and extending to the present day a major tectonic event began to affect S-margin of the lake as well as W-margin of SE-delta. The large-scale regional mechanics of this movement is closely related to slab delamination process, asthenospheric doming and thin crustal structure. The result has been a general W-E right-lateral divergent strike-slip reactivation of the Muş suture zone. Further N, the influence of the right lateral motion along the Muş suture adds a basinal stress regime in W- and N-margins, and considerably complicates the structural configuration in that area. This remarks that the younger oblique-slip faults represent pre-existing lines of weaknesses, which were subsequently reactivated as synthetic/antithetic, left/right-lateral strike-slip faults. In the Çarpanak and the sublacustrine basement block uplifts, these faults grade laterally into first-order thrust structures as their orientation does not change considerably to W-E and stress regime in the lake is reorientated to ENE-WSW.

In general, the syn-extension is characterized by sub-parallel seismic reflector dips towards the border faults. The internal reflectors often show transparent, discontinuous character in deeper portions of the graben and indicate a sharp change of reflection from basement to the syn-extension section. Tectonic and sedimentary interpretation of seismic sections suggests that the development of Lake Van basin was initiated by extensional process that produced a half-graben system, which most probably occurred at the Pliocene times. The development of the extensional half-graben system waned during some time and was followed by basinal transgression, depositing thicker sediments that filled in the grabens and covered the basement platform. The contact between the syn-extension and the angular unconformity along hinge margin of NE-Erek delta and Çarpanak spur zone is locally referred to as boundary Late Miocene and Quaternary. Towards to central graben area and subbasin centers this unconformable contact grades into nonconformity and disconformity. Sediments eroded from the highs were deposited in the central graben, also forming the deposition of the subbasins. This event was followed by a transgressive cycle. The transgression covered the basement and was controlled by the horst-graben tectonic/sedimentation system. The last deformation occurred

during Quaternary time, uplifting the Çarpanak block, and producing a transpression-en echelon fold system in central Tatvan basin. Tectonic elements formed during this phase were the reactivation of block faults to strike-slip faults (with a sinistral in N- and W-margins and a dextral movements in S-margin) which cut the previously formed thrust-fold system.

The Pre-Quaternary basement, the Çarpanak block, is well exposed into the E of the Tatvan basin in Çarpanak spur zone. The basement is classified as a Miocene-aged accretionary terrane, probably composed of limestone and/or metamorphic rock and unconformably overlain by deltaic sequences. The Çarpanak basement block uplift, which occurred at the end of deposition, effectively separated the basin from the deep lake in the E. This block uplift changed the cycle from one of transgression to regressive. The central part of the basin quickly subsided as the result of the continental uplift in the plateau center and the Çarpanak uplift in the E. The formation of this structural high caused intense erosion-deposition activity that produced the paralic and deltaic sedimentation of the NE- and SE-delta settings. These delta settings developed as separated blocks and differentially uplifted, subsided and were subsequently filled by transgressive-regressive sediments. Delta sedimentation occurred and completely formed in a transgressive-regressive cycles with several subcycles and local variation. In delta area, regressive and transgressive system tracts are used to partition sequences. The sediments were laid down in a variety of continental depositional settings, which, for this area includes alluvial fans, distributary plain/flood plain, lacustrine delta front, shallow and deep lacustrine environments. The clastic sediments were derived, for the most part, from local source areas and deposited in nearby subbasins. The forming of graben-subbasins commencing sedimentation is indicated by extensive turbidities and debris flows toward deeper sections, suggesting that sedimentation occurred in a lacustrine environment extensional system.

Widespread uplift of region is associated with river incision of fan systems and subsequent shift of sediment transport towards proximal shelf and deep-offshore areas. Relative changes in base-level controlled the relative position of the alluvial fans on the shelf areas, now partly exposed due to regional uplift, promoting major phases of prograding and/or retrograding in adjacent alluvial fans. Thus, the uplift of Çarpanak and NE-delta block had the effect of providing renewed topography in sediment-source areas, increasing the angle of incision, deposition and relative segmentation of evolving fans. The rapid scarp growth and tilting that is another characteristic feature of the lake caused pervasive slope failure, slumped and slided clinoform wedges. Not interestingly, the largest progradational slumps and slides are near faults or fault bends where the stable side slumps toward the most rapidly subsiding areas. Delta progradation over shelf occurred during lake-level low-stands, promoting downslope transport of sedimentary wedges by slope-slide/-channel systems into deeper depocenter areas. Delta progradation commencing in the Quaternary continues in the present-day modern delta.

General and simplified stratigraphic pattern exhibits the five stage cycle of tectonic phase associating sediment filling in the lake: 1) basement-fault reactivation and basin inversion, 2) regressive period: syn-extensional sedimentation and sag infill, 3) transgressive period: post-extensional sedimentation, onlap and downlap series, 4) deltaic infill (progradation and aggradation) of post-inversion topography and 5) oblique-slip deformation of the entire stratigraphic column. The stratigraphic evolution of Lake Van basin area well reflects the strong influence of intermittent

extensional and contractional tectonic events during the Quaternary time. This clearly shows that the lake was formed by a multiphase deformation resulting from an interaction of varying stress regimes during Plio-Quaternary. The lake well preserved a clear record of strike-slip tectonism in its sediments, often described as "fault-bend basin".

Structural geology and tectonic deformation in the lake is a part of post-collisional tectonic events in accretionary prism of E-Turkey. Seismic data interpretation favors basin-bounding faults as comprising upper crust-linked strike-slip faults throughout the Plio-Quaternary. The basement structure of the lake is highly anisotropic and an assemblage of crustal fragments/slivers, ophiolites, and accretionary wedge blocks. As a result of inversion tectonics that happened, caused tectonic regime change, and reactivated the basement, tectonic instability of accretionary wedge blocks underlying the lake resulted in strike-/oblique-slip movement of the upper crustal flakes intruded by extensional magmatism. Overall deformation furthermore resulted in numerous of discontinuous faults, followed by en-echelon fold forming with sharp corner to fault lines. The resulting oblique-slip structures likely accommodate the horizontal and vertical deformations caused by oblique-slip tectonics in the lake.

Based on faults orientation and kinematics, the faults in Lake Van have three patterns: N-margin transpression, S-margin transtension and W-margin transtension. This obliquity of the fault patterns implies that the lake is highly asymmetric across and along the strike of faults. Central Tatvan block obliquely tilts toward the fault and away from the direction that its side of the fault moves and thus appears to grow only in one direction along the faults. Within this structural framework, typical rift configuration is active margin on the W- and S-sides while flexure margin normally located on the N-side. During their early life, central half-graben area is filled up within continental and lacustrine sedimentary deposits. The peculiar one of graben-subbasins is the pull-apart "sphenochasm" formation developed in W-end of SE-delta. In the central half-graben area, subsidence and sedimentation changed with time, shifting along the faults at the slip rate. Overall geometry and pattern of the entire sedimentary column had a half-graben asymmetry. Horizontal successions such as turbidities, debris flows and sill features, are progressively tilted as the basin continues to grow. Each new deposit reached farther onto the tilted and sinking floor of the lake, forming onlap contacts. Seismic structural and sedimentary geometry of these onlap contacts is symptomatic of the obliquity and slip rate on the faults.

Shortly, Lake Van basin developed on the extensional side of a bend of the border fault in W. Transtensional fault pattern in W acted as controller on developing of central Tatvan basin with transtension and strike-slip sedimentation. Transtensional motion of the border fault downstream of the bend gradually returned to horizontal motion away from the bend in W. This pattern produced the characteristic "shingled" sequence developed in central Tatvan basin. Resulting space constraints required not only localized horizontal extension and thinning in W- and S-sides, but also shortening and thickening in N-side, in addition to strike-slip motion along the faults. The steep faulting along N-margin, the steeper this fault, the faster the subsidence required to accommodate bend-related extension. The role that the fault bend structure played in the lake growth is so clear that the main concern is an effect of asymmetry on lateral transport of the depocenter and strike-slip sedimentation rather than tectonic implications of the basin asymmetry. Asymmetry and unidirectional basin growth of the lake also indicated that dextral transtension in S-margin tracks a pre-existing Muş suture, current tectonic regime reactivated the older thrust faults. In

somehow, these thrust faults had to slip obliquely to accommodate horizontal motion and the lateral migration of depocenters, with both a divergent and convergent component added to the strike-slip motion. This obliquity, thus characterized the segment of the fault as transtensive in W and S or transpressive in N, respectively. This result well explains the presence of central half-graben basin and the abundance of internal and external subbasins in the lake. Block asymmetry and unidirectional growth of the lake, shingled and tilted deposition, rapid subsidence, and subsidence shifting at strike-slip rate are general signatures and the most prominent features in Lake Van as recognized in a number of well-known fault-bend basins.

Plio-Quaternary structural development of the Lake Van basin is the result of two separate stress regimes: a Paleotectonic period of collision-compression and a Neotectonic period of extension/strike-slip deformation. Older structural elements bordering the lake have undergone reactivation as sinistral and dextral strike-slip faults along the basin margins. The consequence of this stress reversal has been tectonic instability of accretionary wedges, a reactivation of convergent basement and a change in kinematic boundary conditions of the lake. As a result, during post-collisional period, Lake Van region has undergone basin block fragmentation and separation, implying an oblique opening of Muş suture, through which extensional magmatism propagated into the lake, intensely deformed lake sediments and created the huge magma-hydrothermal lacustrine system. For these reasons, the form of the early compressional Lake Van basin is quite different from the present-day basin. An interplay of sedimentation and tectonics in Lake Van provided a new angle on basement reactivation, oblique motion of the upper crustal flakes and the strike-slip evolution of accretionary wedge basins in Turkic-type orogenic setting.

VAN GÖLÜ HAVZASININ TEKTONİK VE MAGMATİK YAPISI VE YAPISAL EVRİMİ, DOĞU ANADOLU YIĞIŞIM KARMAŞIĞI (DAYK), DOĞU TÜRKİYE

ÖZET

Yeryüzündeki önemli dağ oluşum kuşaklarından birisi olan Doğu Anadolu Yığışım Karmaşığı (DAYK), yer bilimsel tüm alt disiplinlere ilişkin doğal fenomenleri ve süreçlerini teşkil eden bütüncül bir yer laboratuvarı konumundadır. Dalma/batma-yığışım, litosfer ayrılması ve kabuksal sıkılaşma süreçlerini kapsayan, bir çok yerbilimsel disiplin birbiri ile ilişkili olarak bölgeyi temsil etmektedir. Farklı zaman ölçeklerinde olmak üzere, bu disiplinler, Türkik tipindeki dağ oluşum kuşaklarında gerçekleşen, çarpışma sonrası kabuk oluşum süreçlerine önemli ve kiritik denebilecek katkılarda bulunmaktadırlar. Litosfer ayrılmasının bir sonucu olarak, DAYK, Tetisçevresi süperorojenik sistemlerdeki litosfer ayrılması fenomeninin küresel etkilerine sahip gibi görünmekte ve aynı zamanda, litosfer ayrılmasına bağlı olarak Türkik tipindeki küçük ölçekli ve sıcak dağ oluşum kuşaklarının en belirgin örneğini oluşturmaktadır. Türkik tipinde, çok genç bir dağ oluşum kuşağı olarak DAYK, şiddetli, kıta ortası ince kabuk deformasyonu, doğrultu atımlı havza oluşumu ve orografik çökelme sistemine bağlı olarak gelişen gerilmeli alkalin magmatizması oluşturabilen kabuk tektoniği ve magmatizmasını bünyesinde barindırmaktadır. DAYK'ın, ana tektonik blokları sınırlayan zayıf ve dirençsiz kenet zonlarının bindirme şeklinde dilimlenmelerine neden olan aktif sıkışmalı levha olma özelliği nedeniyle, bu küçük orojenik sistem, çarpışma sonrası süreçler boyunca, tektonik ve magmatik yapısı içerisinde sert gradiyentlere sahip aşırı bir karmaşıklık örneği sergilemektedir.

Anlaşılacağı üzere, DAYK'ın çarpışma sonrası evrimsel gelişimine dair ortaya atılabilecek soru ve sorgulamalar, Türkik tipindeki bir orojenik kuşak içerisindeki yığışım kaması havzalarının deformasyon biçimlerinin ve tektonik oluşumlarının anlaşılmasıyla cevaplandırılabilir. Bu kama havzalarının en belirgin olanı, orojenik doğrultuya paralel olarak gelişmiş olan Van Gölü çukurluğudur. Bu çukurluk, DAYK'ın rotasyonel kısımlarının derinliğine yerleşmiş ve bindirmelerle sınırlanmış bir bölgedir. Bu göl havzası, Bitlis Pötürge masifinin Kuzey sınırına, Muş kenet kuşağı boyunca yerleşmiş ve DAYK'ı, BPM'den ayırmaktadır. Van Gölü, aynı zamanda litosferik yapının bulunmadığı ve sıcak astenosferin yukarı domlaşma gösterdiği bölgede bulunmaktadır, bu nedenle, göl yaklaşık 2 km' lik yüksekliğe sahip dom şeklinde bir morfoloji göstermekte ve Van Gölü Domu olarak bilinmektedir. Gölün dom şeklindeki morfolojisi, kabuk oluşturma, kabuksal yoğunlaşma süreçlerini ve litosferik ayrılmanın yüzeysel etkilerini çok iyi bir şekilde temsil edebilen morfolojik bir paradigma olarak kendisini hissettirmiştir. Van Gölü Domu'nun anatomik yapısı sünek, zayıf, dirençsiz havza oluşumlu orojenik bir yapıyı açıkça gösterebilmekte ve aynı zamanda göl'ün hem morfolojik ve hem de limnolojik karekteristiği, yığışım karmaşığının domlaşma merkezinde plato riftleşmesi fenomenin orojenik özelliklerini ve temel yapının yeniden harekete geçmesini göstermesi bir sürpriz olarak karşılanmamalıdır.

Van Gölü, diğer dağ oluşum kuşaklarında çarpışmayla oluşan benzeri göllerle kıyaslandığında (Baykal gölü), Van Gölü'nün yeteri kadar çalışılamadığı ve jeofizik özelliklerinin ise beklenilen düzeyde olmamakla beraber, henüz anlaşılamadığı görülmektedir. Sonuçta, kompleks bir plato sisteminde yerleşke gösteren Van Gölü'nün gerçek manada bütüncül olarak anlaşılması hala sağlanamamıştır. Bu yetersizlik, önemli bir eksikliğide beraberinde getirmiştir. Bu eksikliğin gösterdiği en önemli unsur şudur ki, Van Gölü ve çevresi aslında, incelmiş sıkışmalı bir kabuk yapısının, ergime magmatizmasının ve gerilmeli magmatizmanın nüfuz edebildiği, çarpışma sonrası açılmış sutur zonlarının önemini göstermektedir. İfade edilen bu süreçler, yükselen magmatik malzemenin kabuğun içerisinden yüzeye doğru nasıl taşındığı ve volkanik ya da magmatik bir ortam içerisinde yakın çevreyle nasıl bir ilişkiye girdiğini göstermektedir. Bütün bu süreçlerin ardışık gelişimi, göl'ün temel yapısındaki bir çok karmaşık ilişkiyi gösteren, bir çok değişken parametreye sahip ve zayıf temel bağlantılı, çok bileşenli bağ sistemlerinin dinamik yapının anlaşılması üzerinde temellenmiştir. Göl temel yapısına ve havza marjin zayıflaşmasına çok yönlü bir yaklaşım, göl altı litosfer ayrışması ve kopması olaylarının, üst kabuk tektoniği ve magmatizmasının göreceli rollerine ışık tutmaktadır. Bu durum, üst kabuk kontrollü sismik aktiviteye ve sismik aktivitelere havzanın verdiği cevaba ilişkin derin bir bakış açısının oluşmasını sağlamaktadır ve aynı zamanda, sıkışmalı kabuğun homojen olmayan, anizotropik değişkenliğine dair önemli bir etkinin varlığınada işaret etmektedir.

Bu araştırmanın bir önceki safhasında, patlama şeklinde gerçekleşen magma akıntılarının ve uzun peryotlu sismik aktivitelerin, göl sınırlarındaki gerilmeli ve yanal-genişlemeli faylar boyunca, sığ sedimanter seviyelere doğru yükselim gösteren magmanin gazını salıvermesi süresince oluşan, yüksek basınçların ve gazca zengin magmatik aktivitelerin sonuçları olduğu ifade edilmişti. Göl havzasında etkinlik gösteren bir takım deformasyonlar, örneğin sismik olarak aktif magma hidrotermal oluşumlar, magmatik malzemenin açığa çıkmasına izin veren, yukarı doğru magma yükselimi ve soğuyan magma kütlesini çevreleyen kırık ve çatlakların oluşumu olarak nitelendirilmiştir. Bu türden belirgin karakteristik oluşumlar, ortamı belirleyen fiziksel ve kimyasal koşullar üzerinde volkano-magmatik girdilerin etkisini yansıtmaktadır. Bu türden girdiler, belirli bir derinlikteki, magmatik bir oluşum tarafından serbest bırakılan akışkanlar ve yeraltı suyu arasındaki ilişkilerden kaynaklanan sıcak gaz ve sıvıları içerebilmektedir. Bu nedenle, Van Gölü havzası, hem Doğu Türkiyedeki kıta içi kabuk deformasyonunun karakteristik doğasını ve hem de Türkik tipindeki bir orojenik kuşak içerisindeki kıta içi deformasyon kuramının farklı görüşlerini daha iyi anlayabilmek için bütüncül bir pencere görevini üstlenmiştir. Böylece, bu araştırma orojenik aktivite sonrası bir takım süreçlerin, bir takım kiritik konularını incelemekte ve yeryüzündeki yığışım kaması havzalarının en belirgin örneğini ve bu örneğin, neotektonik süreç boyunca devam edegelen kabuksal gelişimini tartışmaktadır.

Van Gölü araştırmasının temel amaçları arasında, yığışım prizması şeklinde oluşum gösteren orojenlerdeki tektonik ve magmatik süreçlerin yeniden incelenmesi ve kıtasal kabuğun evrimi ve oluşumundaki rolününü anlaşılması da yer almaktadır. Van Gölünün temel yapısını oluşturan yığışım kamalarının çarpışma sonrası dinamiğini and bu kamaların Van Gölü havzasının oluşumundaki etkin rolünü anlayabilme ihtiyacı, bu çalışma süreci boyunca sürekli olarak kendini hissettirmiştir.

Özellikle, yığışımlı olarak oluşan orojenlerin ve ilgili kama şeklindeki havzaların, neden tektonik bir kararsızlığa doğru evrildiğini, havza sınırlarının neden zayıfladığı

ve temel yapının neden harekete geçtiğine dair bir takım yapısal problemlerin varlığına dikkat çekilmiştir. Ayrıca, bindirme dilimi blok rotasyonuna neden olabilen ve doğrultu atımlı ve gerilmeli havza sistemleri oluşturabilen, yığışım kaması havzalarında, kinematik sınır koşullarınını nasıl ve ne türden değişimler gösterebileceği amaçlanmıştır. Bilimsel verinin elde edilmesi ve araştırma konusunun metodolojisi, Uluslararası Kıta Delme Programının (UKDP) 2004 yılı PaleoVan projesi dahilinde gerçekleşen sismik veri ekipmanına, çok kanallı sismik yansıma profillerine ve yüksek çözünürlüklü GeoChirp sistemine dayanmaktadır. Havza analizi için, sismik sekans stratigrafisinin temel yorumlama teknikleri uygulanmıştır ve tasarlanan havza modeli için, bazı özel yaklaşım teknikleri geliştirilmiş ve bunlar etkin bir şekilde kullanılmıştır. Çok kanallı sismik yansıma ve yüksek çözünürlüklü GeoChirp verisinin analitik olarak değerlendirilip yorumlanması, dalan litosfer ayrılması ve dolayısıyla dalma batma sisteminin yeniden organize olmasına cevaben oluşan bir takım segmentleri belirleyen Neojen ayrılmasının jeolojik sonuçlarını da tartışmayı kapsamaktadır. Bu tür olayların sismik yapısal yorumlanması, bütün bir Türkik tipi orojenik sistemin detaylı anlaşılmasını gerektirmiştir.

Van Gölünün sismik yansıma profillleriyle araştırılmasında, yüksek kaliteli veri setinin, yüksek orandaki hassasiyeti ve ölçüm doğruluğu, tektonik ve magmatik olayların en doğru tahminini verebilmiştir. Sismik yansıma metodu kullanılarak gerçekleştirilen bu çalışma, Van Gölü havzasındaki orojenik yapının tektonik ve magmatik kaydını göstermek ve yorumlamak için bazı ilksel sonuçları ve bu sonuçların gerektirdiği bir takım yapısal olayları aşağıda sıralamıştır. Göl havzası içerisinde ve havza boyunca gözlemlenen deformasyonların sismik yapısal yorumlanması, temel yapının yeniden harekete geçmesi, terslenme tektoniği, kenet zonuna paralel gerilme ve doğrultu atım deformasyonu, ayrıca gerilme magmatizması, magma hidrotermal sediment deformasyonları ve magmatizma sonrası hidrotermal alterasyonların açık delillerine öncülük etmiştir. Bu türden bulgularla ilgili olarak henüz cevaplanmamış bir çok soru varsada, Göl'ün genişlemeli olarak faylanmış kenarlarında göç ederek ilerleyen magmatizmanın yapısal olgunlaşmasına dair bir takım model tasarıları önerilebilmektedir. Örneğin, yapısal olgunlaşma süreci boyunca, Göl su kolonuna sokulum gösteren magmatik yükselimler, magma içeriğini, geçirgenliğini ve bir takım jeofiziksel özellikleri etkilemekte ve böylece, daha önce yapılmış Helyum izotop çalışmaları tarafından da rapor edildiği üzere, Göl suyunun kimyasal içeriğinde ciddi bir etkiye neden olmaktadır. Sismik yansıma verisi, tektonik ve magmatik anomalilerin, kayda değer karmaşıklarını ortaya çıkarabilmiş ve Göl'ün gerilmeli ve yanal-genişlemeli tektonik evrimini açıklayan doğrultu ve/veya oblik atım deformasyonunun yapısal ifadelerini göstermiştir. Sismik yapısal deliller, aynı zamanda, sığ derinliklere yerleşmiş, eğim atımlı genişlemeli faylarda oluşan atımın, Göl'de oluşabildiğini göstermiştir. Fakat, bununla beraber, sığ derinlikli ve küçük açılı genişlemeli sıyrılma faylarındaki atımların varlığına ve mekaniğine dair çelişkiler halen mevcuttur. Bu durum, Van Gölü havzasının yapısal ve sedimanter evriminin bütüncül olarak anlaşılmasını gerektirmiştir. Sismik yansıma ve GeoChirp kesitlerinin karşılaştırmalı tektonik, yapısal ve sedimanter yorumu ve üretilmiş olan tektonik-deformasyon-morfo-topografik haritalar aşağıda sıralanan ilksel sonuçları ortaya koymuş ve Van Gölü'nün, hem tektonik ve hem de sedimanter evrimine ışık tutmuştur.

Tatvan havzasındaki sedimanlar, B-D olarak yerleşke göstermiş yarı-graben sistemini yaratan genişlemeli bir fazın oluşum süresi boyunca çökelmiştir. Merkezi

yarı graben sisteminin ilksel oluşumuna dair herhangi bir hassas yaşlandırma verisi bulunmamaktadır, ama bölgesel korelasyonlar, graben sisteminin Pliyosen boyunca gelişmeye başladığını önermektedir. Merkezi Tatvan havzası, yanal-genişlemeli ve yanal-sıkışmalı bir sistem içerisinde hareket eden doğrultu atımlı faylar tarafından kontrol edilmektedir. Doğrultu atım sistemi, Güney sınırda negatif ve Kuzey sınırda pozitif çiçek yapısına sahiptir, böylece horst şeklindeki yükselimlerin ve graben şeklindeki çukurlukların oluşmasına neden olmuştur. Bu tektonik faz, Kuvaterner döneminde gerçekleşmiştir. Geç Kuvaterner döneminde ise, yanal-sıkışmalı tektonik, merkezi Tatvan havzasının Kuzey sınıra doğru sığlaşmasına neden olmuştur. Böylece, Kuvaterner döneminde maksimuma ulaşan yanal-sıkışmalı tektonik aktivite, Göldeki bütün bir çökel dolgusunun deforme olmasına, kıvrımlanmasına ve faylanmasına neden olmuştur. Sismik yapısal yorumlama, eski döneme ait yaşlı yapıların, Pliyo-Kuvaterner yaşlı genişlemeli ve doğrultu atım süreci tarafından ve özellikle Pliyo-Pleyistosen dönemi boyunca, yeniden hareket geçtiğini göstermiştir. Faylanma ve kıvrımlanmanın zamansal oluşum süreci temel alındığında, merkezi Tatvan havzası ve Van Gölü'nün yapısal evrimi aşağıdaki gibi özetlenebilir:

Genişlemeli faz boyunca belirginleşen en dikkat çekici yapı riftleşme-yarılma sürecidir, bu süreç merkezi yarı-grabeninin, iç havzaların ve horst şeklindeki yükselim yapılarının oluşmasına ve aynı zamanda da eski yapıların yeniden harekete geçmesine neden olmuştur. Bu faz boyunca, havza dolgusu, genişleme süreciyle eş zamanlı olarak gelişen sedimentasyona maruz kalmıştır (genişlemeyle eş zamanlı sedimentasyon). Bu faz'ın Kuvaterner evresi boyunca, riftleşmenin bitişi ve havza genişlemesi süreçlerine, doğrultu atımlı faylanmaya ilaveten, Kuzey sınırında yanal-sıkışmalı and Güney sınırında yanal-genişlemeli faylanma eşlik etmiştir. Faylanma doğrultusu genel hatlarıyla Doğu-Batı olarak gerçekleşmiştir. Aynı evre boyunca, genişlemeli deformasyonun ortaya çıkışı, genişlemeli çatlak ve yarıklara, sıçramalı faylara, yarı-graben oluşumuna ve graben tipindeki iç havzalara neden olmuştur. Merkezi Tatvan havzasının bütüncül olarak yapısal terslenmesini sağlayan genişlemeli evre, daha önce var olan ters fayların doğrultusu boyunca, doğrultu atım yapılarının oluşmasına neden olmuştur. Bu genişlemeli evre, Göl'ün Kuzey ve Güney sınırları boyunca oluşan sol ve sağ yanal doğrultu atım faylarla, yapısal olarak uyumludur, bu uyum özellikle, Güney sınırında yerleşke gösteren kıta içi Muş kenedi boyunca belirgindir.

Sol yönlü yanal-sıkışmalı tektonik rejim, Kuzey sınırı boyunca gözlemlenen, geriye bindirmeleri, kıvrım ve horst yapılarını ve iç havzaları oluştururken, Muş kenedi boyunca uzanan Güney sınırındaki sağ yönlü yanal-genişlemeli tektonik aktivite, Güney Doğu deltasında çökelmeyle eş zamanlı olarak gelişen ve küçük ölçekli sıçramalı faylarla sınırlanmış genç bir çek-ayır iç havzasını oluşturmuştur. Göl'deki iç havzalar, Güney sınırdaki sağ yönlü sıçramalı, yanal-genişlemeli makaslama zonu ve Güney Doğu deltasındaki çek-ayır havza geometrisi ve kinematik yapısı dikkatle incelendiğinde, gerilmeli stresin, Batı sınırdaki genişlemeli ve yanal-genişlemeli rejim boyunca, Doğu-Batı olarak yönlendiğini ve Güney Doğu deltasının Batı sınırında yerleşke gösteren iç havzaların "sfenokazm" adı verilen, çek-ayır mekanizmasıyla oluştuğunu işaret etmiştir. Göldeki yapısal unsurların yeniden hareketlenmelerinin bir sonucu olarak, yanal-genişlemeli gerilme rejimi bütünüyle Göl'e hakim olmuştur.

Güney ve Batı sınırlardaki yanal-genişlemeli rejim, genişlemeli merkezi graben havzası ve iç havzalar serisinin oluşumuna olanak tanımıştır, merkezi havza ve iç havza serilerinin oluşumunu, Geç Kuvaterner dönemine kadar uzanım gösteren

sedimentasyon ve çökme peryotları izlemiştir. Bu süreç boyunca, Güney'de, Muş kenedi boyunca gelişme gösteren, makaslama zonunun Doğu-Batı uzanımlı olarak doğrultu atım mekanizmasıyla ilerlemesi, Bitlis Pötürge-Masifi (BP-M) ve Doğu Anadolu Yığışım Karmaşığı (DAYK) arasındaki sınırda yer alan, eski bir kıta içi sıkışma-kilitlenme zonunu etkileyerek ederek yeniden harekete geçirmiştir. Son Pliyosen döneminden başlayarak günümüze kadar devam eden, önemli bir tektonik olay, Göl'ün Güney sınırını ve Güney Doğu deltasının Batı sınırını ciddi bir şekilde etkilemiştir. Bu tektonik hareketin bölgesel mekaniği, litosferik ayrılma, astenosferik domlaşma ve incelmiş kabuk yapısıyla çok yakından ilgili olmuştur. Sonuç, Muş kenet zonunun, Doğu-Batı doğrultulu sağ yönlü yanal-genişlemeli olarak yeniden hareketlenmesi olmuştur. Muş kenedi boyunca gelişen sağ yanal hareketin etkisi, Göl'ün Batı ve Kuzey sınırları başta olmak üzere, havza ölçeğinde yeni bir gerilme rejimi oluşturmuş ve Göl'ün yapısını ciddi bir şekilde karmaşık hale getirmiştir. Bu durum, genç oblik atımlı fayların, daha önce havzada var olan, eski zayıflık zonlarını temsil ettiğini işaret etmektedir ki, bu zayıflık zonları sintetik/antitetik, sol-yanal/sağ yanal doğrultu-atımlı faylar olmak üzere yeniden hareketlenmişlerdir. Bu faylar, Çarpanak ve Göl içi blok yükselimleri başta olmak üzere, ilksel olarak oluşmuş bindirme yapılarına doğru yanal geçişlilik özelliği gösterirler ve fayların Doğu-Batı doğrultularında ise ciddi bir değişim gözlenmemektedir.

Göl de genişlemeyle eş zamanlı oluşan yapısal durum, sınır faylarına doğru eğimlenen ve bükülüm gösteren, yarı paralel sismik yansıtıcıların varlığıyla karekterize edilmiştir. İçsel sismik yansıtıcılar sıklıkla, merkezi graben havzasının derin kesimlerinde transparan ve süreksiz yansıma özellikleri göstermekte ve temel yapıdan, gerilme ile eş zamanlı olarak oluşmuş kesimlere doğru, sismik yansımada keskin bir değişimi işaret etmektedir. Sismik kesitlerin tektonik ve sedimanter yorumu, Van Gölü havzasının yapısal gelişiminin, büyük bir olasılıkla Pliyosen zamanında gelişmiş yarı graben sistemini üreten genişlemeli bir süreç tarafından başlatılmış olduğunu ileri sürmüştür. Genişlemeli yarı graben sisteminin gelişimine, Gölde'ki temel platformunu tümüyle kaplayan ve iç graben havzalarını dolduran kalın sedimanter tabakaların çökelimine imkan veren havza ölçekli bir transgresyon eşlik etmiştir. Kuzey Doğu Erek deltası ve Çarpanak çıkıntı zonunun sınırları boyunca gelişme gösteren, açısal uyumsuzluk yüzeyi ve genişlemeyle eş zamanlı oluşmuş yapısal durum arasındaki ara dokanak düzlemi, lokal olarak, Geç Miyosen ve Kuvaterner sınırı olarak tespit edilebilir. Bu uyumsuzluk dokanağı, merkezi graben alanına ve iç havzaların merkezine doğru, paralel uyumsuzluk geçişliliği göstermektedir. Sedimanlar, horst şeklindeki yükselimlerden aşınarak merkezi grabende çökelmişler ve aynı zamanda, iç havzaların dolmasını sağlamışlardır. Bu olaya, transgresif bir döngü eşlik etmiştir. Göl temel yapısını kaplayan transgresyon, horst-graben tektoniği ve sedimentasyonu sistemi tarafından kontrol edilmiştir. En son deformasyon Kuvaterner zamanı boyunca oluşmuş, Çarpanak bloğunu yükseltmiş ve merkezi Tatvan havzasındaki transpresyonal bir kıvrım sistemini üretmiştir. Bu dönem boyunca Göl'de oluşmuş tektonik unsurlar, blok faylarının, doğrultu atımlı faylar olarak yeniden hareketlenmerinin bir sonucu olmuştur ki, bu faylar daha önce oluşmuş bindirme-kıvrım sistemini kesmektedir.

Pre-Kuvaterner yaşlı temel kaya olan Çarpanak bloğu Çarpanak burnundan, Tatvan havzasının Doğusuna doğru açığa çıkarak mostra vemiştir. Bu temel yapısı, delta çökelleri tarafından uyumsuz olarak üzerlenmiş metamorfik kayalar veya kireçtaşı yapılarından oluşmuş Miyosen yaşlı bir yığışım bloğu olarak sınıflandırılmaktadır. Sedimentasyon peryodu nun bitiminde oluşmuş olan Çarpanak temel blok yükselimi,

etkili bir şekilde Doğuda bulunan delta sistemini derin göl ortamından ayırmıştır. Bu blok yükselimi transgresyon ve regresyon döngüsünü etkileyerek değiştirmiştir. Tatvan havzasının merkezi, Doğudaki Çarpanak yükselimi ve plato merkezinin, bölgesel kıta yükseliminin sonucu olarak hızlı bir şekilde çökmeye uğramıştır. Bu yapısal yükselimin oluşumu, Kuzey Doğu ve Güney Doğu delta ortamlarının paralel sedimentasyonunu sağlayan şiddetli erozyon ve çökelim aktivitesi neden olmuştur. Birbirinden ayrık olarak gelişerek, farklı yükselim ve çökme süreçlerine maruz kalan bu delta ortamları, transgresif ve regresif sedimanlarla dolmuştur. Sonuçta, delta sedimentasyonu gerçekleşmiş ve tümüyle, lokal bir değişim içerisinde, bir kaç alt döngülü transgresif ve regresif sistemler içerisinde oluşum göstermiştir. Sedimanlar, içsel çökel ortamlarında da yayılım göstermiştir, bu türden yayılım ortamları alüvyal fanlar, dağılım düzlükleri, gölsel delta önleri, sığ ve derin göl çevrelerini içermektedir. Klastik çökellerin bir çoğu lokal kaynak alanlarından gelmiştir ve yakınlardaki iç havzalara çökelmiştir. Sedimentasyon sürecini başlatan graben tipindeki iç havzaların oluşumu, derin kesimlere doğru akma ve yayılma gösteren debris akıntıları ve geniş yayınım gösteren türbiditik çökeller tarafından belirgindir. Bu durum açık bir şekilde, Göl ortamı gerilmeli bir sistem içerisinde oluşum gösteren sedimentasyonu ifade etmektedir.

Bölgesel ölçekli yükselim, delta fan sistemlerinin dereler tarafından derince kazılması ve derin ve sığ çökel ortamlarına doğru çökel taşınımındaki belirgin kayma ile ilişkilidir. Göl taban düzleminde seviye oynamaları, sığ su ortamlarındaki alüvyal fan sistemlerinin göreceli olarak pozisyonlarını kontrol etmiştir ki bu alanlar, bölgesel ölçekli yükselim nedeniyle kısmen ortaya çıkmış, ve yakın alüvyal fanlarda oluşan, delta gerileme ve ilerlemesinin önemli fazlarını oluşturmuşlardır. Böylece, Çarpanak ve dolayısıyla Kuzey Doğu delta bloğunun yükselimi, sediman kaynak alanlarında yeni bir topografyanın oluşumunda önemli bir etkiye sahip olmuş ve bu şekilde derine doğru kazılma açısını yükselterek, çökelme ve fan delta sistemlerinin segmentleşmesine önemli bir etkiye sahip olmuştur. Hızlı skarp yapısı gelişimi ve eğimlenme, Göl'ün bir diğer karekteristik özelliğidir, bu özellik eğimsel kararsızlıklara, kayan ve yuvarlanan delta kamalarının varlığına neden olmuştur. Büyük ölçekli delta kayma ve akma yapılarının, faylara ya da fay bükümlerinin bulunduğu yerlere yakın yerleşke göstermesi bu nedenle bir sürpriz değildir. Faylanmanın kararlı olduğu bölgeler dahi hızlı bir şekilde çökme gösteren alanlara doğru kayma eğilimi göstermiştir. Göl su seviyesinin düşük kademeleri boyunca, şelf alanlarında delta progradasyonu oluşmuş ve bu oluşum, eğim kayması ve dere kanal sistemleri tarafından sedimanter kamaların derin depolanma merkezlerine doğru eğim aşağı taşınımını sağlamıştır. Kuvaterner döneminde başlayan delta progradasyonu günümüzde de halen modern delta sistemi olarak devamlılık göstermektedir.

Basitleştirilmiş genel stratigrafik görünüm, Göl'ün sedimentasyonuna bağlı olarak gelişen tektonik fazın beş aşamalık döngüsünü işaret etmektedir: 1) temel-fay yeniden hareketlenmesi ve havza terslenmesi, 2) regresif peryod: genişleme ile eş zamanlı sedimentasyon ve genişleme dolgusu, 3) transgresif peryod: genişleme sonrası sedimentasyonu, onlap and downlap serileri, 4) terslenme sonrası topografyasının delta dolgusu (progradasyon ve agradasyon) ve 5) bütün bir stratigrafik kolonun oblik-atım deformasyonuna maruz kalması. Van Gölü havzasının stratigrafik evrimi, Kuvaterner zamanı boyunca süreksizlerle gelişen sıkışmalı ve genişlemeli tektonik olayların baskın etkisini çok iyi bir şekilde yansıtmaktadır. Bu durum, Göl 'ün Pliyo Kuvaterner dönemi boyunca değişkenlik

gösteren gerilme rejimlerinin birbiriyle ilişkisinden kaynaklanan çok fazlı bir deformasyon tarafından oluşturulduğunu açıkca göstermektedir. Göl, sıklıkla fay büküm havzası olarak tanımlanan doğrultu atım tektoniğinin açık ve net bir kaydını kendi çökel sistemi içerisinde iyi bir şekilde korumuştur.

Göl'ün yapısal jeolojisi ve tektonik deformasyonu, gerçekte Doğu Anadolu yığışım kompleksinde devam etmekte olan çarpışma sonrası tektonik olayların sadece bir bölümünü oluşturmaktadır. Sismik verilerin yorumu havzayı sınırlayan fayları, Pliyo Kuvaterner boyunca gelişmiş, üst kabuk bağlantılı doğrultu atımlı faylar olarak belirlemiştir. Göl'ün temel yapısı, yüksek oranda anizotropik özelliğe sahip, yığışım kaması bloklarının, ofiyolit ve kabuk dilimlerinin bir araya gelmesinden ibaret olmuştur. Göl'de tektonik rejime değişimine ve temel yapısının yeniden hareketlenmesine neden olan inversiyon "terslenme" tektoniğinin bir sonucu olarak, Göl tabanı yığışım kaması bloklarının tektonik kararsızlığı, genişlemeli magmatizmanın sokulum yaptığı üst kabuk bloklarının doğrultu veya oblik atımlı hareketine neden olmuştur. Ayrıca, genel deformasyon yapısı bir takım süreksiz ve kesintili faylara da neden olmuş ve deformasyona, fay hatları boyunca gelişen keskin kenarlı sıçramalı kıvrımlar eşlik etmiştir. Sonuçta ortaya çıkan oblik atımlı yapılar, Göl içerisinde oblik atımlı tektoniğin neden olduğu yatay ve dikey deformasyonları karşılamıştır.

Fay oryantasyonu ve kinematiği temel alındığında, Van Gölün deki faylar başlıca üç ana yapıya ayrılabilirler: K-sınırı yanal-sıkışmalı, G-sınırı yanal-genişlemeli and B-sınırı yanal-genişlemeli. Fayların oblik gelişimi, Göl 'ün fayların doğrultusu boyunca önemli ölçüde asimetrik bir gelişim gösterdiğini ifade etmektedir. Merkezi Tatvan bloğu oblik bir şekilde faylanmaya doğru eğimlenmiştir ve fayın hareket eden kenarından uzağa doğru meyil kazanmış ve böylece faylar boyunca sadece tek bir yönde ya da tek yönelimli bir oluşum göstermiştir. Böyle yapısal bir çerçeve içerisinde, bükümlü bir sınırı yapısı Kuzey kenarda oluşurken, tipik bir geişleme ya da riftleşme yapısı Batı ve Güney kenarlarında aktif birer sınır yapısı olarak göze çarpmaktadır. Faylanmaların ilksel oluşum süreçleri boyunca, merkezi yarı graben alanı, karasal ve gölsel çökel ortamı içersinde dolmuştur. Graben tipindeki iç havzaların en belirgin olanı, Güney Doğu deltasının Batı sınırında gelişim gösteren, bir çek ayır havzası tipindeki "sfenokazm" oluşumudur. Merkezi yarı graben alanında, çökme ve sedimantasyon zamanla değişkenlik göstermiş ve belirli bir atım oranına sahip faylar boyunca bir takım sapmalara maruz kalmıştır. Bütün bir çökel kolonunun genel geometrisi ve yapısal görünümü yarı graben asimetrisini göstermiştir. Göl havzası gelişim ve oluşum sürecine devam ederken, yatay yayınımlı sedimanter dizilimler, örneğin türbitler, debris akmaları ve sill yapıları, aşamalı olarak ve gittikçe gelişen bir düzeyde eğimlenmişlerdir. Her bir çökelim serisi daha ileri bir düzeye eğimlenmiş ve çökmekte olan göl tabanına doğru uzanım göstererek onlap serilerini ve ilgili kontakt yüzeylerini oluşturmuştur. Bu onlap kontak yüzeylerinin sismik yapısal ve sedimanter geometrisi, faylardaki atım ve ötelenme oranının ve aynı zamanda oblikleşmenin semptomatik karekterini ifade etmektedir.

Van Gölü havzası Batıda ki sınır fayının bükümlenme gösterdiği genişlemeli kenarında oluşmuştur. Batıdaki yanal-genişlemeli faylanma, yanal-genişlemeli ve doğrultu atımlı sedimentasyon gösteren merkezi Tatvan havzasının gelişiminde ana kontrol mekanizması olarak davranmıştır. Sınır fayının büküm aşağı yanal-genişlemeli hareketi aşamalı olarak, Batıdaki bükümden uzağa doğru, yatay bir harekete dönüşmüştür. Bu yapısal oluşum, merkezi Tatvan havzasın da gelişen

karakteristik doğrultu atımlı dizilim sekanslarını oluşturmuştur. Böyle bir yapısallık sonucu oluşan mekansal ve yersel boşluklar, faylanmalar boyunca gelişen doğrultu atımlı harekete ek olarak, hem Batı ve Güney kenarlardaki lokalize olarak gelişen yatay gerilme ve incelmeyi ve hem de Kuzey kenardaki kısalma ve kalınlaşmayı gerektirmiştir. Kuzey sınırı boyunca gelişen dik faylanmaya dikkat edildiğinde, bu fay düzlemi her ne ölçüde dik olarak gelişebilmişse, fay bükümlenmesine bağlı olarak gelişen gerilmeyi karşılayabilmek için gerekli olan çökmede o derece hızlı gerçekleşmiştir. Asimetrik havza yapısı ve Göl'ün tek yönlü yapısal gelişimi aynı zaman da, Güney sınırdaki sağ yönlü yanal-genişlemenin, daha önce var olan Muş kenedini izlediğini ve var olan tektonik rejimin eski bindirme faylarını yeniden harekete geçirdiğini göstermiştir. Bu bindirme fayları ana çökel merkezinin yatay migrasyonunu ve yatay hareketi karşıılayabilmek için oblik olarak, hem genişlemeli ve hem de sıkışmalı olarak atım yapmışlardır. Böylece, bu oblik yapı Batı ve Güney de yanal-genişlemeli ve Kuzeyde yanal-sıkışmalı faylar olarak, fay segmentlerini karekterize etmiştir. Bu durum, net bir şekilde Göl'de içsel ve dışsal havzaların çokluğunu ve merkezi yarı graben havzasının varlığını açıklayabilmektedir. Havza blok asimetrisi ve Göl'ün tek yönlü yapısal gelişimi, çökel dizilimi ve eğimli sedimentasyon, hızlı çökme ve doğrultu atım oranında çökme merkezinin kayma göstermesi, Göl'ün temel yapısal unsurları olmakla beraber, dünyada çok iyi bilinen fay bükümü havzalarında görüldüğü gibi, Van Gölü'nün en belirgin özelliklerini teşkil etmektedir.

Van Gölü havzasının Pliyo-Kuvaterner dönemine ait yapısal gelişimi iki ayrı gerilme rejiminin sonucu olarak gözükmektedir: bunların ilki, çarpışma-sıkışma peryodunun paleotektonik dönemi, diğeri ise, genişleme/doğrultu-atım peryodunun neotektonik dönemidir. Göl'ü sınırlayan eski yapısal elementler, havza sınırları boyunca sağ yanal ve sol yanal doğrultu-atımlı faylar olmak üzere yeniden hareketlenmişlerdir. Bu gerilme terslenmesinin sonucu, yığışım kamalarının tektonik kararsızlığı, sıkışmalı temel yapının yeniden hareketlenmesi ve Göl'ün sınır koşullarının kinematik yapısında önemli bir değişim olarak belirlenmiştir. Sonuç olarak, çarpışma sonrası dönem boyunca, Van Gölü havzası blok parçalanmasına ve ayrışmasına maruz kalmıştır. Bu ayrışma Muş kenedinin oblik olarak açılmasına işaret etmektedir. Kenet boyunca genişlemeli magmatizma Göl'e doğru ilerleme göstermiş, Göl çökellerini şiddetli bir şekilde deforme etmiş ve magma-hidrotermal göl sisteminin oluşmasına neden olmuştur. Bu nedenle, Van Gölü'nün ilksel sıkışmalı oluşum formu, günümüz havza yapısından çok belirgin bir şekilde farklıdır. Van Gölü havzasındaki sedimentasyon ve tektoniğin karmaşık etkileşimi, temel hareketlenmesi, üst kabuğa ait blokların oblik hareketi, ve Türkik tipinde orojenlerde bulunan yığışım kaması havzalarının doğrultu-atımlı gelişimine yeni bir bakış açısı getirmiştir.

1. INTRODUCTION

1.1 Global Impacts of Delamination Phenomena in Tethyside Superorogenic Systems

Convective removal of lithosphere beneath mountain belts has global consequences of lithospheric and/or crustal delamination rather than thermal and mechanical consequences. This views post-collisional involvement of the convergent crustal material in delamination of the lithosphere. The one speculative consequence of lithospheric delamination with continental crust involved is that the lithospheric delamination process has resulted in an enormous loss of continental crust over the last 600 m.y. This loss could have also significantly influenced the climatic and biologic evolution on Earth (Massonne, 2005) and also formation of deeper sedimentary basins with thicker deposits.

A model of lithospheric detachment and slab break off is extremely effective process and well applicable in the magmatism and deformation of collisional orogens (see Platt and England, 1994 and also see its excellent test model in Davies and von Blanckenburg, 1995). The slab detachment, then subsequent uplift, is followed by post-collisional intraplate deformation of weak continental crust (see Variscan tectonics of central Europe in Krohe, 1996) and strike-slip/extensional tectonics (also see Betic-Rif orogeny in Zeck, 1996). At the same time, large volumes of extensional alkaline magma, the formation of which is clearly triggered by ascending hot mantle material causing an increase of the geothermal gradient, intruded the convergent crust (see the Variscan crust in Massonne, 2005 and Nappe tectonics in Matte and Burg, 1981 and Schulmann et al., 1991). Suture-bounded fault and shear zones (Rajlich, 1990; Krohe, 1996) also contribute to a collage of many small basement blocks of different age and metamorphic evolution, and sedimentary rocks.

Convective instability of a thickened boundary layer and its relevance for the thermal evolution of the continental crust also gives the most important consequences of lithospheric delamination. The critical one of these consequences involving

continental crust with respect to the evolution of the continental crust on earth, in general, is the portions of the crust that can be involved in the delamination. This can produce localized crustal thinning and the squashy basement over doming asthenosphere. The warm and weak convergent crust is highly vulnerable intraplate deformation. The local crustal involvement in the lithospheric delamination depends on the quantity of dense, mainly basic, material in the corresponding crustal portions. This involvement can be so intense that only relatively thin crust (20–30 km thick) remains in segments of the formerly equally thickened crust, so that basins suddenly evolve that can be filled with km-thick sequences of sediments (Massonne, 2005). Heterogeneous internal deformation would be evidence for thinning of the continental crust by the delamination process, which would also explain why basins were newly formed despite continuous collision. In these, up to several km-thick sequences of sediments are deposited.

In the Tethyside superorogenic systems (Fig. 1.1), subduction-collision and slab detachment processes play a significant role and control the tectonic evolution of the convergent crust and intraplate sedimentary basins, once the subduction zone is taken as the structure of reference in a plate tectonic framework of orogens (see Şengör and Natal'in, 2007 for orogenic terminology). Superorogenic belts formed by more than one collision between continents contain invaluable records of the plate tectonic history of the Earth and collision-related deep orogenic lakes and hence, have always attracted the attention of extensive studies in orogenesis. The genetic connexion between the two orogenic systems combines them into a single superorogenic system (Şengör and Natal'in, 2007). Mediterranean region has the rich complexity of such an orogenic system. Seismic tomography models reveal that not all subducted slabs in the Mediterranean region are connected to the lithosphere at the surface, which has been interpreted as evidence for slab detachment (Wortel and Spakman, 2000 and Facenna et al., 2006) (Fig. 1.2). In Mediterranean region, how and which portion of crustal material is involved in delamination of the lithosphere during post-collisional period was well studied by Masonne, (2005). In this study, global consequences of lithospheric/crustal delamination with continental crust involved were discussed. This model study with its global pattern was applied to the Cretaceous to Quaternary evolution of the orogenic chains in the Mediterranean region, superorogenesis of the Tethysides (Fig. 1.1).

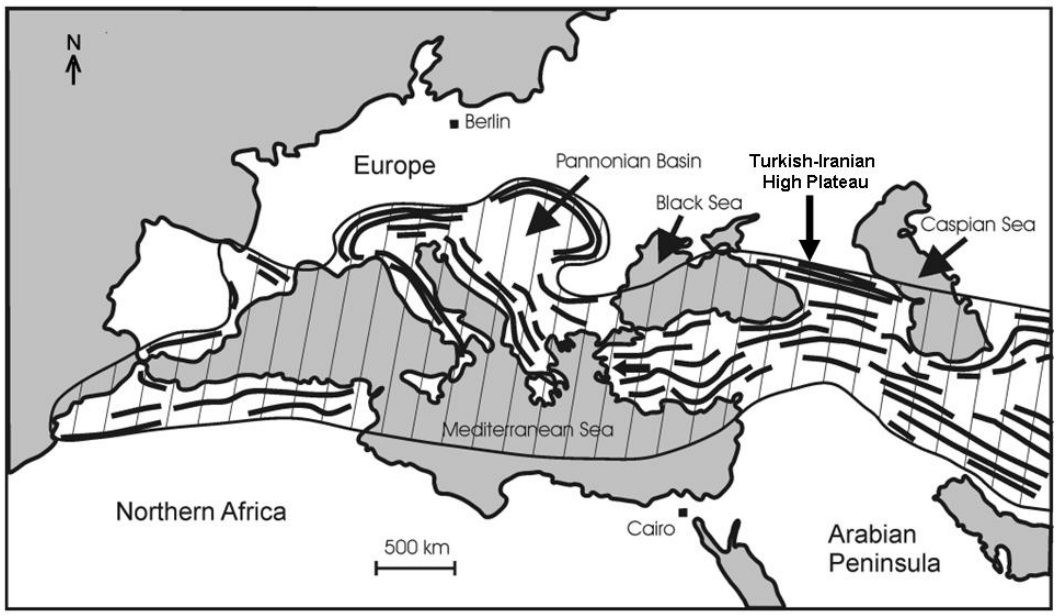

Figure 1.1 : Orogenic region of the Tethysides (marked by the hatched area). This region is subdivided into mountain chains (thick lines) and several basins (Pannonian Basin or those (grey) with surface below sea level). The single thick arrow shows relative motion of the Anatolian plate caused by the Arabian plate indenting into the Tethysides (Masonne, 2005).

Mediterranean region, at present, can be subdivided into mountain chains and several basins (Pannonian Basin or those with surface below sea level). Interestingly, the model concluded that this region entirely underwent extended lithospheric delamination in the late Paleogene (Fig. 1.1). Lithospheric delamination happened in the Late Paleozoic, as outlined and discussed by Masonne, (2005) in a case of the collision of the African plate (formerly part of Gondwana) and the W-part of Eurasia. Then, however, there was a pause of at least 200 m.y. until a very similar continent-continent collision started again. This resulted in the formation of the Tethysides. Surprisingly, Masonne, (2005) stated that a pause of similar time span can be assigned to orogenies in today's China. The remark is that, despite these orogenic pauses, the loss of a significant volume of continental crust since the Late Neoproterozoic is considered (although a quantification of this loss would be highly speculative at present by Masonne, 2005). For a rough estimate, it is assumed that the process of lithospheric delamination (with involvement of continental crust) occurred only 10 times during the last 600 m.y. A mean area equivalent to the present thickened continental crust in the regions of about 4 million km^2 (the Himalaya, Tibetan Plateau, Tien Shan, and Nan Shan) is subjected to this process. The complete lower crust (15 to 18 km thick) of the lower plate on average, such as India, is recycled into the mantle by a delamination process. Then an equivalent of about two-

thirds of the continental crust of the African plate (~30 million km^2, 33 km thick) is lost during the last 600 m.y. As Masonne, (2005) well reported that, however, such events could have occurred more often than 10 times since the Late Neoproterozoic and the mean thickness of delaminated continental crust could be larger than assumed above, as is suggested by the extended basins (= thin continental crust) in the Mediterranean area. The result is that the amounts of continental crust even clearly larger than an equivalent of two-thirds of the continental crust of the African plate are recycled since the Late Neoproterozoic. Thus, it is almost impossible to reconstruct former constellations of crustal plates, for instance, those of the ancestral supercratons (see Bleeker, 2003 and Masonne, 2005).

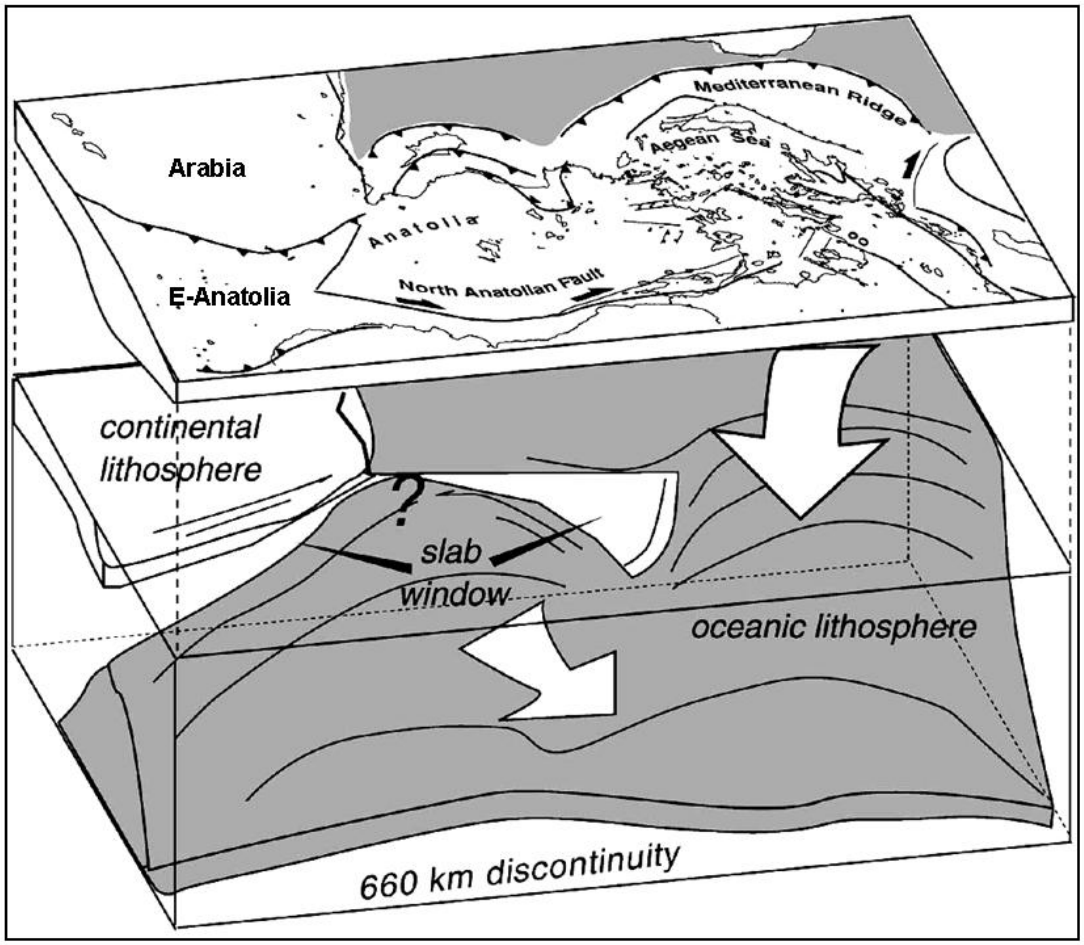

Figure 1.2 : Cartoon illustrating the connections between surface tectonics and the deep upper mantle. The detachment of the slab below E-Anatolia (Bitlis) propagates at least to Cyprus and possibly further to the W to the E-end of the Hellenic arc, favoring indentation and resulting in an increase of the slab pull force on the Hellenic trench. This mechanism is responsible for the Miocene-Pliocene re-organization in the Anatolian-Aegean region that resulted in the W-motion of Anatolia (Faccenna et al., 2006).

The Turkish-Iranian High Plateau (E-Turkey) is the most prominent and complicated one of Tethyside superorogenic systems and the one of global consequences of lithospheric delamination (Fig. 1.1). The plateau is an perfect example of how delamination phenomenon can give a clue to both global impacts of crust consolidation-construction and making a new continent during collisional history of earth and the end episode of a Wilson Cycle (Şengör et al., 2008). The high plateau is one of the broad and the major mountain ranges along the Alpine-Himalayan System, which is characterized by very high strain rates of continental collision (see Fig. 1.3 for second invariant rates).

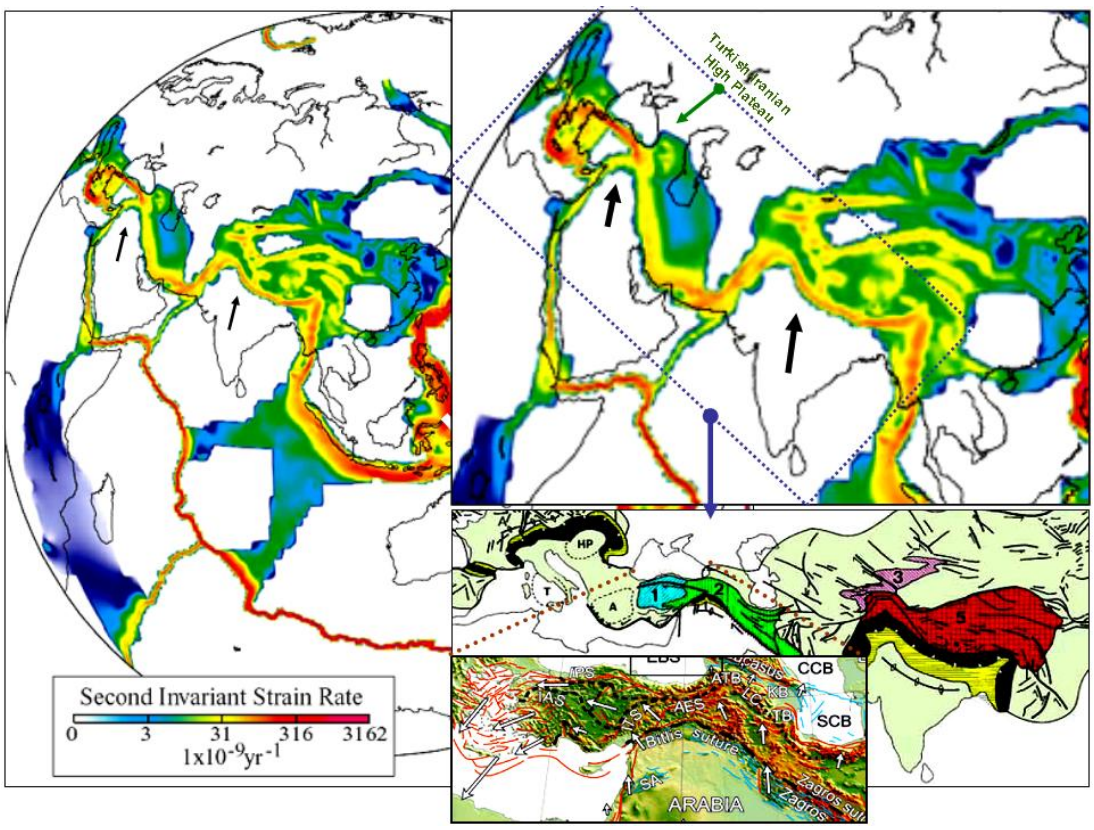

Figure 1.3 : Contours of the second invariant of the model strain field determined using 3000 geodetic velocities world-wide, and Quaternary slip rates in Alp-Himalayan orogen. All areas in white are assumed to behave rigidly (the contour scale is quasi-exponential) (Kreemer et al., 2003). This figure also shows (below) plateaus in the Alpine/Himalayan mountain belt. Black: thrust belts; yellow: foreland and hinterland basins. Numbers refer to the average height of the plateaus. 1: W-Anatolian plateau (1 km); 2: E-Anatolian Plateau (2 km); 3: Tien Shan (3 km); 5: Tibet (5 km) (from Dewey et al., 1986 and Keskin, 2005). Numbers 1 and 2 indicate digital elevation model of Turkey.

This plateau is geographically dome-shaped and confined accretionary system, bounded by major intraplate transform faults (North and East Anatolian faults) (Şengör et al., 2003). E-Turkey is also a typical example of a small and hot Turkic-

type orogen (Şengör et al., 2008). The role of the mantle lithosphere in this small orogeny shows that assimilation of lithosphere by the mantle during contraction is a pivotal problem in continental dynamics, with proposed mechanisms ranging from viscous distributed deformation and Rayleigh-Taylor (RT) type-instabilities through delamination and slab break off, to subduction (see Beaumont et al., 1996; 2000; 2001). Such a case implicates for post-collisional crust-forming processes in Turkic-type orogens, such as in the Arabian Pan-African Turkic-type orogenic system and also surrounding Pan-African Turkic-type orogenic terrains by Şengör et al., (2008).

The plateau is a well-exposed and accessible present-day collisional convergent zone forming a higher elevation averaging some 2 km above sea level, which it has attained since the Serravallian (c. 12 Ma ago). Although extremely complicated and less well-exposed than many other orogenic belts in the world, E-Turkey offers perhaps a unique place for the study of Tethyan geology in particular and collision processes in general and is the most critical portion of the Alp-Himalayan orogeny. Since, it is the last Oligo-Miocene remain of the closed Turkish Tethys. It not only has a representative selection of nearly all of the main Tethyan palaeogeographic elements, but has an amazingly rich assortment of collision-related structures (Şengör and Yılmaz, 1981). For instance, based on Arni's excellent studies, Arni, (1939a, b and 1942) interpreted the geology of entire Anatolia in an imaginative Argandian scheme, using Argand's embryonic tectonics (Argand, 1916), but in a symmetrical fashion (Şengör et al., 2008). Thus, E-Turkey represents embryonic development of a small Turkic-type orogeny, representing clear tectonic evidences of crust-forming processes in Turkic-type orogens and very similar to the Altaids in C-Asia and the Pan-African System in N-Afro-Arabia and to any other Turkic-type orogen (see Şengör and Natal'in, 2007 for similarities). The entire basement of E-Turkey is imbricated in terms of a subduction–accretion complex (Arni, 1939a, b and 1942 and Şengör and Yılmaz, 1981). Arni called this imbricated region of clastics, flysch and limestones Iranides and correlated them, in the best cylindristic tradition of Argand, with the Flysch Nappe, the Radiolarite Nappe and the Metamorphic Nappe of de Bökh et al. (1929), who continued them into Makran (see de Bökh et al., 1929). Şengör et al., (2008) stated that all orogens are accretionary, thus, it is no the need to use the term "accretionary orogeny", which amounts to an uniformative tautalogy and emphasized an definition of Turkic-type orogeny, "the collisional

orogeny involves the growth of very large subduction-accretion prisms (commonly with significant net crustal growth)". Therefore, in this study, it is called the accretionary prism or prism system of E-Anatolia, the Eastern Anatolian Accretionary Complex (EAAC) following Şengör and Yılmaz (1981).

The geological nature of the terrains in E-Anatolia is separated by very steep thrust contacts (see and examine fragments in the map of MURAT region in Şengör et al., 2008) and seems to have the inconsistency of vergences. Overall structural pattern and geometry of accretionary complex is described in a style of "Accordion Tectonics", due to the high-angle steep contacts of mélange wedges (pers. common. Şengör, 2006; 2007). Embryonic tectonic development and accordion-shaped accretion of the small Turkic-type orogeny offer extremely complicated process of its collisional growth. Because, Turkic-type orogens are highly anisotropic, thermally disturbed, and structurally chaotic systems through which fluids, including melts, may pass. That such systems are open suggests that they may be dominated by disequilibrium rather than equilibrium processes and the ultimate trigger for orogeny is likely to be in the mantle. Particularly, relatively smaller Turkic-type orogens formed by subduction–accretion complexes have mechanically anisotropic convergent crust, as well as these orogens are tectono-thermally unstable systems due to their weak and irresistant structure (Şengör and Yılmaz, 1981). Due to a little stress change in plate tectonic setting, orogenic tectono-thermal unstability and mechanical anisotropy of the convergent crust may extremely result in a complicated rheology of basement accretionary complexes and/or mélange wedges, basement reactivation processes and fault-controlled, inverted blocky structures. Inverted blocks are, in general, bounded by extensional and strike-slip faults. High amount of orogenically-concentrated precipitation is focused on and deposited in troughs of inverted wedges. Thus, accordion-like, smaller accretionary orogens stand at an excellent example of both thermal and tectonic disequilibrium processes and also sediment-rich environments.

Fig. 1.4 briefly shows a prominent sample of N-S-trending P-wave tomographic data, track line across Muş-Lake Van region and major Holocene volcanoes in E-Anatolia. The extensive geochemical studies of Keskin, (2003; 2005; 2007) in and around these volcanoes provided essential isotopic data to model delamination and break off events beneath E-Anatolia from Late Oligocene to Quaternary (see evolution and

time scales in Fig. 1.5). Due to the slab delamination and break off events, E-Anatolia is dynamically supported by doming asthenosphere, very high and still rising above a hot mantle (Fig. 1.5e).

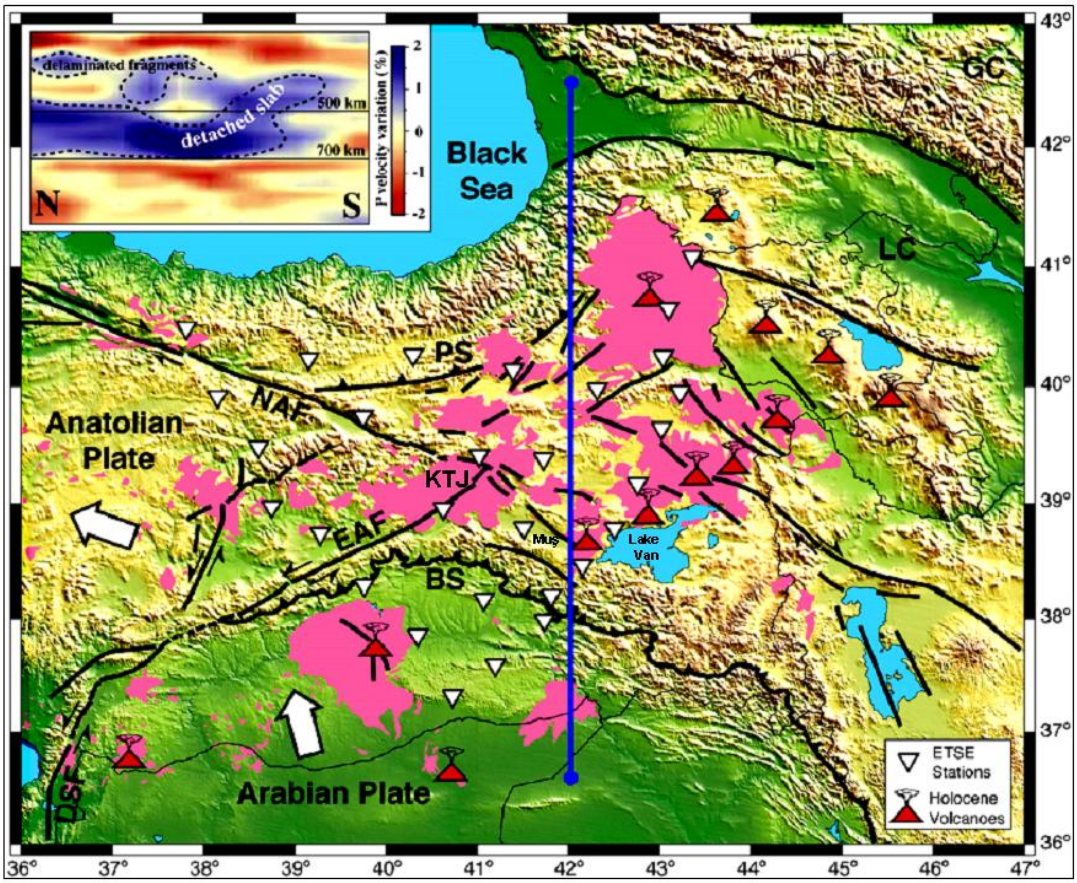

Figure 1.4 : Regional tectonic map of E-Turkey with topographic relief, station locations of ETSE array (inverted triangles), Neogene volcanics (pink area) and Holocene volcanoes (red triangles). Arrows indicate the direction of plate and fault motions. NAF, North Anatolian Fault; EAF, East Anatolian Fault; DSF, Dead Sea Fault; BS, Bitlis Suture; PS, Pontide Suture; LC, Lesser Caucasus; GC, Greater Caucasus. The inset figure shows the tomographic cross-section of Faccenna et al. (2006) based on the seismic model of Piromallo and Morelli (2003). The location of the seismic tomography is shown by a blue line in the map. Enclosed areas characterized by positive anomalies are taken from Keskin, (2007) and represent locations of detached slab and delaminated fragments of lithospheric mantle (Özacar et al., 2008).

It is an extraordinary place, where a thin crust underlies a high plateau undergoing shortening yet being covered by volcanic rocks typical of extensional regions. Therefore, E-Anatolia can be regarded as a spectacular natural laboratory where the stages of subduction-accretion, slab detachment, break off and their effects can be thoroughly studied to understand post-collisional tectonics of the deeper orogenic lakes. Moreover, it forms a typical Turkic-type collisional orogen, albeit a very small

one, yet its structural and magmatic products are very reminiscent of its much larger older cousins in Central Asia and elsewhere.

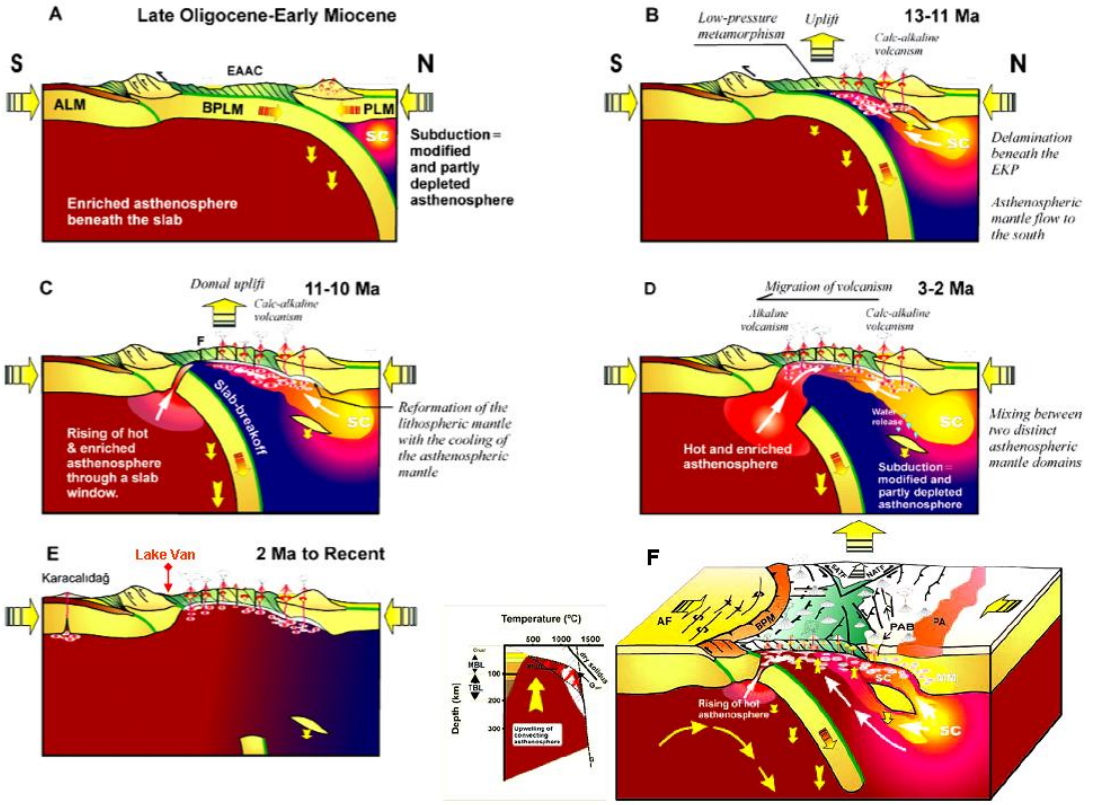

Figure 1.5 : Cross-sections displaying the evolution of the E-Anatolia in time, from L. Oligocene-E. Miocene through 3-2 Ma to recent (see Keskin, 2007 for detailed explanations). Block diagrams illustrate the slab-steepening and break off model. EAAC-Eastern Anatolian Accretionary Complex; ALM-Arabian lithospheric mantle; BPLM-lithospheric mantle of the Bitlis-Pötürge Massif; PLM-lithospheric mantle of the Pontides; SC-asthenospheric mantle containing a subduction component; EKP-Erzurum-Kars plateau. Block diagram in F shows MBL-mechanical boundary layer; TBL-thermal boundary layer; AF-Arabian foreland; BPM-Bitlis Pötürge Massif; PA-Pontide arc; MM-mantle metasomatism; SC-subduction component; SATF and NATF-South and North Anatolian transform faults. In F, the white arrows indicate the possible flow direction of the asthenosphere (modified from Şengör et al. 2003 and Keskin, 2003 and 2007).

The similar processes also dominated the post-collisional tectonics of such orogenic systems as the Pan-African collage of NE-Afro-Arabia and all other Turkic-Type orogens the world over. As it is likely that Archaean collisions were dominated by Turkic-type post-collisional events rather than Tibetan ones (Şengör and Natal'in, 1996a, 2004), which only became common in the Proterozoic. Therefore, E-Anatolia constitutes a marvelous region to study how continental crust is generated and consolidated in Turkic-type orogens since the earliest days of our planet. Additionally, intraplate orogeny of E-Turkey constitutes a unique Geosciences

laboratory hosting natural phenomena and processes on virtually all geosciences sub-disciplines. There are not only many scientific issues specific to each sub-discipline, but also several cross-cutting themes of tremendous scientific interest and practical relevance, such as the climate-geomorphology interactions over different timescales. Due to its origin related to an active convergent-plate margin that causes uplifting and volcanism, E-Turkey shows extreme complexity, with strong gradients in geology and morphological structure. It is, since, an aggregate of island arcs, mélange blocks and accretionary prisms and is characterized by great structural complexity. Since, the intraplate continental collision involves the progressive impingement of buoyant or high standing terranes with subduction zones. All scales and variations exist on this theme between the collision of seamounts and seamount chains with arcs through the collision of oceanic plateaux and microcontinents with arcs to the collision of large continental masses (Dewey et al., 1986). Hence, E-Turkey is the one of the best special areas all along the Alp/Himalayan orogenesis to study the orogenic geometry, accretionary tectonism and collisional magmatism during collision and post-collisional periods. As an example, the unusual aspect of the plateau emerges, on a profile taken E-W from about the middle of the plateau (Şengör et al., 2008) (Fig. 1.6c). Considering the profiles of Şengör et al., (2008), one is driven to the conclusion that E-Anatolian high plateau is really a massive dome (Fig. 1.6a), albeit corrugated by N–S shortening and by the presence of smaller, more local domes such as the Lake Van Dome, and, as a consequence, houses endorheic depressions (Fig. 1.6b). Indeed, the plateau represents the end of a Wilson Cycle and Lake Van Dome, in fact gives the end products of this cycle and shows how this structure is actively deforming.

1.2 Background Theory of Turkic-type Orogeny based on Delamination Event

Delamination event fundamentally contributes to partial melting and intraplate magmatic processes in and around Lake Van Dome. The partial melting of the mantle below the thin crustal zone (38 km) due to hydration-induced lowering of the melting temperature is the primary mechanism by which mantle differentiates to create continental crust in accretion mosaics including island arcs (Şengör and Yılmaz, 1981; Şengör et al., 2008) and it considerably affects the evolution of the convergent crust. Thus, delamination process plays a crucial role in crustal

consolidation and its construction (see Şengör and Natal'in, 2007). It is key to the development and sustainability of crust-forming process in Turkic-type orogeny (Şengör et al., 2008).

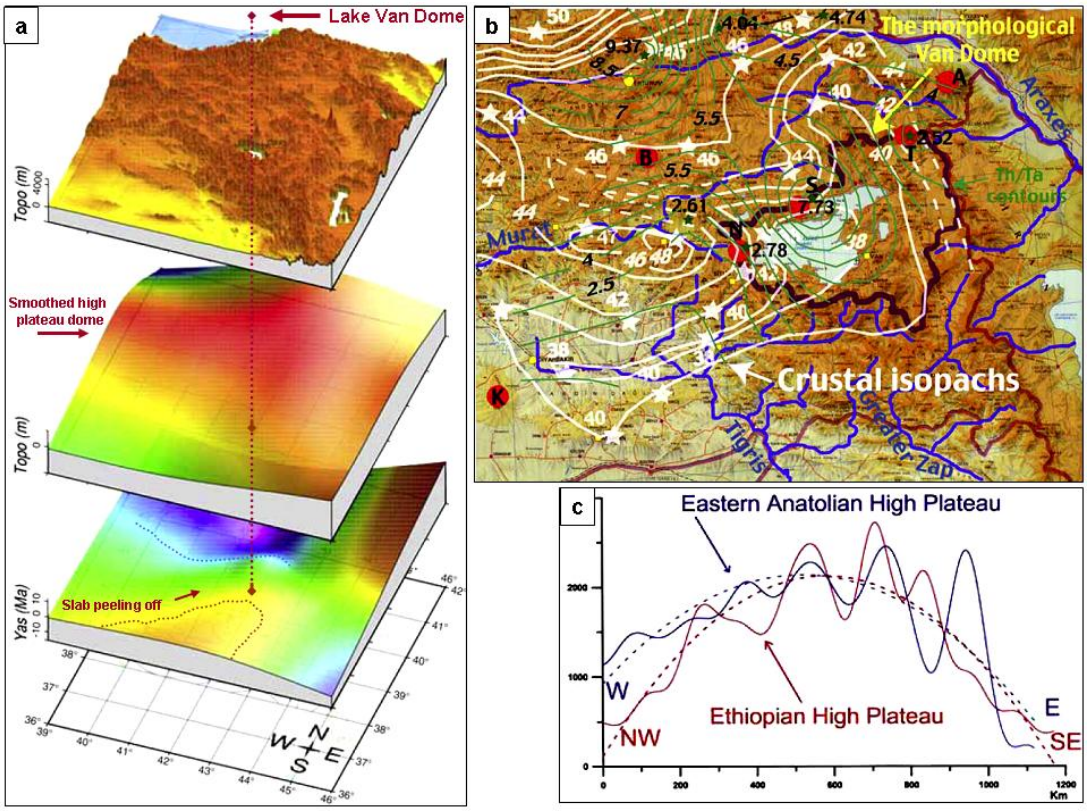

Figure 1.6 : a) block diagrams showing the actual topography (top), smoothed E-Anatolian high plateau dome, and the geometry of the slab immediately underlying E-Turkey just at a time when it began peeling off, while creating the surface that fits the long-wavelength features of the topography (Şengör et al., 2008). Brown dashed line indicates a morphological projection of Lake Van Dome. b) Lake Van Dome showing topography, drainage, crustal thickness contours and Th/Ta ratio contours displaying the distribution of Th/Ta ratio in primitive basaltic lavas across the region. Notice that the centre of the dome, now occupied by Lake Van, coincides with the thinnest crust (38 km) with volcanic rocks containing the highest enriched asthenospheric mantle component in their composition as shown by the low Th/Ta (2.5) ratios. c) W-E topographic profile along the 40°N parallel in E-Anatolia from 44°30'E, low-pass filtered at 125 km to eliminate crustal structures affecting topography and its comparison with a similar curve across the Ethiopian High Plateau. Notice the surprising similarities between the two topographic profiles and the simplified smooth lines (Şengör et al., 2008).

In E-Turkey, delamination obviously shapes the plateau morphology, and it is thought to facilitate sub-crustal flows, flow stresses, upper mantle anisotropy and intraplate magmatism beneath Muş-Lake Van region. Delamination dramatically affects the evolution of intraplate accretionary basins, styles, and patterns of intraplate deformation by profoundly influencing geothermal heat flow and cooling,

and contributes to processes that weaken faults, including master faults at suture boundaries and inverts sedimentary basins. Understanding the effects of delamination on current upper mantle processes, crustal tectonics, basin formation, and evolution has spawned scientifically rich multidisciplinary on-going observational and theoretical efforts employing continental scientific drilling program (ICDP), multi-channel seismic reflection and high-resolution data, seismic tomography, seismology, volcanic geochemistry, and geodynamics.

1.2.1 The surficial effects of delamination event

The slab detachment occurrence conducts to major plate reorganization. A discontinuity in the slab, such as a detachment, is related to a sharp superficial decoupling zone between the collision and the subduction. Conversely, continuity in the shape of the slab should permit to transfer progressively the deformation from the collision to the subduction domains (Regard et al., 2005). Thus, the slab delamination provides an interesting overview to highlight the causes of differences between the collision and post-collision in E-Anatolia. Since, active surface deformation may be caused by slab detachment. It is observed from 2D-simulations from Buiter et al., (2002) that surface deformation is caused by the effective control of deep-seated processes (slab detachment) on the evolution of convergent plate boundary from subduction-collision to post-collision by Regard et al., (2003). In a point of this view, the post-collisional deformation can be considered in regard to the upper plate tectonics. The effects of deep processes related to the slab delamination on the upper crustal deformation have been ignored by Keskin, (2007) and Şengör et al., (2008). These deep processes involved can be a slab break off or, a flexure of the slab without any discontinuity. These processes must play a first order role in the way E-Turkey is deforming. The slab detachment and break off process results in a tremendous difference in the way both sides accommodate the transition between subduction and collision by a relative coupling before detachment (collision) or by a decoupling of the subducting and colliding parts after break-off (post-collision) (Regard et al., 2005). This highlights the first-order major role of deep processes on crustal tectonics. Lithospheric plate rheology seems to act only as a second-order role controlling parameter (Regard et al., 2005). For example, in Iran, lithospheric plate rheology only governs the structures that are reactivated (such as the N-trending

Nayband-Gowk fault system that separates central Iran and the Lut Block in Walker and Jackson, 2002; Regard et al., 2004).

The behavior of subduction-collision transition is investigated, using laboratory experiments by Regard et al., (2005). These experiments for the Iranian tectonics provide evidence for surface deformation in front of the indenter and above the oceanic subduction zone that depend on the behavior of the slab below the collision zone. This study clearly remarks that hinterland deformation extremely depends on whether or not the slab deforms below. This case results in heterogeneous or homogeneous hinterland deformation. When the slab significantly deforms at depth, the closure of the oceanic domain in front of the indenter (Arabia) is no more followed by the subduction, during which the tectonic regime within the continent (E-Anatolia) remains quite "heterogeneous". However, if the slab does not deform significantly at depth, in contrast, the closure of the oceanic domain in front of the indenter is followed by a longer period of the subduction, during which the tectonic regime within the large continent remains quite "homogeneous".

In E-Anatolia, the slab breaks off and the subducting oceanic lithosphere detaches from the continental part of the slab (Şengör et al., 2008) (see Fig. 1.5b). Afterwards, the detachment progresses from N to S, towards the further S, under the suture boundary between the BP-M and EAAC (Facenna et al., 2006; Şengör et al., 2008) (Fig. 1.5c, d and e). It is difficult to establish the rate of lateral propagation of the detachment, but it seems to have occurred quite rapidly. Indeed, it is noted that in surface, on the E-side of the Karlıova triple junction, W-E-striking folds, ramp-thrust basins (Muş-Lake Van region) and thrust/reverse-faults, just after the slab detachment, reactivate and invert normal and strike-slip faults related to the present stage. This demonstrates that active tectonic deformation at the surface is then strongly influenced by the detachment process (see and examine analogue experiments in Regard et al., 2005). This result well views that the way the upper plate deforms during post-collision depends much on the present characteristics of the subduction system and also on the history of subduction. During post-collisional period, the different efficiency and/or inefficiency of the subduction system is accommodated in the surface with internal deformation and/or by the rigid rotation of the upper continental block.

1.2.2 Crustal consolidation and crust-forming process

In small and hot Turkic-type orogens, it is assumed that the initial collision causes the accretionary prism system, forming mountain range and then, post-collisional period may cause tectonic unstability of accretionary wedges and complete structural inversion. The weakness and irresistant dynamics of accretionary wedges may result in intraplate fragmentation, separation and differentiation of suture complexes (that is post-collisional suture zone opening). Differential disintegration of accretionary wedge blocks is followed by strike-slip and extensional faults, accompanied by extensive alkaline magmatism. The end-members are fault-controlled internal and external sedimentary basins covered by magmatic occurrences in intraplate compressional setting. Faulting and sedimentary basin formation is mainly driven by mechanical anisotropy of the convergent crust and main tectonic trends. These trends are such likely suture-bounded basins or massive tectonic blocks. In contrast to compressional stresses originated by plate boundary forces, however, the origin of intraplate stresses causing extensional/strike-slip deformation, sedimentary basin formation and extensional alkaline magmatism is questionable. Especially, the remark is that suture-bounded compressional ramp basins may be covered by extensional alkaline magmatism and related volcanic dome-cone complexes, suggesting the reactivation of pre-existing shear zones, basin inversion and tectonic regime transition.

Dewey and Burke, (1973) reported collision-related basement reactivation and related magmatism. This study argued that collisions create major magmatism that, dominantly of intermediate and felsic type, spreads across vast areas, not uncommonly on both sides of terminal sutures welding the apposed continents (Şengör et al., 1991, 1993, 2008). Collisional reactivation of the continental crust in the model of Dewey and Burke (1973) involves generation of Tibet-type high plateaux with considerable crustal thickening (Dewey et al., 1988), loss of lithospheric mantle (Bird, 1978; Houseman et al., 1981; Molnar et al., 1993) and/or eclogite to granulite transformation of the lower crust (Le Pichon et al., 1997) and consequent crustal melting (Nelson et al., 1996). The resulting magmatism is dominantly of calcalkalic type and rich in K (Pearce and Mei, 1988; McKenna and Walker, 1990). However, not all post-collisional magmatism involves generation of Tibet-type high plateaux or calc-alkalic magmatism (Şengör et al., 2008). It is well

documented by Şengör et al., (2008) that the magmatic products are dominantly alkalic to peralkalic in Turkic-type post-collisional magmatism. These magmatic products greatly resemble those of extensional regions giving rise to much confusion especially in interpreting old collisional orogenic belts. In general, post-collisional magmatism is generated by extensive crustal melting in Tibet-type collisional environments. However, this magmatism is also generated by falling out of slabs from under giant subduction–accretion complexes in Turkic-type collisional orogens. This gives rise to decompression melting of the asthenospheric mantle replacing the removed oceanic lithosphere. For example, in C-Asia, post-collisional felsic magmatism in Turkic-type orogens (Şengör et al., 2008) contains not only calc-alkalic, but also alkalic to peralkalic rocks erupted onto or intruded into continental crust (Şengör and Natal'in, 1996a,b; Vinogradov, 1969; Wang,1985; Şengör et al., 2008). Although some of these rocks formed in settings unquestionably extensional (Allen et al., 1995; Wartes et al., 2000, 2002), others originated in orogenic segments not subsequently stretched (Kurchavov,1983; Kurchavov and Yarmolyuk, 1984; Jahn et al., 2000a,b). Similarly, the alkalic and peralkalic post-collisional magmatic rocks of the Pan-African Arabian Shield that were extruded and intruded into crust (see Stoeser,1986; Jackson,1986; Brown et al.,1989 and Schandelmeier et al., 1997). Also, in E-Australia, a similar evolution is well known and commonly attributed to regional extension following orogeny (Vandenberg, 1978; Foster and Gray, 2000), although delamination of the lithospheric part from under this area was proposed by Coney (1992) and recently has been resuscitated in the form of the falling off of the oceanic lithosphere in a doubly-vergent subduction zone (Soesoo et al., 1997). These considerations based on examples show the widespread occurrences, and possible dominance during the Archaean of Turkic-type orogens (Şengör and Natal'in, 1996b). This clarifies how the continental crust forms and evolves and also provides an understanding of the origin of such problematic post-collisional magmatic rocks critical.

It is likely that Archaean collisions were dominated by Turkic-type post-collisional events rather than Tibetan ones that only became common in the Proterozoic. Hence, there is a strong tectonic importance in understanding overall structures and features of collisional environments, such as non-Tibet-type, or Turkic-type and how post-collisional magmatism is recognised and also how they form. The best approach to

solve the problem of the origin of the Turkic-type post-collisional magmatism is to find a place in the world, where they are now forming, and have done so in the very recent past, and to try to elucidate their formation (Şengör et al., 2008). E-Turkey is the one of such a place in the NW-segment of the Turkish–Iranian high plateau (Şengör and Kidd, 1979).

In the absence of seismic information, Şengör and Kidd (1979) had assumed a 55-km thick crust to support the high elevation on the basis of a comparison with Tibet. The results of the Eastern Turkey Seismic Experiment showed that this assumption was clearly wrong. It is emphasized that the convergent crust under E-Turkey is not only not as thick as expected, but actually too thin for its elevation (see crustal isopachs in Fig. 1.6b). In fact, the culminating part of the high plateau, the Lake Van Dome, is on the thinnest part of the crust and where the observations on He isotopes in the volcanic rocks indicate the highest mantle contribution in the whole of Turkey (Güleç et al., 2002). Such a thing is only expected in an extensional region, not in one of the great shortening regions at the apex of the Turkish Syntaxis of the Alpides, one of the four great syntaxes of this largest active orogenic system of our planet (see Şengör, 1990b). In the entire region, there are very few normal fault-plane solutions and they are not on the highest ground. The hypothesis of a slab fall-off from under the accretionary prism upon collision with the Arabian continent appeared a very attractive solution by Şengör et al., (2003). Şengör et al. (2003) proposed this alternative, Şengör et al., (2008) improved this model and Keskin (2003, 2007) and Keskin et al. (2006) explored its petrological and geochemical implications. However, their geological evolution scenario is not entirely accurate for Muş-Lake Van basin system, since they remained ignorant of the complex tectonic and magmatic history of the Lake Van region. The presumed presence of such slab-driven asthenospheric flows beneath Muş-Lake Van region may provide an answer to the question of why the volcanic activity initiated much earlier in the N and migrated to the S in time, towards Lake Van region. Similarly, it explains better why the volcanic products are calc-alkalic with a distinct subduction signature in N while they are alkalic with a distinct within-plate signature in S (Keskin, 2003, 2007), and they also explain why a lithospheric keel under eastern Turkey failed to form.

1.2.3 Lake Van Dome as a morphological paradigm

Time-dependent effects of perturbated heat sources such as upwelling mantle on orogenic thermal structure considerably affect both regional morphology and thermal profile of sedimentary basins. In E-Turkey, the rise of the topography is due to the doming, as it also rises where the ramp faults do not exist, especially on the E. Viewing a series of N–S and E–W topographic sections in Şengör et al., (2008), a topographic swelling appears and becomes the vertex of the high plateau, implying Lake Van Dome (Fig. 1.6). Fig. 1.6b shows crustal thickness (38 km) beneath Lake Van region and Fig. 1.6a shows original and smoothed topographic projections of E-Anatolia and age-based slab geometry. As seen in Fig. 1.6, Lake Van region developed as a local dome on the regional massive dome of E-Anatolia, suggesting that the development of the highlands sedimentary basins is resulted from catastrophic doming of E-Anatolia. This implies density compensation within the mantle, and explains singular features of the region as the highlands topography compared with modest crustal thickening.

The Lake Van is a suture-bounded depression, actively doming. Its setting is limited by Muş and Cryptic sutures at N-end of BP-M and bounded by pre-existing structural lineaments and accretionary blocks (see Fig. 1.7 for Muş suture zone). Fig. 1.8c shows intralake cryptic suture zone trending W-E and Fig. 1.8b shows cross sectional profile of Cryptic suture. Figs. 1.7 and 1.8 well illustrate complex structural relations between thinned crust, Holocene volcanoes and their ages, accretion geology and suture trends. In Fig. 1.7, Lake Van setting seems to be a structural boundary, separating EAAC from BP-M, thus it forms intraplate boundary along Muş and/or Cryptic suture zones. Cryptic suture zone passes trough the lake, forming intralake structural boundary. Both sutures form major structural weaknesses. These are pre-existing thrust contacts of accretionary wedges underlying Muş-Lake Van setting. This shows that this lake is located over structural weaknesses created by accretionary wedge dynamics.

The Lake Van, almost completely confined by faults, is geographically restricted area, resulting in incompatibility problems of strains and a complicated pattern of shear zones. It also seems to result from continuous gradual subsidence accompanying faulting (Degens et al., 1984). Sonobuoy profiles suggest a thick sequence (up to 600 m) of unconsolidated sediments in the Tatvan Basin (Wong and

Finckh, 1978). Depositional sensitivity of these softer sediments is so subject to various deformational patterns. This makes morpho-physiographic framework more complicated. The lake developed as a suture-bounded, elongated and deeper sedimentary trough within the central top of the high plateau and is surrounded by active volcanic dome-cone complexes. Hence, Lake Van is the best place to implicate for crust-forming processes in a higher elevation and to show seismic structural expressions of these processes.

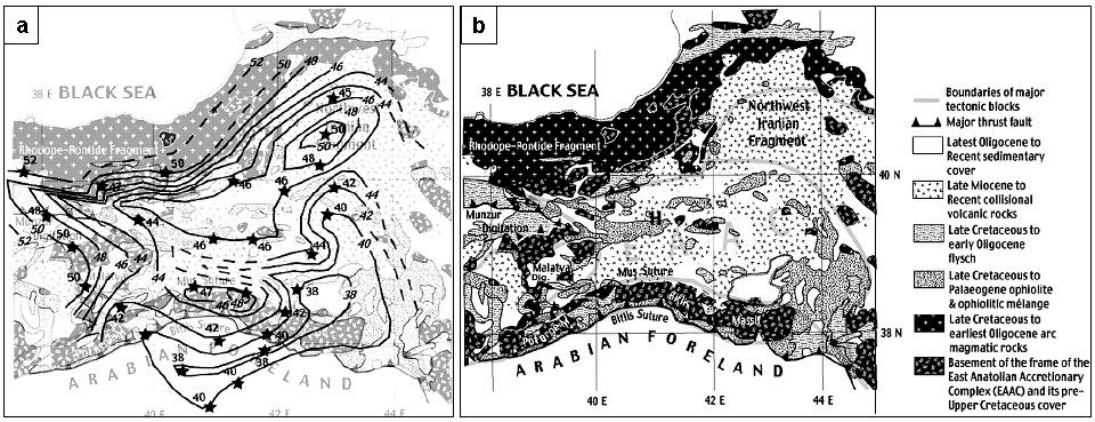

Figure 1.7 : a) crustal thickness map of E-Turkey, modified from Şengör et al. (2003). The modification is undertaken by making inferences on the basis of surface geology without violating the seismic observations. The crustal isopachs are drawn on a base map formed from the simplified tectonic map of E-Turkey showing the main Alpide tectonic units with a view to illustrating the agreement between the observed crustal geometry with the tectonics as inferred from surface geology. The crust is nowhere thicker than 46 km, east of 42°E m0000000eridian generally thinner than 42 km. and beneath the Lake Van Dome, it is generally thinner than 38 km. b) highly simplified tectonic map of E-Turkey showing the main Alpide tectonic units. The map is simplified from Şengör and Yılmaz (1981) with appropriate revisions according to Şengör et al. (1982) (see Şengör et al., 2008).

The Lake Van is in a critical region where the Afro/Arabian Plate from S meets the Eurasian Plate from N and E (Fig. 1.4). The lake is near a tectonic plate triple junction of Karlıova that allows fluids from the Earth's mantle to accumulate in Lake Van and the nearby crater lake of Nemrut volcano (Kipfer et al., 1994). The lake and the surrounding areas are of special interest as they are located almost above the rifting of inferred slab-break off or above the edge of the lithospheric delamination (Fig. 1.5e and f). This consideration seems to be consistent with the results of previous geophysical studies and the presence of a number of big volcanic edifices (mainly stratovolcanoes), some of which (Nemrut and Süphan volcanoes) have been recently active during the sedimentation (volcanic ashes, tephras and pyroclastic

deposits) in Lake Van. Former tracer investigations from 1990 to 1991 showed that Lake Van accumulates He from a depleting Earth mantle source (Kipfer et al., 1994). Further the accumulation of ^{3}He from the decay of water-bound ^{3}H (tritiogenic ^{3}He) did not add significantly to the observed ^{3}He abundance, which indicated rapid deep-water exchange, e.g. in the early 90s up to 50% of Lake Van's deep water was renewed annually (Kipfer et al., 1994).

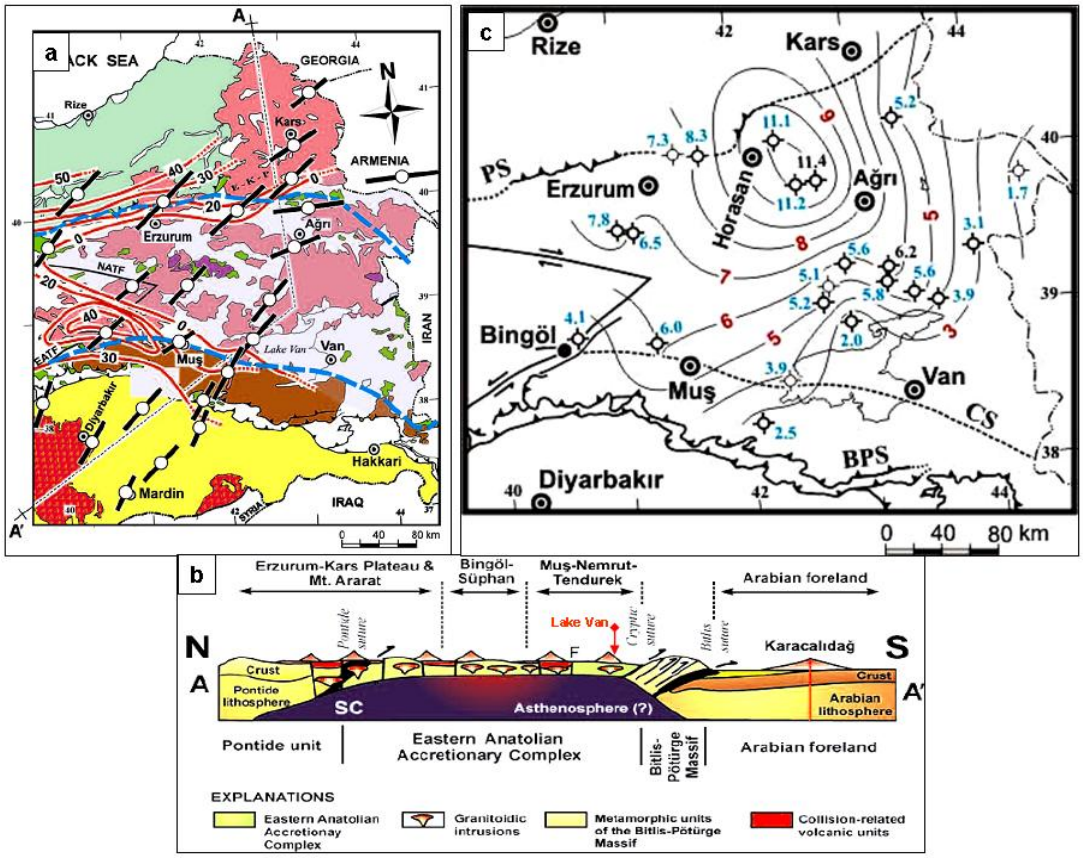

Figure 1.8 : a) map showing collision-related volcanic and tectonic units, mantle lid thicknesses, and shear wave-splitting fast polarization directions (from Sandvol et al., 2003b) in E-Anatolia. The contours (red) indicate the mantle lid thicknesses in km (Şengör et al., 2003). The light bluish-colored triangular area surrounded by the cities of Ağrı, Erzurum, Muş, and Van in the center of the figure represents the area with no mantle lid. The thick, dashed dark blue lines represent the N-and S-borders of the EAAC. Note that areas of inferred complete lithospheric detachment almost exactly coincide with the extent of the EAAC. b) N-S cross-section summarizes the lithospheric structure across E-Anatolia (not to scale). The crustal and lithospheric thicknesses are from Şengör et al. (2003) and Zor et al. (2003). The direction of the cross-section (A-A′) is shown in a. SC-subduction component; F-strike-slip faults. c) distribution of the oldest radiometric ages of the volcanic units. Initiation ages of the volcanism are contoured in 1-Myr intervals. PS: Pontide suture, BPS: Bitlis-Pötürge suture, CS: inferred cryptic suture across Lake Van, between the EAAC and BPS (Keskin, 2003 and 2005).

Results of He isotopic studies (Kipfer et al., 1994) revealed that waters of Lake Van contain excessive amount of helium derived from a depleted mantle source, indicating that magmatic activity is still in progress beneath Lake Van part of this domal region. This results in extensive hydrothermal activity of magmatism and also of travertine deposits in SE-part of lake. Evaporation processes, hydrothermal activities and chemical weathering of volcanic rocks create extreme alkalinity of the lake water (alkalinity 155 m eql^{-1}, pH 9.81, salinity 21.4 ‰ Kempe et al., 1991) and make Lake Van the greatest soda-water lake in the world (Kadioglu et al., 1997).

Lake Van Dome fills a tectonic depression within an active fault system that causes regional volcanism, earthquakes and hydrothermal activity (Degens and Kurtman, 1978; Kipfer et al., 1994; Keskin, 2003; Sengör et al., 2003). Lake Van forms the base level of a small endorheic basin of some 12,520 square kilometers (also see profiles in Şengör et al., 2008). All the major rivers of the region (Euphrates, Tigris, Greater Zap and the Araxes and its right-hand tributaries) originate on the flanks of the Lake Van Dome. Erinç, (1953) in fact pointed out that this dome is one element of the water divide between the drainage systems of the Atlantic and the Indian Oceans (Şengör et al., 2008). Tributary rivers display various water types, a common feature is a bicarbonate content surpassing that of the alkaline earth metals. This soda-chemistry is indicative of a postvolcanic CO_2-activity (see Kempe et al., 1978 for details). The soda character of the lake and the chemistry of the rivers proved that the lake has developed under the influence of postvolcanic CO_2-activity which must still be present throughout the N- and E-parts of the lake. High contents of sodium, potassium, and lithium and a deficiency of alkaline earth metals characterize its hydrochemistry. Thus, large scale postvolcanic CO_2-activity has determined the lake to develop into a soda-lake. A considerable amount of juvenile CO_2 must be released here from the crust into the atmosphere (Schoell, 1978). Within the dome, Lake Van region lies in a depression that has formed through a combination of normal and strike-slip faulting and thrusting (see Şengör and Kidd, 1979; Şengör et al., 1985; Dewey et al., 1986; Toker, 2006 and Şengör et al., 2008). The dome also contains three of the five sub-active volcanic centres in E-Turkey. The Th/Ta ratios indicate that the volcanoes within the dome have been fed by an enriched asthenosphere (with the exception of the Mt. Süphan volcano). Güleç et al. (2002) found, in the water samples from the Nemrut caldera lake and Lake Van, the highest R/R_A values (R=

sample $^{3}He/^{4}He$ and R_A=air $^{3}He/^{4}He$) in Turkey, namely 6.15, 6.58, 7.04 (Nemrut) and 7.54 (Van). This data clearly indicate more than 75% mantle He. However, all these results suggest an extensional tectonic setting. Lake Van lies mainly in a major shortening structure, a sort of "ramp valley" (Şengör et al., 1985), but with significant strike-/oblique-slip faulting along its N- and S- sides with some as yet unspecified amount of attendant E–W extension (Toker, 2006 and Toker et al., 2009a, b). All these results are unusual in an orogenic belt, indicating a cryptic area of the research and a new paradigm

The study of tectonic history of Lake Van may help to resolve some critical options remained unanswered. Geophysical studies (Sandvol et al., 2003; Piromallo and Morelli, 2003; Maggi and Priestly, 2005), coupled with geologic (Sengor et al., 2003), geochemical (Keskin, 2003) and experimental (Faccenna et al., 2006) findings support the view that both domal uplift and extensive magma generation can be linked to the mechanical removal of a portion or the whole thickness of the mantle lithosphere, accompanied by passive upwelling of normal-temperature asthenospheric mantle to a depth as shallow as 40-50 km (Keskin, 2003). This process is argued to have occurred either by delamination (Pearce et al., 1990; Keskin et al., 1998), slab-steepening and breakoff (Keskin, 2003; Sengör et al., 2003), or a combination of both (Keskin, 2006). One of the explanations proposed for asthenospheric upwelling and lithospheric thinning is the break-off of the Arabian slab under Anatolia (Keskin 2003; Sengör et al. 2003). Following slab delamination and break off process, the remark is that fast velocity vectors of asthenospheric flows are observed just beneath Lake Van and probably one of these flows is pooled in the bottom of BP-M and channelized through Muş suture complex. This opens a question of whether asthenospheric flows beneath the lake may directly contribute to the present-day structural and sedimentary development of Lake Van Dome or these flows show the independent growth in affecting upper crustal deformation. This question is related to a complicated origin of intraplate strain patterns in E-Turkey.

1.3 Various Extensional Aspects of the Theory of Intraplate Deformation based on Turkic-type Orogeny

1.3.1 Nature and characteristics of intraplate deformation in E-Turkey

Continental convergent plate boundaries such as the Alpine/Himalayan system, are wider, more diffuse and complicated zones where relative plate displacements are converted into complex and variable strains and smaller block-bounding displacements (Dewey et al., 1986). Intraplate earthquakes, uplifts, and basins are more common (Dewey, 1982; Dewey, 1988). Extension is, hence, the commonest form of intraplate deformation. This contrasts with oceanic plate boundaries, which are generally narrow, relatively simple zones in which only a small portion of relative plate motion is converted into strain and smaller displacements (McKenzie, 1972). This is probably due to the relative weakness and buoyancy of quartz and the relative strength and negative buoyancy of olivine as the principal mineral phases in the continents and oceans respectively. The great inhomogeneity and anisotropy of the continental crust, riddled with zones of low strength, generated and modified by many varied mechanisms, contrasts with the relative homogeneity of the oceanic lithosphere generated by plate accretion with fracture zone modifications (Dewey 1982; Dewey et al., 1986).

Colliding continental margins are irregular and strain sequences are usually diachronous along great strike lengths along suture zones (Dewey and Burke 1973; Dewey et al., 1986). As in E-Anatolia, prior to terminal continental collision, one or both continental margins may have had a long and complex history of exotic terrane assembly (Coney et al., 1980). Post-collisional strains within plate are very much smaller than those in plate boundary zones, but are a very subtle barometer of tectonic stress conditions within the plates, and may be of great importance in making and interpreting past plate reconstructions. Since, the global configuration of plates and the nature of their boundaries have the most profound influence on intraplate geology (Dewey, 1988). Intraplate deformation, although much subtler and characterized by smaller strains and displacements than those of plate boundary zones, is widespread, particularly in the continental lithosphere (Dewey 1982) as witnessed by earthquakes, rifts, zones of compressional and wrench deformation, uplifts, and basins (Dewey, 1988).

The smaller scale collision of E-Turkey dictates the style, duration and intensity of the resulting strain systems and sequences (Dewey, 1977), and these parameters of continental contraction produce a wide range of intraplate deformation and deep sedimentary basins in the plateau (Fig. 1.9). Since, E-Turkey is thermally young collision zone with its thinned crust and delaminated lithosphere, thus, particularly susceptible to intraplate deformation. E-Turkey does not show considerable mild tectonism, and much of its topography has been generated recently by intraplate stresses that are relieved by small-moderate sized earthquakes. Collisional assembly E-Turkey is followed by widespread partial melting in thrust-shortened collisional zones, and the anomalous intrusions of melting materials. However, E-Turkey is affected, pervasively, by extension zones of many ages in a wide variety of collisional intraplate tectonic setting, where magmatism, volcanic domes and forceful diapiric intrusion of granites-plutons cause compression in the injected country rock (Fig. 1.9). Magma pressure at dyke-tips induces very high localized tensile stresses that cause rapid crack propagation (Dewey, 1988). More passive magma intrusion, for example, causes tension that leads to collapse of magma-chamber walls and stopping. Structural compatibility problems (Şengör et al., 1985; Dewey et al., 1986; Dewey, 1988) at intraplate settings, plate boundaries and triple junctions can cause substantial stresses and complex sedimentary basins recognized in E-Turkey. Gaps and overlaps arise from geometric complexities and/or space problems at intraplate settings and plate boundaries, and the growth of these induces tension and compression respectively. At the marginal contact regions of collided terrains (Muş-Lake Van region) suffering differential uplift or subsidence and shear generates oblique stress fields (Dewey, 1988). The most excellent examples are transpressive and transtensional segments of, and flake rotation within, continental transform zones, gaps at TTT-triple junctions, and gaps at the termination of strike-slip bounded wedges in convergent zones (Dewey et al., 1986; Dewey, 1988). These resulting stresses cause relatively localized deformation and can be considered as local tectonic weather in a more regional tectonic climate (Dewey, 1988).

Shallow deviatoric tension can be developed in uplifts that are compensated in the crust, with a different stress regime in the upper mantle. This is the best exampled in Lake Van, where compensation occurs within the crust, the resultant horizontal tension is thin skinned and confined to the crust (Toker, 2006 and Toker et al.,

2009a, b). Similarly, flake rotation in shear zones (Karner and Dewey 1986; Dewey et al., 1986; Dewey, 1988) generates complex variation between shallow tension and compression. Plateaux and uplifts, therefore, may exist in a variety of tectonic settings with different vertical stress profiles, depending upon whether compensation is in the crust or mantle and whether the plate is in background deviatoric tension or compression (Dewey, 1988). Grabens and depressions may be, for example, deep-rooted in a delaminating lithosphere where compensation is in the mantle and associated magmatism is therefore more likely, shallow-rooted where compensation is in the crust (Dewey, 1988). In a highlands-compressional ramp setting, these strain patterns shape and form structural framework of Lake Van Dome. However, these patterns are also related to strong mechanical anisotropy of the convergent crust in E-Turkey. Since, a young and hot accretionary orogenic setting is seamed with zones of weakness and inhomogeneity, including weak orogenic zones, accreted terrains, block provinces and boundaries (Glazner and Bartley, 1985) and recent zones of crustal stretching (Figs. 1.7 and 1.9).

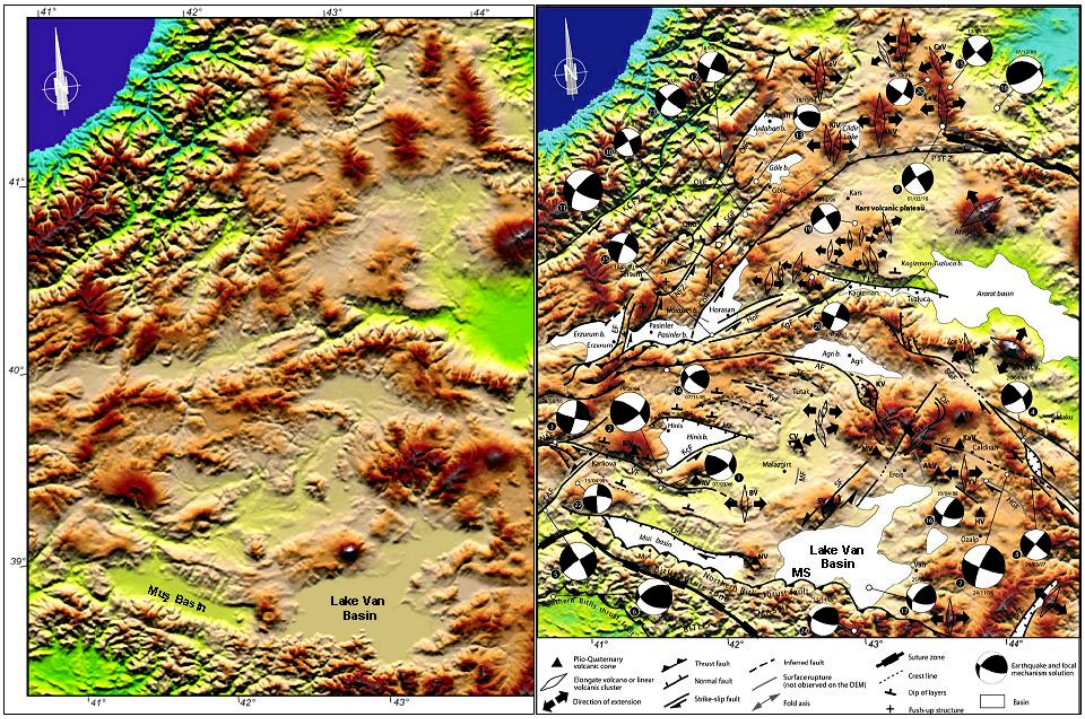

Figure 1.9 : Shadowed image of a digital elevation model (DEM) of the EAAC (left). It is generated by linear interpolation of digitized elevation contour lines of the 1:250,000 scale topographic chart of Turkey. Pixel size is 250 m and illumination is from the N. Structural and morpho-tectonic analysis of the DEM (right) show the main faults, extensional fissures, strike-/oblique-slip basins and fault mechanisms (see Dhont and Chorowicz, 2006 for details).

A particularly good example of the relative weakness of the thin crust and delaminated lithospheric mantle is seen in the structural relationships in Lake Van (Fig. 1.8a and b). Lithospheric delamination process and its end-members discussed by Bird, (1978), Houseman et al., (1981) and Dewey, (1988) clearly resulted in the rapid and lately morphotectonic uplifts and doming of E-Turkey with associated volcanism and magmatism in high-level extensional environments along E-Turkey. These morphotectonic uplifts, and the weakened orogenic uplift zones, enhance tension and are the likely preferential sites of extensional tectonics, leading to lithospheric failure (Dewey, 1988). Alkaline intrusions, for example, are encouraged by deviatoric tension and are preferentially sited in plateau uplifts and rifts (Bedard 1985; Dewey, 1988). Increasing deviatoric tension leads to accelerating continental extension accompanied by widespread dyke swarms and the eruption of flood basalts (Cox, 1978), immediately followed by lithospheric splitting, and tension being enhanced by plateaux generated by basaltic underplating (McKenzie 1984; Dewey, 1988). For example, even where hot-spot advective uplifts or volcanic edifices occur in the oceans they generate insufficient tension to offset ridge push forces, whereas those in the continents can generate deviatoric tension even against a background of deviatoric compression (Crough 1983; Dewey, 1988). Therefore, intraplate convergent settings are very important environments in understanding post-collisional, intraplate extensional processes, particularly in dome-shaped lacustrine basins.

If lithospheric delamination (Bird 1978; Houseman et al., 1981) beneath an orogen occurs, shallow tension may give way to lithosphere-penetrating tension in a rapidly uplifted region (Dewey, 1988). This uplifted region is the squashy zone, in which Lake Van is rapidly domed by rising asthenosphere (Şengör et al., 2008). This shows that the slab delamination induces the rapid plateau uplift and asthenospheric doming. This process strongly controls the distribution and localization of extensional strains all over suture boundaries of the lake. As the lithosphere delaminates and the crust thins, tensional stress increases, and stress amplification in a thinning crust further concentrates tension, as proposed by Kusznir and Bott, (1977) and Dewey, (1988). Delamination-dependent extensional strains result in more complicated deformation patterns and strain incompatibility problems. Since, an uplift compensated in the crust affects stress conditions only in the crust, and thus

extension may be shallow-rooted. Extensions of crust-compensated uplifts such as Lake Van Dome, are buffered by compatibility problems between the extending crust and non-extending mantle (see also shear wave-splitting and anisotropy studies ETSE project, 2003). These extensions are unlikely to exceed about 20 per cent, and extension of some uplifts is buffered by crustal compensation and leads to aborted rifts (Dewey, 1988). This may implicate for rift-related origin of Lake Van Dome at crustal depths. Strains are localized through pre-existing structural lineaments. Strong localization of extensional strains all along suture complexes may cause the post-collisional oblique opening of sutures. This may imply the Highlands extension of Lake Van Dome, and hence, is extremely unusual (see Fig. 1.8b for doming and suture relations).

The more obvious evidence for the aborted rifting event comes from a style of "Accordion Tectonics" as given earlier. "Accordion Tectonics" is the terminology for superimposed phases of extensional and contractional tectonics (Beaumont et al., 1996; 2000 and 2001). It follows naturally from orogenesis and rifts to investigate the effects of superposition and proposes a unified model of orogenesis and continental rifts. The Alpine evolution of the Pyrenees is a particularly good example of inversion tectonics, including rift inversion and rifting of collisional orogens (Beaumont et al., 1996; 2000 and 2001). Thus, this proposes to investigate the correlation between the tectonic characteristics of the Plio-Quaternary extension and the tectonic style of the superimposed Turkic-type orogen as a function of position along the Arabia/Anatolian plate boundary. Thematic framework and structural concepts of extensional tectonics in continental rifts and rifted continental margins presented by (Huismans and Beaumont, in prep., and Huismans and Boutilier, in progress.) are widely considered in a scheme of "Accordion Tectonics" (Beaumont and Pedreira, in progress). Thematic framework can be arranged by a wide range of primary structural processes. These are faults/shears, strain localization, inheritance and reactivation of structures, fluid interactions, strain partitioning as well as decompression melting, small-scale convection, active/passive rifting and gravitational instabilities (also see Beaumont et al., 1996; 2000 and 2001). This scheme well summarizes primary structural events, possibly in "Accordion Tectonics" in and around Lake Van Dome.

1.3.2 Morphological and limnological characteristics of the Highlands rifting in Lake Van

Considering the various limnological aspects of the Lake Van (Schoell, 1978; Kempe et al., 1978; Degens et al., 1978 and Degens and Kurtman, 1978), there are many which remind of an ocean rather than of an inland lake. For instance, the water balance is sensitive only to climate, the evaporation is similar to that of the ocean (Kempe et al., 1978). The hydrological features also have similarities with those in the open oceans. Surprisingly, the morpho-tectonic framework of Lake Van Dome resembles that of the East-African rift lakes (Kempe et al., 1978). A good measure for the steepness of the basin is the ratio of area against volume. For the lake, this ratio is 5.3, graphically deduced by Kempe et al., (1978). Typical rift lakes such as Lake Tanganyika and Lake Kivu (Hecky et al., 1973) have ratios of 1.5 and 3.0 respectively (Kempe et al., 1978). This is in the same range as Lake Van. Lakes in tectonically stable regions are characterized by shallow depth and relatively large area. Their area to volume ratio is one or two orders of magnitudes greater than those of the rift lakes. Kempe et al., (1978) concluded that Lake Van belongs morphologically to the group of the rift lakes which are situated at the margins of crustal plates. This is a strange result for the lakes that developed in collisional settings. However, this result may argue a kind of extension in the lake.

Hydrologically lakes are divided into two classes: open and closed lakes (Langbein, 1961). “Open lakes” have an outlet, mostly rivers but sometimes the underground is also porous enough to serve as an outlet. “Closed lakes” lose their water by evaporation only. Within this group, Lake Van is not among the ten largest lakes of the world by area (Kempe, 1977), but by volume it is surpassed only by the Caspian Sea, Lake Aral and Lake Issykul (Russia). This difference in position is explained by the difference between the shallow continental basin lakes and the steep rift lakes. Closed lakes with a morphology of rift lakes are comparatively seldom. The largest are Lake Issykul, Lake Van and the Dead Sea. Most other closed lakes are of the shallow type termed as playa lakes (Langbein, 1961 and Kempe et al., 1978). Interestingly, this may indicate that Lake Van Dome is “Open lake” with a typical steep rift morphology. The steep morpho-tectonic structure, and the lower-lying basement suggest that the central Tatvan basin has been undergoing a steady subsidence that is still active today (Wong and Finckh, 1978). However, it is

unknown that the process is gradual and continuous, episodic. It is reported that the underlying cause may reside in the repeated partial emptying and gradual collapse of the magma chamber that feeds the Nemrut (Degens et al., 1978). The fact that over 210 km^3 of volcanic material (calculated from map in Blumenthal et al., 1964) have been extruded from this volcano while only about 50 km^3 of additional lake volume has been created by subsidence makes this concept physically admissible. Thus, subsidence gives rise to slow lake level variations, while those caused by a water imbalance are catastrophic (Degens et al., 1978).

Kempe et al., (1978) and Degens et al., (1978) postulated that morpho-tectonic and hydrological features of Lake Van are intimately connected to global plate tectonics. Since, at plate margins, the morphology tends to develop rapidly. These authors also noted that this explains the rift-valley-like basin form of the lake, although no rifting has ocurred here but rather convergence of plates. However, the possibility of rifting in the lake is still an open question to be answered. These plates movements are also the ultimate reasons for the volcanic events which barred the former outflow of the basin by a lava dam, thus turning Lake Van into a "Closed lake". This may propose an hydrological inversion of the lake from opened into closed lake form. Another feature associated with the plate tectonics is the thermal balance within the hypolimnion, which appears to be influenced by an unusually large geothermal gradient (Kempe et al., 1978). The calculations on heat transfer indicate (Kempe, 1976 and Kempe et al., 1978) that there is an excess in heat which can only be linked to geothermal processes (see Degens et al., 1978 for calculated values). Heat flow values of a large magnitude have been reported from some oceanic rifts (Erickson and Simmons, 1969). The data from Degens et al., (1978) suggests that a heat source must be located close to the lake bottom. The same source could be responsible for the Nemrut volcano, which has been active in historic times (Degens et al., 1978). From hydrographic data (Kempe et al., 1978) it is concluded that heat flow in the Lake Van basin must be substantial, exceeding world average by about 40 times (Degens et al., 1978). This is significant for questions of the hydrothermal activity, the oil and gas seeps, because organic matter can be more rapidly converted into hydrocarbons. Heat flow appears to be partially responsible for the effective deep-water mixing of the lake which inhibits a possible accumulation of gaseous hydrocarbons at depth and for the hydrothermal discharge below lake level (Kempe et al., 1978 and Degens et al., 1978). Furthermore, the influence of postvolcanic

CO_2-activity must still be present throughout the N- and E-parts of the lake. A considerable amount of juvenile CO_2 must be released here from the crust into the atmosphere (Schoell, 1978). High heat flows, hydrothermal discharges and CO_2-emissions in the lake may give some evidences of the events in the upper crust beneath the lake and these are closely related to extensional processes in and around the lake.

Studying all these limnological parameters from the lake (see Degens and Kurtman for full data set of these parameters and discussion), there are more indications than one, giving a evidence of an oceanic lake form rather than of an inland lake. If it is so, this surprisingly brings a possibility of the rifting event, in somehow, into the lake. As referred to Archean and Pan-Afro-Arabian collisons as Turkic-type orogens, classified by Şengör et al., (2008), it is quiet reasonable to consider that Lake Van Dome with its high heat flow and subsequent hydrothermal activity, indeed, resembles the East-African rift lakes. This makes this research extremely interesting with a question is whether or not Lake Van Dome experiences the highlands extension or let's to say that, the post-collisional rifting. Probably, this is the way Lake Van implicates for post-collisional crust-forming and consolidation processes in a Turkic-type orogen as in the Pan-African orogens.

1.4 Outline Anatomy of Lake Van Orogenic Structure with a brief review of the Theory of the Squashy Basin

The quest for understanding Lake Van orogenic structure, form and role of deformation mechanisms in Turkic-type orogeny requires a multi-disciplinary effort, at the intersection of accretionary orogens, and accretionary basins. It is a timely and relevant subject for a multi-disciplinary research. It is potentially a very broad topic and consists of a focus on shallow structure, including fault zones/suture contacts and types of fault deformation. It also consists of a separate focus on partial melting, magma propagation, and upper mantle/lower crust decoupling, as focus on processes in the transition zone within-plate magmas, and finally a focus on magma-hydrothermal deformations, sediment dynamics and crustal emplacement mechanism of magmatism in the convergent crust.

It is necessary first to review briefly a kind of the deformations of the Turkic-type orogens in depicting and understanding structures and to provide a comprehensive

treatment of the question: if Lake Van region is an area of germanotype deformation or this region can represent germanotype area of Turkic-type orogenic system?. This question builds the philosophy of a basic problem related to the theory of the squashy basin and thus, highlights extensional reactivation of accretion mosaics in a Turkic-type orogeny. Tectonic unstability and mobility of accretion mosaics are interpreted as indicating irresistant and weakening intraplate basins, which are deeper troughs resulting from fragmentation and separation of bounding thrusts or sutures. Consideration of the rheology of Turkic-type orogenic structure (accretion rheology) and reactivation of pre-existing structural lineaments along with the delamination, thin crust and other structural complexities requires some specific points and new approaches to be taken into account, such as the squashy basin.

Turkic-type orogeny is important for both Lake Van region and E-Turkey, since much of the Archaean orogeny appears to have been of that kind (Şengör and Natal'in, 2007 and Şengör et al., 2008). The continental crust has been constructed largely through Turkic-type orogeny and it is today what happens in E-Turkey (Şengör et al., 2008). On the other hand, to understand some specific points with Turkic-type orogeny as a process, much attention to an outline anatomy of Lake Van orogenic structure is necessary. Therefore, in what follows, a brief review of the theory of the squashy basin is presented. In the following paragraphs, the basic characteristics and orogenic type of Lake Van are outlined with a view to placing the Turkic-type orogeny into a proper perspective. Most of what is pronounced below has been taken from Şengör (1990a), Şengör and Natal'in (2007) and Şengör et al., (2008), to which the problems are referred.

When orogens finish their evolution they end up as parts of continents, concerning with defining and naming dead orogenic systems (Şengör and Natal'in, 2007). From this viewpoint, two major dichotomies seen on regional geology and deep structure of the lake are fundamental: (1) the difference in rheology of accretion mosaics between EAAC and BPM regions (Fig. 1.7) and (2) the difference in thermo-mechanical relations between the crust and the uppermost mantle (Fig. 1.8b). Both produce considerable differences in deformational characteristics of bounding sutures, such as Muş and/or Cryptic sutures and plate interiors, such as Lake Van basin. The differences in deformational patterns are mainly based on a major distinction between past (collision) and present (post-collision) tectonic regimes.

Because, in Turkic-type orogens, it is very common to confuse presently-active tectonic regimes with tectonic regimes that long ceased to be active (Şengör and Natal'in, 2007). Therefore, it is important to distinguish the presently active tectonic regime in a region of interest from those regimes that preceded it. Şengör and Natal'in, (2007) state that, in defining tectonic units in a region, it is generally convenient to group those structures that formed through "fossil strain systems" (Harland and Bayly, 1958) under palaeotectonic units and those that have formed and are now forming by "active strain systems" under neotectonic units (Şengör, 1980). This distinction also implies the superimposed pattern of fossil and active strain systems bounding any region. In such a case, the distinction is too difficult to differentiate the resulting strains and the faults. Lake Van region forms such a complicated pattern of heterogeneous strain systems superimposed on its bounding faults.

Orogenic systems include both regions of alpinotype and germanotype deformation resulting from one orogeny (Şengör and Natal'in, 2007), revealing the nature and characteristics of intraplate deformation during post-collisional period (after delamination). This suggests that, from the completion of one major Wilson Cycle, with all its attendant phenomena of opening and closing of multiple back-arc basins, coastwise strike-slip transport also including both secondary extensional (Gulf of California) and shortening phenomena (Transverse Ranges: Dickinson, 1996) (Şengör, 1984, Şengör and Natal'in, 1996a). This definition of nature of intraplate deformation in an orogenic system is important, since orogens complete their construction when their creative subduction zone ceases its activity (Şengör and Natal'in, 2007). It relates the orogenic system as a concept to the final closure of an ocean that essentially eliminates one or more subduction zones and thus refers to the fundamental nature of the subduction zone in an orogen, such as delaminaton and break off, as defining feature of an orogen. In areas, where orogenic deformation creates non-penetrative, blocky structures (Accordion-type features) with some alkalic magmatism in places, such as Muş-Lake Van region, show germanotype deformation. This deformation commonly accompanies orogenic zones in their neighbouring cratons and result from orogenic stresses affecting the craton (Şengör and Natal'in, 2007). As referred to the strike-slip deformation and collisional studies of Şengör et al., (1985), Dewey et al., (1986), Şengör et al., (2003) and Şengör et al.,

(2008) in E-Turkey, in fact, E-Turkey may imply clear evidences and typical styles of germanotype deformation. Because, many of the germanotype structures are either resurrected (resurrection) or replaced (replacement) structures (see palaeo- and neotectonic classification of structures in E-Turkey in Şengör et al., 1985) with respect to the Cimmeride and the Alpide germanotype structures (Şengör, 1984, 1985, Şengör et al., 1988 and Şengör and Natal'in, 2007). Such a consideration of deformation types and distinction of structures makes a rapid overview of orogenic systems possible and allows powerful insights into the historical geology of continents, particularly of Turkic-type orogens. As given much earlier, the nature, geometry and type of delamination and break off process and its surficial consequences in E-Turkey are important, since the fundamental orogenic structure is the subduction zone and the entire orogenic architecture is best described with reference to it (Şengör and Natal'in, 2007). Lake Van Dome as a morphological paradigm is the most prominent result of such a delamination and break off event and the most peculiar example of how such a dome-shaped basin can give a clue to both basin type and history and also deformation type and history. Deformation type and history also give some certain clues about magmatic periods and tectonic intensity, which control depositional characteristics and structural architecture. Consideration of deformation mechanisms and styles along with the orogenic complexities explains and describes outline anatomy of Lake Van, as an orogenic structure, with a review of the theory of the squashy basin.

If it is assumed that E-Turkey is an area of germanotype deformation, it is recognized that, in germanotype areas of orogenic systems, the flanking continents commonly get deformed during both collisional and compressional magmatic arc-related orogeny (see Şengör et al., 2008 for description of MURAT region). In these areas, deformation is characterised by blocky structures that do not create penetrative structures (see Dewey et al., 1986 for upper crustal flakes). As mentioned above, these blocky structures seem to have arranged in accordion-shaped features. These blocky structures take the shape of chains of thrust-bound basement uplifts within cratons marginal to orogenic belts (Rodgers, 1987 and Şengör and Natal'in, 2007), very similar to the Muş-Lake Van uplift and other uplifts in E-Turkey. In addition to such uplifts, rift clusters and rifting are also possible, resulting from orogen-parallel extension. Conjugate and discontinuous strike-slip faults are clearly observed,

resulting from an overall orogen-normal shortening of the fore- and hinterlands (Şengör and Natal'in, 2007). Rift clusters, rifting and strike-slip faults with normal or reverse components accompany orogeny in the germanotype fore- and hinterland fields of collisional and compressional arc-type orogens (Şengör, 1995 and Şengör and Natal'in, 2007). These features are shown to be common to deformations taking place on a regional scale of E-Turkey and prevailing on all scales (see Dhont and Chorowicz, 2006). This case reveals a dominant style of germanotype deformation in a smaller Turkic-type orogeny and gives a different view to understanding overall structure and mountain architecture of E-Turkey as one of a long and narrow edifice created at the expense of a pre-existing basin of more-or-less similar plan (see Şengör and Yılmaz, 1981). Its small size is a function of the mode of its formation.

It seems that E-Turkey is squashed between two continental pieces in N and S (see Şengör et al., 2008 for continental fragments of MURAT region) and that Lake Van appears to be squeezed out of a small basin (pers. comm., Şengör, 2006). The fact that a basin had been squeezed between its two walls to make E-Turkey is a cryptical research concept (see Şengör and Natal'in, 2007 for discussion). Because, squashing basins to make mountains became a dogma as soon as it was thought that thermal contraction was a good (Şengör and Natal'in, 2007). However, the sedimentary basins may be more susceptible to being squashed by their walls and that seems to explain why there are more mountains squeezed out of basins than not. In fact, this describes "the jaws-of-the-vise analogy of mountain-building", rather than the old vertical uplift models. If one squeezed any part of the crust it would inevitably create a bump on it, either by breaking or buckling (Şengör and Natal'in, 2007). Following Suess's famous metaphor for mountain building, volcanoes (the blood), the folds of the mountain belt (the crowded skin) and the normal faults (the wound) that commonly ended up bounding the internal sides of mountains (Suess, 1875, 1878 and Şengör and Natal'in, 2007). For example, as indicated by studies of shear wave anisotropy beneath Muş-Lake Van region, due to delamination and break off event, disturbed convection currents (Rayleigh-Taylor instabilities) in the interior of the earth to provide the necessary friction to fold and tear the crust in the way Suess had imagined (England et al., 2007) are contemplated (Şengör and Natal'in, 2007). Since, this could create a similar wound in the crust and such a simple way of mountain-making is also easy to imagine.

Suess's definitions reveal and clarify a kind of mountain-building different from the classically-known ones in the other mountains of the earth (Şengör and Natal'in, 2007) and hence, his descriptions are still very relevant to an understanding of tectonic structure of Lake Van and E-Turkey. Suess's studies also give a basic theory of the squashy basin formation and the squashed structure of weaker accretionary complex materials in E-Turkey and provide certain clues about crustal consolidation and crust-forming processes (Şengör et al., 2008). These processes control outline anatomy of Lake Van orogenic structure, together with mountain-building processes in E-Turkey. Therefore, it is considered that Lake Van region is an area of germanotype deformation and represents germanotype area of Turkic-type orogenic system. This consideration contructs a basic problem of how crust is formed and continent is made, related to the theory of the squashy basin. This problem seems to indicate extensional reactivation of accretion mosaics in a Turkic-type orogeny and intraplate magmatism with a high amount of alkaline component.

In the light of the previous studies, particularly of Şengör et al., (2003), Şengör and Natal'in, (2007) and Şengör et al., (2008), a rough definition of orogenic anatomy of Lake Van with a structure of the squashy basin underlines simply the significance of the Turkic-type orogens in continent construction and provides a way of how to express the peculiarities of orogenic systems. The term "orogen" alone is no longer adequate to describe many major orogenic areas, which are formed as a result of the activity of a large number of convergent plate boundaries in space and in time, such as the Tethysides (Şengör, 1990a and Şengör and Natal'in, 2007). The Tethysides are examples of superorogenic systems and are constructed by two major Wilson Cycles (Şengör and Natal'in, 2007). Such orogenic zones consist of more than one orogen and the term "orogenic collage" has been in use for it. An excellent active example of such a major orogenic area now in construction is E-Turkey. Smaller orogenic structure of E-Turkey is not simply another fold-thrust belt, such as E-Anatolian foldbelt or a collisional zone, is the accretionary complex structure with a higher plateau, where Lake Van region contributes to crustal consolidation process. Hence, Lake Van region is not simply another compressional thrust-ramp basin. This region has not only a morphological paradigm, but also a wide range of tectonic and magmatic peculiarities of the squashy phenomena.

1.5 Focus and Objectives of Lake Van Basin Research

Although the extensive geophysical researches have been carried out by various teams on diverse topics and in different areas, an overall understanding of E-Turkey as a complex orogenic system is still lacking, implying a morphological paradigm, Lake Van Dome. No definitive agreement has yet been reached among geoscientists on the fundamental nature of the sub-crustal dynamic processes that drive the accretionary basins and shape Turkic-type orogeny. There are still vigorous debates about extensional and strike-slip basin formation within thrust-ramp setting; about the depths to which the convergent crust is mechanically stratified and drives basin formation. Some of these debates is about the delamination or break off origin and even the existence of mantle thermal plumes rising through Lake Van Dome; the thermal/mechanical nature and origin of heterogeneity in the convergent crust; the nature and importance of mechanical decoupling between the upper mantle and the lower crust. Scientific motivation is mainly based on these debates to understand the Highlands morphological paradigm of Lake Van.

The Highlands morphology and possible rifting phenomena of Lake Van offer a new window into the doming asthenosphere, just beneath it with unknown implications. Combining information about the properties of Turkic-type orogeny, as derived from the correlative orogenic researches (Şengör et al., 2003; Şengör and Natal'in, 2007 and Şengör et al., 2008), the full range of geological, geophysical and geochemical observations are interpreted through geodynamical models. Ultimately, fundamental understanding of Lake Van's evolution, present dynamics and an integrative framework is necessary to better address key issues of societal relevance and to achieve progress on the cutting-edge topic of upper mantle and thin crustal dynamics. The different types of problems that arise in Lake Van basin research are building scientific motivation and challenging to solve for several reasons. Orogenic peculiarities, thermal and mechanical heterogeneities and thermo-mechanical decoupling are now recognized to play essential roles, with evidence for alkaline magma reservoirs in the anisotropic crust, delaminating and sinking chemically distinct slab, upper mantle/lower crust differences in deformation style of upper crust, magmatism transitioning from subduction to intraplate driving forces upon upper crustal nucleation of deformations, among others. All these events on scales ranging from regional to local characterize tectonic and magmatic activity and

seismic expressions of their structural styles are expected in and around Lake Van region. Indeed, the action of thermal perturbation, upward mass transport of decompressional melting magmatism at the surface, and infiltration of alkaline magma, its volatile components and other fluids at crustal depths offer dramatic examples of Lake Van's ongoing geological evolution in a small Turkic-type orogeny. It is thought that the deformation record provides an integrated history of Lake Van's magmatism and tectonics during post-collisional period. Hence, scientific motivation and objective of this research appear the most critically and underline the relevance and significance, for ideas on mountain-building and associated continent-generation, of the recognition of the difference in magmatic composition and tectonic structure of Lake Van from those of such classical compressional thrust-ramp basins. Such a distinction lies the key to understanding of how continents are made and of how Lake Van contributes to it.

Lake Van is the deepest lacustrine system emplaced in N-side of Muş suture (N-end of BP-M). Perhaps, more remarkable one than those pronounced above is that, Lake Van is the squashed orogenic basin at the domal center of the high plateau, surrounded by Karlıova (unstable) triple junction in W, isolated metamorphic blocks (BP-M) with bounding-suture complexes in S and accretionary-ophiolitic complexes in N and E. Unusual structural emplacement and obliquity of Lake Van (also with Muş basin) leaves it in complicated tectonic interactions with unstable structural trends around it. Hence, a wide range of geophysical and geological importance and motivations of this research essentially imply that Lake Van is prone to major magmatic and tectonic anomalies within a convergent zone, whose examination and interpretation require a comprehensive understanding of both the entire E-Turkey and its accretionary complex.

The main scientific focus of this study is that accordion tectonism-dependent factors, such as basement reactivation, structural inversion (inversion tectonics of mélange wedges) and basement mechanical anisotropy, may result in tectonic unstability of accretionary wedges. Shear-wave anisotropy and multi-directional flows of asthenosphere beneath thin crust show distinct distributional patterns of heterogeneous flow, directly beneath Muş-Lake Van region and through suture complexes (see data in ETSE project, 2003). The heterogeneous flow may suggest the extension phenomenon within a compression thrust-ramp basin, implying the

Highlands extension of Lake Van Dome. The extensional phenomenon in E-Turkey has not been clearly observed and reported, particularly in suture complexes since the extensive studies of Şengör et al., (1985), Dewey et al., (1986), Koçyiğit et al., (2001) and Dhont and Chorowicz, (2006), which only reported tectonic framework of E-Turkey. The extension phenomenon remarks the possibility that the opening of accreted terrains all along sutures causes a structural inversion of compressional thrust-ramp basins into the wedge-shaped extensional basins in a form of aborted rifts (Dewey, 1988). Thus, Lake Van stands at a complex form of intraplate fragmentation and separation events all along Muş and Cryptic suture zones in S, separating EAAC in N from BP-M in S.

Post-collisional highlands extension of Lake Van, the fragmentation and separation of bounding sutures have to be densely followed by the highlands alkaline/ultra-alkaline magmatism (Şengör et al., 2003 and 2008). This suggests converting accretions into the new crust, indicating a crust-forming and consolidation process, confirming the arguments by Şengör et al., (2008). According to Şengör et al., (2003 and 2008), the vast amount of the magmatic cover in and around Lake Van implies a corresponding abundance of alkaline magma, injecting into the wet accretionary complex rocks and there became solidified. This well evident how continental crust forms and begins its journey towards complete consolidation in the form of a craton. This event of crust-forming process clearly put Lake Van into the most critical case due to its having a large amount of tectonic and magmatic evidences.

New insight has been triggered primarily by available seismic data and preliminary results of structural deformation in the lake. Within this context, this study is organized to examine processes that contribute to the evolution of the convergent crust. The origin and structural evolution of the convergent crust pose intriguing questions that are being addressed by this study and research ideas on how melt segregates, extends and migrates through the crust into the lake and on how this lake can seismically represent the upper crustal effects of delamination process. The question of how accretionary wedges are deformed by processes of crustal differentiation and their implication for transition to post-orogenic squashy basin formation is also noticed and addressed to improve a unique perspective from E-Turkey. Some questions seem to have been most critically arranged. The one is when and how Lake Van is rifted or has such a rift-related origin in an orogen. If it is so,

how its rift-related origin, although it is aborted, implicates for post-collisional crust-forming process. Why and how the sutures complexes are obliquely fragmented and separated. How dome-shaped lake basin extensionally forms in a higher elevation with 2 km, how such a basin shows strange tectonic and magmatic patterns, in contrast to collisional products and contributes to a complete consolidation of the convergent crust. Tectonic and magmatic basics of all these unusual events in the lake are, in fact, the main objectives of this study.

A unique perspective requires an understanding of delamination-dependent extensional phenomenon in the lake. Since, an understanding of this phenomenon will highlight some structural problems within a setting of intraplate deformation and provide an insight into accretionary wedge deformation and extensional basin formation. Hence, post-collisional tectonics and magmatism of Lake Van from its crustal basement to upper sedimentary sections are completely investigated. In terms of searching for the collision-related lakes, such as Asia lakes of convergent high plateau systems along the youngest Alp/Himalayan orogenesis, this study will be a beginning and great opportunity for the further collision-related researches from various scientific disciplines to examine, correlate and exchange ideas for reaching a better understanding of causal links between the structural, sedimentary and volcanic processes. Thus, this study expects to obtain a reasonably clear idea of tectonic, magmatic and sedimentary outlines of Lake Van evolution as an unusual end-member product. In this study, the evolution of the continental crust of E-Turkey orogen is also reviewed in the context of a delamination process. The main tectonic and magmatic consequences of lithospheric delamination in a global context are identified. For that purpose, the tectonic and magmatic evolution of Lake Van and the current situation of E-Turkey orogen are combined by integrating the previous and present data to show that indeed, Lake Van is underlain by a late subduction-accretion complex and to prove that the post-collisional evolution of the lake is the result of the removal of the subducting slab from under it.

Shortly, the ultimate goal of this research is to develop an integrated approach with a multi-component and an integrative conceptual model drawing upon all contributing disciplines to understand Plio-Quaternary tectonic and magmatic evolution, and upper crustal dynamics of Lake Van and, by extension, accretionary structure of E-Anatolia and other similar Turkic-type orogens. The practical objectives are to

address the most important and difficult problems that have defied solution and to contribute a seed-bed for previous geophysical and geological ideas within an integrative conceptual framework. This framework identifies the next generation of critical experiments and observations in the research of Turkic-type orogens and builds support and appreciation for them. One last attempt is to provide an effective mechanism for the Highlands rifting phenomena in accretionary basins of Turkic-type orogens at all scales with a view to understanding how voluminous alkaline magmatism and extensive magmatic intrusions formed and whether this magmatism, indeed, constitutes a present-day example of the products of a Turkic-type (or non-Tibet-type) post-collisional development.

1.6 Methodology of Research Framework and Specific Approaches into Basin Model Assumption

The anticipated significance of this research work is the provision of a testable quantitative framework that describes and predicts upper crustal tectonics, affected by slab break off and delamination events. As given above, it is focused on several topics and main objectives of this research that the attempts are made here to derive a general scheme for the prevailing processes on Lake Van. These strongly depend on delamination events and the consequences of these events during post-collisional period and show the prominent tectonic and magmatic events, where the delamination process settled within an orogenic development.

The further progress is made in understanding a present-day dynamic evolution of Lake Van in a smaller and hot Turkic-type orogenic area. Hence, this research needs to improve a complete framework, including some orogenic peculiarities of E-Turkey. These make Lake Van region an attractive research area to solve tectonic problems and recognize its significance and place in an aspect of small Turkic-type orogeny. As mentioned earlier, much attention is paid to these orogenic peculiarities of E-Turkey. The following are examples of fundamental orogeny themes that should be considered in advancing outstanding research: a) subduction-accretion structure and its correlation with other similar accretionary orogens. b) delamination structure, its global geodynamic consequences and surficial tectonic effects. c) asthenospheric upwelling, its thermo-mechanical, volcanological and morphological effects. d) squashing phenomena and its effects in softening faults and weakening basins. e) Rift

clusters, rifting and extensional/strike-slip deformation in reactivating of accretionary wedges, and g) germanotype deformation in a small Turkic-type orogeny and its implications for crustal consolidation and construction and making a new continent. These give a clear way of constructing the methodology of research framework and provide certain clues about specific approaches into basin model assumption.

The research framework is, thus designed to demonstrate a coherent relation of shallow- and deep-seated processes in the basin. This is organized to improve a unique perspective from the lake and to search for the surficial effects of deep-seated events on the lake and their active control within unstable orogenic boundary. Some critical concepts of post-collisional intraplate tectonism, such as kinematics of faulting and several structural problems are identified to understand dynamic evolution and then accurately to reconstruct basin dynamics. During the progress of this research, the framework is widely ranged to be involved in differing styles of crustal deformation. This improves an understanding of crustal tectonic processes over a range of upper crustal scale through delamination, in which basic, underlying processes are combined in an analysis of structural framework. Hence, the intention is developed to understand the deformation mechanics and styles of margin boundary faults that were imbricated stacks and the controls on their development. The interest is to emphasize in the way Lake Van Dome's grow dynamically, the dependence of its tectonic structure on the crustal rheology and its response to extensional magmatism.

The sensitivity of the results to various tectonic and magmatic hypotheses is also examined. Comparisons and observations are made with the other sedimentary basins in the world, for which there are extensive data and interpretation experiences. In doing this, the results are compared and contrasted with these examples. Thus, tectonic model is refined in and how applicable the lake might be to tectonic structures of the other sedimentary basins in the collisional settings. The tectonic and magmatic framework of proposed model is mainly based on a parsimonious set of model assumptions. According to seismic reflection data and related maps, all these model assumptions are accurately integrated and combined to reconstruct dynamic model of the lake. For that reason, the research frame of a typical accordion tectonics is preferred due to that it has differential blocky structure of accretionary wedges.

Model assumptions are initially from Şengör et al., (1985) for strike-slip basin formation, basin classification and rhomb-shaped block models, and Dewey et al., (1986) for upper crustal flake-wedge tectonics, internal and external rigid body-block rotations. These model assumptions are reconsidered and reformed within a tectonic framework of the irresistant mechanics and weak rheology of accretionary wedges in E-Turkey by Şengör and Yılmaz, (1981). Thus, the presumed model is designed in an accretionary wedge-block. Mechanics and kinematic boundary conditions of faulting is considered in a relation to and compared with model studies of oblique faulting from Dewey et al., (1998) and examined in the light of flake-wedge tectonism and block rotations. Overall tectonic and sedimentary framework of graben-like structure of Muş-Lake Van region at crustal depths is highlighted by studies of regional wave propagation by Gök et al., (2000) and reviewed in relations with bounding suture complexes. These models are also constrained by geological time scales and periods of inversion process within a context of tectonic regime transition from Koçyiğit et al., (2001). Morphologic and morpho-tectonic applicability of these models to Muş-Lake Van region is examined and tested by morphological studies from Dhont and Chorowicz, (2006).

These model assumptions and designs are superimposed by asthenospheric doming, development of the squashy zone and an evidence of alkaline/ultra-alkaline magmatism during post-collisional period from Şengör et al., (2003). The orogen-wide delamination and break off models from Faccenna et al., (2006) for the low resolution 3D-delamination and slab windows model and Şengör et al., (2008) for the high resolution 2D-delamination and break off model are extensively used to confirm a close structural interaction of suture complexes with the model in design. Furthermore, both model studies from Faccenna et al., (2006) and Şengör et al., (2008) are correlated with a model of collisional delamination by Cloos et al., (2005) to understand time periods of crustal deformation after break off and confirm upper crustal strike-slip faulting and alkaline magmatism. In this way, the model study of Cloos et al., (2005) is extended to apply with suture belts in S of the lake. Locally uplifted domal zone in a confined area of the mid-plateau is morphologically well investigated by Dhont and Chorowicz, (2006). The results of this morphological analysis are constrained for doming of the lake. For this reason, the receiver functions data set from Angus et al., (2006) are interactively used as combined with

the moho variations from Zor et al., (2003) and geologically interpreted to observe possible offsets of moho thickness beneath the lake and thus, to understand crustal basement for model design. Crustal emplacement and distribution model and feed back mechanism of rising alkaline magmatism are considered in a close relation to the effects of mechanical anisotropy of the crust from a wide range of previous model studies that are cited and given during this study.

Regional geodynamic models of E-Turkey give acceptable thermo-mechanical consequences in affecting crustal deformation and thus, in determining the characteristics of the deep-seated process beneath the lake. The predictions can then be compared and contrasted with those from approaches based on other assumptions and with observations. Tectonic model assumptions, particularly by Dewey et al., (1986) are very useful. Since, they provide insight into system behaviour and point to key data necessary to discriminate among competing hypotheses. The general approach in which deformation properties, styles and structural patterns that are considered important are incorporated in tectonic patterns and structural styles of upper crustal deformation to address specific tectonic applications pronounced in Şengör et al., (1985) and Dewey et al., (1986).

Tectonic deformation of Lake Van is, due to its squashy basement, extended to investigate the relationships between overall deformation, faulting and magmatism, such as thermo-mechanically coupled or uncoupled systems. Several factors of this research make this an opportune time to investigate the role of weak reactivated faults and suture-related shear zones, partial melts and other weak and softer materials, such as lacustrine sedimentation, in upper crustal deformation. Persistent weak boundary faults and suture-related shears have long been considered to have a significant influence on the architecture and patterns of strain partitioning within the crust (Sibson, 1977; Handy, 1989; Holdsworth et al., 1997). Although arguments exist against weak boundary faults (Scholz, 2000; Townend and Zoback, 2000), the research framework of this study recently begins to point to specific weakening mechanisms based on a orogenic field (Braun et al., 1999; Holdsworth et al.,2001 and Bos, 2001). These results lead to rheological deformation of accretions and/or accretionary wedges that well predict how the crust may strain soften. For example, for accretionary fault/shear zones, the thinned and warm crust may determine the frictional-viscous behaviour and can lead to strain- and strain-rate weakening of a

fault zone by factors of four, and possibly much more (Bos, 2001). In continental rifts and rifted continental margins, Huismans and Beaumont (in revision for Geology) uses the thermal-mechanically coupled model to demonstrate that strain softening of the Coulomb regions of the crust naturally leads to asymmetry during rifting. This result indicates the potential importance of all processes that weaken specific parts of the crust. Hence, as asymmetric faulting of margin boundaries and basin asymmetry is taken into account, the current focus is on the effect of upper crustal deformation on the basin geometry, in particular, the wedge-shaped geometry and the faulting of margin boundaries. By using the same approach, proposed mechanisms for upper crustal deformation and transitions in deformation mechanisms, for example accompanying strength reduction on basin-scale strain partitioning, shear zone development, and faulting are also investigated. Suture-bounded tectonic blocks and suture-related shear zones represent structural framework of accretionary complex beneath the lake. This complexity of thrust fault contacts of accreted terrains allows the effects of localized weakening on deformation to be recognized accurately. The intent is to understand how localization occurs dynamically and how/when weak zones are abandoned as loci of deformation when they lose geometrical compliance. Because, decompressional magmatism and partial melting reduce the effective bulk viscosity of the crust and demonstrates the potential importance of this reduction on tectonic processes. In deep sedimentary basins of thin-skinned fold and -thrust belts of intraplate orogenic settings, unconsolidated, softer lacustrine sediments subject to high fluid pressures are special weak materials that profoundly alter the deformation style, especially in deltas. These weakening effects of depositional system are also investigated as part of the deformation of deltaic provinces.

1.7 Geography, Geology, and Limnology

1.7.1 Geological background of EAAC

The active tectonics of EAAC is characterised by N-S shortening expressed by widespread flexural slip folds with steep axial planes striking generally E-W, thrust faults of similar orientation, strike-slip faults that strike NE-sinistral and NW-dextral (Şengör et al., 1985; Dewey et al., 1986; Koçyiğit et al., 2001 and Dhont and Chorowicz, 2006) (Fig. 1.9). The EAAC exercised a very profound influence on the

neotectonics of E-Turkey (Şengör and Kidd, 1979; Şengör, 1980; Şengör and Yılmaz, 1981; Şengör et al., 1985; Dewey et al., 1986). It experienced the strong internal deformation as different from the Anatolian plate ("scholle", ova regime) escaping to the WSW, and is subjected to high plateau diffuse convergent regime (Şengör et al., 1985) (Fig. 1.10).

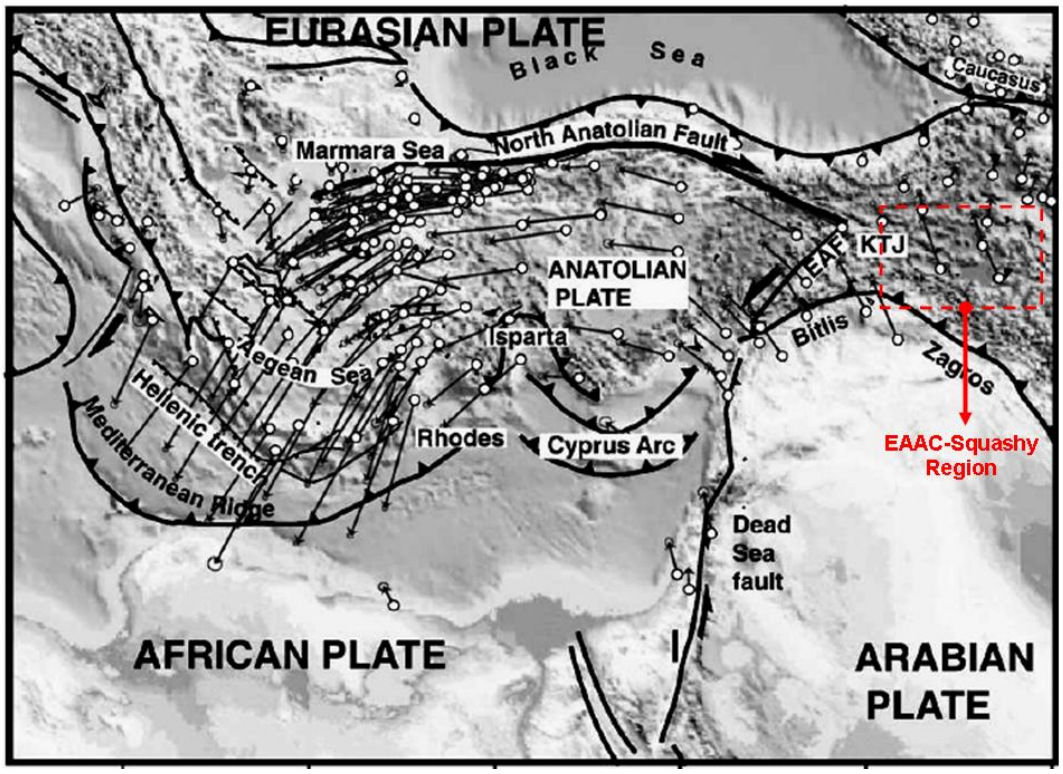

Figure 1.10 : The GPS velocity field relative to Eurasian reference frame in the E-Mediterranean region, where the Arabian, African, and Anatolian plates meet, shows an anticlockwise rotation of a large region, compromising the Arabian, Anatolian and Aegean regions (GPS data from Reilinger et al., 2006). GPS velocities along the NAF present also an increase from E to W. The N-movement of the Arabian plate along the Dead Sea Fault (DSF) causes the Anatolian plate to escape westwards via the right-lateral North Anatolian Fault (NAF) and the left-lateral East Anatolian Fault (EAF) (Faccenna et al., 2006). Dashed red square shows EAAC-squashy region.

The neotectonic phase of collisional convergence began about 12 Ma ago in which the N-convergence of Arabia with Eurasia produced shortening and thickening of the crust and caused a wedge-shaped Anatolian "block" to migrate westwards over the subducting oceanic lithosphere of the E-Mediterranean (Şengör and Kidd, 1979; Şengör and Yılmaz, 1981; Şengör et al., 1985; Dewey et al., 1986). Şengör et al., (1985) and Dewey et al., (1986) discussed that to avoid excessive thickening by shortening, the EAAC "wedged-out" a considerable piece of the Anatolian Orogen along two new boundaries, the N- and E-Anatolian Transform Faults, towards the

more readily subductable oceanic region of the E-Mediterranean (McKenzie 1972a, b; Dewey and Şengör, 1979), thereby giving birth to the Anatolian "Block" or "Wedge". This model has the particular merit of explaining E-W lateral wedging and extension as a late stage consequence of crustal thickening. The fault ends in two continental triple junctions where incompatibility has led to the formation of complex intracontinental basins (Karliova and Adana) (Şengör et al., 1985) (Fig. 1.10).

The N-S collision initiated a new tectonic episode mainly characterized by compressional tectonics. During this new episode, the E-W-extending folds, reverse-thrust and left (NE-SW striking) and right lateral strike-slip (NW-SE striking) faults and large-scale pull-apart type of extensional fractures are formed in the neotectonic episode (Şaroğlu and Yılmaz, 1986) (Fig. 1.9). In places where strike-slip faults step up in en echelon character, there are some volcanoes existed as a result of the effective tectonism. These structures led to the narrowing and subsequent widening of the region in N-S and E-W directions, respectively and also caused the thickening of continental crust, thus subsequent uplifting of the region. In general, synclines and anticlines trending E-W in the region correspond to and are overlain by E-W trending basins and elongate ridges (Şaroğlu and Yılmaz, 1986). Due to N–S compressional regime, the E-Anatolia alkaline volcanism, especially the fissure eruptions, is closely related to N-S striking tension fractures formed by the compressional regime (Şaroğlu and Yılmaz, 1984). The upper volcanic units are either observed in the form of intrusions following the ENE- and WSW-striking faults and E-W striking fold axis or in the form of fissure lava flows W, SW, and S of the Varto region (Buket and Görmüş, 1986; Buket and Temel, 1998). The trends of dykes are parallel to the general trend of the NAFZ. There are also quite a number of parallel, right-lateral, strike-slip faults between Karliova and Varto (Gülen, 1984; Şaroğlu et al., 1992). According to Şengör et al., (1985) and Dewey et al., (1986), these faults follow the same trend as the NAFZ from the E of Karlıova to the E of Varto and they have combined strike-slip, and thrusting mechanism due to the regional compressional forces. The presence of dykes along segments of the fault zone denotes not only the compressional regime, but also the presence and effects of a tensional regime (Buket and Temel, 1998).

The relations between structural elements and the basins formed in the neotectonic episode. Şaroğlu and Yılmaz, (1986) well documented geological evolution and basin models during neotectonic episode in the E-Anatolia (also see Yılmaz, 1984; Şaroğlu and Yılmaz, 1984; Yılmaz et al., 1986; Şaroğlu, 1985). These studies have also provided information on the tectonically related structures and their subsequent deformational geometries that are shaped up in the period between the last change in tectonic regime and the present time. Şaroğlu and Yılmaz, (1986) showed that different type of basins are also formed along the N-S trending extensional fractures and in areas where strike-slip faults step up in en-echelon character (Şaroğlu and Yılmaz, 1986). En echelon character of strike-slip faults is well observable pattern in Muş-Lake Van region, particularly in and around Nemrut volcanic dome-cone complex (Dhont and Chorowicz, 2006). Some pull-apart types of basins are formed between strike-slip faults in the region (Şaroğlu and Yılmaz, 1986) (Fig. 1.9). Another different type of basins in the E-Anatolia is the intermountain basins which generally extend E-W and correspond to the synclines. Such intermountain basins can be bounded on one side by a thrust fault. There are also basin-like localities between compressional features or along the extensional fractures. But these are relatively small in scale. Thus the two basin types in the E-Anatolia are given by Şaroğlu and Yılmaz, (1986) as pull-apart and intermountain basins.

The range of crustal structures characterizing collisional orogens and their forelands, most of which occur in E-Anatolia (Fig. 1.11). The pre-collisional geology of the EAAC is characterized by three terranes separated by suture zones containing mélanges, accretionary complexes and flysche-molasse basins; the S-terrane is the para-autochthonous Arabian foreland. The C-terrane is the Bitlis Massif, an allochthonous terrane of Palaeozoic metamorphic rocks, predominantly metasediments (Hall, 1976). The N-terrane is the Pontide belt, which comprises a metamorphic basement of Palaeozoic age overlain by Mesozoic shelf sediments. Rocks of the Arabian foreland are separated from the Bitlis Massif by a complex imbrication zone, the Bitlis Thrust (or Suture) zone, which contains ophiolitic and island arc assemblages of probable late Cretaceous age (Robertson and Aktaş, 1984). The pre-Neogene geology of this zone is dominated by an accretionary complex of Eocene or younger age (Şengör and Yılmaz, 1981; Pearce et al., 1990). Major tectonic blocks of the E-Turkey orogen (Şengör et al., 2003) are involved in the five

provinces seen in Fig 1.11a, namely Rhodope-Pontide fragment, NW-Iranian fragment, Eastern Anatolian Accretionary Complex (EAAC), Bitlis-Pötürge Massif and Arabian foreland. In Fig. 1.11b, topographic map of the EAAC over which the main tectonic units as well as collision-related volcanics are also superimposed (Keskin, 2005 and 2007).

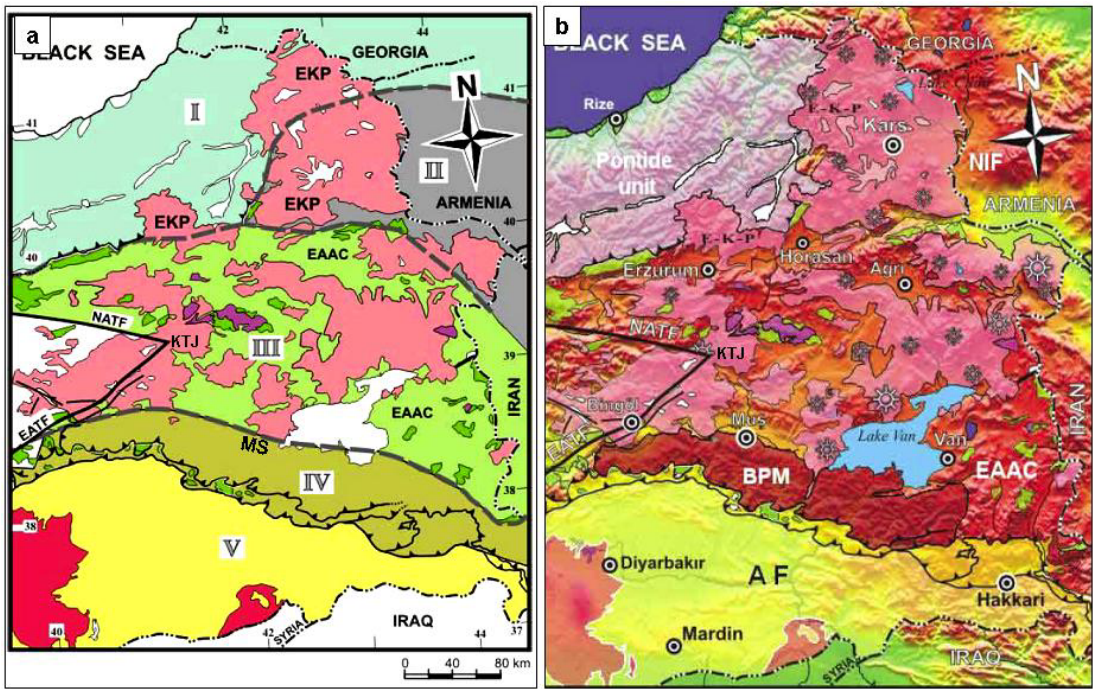

Figure 1.11 : a) major tectonic blocks of E-Anatolia. The borders are modified from Şengör et al. (2003). I: Rhodope-Pontide fragment, II: Northwest Iranian fragment, III: Eastern Anatolian Accretionary Complex (EAAC), IV: Bitlis-Pötürge Massif, V: Arabian foreland. Dark green areas: outcrops of ophilitic melange, Pink and red areas: collision-related volcanic units, white areas: undifferentiated units or young cover formations. EKP: the Erzurum-Kars Plateau in the N (Keskin, 2005). b) topographic map of E-Anatolia, over which the main tectonic units as well as collision-related volcanics are superimposed. NIF: NW-Iranian Fragment, BPM: Bitlis-Pötürge massif, AF: Arabian Foreland (for more explanation, see Keskin, 2005 and 2007).

In E-Turkey, the present-day motions are about 2.5 cm/a in a broad region between Erzurum in N and Bitlis in S and they decrease abruptly to about 0.5 cm/a N of Erzurum (Fig. 1.12). The broad region corresponding with high surface velocities are underlain by slow seismic velocitis and appears to be bereft of a mantle lithospheric lid. This regions is termed as Muş-Lake Van squashy zone (see cross sectional profile of the squashy region in Fig. 1.12). An integrated geophysical survey across the EAAC clearly demonstrates that the 2 km high topography of the E-Turkey is isostically undercompensated (Al-Lazki et al. 2003; Gök et al. 2000; Sandvol et al.

2003; Örgülü e al., 2003; Türkelli et al. 2003; Zor et al. 2003). These studies documented that E-Turkey, is not supported by thick crust but by hot mantle, and this leads to a model of active extension and lithospheric thinning. The falling off of the slab exposed the underbelly of the EAAC to at least asthenospheric temperatures, which resulted in its widespread partial melting (Şengör et al., 2003 and 2008).

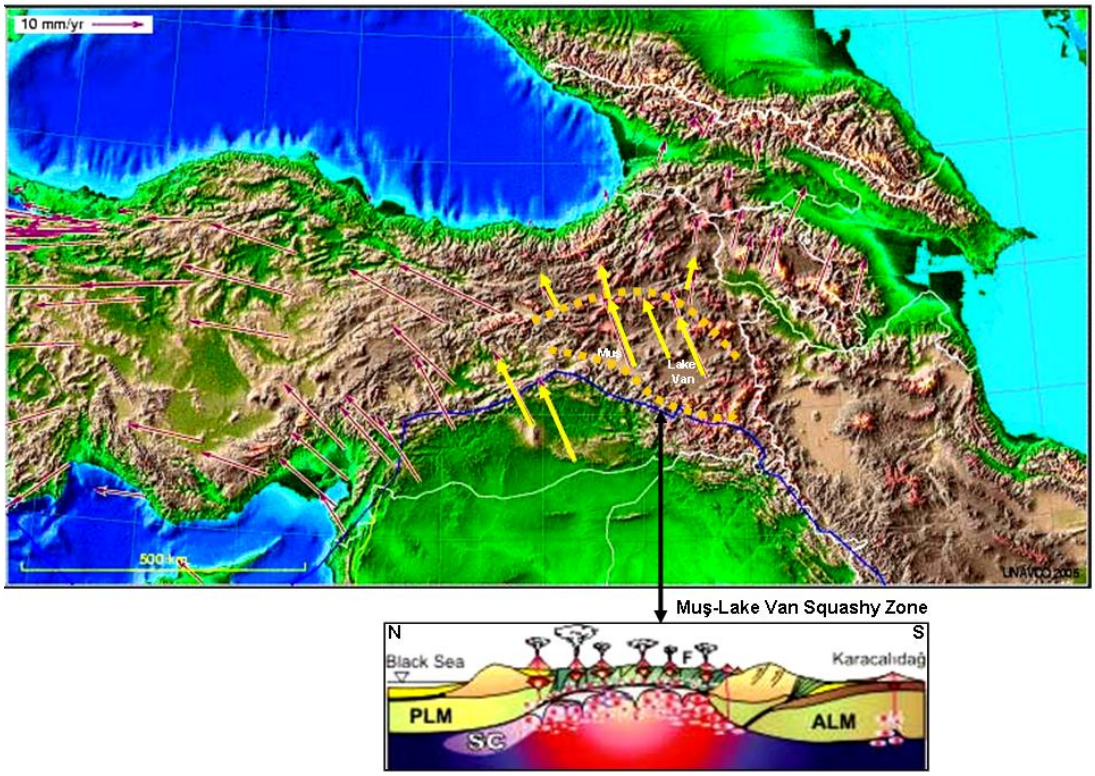

Figure 1.12 : Detailed GPS vectors of E-Anatolia (see Şengör et al., 2008). Faster vectors (long yellow arrows) show the squashy zone of Muş-Lake Van region and slower vectors (shorter yellow arrows) show relatively slow motions. Dashed orange lines bound the Muş-Lake Van squashy zone in N and S. Note that abrupt velocity changes in the region. Small section shows N-S trending cross sectional profile of the squashy region (Keskin, 2007).

Sedimentary rocks and coeval volcanites cover very wide areas (Fig. 11b). The young volcanism in the region has displayed some changes depending on the evolution of the continental crust. The nature of the volcanism has changed with time as continental crust has been evolved by the persistent tectonic effect (Yılmaz et al., 1986). Eruptions have mostly followed the extentional fractures and chosen them as paths to get out (Fig. 1.9). N-S trending deep valleys and E-W trending meandering rivers are among other features formed during this neotectonic episode (Şaroğlu and Yılmaz, 1986). Şengör, (2006) stated that the volcanicity started about 11 Ma ago in the N and migrated S, became more alkaline with time and southward, where it

remains active (last eruption in Mt. Nemrut in AD 1443). The late Miocene to present volcanicity of E-Turkey exhibiting a complex composition and geochemistry ranging from andesitic-rhyolitic crustal melts to alkalic olivine basalts probably reflect the rise of the asthenosphere, its adiabatic melting and heating up of the overlying crust (Şengör et al., 2003). The model proposed by Şengör et al., (2003) has important implications for other regions underlain by very large subduction-accretion complexes, such as wide areas of the Altaids in Central Asia (Şengör and Natal'in, 1996) or the Songpan-Ganzi system in China (Şengör, 1984).

The structural evolution and geodynamics of E-Anatolian volcanism during post-collisional period are studied by Pearce et al., (1990), Yılmaz, (1990), Notsu et al., (1995), Buket and Temel, (1998) and Yılmaz et al., (1998). In the study of Yılmaz et al., (1998), four well-developed Quaternary volcanic centers are introduced and outlined in much detail. These are; the Mounts of Ararat, Süphan, Tendürek and Nemrut. They well described the volcanic centers from a volcanological perspective to review their petrogenetical nature and to discuss their tectonic significance. Buket and Temel, (1998) proposed that generation of the magmas from a depleted mantle source and/or their emplacement within the continental crust with variable degrees of contamination and fractional crystallization has been related to a detached sinking slab following Miocene continental collision along the Bitlis Suture Zone.

1.7.2 Limnological background of Lake Van basin

Lake Van basin is within a tectonically active boundary region, and the E-continuation of the Muş ramp basin with the Nemrut volcano in between (Şengör et al., 1985) (Fig. 1.13). Lake Van is thrust-bounded compressional ramp basin and located in a restricted area, in the N-branches of the Bitlis-Zagros suture zone (Dhont and Chorowicz, 2006). This lake represents a structural boundary between the EAAC and Bitlis-Pötürge Massif (BP-M) and is bounded by Muş and Cryptic sutures in S (Fig. 1.13). Thus, the lake experiences the collision-related structural phenomenon and tectonic inversions (see Şengör et al., 1985 and Dewey et al., 1986 for a tectonic interpretation and marginal faulting of Muş-Lake Van region). The lake seems to be younger and deeper sedimentary wedge as a product of post-collisional processes. Lake Van is also known as a very active seismic zone and about 30 earthquakes with magnitude ≥ 5.0 occurred in the vicinity of Lake Van since 1900 (Fig. 1.9). Recent small and moderate earthquakes suggest that the lake is tectonically still active and

compromise notable strike-slip motion (Tan and Taymaz, 2001; Pınar et al., 2002). The S-shore of the lake is formed by the Bitlis massif (3,500 m) and the area N and W of the lake is influenced by volcanic eruptions in the Pliocene and Quaternary age. (Fig. 1.13) Two semi-active volcanoes rise in the immediate vicinity of the lake (1674 m a.s.l.) at Nemrut Dagı (3050 m a.s.l.) and Süphan Dagı (3800 m a.s.l.) (Karaoglu et al., 2005). There are also a number of collapsed parasitic cones and domes in SSW-part of the lake (Yılmaz et al., 1987 and Dhont and Chorowicz, 2006 for an updated map of this region). The Nemrut built a lava dam across the Muş Basin probably between 100,000 and 200,000 years ago. Later, subsidence formed a large drainage basin (Degens et al., 1984). Rivers within this basin discharged water and sediments into the lake, which has no significant outflow today.

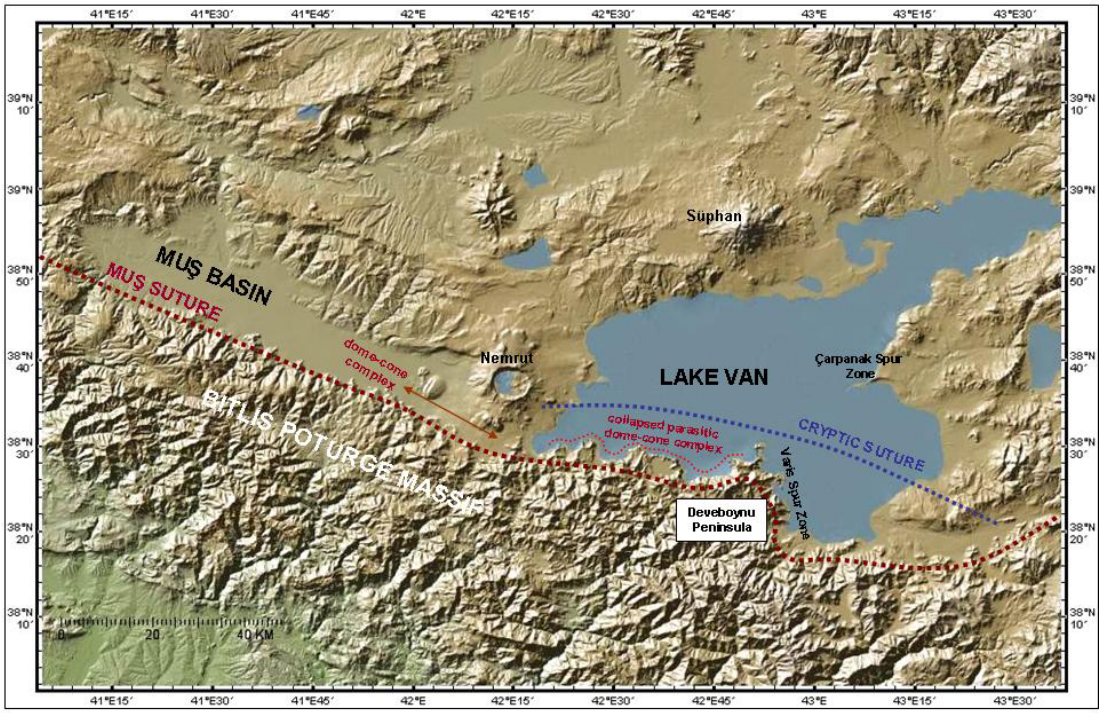

Figure 1.13 : Detailed morphological model of Muş-Lake Van region, bounded by Bitlis-Pötürge Massif (BP-M) in S. Dashed brown line shows Muş suture in S. Dome cone-complex around Nemrut volcano and collapsed parasitic dome-cone complex in S-coast of the lake are also indicated. Dashed blue line indicates Cryptic suture across the S-part of the lake (see also Fig. 1.8c). Note that Deveboynu Peninsula in S and Çarpanak Spur Zone in E of the lake are important morphological features.

The first acoustic data of Lake Van collected in 1974 (Wong and Degens, 1978; Degens et al., 1984), indicate its division into three distinct physiographic provinces by Kempe et al., (1978). a) a lacustrine shelf (27 % of the lake area), extending from the lakeshore to a sharp break in the bottom slope; b) a steeper lacustrine slope

(sublacustrine slope, 63 % of the area) c) a deep, relatively flat-plain basin province (10 % of the area) in the center of the lake. The deepest part of the lake, the Tatvan basin, is almost completely controlled by faults (Wong and Finckh, 1978). This basin is bounded by a combined delta system in the E (NE-Erek and SE-Eastern delta systems), by irregular spur zone (S-spur zone) in the S, by Tatvan delta and Adabağ spur zone in the W and by sublacustrine slope in the N. The most important spur zones around the Tatvan Basin are Çarpanak spur in the E, Adabağ spur in the W, S-spur zone in the S and Varis spur zone surrounding Deveboynu peninsula in the SE (Fig. 1.14). Varis spur zone and Deveboynu peninsula are seismically most active regions of the lake (see an collection of papers in the Geology of Lake Van book by Degens and Kurtman, 1978 for a full discussion of morpho-physiographic and topographic, sedimentary and structural outlines of the lake).

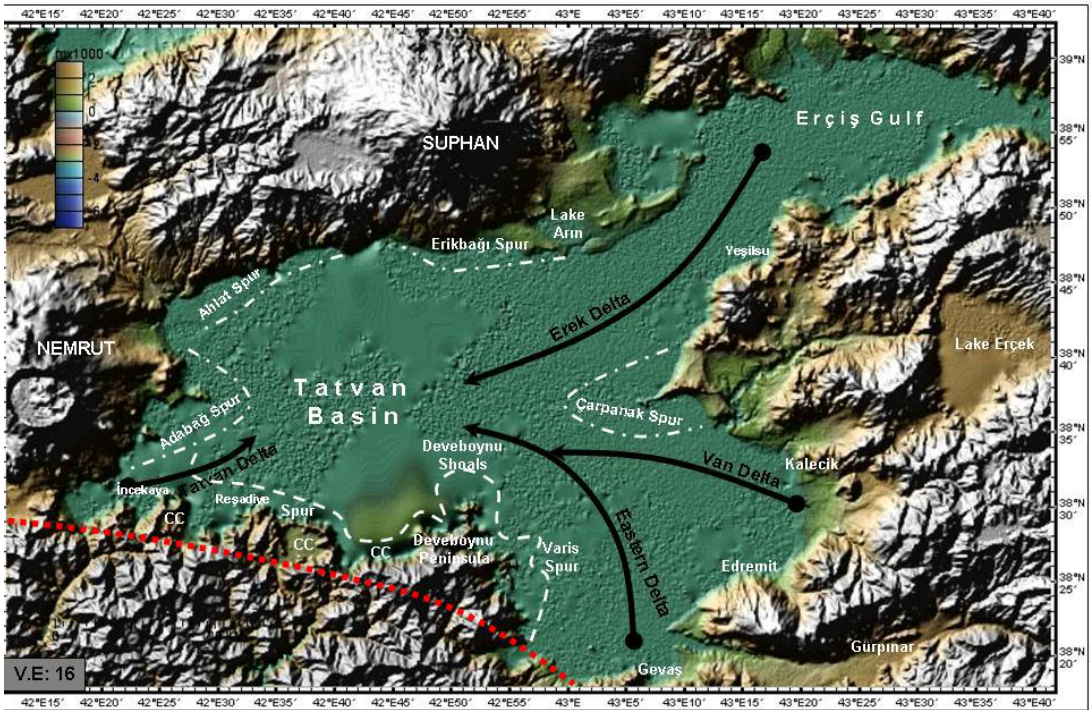

Figure 1.14 : Morpho-physiographic and topographic provinces of Lake Van showing the main deltaic areas, coastal sections, spur zones (modified after Wong and Degens, 1978). Black Arrows show the SW-corner of Tatvan delta, NE-Erek delta and SE-Eastern-Van delta systems. Note that locations of spur zones, Nemrut volcano at W and Süphan volcano at N. Deep lake center is central Tatvan Basin. Scale (x 1000 m) at the top left corner is the elevation and vertical exaggeration of map (V.E) is 16. Red dashed line indicates a part of Muş suture zone and collapsed cones (CC).

Lake Van is the fourth largest of all terminal lakes in the world (Erinç, 1974). It is also the largest soda lake with the present water level at 1648 m.a.s.l., with a surface area of 3522-3570 km^2 (3713 km^2 according to Wong and Degens, 1978), a volume of 576-607 km^3. The bathymetric map of the lake (Wong and Degens, 1978) permitted the calculation of its volume for the first time (Kempe et al., 1978). This volume makes the lake the fourth largest closed lake, having a maximum water depth of 445-460 m (Wong and Degens, 1978 and Litt et al., 2009), extending roughly for 130 km WSW–ENE. In present time the lake level is at 1,648 m above sea level. Catchment area is 12,522 m^2 (Kempe et al., 1978). The drainage basin covers 16,096 km^2 (Kempe and Degens, 1978) and encompasses the E-part of the Muş Basin. The lake water is highly alkaline, the Ph reaches 9.8, salinity is 22 parts per thousand and calcium concentration is low (Kempe et al., 1991). The climate of the area is characterized by continental conditions, with hot and dry summers and cold winters, and water level control is unregulated (Kempe et al., 1978).

Degens et al., (1978) reported that large amount of oil and gas seepage occurs abundantly in the lake. It was, therefore, of interest to get information on the structure of the lake basin. Due to its depth and salinity pattern, water stratification similar to Lake Kivu/East Africa, was expected (Degens et al., 1978). For example, data from Kivu have shown substantial methane accumulation at a water depth below 300 m (Degens et al., 1973; Deuser et al., 1973). 50 km^3 of methane (at standard temperature and pressure) are presently contained in its deep water and can readily be extracted (Degens et al., 1978). It is added that, furthermore, a number of major faults border the Tatvan basin, and the E-shelf is dissected by numerous extension fractures. No major synclines or anticlines are reported within the upper two kilometers of the Lake Van basin. The Upper Cretaceous limestone beneath the lake dips NW at about 5^o, again, its W-flank is truncated by a near vertical fault (Degens et al., 1978). Although the oil-gas generating potential of the whole region appears to be quite substantial, the tectonic setting beneath and around the lake shores is unfavorable for large accumulation of oil deposits (Degens et al., 1978). This shows a clear evidence of strong tectonic activity in the lake. However, the various oil and gas seepages and related deformation structures should only be viewed as an expression of the fractured subsurface structure, rather than an indication of large reservoirs at depth (Degens et al., 1978).

The lake's position at the junction of the atmospheric SW-jet stream and N-branch of the Subtropical High makes it climatically sensitive (see related map in Litt et al., 2009). The jet stream steers the cyclone tracks that are responsible for supplying moisture from Mediterranean air masses during winter. The location of the Subtropical High controls the southward extension of the dry continental air masses of NE-Europe and Asia (La Fontaine et al., 1990; Akcar and Schlüchter, 2005). Within the sensitive climate region of NE-Anatolia, the Lake Van record represents an excellent continental climate archive between the Black Sea, the Arabian Sea and the Red Sea (Roberts and Wright, 1993; Cullen and de Menocal, 2000; Lamy et al., 2006). Subaerial terraces and sedimentological evidence demonstrate that lake level changes of up to several hundred meters occurred during the last 20 kyr (Litt et al., 2009). This indicates that the lake reacts sensitively to alteration of the hydrological regime in response to climate change (Landmann et al., 1996a and Litt et al., 2009). The one important thing is that Lake Van sediments have a water content of about 60% (Kempe, 1977 and Kempe et al., 1978). Furthermore, the sediments of Lake Van are annually laminated for nearly 14 kyr (Kempe and Degens, 1978; Lemcke, 1996; Landmann et al., 1996b; Wick et al., 2003), which is ideal for creating high-resolution climate, tectonic and volcanic histories (Litt et al., 2009), particularly for understanding earthquake-related soft sediment deformations and sediment-gas-fluid mixture products in deltas.

Lake Van presently seems to be in hydrologic equilibrium (Kempe et al., 1978). Thus, terraces above the present lake level document that the input of water to the lake exceeded the evaporation (Schoell, 1978). Annualy 4.2 km^3 water is lost by evaporation which are recharged by rivers (2.5 km^3) and precipitation (1.7 km^3). The lake level oscillates with the frequency of the solar cycle. In April a warm surface layer starts to develop, while in February and March the entire volume convects. The losses of heat due to winter cooling indicate a high geothermal gradient in the Van region. Due to winter convection, no stratification can build up in the lake. However, such stratification might have existed at the height of the last ice age, where deep water mixing was inhibited (Degens et al., 1978). Because of winter-convection chemical composition of water is homogeneous throughout the lake. The hydrological features have similarities with those in the open oceans, in winter arctic downwelling occurs, in summer an equatorial warm surface layer is formed, and in

autumn or early winter upwelling is encountered in the lake. Contrary to the open oceans the influence of the solar activity on weather is displayed by a fluctuation in lake level (Kempe et al., 1978). Climatic changes have caused the lake level to alter since glacial times to a great extent, but were insufficient to dry the lake up (Litt et al., 2009).

Site survey results and perspectives of "PALEOVAN" project, International Continental Scientific Drilling Program (ICDP): as preparation for an ICDP drilling campaign, a site survey was carried out during the past years and cored 10 different locations to water depths of up to 420 m (Fig. 1.15). Multidisciplinary scientific work at positions of a proposed ICDP drill site included measurements of magnetic susceptibility, physical properties, stable isotopes, XRF scans, and pollen and spores (see Litt et al., 2009 for details).

The lake's size and depth suggest that the lake may have deep sedimentary deposits spanning multiple glacial-interglacial cycles (Degens and Kurtman, 1978 and Litt et al., 2009). The combination of climatic sensitivity and a varved sediment lithology makes the lake a suitable candidate to disentangle and isolate processes and patterns of climate and environment. The sedimentary record of Lake Van, partly laminated, has the potential to obtain a long and continuous continental sequence that covers several glacial-interglacial cycles (ca 500 kyr). Therefore, Lake Van is a key site within the International Continental Scientific Drilling Program (ICDP) for the investigation of the Quaternary climate evolution in the Near East ("PALEOVAN").

The ICDP project attempts to analyze the depositional regimes of Lake Van, characterize the Holocene and last glacial sediments, and evaluate the potential of Lake Van for long continuous sedimentary records (see and examine the most important results of these surveys in Litt et al., 2009). Litt et al., (2009) stated that the core extends back to the Last Glacial Maximum (LGM), a more extended record than all the other Lake Van cores obtained to date. Both coring and seismic data do not show any indication that the deepest part of the lake (Tatvan Basin, Ahlat Ridge) was dry or almost dry during past times. These results show potential for obtaining a continuous undisturbed, long continental palaeoclimate record (Litt et al., 2009). The research potential of "ICDP PALEOVAN" project also establishes new results on the dynamics of lake level fluctuations, noble gas concentration in pore water of the lake

sediment, history of volcanism and volcanic activities based on tephrostratigraphy, and paleoseismic and earthquake activities.

Late Quaternary depositional settings, water level changes combined with climatic effects are investigated by Karabıyıkoğlu et al., (2007). A contribution to identifying climate forcing, recent tectonic impact and relationships to volcanic activity during Upper Pleistocene by Kuzucuoğlu et al., (2007) showed the evidences of high magnitude low and high stands of Van lake level. Akköprü et al., (2007) also presented some preliminary results of modelling Lake Van level and water budget variations in the past and out of the interpretation of coastal deposits and DEM. Past lake levels are also presented as elevations relative to recent measurements (Litt et al., 2009). A highstand of 90 m is documented in coastal outcrops along the lake (Schweizer, 1975; Landmann et al., 1996a). Several lowstands also occurred, the lowest of which (200 m), occurred 12 kyr ago during the Younger Dryas. During the 3rd millennium aridity crisis (3 kyr BP), lake level dropped to 80 m (Landmann et al., 1996a; Lemcke and Sturm, 1997). No lithologic or seismic data, however, indicate that the lake ever dried out completely as assumed by Landmann et al. (1996a) (Litt et al., 2009).

2. ICDP-SEISMIC DATA EQUIPMENT AND MATERIALS

2.1 Multi-Channel Seismic Reflection Profiling and High-Resolution GeoChirp System

During the meeting of the European Lake Drilling Program in 2001, it was suggested to start with a proposal development for large lake drilling with the ICDP (International Continental Drilling Project) equipment pool GLAD 800. In this framework a seismic pre-site survey at Lake Van was carried out from June 1 to June 15, 2004. In total 50 profiles with a length of ~ 850 km are collected by means of a high resolution multi-channel seismic and a GeoChirp system (Fig. 2.1). The GeoChirp system generated a sweep signal (2–8 kHz), which was recorded by a ministreamer, amplified, correlated, and written on to magnetic tape. The high-resolution multi-channel seismic system consists of a 100 m-long 16-channel streamer, a Mini-GI-Gun (frequency range 80–400 Hz) and a recording unit. Processing included trace editing, binning, velocity analysis, normal move-out corrections, bandpass frequency filtering (frequency content: 55/110–600/800 Hz), stacking and time-migration. A bin spacing of 10 or 15 m was applied throughout.

Guided by the seismic results, 10 different locations in Lake Van with water depths ranging to 420 m (July 24 to August 10, 2004) are selected and cored (Fig. 2.1). The cores were collected using a 60 mm diameter deep-water, percussion-style, piston corer (UWITEC). This operation in water depths around 400 m was a milestone in testing this coring system for very deep lakes, such as Lake Van. Subsequently, a Kullenberg piston corer (63 mm diameter, Kelts et al., 1986) sampled additional sediment along the seismic lines at seven locations. All sampling locations include 1.5 m-long gravity cores that provide undisturbed samples of the uppermost soft and water-rich sediments (see Litt et al., 2009 for details of methods of the site survey).

The processed seismic data were the basis for the ICDP workshop proposal “Lake Van Drilling Project- PaleoVan”, which was submitted in early 2005. The main goal of the proposed project is the detailed interpretation of the acoustic data in order to

locate the best possible locations for potential ICDP-sites and to analyze the evolution of Lake Van. This is the basis for an ICDP-proposal for Lake Van and is independently used for a reconstruction of the tectonic evolution, structure and structural origin of Lake Van. For this study, some special seismic profiles are selected colored in red and blue, showing the most critical structures and related deformations all over the lake (Fig. 2.2). First acoustic data of Lake Van were collected in 1974 during a research cruise aboard the cargo ship Erek. Bathymetric data were collected with a 3.5 kHz echosounder (Wong and Degens, 1978; Degens et al., 1984). Three distinct provinces were detected: a) the lacustrine shelf defined as the portion of the lake extending from the lakeshore to where a sharp break in the bottom slope occurs; b) the sublacustrine slope; and c) the lake basin (Tatvan basin). The maximum measured water depth is 451 m. In addition to the echosounder profile, seismic profiles were collected along seven profiles using a Bolt Airgun (Wong and Finckh, 1978; Degens et al., 1984). These seismic profiles showed that the lake basin is almost completely bounded by faults and it seems to be the result of a continuous, gradual subsidence accompanying faulting. This interpretation is consistent with velocity-depth sections determined by sonobuoy profiles (Wong and Finckh, 1978). The acoustic basement lies at greater depth in the basin. All sonobuoy profiles suggest a thick sequence (up to 600 m) of unconsolidated sediments. The seismic data collected during the 1974 research cruise are only available in analogue form. A major problem during the survey was the navigation accuracy. Navigation was executed exclusively by dead reckoning, visual sighting, and sextant fixes. Navigation accuracy was typically ± 1.5 km, but could be as poor as ± 3 km. In the seismic study of the lake, kinematics of faults and faulting (e.g., sense of shear), tectonics and structural development of the lake have remained unknown.

The new acoustic data at Lake Van is high resolution and multi-channel seismic system used for this survey, consisting of a 100-m-long 16-channel streamer, a Mini-GI-Gun, and a Bison-Recording Unit and the navigation was GPS system. The new seismic net gives a good coverage of most parts of the lake and allows a detailed analysis of the sedimentary and tectonic evolution of Lake Van. Based on the preliminary results of the seismic survey 10 different locations were cored in water depth up to 420 m during an expedition led by T. Litt (July 24th to August 10th 2004). This was performed by using a specially designed aluminum platform.

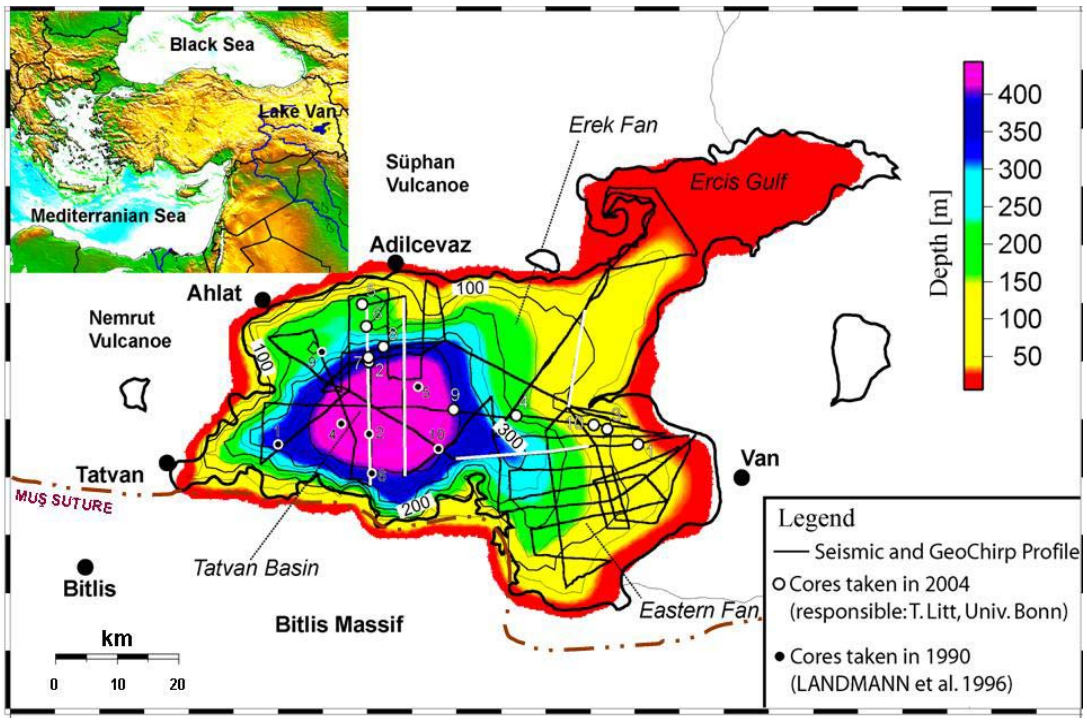

Figure 2.1 : Cruise track lines of the seismic reflection survey and core locations at Lake Van. The black lines show the locations of the new seismic and GeoChirp profiles, superimposed with bathymetry. Note that the locations of cores are taken by studies in 1990 and 2004, the deepest part of the lake is more than 450 m water depth and Muş suture indicates the N-end of Bitlis Massif.

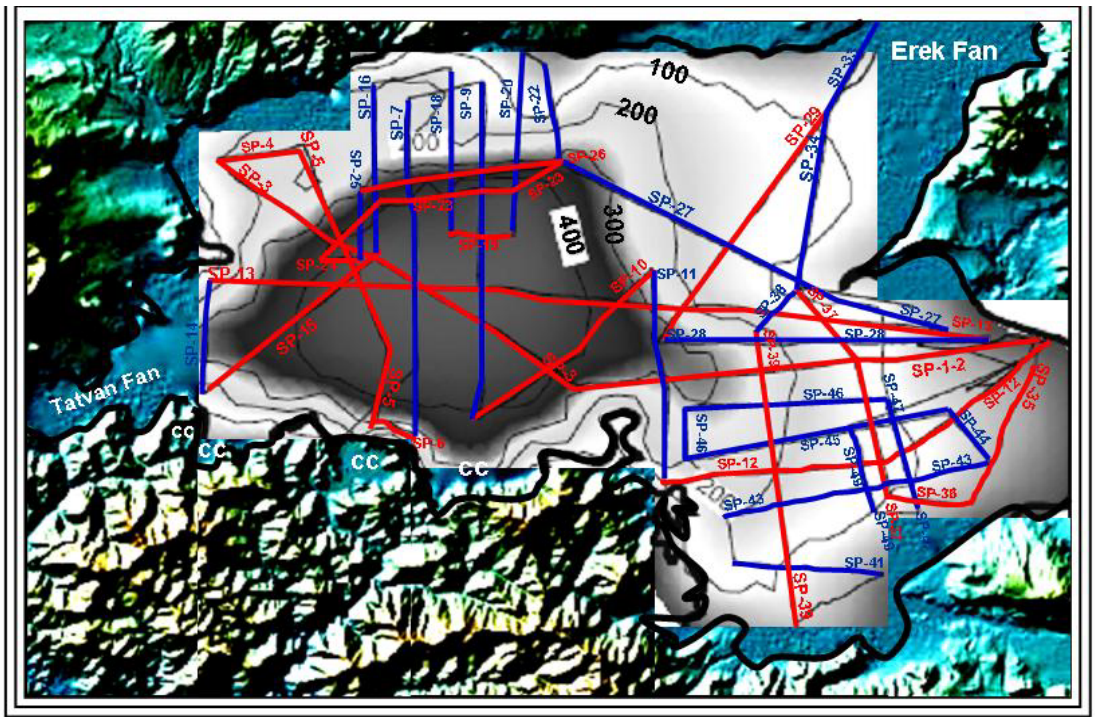

Figure 2.2 : Map shows seismic reflection track lines (red and blue) and seismic profiles selected for this study. Seismic profile numbers (SP) are indicated in the red and blue track lines. 2D map (Fig. 2.1) is combined with digital elevation model (DEM) along the surroundings of the lake and coastlines are redrawn. Collapsed parasitic cones (CC) are also shown in S-coastal sections.

The multi-channel seismic and GeoChirp data were processed. The processing was carried out in the laboratory of the Bremen University and was made with a combination of in-house software of the department and the commercial software package VISTA. A CMP-processing was carried out for all seismic profiles. The processing includes editing of bad traces, set up of geometry, binning, velocity-analysis, NMO-correction, and stacking. For the CMP-stacks, we chose a bin-distance of 15m. After stacking the profiles were filtered and time migrated. These processing steps lead to a significant increase of the lateral resolution and the signal-to-noise ratio in comparison to the brutestacks already produced while being on the lake. The GeoChirp data consisted of segments divided by numerous delay jumps, which make the interpretation difficult. The delay jumps were corrected, and the gain inside each segment was automatically adjusted. This processing allows an overall interpretation of the data and a joint interpretation with the seismic profiles. All processed data (seismic and GeoChirp data) were loaded into the seismic interpretation package 'Kingdom Suite'. This system allows sophisticated visualization of the seismic and GeoChirp data. Thus, the mapping of the fully processed data and seismic interpretation was done.

For seismic structural interpretation, seismic sequence stratigraphy techniques were effectively used and acoustic characteristics of seismic reflection configurations were analysed. During the mapping processes, both digital (Kingdom software) and also classical mapping techniques were used. Hand-made mapping works and digitized data benefited for contouring of structural discontinuities and well controlled bathymetric correlation by digitizing contour lines. Then, all maps with the previous ones were compared. In the first step of the seismic interpretation, the main morphological and physiographic provinces of the lake bottom and mapped morpho-physiography of the lake were identified. NE- and SE-delta system of the lake and mapped sequence stratigraphic boundaries, facies and soft sediment deformation structures were analyzed. Then, the main fault systems at various scales, their kinematic characteristics and deformation style of the lake were determined. At last, the major structural elements, faults, structures, structural deformations and related basin formations from seismic profiles were completed to map. Some structural features identified in the data collected in 1974 (Degens et al., 1984) were re-examined, included and tectonically described in maps.

First results of this survey were presented during the 2005 EGU meeting (Demirel-Shlueter et al., 2005; 2006) and also presented in a wide range of studies. These are documented by Toker et al., (2006) for tectonic and kinematic structure, Krastel et al., (2006) for sedimentary structure, Toker, (2006) for earthquake-related soft sediment deformations, Toker, (2007) for volcano-seismicity analysis by using 3D-seismogram data and Toker et al., (2007; 2009a, b) for volcano-seismogenic analysis and earthquake characteristics of boundary faults.

3. TECTONICS OF LAKE VAN

3.1 Seismic Structural Interpretation of Reflection Data

3.1.1 N-margin

N-S, NW-S, NW-SE and W-E trending seismic sections shown in Figs. 3.1-3.11 morphologically show lacustrine shelf, sublacustrine slope and Tatvan basin in a cross sectional area bounded by Ahlat-Adabağ-Erikbağı spur zones in NNW and southern spur zone, collapsed dome-cone complexes in S and offshore Deveboynu peninsula in SE. These seismic sections connect related faults existing on the parallel and sub-parallel seismic cross sections (Figs. 3.1-3.11). Seismic sections are the longer basinal lines covering central Tatvan basin, shown in Figs. 3.3, 3.5, 3.8 and 3.9. These longer lines are an attempt to provide constraint on the location of deformed sections in N and S.

The morphology of the active faults is well preserved on the lake floor as a deformation zone between Fig. 3.1 and Fig. 3.7. There are several faults in this uplifted zone, formed by the master fault (PDZ) in N (Figs. 3.1-3.7). The fault planes providing the displacement have vertical slope or steeper angles. Indication of the deformation zone and an active oblique fault with reverse displacement bounding the N-edge of the basin is apparent at Figs. 3.1-3.7. This fault at Figs. 3.1-3.7 shows reverse fault activity with strike-slip displacement in the shallow layers of the lakefloor. The secondary deformation becomes more pronounced in this margin. The secondary faults present on Figs. 3.1-3.7 are oblique faults related with the master fault (PDZ). The other oblique faults existing on Figs. 3.1-3.7 are also related with the master fault. These oblique faults with reverse component are interpreted as the W-E continuation of the master fault in the sense of sinistral shear. The faults observed on both sides of the deformation zone in N (Figs. 3.1-3.7) are also products of sinistral shear. These sections shown in Figs. 3.1-3.7 indicate that the sinistral shear in N strongly controls the present-day stratigraphy of Tatvan basin and the sublacustrine basement block and deforms it in a complicated way.

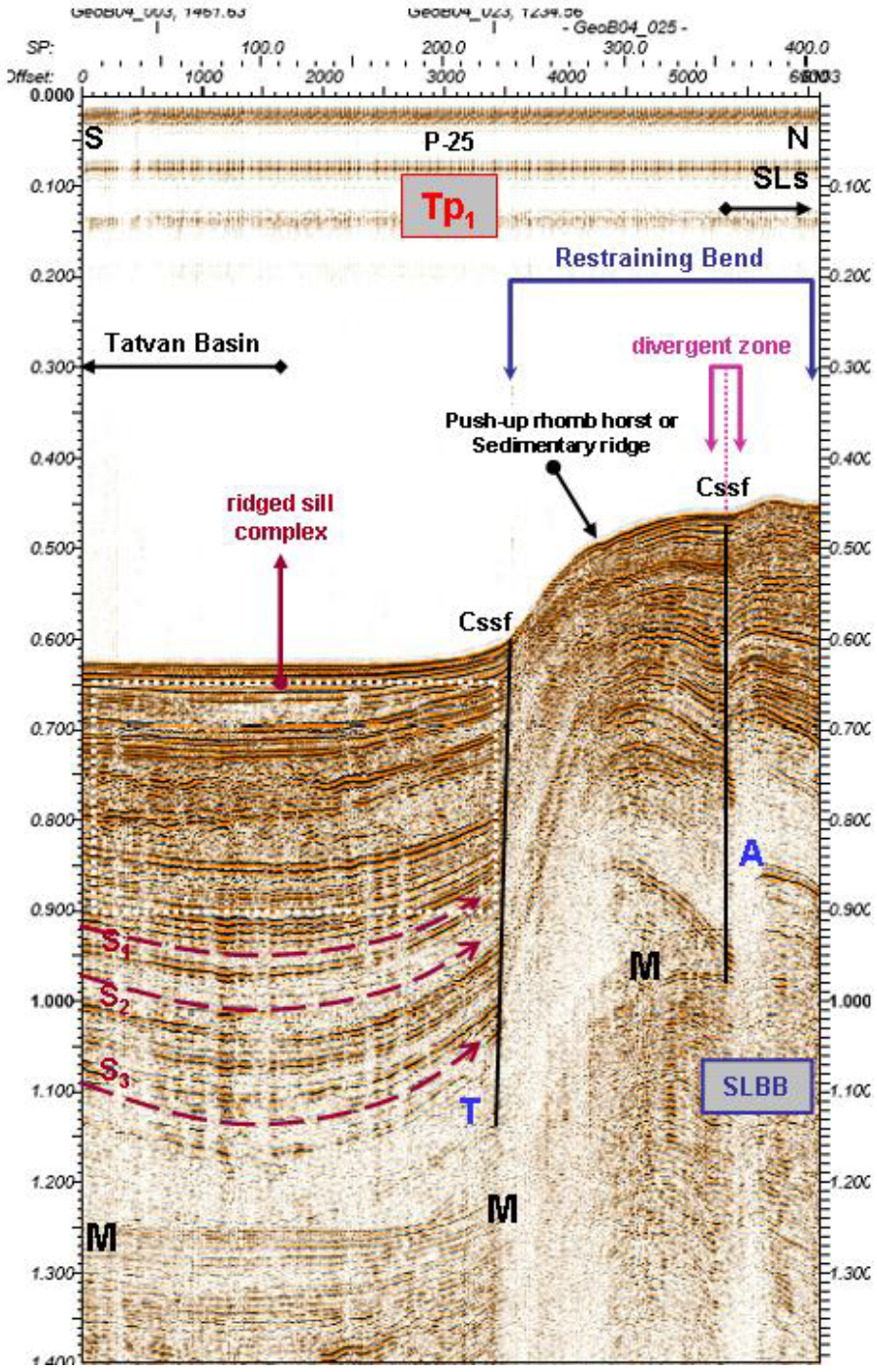

Figure 3.1 : N-S seismic section from N-margin boundary of central Tatvan basin across a zone of restraining bend through sublacustrine slope (SLs) and sublacustrine basement block (SLBB) cut by convergent strike-slip faults (Cssf). Seismic profile number of this section is 25 (P-25), as seen at the top center (see the location of this profile in Fig. 2.2). M: multiple, T: toward, A: away. Tp_1 (transpression-1, red colour) describes the initial evolutional stage of seismic structural interpretation of transpression in N-margin boundary. Note the divergent zone that separates the blocks and forms subbasin in the next stages. Dashed thin arrows (dark red colour) show magma flow paths and directions (S_1, S_2, S_3: sill sequences) from S to N. Dotted thin square (white colour) shows ridged sill complex (max. sediment thickness: 527 m, max. water depth: 473 m, offset: 6 km, two-way travel time in sec).

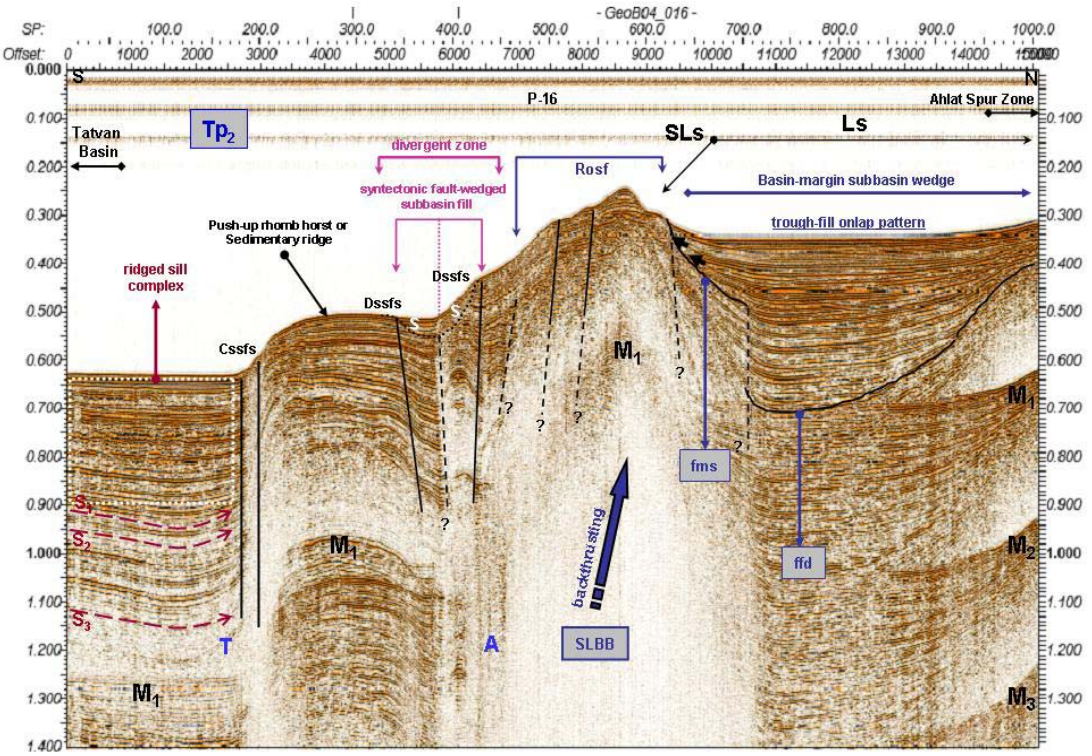

Figure 3.2 : N-S seismic section from N-margin boundary of central Tatvan basin across a zone of convergent-divergent strike-slip faults (Cssfs-Dssfs) through sublacustrine slope (SLs), lacustrine shelf (Ls) and sublacustrine basement block (SLBB) cut by divergent (Dssfs) strike-slip and reverse oblique-slip faults (Rosf). Seismic profile number of this section is 16 (P-16), as seen at the top center (see the location of this profile in Fig. 2.2). M: multiple, T: toward, A: away, fms: fault margin sag, ffd: fault flank depression, S: sagging. Tp_2 (transpression-2, blue colour) describes the second evolutional stage of seismic structural interpretation of transpression in N-margin boundary. Note the divergent zone that separates the blocks and forms subbasin in the stage. Dashed thin arrows (dark red colour) show magma flow paths and directions (S_1, S_2, S_3: sill sequences) from S to N. Dotted thin square (white colour) shows ridged sill complex (max. sediment thickness: 527 m, max. water depth: 473 m, external subbasin is 315 m thick, offset: 15 km, two-way travel time in sec).

Seismic profiles seen in Figs. 3.1-3.7 show W-E progressive development of deformation zone in N-margin across reverse oblique faults and secondary structures. These structures are produced by different combinations of syn- and antithetic accommodation faults. Complex combination of the synthetic and antithetic fault planes are clearly observed in N-end of Tatvan basin near N-margin-side (Figs. 3.2-3.5). In these sections, complex combinations of syn-faults and antithetic accommodation faults, including reverse and normal oblique faults, occur with sets of strike-slip faults of deformation. Sublaccustrine slope and lacustrine shelf seem to be a faulted crestal terrace with a number of reverse oblique faults (Figs. 3.2-3.7). Convergent strike-slip faults control fault-wedged sedimentary high or ridge,

appearing as a horst (Figs. 3.1-3.5). Divergent strike-slip faults control fault-wedged sedimentary trough, appearing as a graben or horst-foot graben (Figs. 3.2-3.5).

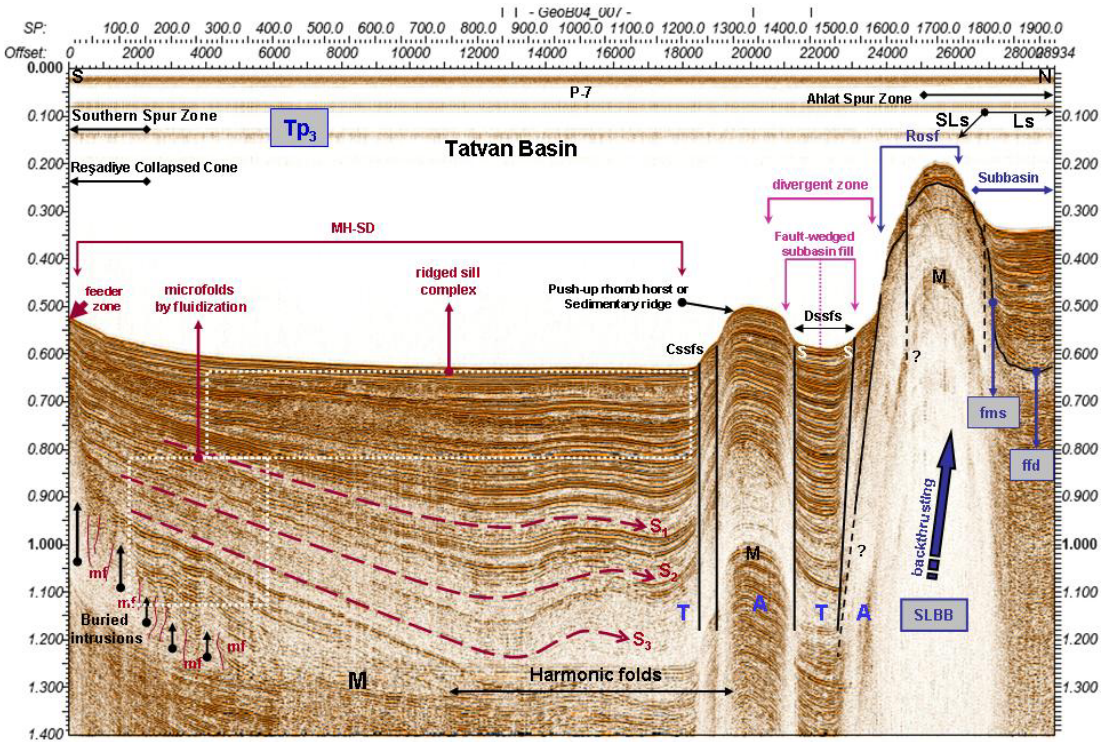

Figure 3.3 : N-S seismic section from N-margin boundary of central Tatvan basin across a zone of convergent-divergent strike-slip faults (Cssfs-Dssfs) through sublacustrine slope (SLs), lacustrine shelf (Ls) and sublacustrine basement block (SLBB) cut by divergent (Dssfs) strike-slip and reverse oblique-slip faults (Rosf). Seismic profile number of this section is 7 (P-7), as seen at the top center (see the location of this profile in Fig. 2.2). M: multiple, T: toward, A: away, fms: fault margin sag, ffd: fault flank depression, S: sagging, mf: microfaults-fractures. Tp_3 (transpression-3, blue colour) describes the third evolutional stage of seismic structural interpretation of transpression in N-margin boundary. Note that the divergent zone forms internal subbasin in the stage. Dashed thin arrows (dark red colour) show magma flow paths and directions (S_1, S_2, S_3: sill sequences) from S to N. Dotted thin squares (white colour) show seismic structural patterns of magma hydrothermal-sediment deformations (MH-SD), (max. sediment thickness: 575 m and min. thick. is 328 m, max. water depth: 443 m, external subbasin is 250 m thick, offset: 29 km, two-way travel time in sec).

A single fault is considered as master fault, composed of numerous parallel to sub-parallel and discontinuous fault segments (Figs. 3.1-3.7). The morphological and structural arrangement of these fault segments show a typical strike-slip fault control with reverse component and stepped-like morphology indicating the oblique nature of the faults shown in Figs. 3.1-3.7. W-E continuation of this fault zone is considered as a principal displacement zone (PDZ) crossing the N-edge of Tatvan basin (see also Fig. 3.7). This represents N-margin boundary fault of Lake Van basin. Figs. 3.1-3.7

show that lacustrine shelf, sublacustrine slope and its basement block are an active tectonic zone, characterized by the sinistral oblique-slip regime with reverse component of the master fault in N. This master fault is the main structural element controlling the morphological and structural features in the area. A single trough-going master fault and several secondary faults parallel to the single fault are well traced in N-margin. It passes through the sublacustrine slope and basement block and enters the NW-end of Erek delta (Fig. 3.7). This fault terminates against NE-Erek delta, but probably continues to the further ENE (Fig. 3.12).

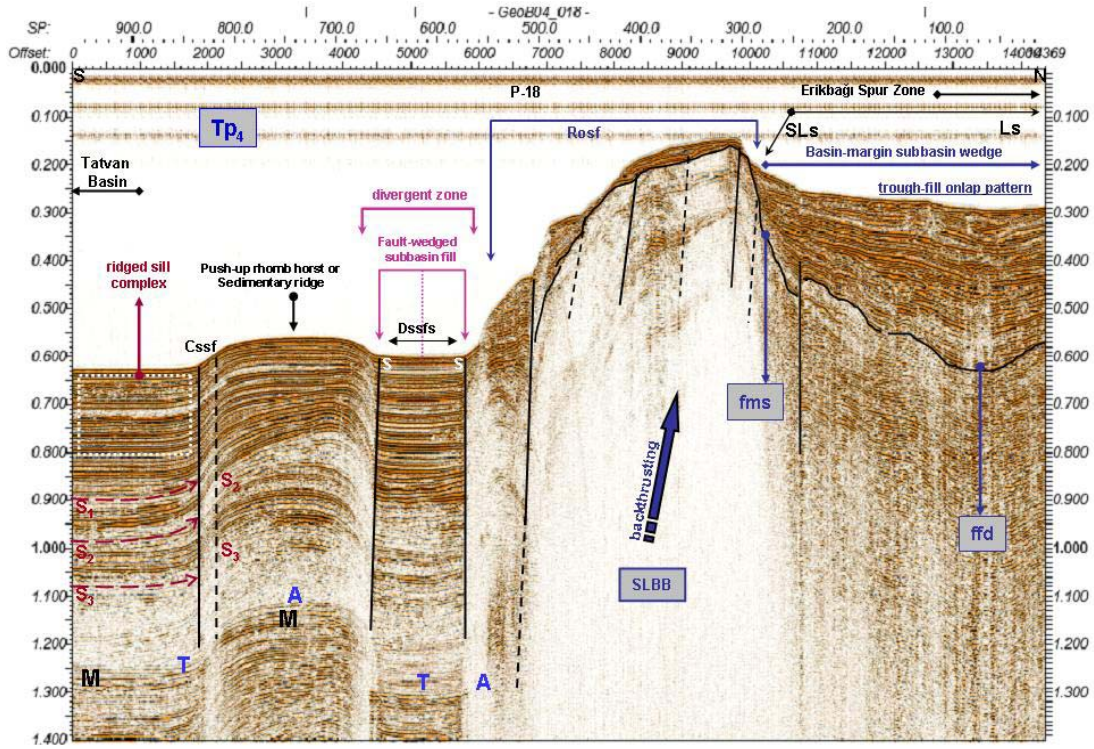

Figure 3.4 : N-S seismic section from N-margin boundary of central Tatvan basin across a zone of convergent-divergent strike-slip faults (Cssfs-Dssfs) through sublacustrine slope (SLs), lacustrine shelf (Ls) and sublacustrine basement block (SLBB) cut by divergent (Dssfs) strike-slip and reverse oblique-slip faults (Rosf). Seismic profile number of this section is 18 (P-18), as seen at the top center (see the location of this profile in Fig. 2.2). M: multiple, T: toward, A: away, fms: fault margin sag, ffd: fault flank depression, S: sagging. Tp_4 (transpression-4, blue colour) describes the fourth evolutional stage of seismic structural interpretation of transpression in N-margin boundary. Note that the divergent zone forms internal subbasin in the stage. Dashed thin arrows (dark red colour) show magma flow paths and directions (S_1, S_2, S_3: sill sequences) from S to N. Dotted thin square (white colour) shows ridged sill complex, (max. sediment thickness: 531 m, max. water depth: 469 m, external subbasin is 280 m thick, offset: 14.5 km, two-way travel time in sec).

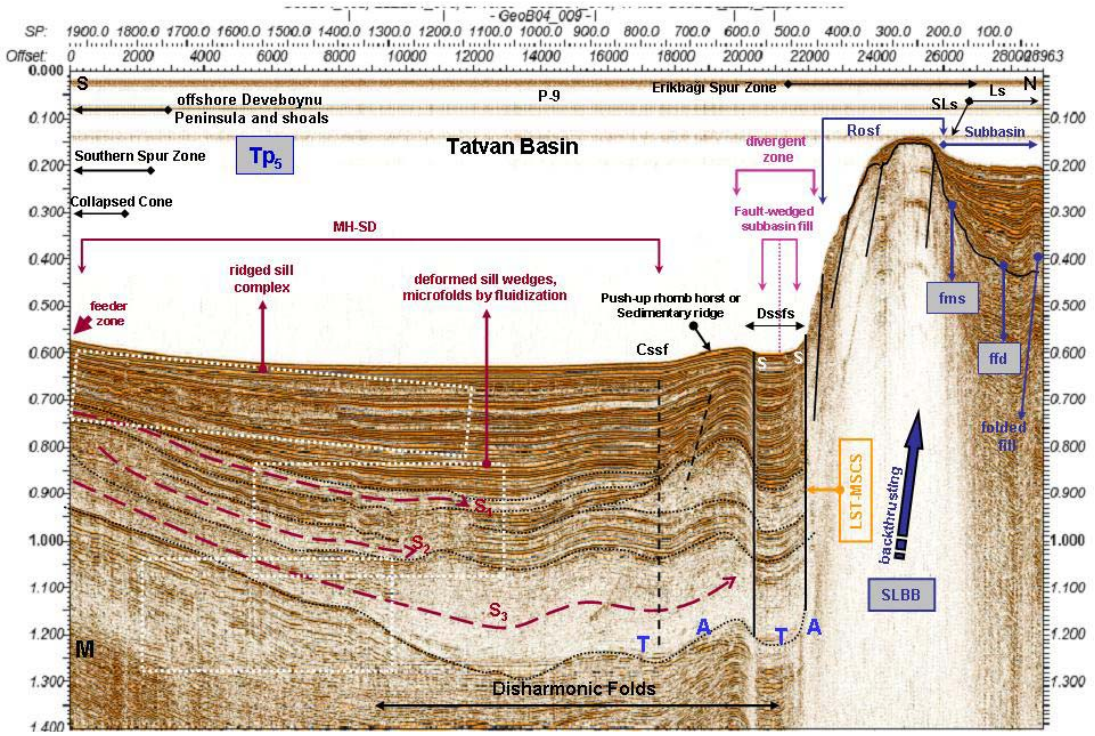

Figure 3.5 : N-S seismic section from N-margin boundary of central Tatvan basin across a zone of convergent-divergent strike-slip faults (Cssfs-Dssfs) through sublacustrine slope (SLs), lacustrine shelf (Ls) and sublacustrine basement block (SLBB) cut by divergent (Dssfs) strike-slip and reverse oblique-slip faults (Rosf). Seismic profile number of this section is 9 (P-9), as seen at the top center (see the location of this profile in Fig. 2.2). M: multiple, T: toward, A: away, LST-MSCS: lowstand system tract-multiple slumping of clinoform successions, fms: fault margin sag, ffd: fault flank depression, S: sagging. Tp_5 (transpression-5, blue colour) describes the fifth evolutional stage of seismic structural interpretation of transpression in N-margin boundary. Note that the divergent zone forms internal subbasin in the stage. Dashed thin arrows (dark red colour) show magma flow paths and directions (S_1, S_2, S_3: sill sequences) from S to N. Dotted thin squares (white colour) show seismic structural patterns of magma hydrothermal-sediment deformations (MH-SD), (max. sediment thickness: 544 m and min. thick: 332 m, max. water depth: 458 m, external subbasin is 196 m thick, offset: 29 km, two-way travel time in sec).

Although the seismic data are generally of good quality resulting in clear images of faults cutting recent lake floor sediments, at some sites the quality deteriorated due to interference from strong multiple reflections (Figs. 3.1-3.10). These strong multiples suggest a large impedance contrast between the water and lakefloor, indicating that the sublacustrine basement block in N-margin is made of older, more strong basement rocks. This result implies the pre-existing thrust block nature of N-margin. The uplifted deformation zone of N-margin, controlled by sinistral reverse oblique-slip faults, shows a geometry similar to a positive flower structure, as is clear from the interpretation of the seismic profiles (Figs. 3.1-3.7). The master fault and secondary faults observed in N-margin are part of this geometry. These faults have

vertical slope angles and are the determinative structural elements which form N-margin in its present shape (Figs. 3.1-3.7). The fault geometry is supported by the antithetic and synthetic faults, depending on the displacement of the master fault.

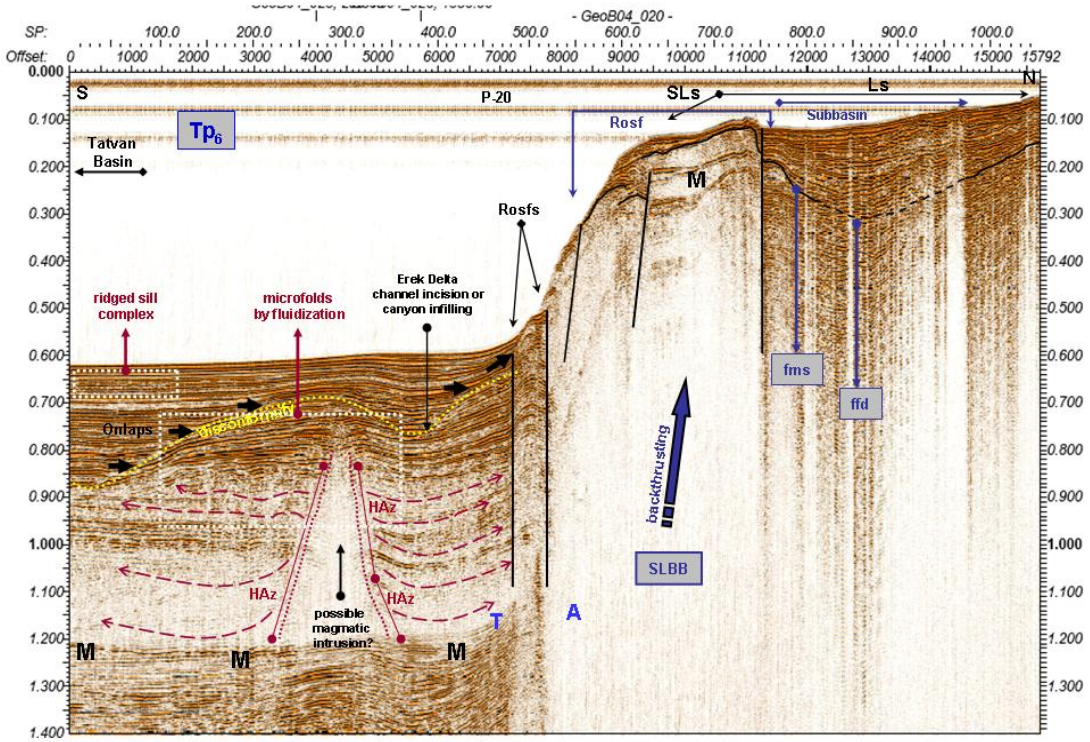

Figure 3.6 : N-S seismic section from N-margin boundary of central Tatvan basin across a zone of reverse oblique-slip faults (Rosfs) through sublacustrine slope (SLs), lacustrine shelf (Ls) and sublacustrine basement block (SLBB) cut by reverse oblique-slip faults (Rosf). Seismic profile number of this section is 20 (P-20), as seen at the top center (see the location of this profile in Fig. 2.2). M: multiple, T: toward, A: away, HAz: hydrothermal alteration zones, fms: fault margin sag, ffd: fault flank depression. Tp_6 (transpression-6, blue colour) describes the sixth evolutional stage of seismic structural interpretation of transpression in N-margin boundary. Note that possible magma intrusion produces localized sills along HAz (dashed thin arrows in dark red colour). Dotted thin squares (white colour) show ridge sill complex and microfolds by fluidization (onlap thickness: 221 m, max. water depth: 465 m, external subbasin is 153 m thick, offset: 16 km, two-way travel time in sec).

3.1.2 W-margin

The W-continuation of the oblique fault in N-margin sharply bends towards WSW and connects the other fault and deformation zone in W-boundary of Tatvan basin (Fig. 3.1). The small area shown in Fig. 3.1 at NNW-corner of Tatvan basin seems to be a restraining bend, representing a structural boundary between deformation zones in N- and W-margins of Tatvan basin.

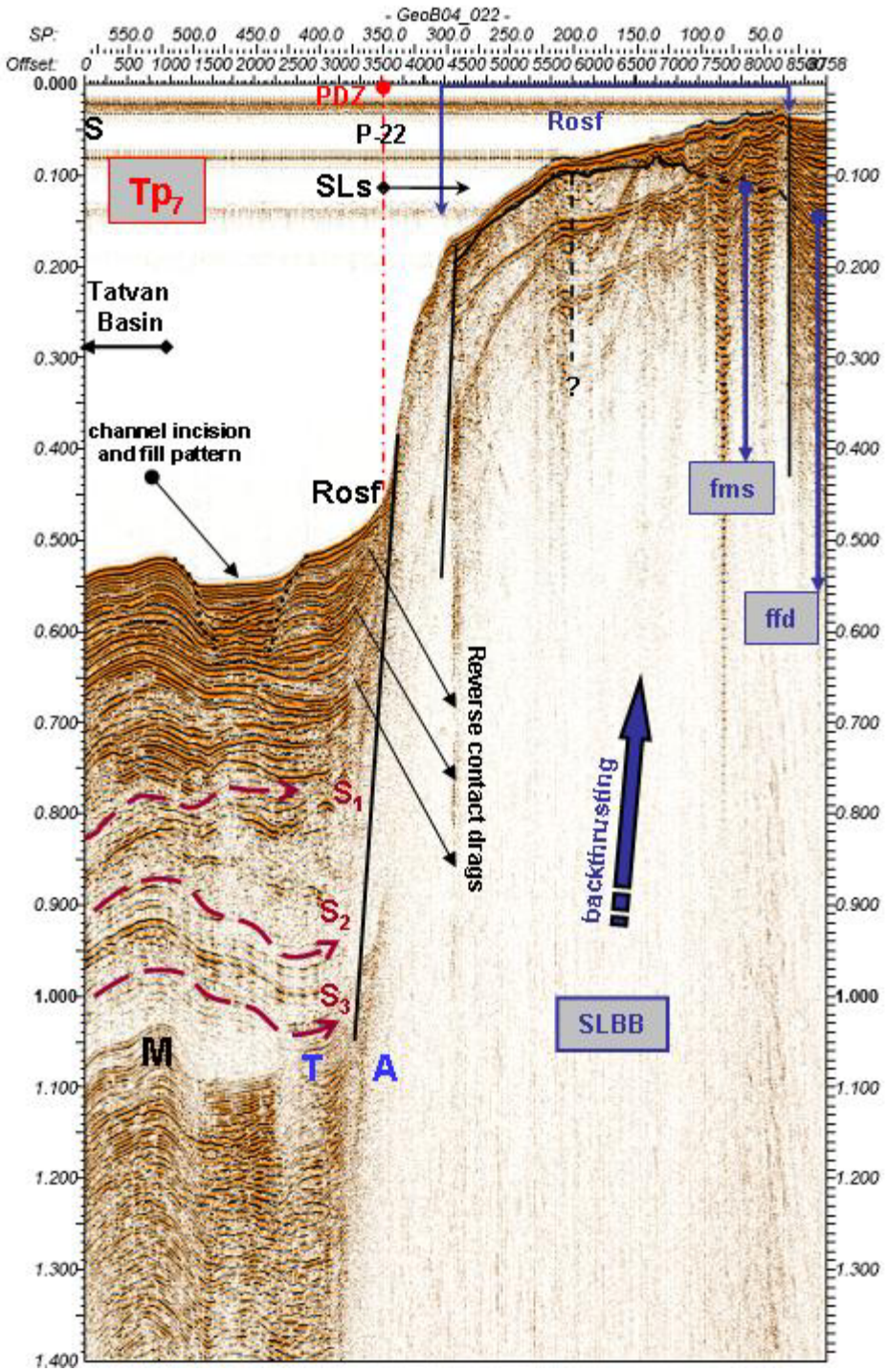

Figure 3.7 : N-S seismic section from N-margin boundary of central Tatvan basin across a zone of reverse oblique-slip faults (Rosf) through sublacustrine slope (SLs), lacustrine shelf (Ls) and sublacustrine basement block (SLBB) cut by reverse oblique-slip faults (Rosf). Seismic profile number of this section is 22 (P-22), as seen at the top center (see the location of this profile in Fig. 2.2). M: multiple, T: toward, A: away, fms: fault margin sag, ffd: fault flank depression. Tp_7 (transpression-7, red colour) describes the seventh evolutional stage of seismic structural interpretation of transpression in N-margin boundary. Note that principle displacement zone (PDZ) is reverse oblique-slip fault (Rosf). Dashed thin arrows (dark red colour) show magma flow paths and directions (S_1, S_2, S_3: sill sequences) from S to N (max. water depth: 405 m, external subbasin: 110 m thick, offset: 8.75 km, two-way travel time in sec).

There are several faults in this uplifted zone shown in Figs. 3.8-3.11, formed by the master fault (PDZ) in W-margin. Indication of an active oblique fault with normal displacement bounding W-edge of Tatvan basin is apparent at Figs. 3.8-3.11. The fault planes providing the displacement have vertical slope or steeper angles. Normal displacement of this oblique fault gradually increases in W-E seismic sections (Figs. 3.10 and 3.11). The active oblique faults with reverse displacement observed on Figs. 3.8 and 3.9 are also evident on Fig. 3.10. The fault shown at Figs. 3.8-3.11 shows normal fault activity with strike-slip displacement in the Tatvan basin. The secondary deformation also becomes more pronounced in this margin. The faults observed between Fig. 3.8 and 3.10 are oblique faults related with the master fault. These oblique faults with reverse component are interpreted as the continuation of the master fault in N-margin and they seem to be an important part of deformation zone in N-margin. The fault and deformation zone seen in Figs. 3.8-3.11 is considered as the SW-NE continuation of the master fault in this margin. The sinistral shear in W-margin also controls the present-day stratigraphy of Tatvan basin and the sublacustrine basement block and deforms it in a complicated way (Figs. 3.8-3.11). The oblique faults observed on both sides of the deformation zone are also products of sinistral shear.

Lacustrine shelf, sublacustrine slope and its basement block is also an active tectonic zone in W-margin, characterized by the sinistral oblique-slip regime with normal component of the master fault in W (Figs. 3.8-3.11). As recognized in N-margin seen in Figs. 3.1-3.7, this master fault is the main structural element controlling the morphological and structural features in W-margin. In this margin, a single fault is considered as master fault, composed of numerous parallel to sub-parallel and discontinuous fault segments (Figs. 3.8-3.11). A single trough-going master fault and several secondary faults parallel to the single fault are well traced toward NNW-corner of Tatvan basin (Figs. 3.8 and 3.9). The master fault passes through the sublacustrine slope and basement block and enters the N-margin boundary. The SW-NE continuation of the fault zone in W-margin is considered as a principal displacement zone (PDZ) crossing the W-edge of Tatvan basin, representing W-margin boundary fault of Lake Van basin.

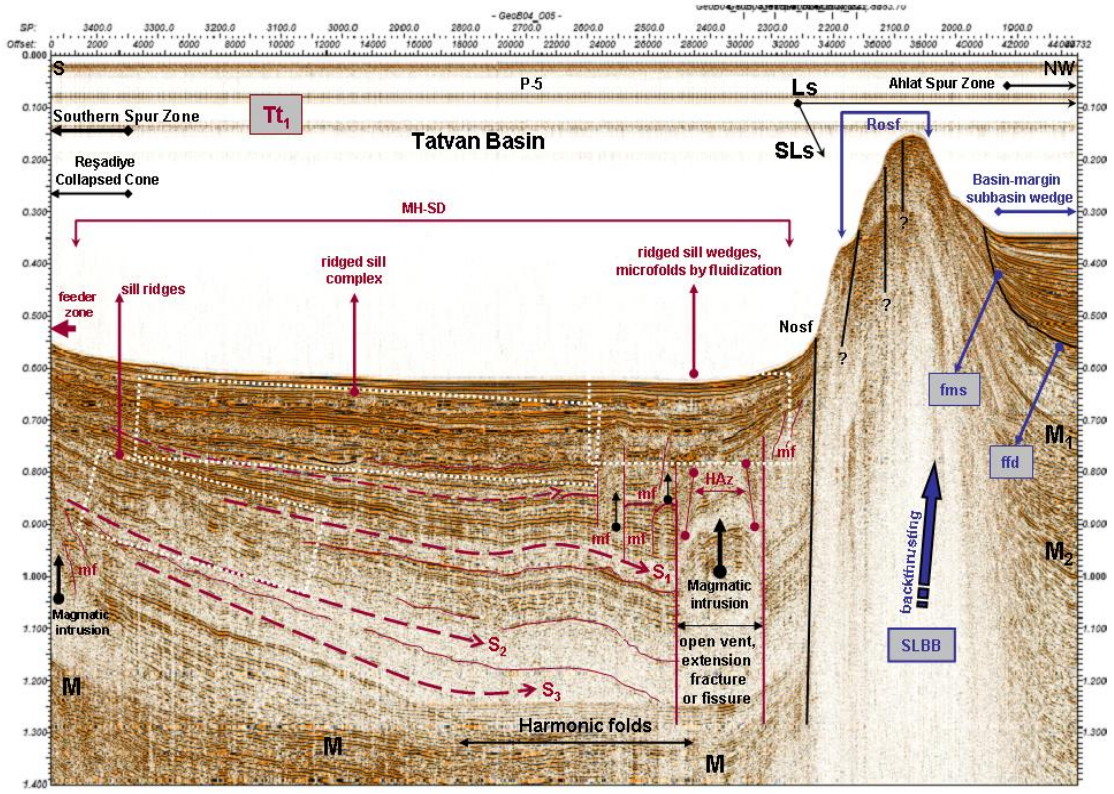

Figure 3.8 : NW-S seismic section from W-margin boundary of central Tatvan basin across a zone of normal oblique-slip fault (Nosf) through sublacustrine slope (SLs), lacustrine shelf (Ls) and sublacustrine basement block (SLBB) cut by reverse oblique-slip faults (Rosf). Seismic profile number of this section is 5 (P-5), as seen at the top center (see the location of this profile in Fig. 2.2). M: multiple, fms: fault margin sag, ffd: fault flank depression, mf: microfaults-fractures, HAz: hydrothermal alteration zones. Tt_1 (transtension-1, brown colour) describes the initial evolutional stage of seismic structural interpretation of transtension in W-margin boundary. Note that magma intrudes through thick sedimentary section from an opening vent, point source, or extension space and that tilted sedimentary section, intrusive activity and feeder zone indicate a normal oblique-slip fault (W-segment of S-margin boundary fault) in the S-end of this section. Dashed thin arrows (dark red colour) show magma flow paths and directions (S_1, S_2, S_3: sill sequences) from S to NW. Dotted thin squares (white colour) show seismic structural patterns of magma hydrothermal-sediment deformations (MH-SD), (max. sediment thickness: 557 m and min. thick: 366 m, max. water depth: 450 m, external subbasin is 175 m thick, offset: 45 km, two-way travel time in sec).

The morphological and structural arrangement of the master faults and secondary fault segments in N- and W-margins show a typical strike-slip fault control with reverse and normal components and stepped-like morphology indicating the oblique nature of the faults shown in Figs. 3.1-3.11. It is interesting to note that oblique-slip faults with reverse and normal components in N- and W-margins have the restraining-releasing bend relationships in NNW-corner of Tatvan basin (Fig. 3.1, 3.8 and 3.9). This implies sublacustrine basement block is a backthrusted feature by

these oblique-slip faults (Figs. 3.2-3.10). Backthrusting in N- and W-margins probably results in extensional half-graben geometry and syn-tectonic sedimentation in Tatvan basin (Figs. 3.3, 3.5, 3.8-3.10). This is very clear as recognized in seismic sections in W-margin boundary (Figs. 3.8-3.10). These seismic sections well express the intrusive-extrusive activity through the fault planes and vent-fissure structures (Figs. 3.8-3.10).

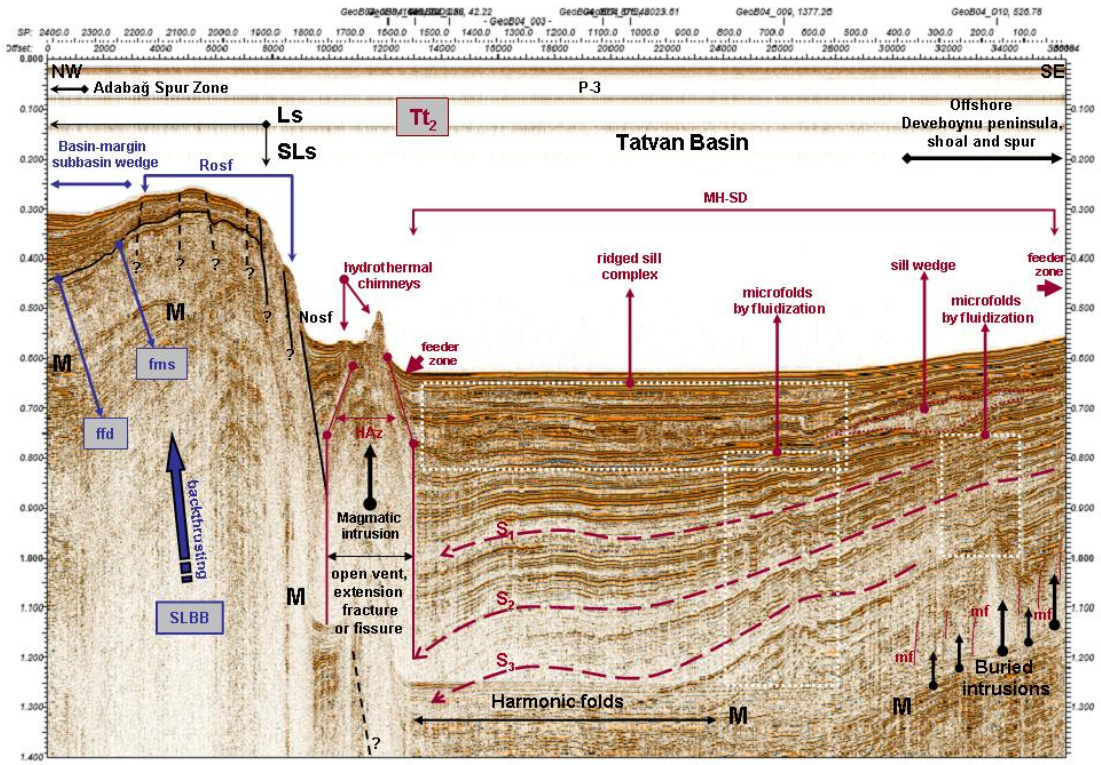

Figure 3.9 : NW-SE seismic section from W-margin boundary of central Tatvan basin across a zone of normal oblique-slip fault (Nosf) through sublacustrine slope (SLs), lacustrine shelf (Ls) and sublacustrine basement block (SLBB) cut by reverse oblique-slip faults (Rosf). Seismic profile number of this section is 3 (P-3), as seen at the top center (see the location of this profile in Fig. 2.2). M: multiple, fms: fault margin sag, ffd: fault flank depression, mf: microfaults-fractures, HAz: hydrothermal alteration zones. Tt_2 (transtension-2, brown colour) describes the second evolutional stage of seismic structural interpretation of transtension in W-margin boundary. Note that magma intrudes through thick sedimentary section from an opening vent, point source, or extension space and that tilted sedimentary section, intrusive activity and feeder zone indicate a normal oblique-slip fault (W-segment of S-margin boundary fault) in the SE-end of this section. Dashed thin arrows (dark red colour) show magma flow paths and directions (S_1, S_2, S_3: sill sequences) from SE to NW. Dotted thin squares (white colour) show seismic structural patterns of magma hydrothermal-sediment deformations (MH-SD), (max. sediment thickness: 550 m and min. thick: 340 m, max. water depth: 465 m, external subbasin is 111 m thick, offset: 36 km, two-way travel time in sec).

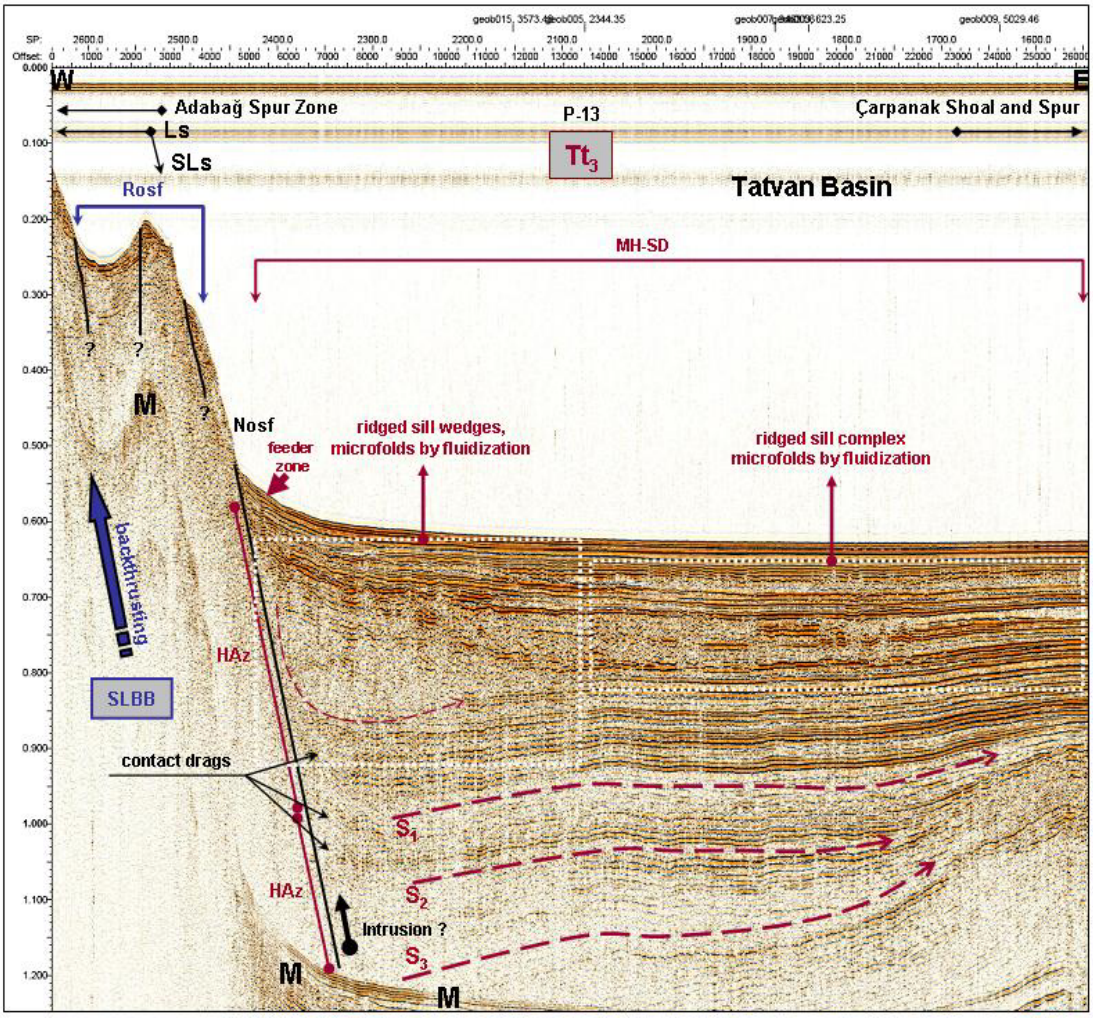

Figure 3.10 : W-E seismic section from W-margin boundary of central Tatvan basin across a zone of normal oblique-slip fault (Nosf) through sublacustrine slope (SLs), lacustrine shelf (Ls) and sublacustrine basement block (SLBB) cut by reverse oblique-slip faults (Rosf). Seismic profile number of this section is 13 (P-13), as seen at the top center (see the location of this profile in Fig. 2.2). This profile is a W-portion of P-13. M: multiple, HAz: hydrothermal alteration zones. Tt_3 (transtension-3, brown colour) describes the third evolutional stage of seismic structural interpretation of transtension in W-margin boundary. Note that possible magma intrudes through the fault plane from an opening vent, point source, or extension space. Dashed thin arrows (dark red colour) show magma flow paths and directions (S_1, S_2, S_3: sill sequences) from W to E. Dotted thin squares (white colour) show seismic structural patterns of magma hydrothermal-sediment deformations (MH-SD), (offset: 26.5 km, two-way travel time in sec).

Sublacustrine basement block uplift is response to downfaulting of the Tatvan basin (Figs. 3.2-3.11). This block uplift produces a steeper bathymetric high leading to reduced sedimentation. An erosional unconformity and related subbasin structure develop over this block (Figs. 3.2-3.9), since the block uplift is sufficient to raise the upthrown block above storm-wave base. The subbasin structure well characterizes

trough-filling onlap pattern with the basal onlap and horizontal continuous toplap relations (Figs. 3.2-3.9). This subbasin is a basin-margin sedimentary wedge, forming a gentle synclinal trough subsiding as sediment accumulates. The horizontal upper surface of the topmost layer indicates that subsidence ceased. The subbasin fill is 250-320 m max. thickness in W- and 100-200 m max. thickness in E-parts of N-margin and gradually thinning to the further E (Fig. 3.7). Thickness in the subbasin fill also ranges from 111 to 175 m in W-margin and terminates against the further SW (Fig. 3.10 and 3.11). This shows that the subbasin fill is a localized depositional feature emplaced at sublacustrine slope and lacustrine shelf. The subbasin development is controlled by a complex oblique fault zone with repeated movements as shown in seismic sections (Figs. 3.2-3.9). Thus, the syn-fault sedimentation occurs over the subbasin, depositing more than 200 m thick. The corresponding subbasin interval on the block is represented by an erosional surface extending into the lacustrine shelf towards an area of spur zones. The erosion indicated by the unconformity is interpreted to have been the result of the block uplift during syn-fault sedimentation.

It is important to note that the role of sublacustine basement block uplift has an structural significance in a review of the geometrical evolution of extensional normal faults with strike-slip component along W- and N-margins. Especially, initial structural control of N-margin is interpreted to have been an extension with strike component during the block uplift and recently an compression with strike component. This hybrid structural control observed in seismic sections from N-margin (particularly in Figs. 3.3 and 3.5) is well recognized in downfaulting of Tatvan basin associated to fold, horst-graben structures and reverse oblique-slip motions (Figs. 3.2-3.7). Moreover, seismic sections in N- and W-margins show an example of strike-slip faults with reverse and normal component associated with a major tilted block in Tatvan basin (Figs. 3.3, 3.5 and 3.8-3.11). These seismic sections well show the deformational relations of the oblique-slip faults with secondary faults in N- and W-margins and reverse and normal patterns of fault-controlled sediments, indicating that marginal fault activity is extremely polyhistoric.

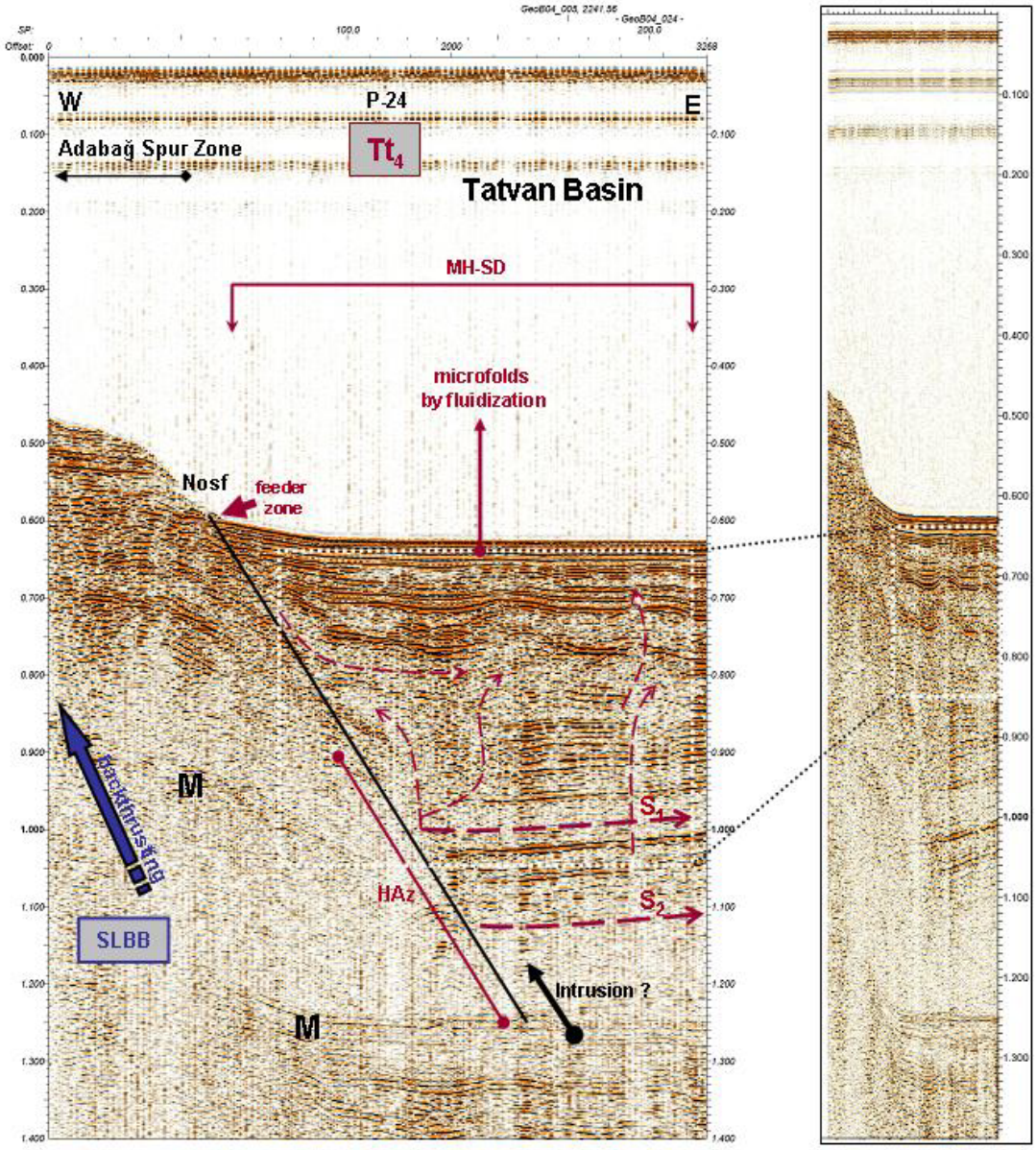

Figure 3.11 : W-E seismic section from W-margin boundary of central Tatvan basin across a zone of normal oblique-slip fault (Nosf) through sublacustrine basement block (SLBB) cut by normal oblique-slip fault (Nosf). Seismic profile number of this section is 24 (P-24), as seen at the top center (see the location of this profile in Fig. 2.2). M: multiple, HAz: hydrothermal alteration zones. Tt_4 (transtension-4, brown colour) describes the fourth evolutional stage of seismic structural interpretation of transtension in W-margin boundary. Note that possible magma intrudes through the fault plane from an opening vent, point source, or extension space and that dashed thinner arrows (vertical-curved lines in dark red colour) indicate deformation patterns of hydrothermal fluids or volatiles. Seismic section at the right is vertically exaggerated section of this profile, indicating a tilted sedimentary block. Dashed thin arrows (dark red colour) show magma flow paths and directions (S_1, S_2,: sill sequences, S_3 is absent due to multiple) from W to E. Dotted thin squares (white colour) show seismic structural patterns of magma hydrothermal-sediment deformations (MH-SD), (max. sediment thickness: 523 m, max. water depth: 465 m, offset: 3.27 km, two-way travel time in sec).

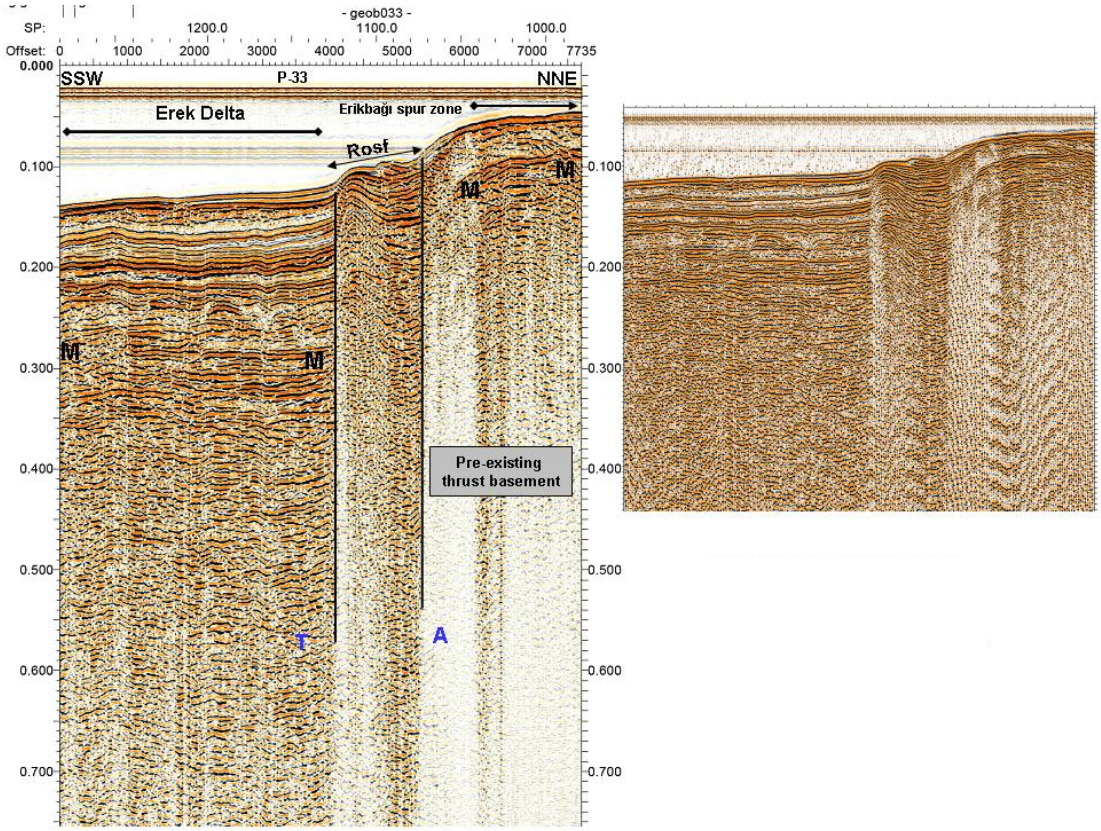

Figure 3.12 : SSW-NNE seismic section from NE-Erek delta setting across a zone of reverse oblique-slip faults (Rosf) through pre-existing thrust basement cut by reverse oblique-slip faults (Rosf) in Erek delta. Seismic profile number of this section is 33 (P-33), as seen at the top center (see the location of this profile in Fig. 2.2). M: multiple, T: toward, A: away. This reverse oblique-slip fault (Rosf) is a structural continuation of Tp_7 (transpression-7 seen in Fig. 3.7) from N-margin boundary of central Tatvan basin across NE-Erek delta, indicating transpression in N-end of Erek delta. Seismic section at the right is less exaggerated section of this profile, clearly indicating uplifted basement structure of Erek delta (max. water depth: 105 m, max. sediment. thick: 111 m, offset: 7.7 km, two-way travel time in sec).

3.1.3 W-portion of S-margin

There seems to be an important deformation zone located in S-edge of Tatvan basin, only partly shown in S and SE-ends of the longer seismic sections at Figs. 3.3, 3.5, 3.8, and 3.9. These sections show that this deformation zone is apparently fault-related, affecting the entire sediment column, since the thickness of sediments changes in the fault-related zone. In Figs. 3.3, 3.5, 3.8, and 3.9, the thick sedimentary section ranges from 520 m to 580 m in N-margin, gradually thins toward S-margin and reaches the values ranging from 320 m to 370 m. This asymmetric depositional control indicates tilted block geometry of Tatvan basin, suggesting an structural active zone in S- and SE-ends of the profiles shown in Figs. 3.3, 3.5, 3.8, and 3.9. This is also well evident by strong intrusive and extrusive activity of magma-related

products in S-margin (also see S- and SE-ends of seismic sections in Figs. 3.3, 3.5, 3.8, and 3.9). This activity is easily traced through S- and SE-ends of the longer seismic profiles into the deeper parts of Tatvan basin. These seismic sections also show extensional fault-controlled block geometry of Tatvan basin and is considered as asymmetric half-graben depositional center.

Active structural control in S-margin may also indicate why the shelf and slope are not developed in this area. However, the faulting and intrusive-extrusive activity in S-margin do not seem to be controlled directly by a master fault in this area. The evidence comes from N-S, SW-NE and W-E trending seismic sections seen in Figs. 3.13-3.15. These sections show that the faulting in S-margin has a structural complexity and the deformation recognized is caused by the secondary or segmentary fault being the en echelon extension of the master fault (PDZ) in S (Figs. 3.13 and 3.14). The faulting may terminate against Deveboynu peninsula (Figs. 3.5 and 3.9) and thus, deforms only the S-edge of central Tatvan basin. Seismic sections seen in Figs. 3.13 and 3.14 show fault-controlled intrusive-extrusive activity in a cross sectional area bounded by Adabağ-Southern spur zones and collapsed dome-cone complexes in S. The intrusive activity in Fig. 3.15 is also the fault-related product.

Seismic sections show that the deformation zone in S-margin seems to be controlled by secondary oblique faults with normal component (Figs. 3.13 and 3.14). These normal oblique faults are interpreted as the continuation of the master fault in this margin. W-E continuation of this fault zone in S-margin is considered as a principal displacement zone (PDZ) crossing the S-part of Tatvan basin (Figs. 3.13 and 3.14). A combined interpretation of seismic sections shown in Figs. 3.3, 3.8, 3.9 and 3.13-3.15 indicate that a single fault is considered as master fault, composed of numerous parallel to sub-parallel and discontinuous smaller fault segments, through which the intrusive-extrusive activity is the prominent. The one of these segments represents W-segment of S-margin boundary fault (PDZ). The W-segment is highly characterized by not only the intrusive-extrusive activity in Tatvan basin, by but also collapsed dome-cone complexes in southern spur zone (well seen in Figs. 3.13-3.15).

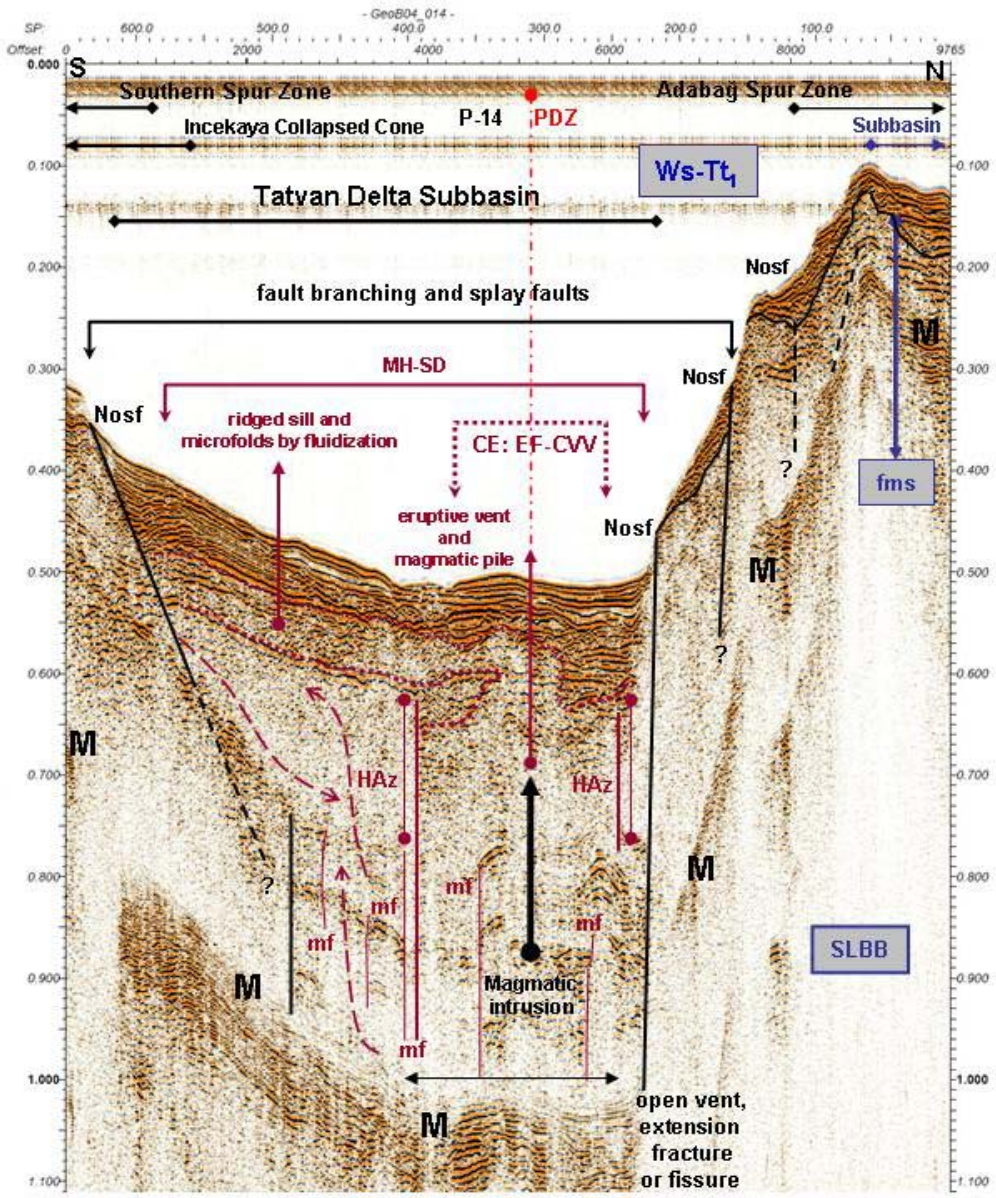

Figure 3.13 : N-S seismic section from S-margin boundary of central Tatvan basin across a zone of normal oblique-slip faults (Nosfs) through Tatvan delta and sublacustrine basement block (SLBB) cut by normal oblique-slip faults (Nosf). Seismic profile number of this section is 14 (P-14), as seen at the top center (see the location of this profile in Fig. 2.2). M: multiple, fms: fault margin sag, mf: microfaults-fractures, HAz: hydrothermal alteration zones, CE: cryptoexplosion, EF-CVV: explosive fissure-central vent volcano. Ws-Tt_1 (W-segment-transtension-1, blue colour) describes the initial evolutional stage of seismic structural interpretation of transtension in S-margin boundary and Tatvan delta internal subbasin. Note that magma intrudes through thin sedimentary section from an opening vent, point source, or extension space, experiencing brecciation of the crystalline rind (cryptoexplosive breccia type). This section shows seismic structural patterns of magma hydrothermal-sediment deformations (MH-SD) and dashed thinner arrows (vertical-curved lines in dark red colour) indicate deformation patterns of hydrothermal fluids or volatiles (max. sediment thickness: 100-150 m, max. water depth: 370 m, external subbasin is 51 m thick, offset: 9.7 km, two-way travel time in sec).

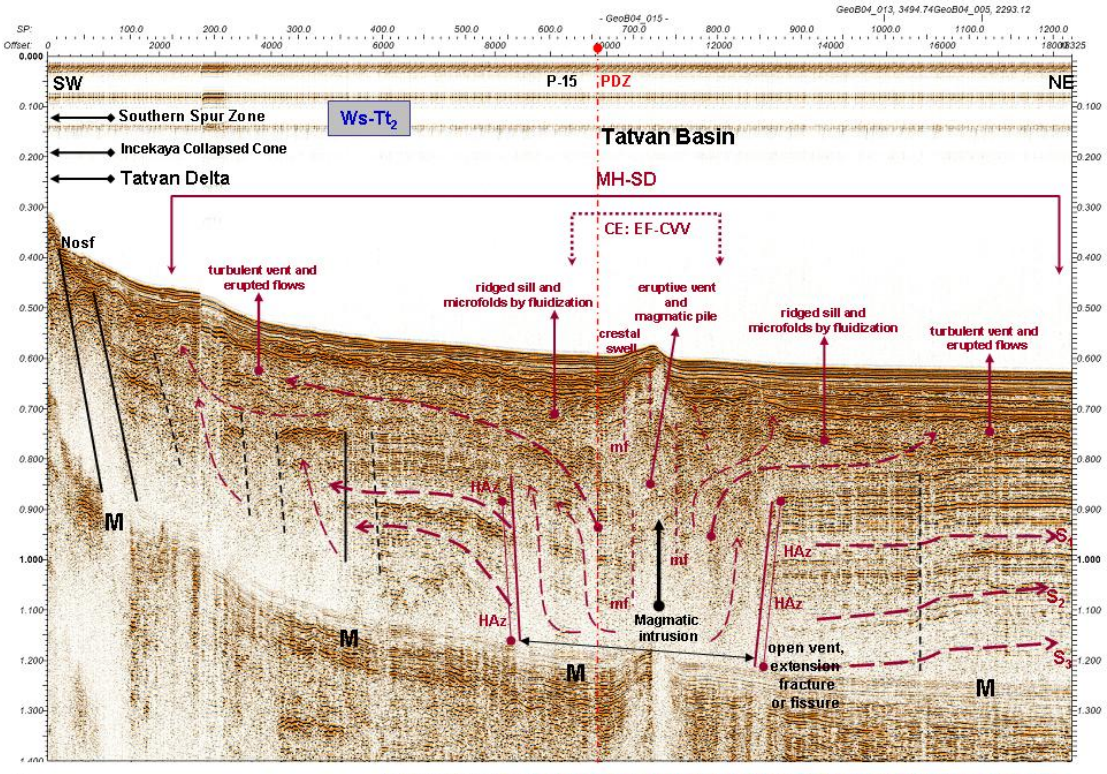

Figure 3.14 : NE-SW seismic section from S-margin boundary of central Tatvan basin across a zone of normal oblique-slip faults (Nosfs) through Tatvan basin intruded by rising magma. Seismic profile number of this section is 15 (P-15), as seen at the top center (see the location of this profile in Fig. 2.2). M: multiple, mf: microfaults-fractures, HAz: hydrothermal alteration zones, CE: cryptoexplosion, EF-CVV: explosive fissure-central vent volcano. Ws-Tt_2 (W-segment-transtension-2, blue colour) describes the second evolutional stage of seismic structural interpretation of transtension in S-margin boundary. Note that magma intrudes through thick sedimentary section from an opening vent, point source, or extension space, experiencing brecciation of the crystalline rind (cryptoexplosive breccia type). Dashed thick arrows (dark red colour) show magma flow paths and directions (S_1, S_2, S_3: sill sequences) from SW to NE and dashed thin arrows (vertical-curved lines in dark red colour) indicate deformation and dispersal patterns of hydrothermal fluids or volatiles. Dashed thin lines (black colour) indicate inferred fractures-faults. This section shows seismic structural patterns of magma hydrothermal-sediment deformations (MH-SD) (max. sediment thickness: 530 m, max. water depth: 469 m, offset: 18 km, two-way travel time in sec).

Seismic sections show that Tatvan delta subbasin seems to be controlled by a flower structure associated with intrusive-extrusive activity through the open vents-fractures or fissures (Fig. 3.13). This subbasin has 6 km morphological width with a sediment thickness much less than 150 m (Fig. 3.13). Seismic interpretation shows that Tatvan delta subbasin is probably an uplifted erosional product and recently controlled by the master fault. It is assumed that the faulting and intrusive-extrusive activity in these seismic sections seen in Figs. 3.13-3.15 as an secondary effect consists of en echelon-like discontinuous and several small-scale fault segments. Seismic structural

interpretation reveals that these fault segments are splay faults as a result of fault branching of the master fault (PDZ) in S-margin (Figs. 3.13 and 3.14). This implies a complicated discontinuous faulting pattern of W-segment, representing a releasing en echelon bend of S-shear zone.

The dextral shear in W-segment controls the present-day stratigraphy of Tatvan basin and deforms it in a complicated way. The oblique faults observed on both sides of the deformation zone are also products of dextral shear. W-segment is probably detached adjustment structure developed under the combined influence of gravitational instability processes and ductile events at deeper sedimentary sections.

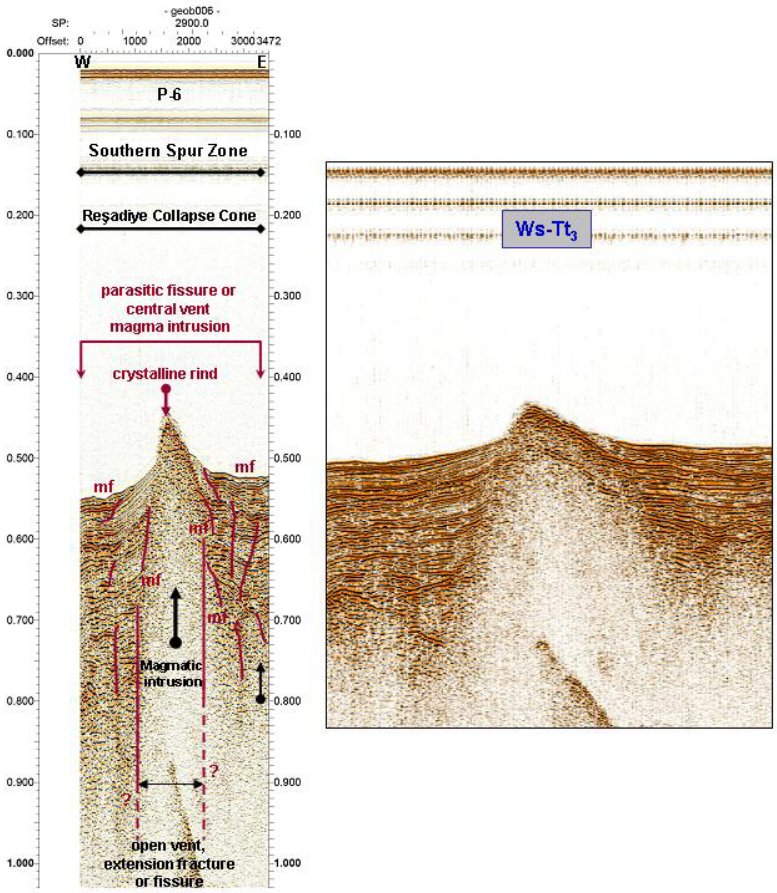

Figure 3.15 : W-E seismic section from S-margin boundary of central Tatvan basin across S-coast of the lake (collapse cone) through S-spur zone intruded by individual magma through microfaults-fractures (mf). Seismic profile number of this section is 6 (P-6), as seen at the top center (see the location of this profile in Fig. 2.2). Ws-Tt_3 (W-segment-transtension-3, blue colour) describes the third evolutional stage of seismic structural interpretation of transtension in S-margin boundary. Note that magma intrudes through coastal section from an opening vent, point source, or extension space, solidifying and forming its crestal crystalline rind. Seismic section at the right is less exaggerated section of this profile, clearly indicating crestal swelling of crystalline rind of parasitic intrusion (max. water depth: 413 m, offset: 3.5 km, two-way travel time in sec).

3.1.4 Structural implications for marginal and basinal sections

Seismic structural analysis and some findings of seismic reflection interpretation illustrate several important implications for structural reactivation of margin-bounding faults. They provide very useful seismic information for understanding structural development of the oblique-slip fault systems in margins.

Three sets of faults control the structural and sedimentary evolution of central Tatvan basin. One set trends W-E parallel to the master fault, showing a restraining bend in N-margin (Figs. 3.1-3.7). The geometry and kinematic indicators of these faults imply that their movements are mainly sinistral reverse oblique. The second set of faults trends in a SW-NE direction, showing evidence of sinistral normal oblique motion and a releasing bend in W-margin (Figs. 3.8-3.11). Some of these faults show evidence of vertical displacements. The third set of faults trends approximately W-E parallel to the master fault, showing a releasing bend in S-margin (Figs. 3.13-3.15). The geometry and kinematic indicators of these faults imply that their movements are mainly dextral normal oblique. All marginal fault systems appear to develop coevally, because they cut across one another.

The oblique-slip faults in N- and W-margins are cut by the master faults and interpreted as the pull-apart boundary faults which shifted Tatvan basin block. The master faults observed in N- and W-margins have vertical dips and more than a kilometer or so in length they are invariably basement involved. The sense of oblique-slip displacement is described as sinistral. On the other hand, releasing bends in W- and S-margins are well observed in marginal edges of the central Tatvan basin, affecting the entire sedimentary section. This shows that the margin boundary faults strongly control the fault geometry and stratigraphy, causing oblique deformation in the basin. The structural geometry and kinematic indicators of the secondary faults existing in these fault zones suggest that their movements are oblique with normal component, and that they are related to the extensional tectonics occurring in Tatvan basin (see seismic sections in Figs. 3.8-3.11).

It is recognized from seismic structural interpretation that the oblique faults in N- and W-margins show evidence of repeated movements (Figs. 3.1-3.11). Seismic sections show a part of several seismic lines through a fault and deformation zone in N-margin, and there is a clear evidence of several episodes of movement (Figs. 3.1-3.7). The segments of the fault planes are steeply inclined but the structural geometry

of the shallowest faulted zone indicates a subbasin formation with local tilting, reverse drags, and reverse movements with strike components. Repeated movements involving a change in faulting type in N- and W-margins are often recognized by a relation of the master faults with secondary fault sets and downfaulted Tatvan basin. This suggests that a steeper reverse fault in margin boundary reactivated as a high-angle normal fault with strike component. Deformation activity in N- and particularly in W-margins well reflects this situation (Figs. 3.1-3.10). For example, the master fault in N-margin propagates up through the cover sequence, maintaining its dip (Figs. 3.1-3.7). This shows that the fault reactivation occurs during sedimentation. It is also observed from seismic sections that a significant sedimentary cover does not overly possible older faults before they are reactivated. Therefore, a change in fault geometry is seen only within contact drags of the fault planes, the shallowest faults controlling the subbasin and sedimentation style in Tatvan basin. Indeed, seismic sections show a structural situation where the high-angle reverse faults in the basement are reactivated (Figs. 3.1-3.10). Faulting in the basement produces extensional stress in the sedimentary section of Tatvan basin. The maximum extensional stress is oriented vertically. Any fault developing in the sedimentary cover develops at an angle to the vertically oriented maximum stress. The initial movements are likely to occur in N- and W-ends of the Tatvan basin, producing an incipient high-angle steeper reverse fault with a considerable strike-slip component in N-margin seen in Figs. 3.1-3.7 and an incipient high-angle normal fault with a considerable strike-slip component in W-margin seen in Figs. 3.8-3.10. It is clear that deformation zone in N-margin has already experienced the recent deformation style in W-margin, before N-margin is controlled by reverse oblique motions. As a result, W-margin recently experiences normal oblique-slip deformation, while N-margin experiences reverse oblique-slip deformation. Both margins obliquely control sedimentation pattern in Tatvan basin.

As there can be no net extension or compression in the sedimentary cover due to the oblique faulting in N- and W-margins, any reverse movements are balanced by normal faulting or any normal movements are balanced by reverse faulting. This structural situation is perfectly imaged by seismic sections in W-margin (Figs. 3.8-3.10), where initial normal fault with strike component (pre-existing steeper reverse fault) develops and high-angle reverse oblique faults occur in sublacustrine slope.

Since, there is no net extension or compression across the fault zone. This case also shows the effects of fault reactivation on a normal fault and the same for N-margin. Seismic sections well image these cases where the reactivated faults have a dipping fault plane, the propagating faults have a steeper dip in the sedimentary cover than the original fault. As a result, the faults in both N- and W-margins are reactivated oblique faults, showing several episodes of movement. W-segment as an en echelon feature of the master fault (PDZ) in S-margin is also interpreted to have been an reactivated product, controlling S-end of Tatvan basin (Figs. 3.13-3.15). Seismic structural interpretation suggests that W-segment in S-margin, reverse and normal oblique faults in N- and W-margins develop in response to reactivation of deeper, high-angle vertical faults, in association with extensional or strike-slip faulting and/or by rotation of originally steeper reverse faults. This confirms that faulting and deformation activity along margin boundaries of Tatvan basin are extremely partitioned.

It is well observed that the structures associated with oblique-slip faults are more diverse than those associated with any other fault type. Frequently, folds, secondary faults, horsts-grabens, subbasins can occur in association with oblique-slip faults (Figs. 3.1-3.10). Since, these oblique faults occur in basement rocks with an overlying sedimentary cover. In such a situation, the fault movement is not directly relayed into the cover sequence, but manifests in a variety of structures ranging from en echelon grabens to folds, their axes inclined at an angle to the direction of fault movement in N-margin (Figs. 3.1-3.5). Flower structures are supposedly characteristic of strike-/oblique-slip movements, but they can also occur above reactivated reverse faults, as recognized in N-margin (Figs. 3.1-3.7).

The fold structures are observed in and along Tatvan basin (Figs. 3.3, 3.5, 3.8 and 3.9). These folds are roughly trending N-S and smaller-scale features associated with local compression that has only basinal significance. Amplitude of these folds increases from S to N and accelerates into deformation zone in N-margin (Fig. 3.3 and 3.5). Gentle folds in S sharply become high amplitude folds in N and cut by vertical faults in N-margin. Figs. 3.2-3.5 show that the folding of sedimentary layers in Tatvan basin is completely confined within deformation area in N-margin and controlled by secondary faults. Thus, strong folding are involved in horst-like sedimentary ridge structure in N-margin (Figs. 3.2-3.5). This suggests that these

folds are anticlinal features with varying amplitudes associated with strike-slip faulting and that folding of sedimentary layers overlies a reactivated deeper fault. The fault planes are approximately vertical in N- and W-margins and thus, the faulting does not produce net extension or net compression of the faulted strata. As a result of this, these folds are a direct result of the oblique deformation in margins. This indicates that folding and normal-reverse drags are directly related to oblique faulting and associated with frictional forces on fault planes. The rise of underlying intrusive features and also lateral extensive sheet-like extrusive features can cause smaller-scale folding or upbending (Figs. 3.3, 3.5, 3.6, 3.8 and 3.9). Seismic structural interpretation implies that internal and external geometry of the fold forms is dependent on the nature and layer thickness of the depositional sequences being folded. The folding of these sequences are intercalated with the extensive sheet-like features. This indicates that ductility contrasts between differing sedimentary sequences produce these differing fold styles within the same sequence. These folds developed in multilayered depositional sequences are generally controlled in their distribution and wavelength by the more competent members of the sequence.

3.1.5 E-portion of S-margin and NE-delta

There seems to be an complicated deformation zone in E-delta setting of Lake Van shown in Figs. 3.16-3.25. This deformation zone completely affects the shallow water delta setting and partly E-continuation of Tatvan basin. The distinct morphology of the active faults is well preserved on the lake floor as a deformation zone between NE-Erek delta and Eastern and Van delta settings in SE (Figs. 3.16-25). Seismic sections image that the deformation zone observed between NE- and SE-delta settings is characterized by an uplifted structural feature, known as Çarpanak basemen block uplift (Figs. 3.16-3.21 and 3.23-3.25). This uplift appears to have been a result of prominent faulting activity striking W-E, formed by the master fault (PDZ) located between NE- and SE-delta settings (Figs. 3.16-3.25). This indicates that W-E trending master fault is a structural boundary separating NE- and SE- delta settings. The fault planes providing the displacement have vertical slope or steeper angles (Figs. 3.16-3.25).

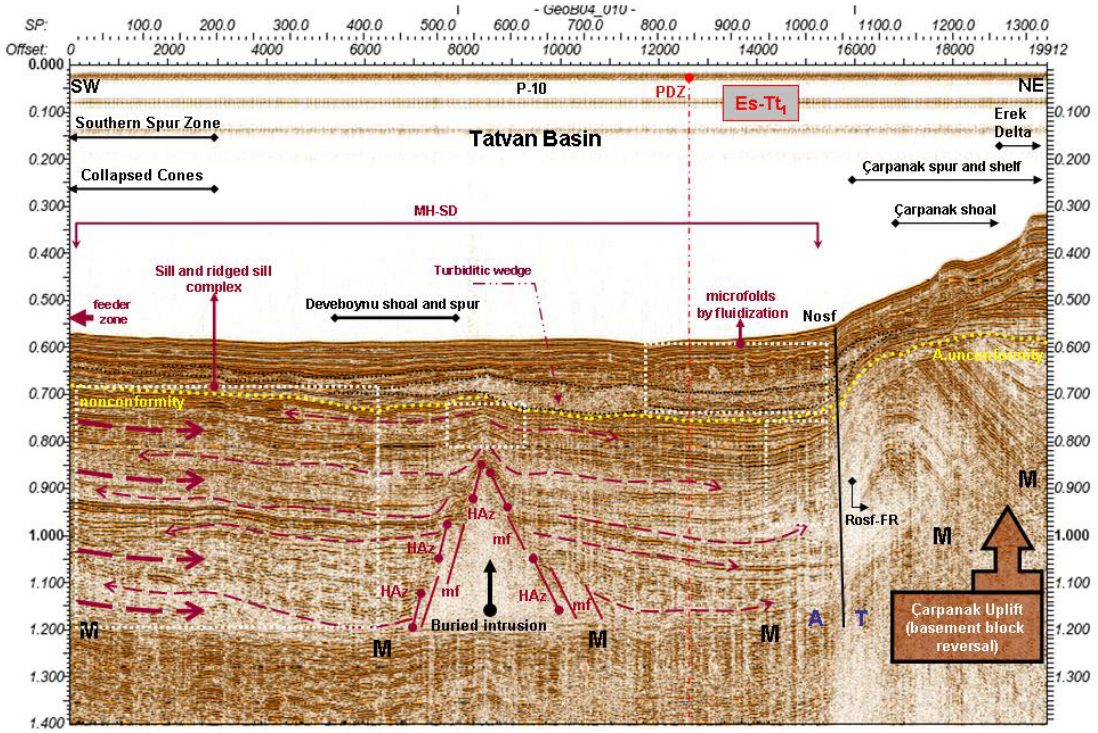

Figure 3.16 : SW-NE seismic section from S-margin boundary of central Tatvan basin across a zone of normal oblique-slip fault (Nosf) through Tatvan basin intruded by a buried intrusion. Seismic profile number of this section is 10 (P-10), as seen at the top center (see the location of this profile in Fig. 2.2). M: multiple, PDZ: principal displacement zone, T: toward, A: away, mf: microfaults-fractures, HAz: hydrothermal alteration zones. Es-Tt_1 (E-segment-transtension-1, red colour) describes the initial evolutional stage of seismic structural interpretation of transtension in S-margin boundary. This seismic section clearly shows pre-existing basement block reversal (Çarpanak uplift with overlying delta sedimentation), fault reactivation process (reverse oblique-slip fault-fault reactivation shown as Rosf-FR), and formation of angular unconformity-nonconformity (dotted round lines in yellow colour). Note that magma intrudes through thick sedimentary section from an opening vent, point source, or extension space and radially deforms depositional sequences. Dashed thick arrows (dark red colour) show magma flow paths (sill features) of collapsed cones in S-spur zone, trending from SW to NE. Dashed thin arrows (dark red colour) indicate deformation and dispersal patterns of sill features, hydrothermal fluids or volatiles. Dotted round thin lines (black colour) indicate block faulting-related turbiditic wedge deposits. This section shows seismic structural patterns of magma hydrothermal-sediment deformations (MH-SD) (max. sediment thickness: 532 m, min. sediment thickness: 150-250 m, max. water depth: 430 m, offset: 20 km, two-way travel time in sec).

Seismic section seen in Fig. 3.16 morphologically shows E-continuation of Tatvan basin bounded by an area of collapsed dome-cone complex and southern spur zone in SW and Çarpanak spur zone in NE. The fault appearing in this seismic section controls max. sediment thickness 532 m of Tatvan basin, resulting in basement block uplift of Çarpanak spur zone and related secondary features and donwlift of Tatvan basin. Sediment thickness in Tatvan basin gradually thins and reaches a value of 408

m at the fault plane (Fig. 3.17). N-S trending seismic section seen in Fig. 3.18 perfectly shows internal development of sedimentary subbasins bounded by Çarpanak spur zone in N and Varis spur zone offshore Deveboynu peninsula in S.

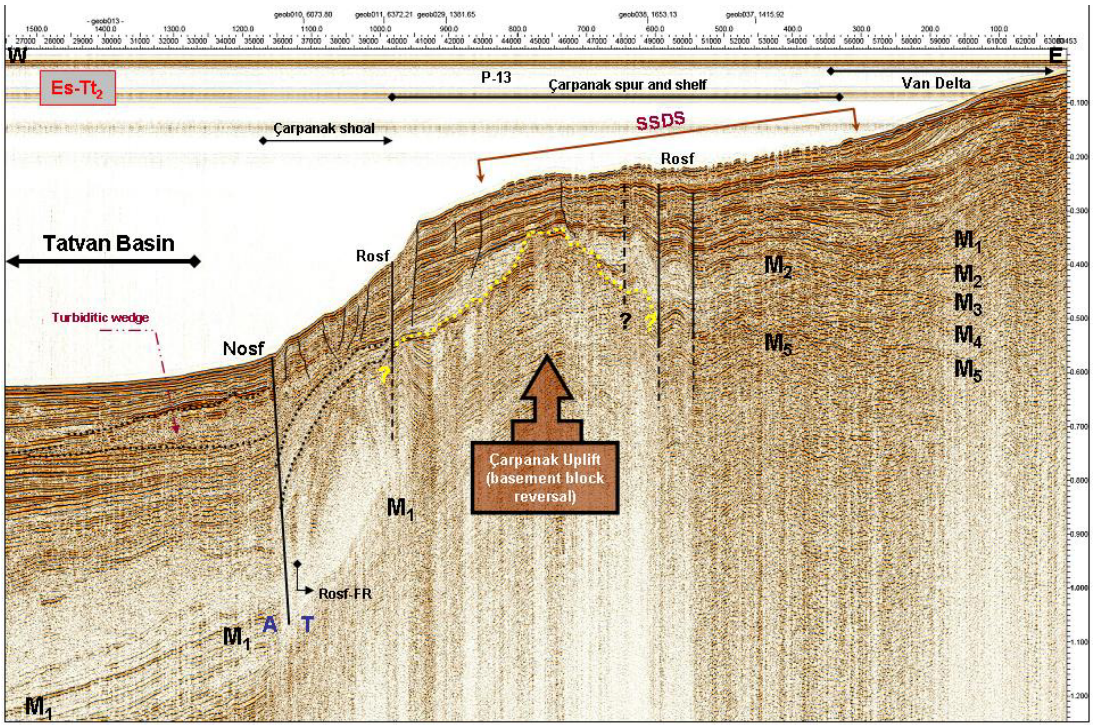

Figure 3.17 : W-E seismic section from S-margin boundary of central Tatvan basin across a zone of normal and reverse oblique-slip faults (Nosf-Rosf) through Tatvan basin and Çarpanak spur zone. Seismic profile number of this section is 13 (E-portion of P-13), as seen at the top center (see the location of this profile in Fig. 2.2). M_1, M_2, M_3: first, second and triple multiple sequences, T: toward, A: away. Es-Tt_2 (E-segment-transtension-2, red colour) describes the second evolutional stage of seismic structural interpretation of transtension in S-margin boundary. This seismic section clearly shows pre-existing basement block reversal (Çarpanak uplift with overlying delta sedimentation), fault reactivation process (reverse oblique-slip fault-fault reactivation shown as Rosf-FR), and formation of angular unconformity (dotted round line in yellow colour). Note that soft sediment deformation structures (SSDS) are localized in Çarpanak spur zone and shelf and Van delta. Dotted round thin lines (black colour) indicate block faulting-related turbiditic wedge deposits. This section as a E-portion of P-13 requires W-E trending cross sectional correlation of Figs. 3.10 and 3.31 (max. sediment thickness: 408 m, min. sediment thickness: 150-300 m, max. water depth: 450 m, offset: 37 km, two-way travel time in sec).

These internal subbasins shown in Fig. 3.18 are deformed and divided by a peculiar intrusive-extrusive activity into two separate internal basins; Varis spur zone and Deveboynu subbasins. The widths of these subbasins are morphologically ranged from 6-7 km, suggesting broadly widening internal depositional trough with an averaged width value of 12-14 km.

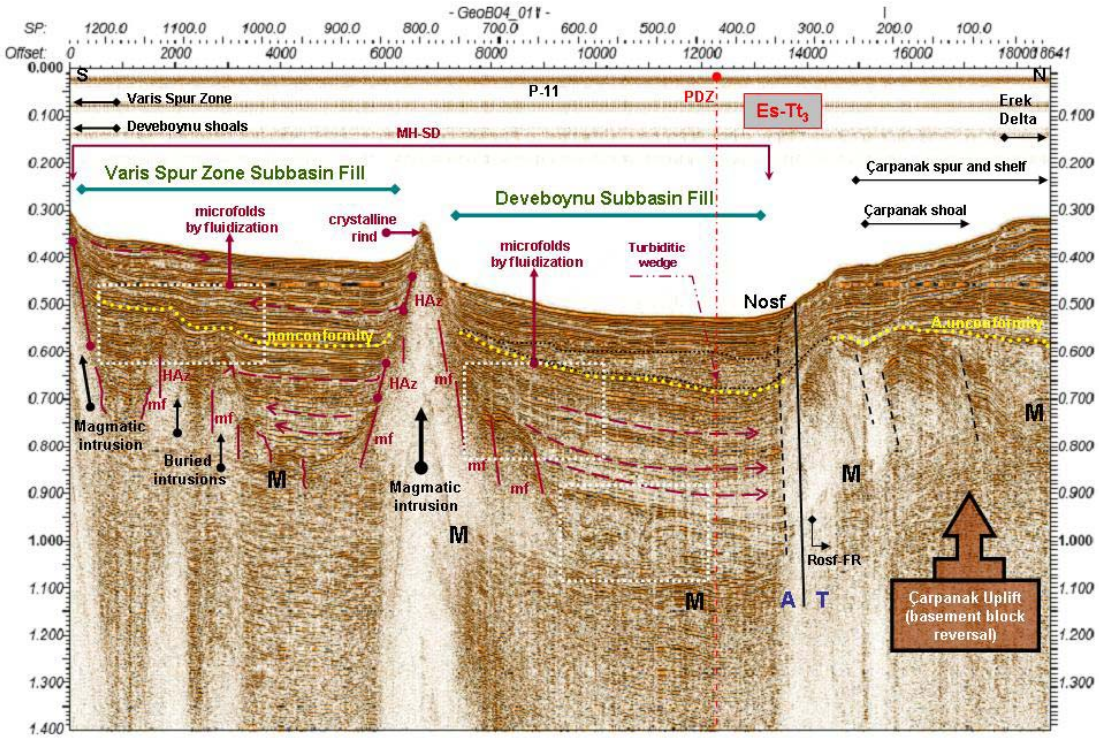

Figure 3.18 :N-S seismic section from S-margin boundary of central Tatvan basin across a zone of normal oblique-slip fault (Nosf) through Varis spur zone and Deveboynu subbasins separated by a magmatic intrusion. Seismic profile number of this section is 11 (P-11), as seen at the top center (see the location of this profile in Fig. 2.2). M: multiple, PDZ: principal displacement zone, T: toward, A: away, mf: microfaults-fractures, HAz: hydrothermal alteration zones. Es-Tt_3 (E-segment-transtension-3, red colour) describes the third evolutional stage of seismic structural interpretation of transtension in S-margin boundary. This seismic section clearly shows pre-existing basement block reversal (Çarpanak uplift with overlying delta sedimentation), fault reactivation process (reverse oblique-slip fault-fault reactivation shown as Rosf-FR), and formation of angular unconformity-nonconformity (dotted round lines in yellow colour). Note that rising magmas intrude through thick subbasin fill from an opening vent, point source, or extension space and radially deforms depositional sequences. Dashed thin arrows (dark red colour) indicate deformation and dispersal patterns of sill features, hydrothermal fluids or volatiles. Dotted round thin lines (black colour) indicate block faulting-related turbiditic wedge deposits. This section shows seismic structural patterns of magma hydrothermal-sediment deformations (MH-SD) in subbasinal zone (max. sediment thickness of Varis spur zone and Deveboynu subbasins: 383 m and 438 m, min. sediment thickness: 150-250 m, max. water depth: 385 m, offset: 18.5 km, two-way travel time in sec).

The overlying max. sediment thicknesses in these troughs, Varis spur zone and Deveboynu subbasins, are 383 and 438 meters respectively. These values are approximately ranged from 400-450 m due to the effects of multiple reflections. This shows that a higher amount of sedimentation, overloading and rapid subsidence occur in these subbasins. SW-NE trending seismic section in Fig. 3.19 shows a cross sectional area characterized by a part of Deveboynu subbasin with 380 m max.

sediment thickness, Çarpanak spur zone and shelf and NE-Erek delta. This section well images structural dimensions of Çarpanak basement block uplift associated with NE-Erek delta.

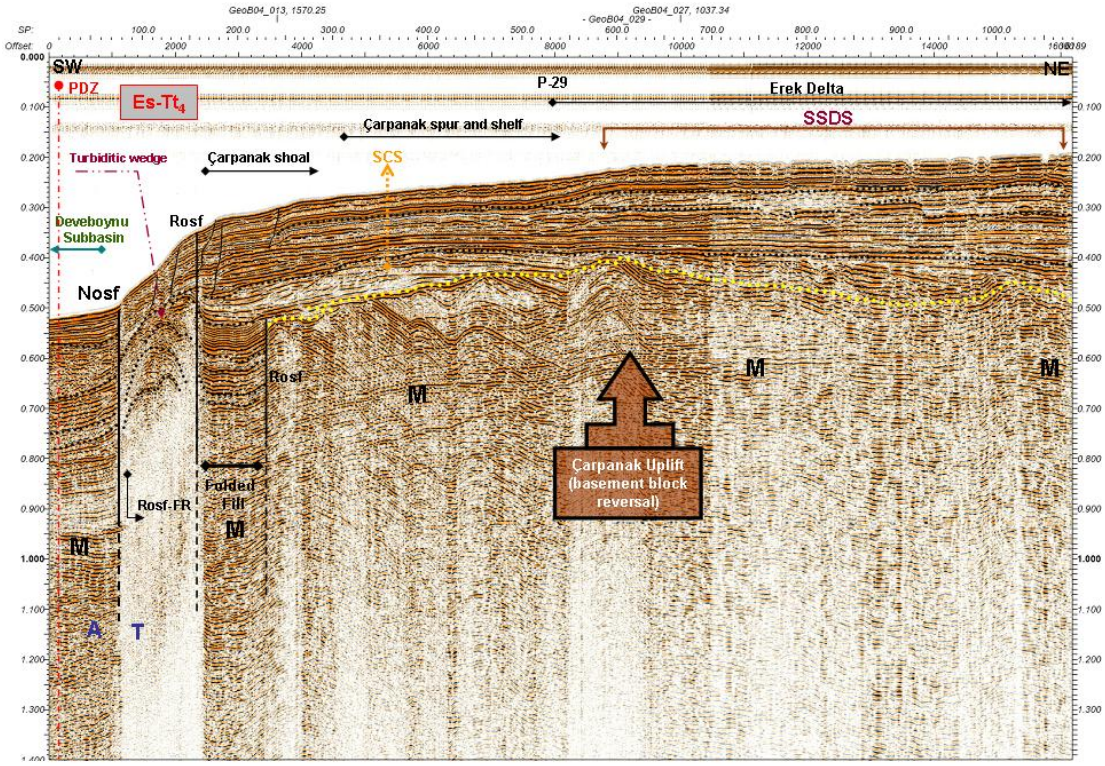

Figure 3.19 : SW-NE seismic section from S-margin boundary of central Tatvan basin across a zone of normal and reverse oblique-slip faults (Nosf-Rosf) through Çarpanak spur zone and NE-Erek delta. Seismic profile number of this section is 29 (P-29), as seen at the top center (see the location of this profile in Fig. 2.2). M: multiple, T: toward, A: away, PDZ: principal displacement zone, SCS: slumping of clinoform succession. Es-Tt_4 (E-segment-transtension-4, red colour) describes the fourth evolutional stage of seismic structural interpretation of transtension in S-margin boundary. This seismic section clearly shows pre-existing basement block reversal (Çarpanak uplift with overlying delta sedimentation), fault reactivation process (reverse oblique-slip fault-fault reactivation shown as Rosf-FR), and formation of angular unconformity (dotted round line in yellow colour). Note that soft sediment deformation structures (SSDS) are localized in NE-Erek delta. Dotted round thin lines (black colour) indicate block faulting-related turbiditic wedge deposits (max. sediment thickness: 380 m, min. sediment thickness: 150-300 m, max. water depth: 390 m, offset: 16 km, two-way travel time in sec).

NE-SW and S-N trending seismic lines seen in Figs. 3.21 and 3.22 are connected to obtain a complete cross sectional profile across Eastern delta setting towards Çarpanak spur zone in S-NNE direction shown in Fig. 3.20. Fig. 3.20 well images Deveboynu subbasin system with 378 m. max. sediment thickness, bounded by Çarpanak spur zone in N and several secondary faults in Eastern delta towards S.

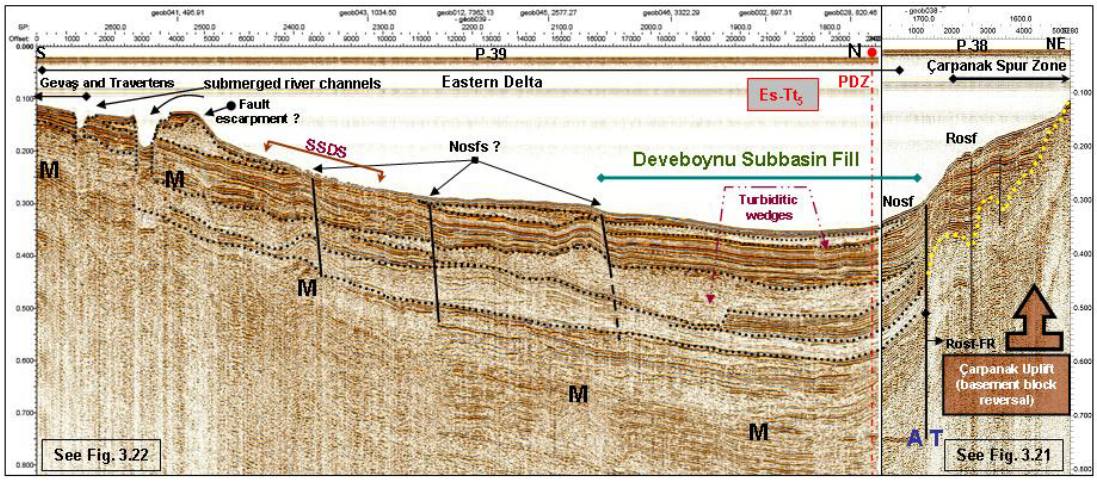

Figure 3.20 : S-NNE seismic section, a combination of S-N and SW-NE trending seismic profiles, from SE-delta across a zone of normal and reverse oblique-slip faults (Nosf-Rosf) through Deveboynu subbasin and Çarpanak spur zone. Seismic profile numbers of this combined section are 38 and 39, (P-38 and P-39, also see Figs. 3.21 and 3.22 for detailed sections), as seen at the top center (see the location of this profile in Fig. 2.2). M: multiple, T: toward, A: away, PDZ: principal displacement zone. Es-Tt_5 (E-segment-transtension-5, red colour) describes the fifth evolutional stage of seismic structural interpretation of transtension in S-margin boundary. This seismic section clearly shows pre-existing basement block reversal (Çarpanak uplift), fault reactivation process (reverse oblique-slip fault-fault reactivation shown as Rosf-FR), and formation of angular unconformity (dotted round line in yellow colour). Note that soft sediment deformation structures (SSDS) are localized in tilted half-graben structure of Eastern delta. Dotted round thin lines (black colour) indicate block faulting-related turbiditic wedge deposits. Dotted round thick lines (black colour) indicate block faulting-related sediment disruptions (max. sediment thickness: 378 m, min. sediment thickness: 150-300 m, max. water depth: 250 m, offset: 29 km, two-way travel time in sec).

The morphological width of Deveboynu basin in this section is approximately 7-9 km. In fact, Fig. 3.20 significantly represents not only Deveboynu subbasin, but also possible asymmetric half graben structure between Çarpanak spur zone in N and Gevaş area in S. Hence, this section may also represent extensionally tilted basement geometry of Eastern and Van delta settings as a SE-delta system. W-E trending seismic section in Fig. 3.23 is parallel to W-E continuation of the master fault (PDZ), therefore, PDZ is not observed in this section. Fig. 3.23 shows a part of Deveboynu subbasin, Çarpanak spur zone and shelf, Eastern and Van delta settings. In Fig. 3.23, sediment thickness in Deveboynu subbasin thins and reaches a value of 290 m. due to fault-controlled Çarpanak uplift. The fault-related folding, uplifting and slumped-slided progradations are also recognized (Fig. 3.23). Seismic sections seen in Fig. 3.24-3.25 show Çarpanak spur zone, Erek and Van delta settings.

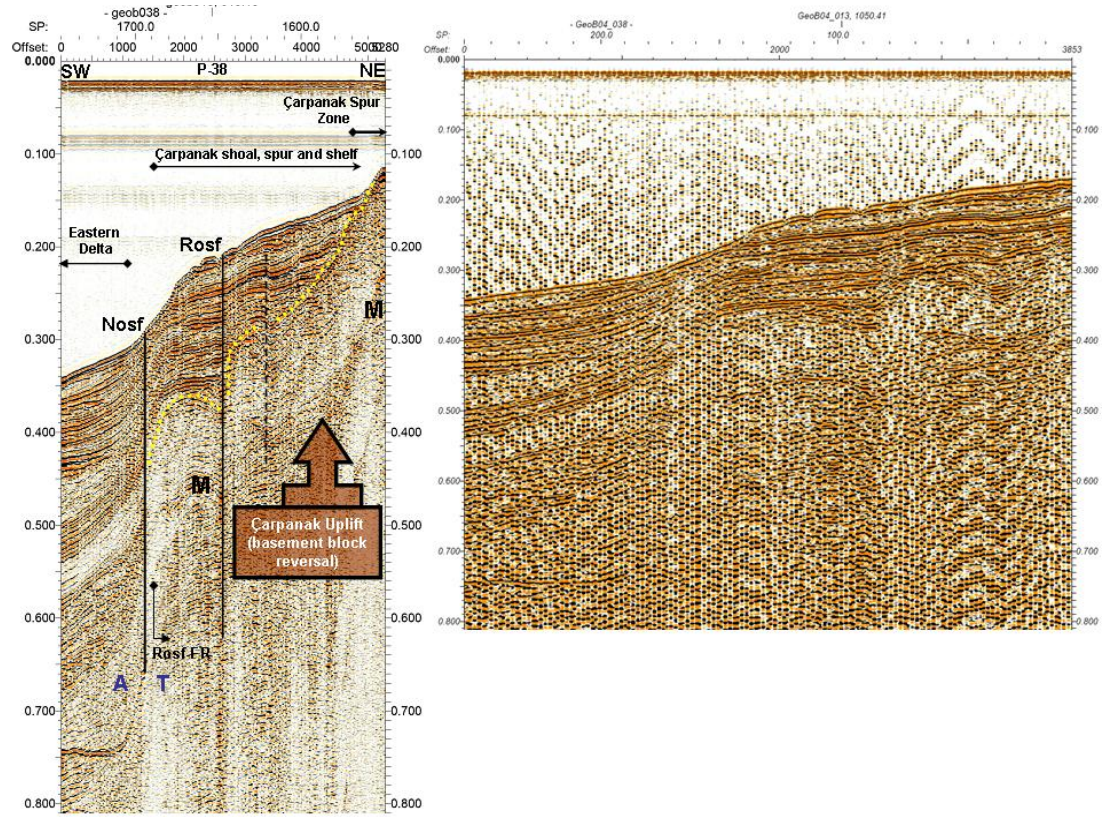

Figure 3.21 : A detailed image of seismic section shown in Fig. 3.20 well illustrates contact drag of folded sediments in Çarpanak spur zone.

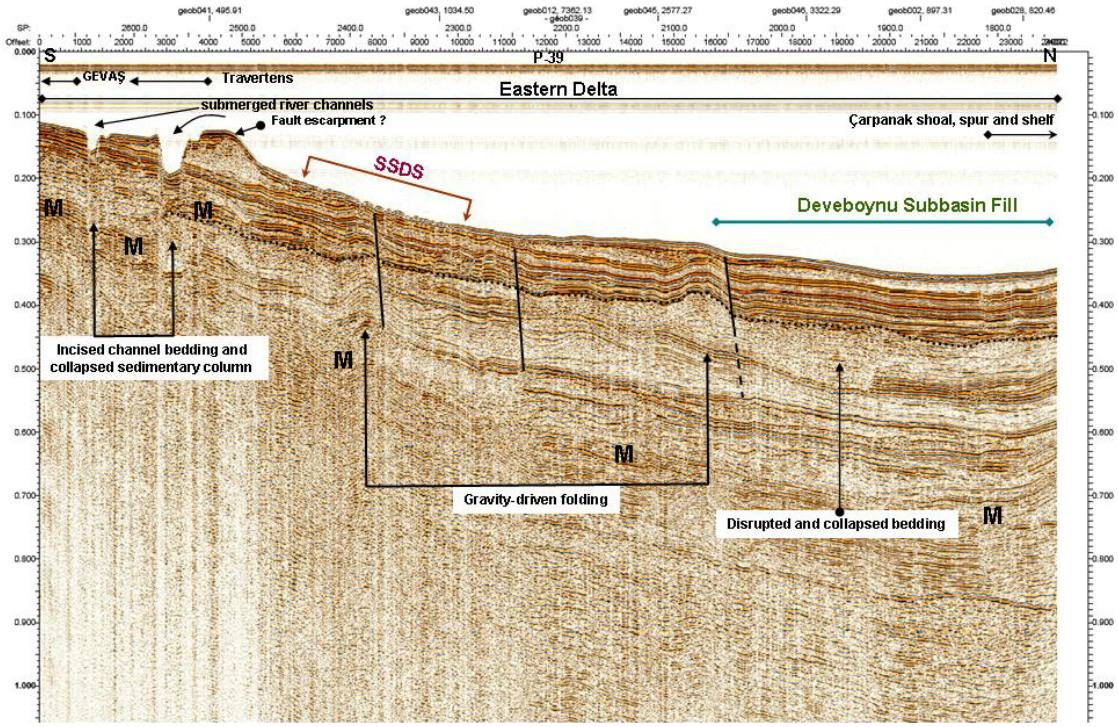

Figure 3.22 :A detailed image of seismic section shown in Fig. 3.20 well illustrates block faulting and subsidence-related sediment deformations, faulting, folding and disrupted beddings.

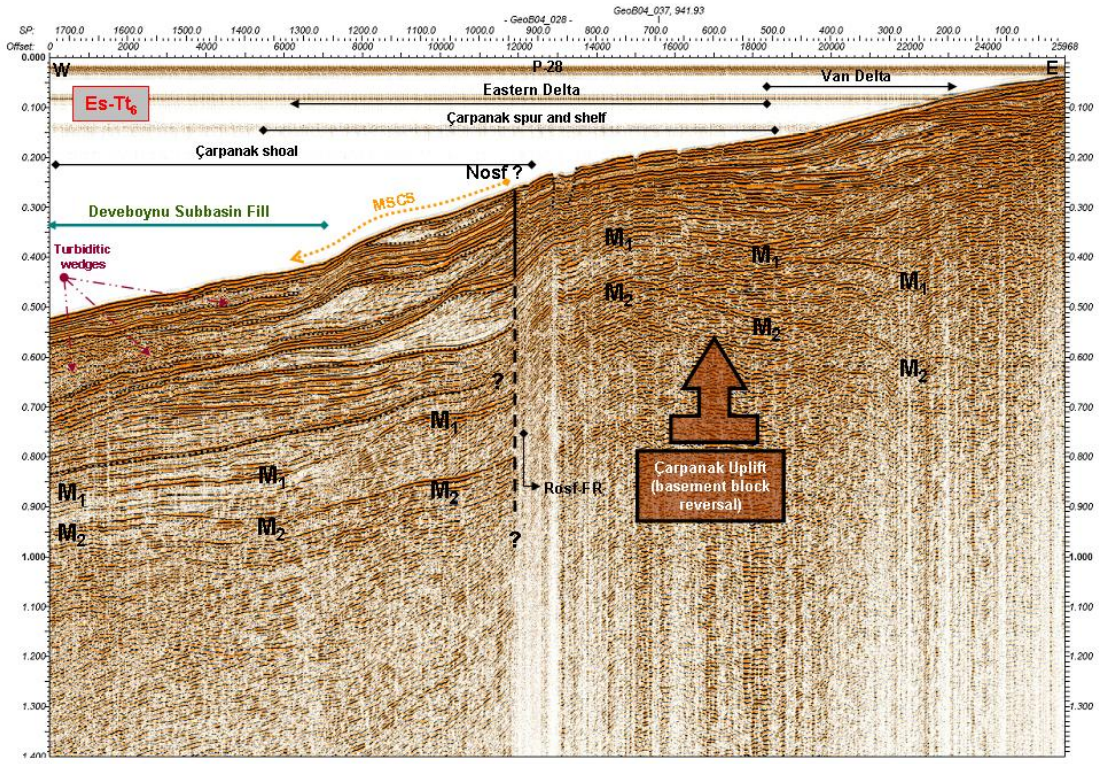

Figure 3.23 : W-E seismic section from S-margin boundary of central Tatvan basin across a zone of normal and reverse oblique-slip faults (Nosf-Rosf) through Deveboynu subbasin, Çarpanak spur zone, Eastern and Van delta. Seismic profile number of this section is 28 (P-28), as seen at the top center (see the location of this profile in Fig. 2.2). M_1 and M_2: multiples, MSCS: multiple slumping of clinoform successions. Es-Tt_6 (E-segment-transtension-6, red colour) describes the sixth evolutional stage of seismic structural interpretation of transtension in S-margin boundary. In this section, block motions and sense of shear are not shown due to its being parallel to PDZ of S-margin boundary fault. This seismic section clearly shows pre-existing basement block reversal (Çarpanak uplift with overlying delta sedimentation), fault reactivation process (reverse oblique-slip fault-fault reactivation shown as Rosf-FR), and strong folding of delta sediments. Note that MSCS is triggered and driven by Çarpanak block uplift. Dotted round thin lines (black colour) indicate block faulting-related turbiditic wedge deposits (max. sediment thickness: 290 m, min. sediment thickness: 150-300 m, max. water depth: 390 m, offset: 26 km, two-way travel time in sec).

The fault-controlled sedimentary folding, Çarpanak uplift, slumped-slided progradations and river channel incisions are also clearly observed in these sections, in which Çarpanak spur zone appears as a peculiar cone-shaped structural high.

The calculated sediment thicknesses from complete set of seismic profiles show that Çarpanak spur zone is a fault-controlled basement block uplift characterized by erosional unconformity surface in which sediments thickness values range from 200 to 250 m and much less than 300 m max (Figs. 3.16-3.20, 3.24 and 3.25). Erek delta has also approximately the same averaged values of 200 to 250 m, because it overlies

Çarpanak uplift and has a same sediment section (Figs. 3.19 and 3.24 at top). However, thick progradational wedge complexes of Erek delta have a value of approximately 400-425 m in thickness, due to slumping-sliding toward deep Tatvan basin (Fig. 3.25). Sediment thickness in Van delta ranges from 150 to 180 m and much less than 200 m max (Figs. 3.17, 3.23, 3.24 at the bottom and 3.25). Thickness in Eastern delta reaches a max. value of 378 m due to Deveboynu depression toward Çarpanak uplift and gradually thins towards the further S by ranging from 300 to 100 m (Fig. 3.20). These values in Eastern delta indicate asymmetric sedimentary wedge, thickening in N and thinning in S, suggesting a strong structural control (Fig. 3.20).

Indication of the deformation zone and an active oblique fault with normal displacement bounding the E-edge of the Tatvan basin is apparent at Figs. 3.16 and 3.17 and also observed in Figs. 3.18-3.21, 3.24 at the bottom and 3.25. This fault shows strike-slip displacement with normal fault activity in the delta settings and is clearly observable through all seismic sections. The secondary deformation also becomes more pronounced in and around the Çarpanak spur zone. The secondary faults present on the. Figs. 3.16-3.21 are oblique faults related with the master fault. The folding, uplifting and the strong disturbance of progradational sedimentary wedges existing on seismic sections seen in Figs. 3.16-3.21 and 3.23-3.25 are also related with the master fault. This shows that the deformation zone in delta settings seems to be controlled by secondary oblique faults with normal component. These faults are interpreted as the W-E continuation of the master fault in the sense of dextral shear. The faults observed on both sides of the deformation zone in NE- and SE-delta settings are also products of dextral shear. The dextral shear in this region strongly controls the present-day stratigraphy of Tatvan basin, delta settings and the Çarpanak basement block uplift and deforms it in a complicated way.

Seismic structural interpretation suggests that a single fault is considered as master fault, composed of numerous parallel to sub-parallel and discontinuous fault segments (Figs. 3.16-3.21 and 3.23-3.25). The morphological and structural arrangement of these fault segments show a typical strike-slip fault control with normal component, stepped-like morphology of Çarpanak spur zone and NE-Erek delta, indicating the oblique segmentary nature of the faults shown in Figs. 3.16-3.21 and 3.23-3.25. The normal oblique faulting seen in these seismic sections controls the asymmetric depositional pattern in delta settings and indicates tilted basement

block geometry of Çarpanak uplift. This suggests an structural active zone between NE- and SE-delta settings well seen in Figs. 3.20 and 3.24. This structural activity is characterized by a formation of depositional graben-like troughs, known as subbasins in Figs. 3.18-3.20 and 3.23.

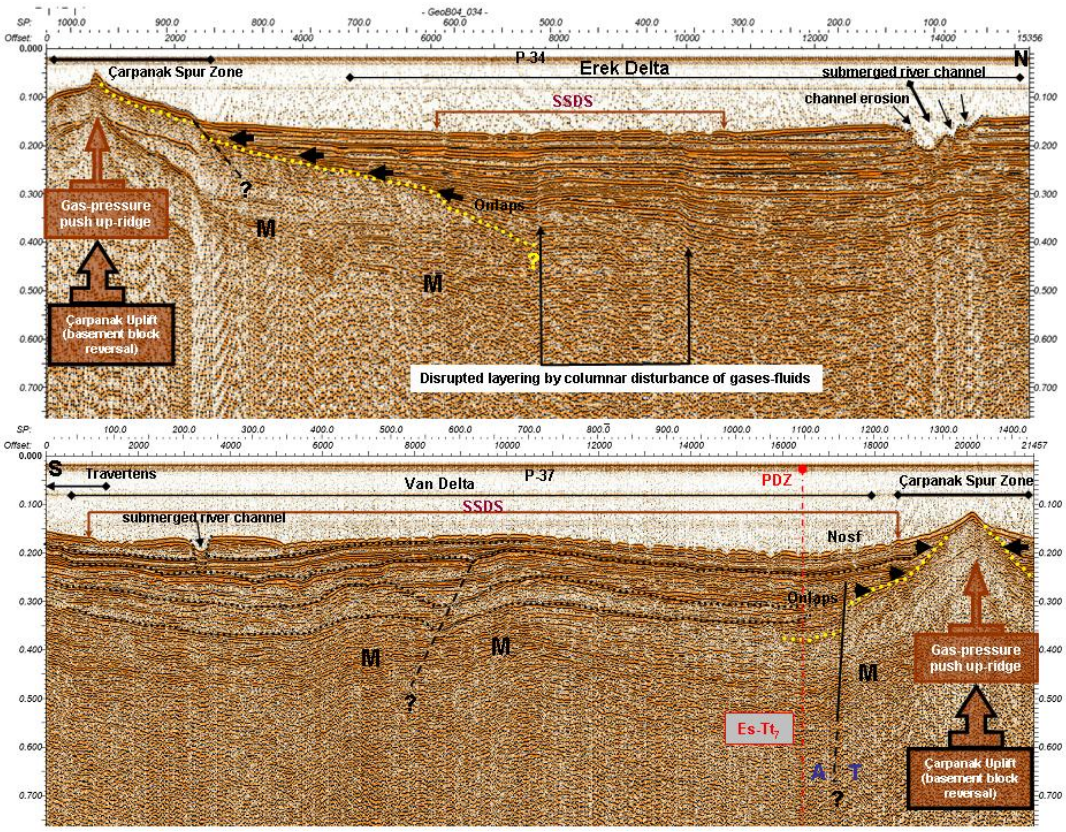

Figure 3.24 : S-N seismic section from NE-Erek and Van delta across a zone of normal oblique-slip fault (Nosf) through Çarpanak spur zone. Seismic profile numbers of these sections are 34 and 37 (P-34 and P-37), as seen at the top center (see the location of these profiles in Fig. 2.2). M: multiple, T: toward, A: away, PDZ: principal displacement zone. Seismic section at the top shows progressive onlap of wedge-shaped sediment package onto the foot of Çarpanak spur zone during uplifting and deep channel incision in N-end of Erek delta. Seismic section at the bottom also shows progressive onlap of wedge-shaped sediment package onto the foot of Çarpanak spur zone during uplifting and channel incision in S-end of Van delta. Es-Tt_7 (E-segment-transtension-7, red colour) describes the seventh evolutional stage of seismic structural interpretation of transtension in S-margin boundary. Both sections clearly show pre-existing basement block reversal (Çarpanak uplift with overlying delta sedimentation), fault reactivation process, and formation of angular unconformity (dotted round line in yellow colour). Note that a prominent structural feature in Çarpanak uplift indicates gas-pressure push up-ridge and that soft sediment deformation structures (SSDS) are widely distributed in both delta settings. Dotted round thin lines (black colour) in the section at the bottom indicate folded sequences of Van delta (max. sediment thickness: 150-300 m, min. sediment thickness: 50-100 m, max. water depth: 100-150 m, offset: 15.5 km (top) and 21.5 km (bottom), two-way travel time in sec).

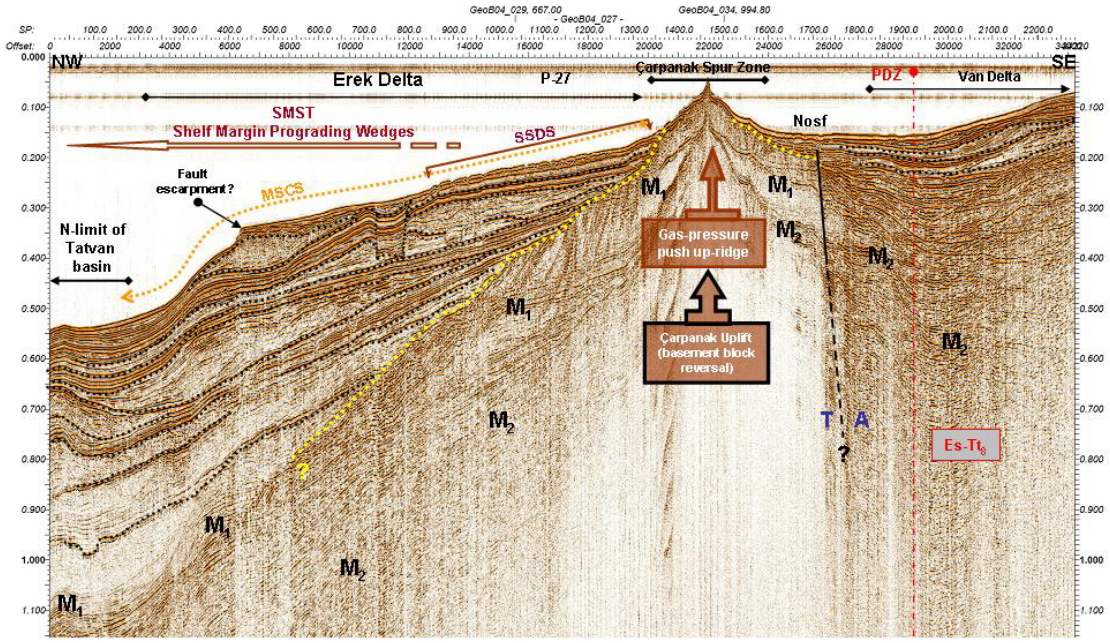

Figure 3.25 : NW-SE seismic section from Erek and Van delta across a zone of normal oblique-slip fault (Nosf) through Çarpanak spur zone. Seismic profile number of this section is 27 (P-27), as seen at the top center (see the location of this profile in Fig. 2.2). M_1 and M_2: multiples, T: toward, A: away, PDZ: principal displacement zone. MSCS: multiple slumping of clinoform successions, SSDS: soft sediment deformation structures. Es-Tt_8 (E-segment-transtension-8, red colour) describes the eighth evolutional stage of seismic structural interpretation of transtension in S-margin boundary. In this section, shelf margin system tract (SMST) shows shelf margin prograding wedges which are gently warped toward N-limit of Tatvan basin. This seismic section clearly shows pre-existing basement block reversal (Çarpanak uplift with overlying delta sedimentation), fault reactivation process, and formation of angular unconformity (dotted round line in yellow colour). Note that MSCS is triggered and driven by Çarpanak block uplift, in which a prominent structural feature indicates gas-pressure push up-ridge (max. sediment thickness: 390 m, min. sediment thickness: 100-130 m, max. water depth: 410 m, offset: 34 km, two-way travel time in sec).

In Fig. 3.18, there is an strong evidence of the intrusive and extrusive activity of magma-related products through the fault planes and vent-fissure or fractures. This activity is easily traced through the subbasins (Figs. 3.18-3.20 and 3.23) into Tatvan basin (Figs. 3.16 and 3.17).

The faulting activity controlling deformation in delta settings indicates an complicated pattern of extensional and transtensional block geometry of SE-delta (downlifting) and NE-delta (uplifting) (Figs. 3.17, 3.19 and 3.20). For example, Fig. 3.20 shows that SE-delta is asymmetric half-graben depositional center through Deveboynu subbasin into Tatvan basin in W. On the other hand, active structural control indicates that Çarpanak spur zone is a uplifted basement block controlling an

depositional emplacement of NE-Erek delta and progradational successions (Figs. 3.16-3.19, 3.24 and 3.25). It is clear that Çarpanak spur zone with NE-Erek delta is uplifted by normal oblique-slip faulting, associated with downlifting of Deveboynu subbasin and SE-delta. Hence, internal sedimentary subbasins, secondary features and the intrusive-extrusive activity seem to be controlled directly by extensional-transtensional events in delta regions. Seismic intepretation suggests that the faulting as a boundary between NE- and SE-delta settings is interpreted as the secondary or segmentary fault being the en echelon extension of the master fault in S-margin (Figs. 3.16-21 and 3.23-3.25). This fault terminates against Tatvan basin (Figs. 3.16 and 3.17) and deforms only the E-edge of central Tatvan basin into the delta settings where this fault results in a distinct sedimentary troughs well seen in Fig. 3.18. In Fig. 3.18, the fault-controlled intrusive-extrusive activity is seen within an area, bounded by Varis spur zones offshore Deveboynu peninsula in S and Çarpanak spur zone in N.

It is interpreted from a complete set of seismic sections that NE- and SE-delta environments are active tectonic zones, characterized by the dextral oblique-slip regime with normal component in S-margin. The observed fault obliquely cuts the E-edge of Tatvan basin (Figs. 3.16 and 3.17), passes through Varis spur zone and Deveboynu subbasins (Figs. 3.18-3.20) and entering into Eastern and Van delta settings (Figs. 3.23-3.25). This fault is buried by a thin depositional section of Van delta and terminates in the furher E, but probably continues to the land area (Kalecik area) in E (Figs. 3.24 at bottom and 3.25). This fault represents E-segment in S-margin. The PDZ of the master fault is, in fact, the main structural control driving the observed morphological and structural features through S-margin. This is a single trough-going master fault with several secondary faults parallel to the single fault, well traced in seismic sections. The PDZ directly crosses the shallow water (NE- and SE-deltas) through deep water (Tatvan basin) into Tatvan delta graben basin in the further W. The W-E continuation of the PDZ represents S-margin boundary fault of Lake Van with its E- and W-segments (see PDZ continuation through seismic sections in Figs. 3.16-3.20, 3.24 at the bottom, 3.25, 3.13 and 3.14). E- and W-segments subparallel each other suggest a close structural relation to PDZ. This relation indicates that W-E oblique continuations of W- and E-segments in S-margin are considered as splay faults or branching of a principal displacement zone (PDZ). Seismic structural interpretation suggests that E-segmentary fault in delta settings is

the releasing en echelon bend of S-shear zone, as interpreted in W-segment. This segmentary fault in S-margin is a distinct structural feature, separating delta settings into two different sub-deltas, developed under the combined influence of transtensional processes and ductile events at deeper sedimentary sections. This is also recognized in seismic sections crossing W-segment. Faulting and deformation styles from W- and E-segments, particularly internal subbasins, are controlled by dextral normal oblique-slip regime through a single trough-going master fault with several secondary faults. This clearly shows a geometry similar to a negative flower structure, as is clear from the structural interpretation of the seismic profiles. The master fault (PDZ) and W- and E-segmentary faults observed in S-part of the lake are part of this geometry. The faults in E-segment have vertical slope angles and are the determinative structural elements which form NE- and SE-delta settings in its present shape. The deformation geometry shaping faulting and subbasin development is also supported by negative flower structure. This shows that splay faults or branches (W- and E-segments) of the master fault (PDZ) in S-margin of the lake are the releasing en echelon bends. The one controls S-edge of deep Tatvan basin, while the other controls the NE- and SE-delta settings, resulting in internal sedimentary subbasins. The releasing en echelon characteristics of these segmentary faults form an strong evidence of the extreme intrusive-extrusive events through the vents-fissures or fractures into the subbasins. This evidence of deformational events is well recognized in seismic sections through the PDZ in W- and E-segments (Figs. 3.13-3.20, 3.24 at the bottom and 3.25).

3.1.6 SE-delta

Graben-like depression geometry of Deveboynu and Varis spur zone subbasins seen in Fig. 3.18 is also well reflected in seismic sections taken from SE-delta setting toward Deveboynu peninsula in W (Figs .3.26-3.29 and 3.30 at the top). These seismic sections morphologically indicate Varis spur zone parallel offshore Deveboynu peninsula and shoals. Varis spur zone has an axial elongation, trending NNW-SSE and located at the W-end of Eastern delta, forming W-margin boundary of SE-delta.

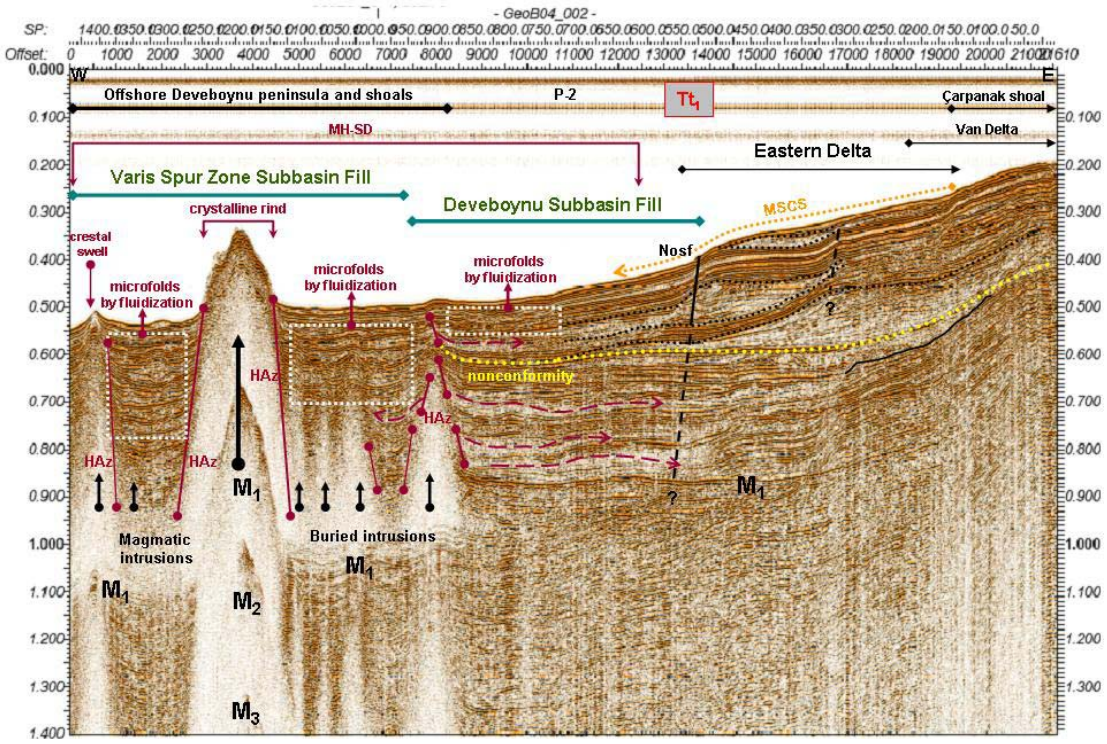

Figure 3.26 : W-E seismic section from SE-delta across a zone of normal oblique-slip fault (Nosf) through Varis spur zone and Deveboynu subbasins intruded by a wide range of magmatic intrusions. Seismic profile number of this section is 2 (P-2), as seen at the top center (see the location of this profile in Fig. 2.2). M_1 and M_2: multiples, HAz: hydrothermal alteration zones. Tt_1 (Transtension-1, red colour) describes the initial evolutional stage of seismic structural interpretation of transtension in W-margin boundary of SE-delta (offshore Deveboynu peninsula and Varis spur zone). This seismic section clearly shows that multiple slumping of clinoform successions (MSCS) is recently cut by Nosf, resulting in transtensional formation of Varis spur zone and Deveboynu subbasins. Note that rising magmas intrude through thick subbasin fills from an opening vent, point source, or extension space and radially deform subbasinal sequences. Dashed thin arrows (dark red colour) indicate deformation and dispersal patterns of sill features, hydrothermal fluids or volatiles. Dotted round thin lines (black colour) indicate slumped progradations. This section shows seismic structural patterns of magma hydrothermal-sediment deformations (MH-SD) in subbasinal zone (max. sediment thicknesses of Varis spur zone and Deveboynu subbasins: 315 m and 357 m, max. water depth: 413 m, offset: 21.5 km, two-way travel time in sec).

Morphological widths of Varis spur zone and Deveboynu subbasins are ranged from 6-7 km and sediment thicknesses are 315 and 357 m respectively (Fig. 3.26). The basinal widths of Varis spur zone and Deveboynu subbasins are narrowing toward S, reaching 4 km and sediment thicknesses are 362 and 327 m respectively (Fig. 3.27). The basinal width of Varis spur zone subbasin are much narrower toward the further S, reaching 2 km with a value of 306 m in thickness (Fig. 3.28). 8 km and 5 km basinal widths of Varis spur zone subbasin with 350 m and 264 m in max. sediment thickness are characterized by seismic sections in the S-end of Eastern delta (Figs.

3.29 and 3.30 at the top). These values indicate that the subbasinal widths of Varis spur zone along an axial elongation trending NNW-SSE are between 2-8 km with a relatively thick depositional pattern ranging from 250 to 370 m. Seismic structural interpretation shows that Varis spur zone and Deveboynu subbasins are internally formed and broadly widening (4-9 km) sedimentary depressions with the sediment thicknesses from 250 to 450 m (Figs. 3.18 and 3.26-3.30 at the top).

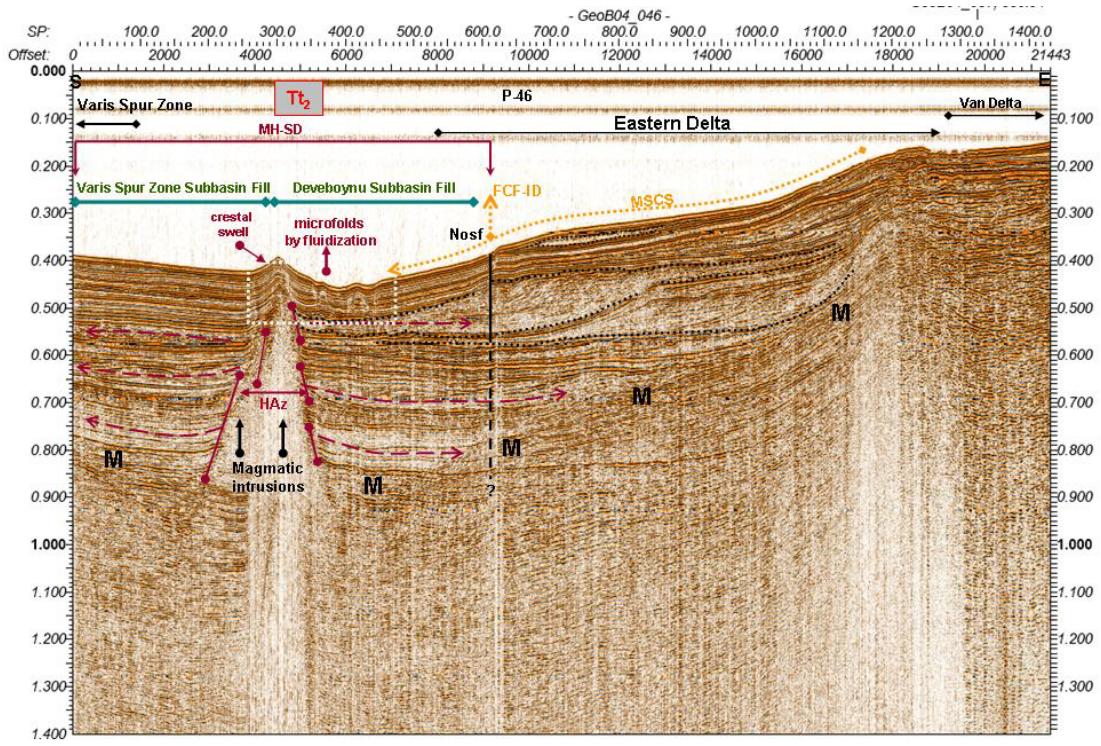

Figure 3.27 : S-E seismic section from SE-delta across a zone of normal oblique-slip fault (Nosf) through Varis spur zone and Deveboynu subbasins intruded by an individual intrusion. Seismic profile number of this section is 46 (P-46), as seen at the top center (see the location of this profile in Fig. 2.2). M: multiple, HAz: hydrothermal alteration zones. Tt_2 (Transtension-2, red colour) describes the second evolutional stage of seismic structural interpretation of transtension in W-margin boundary of SE-delta (offshore Deveboynu peninsula and Varis spur zone). This seismic section clearly shows that multiple slumping of clinoform successions (MSCS) is recently cut by Nosf, resulting in transtensional formation of Varis spur zone and Deveboynu subbasins, faulted clinoform failures (FCF) and internal destabilization of clinoform packages (ID). Note that rising magma intrudes through thick subbasin fills from an opening vent, point source, or extension space and radially deforms subbasinal sequences. Dashed thin arrows (dark red colour) indicate deformation and dispersal patterns of sill features, hydrothermal fluids or volatiles. Dotted round thin lines (black colour) indicate slumped progradations. This section shows seismic structural patterns of magma hydrothermal-sediment deformations (MH-SD) in subbasinal zone (max. sediment thicknesses of Varis spur zone and Deveboynu subbasins: 362 m and 327 m, max. water depth: 340 m, offset: 21.5 km, two-way travel time in sec).

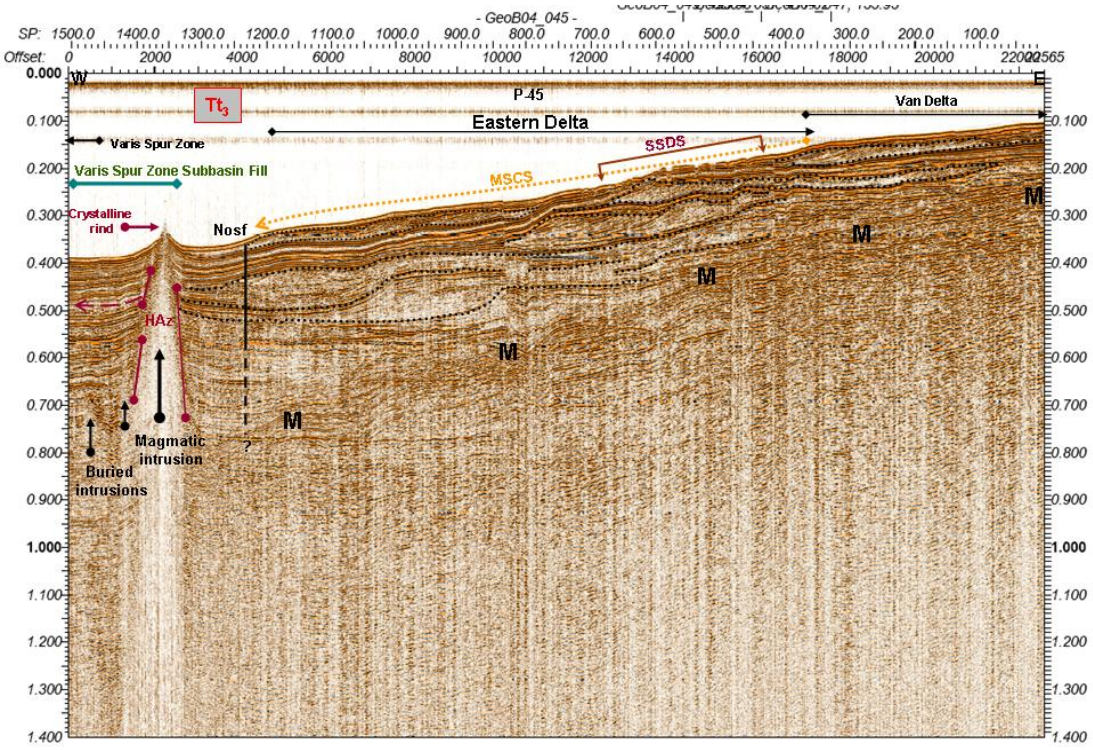

Figure 3.28 : W-E seismic section from SE-delta across a zone of normal oblique-slip fault (Nosf) through Varis spur zone subbasin intruded by an individual intrusion. Seismic profile number of this section is 45 (P-45), as seen at the top center (see the location of this profile in Fig. 2.2). M: multiple, HAz: hydrothermal alteration zones, SSDS: soft sediment deformation structures. Tt_3 (Transtension-3, red colour) describes the third evolutional stage of seismic structural interpretation of transtension in W-margin boundary of SE-delta (offshore Deveboynu peninsula and Varis spur zone). This seismic section clearly shows that multiple slumping of clinoform successions (MSCS) is recently cut by Nosf, resulting in transtensional formation of Varis spur zone subbasin. Note that rising magma intrudes through thick subbasin fill from an opening vent, point source, or extension space and radially deforms subbasinal sequences. Dashed thin arrow (dark red colour) indicates deformation and dispersal patterns of sill features, hydrothermal fluids or volatiles. Dotted round thin lines (black colour) indicate slumped progradations (max. sediment thickness of Varis spur zone subbasin: 306 m, max. water depth: 290 m, offset: 22.5 km, two-way travel time in sec).

Seismic sections seen in Figs. 3.18 and 3.26-3.30 at the top show that the higher amount of intrusive-extrusive activity deforms the sediments deposited in Varis spur zone and Deveboynu subbasins and progradational wedges in Eastern delta. Particularly, W-E trending seismic section in Fig. 3.26 clearly shows this deformation activity occurring offshore Deveboynu peninsula (also see Fig. 3.18). The intrusive activity also causes the formation of high and lows in the lake floor. Progradational clinoform packages from Eastern delta are gently inclined into the subbasinal troughs (Figs. 3.26 and 3.27). This suggests the faulting activity trending NNW-SSE, parallel Varis spur zone and Deveboynu peninsula. The faulting activity

seen in Figs. 3.26-3.30 at the top strongly deforms and vertically cuts progradational wedges and also Eastern delta, resulting in Varis spur zone subbasin, parallel Deveboynu peninsula. Seismic structural interpretation suggests that structural deformation controlling Varis spur zone and Deveboynu subbasins are related to the strike-slip faults with a distinct normal displacement in a sense of dextral shear (Figs. 3.26-3.30 at the top). These oblique faults are the secondary, smaller and discontinuous fault segments, segmenting offshore Deveboynu peninsula and causing Varis spur zone and Deveboynu subbasins (Figs. 3.18 and 3.26-3.30 at the top). The subbasin formation indicates the W-end of Eastern delta.

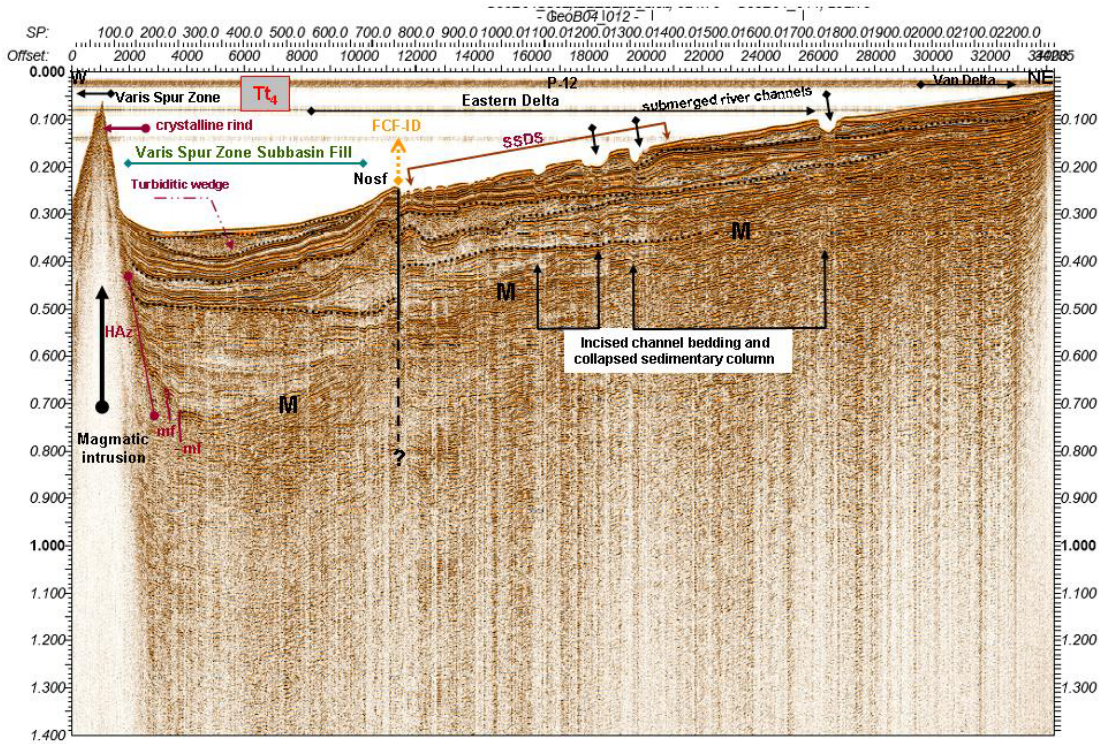

Figure 3.29 : W-NE seismic section from SE-delta across a zone of normal oblique-slip fault (Nosf) through Varis spur zone subbasin intruded by an individual intrusion. Seismic profile number of this section is 12 (P-12), as seen at the top center (see the location of this profile in Fig. 2.2). M: multiple, HAz: hydrothermal alteration zones, mf: microfaults-fractures, SSDS: soft sediment deformation structures. Tt_4 (Transtension-4, red colour) describes the fourth evolutional stage of seismic structural interpretation of transtension in W-margin boundary of SE-delta (offshore Deveboynu peninsula and Varis spur zone). This seismic section clearly shows that clinoform package is recently cut by Nosf, resulting in transtensional formation of Varis spur zone subbasin, faulted clinoform failure (FCF) and internal destabilization of clinoform package (ID). Note that rising magma intrudes through thick subbasin fills from an opening vent, point source, or extension space and radially deforms subbasinal sequences. Dotted round thin lines (black colour) indicate destabilized progradations (max. sediment thickness of Varis spur zone subbasin: 350 m, max. water depth: 250 m, offset: 34 km, two-way travel time in sec).

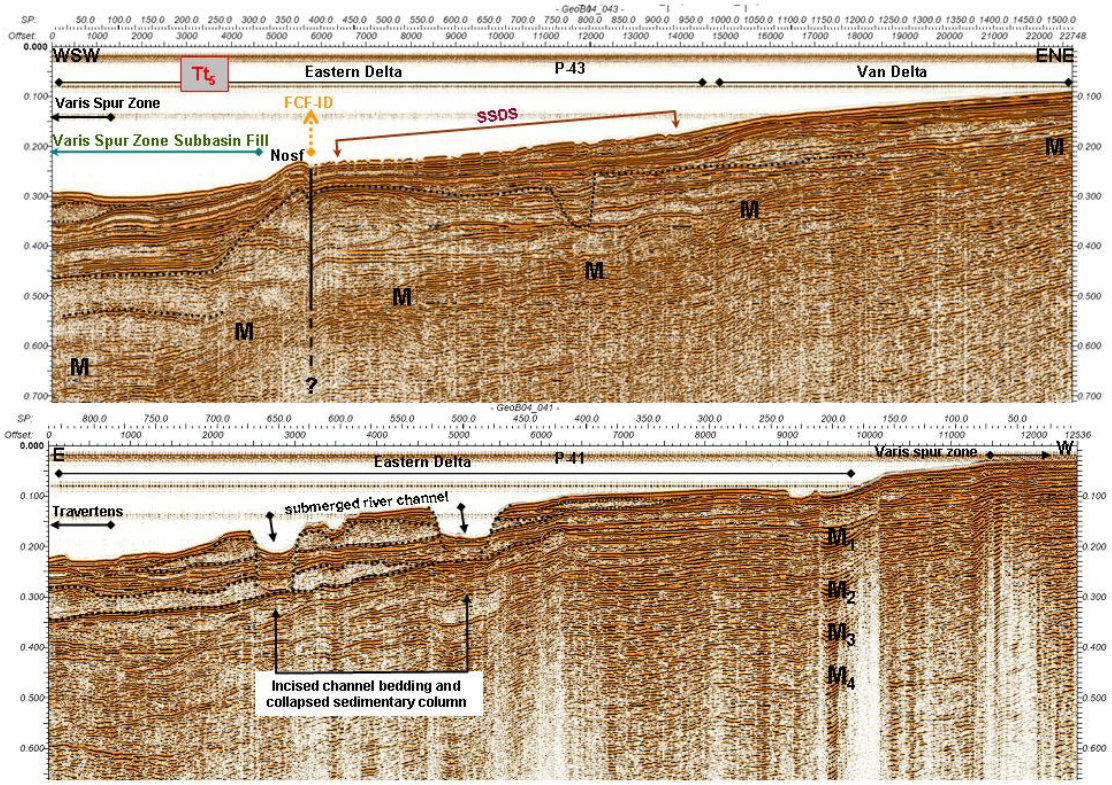

Figure 3.30 : WSW-ENE seismic section at the top from SE-delta across a zone of normal oblique-slip fault (Nosf) through Varis spur zone subbasin. Seismic profile number of this section is 43 (P-43), as seen at the top center (see the location of this profile in Fig. 2.2). M: multiple, SSDS: soft sediment deformation structures. Tt_5 (Transtension-5, red colour) describes the fifth evolutional stage of seismic structural interpretation of transtension in W-margin boundary of SE-delta (offshore Deveboynu peninsula and Varis spur zone). This seismic section clearly shows that clinoform package is recently cut by Nosf, resulting in transtensional formation of Varis spur zone subbasin, faulted clinoform failure (FCF) and internal destabilization of clinoform package (ID). W-E seismic section at the bottom from SE-delta across a zone of incised channel beddings shows SSE-end of SE-delta system and deeply incised river channels. Seismic profile number of this section is 41 (P-41), as seen at the top center. Dotted round thin lines (black colour) indicate destabilized progradation (top) and incised sedimentary beddings (bottom) (max. sediment thickness: 150-300 m, min. sediment thickness: 50-100 m, max. water depth: 150-225 m, offset: 23 km (top) and 12.5 km (bottom), two-way travel time in sec).

The integrated structural interpretation of seismic sections from E-segment and delta settings (Figs. 3.16-3.20 and 3.23-3.25) suggests that these oblique faults are en echelon in character and extensional and transtensional fault segments as a part of a dextral shearing in S-margin of the lake. These smaller fault segments seem to be horse-tail splay faults, suggesting horse-tail or imbricate fan-shaped termination of S-margin boundary fault (PDZ). Termination of the dextral shear zone in S-margin causes the extensional and transtensional formation of both Deveboynu and also Varis spur zone subbasins. This suggests that these subbasins are the releasing bends

and graben-like sedimentary depressions. The deformation style and faulting geometry of Varis spur zone subbasin indicates that the W-end of Eastern delta represents a small pull-apart boundary as a W-margin of SE-delta. This may imply that Varis spur zone subbasin seems to have been a dextral pull-apart subbasin as a result of the horse-tail or imbricate fan-shaped termination of S-margin boundary fault (PDZ).

3.1.7 Deep basin centre

W-E trending seismic section in Fig. 3.31 shows a depositional and structural geometry of Tatvan basin between Adabağ spur zone in W and Çarpanak spur zone in E. Parallel and subparallel seismic sections in the further N show an complicated structural and depositional relation of Tatvan basin to deformation in N-margin and to progradational wedges in NE-Erek delta system (Figs. 3.32-3.34).

W-E trending seismic section in Fig. 3.31 shows wedge-shaped depositional pattern of Tatvan basin, characterized by thicker onlapping sequences and that onlap is the predominant infill mechanism in deep water setting. In Fig. 3.31, onlapping sedimentary wedge having a tilted geometry, is strongly controlled by normal oblique-slip faults in W-margin and E-segment in S-margin. These seismic section perfectly shows how the fault-controlled shape of basement block of Çarpanak uplift can influence subsequent sedimentation. Thicker sedimentary wedge unconformably overlies the Çarpanak uplifted block and shows strong onlap onto the edge of Çarpanak high (Fig. 3.31). It consists of thick deep basin sediments and occasional interbedded extrusive lateral sheets. Fig. 3.31 also shows that sediment transport is from W to E and is thickest in the W-part of Tatvan basin. It gradually thins in an area of E-segment and thins rapidly in Çarpanak uplift. Wedge-shaped sedimentary package in Tatvan basin also onlaps onto lowstand progradational wedges at the edge of Erek delta body in NE (Figs. 3.32-3.34). This progradational wedge is approximately 190 m in thickness, onlapped by max. 365 m (Fig. 3.32) and by min. 230 m and max. 370 m. thicker sediments (Fig. 3.33). Lowstand progradational wedge seen in Fig. 3.32 is a member of basin floor-slope prograding complex of lowstand system tract (LST). This indicates that regressive conditions promote the formation of prograding clinoforms in this area (see also Figs 3.33 and 3.34). This area shown in Figs. 3.32-3.34 well illustrates onlap of wedge-shaped sedimentary package onto a rapidly deposited and slumped feature, for example, a progradational

lowstand wedge, a part of NE-Erek delta front, abandoned by avulsion of the main delta. In NE-Erek delta setting, shelf-break-slope bypassing results in the development of the basin floor wedge, forming lowstand extent (Figs. 3.25 and 3.32-3.34).

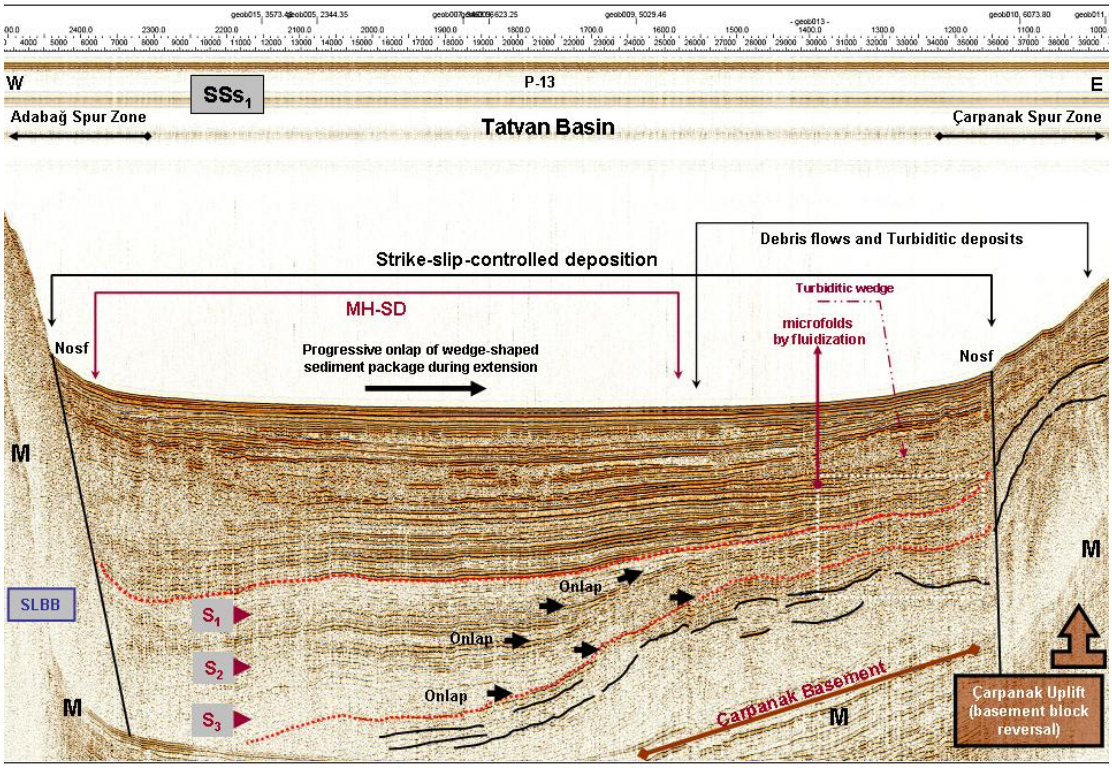

Figure 3.31 : W-E seismic section from central Tatvan basin across a zone of normal oblique-slip faults (Nosf) through Adabağ spur zone in W-margin (sublacustrine basement block-SLBB) and Çarpanak spur zone in S-margin (E-segment in Çarpanak basement block). Both blocks are cut by inter-marginal oblique-slip faults. Seismic profile number of this section is 13 (central portion of P-13), as seen at the top center (see the location of this profile in Fig. 2.2). M: multiple. SSs_1 (strike-slip sedimentation-1, black colour) describes the initial evolutional stage of seismic structural interpretation of strike-slip-controlled deposition in central Tatvan basin. Note that wedge-shaped sedimentary section of central Tatvan basin onlaps onto the foot of Çarpanak uplift during extension and that sill sequences (S_1, S_2, S_3:) from W to E are intercalated with onlapping series. Dotted thin squares (red colour) show sequence boundaries and discontinuous thick lines (black colour) indicate basement boundary of Çarpanak block. This seismic section clearly shows that the extensional tilted geometry of central Tatvan basin, differential uplift and asymmetric subsidence are accompanied by magma hydrothermal-sediment deformations (MH-SD), debris flows and turbiditic wedge deposits. This section as a central portion of P-13 requires W-E trending cross sectional correlation of Figs. 3.10 and 3.17 (max. sediment thickness: 527 m, min. sediment thickness: 336 m, onlap thickness: 250-300 m, max. water depth: 470 m, offset: 36.5 km, two-way travel time in sec).

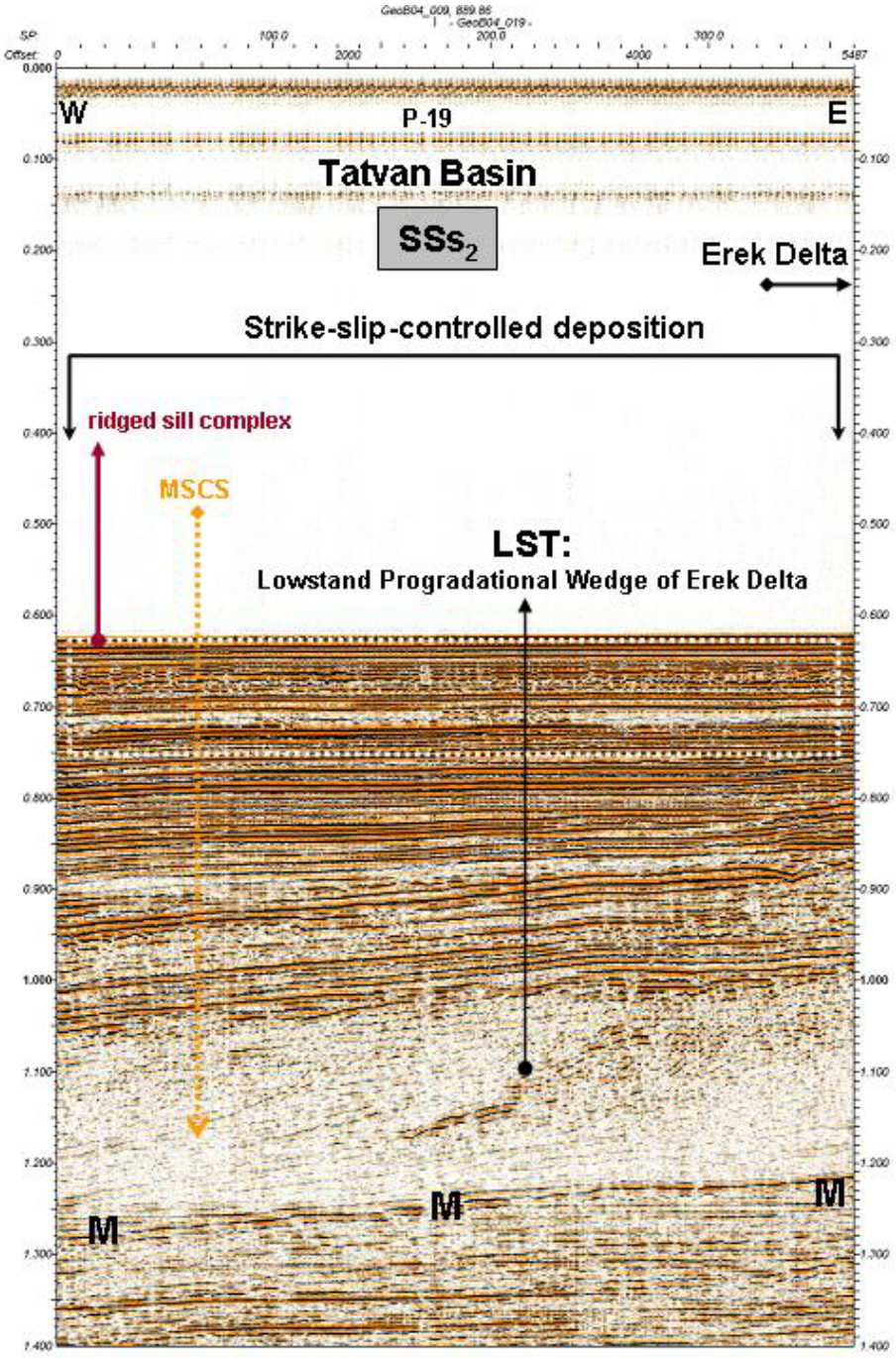

Figure 3.32 : W-E seismic section from central Tatvan basin through strike-slip-controlled deposition. Seismic profile number of this section is 19 (P-19), as seen at the top center (see the location of this profile in Fig. 2.2). M: multiple. SSs_2 (strike-slip sedimentation-2, black colour) describes the second evolutional stage of seismic structural interpretation of strike-slip-controlled deposition in central Tatvan basin. Note that well stratified and uniformly deposited sedimentary section of central Tatvan basin onlaps onto the edge of NE-Erek delta body during extension and that ridged sill complex from W to E is seen in the upper series. In this section, lowstand system tract (LST) refers to lowstand progradational wedge formed as a result of multiple slumping of clinoform successions (MSCS) from Erek delta. Progradational wedge complex clearly underlies the sedimentary section (max. sediment thickness: 560 m, onlap thickness: 375 m, max. water depth: 465 m, offset: 5.5 km, two-way travel time in sec).

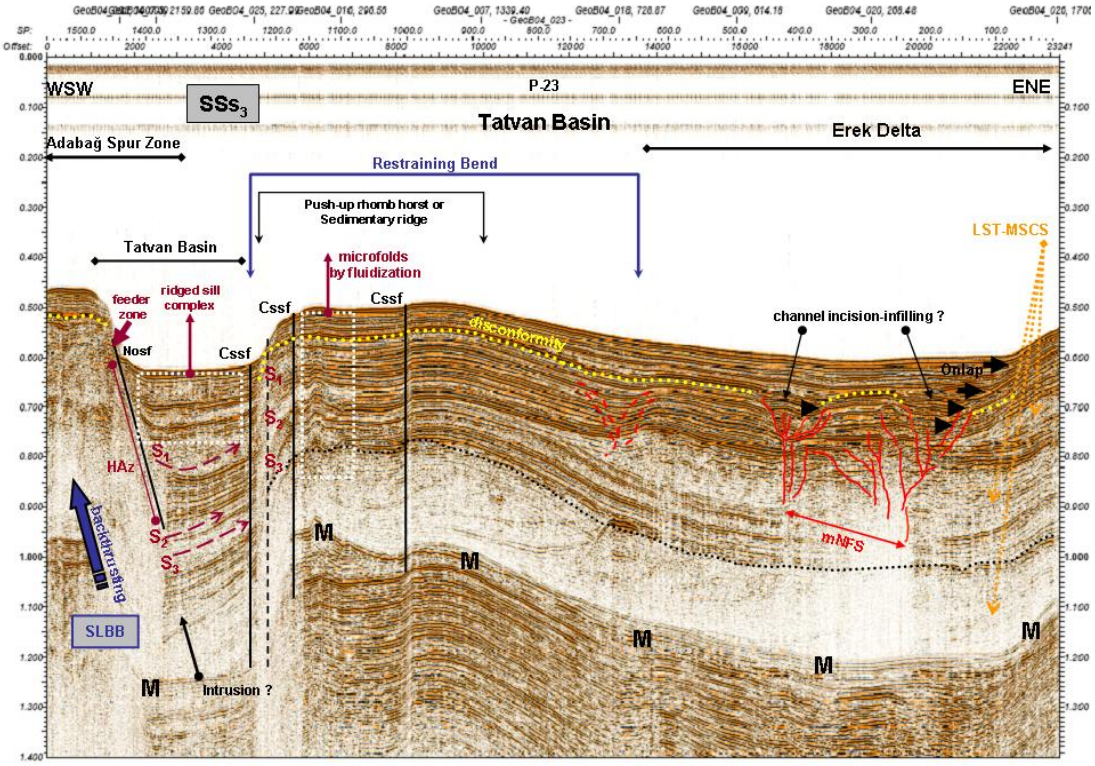

Figure 3.33 : WSW-ENE seismic section from N-part of central Tatvan basin across a zone of convergent strike-slip (Cssfs) in N-margin and normal oblique-slip faults (Nosf) in W-margin (Adabağ spur zone) through the restraining bend and NE-Erek delta. Seismic profile number of this section is 23 (P-23), as seen at the top center (see the location of this profile in Fig. 2.2). M: multiple, SLBB: sublacustrine basement block, HAz: hydrothermal alteration zones, mNFS: mini negative flower structure. SSs_3 (strike-slip sedimentation-3, black colour) describes the third evolutional stage of seismic structural interpretation of strike-slip-controlled deposition in central Tatvan basin. This section shows an image of the restraining bend in N-margin, the releasing bend in W-margin boundaries and Erek delta. Note that restrained sedimentary section onlaps onto the edge of NE-Erek delta body during extension in W-margin and that magma flow paths (S_1, S_2, S_3: sill sequences) show lateral wedge termination in push-up rhomb horst structure. In this section, lowstand system tract (LST) refers to lowstand progradational wedges formed as a result of multiple slumping of clinoform successions (MSCS) from Erek delta. Slumped progradational wedges clearly underlie the onlapping series. Dotted thin squares (white colour) show seismic structural patterns of magma hydrothermal-sediment deformations (MH-SD), (max. sediment thickness: 350 m-510 m, max. water depth: 465 m, onlap thickness: 100 m, offset: 23 km, two-way travel time in sec).

These sections show that slope failure leads to the formation of sediment slides, slide scars and resedimented deposits at the toe of slope of NE-Erek delta and into the basin floor, showing downslope resedimentation of large volumes of slope (also examine Figs. 3.25 and 3.32-3.34). These types of deposits are invariably onlapped by deep basin sediments, suggesting that such a situation results in the delta body being onlapped by the sediments in Tatvan basin. This type of onlap situation is quite

distinct from the more widespread onlap of basin margins, which is a result of basic subsidence processes in Tatvan basin. Seismic structural interpretation suggests that the deep basin onlap geometry reflects early highstand deposits in central Tatvan basin (Fig. 3.31) and that possible downlap geometry at deeper sections reflects late highstand deposits. However, downlap series are not identified in the seismic sections due to multiple effects (Fig. 3.31).

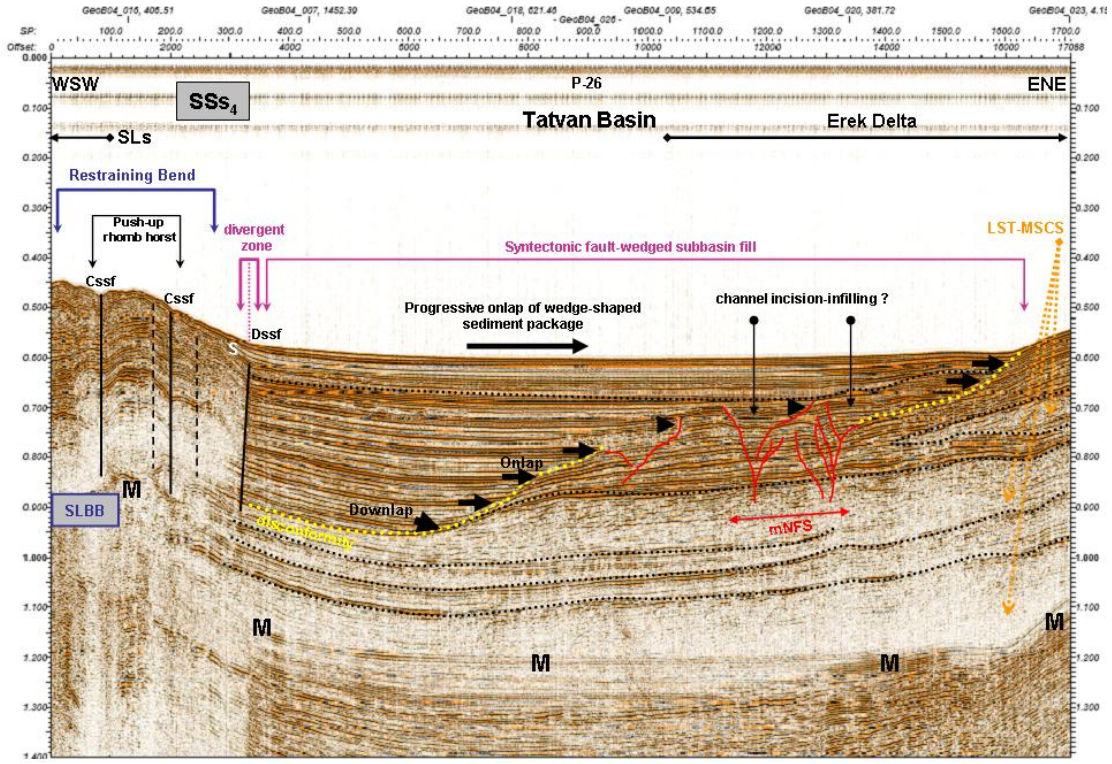

Figure 3.34 : WSW-ENE seismic section from N-margin of central Tatvan basin across a zone of convergent-divergent strike-slip faults (Cssfs-Dssfs) in N-margin boundary through the restraining bend, the fault-wedged subbasin fill and NE-Erek delta. Seismic profile number of this section is 26 (P-26), as seen at the top center (see the location of this profile in Fig. 2.2). M: multiple, SLBB: sublacustrine basement block, SLs: sublacustrine slope, S: sagging, mNFS: mini negative flower structure. SSs_4 (strike-slip sedimentation-4, black colour) describes the fourth evolutional stage of seismic structural interpretation of strike-slip-controlled deposition in central Tatvan basin. This section shows an image of the restraining bend and the divergent zone (fault-wedged subbasin fill) in N-margin boundary and Erek delta. Note that the fault-wedged subbasin fill progressively onlaps onto the edge of NE-Erek delta body. In this section, lowstand system tract (LST) refers to lowstand progradational wedges formed as a result of multiple slumping of clinoform successions (MSCS) from Erek delta. Slumped progradational wedges clearly underlie the onlapping series, (max. sediment thickness in subbasin: 310 m, max. water depth: 435 m, onlap thickness: 100 m-300 m, offset: 17 km, two-way travel time in sec).

Seismic section in Fig. 3.31 shows that beds terminate at the onlap surface, but do not terminate at the downlap surface. Since, deposition continues into the basin as thin beds parallel to the basin floor (Figs. 3.31 and 3.32). It is interpreted from Fig. 3.31 that possible downlap surface is only where beds downlapped against a topographic high that is Çarpanak uplift. This suggests that downlapping strata locally appear to be onlapping at the deeper parts of basin. This implies that onlap and possible downlap surfaces are base-discordant patterns of depositional geometry of deep Tatvan basin (Fig. 3.31).

Marked depositional changes in sedimentary section and the filling patterns are evident in the trends of main basin-bounding faults controlling asymmetric subsidence of Tatvan basin (Figs. 3.3, 3.5, 3.8, 3.9, 3.11, 3.16 and 3.31-3.33). Sediment thickness is measured from these seismic sections showing central Tatvan basin. The results show that basin fill in Tatvan basin ranges from min. 320 m to max. 580 m in thickness. The average thickness values change between min. 300 m and max. 600 m. This implies that, at least an half of thickest depositional section is structure-controlled. The faulting activity in N- and W-margins controls, at least 500 m sediment thickness, while the faulting in S-margin controls, at least 300 m sediment thickness. Thickness values are between 320 m and 370 m along W- and E-segments in S-margin and these values are between 520 m and 580 m along N- and W-margins. These abrupt variations in sediment thickness show that sedimentation in Tatvan basin is strongly fault-controlled and its N- and W-edges are represented by a thickest value 580 m, while its S-edge is represented by a thinnest value 320 m. This significantly implies a sharp thinning of depositional section from N- and W-margins into W- and E-segments in S-margin. N-S trending seismic sections in Figs. 3.3, 3.5, 3.8 and 3.9 show asymmetric depositional geometry of half-graben sedimentation with the extrusive sheet-like products in Tatvan basin, while W-E trending seismic sections in Figs. 3.10, 3.11 and 3.31-3.34 show onlapping depositional geometry of strike-slip sedimentation with the extrusive sheet-like products in Tatvan basin. 3D-seismic interpretation of the N-S and W-E trending seismic sections suggest strike-/oblique-slip sedimentation pattern, intercalated with the extrusive lateral sheet-like products of deep Tatvan basin (well seen in Figs. 3.10 and 3.31-3.34).

Marked deformational changes are also well evident in the trends of main basin-bounding faults, particularly in N- and W-margins (Figs. 3.1-3.11). WSW-ENE

striking seismic sections show a depositional trend into the deformation zone in N-margin (Figs. 3.33 and 3.34). This trend implies that that onlapping sequences of Tatvan basin and prograding wedge complexes are deformed in a complicated way by reverse oblique-slip, convergent and divergent strike-slip faults (Figs. 3.33 and 3.34). These seismic sections shown in Figs. 3.33 and 3.34 well illustrate a WSW-ENE striking cross sectional profile of horst, horst-foot graben or graben structures and the subbasin fills observed in and along N-margin. Seismic data in Figs. 3.33 and 3.34 depict Tatvan basin to be confined to the N by steep fault-bounded structures cut by transverse seismic sections. Such a configuration highlights the subsident character of Tatvan basin, revealed in seismic data by active oblique faults cross-cutting the lakefloor. Seismic structural interpretation suggests that Tatvan basin is segmented by active oblique faults along marginal sections and basin segmentation results in the deposition of deep basin strata in evolving internal sedimentary depressions or subbasins well observed in basin margins.

The seismic information from marginal and basinal sections and structural interpretation presented above, together with the sedimentation observed in Tatvan basin, proves that lateral facies distribution is closely dependent on the major tectonic events affecting the margins. In fact, several types of stratigraphic pinch-outs onto basin-margin structures are observed on the seismic record. Lateral variations and lateral pinch-outs onto structural highs mark significant lateral facies variations (Figs. 3.6, 3.24, 3.31, 3.33 and 3.34). Moreover, it is assumed that depocenter migration in Tatvan basin denote the lateral shifting of depocentres with time, with emphasis to the base of the onlapping strata and lateral extent of progradational wedges into the basin floor (see and examine Figs. 3.31-3.34). The depositional geometry and internal character of overall sedimentation in Tatvan basin from N-S and W-E trending seismic sections reveals that a major period of subsidence and subsequent basin infill occurred. These seismic sections also show that basin-bounding faults are particularly active during the deposition of deep lake sediments, as shown by significant onlap and thinning of strata onto major structures seen in seismic sections (Figs. 3.31-3.34). Moreover, the strong internal reflections as multiples are seen in seismic sections in Figs. 3.31-3.34. These ringing multiples are mainly developed in basement block uplifts in N-margin, Çarpanak spur zone and delta settings.

So care must be taken that these basement features are not confused with other lithologies that can also produce a similar seismic response, for example, intrusive-extrusive activity and laterally extensive sheet-like products. This case is perfectly imaged in W-E trending seismic section of Tatvan basin, showing lateral sheet-like features and the edge of Çarpanak basement separated by an onlap surface (Figs. 3.31). This is also a case recognized between sheet-like features in W-margin and progradational wedges from NE-Erek delta seen in Figs. 3.33. In seismic structural interpretation, a particular attention is given for structural discrimination of lithologies having similar seismic response.

Seismic sections in Figs. 3.3, 3.5, 3.8-3.10 and 3.31-3.34 show distinct seismic characters and vertical stacking patterns for the strata filling the depocenters involving subbasins. This case stresses that different tectonostratigraphic records should exist. Striking spatial variations in basin-margin morphology and relative sediment thickness are also noted in these seismic sections. Structural differences between the seismic sections from different marginal sections reveal major changes in depocenter and subbasin development and also morpho-physiography. Subbasins or graben-like depositional troughs seen along margin-bounding faults evolved through the oblique faulting as structurally segmented depocenters, at places connected by active faulting (Figs. 3.2-3.9, 3.13, 3.18-3.20, 3.23, 3.26-3.29 and 3.30 at the top). As a result of this complex setting, eight types of stratigraphic contacts in basin-margin structures are recognized by evaluating the lateral changes in geometry on seismic data. An important characteristic of these types of contacts is to enable basinal correlations of vertically stacked fills. Particular attention is given to the recognition on seismic data of the stratigraphic surfaces marking the significant structural and depositional events shaping the Lake Van basin. These contacts are recurrent throughout the basin with type of pinch-out onto gentle basin-margin structures clearly predominating and thickening onto abrupt basin-margin features, mostly on fault-bounded slopes. These contacts are well identified in Tatvan basin and margin-bounding faults (for example Figs. 3.10, 3.11 and 3.31). Onlap of buried topography, laterally migrating pinch-out and thickening (growth) geometries characterize the contact type identified in W- and E-parts of Tatvan basin (Fig. 3.31).

Truncation within incised valleys and onlap and pinch-out within incised valleys or paleo-river incisions and also pinch-out due to erosional truncation are recognized NNW-part of Tatvan basin and NE-Erek delta setting (Figs. 3.6, 3.7, 3.24, 3.33 and 3.34). Amalgamated contacts as complex interfingering are well reflected by intrusive activity in W- and S-margins (Figs. 3.8, 3.9, 3.15, 3.16, 3.18, 3.26 and 3.27). These types of contacts are more frequent in the lake, indicating active structural and depositional evolution.

These findings of seismic structural interpretation have important implications for tectonic and kinematic models of margin boundary faults and provide very useful information for understanding structural development of Lake Van basin. As well known, an important aspect of seismic structural interpretation is to attempt to understand the causes of the structuring. A correct tectonic interpretation of structures identified in seismic records and their causes is also fundamental to understanding structures, structural relations and tectonic framework in deformed zones of lake margins. Hence, the observed structures are, at a basic level, grouped into three broad categories: 1- Margin-bounding faults are primary structures and basement involved. 2- Subsidiary-splay faults or fault branching, folds developing in the sedimentary cover and subbasins or mini-basins are seconday structures developed by major basement-involved structures and directly related to the primary structures. 3- Intrusive-extrusive activity, laterally extensive sheet-like products and related deformation patterns and delta progradation-related deformations are passive or adjustment structures developed as a consequence of, or as an after effect of, primary and secondary structural effects. This subdivison into such a seismic structural scheme provides an appreciation of cause and effect and so be used predictively.

3.2 Structural Description of Seismic Reflection Images and Tectonic Interpretation of Structural Domains

Seismic expressions of structural styles, image analysis of reflection profiles and seismic structural interpretation reveal that deformation style in N-margin is characterized by a relatively shorter (roughly 15-20 km in length) restraining bend, seismically reflecting a well defined positive flower structure. Branching faults and fault splays control the external and internal subbasin development.

N-margin is a complicated shear zone of sinistral transpressional regime producing typical secondary features of the oblique deformation. Seismic reflection profiles showing the deformation in N-margin (Figs. 3.1-3.7) are numbered and respectively ranged from Tp_1 to Tp_7 (Transpression) to underline predominant deformation style and faulting activity in the margin. This provides an easy way to examine and review seismic structural continuity and seismic evolution of deformed zone in and along parallel and subparallel sections.

Deformation style in S-margin is characterized by a relatively longer (roughly 70 km in PDZ-length) releasing bend, structurally reflecting en echelon arrangement of W- and E-segments of the faulting in S-margin and a well defined negative flower structure. W- and E-segments are respectively 30 km and 33 km in lengths. Branching faults and fault splays control the internal subbasin development. S-margin is a complicated and broadly widening shear zone of dextral transtensional regime producing typical secondary features of the oblique deformation. Seismic reflection profiles showing the deformation in W- (Figs. 3.13- 3.15) and E- (Figs. 3.16-3.25) portions of S-margin are numbered and respectively ranged from $Ws\text{-}Tt_1$ to $Ws\text{-}Tt_3$ (W-segment-Transtension) and from $Es\text{-}Tt_1$ to $Es\text{-}Tt_8$ (E-segment-Transtension) showing predominant deformation style and faulting activity in the margin. Both N- and S-margin boundary faults perfectly represent a typical structural development of flower-shaped complex faults associated with internal-external subbasins.

Deformation style in W-margin is characterized by a relatively shorter (roughly 13-15 km in length) releasing bend, seismically reflecting WSW-continuation of N-margin boundary fault. Branching faults and fault splays control the external subbasin development. W-margin is a complicated shear zone of sinistral transtensional regime producing typical secondary features of the oblique deformation. W-margin may imply the pull-apart boundary of central Tatvan basin in its W-end. Seismic reflection profiles showing the deformation in W-margin (Figs. 3.8-3.11) are numbered and respectively ranged from Tt_1 to Tt_4 (Transtension), showing predominant deformation style and faulting activity in the margin.

Deformation style in W-edge of SE-Delta is characterized by a relatively shorter (roughly 20-25 km in length) releasing bend, structurally reflecting SSE-termination of S-margin boundary fault (PDZ) associated with E-segment. The fault termination

is horse-tail or imbricate fan-shaped. Branching faults and horse-tail splay faults seem to be discontinuous and en echelon-like smaller fault segments controlling an axial elongation of the internal subbasin development. The subbasin formation causes W-end of SE-delta. This edge of SE-Delta is a complicated shear zone of dextral transtensional regime producing typical secondary features of the oblique deformation. Deformation may imply the pull-apart boundary in its W-end of SE-Delta. Seismic reflection profiles showing the deformation in W-edge of SE-Delta (Figs. 3.26-3.29 and 3.30 at the top) are numbered and respectively ranged from Tt_1 to Tt_5 (Transtension), showing predominant deformation style and faulting activity in the margin.

Seismic structural view is that N- and S-margin boundaries of Lake Van are shaped by flower structures. W-margin boundaries of the lake, such as central Tatvan basin and SE-delta setting, are shaped by pull-apart structures. This indicates that Lake Van is a rhombic-shaped basin block, subjected to the oblique-slip deformation. Seismic reflection profiles showing deformational and depositional styles in central Tatvan basin (Figs. 3.31-3.34) are numbered and respectively ranged from SSs_1 to SSs_4 (Strike-slip sedimentation), showing predominant deformation and deformation-controlled sedimentation in Tatvan basin. These seismic sections taken from central Tatvan basin, in fact, well summarize how transpressional (N-margin) and transtensional regimes (W- and S-margins) have resulted in a complicated tectono-sedimentary/-stratigraphic development of Lake Van. Therefore, structural description of seismic reflection images and tectonic interpretation of structural domains is mainly based on the complexity and variety of seismic structures. This structural complexity individually or in combination has five main aspects in basinal and marginal domains of Lake Van region: (1) divergent and convergent nature of N-margin transpressional fault as a “palm tree structure”, (2) the en echelon and divergent nature of S-margin transtensional fault as a “tulip structure”, N- and S-margins have structural complications due to component of reverse or normal dip-slip on the basement fault and lateral offsets of basement-involved strike-slip faults which create local extensile (graben-subbasins) or shortening (horst-shaped uplifts) structures. (3) internal and external subbasin or mini-basin formations and structural geometries through N- and S-margin boundary sections, (4) gravity-driven folding of the sedimentary cover in central Tatvan basin, (5) prominent strike-slip

sedimentation in central Tatvan basin. Seismic image analysis of these structural styles, their structural descriptions and general tectonic interpretation of reflection data are given below in much detail.

3.2.1 Marginal domain

Figs. 3.1-3.7 are grouped sections of seismic track lines from N-margin across sublacustrine basement block through a complex shear zone of reverse oblique-slip faults. Thus, these figures well express a seismic structural arrangement of grouped seismic sections and manifest an axial and marginal elongation of the observed faults in N. Grouped seismic sections from parallel track lines give a descriptive and conceptual clue to both the deformation type and the faulting history in N-margin. A grouped illustration of parallel seismic sections provides a tectonic overview in understanding and modeling evolutionary domains of lake.

A seismic structural interpretation of the fault systems (particularly in Figs. 3.1-3.11) in marginal sections suggests that these fault systems form a type of branching and braided strike-slip zones. These braided fault zones consist of anastomosing faults and obliquely trending folds. These faults display local complexities that have only obscure kinematic relations to strike-slip origin (Crowell, 1974a). As shown in Figs. 3.8-3.11, individual faults exhibit dip-slip and dip-separations. As shown in Figs. 3.1-3.7, those originated as wedges within the zone are squeezed upward and others, during sagging of wedges downward (Wilcox et al., 1973; Crowell, 1974a). The N-margin boundary fault zone in Figs. 3.1-3.7 shows these complicated patterns very well. This margin boundary, as a pre-existed thrust fault contact, on a basin scale is weak, so that when a crustal block is pressed upward beside a nearly vertical fault, the hanging wall sags outward and downward, indicating a reversed oblique-slip fault. Such an origin for local complexities is described, especially in places where horsts and grabens are associated with strike-slip zones by Wilcox et al., (1973) and Crowell, (1974a). Braided zones are also recognizable in diagrammatic map by Crowell, (1974a) showing progressive development of fault splays and wedges on a right-slip fault. Straight fault gradually develops a bend through time and eventually forms a fault wedge. Based on seismic structural interpretation, oblique slip-controlled structures are examined and described below.

3.2.1.1 Fault systems: convergent and divergent strike-slip faults

Seismic structural interpretation indicates that Lake Van basin is an elongate block in the zone of strike-/oblique-slip faulting. Its N- and S-margins are bounded by various arrangements of convergent (transpressive) and divergent (transtensive) strike-slip faults and related uplifts and subsidence (Figs. 3.1-3.7 and 3.13-3.25). The geometry and style of structures associated with strike-/oblique-slip faulting depend greatly on several factors at different places along and within a strike-slip fault zone. This includes the nature of the rocks being deformed, the configuration of pre-existing structures, the amount of horizontal slip, the contribution of the vertical component of slip, and the strain rate (Sylvester, 1988). The most important factor governing uplift or subsidence along a strike-slip fault in N-margin is the bending geometry of the fault surface relative to its slip vector, because this determines whether, local convergence or divergence will occur (Crowell, 1974b; Sylvester, 1988). Where strike-slip movement is inhibited by restraining bends (Crowell, 1974b), convergent strike slip or transpression (Harland, 1971) occurs associated with crowding, crustal shortening, and uplift (Figs. 3.1-3.7). Releasing bends (Crowell, 1974b) provide for transtension (Harland, 1971) or divergent strike slip accompanied by stretching, crustal extension, subsidence, and formation of pull-apart basins (Figs. 3.8-3.11, 3.13-3.29 and 30 at the top). As well known, strike-slip faults in domains of pure shear do not evince offsets measurable in hundreds of kilometers, because of room problems that result from convergence of large crustal masses. However, simple shear has a monoclinic symmetry of strain because it is rotational, and a greater variety of structures forms in simple shear than in pure shear (Sylvester, 1988). The structures in these simple shear systems typically form en echelon arrangements in relatively narrow zones. Therefore, an appreciation of crustal mobility and flexibility, both vertical and horizontal, is of particular importance for arriving at tectonic understanding of deformation in strike-/oblique-slip fault zones (Crowell and Sylyester, 1979 Sylvester, 1988). Because, crustal blocks move laterally over time, they may alternately rise and sink.

N-margin shows very steep and regular sublacustrine slope, along which N-margin boundary fault emplaces and cuts this steep slope. It is also bathymetrically clear that the N-part of the lake is tectonic-controlled (Figs. 3.1-3.7). The oblique-slip boundary in N-margin is where strike-slip movement is convergent. This shows that

strike-slip fault is a typical belt of braided, nearly vertical shears, bounding elongate block (push-up rhomb-shaped horst). This horst block is squeezed upward along those shears to make high-standing source areas for sediments (Crowell, 1974b; Sylvester, 1988). The oblique-slip boundary in S-margin is where strike-slip movement is divergent. This shows that crustal block sags, subsides, or tilts between or adjacent to bounding faults. (Figs. 3.13, 3.14, 3.16-3.20 and 3.23-3.25). This makes local sites for deposition of sediments whose stratigraphic characteristics reveal much about the related tectonic activity (Balance and Reading, 1980; Sylvester, 1988). The uplift and subsidence of elongate ridges of rocks, bounded by steep, inward-dipping minor faults in strike-/oblique-slip fault zones (see Willis, 1938b) is a common mechanical result of continued pressure in a zone traversed by vertical shears. This case is well imaged along Figs. 3.1-3.7. In these sections, the crushed sedimentary rock in the zone is both squeezed up (pushed-up rhomb-horst) and down (fault-wedged mini-basin), with the result that the stresses are carried back into the adjacent masses. Reversed oblique-slip faults are thus, developed in the latter. They curve upward (upthrust) in the direction of least resistance (Figs. 3.2-3.10). They thus become up-curving thrusts or ramps, and blocks. Blocks within such an obliquely faulted zone are completely isolated by minor faults. They are pushed about, mayhap up or down, mayhap over or under, and lengthwise along strike. This process is “wedge-block faulting,” as termed by Willis, (1938a). Thus, the uplift can be regarded as wedge both in horizontal and vertical views (similar to the notions, “center-trough ridge” or “pressure ridge” in Sylvester, 1988).

PDZ in S-margin boundary passes through the S-portion of central Tatvan basin from W to E (Figs. 3.13, 3.14, 3.16-3.20 and 3.23-3.25). It is broadly widening shear zone, having two important en echelon segments; W and E-segments. W-segment is located in SSW at the W-part of Deveboynu peninsula (Figs. 3.13-3.15) and E-segment is located in SSE at the E-part of Deveboynu peninsula offshore Çarpanak spur zone (Figs. 3.16-3.20 and 3.23-3.25). W-segment shows highly irregular coastal morphology, implying the strong kinematic links with irregular coastal and morphological ranges. In and through W-segment, a group of passive (peripheral collapses) and active (younger intrusions) dome-cone complex is both morphologically and also seismically recognized. It is clear that W-segment from SSW-corner (Tatvan delta) to further E (offshore Deveboynu peninsula) is

magmatism-controlled. The interpretation of seismic sections from W- and E-segments suggests that the faulting in S-margin evidently evolved from the Nemrut volcanic dome-cone complex in W through Tatvan delta to Çarpanak spur zone in E, between two or more, right-stepping en echelon dextral oblique faults of a larger dextral oblique-slip fault system (PDZ). The dominant focal mechanism of the earthquake sequence is dextral transpression (Dhont and Chorowicz, 2006; Pınar et al., 2007). This shows that S-margin boundary is overstepped and discontinuous pattern from W to E and broadly widening transtensional shear zone rather than a single boundary fault. Discontinuity in this fault is composed of interacting segments (see also discussion for overstepped strike-slip faults in Mann et al., 1983; Hempton and Dunne, 1984; Sylvester, 1988). The structural geometry of the overstep offshore Deveboynu peninsula between W- and E-segments, depends on the length overlap, the width of the gap between the fault segments, and the depth to the PDZ in the basement.

It is interpreted that kinematic nature of S-margin boundary fault (PDZ) is "Helicoidal" form of individual Riedel shears in right simple shear (see and examine Fig. 3.35). Structural pattern in Fig. 3.35 suggests that W- and E-segments are the main R shears, and R shears or fractures have a "Helicoidal" shape in three dimensions. In fact, this geometry is a consequence of three factors (Naylor et al., 1986; Sylvester, 1988): (1) the en echelon nature of the shears at the surface; (2) their concave-upward geometry when formed in shear without components of convergence or divergence; and (3) the need to join a single basement fault at depth. It is important to note that the strike-slip fault at depth is sufficiently "small or deep" that a through-going fracture fails to develop at the surface (Naylor et al., 1986). Instead, only a long, narrow zone of en echelon normal faults or R shears forms (Erdlac and Anderson, 1982), associated with en echelon folds (Figs. 3.3, 3.5, 3.8, 3.9 and 3.35).This reveals that en echelon arrays composed only of extension fractures, gash-fractures, vents or normal faults are common above a buried strike-slip fault (Sylvester, 1988). It can be considered that synthetic Riedel shears are initially formed in S-margin boundary fault. Soon after the initial formation of the R shears, the incremental strain field is locally modified in the deformation zone. This gives rise to the development of short-lived splay faults (Figs. 3.13 and 3.14). Splay faults form at the tips of the R shears and curve toward parallelism with the extension

fractures (Fig. 3.15) so that an R shear will be a strike-slip fault in the central part of the deformation zone (see and examine PDZ line in Figs. 3.13, 3.14, 3.16, 3.18-3.20, 3.24 at the bottom and 3.25). Figs. 3.3, 3.5, 3.8, and 3.9 show the folding across central Tatvan basin close to N-margin boundary fault. The folding trends WSW-ENE subparallel to N-margin. The folding, together with the en echelon faults in S-margin has an en echelon arrangement (see Fig. 3.35 for this geometry). This is related to syn-tectonic strike-/oblique-slip motion, associated with the opening of the basin from S-margin boundary (see related text in Sylvester, 1988). As a result, central Tatvan basin floor tilts in the form of a half-graben so that the stratal thicknesses are asymmetric, being thickest on N- and W-sides of the basin (also see Figs. 3.10, 3.11, 3.31). The extended shear domains within the releasing bends in W- and S-margins (W- and E-segments) can be depicted as having a mesh-like arrangement of various extension fractures (Figs. 3.3, 3.5, 3.8-3.11, 3.13-3.16 and 3.18). These extension fractures are characterized by opening vents, volcanic cones, linear volcanic clusters, magmatic intrusions and peripherally collapsed parasitic cones on S-shore.

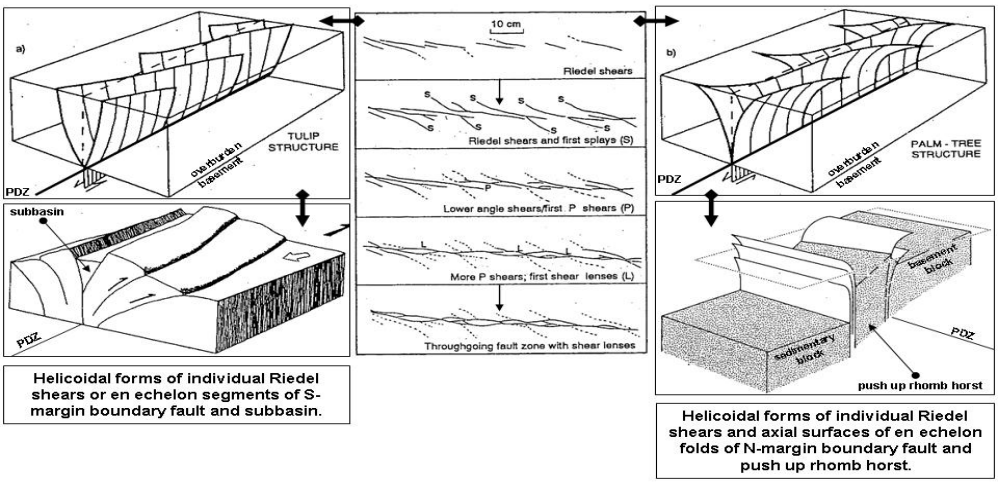

Figure 3.35 : Conceptual 3D-block diagrams of flower structures in S- and N-margin boundaries of the lake illustrate tulip structure (negative flower structure) with axial graben (subbasin) in divergent strike-slip shear zone of S-margin boundary (the left column) and palm tree structure (positive flower structure)with axial push up rhomb horst (sedimentary ridge) in convergent strike-slip shear zone of N-margin boundary (the right column) (modified after Sylvester and Smith 1976; Steel et al., 1985 and Sylvester, 1988). Sequences of Riedel shear fracture development in plan view of a sand box experiment above a strike-slip fault (Naylor et al., 1986) show possible progressive development of Riedel shears in N- and S-margins (the center column). At the top left, transtensional shear zone in S-margin is the similar as helicoidal forms of Riedel shears in sandbox experiment (Naylor et al., 1976). At the top right, transpressional shear zone in N-margin is the similar as helicoidal forms of axial surfaces of en echelon folds (Sylvester, 1988).

Splays or secondary faults controlling subbasins (Tatvan delta graben basin, Deveboynu and Varis spur zone basins) are also present within these seismic sections in a geometrical arrangement that mimics the pattern of PDZ in S-margin.

Rising magmatic materials and related deformations along and through the oblique fault in W-margin are recognized (Figs. 3.8-3.11). S-margin boundary fault also gives evidence that the magmatic intrusions, together with collapsed parasitic dome-cone complex, formed in a long-lived extensile tectonic regime related to transtensional regime in W- and S-margins (decompressional alkaline magmatism. in Şengör et al., 2003) (Figs. 3.13-3.16 and 3.18). However, it is interesting to note that there is a peculiar intrusive activity seen in Fig. 3.6, very close to reverse oblique slip fault in N-margin. It is assumed that transtensional activity across zones of normal oblique-slip faults in W- and S-margins must have been related to orogen-parallel strike slip activity (Tobisch et al., 1986; Sylvester, 1988). The orogen-parallel activity may imply Muş or Cryptic suture-parallel oblique-slip regime (see Şengör et al., 2008 for the sutures). This is supported by the syn-kinematic intrusion of granitic plutons into pull-apart structures along major transform fault zones by Michard-Vitrac et al., (1980). These fault zones provide a domain of extension for the intrusions (Castro, 1985; Gapais and Barbarin, 1986; Guineberteau et al., 1987; Sylvester, 1988), as shown in W- and S-margins. Suture-parallel transtension and also syn-kinematic intrusion of magmatic materials imply tectonic importance of S-margin boundary fault (PDZ). An axial elongation of W-segment is entirely covered by collapsed parasitic cones and active ones, which are located on the N-end of BP-M (the S-shore of lake) (Figs. 3.3, 3.5, 3.8 and 3.9). These passive cones are also morphologically defined and clearly represented by pre-existing intrusive domes. This suggests that W-segment of S-margin boundary fault is extended over this collapsed dome-cone complex. The activation of this segment is accompanied by these collapsed cones. W-segment is contemporaneously activated with volcano-magmatic activity along S-shore of the lake. This proposes the presence of syn-tectonic magmatic activity notably through S-margin boundary.

Seismic structural interpretation through fault systems in marginal sections shows the oblique-slip nature of margin-bounding faults. N-margin boundary are morphologically regular and tectonic-controlled (tectonic margin), while S-margin boundary is morphologically irregular and magmatism-controlled (magmatic

margin). W-margin is also interpreted as a magmatism-controlled pull-apart boundary. Margin-bounding faults are well recognized in both bathymetric and morphological maps. The tectonic interplay between the W-, N-and S-margin boundary faults outlines domains of uplift and subsidence within the basin. This indicates that basin terminates in a detachment at a relatively shallow level. This proposes that the lake as a wedge-block obliquely moves toward the ENE. It seems that margin boundary faults are discontinuous intra-plate faults and most probably restricted to the upper crust. Intra-plate faults typically separate regional domains of extension, shortening, or shear (Sylvester, 1988). Hence, there may be some possible relations between strike-/oblique-slip faults and crustal delamination process at or near the seismogenic zone. This gives a mechanism for regional rotation and translation of crustal slabs and flakes (Dewey et al., 1986; Sylvester, 1988). However, how general and widespread are intra-crustal process, and how the mechanisms operate that drive this detachment tectonics is questions that require additional seismic observations, seismic data and 3D-modeling.

3.2.1.2 Fault deformation systems: flower structures, fault wedge-subbasins, block uplifts, and backthrusts

Seismic structural interpretation and kinematic indicators show that N-margin boundary is typical example of positive flower structure within a narrow shear zone, associated with internal and external subbasins (Figs. 3.1-3.7). However, S-margin boundary is negative flower structure within a widening shear zone, associated with internal subbasins (Tatvan delta graben basin, Deveboynu and Varis spur zone subbasins) (also examine particularly Figs. 3.13, 3.14 and 3.16-3.20).

Structural terminology to describe kinematic features of the observed tectonic styles in N- and S margins is frequently used, as defined by Sylvester, (1988). Descriptions of the two-dimensional arrangement of the faults in interpretations of seismic sections and structural cross sections have a variety of botanical appellations, including “flower structures” by Sylvester, (1988) (see also kinematic description and classification of these structures in Sylvester, 1988). Flower structures are classified into two classes; “positive” and “negative”. The former is “positive flower structure” (Wilcox et al., 1973) or “palm tree structure” (Sylvester and Smith, 1976) (Fig. 3.35), as well as “pop-up,” “squeeze-up,” and “tectonic wedge” in convergent strike slip (Sylvester, 1988).

The latter is “negative flower structure” (Harding and Lowell, 1979) or “tulip structure” (Naylor et al., 1986) (Fig. 3.35) in divergent strike slip (Sylvester, 1988).

Fig. 3.35 well illustrates that the term “palm tree structure” is preferred to describe the convex-upward geometry of faults in profile that bounds an uplifted block in a strike-slip fault zone. The term “tulip structure” is preferred to evoke a clear image of the concave-upward geometry of faults in profile that form in divergent strike-slip. “Tulip structure” is also used in place of “negative flower structure” (Sylvester, 1988). Detailed structural interpretation of seismic sections suggests that the N-margin boundary fault associated with a style of folding is a prominent product of “palm tree structure” and the S-margin boundary fault associated with E- and W-segments is a product of “tulip structure” (see Fig. 3.35). “Palm tree structures” and “tulip structures” (see also Harding and Lowell, 1979; Bally, 1983; Harding 1985 for terminology) are typified by having reverse-and dip-separation faults (convergent and divergent strike-slip faults) side by side across the crest of the structure (Fig. 3.35). This conceptual diagram of palm tree structures (positive flower structure) in right simple shear is well documented by Sylvester, (1988). The presence of divergent and convergent strike-slip faults in N-margin boundary suggests that some of the faults of oblique-slip motion are indeed thrusts that reflect the overall uplift of the central block and shortening across it (convergent strike-slip faults in Figs. 3.1-3.7). However, some others are just as clearly normal faults, reflecting the extension across the top of uplifted and laterally spreading block (divergent strike-slip faults in Figs. 3.1-3.7) (Sylvester and Smith, 1976; Sylvester, 1988) shown diagrammatically in Fig. 3.35. Pushed-up, rhomb-shaped horst geometry (sedimentary ridge) in between central Tatvan basin and sublacustrine platform is very similar to palm tree geometry in Sylvester and Smith, (1976) and in Sylvester, (1988). The presence of divergent strike-slip faults in the S-margin boundary suggests that the faults of oblique-slip motion are just as clearly normal faults, reflecting the extension (divergent strike-slip faults in Figs. 3.13, 3.14, 3.16-3.20, 3.24 at the bottom and 3.25) shown diagrammatically in Fig. 3.35. This represents tulip structure (negative flower structure) or palm tree structure with axial graben by Steel et al., (1985). Central graben structure in Fig. 3.35 represents the subbasins or mini-basins through the PDZ in S-margin. It is clear from seismic sections that in E-segment, Çarpanak spur zone and Deveboynu peninsula are transpressed uplifts by tulip structure or

palm tree structure with axial graben. This axial graben is controlled by splays or secondary faults and characterized by Deveboynu and Varis spur zone internal subbasin systems. These subbasins are located in this axial graben system. In W-segment, Tatvan delta graben basin also seems to have been controlled by the same tulip structure. En echelon oblique motion of the S-margin boundary fault can be structurally represented by a broadly widening shear zone of tulip-type negative flower structure with axial grabens (Fig. 3.35).

In the N-margin boundary, and especially within its border-shear zone, rhomboidal wedge-shaped subbasin is associated with similarly shaped high-standing block uplift, bank or sedimentary ridge, which is pushed up, rhomb-shaped horst block (Figs. 3.1-3.5). Such a fragmented portion of the sedimentary cover can be visualized theoretically as forming within a strike-slip regime if the major strike-slip faults converge and diverge in map view (Crowell, 1974a). In a left-slip system of the N-margin boundary (Figs. 3.1-3.7), where two major left-slip faults converge, assuming concurrent or intermittently alternating movement on each. The wedge between the faults will be compressed and elevated where the faults diverge, the block is extended and terrane subsides (Crowell, 1974a). Many faults in a broad and anastomosing system probably do not all move at the same time. Those that predominate become straighter and longer, whereas some early faults are bent and rotated out of an orientation conducive to easy slip. Sketch map illustrated in Fig. 3.36 by Crowell, (1974a) shows an uplift of tip of fault wedge with convergence of strike-slip faults, and an subsidence of tip with divergence (see text for discussion in Crowell, 1974a). In Fig. 3.36, only some situations from a range of possible topographic results of slip along a bifurcating dextral fault give fault-wedge basins. Figs. 3.35 and 3.36 diagrammatically show that in N-margin, an uplifted central block appears to be pushed-up, rhomb-shaped horst and/or uplifted sedimentary ridge, nearly 2-3 km wide between the two sub-parallel oblique-slip faults (divergent and convergent strike-slip faults). This horst uplift necessitated by the convergent strike-slip is accommodated by the folding and by a variety of secondary or splay faults. Some of these faults project into the main fault that bounds this uplifted central block (convergent strike-slip faults).

Some others dip away from the central block as back-thrusts or up-thrusts (reversed oblique-slip faults) and die out in bedding surfaces (toward lacustrine shelf) (see for the sample in Sylvester and Smith, 1976).

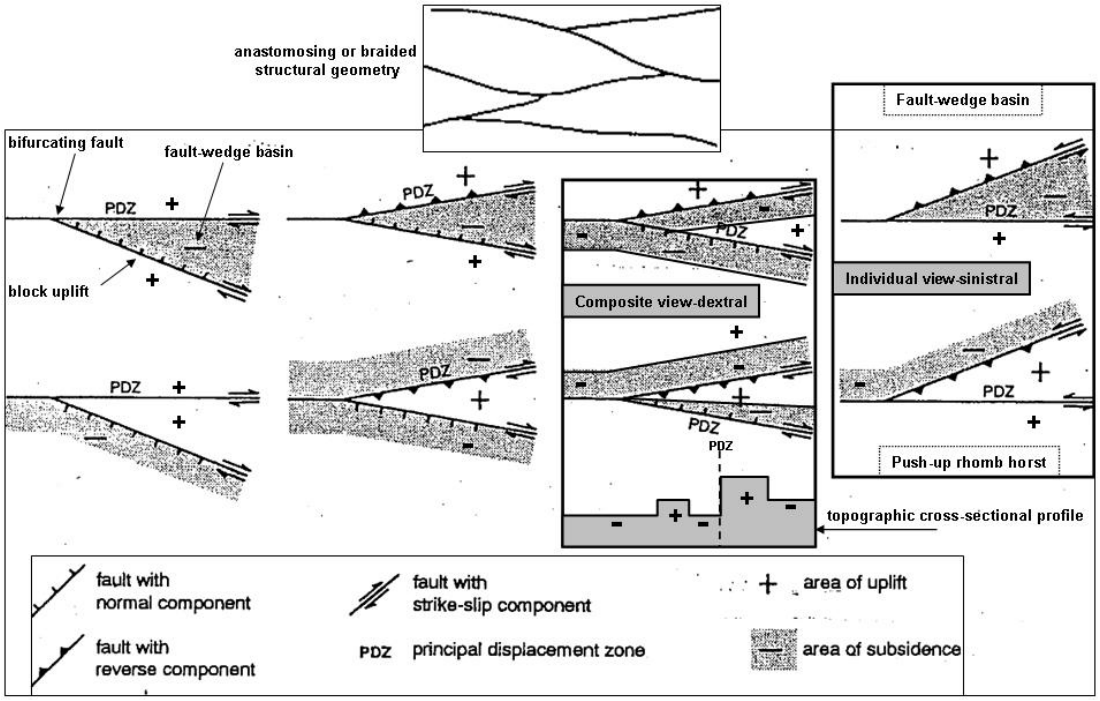

Figure 3.36 : Range of possible topographic results of slip along a bifurcating oblique-slip fault (after Christie-Blick and Biddle, 1985) illustrates that only some situations give fault-wedge basins *sensu stricto* (Woodcock and Schubert, 1994). Topographic composite views of push-up rhomb horst structure (+) and fault-wedge subbasin (-) through N-margin boundary fault show different plan views of a topographic cross-sectional profile (see Figs. 3.3 and 3.4). Topographic individual views of push-up rhomb horst structure and fault-wedge subbasin are respectively shown in the right column (see Figs. 3.3 and 3.4 for structural and topographic correlation).

Ideas developed by Crowell, (1974a) to explain horsts and grabens and changing fault dips along strike-slip fault zones in some regions can be modified to apply to the structural complexity between N- and W-margins. Structural interpretation of Figs. 3.1-3.11 as combined with Figs. 3.35 and 3.36 suggests that all of the faults bound a rhomb-shaped domain of folded strata, which resembles the push-up seen at the toe of some overthrust faults. The axes of the folds in the rhomb-shaped domain along convergent and divergent strike-slip faults are oriented at low angles to the main fault and rhomb-shaped structure. They constitute a transected series of en echelon folds (see also convergent strike-slip faults, offshore oil fields of S-California and in the Taranaki basin of New Zealand in Sylvester, 1988).

The N-margin boundary in a transpressional regime shows tipped fault wedges where left-slip faults converge or diverge (see text for discussion in Crowell, 1974a) (Fig. 3.36).

Braided zones apparently develop in a boundary region of weak block edges between rigid blocks. In these complex systems, some faults lie parallel to the direction of relative plate movement whereas others lie at an angle, usually a small angle. In general, those parallel to the plate movement direction predominate and grow longer and those at an angle may rotate even farther out of alignment. The long predominating faults develop nearly vertical dips and those rotated out of alignment develop dips that depart considerably from the vertical. Strike-slip faults curving or bending away from the plate-movement direction gradually change from pure strike slip upon a vertical fault surface to those with first gentle oblique slip and then steep oblique slip as the fault strike bends more and more. The fault strike sharply bends at NNW-corner of Tatvan basin (see this relation from Fig. 3.1 into Fig. 3.8). If the curvature carries the fault into a region of extension, the fault becomes a normal oblique-slip fault (Figs. 3.8-3.11). If the curvature carries the fault into a region of compression, the fault becomes a reverse oblique-slip fault (Figs. 3.1-3.7). Such geometric relations are especially easy to envisage along braided zones of single major strike-slip faults where all slices occur in surficial rocks. Along such master faults, the faults bounding the slices converge at depth to rejoin the strike of the through-going fault. Most probably, the major faults meet at depth, but presumably end in the upper crust in approaching the detachment zone where ductile shears may predominate. This kind of system includes branching and braided strike-slip zones, the highs (push up, rhomb-shaped horst blocks) owing to convergence, and the lows (fault-wedge subbasins) owing to divergence between major left-slip faults. Such a system is perfectly expressed within a curvature relation of N-margin boundary fault to W-margin boundary fault (see Fig. 3.1 at NNW-corner).

Reversed oblique-slip faults along the main trend of N- and W-margin boundary faults are clearly seen as surficial thrusting (Figs. 3.2-3.10). They are backthrusts flattening toward the lacustrine shelf. The near-surface, low-angle segments of strike-slip faults are common along many major convergent strike-slip faults, particularly where the faults mark the base of a steep mountain front (Sylvester, 1988) or steep sublacustrine slope structure.

The upward flattening of strike-slip faults in zones of transpression is also documented (Davis and Duebendorfer, 1982; Craddock et al., 1985; Sylvester, 1988). It is proposed by Wellman, (1955) that the surficial thrusting observed results from downslope creep under gravity, which bends the fault in mass movement. However, Allen, (1965) indicated another important causal factor that it may be related to the origin of the steep mountain front itself or steep sublacustrine slope. This implies that the presence of the steep sublacustrine front is caused by a local vertical component of displacement along the predominantly fault. Then vertical motion constrained at depth to a vertical plane must necessarily result in localized low-angle thrusting at the surface (reversed oblique slip fault), as demonstrated in models by Sandford, (1959). These surfical thrusts may conceal the major underlying strike-slip faults and may have delayed recognition of the dominance of horizontal displacements on faults (Allen, 1965). This hypothesis well explains the local surfical flattening of strike-slip faults. However, it is also argued that the larger-scale thrusting results from "a mechanical delamination" of an uplifted block coupled with shortening. This permits thin structural flakes (Dewey et al., 1986) to move obliquely across the adjacent block and appear as though they have been thrust up (up-thrusting) and out of the deformation zone. This is an explanation for those thrust segments which seemingly have come out of a strike-slip fault zone which is very much narrower than the thrust segment itself, as recognized from maps. Thus, the overlying sedimentary sequence between the faults deforms passively in response to gravity-driven flow and differential uplift of the basement (see text in Sylvester and Smith, 1976).

3.2.1.3 Faults-induced sedimentary basin systems: internal and external subbasins (mini-basins)

A system of anastomosing strike-slip faults, converging and diverging in map view, may give rise on a regional scale to wedge-shaped basins separated by uplands (Fig. 3.36). Therefore, modes of basin formation in and adjacent to strike-slip fault zones are discrete. Displacement along converging and diverging strike-slip faults bounding such wedges results in shortening and elevation, or in stretching and subsidence, respectively. For example, in a soft crust, convergence of faults will result in squeezing of the terrane between the faults and in its deformation and uplift owing to isostatic compensation. Divergence of strike-slip faults will result in

stretching and sagging, and the development of down-tipped triangular basins and pull-apart basins (Crowell, 1974a).

As mentioned above, fault-wedge basin, intervening bank uplift or sedimentary ridge in N-margin boundary originate in a broad left-slip regime where strike-slip faults converge and diverge in plan view to slice the terrane into wedge-shaped segments. Many of these basins will be rhombic in shape. Some of these may have floors composed of volcanics intermixed with infilled sediments with few or no remnants of previously existing crustal rocks (Crowell, 1974a). Inasmuch as much stretching, sagging, squeezing and uplift goes on hand in hand with sedimentation, complicated unconformities and overlaps are to be expected within the basins, and especially around their margins (Crowell, 1974a). Kinematics interpreted from local structures may therefore reveal only remotely their connection to a broad strike-slip regime. Hence, the formation mechanisms of internal and external basins through the margin-bounding faults are discussed in the following.

Internal and external basins, with respect to S-transtensional and N-transpressional zones, are termed as “subbasins” or “mini-subbasin formations” (or only mini-subbasins) evolved within strike-/oblique-slip setting of Lake Van basin. Basin formations in strike-/oblique-slip settings are well reviewed and reported by Crowell, (1974a), Reading, (1980), Christie-Blick and Biddle, (1985). The resulting structural geometries of margin-bounding faults are characterized by subbasinal sedimentary wedges, fault-wedged subbasins, graben-like subbasins or en echelon-like segmented grabens/half grabens. Since, any segments of a strike-slip fault that is oblique to the regional slip vector will contain a component of dip-slip. Whether this component is normal or reverse, sediments may accumulate in the topographic depressions on the downthrown side of the faults, and the upthrow side may provide a convenient local source. The subbasin development observed through margin boundary faults is classified into subdivisions to understand their formation mechanisms. Two sites of basin formation in strike-slip belts can be distinguished; “internal and external” basins. The former is related to basins internal to the strike-slip zone. These form in local transtensional areas along active faults strands (at releasing bends of offsets) (see and examine Figs. 3.13, 3.18-3.20, 3.26-3.29 and 3.30 at the top). The latter is related to basins external to the strike-slip zone.

These form in local transpressional areas, either due to folding of adjacent cover rocks or by blocks thrust out from transpressional areas or by sediment eroded off internal push-ups (see and examine from Fig. 3.1 to Fig. 3.9).

These seismic sections from Fig. 3.1 to Fig. 3.9 imply that faults in the restraining bend in N-margin define a compressional uplift called a “push-up block or rhomb horst” This horst uplift forms “fault-margin sags” on both sides of the main fault zone (Mann et al., 1983, Aydın and Nur, 1982). The sediment fill to these sags commonly becomes deformed and may eventually be buried, sliced, or uplifted as part of the push-up block. The push-ups themselves provide fast-rising local sources of sediment in continental settings (Mann et al., 1985). The other kind of external basins is the “fault-flank depressions” formed by the synclines in fold systems adjacent to a strike-slip fault belt (Crowell, 1976). These folds will usually be oblique to the main fault zone, as described by Harding, (1974). In higher sedimentation rates and subsidence, these depressions can be filled and smoothed with deep water sediments and eventually be buried beneath the recent sediments. Internal basins also form at branches in strike-slip faults, as illustrated in Figs.3.2-3.5. These “fault-wedge basins (wedge grabens)”, proposed by Crowell, (1974b) are originally assigned to sites where faults “diverge” with uplift occurring at sites where faults “converge” (in a combination of convergent and divergent strike-slip faults). This means that faults converge in one direction, diverge in the opposite direction, as pointed out by Christie-Blick and Biddle, (1985) (also see Fig. 3.36). It seems that the tendency of a fault wedge to subside depends, in fact, on the orientation of both the branch faults to the slip vector and to their relative displacement magnitudes. A range of topographic effects may result for this, such as very steep sublacustrine slope in N-margin. Fig. 3.36 well summarizes this effect that only some situations give “fault-wedge basins” from a range of possible topographic results of slip along a bifurcating dextral fault (Woodcock and Schubert, 1994, after Christie-Blick and Biddle, 1985).

Internal basin formation also occurs at releasing bends or stepovers across S-margin boundary fault into offshore Deveboynu peninsula in SE-delta. Tatvan delta graben basin in Fig. 3.13 and Deveboynu and Varis spur zone basins in Figs. 3.18-3.20, 3.23, 3.26-3.29 and 3.30 at the top are defined by strike-slip strands parallel to the slip vector and by normal oblique-slip faults across the ends of the basin. S-margin

boundary fault (PDZ) is terminated as horse-tail or imbricate fan-shaped against SE-delta setting. Therefore, vertical and lateral components of strike-slip-controlled basins can vary in place to place. As a result, basins form above "imbricate fans or horse-tails (horse-tail splays)", and can be regarded as "hybrid basins" between pull-apart and fault-wedge basins, illustrated in Figs. 3.26-3.29 and 3.30 at the top. This situation is also sampled in and around Nemrut volcanic dome-cone complex in SW-corner (examine Fig. 3.13 and also Fig. 3.14). En echelon type segmented graben-like subbasins through S-margin boundary fault and horse-tail splay faults-controlled subbasins through offshore Deveboynu peninsula (W-end of SE-delta) are internal basins in S-margin of lake.

A wide range of all these subbasins locally developed in strike-/oblique-slip related setting is both morphologically and seismically observed through N- and S-margin boundary faults. Their size and shape tend to be smaller, more elongated and deeper in relation to their width than basins formed by thermal subsidence or flexural loading. Their subsidence on steep faults tends to be localized, and hence, small strike-slip basins subside very rapidly. It is assumed that all subsidence and uplift is compensated in the crust, and no long-wavelength thermal effects need occur. Depositional environment and characteristic fill patterns of these strike-slip subbasins are almost entirely based on continental environments. As a result, sediment starvation is common, due to subsidence rates exceeding sediment supply rates. Fault-controlled facies patterns are also common (see Fig. 3.31). This seismic section shows that sedimentation and sedimentary patterns observed across central Tatvan basin are clear indication of strike-/oblique-slip deformation and related subbasin formation. However, it is generally impossible from the sedimentary record alone to decide whether the contemporary faults are dominantly strike-slip or dip-slip. Thus, sedimentation within a depositional setting of asymmetric half graben structure of central Tatvan basin is viewed and examined on a basin scale.

3.2.2 Basinal domain

Basinal domain only includes the wedge-shaped structural pattern of central Tatvan basin, well reflecting the sedimentation patterns and sedimentary expressions of strike-slip deformation in the lake. This implies gravity-driven folding geometry of the sedimentary cover in central Tatvan basin.

3.2.2.1 Fold systems: gravity-driven folding

The folds are distributed in a relatively narrow and persistent zone above or adjacent to a master strike-slip fault in N-margin (Figs. 3.3, 3.5, 3.8 and 3.9). It is interpreted that these are en echelon folds, strongly deformed and cut by convergent and divergent strike-slip faults across N-margin (Figs. 3.1-3.5 and also see Fig. 3.33). These folds are popularly called “drag folds” (Moody, 1973; Sylvester, 1988) where they curve into parallelism with a strike-slip fault. These folds are born in an en echelon orientation as many model studies show (Pavoni, 1961b; Wilcox et al., 1973; Dubey, 1980) (Fig. 3.35). Hence, they are rotated and also internally sheared by piecemeal slip on R fractures and smeared, thereby, into a “dragged” appearance (Sylvester, 1988). These observed folds across central Tatvan basin are confined features at N-margin boundary. Therefore, they seem to be useful structural indicators to identify the associated fault, the fault type, its related structures and deformations. Detailed seismic structural observation of these folds reveals that in N-margin, a strike-slip fault is probably nearby laterally or at depth and that the direction of slip on that fault is by the overstepping direction of the folds and the expected orientations of related faults.

The WSW-ENE striking folding in central Tatvan basin associated with N-margin boundary fault is typically arranged in en echelon pattern, oblique to the principal direction of shear (PDZ in N-margin). En echelon folding may reflect the complex influence of basement structures at depth, or it may represent the superposition of differently oriented folds in time and space (Harding, 1988; Sylvester, 1988). Seismic structural interpretation suggest that the axial surface of this folding has a “helical” geometry, similar to that of an R shear (Naylor et al., 1986) (Fig. 3.35), except that an R shear steepens upward, whereas a fold axial surface flattens upward (Sylvester, 1988). Helicoidal form of axial surfaces of en echelon folding in left simple shear implies that the observed angular relation between en echelon fold axes and PDZ in plan view depends locally on the amount of internal rotation within the shear zone (Sylvester, 1988). In convergent strike-slip, en echelon folds may have any or all of the profile geometries found in other convergent tectonic styles, even thrust-associated types. In and along N-margin boundary fault, the crestal trace of folding is typically parallel to the PDZ. Figs. 3.3, 3.5, 3.8 and 3.9 across central Tatvan basin show that this folding has a cross-sectional geometry and evolution

similar to those of drape, or forced folds. These folds form above normal fault blocks complete with anticlines or monoclinal knees next to, and parallel with, the relatively higher side of the PDZ. Folding also has synclines or monoclinal "ankle flexure" adjacent to, and parallel with, the edge of the apparently down-dropped fault block (Harding, 1974; Harding et al., 1985; Sylvester, 1988).

The maturation of N-margin boundary fault zone and its associated structures from their evolutionary sequence are clearly observed from seismic data through N-margin (Figs. 3.1-3.7). Thus, the factors controlling the style and development of folding in simple shear can be easily defined to a certain degree. Since, the features of the observed folding, such as the fold spacing, orientation, size, and rate of growth, depend on the cohesion, the strain rate, and the degree of strike-slip convergence across N-margin (Wilcox et al., 1973). Both seismic structural and tectonic interpretation across central Tatvan basin through N-margin boundary fault considers that initially folding form perpendicular to the shortening axis within a shear couple. However, its formation requires a ductile material or inter-layered member, such as a thin sheet. Since, the ductility will deform continuously rather than by shearing (see discussion in Wilcox et al., 1973; Sylvester, 1988). Therefore, in convergent strike slip, a component of shortening is imposed above the zone of strike-slip deformation, and the folds form readily and in a distinct, consistent en echelon arrangement (Wilcox et al., 1973; Babcock, 1974; Sylvester, 1988). The folds and thrust faults, in principle, form initially perpendicular to the axis of shortening. If deformation continues then the fold axes and faults will rotate according to the amount of shearing. The end result is that the folding and faulting will form or be rotated into orientations parallel to the PDZ. The resultant faults will look like dip-slip growth faults, and the folds will have all of the characteristics of "drape folds" when viewed in two-dimensional seismic or structure sections (Harding et al., 1985; Sylvester, 1988).

An en echelon array of simple folds is early formed in the deformation history. With more deformation, R shears break the surface and deform the folds into sedimentary ridges, half anticlines, and synclines. Then the deformation zone broadens, and parts of the early-formed structures are deeply eroded and also faulted out of the picture. This leaves vestiges of steep, secondary faults and parts of folds recently cut complexly by thrust and normal faults and by R shears (Harding et al., 1985).

Folding extends progressively farther from the PDZ with increasing displacement over time. The largest amplitude folds are at depth near the fault, and the most recent folds are farthest from the fault at the margins of the deformation zone (Wilcox et al., 1973; Harding, 1976; Harding and Lowell, 1979). All these structural effects are summarized through seismic sections from Fig. 3.1 to Fig. 3.7 and even partly in Figs. 3.8-3.9. Through the folding across N-margin boundary fault, the present maximum stress is inferred to be oriented nearly perpendicular to the fault. Therefore, "transpressive tectonics" is better described as "decoupled transcurrent and compressive deformation", operating simultaneously and largely independently" (see example from Mount and Suppe, 1987). "Decoupled transcurrent and compressive deformation" views that separate and largely independent thrusting and strike-slip faulting implies a "mechanically layered crust". On a basin scale, this reveals that the state of stress is thought to have changed abruptly from compressional-contractional episode to compressional-extensional episode into strike/oblique-slip episode (see detailed time episodes in Koçyiğit et al., 2001 for basin formations). Regime change caused departure from pure strike-slip motion on the N- and S-margin boundary faults to oblique-slip across central Tatvan basin, contemporaneous with the main episode of crustal shortening and folding. This created complex structural ranges of the N-margin boundary.

3.2.2.2 Strike-slip-controlled depositional system

W-E and WSW-ENE striking seismic sections across central Tatvan basin illustrated in Figs. 3.31-3.34 are an example of how a group of seismic track lines can give a clue to both strike-/oblique-slip basin type, basin and sedimentation history. Fig. 3.31, a seismic section through central Tatvan basin, especially shows normal oblique-slip faults-controlled margins (W-margin and E-segment in S-margin). These oblique-slip faults control wedge-shaped sedimentation pattern. Fig. 3.10 and Fig. 3.17 are respectively W- and E-seismic sections of Fig. 3.31. Seismic structural interpretation and sedimentation patterns shown in Figs. 3.10, 3.17 and 3.31-3.34 indicate that strike-/oblique-slip basin is typified by high sedimentation rates, scarce intrusive and extrusive activity, abrupt facies changes, abrupt thickening of sedimentary sequences over short distances (also see Sylvester, 1988). These seismic sections show that sedimentary facies is telescoped or "stretched" and great mismatches in sedimentation history are locally juxtaposed across the oblique faults.

Numerous unconformities reflect “syn-tectonic sedimentation” and the presence of a locally derived, skewed fan-body of fault-margin breccia facies represents talus detritus or alluvial fans (Figs. 3.32-3.34) (Hempton et al., 1983; Dunne and Hempton, 1984; Nilsen and McLoughlin, 1985; Sylvester, 1988). This shows that sedimentation pattern across central Tatvan basin is typical depositional setting related to strike-slip faults.

Sedimentation related to strike-slip faults is clearly reflected by basinward extent of progradational wedges from NE-Erek delta (Figs. 3.32-3.34). These wedges extent toward NNE-edge of central Tatvan basin, very close to N-margin boundary (see and examine Figs. 3.25, 3.33 and 3.34). Then, these progradational wedges are strongly deformed by convergent and divergent strike-slip faults in N-margin (Figs. 3.33 and 3.34). These seismic sections perfectly reflect thick sedimentary sequences, onlapping onto the foots of NE-Erek delta and Çarpanak uplift. This suggests that onlapping of sedimentary sequences starts in central Tatvan basin because of the long-way extent of NE-Erek delta toward the deep basin. It can be assumed that the coarse, basin-margin facies form a narrow band along the fault at the edge of the basin. This is volumetrically subordinate to, and contrasts strongly with the main sequence of flood basin and lacustrine strata with which it interfingers and mixes in the basin. This is much finer grained, farther traveled, and commonly deposited by turbidity currents. Resultant local uplift and erosion of fault-controlled blocks (Çarpanak block uplift) and slices yield angular unconformity of the same age as thick, and laterally extensive (see Figs. 3.16, 3.17, 3.19, 3.24 and 3.25). Sedimentary sequences are very rapidly deposited on adjacent subsided blocks such as Deveboynu, Varis spur zone subbasins (Figs. 3.18-3.20, 3.26-3.29) and central Tatvan basin (Figs. 3.16 and 3.17). Probably, a great discordance between clast size or lithology of detritus in sedimentary units and possible sources across faults typically reflects the horizontal translation of the source relative to the deposits.

The most prominent and distinctive stratigraphic feature of central Tatvan basin that forms in association with strike-slip is the extreme thickness of onlapping sedimentary sequence in oblique-slip basin relative to their area (Fig. 3.31). In this seismic section, W-E arrangement of stratal units in central Tatvan basin is viewed parallel to the depositional basin and parallel to oblique-slip boundary faults in N- and S-margins, which lie in the basin from the source area to basin.

The center of deposition clearly migrates toward the principal source area which lies E of the basin (toward the Çarpanak spur zone and NE-Erek delta) and across the oblique fault behind the basin (see and examine Fig. 3.37 as analogue sample of seismic section in Fig. 3.31). This happens because of "migration of the depocenter" by means of syn-depositional strike/oblique-slip (see also Crowell, 1974b, 1982a; and Sylvester, 1988). The center of deposition migrates in the direction opposite to that of strike-slip movement of the basin, so that the basin lengthens over time. This indicates that thick deep-water sediments lengthen and relatively thin toward the deltaic source areas. Thus, the sediments are deposited in an overlapping "venetian blind" arrangement or "stratal shingling" which youngs toward the depocenter (Hempton and Dunne, 1984; Sylvester, 1988). Such thick, asymmetric and onlapping sedimentary fillings are strike-/oblique-slip depositional characteristics of central Tatvan basin. This gives the best evidence of lacustrine sedimentation related to strike-slip faults. Strike-slip related sedimentation in central Tatvan basin is extremely similar to the lake in Hornelen basin of W-Norway in Steel and Gloppen, 1980 and Ridge basin, S-California, in Fig. 3.37 from Crowell and Link, 1982 and Nilsen and McLaughlin, 1985.

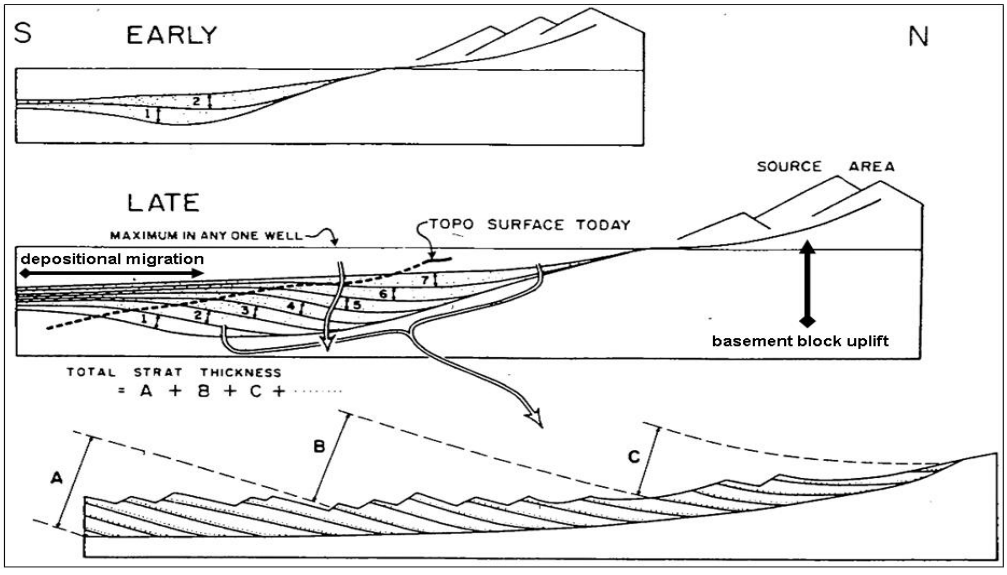

Figure 3.37 : Diagrammatic arrangement of stratal units in strike-slip basin (Ridge), viewed parallel to the depositional basin and perpendicular to dextral fault, which lies between the source area and the basin (from Crowell, 1982a). The center of deposition migrates toward the principal source area which lies N of the basin and across the fault behind the basin (Sylvester, 1988), the same as strike-slip sedimentation in central Tatvan basin (see Fig. 3.31 for correlation basinal sections). The lower cross section shows the way the region is recently exposed after uplift and erosion. This is the case observed in Çarpanak uplift and NE-Erek delta.

The criteria for determination of the magnitude of horizontal displacement on a strike-slip fault are those that are least affected by depth of erosion (Gabrielse, 1985; Sylvester, 1988). These are offsets of geologic lines that yield piercing points (Crowell, 1962; Sylvester, 1988), such as strand lines and shelf-to-basin transition zones (Addicott, 1968) (Çarpanak spur zone). Some others are the surfaces of considerable vertical extent, such as magmatic intrusions (Speight and Mitchell, 1979), and even suture zones (Şengör, 1979; Sylvester, 1988). Suture zones (Muş and Cryptic sutures in Keskin, 2003; Şengör et al., 2008) are very critical reference lines to recognize horizontal displacement. This provides an evidence of oblique displacement of S-margin boundary fault (PDZ). This suggests that wedge block geometry of central Tatvan basin and Çarpanak spur zone laterally displaces toward the ENE.

3.2.3 Tectonic implications for seismic structure of basinal and marginal domains

Seismic expressions of structures, structural description, and tectonic interpretation of reflection profiles showed two distinct domains of the lake setting. Seismic structure of marginal domain is characterized by convergent and divergent strike-slip fault systems, fault deformation systems such as flower structures, fault wedge-basins and block uplifts, accompanied by faults-induced sedimentary basin systems such as internal and external subbasins. Seismic structure of basinal domain is characterized by gravity-driven folding and strike-slip faults-controlled depositional systems. Seismic image analysis of reflection profiles and seismic characterization of structural styles and structural domains showed a complicated seismic and tectonic structure of Lake Van. The presence of shortening structures (folds, reversed oblique-slip faults and block uplifts) and, of extensile structures (normal oblique-slip faults, vent systems, linear volcanic clusters, intrusive-extrusive activity and structures with horizontal shear on nearly vertical surfaces), all together in a strike-slip regime is involved in the concept of “strike-/oblique-slip tectonics” (Wilcox et al., 1973; Naylor et al., 1986; Sylvester, 1988).

The presence of strike-/oblique-slip faults in the marginal sections is frequently indicated by en echelon arrays of fractures, faults, and folds in narrow elongate zones. The magnitude and rate of shear strain varies greatly from place to place within the basin. The entire marginal domain of strike-/oblique-slip is made up of

many subzones or segments, each undergoing simple shear with vertical components at a particular rate. Across marginal domains, the apparent simultaneous development of extended and shortened structures, together with the variable vertical separation along strike, is typical aspects of strike-slip faults (Sylvester, 1988). These features are caused by localized and alternating convergent and divergent components of lateral displacement along the fault in combination with alternating local uplift and subsidence of blocks and slices developed within the fault zone over time. Seismic structure of basinal and marginal domains implicates for a relatively long-lived strike-slip tectonic development of Lake Van. This implies a progressive deformation history. Progressive deformation superimposes structures of brittle and ductile rheologies, from newly initiated and strongly rotated generations, and from varying obliquities and senses of displacement vector across the zone (Woodcock and Schubert, 1994). Seismic image analysis of the observed structural styles, deformation patterns, and overall interpretation of seismic reflection data significantly imply some tectonic implications for seismic structure of basinal and marginal domains. The following section briefly outlines some commonly observed structures and structural geometries within planar strike-/oblique-slip zone of the lake.

Marginal domain through its evolutionary stage in strike-/oblique-slip zone indicates that the first formed structures are en échelon R shears. They have a component of synthetic strike-slip, but also a small dip-slip component, which changes downthrow sense at the mid-point of the shear. Therefore, each R shear is also a “scissor fault”. “Splay faults”, linking to a genetically related master fault (PDZ), form at the tips of the R shears, at a higher angle to the zone. At higher displacements, the R shears become linked by synthetic low-angle shears (P shears) (Tchalenko, 1970). These form in response to the locally rotated stresses within the array of R shears. Yet further displacement links segments of R and P shears into a through-going synthetic “principal displacement zone” (PDZ), a narrow zone that accounts for most of the displacement (Tchalenko and Ambrayses, 1970). Hence, structural patterns in strike-/oblique-slip zone are discrete with either an en echelon arrangement in map view (S-margin), or they are interconnected into anastomosing or braided patterns (N-margin).

Anastomosing or braided patterns refer to branching and rejoining of a network of surfaces or surface traces, particularly faults. En echelon describes a consistently overstepping and overlapping arrangement of structures, sub-parallel to each other but oblique to the planar zone in which they occur (Campbell, 1958). The sense of overstep (discontinuity between two parallel faults, commonly in map view in Aydin and Nur, 1982 from one structure to the next) is described as right-stepping. The overstep sense, where it is consistent along a zone of faults, can be used to tell the displacement sense on the zone. Overstepping faults are commonly overlapping, that is, the normal to one fault tip intersects the other fault (Pollard and Aydin 1984; Gamond, 1987). A discontinuity (stepover) in a fault trace may be either releasing or restraining, depending on their sense of overstep with respect to the overall shear sense. As well recognized in the formation of internal and external subbasins through the marginal sections, releasing stepovers or bends tend to subside vertically. If faults isolate the subsiding area, it becomes a fault wedge subbasin or a graben subbasin or a wide range of subbasin formations. This is an important mode of basin formation and releasing. This is the equivalent at a restraining stepover or bend. If faults isolate the uplifting area, it becomes a rhomb horst or push-up (or pop-up). This is an important mode of basin uplifting and restraining (Woodcock and Schubert, 1994).

Open vents, extension or tensile fractures or fissures also develop in small-scale shear zones. They are particularly favoured at low differential stresses and high pore fluid pressures. Extension fractures, volcanic conduits or vent systems, similar to “in-line structures” on map view, are more common and parallel to strike-slip zones. These structures are directly related to the PDZ; either as shear lenses along PDZ or as forced folds generated by draping of the cover over the faulted basement. These structures away from or between major faults can result from partitioning of oblique displacements. Partitioning is the physical resolution of displacements or strain in to several components, reflected in several different structures. For example, oblique shortening across N-margin is physically resolved into strike-slip and shortening normal to intervening folds and thrusts. This partitioning presently operates in zones containing faults too weak to support much shear stress (Mount and Suppe, 1987, Zoback et al., 1987). Oblique extension across S-margin is physically resolved into strike-slip and extension normal to intervening folds and thrusts. This partitioning

also presently operates in a zone containing faults too weak to support much shear stress. This zone seems to have been a complex of Muş and Cryptic sutures.

Vertical cross-sections through strike-slip zones from seismic reflection data commonly show diverging from a steep fault system (the stem). A pattern of upward-diverging faults is termed a "flower structure" (Harding and Lowell, 1939). "Helicoidal" forms of Riedel shears in sandbox experiment (Naylor et al., 1976) and axial surfaces of en echelon folds (Sylvester, 1988) are shown in three dimensions by Woodcock and Schubert, (1994). The Riedel shear and related fractures are seen not to be vertical, but to have a helicoidal geometry, twisting to merge with the basement fault at depth. "Tulip structures" in cross-section are concave upwards (Naylor et al., 1986) as interpreted through S-margin. This geometry contrasts with the convex upwards "palm-tree structures" (Slyvester, 1984), which are described from en echelon fold/fault zones (Gamond and Odonne, 1984) as interpreted through N-margin. These are characteristic of transpression rather than simple shear or transtension (Naylor et al., 1986). Positive flower structures or palm tree structure with convex-up fault geometries are dominated by reverse oblique-slip faults. Negative flower structures or tulip structure with concave-up fault geometries are dominated by normal oblique-slip faults (Harding, 1985). Thus, whilst tulip structures are common in transtension and palm tree structures are in transpression (compare Naylor et al., 1986, Sylvester, 1988).

Any fault-bounded sliver in a fault zone can be termed a horse, if subject to near-surface uplift. This can be a pressure ridge or fault-slice ridge, or a linear topographic high (Crowell, 1974b). These highs are Nemrut volcano in W and Deveboynu and Çarpanak highs in E. E-termination of S-margin boundary fault offshore Deveboynu high clearly shows "imbricate fans or horse-tail splays" across the W-edge of SE-delta setting, resulting in the subbasin formation. Horse-tail or imbricate fan-shaped termination of S-margin boundary fault is also recognized in and around Nemrut volcanic dome-cone complex (see Dhont and Chorowicz, 2006). Imbricate arrays of sub-parallel curved oblique-slip faults, each one is linked to the main strike-slip fault at one end but losing displacement to a fault tip at the other (Woodcock and Fischer, 1986). Based on consideration of the upper crustal continuation of margin boundary faults (PDZ) and related basin type of Lake Van region, "flake", a low-angle fault-bounded element (basin), is suggested by Dewey et al., (1986) for strike-/oblique-slip

basin formations. The reason is that a flake is a volume of rock (basin) along a low-dipping fault (Dewey, 1982). This low-angle fault is a detachment fault at upper crustal levels (Dewey et al., 1986) and drives rigid body block rotation of the basin.

A brief outline of structural descriptions through seismic cross sections and tectonic implications for seismic structure of marginal and basinal domains give some clues to both overall deformational patterns and their evolutionary stages through time. A wide range of structures produced by the strike-/oblique-slip shear themselves strongly forms anisotropies (Woodcock and Schubert, 1994), affecting later deformation in the basin.

3.3 Active Tectonic Provinces and Overall Deformational Patterns of Structural Domains

3.3.1 N-Margin boundary fault (tectonic margin)

The Lake Van basin illustrates how major oblique slip faults can influence basin development and sedimentation as well as the tectonic history and structural style of a region. Along N-margin boundary, principal displacement zone (PDZ) of the main fault is reversed oblique slip faulting (Figs. 3.1-3.7). This faulting is characterized by positive flower structure and associated convergent and divergent strike slip faults (Figs. 3.1-3.7, 3.33 and 3.34). Seismic sections from Tp1 (red) in Fig. 3.1 to Tp7 (red) in Fig. 3.7 illustrate the evolutionary stages of convergent and divergent strike slip faulting across the N-margin boundary. Four general styles of oblique slip faulting are recognized from seismic sections (Figs. 3.1-3.7 and also see 3.33 and 3.34 for the oblique views): (1) simple parallel strike slip faults, in which crustal blocks do not move parallel with the main strike slip fault and produce anastomosed and/or braided patterns. (2) convergent strike slip faulting is caused by blocks moving obliquely toward the main fault (Figs. 3.1-3.7 and 3.33) and produce push up rhomb horst structure (Figs. 3.2-3.5). (3) divergent strike slip faulting results from oblique movements of the blocks away from the main fault (Figs. 3.2-3.5, 3.33 and 3.34) and produce the fault-wedged subbasin. (4) the main fault, reversed oblique slip fault (Figs. 3.1-3.7), continues toward ENE along PDZ. All these styles developed on local scale across the N-margin boundary.

These seismic sections clearly reveal that changes in the strike of an active fault lead to additional deformation of the wall rocks as strike slip continues. Thus, the parallel strike slip motion becomes a convergent or a divergent strike slip, at least locally. This produces a complex form of anastomosing pattern localized across N-margin boundary (Figs. 3.1-3.7, 3.33 and 3.34) and both convergence and divergence also develop locally along a strike slip in N-margin. Since, opposed crustal blocks that do not move parallel with a strike slip fault either converge or diverge as strike slip proceeds. These oblique movements are clearly related to non-parallel displacements of crustal blocks on a regional scale, or they are due to local changes in strike of a generally parallel strike slip motion. Changes in the fault strike imply that strong convergence can cause reverse faulting and thrusting or reversed oblique slip faulting. A cross sectional view of seismic sections reveals the complex thrusting of the wedges squeezed up (or pushed up rhomb horst) and out of the strike slip zone by the strong convergence. As these pushed-up blocks rose, they are bounded by vertical or high angle reverse synthetic faults, and they resemble upthrust blocks (Figs. 3.2-3.7). Convergent strike slip faulting, on whatever scale, also tends to enhance compressive strike slip zone structures, namely, en echelon folds and conjugate strike-slip faults. Moreover, the formation of tensional structures, mainly normal oblique faults, is typical of divergent strike slip faulting (Figs. 3.2-3.5, 3.33 and 3.34). The size and extent of the resulting compressional (push up rhomb horst by convergent strike slip faulting) and extensional structures (fault-wedged subbasin by divergent strike slip faulting) depend on the amount of change in fault strike. It also depends on the amount of displacement along the curved fault surface within the anastomosed and/or braided system across the N-margin boundary.

Seismic sections show that nearly all strike slip displacement is concentrated on the synthetic faults, along which the fold axes are offset (Wilcox et al., 1973). A seismic structural interpretation suggests that initial stage is characterized by convergent strike slip faults (Fig. 3.1). The oblique slip fault zone widens as the strike slip fault splays upward (Figs. 3.2-3.5) and produces the first stage of fault-wedge subbasin that is initially syntectonic basin fill (Fig. 3.2). Then fault-wedged subbasin is fully developed (Figs. 3.3-3.5) and it is ended (Figs. 3.6 and 3.7). Individual faults have normal or reverse dip-slip separation. This depends on how adjacent fault blocks are displaced within the strike slip zone (see and examine Figs. 3.1-3.7, 3.33 and 3.34).

Reverse faults with strike slip components (reversed oblique slip fault in Figs. 3.1-3.7) well characterize structure of the N-margin boundary and attest to the lateral strike slip faulting combined with compression and high-angle thrusting or high-angle reverse faults. These high-angle faults are upthrust structures, caused by reversed oblique slip faulting (see cross sectional view of upthrusts as illustrated in Figs. 3.2-3.10). These sections show the reversals of vertical separation on synthetic faults and dominant strike slip offset of fold axes.

An important result of divergent strike slip faulting illustrated in Figs. 3.2-3.5, 3.33 and 3.34 is an overlay of extensional block faulting on the simple strike slip pattern (Wilcox et al., 1973). Asymmetric half-graben geometry of central Tatvan basin is also an evidence of extensional block faulting. Fault-wedged subbasin and/or horst-foot graben form in preference to pushed up rhomb horst. Nearly all fractures have a tendency to develop into high-angle normal faults with oblique slip (see Figs. 3.8-3.10). The warping of obliquely faulted blocks (Figs. 3.1-3.10 and 3.33) to produce closures between the faults is possible as well. The best example of divergent strike slip faulting is the Fitzroy trough, NW-Australia (Wilcox et al., 1973) and is similar to the fault-wedged subbasin structure across the N-margin boundary, but basin scales are different. The Fitzroy trough is formed by divergent strike slip faulting and then folds are developed within the basin trough fill. Fault-wedged subbasin structure, as for the Fitzroy trough, is a divergent strike slip subbasin. It appears that strike slip faulting formed this subbasin, which filled with sediments, and a final episode of minor oblique slip faulting deformed the basin fill.

Overall deformation pattern across the N-edge of central Tatvan basin through N-margin boundary as a active tectonic province gives an strong evidence of kinematic boundary conditions in a sinistral transpressive regime. Woodcock and Rickards, (2003) modelled kinematic structure of sinistral transpression and documented its evolutionary stages (see and examine Fig. 3.38). According to this kinematic model, it is clear that both the folds and faults bordering N-margin boundary result from sinistral transpression, resulting in some distinct products, such as linked duplex, flower, and push-up anticline and horst. In this model, comparing the fold and fault patterns reveals two further geometric relationships. First, that the central part of the strike-slip duplex is closely superimposed on the periclinal anticline. Second, that cross-sections through this part of the duplex show a flower-structure whose faults

have displacements in broad kinematic harmony with the anticline that they cut (also examine and compare Figs. 3.1-3.7 with Fig. 3.38). These fold/fault relationships are unlikely to be coincidental, but probably record sequential ductile and brittle responses to the same transpressive regime (see Figs. 3.3 and 3.5 as distinct samples).

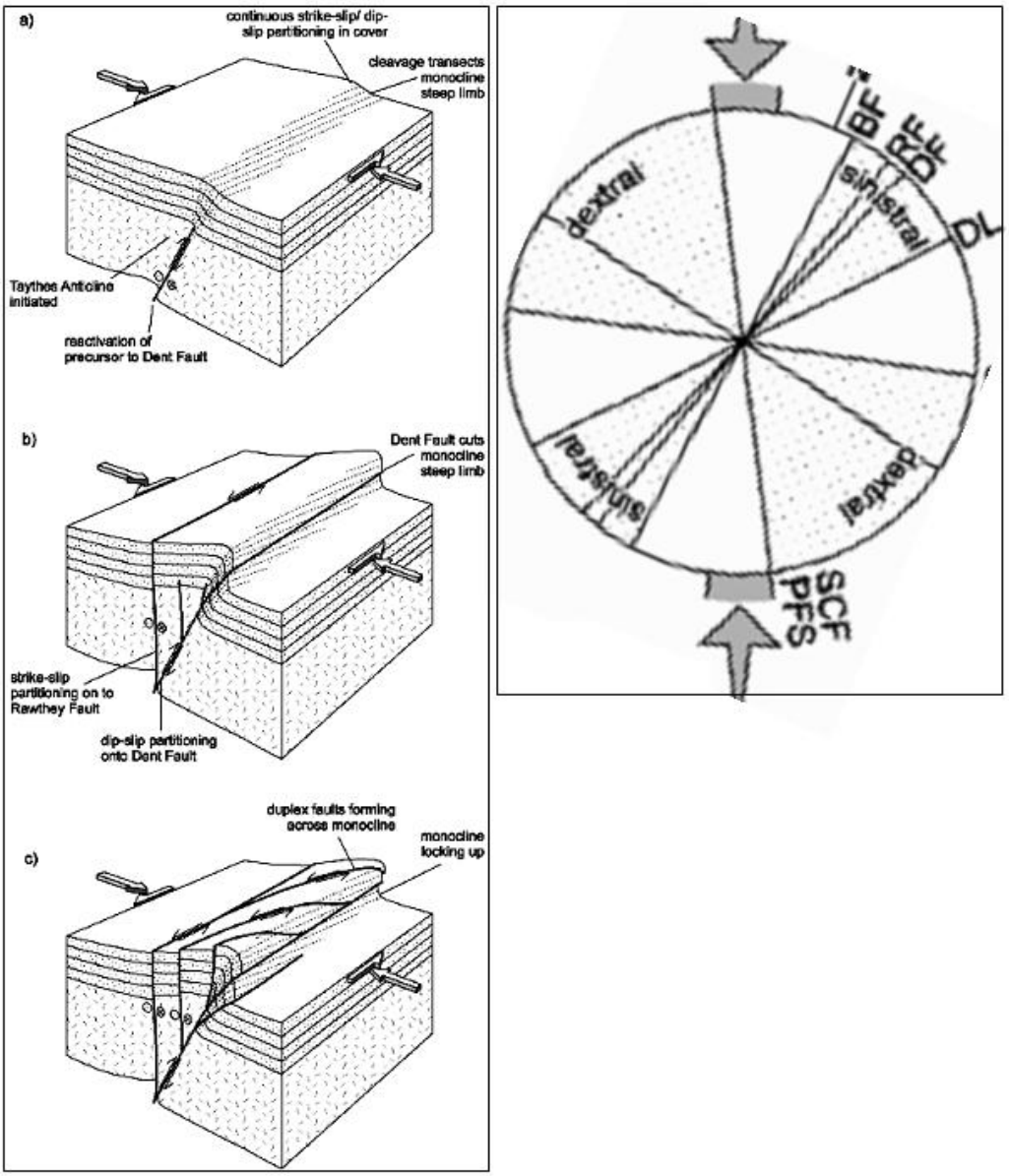

Figure 3.38 : Schematic 3D-block interpretation of the formation of the positive flower structure and contractional duplex by sinistral transpression (Woodcock and Rickards, 2003) indicates complicated kinematic structure of the faulting and the subbasin formation across a zone of convergent-divergent strike-slip faults (Cssfs-Dssfs) through N-margin boundary fault. The periclinal nature of the anticline, due to interference with pre-existing folds, is ignored (Woodcock and Rickards, 2003). Figüre at the right column indicates the N-S compression, the location of the duplex at a restraining overlap and the kinematic constraints on the best-fit regional shortening direction (see Woodcock and Rickards, 2003 for details).

An interpretation of the structural evolution from Fig. 3.1 to Fig. 3.7 suggests that early folding (Fig. 3.38a) is partly forced by bending above the reactivated fault, and enhanced by buckling in response to layer parallel transmission of the regional transpression. Later faults propagate up through the resultant monocline (Figs. 3.38b and 3.38c), but their reverse displacements continue to take up shortening as well as a component of strike-slip. The anticline, and then the larger duplex within which it is nested, is therefore transformed into a fault-bounded push-up horst in the transpressive zone. This shows that fault-wedged subbasins are squeezed upwards (or downwards) in the restraining overlap zone "as a push-up horst" (Woodcock and Rickards, 2003). Figs. 3.33 and 3.34 well illustrate the oblique cross sectional views of the pushed up horst block, the fault-wedged subbasin and its trough-fill pattern and related convergent and divergent strike-slip faults. It seems that wedge-shaped sedimentary package or the subbasin fill pattern onlaps onto the edge of NE-Erek delta. Progradational wedges from NE-Erek delta are strongly upwarped by transpression and involved in deformation of N-margin (examine and compare Fig. 3.33 with Fig. 3.34).

The contrasts across the faults (for example Fig. 3.1 and Fig. 3.3) point to strain and displacement partitioning (see also Fig. 3.38). The strike-slip components are concentrated in the hanging wall, and the dip-slip components in the footwall and possibly along the fault itself (Figs. 3.1-3.7). The degree of strain partitioning probably increases through time, with more continuous accommodation of variable strains during early folding (Fig. 3.38a) and later concentration of strike-slip in the duplex faults as they propagate through the hanging wall block (Figs. 3.38b and 3.38c). The view is that all these faults are most probably a response to kinematic boundary conditions in N-margin rather than to the regional stress system (see Woodcock and Rickards, 2003 for details). This reveals that the independent evidence for sinistral displacement is strong and that the fault splays most probably owe their origin to kinematic constraints rather than a simple dynamic response. An complete examination of Figs. 3.1-3.10 with Fig. 3.38 suggests the kinematic relationship of the strike-/oblique-slip faults in both N- and W-margins. As previously described, N-margin boundary fault sharply bends in NNW-corner, extends to SW and merges with W-margin boundary fault. The sublacustrine basement block shows this relation very clearly.

The faulting across W- and N-margin boundaries seems to transmit sinistral strike slip to the NNE from the W-end of the central Tatvan basin. The sinistral slip on faults also diminishes to N. It is also probable that its strike-slip displacement is transferred to NE-Erek delta from W. The intervening transfer zone contains a number of kinematically suitable NNE-striking faults. The strengthened evidence for sinistral transpression on the faults allows a more quantitative estimate of the regional shortening direction (Woodcock and Rickards, 2003) (Fig. 3.38).

Marginal transpressive kinematics through seismic sections in Figs. 3.1-3.7 across the N-edge of central Tatvan basin and an kinematic analysis of model structure in Fig. 3.38 clearly show that an intimate geometric relationship between a strike-slip fault and an anticline on which the fault are superimposed. The structures are all isolated within a push-up horst in the hanging wall. The geometric interrelationship of this suite of structures is often postulated as a feature of strike-slip influenced deformation (Woodcock and Rickards, 2003). These structures are kinematically related and not just geometrically. Ductile strains, taken up by forced folding early in transpressive deformation, are later replaced by brittle faults that took up the same bulk shape change (Woodcock and Rickards, 2003) (Figs. 3.3 and 3.5). The observed faults across N-margin are interpreted as kinematically induced linkage faults, progressively transferring strike-slip displacement to NNE in the overlap zone. This kinematic explanation is in harmony with growing realization stated by Woodcock and Rickards, (2003) that many structures in transpression zones are more influenced by kinematic boundary conditions than by regional stress orientations. Across both N- and W-margin boundaries, strike-slip deformation is preferentially partitioned into the hanging wall block, particularly those bounding the duplex. However, the footwall preserves predominantly dip-slip displacements. This partitioning mimics closely that seen in larger-scale tectonic settings, for instance at subduction zones (Fitch, 1972; Molnar, 1992) and in continental collision belts (Avouac and Tapponnier, 1993 and Woodcock and Rickards, 2003). It is essential to note that partitioning on the small scale of the N-margin boundary can be ascribed to its greater energy-efficiency compared with oblique-slip faults (Michael, 1990 and Woodcock and Rickards, 2003) and to the influence of a pre-existing basement weakness suitably oriented to take up one component of deformation (Jones and Tanner, 1995 and Woodcock and Rickards, 2003). This implies that N- and W-

margin boundary faults controlling the sublacustrine basement block are the pre-existing basement weaknesses (pre-existing thrust contacts) and reactivation structures (see Şengör and Yılmaz, 1981 for retrocharriage phenomena in compressional ramp basins in E-Anatolia, Şengör et al., 1985 and Dewey et al., 1986 for strike-slip basin formation in E-Anatolia). The result is, on a regional scale of Muş-Lake Van basin system that the N-margin boundary of the Muş basin is controlled by a transform/thrust dextral flower structure. This flower structure is described as a structure in which a narrow zone of strike-slip displacement at depth widens or flowers upwards into a zone of en echelon thrusting (Dewey et al., 1986). The N-margin boundary of Lake Van is controlled by a transform/thrust sinistral positive flower structure. This flower structure is described as an anastomosed or braided pattern of oblique-slip faulting, sinistral transpression. Transpression across N-margins of both basins may imply the pre-existing basement weakness and the present tectonic relationships in the formation of these basins. Dextral transpression in the N-margin boundary of Muş basin is recently described as dextral transtension, namely "Otluk fault" by Dhont and Chorowicz, (2006). Dextral transtension (Otluk fault) is terminated as horse-tail or imbricate fan-shaped in and around Nemrut volcanic dome complex in W. This fault, most probably continues toward the SSW-corner of the lake (Tatvan delta) and may form the en echelon arrangement of S-margin boundary fault.

3.3.2 S-margin boundary fault (suture-parallel magmatic margin)

The S-margin boundary fault is characterized by an large scale en echelon segment through S-margin from Tatvan delta in the SSW-corner (Figs. 3.13-3.15) to Deveboynu peninsula into an area of Çarpanak spur zone in E (Figs. 3.16-3.20) and even into Van delta in the further E (Figs. 3.23, 3.24 at the bottom and 3.25). Across this axial elongation of the PDZ in S-margin, the various scales of en echelon segments appear. These segments entirely cover a huge area of shear zone in S-margin from W to E, characterized by a negative flower structure and related splays (see and examine model structure in Fig. 3.39). This model structure diagrammatically represents 3D-structural geometry of this negative flower structure, branching faults or fault splays, segmented discontinuous faults and internal subbasins.

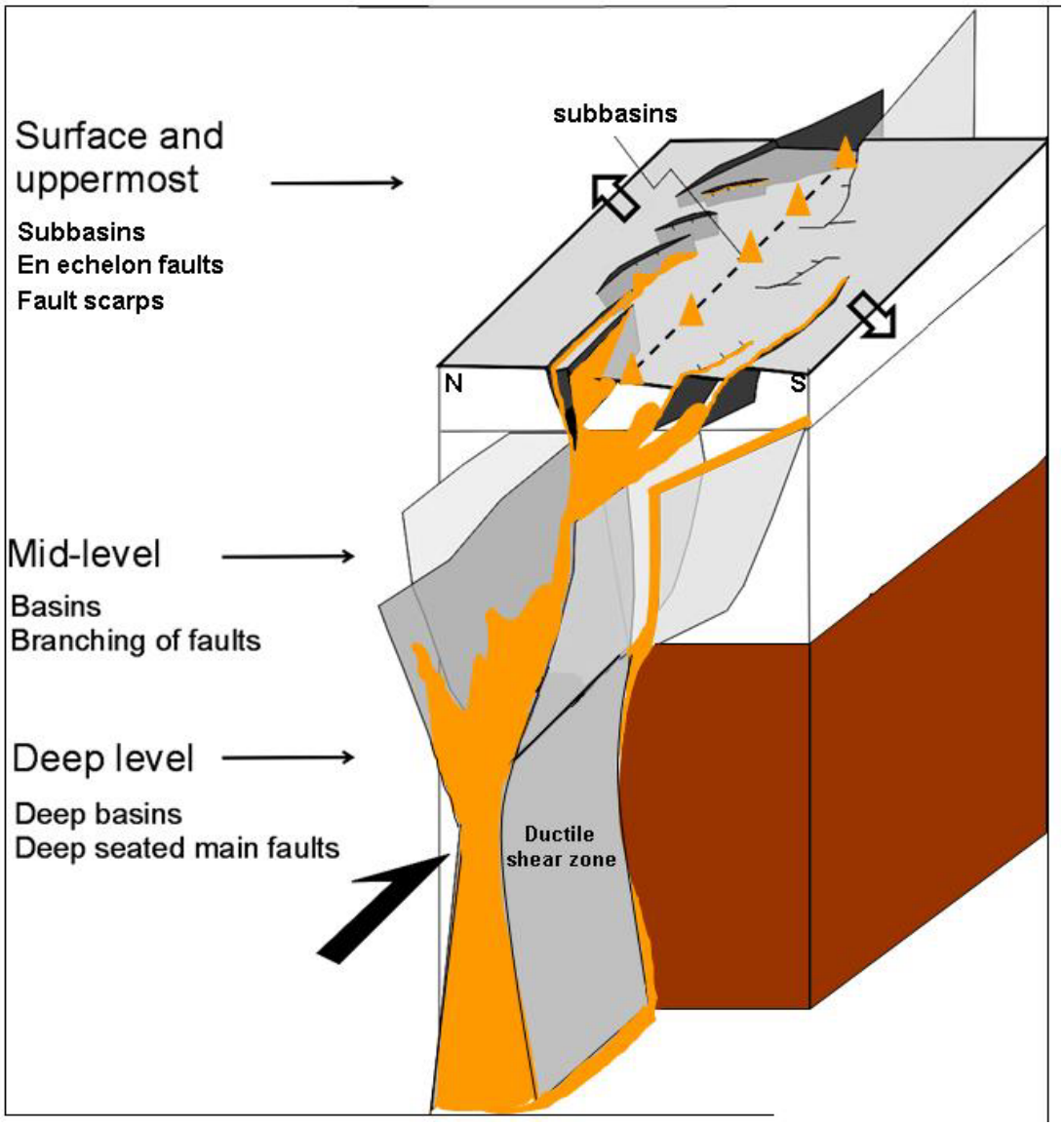

Figure 3.39 : Schematic 3D-block interpretation of the formation of the negative flower structure and extensional duplex by dextral transtension indicates complicated kinematic structure of the faulting, the subbasin formation and extensional magmatism (light orange colour and triangles) across a zone of normal oblique-slip faults (Nosfs) through S-margin boundary fault. En echelon and branching nature of the splay faults, due to interference with ductile shear zone, is highligthed. In this block diagram, the location of the extensional duplex at a releasing overlap (W- and E-segments) and the kinematic constraints on the best-fit basinal extending direction (see text for discussion).

This long-way shear zone coverage is accompanied by extensional and transtensional en echelon stepovers (also from field observations), horse-tail faulting patterns, extensional fissures and variously scaled irregular, shorter and discontinuous faults in W (also examine Figs. 3.13-3.15 and land data from morphological observations by Dhont and Chorowicz, 2006). Most of these faulting patterns seem to be dextral normal oblique-slips according to Dhont and Chorowicz, (2006).

These fault patterns in and around the Nemrut dome complex have complicated kinematic relations to S-margin boundary fault, particularly to its W-segment (Fig. 3.13). These relations imply that this fault is most probably a kinematic continuation of the Otluk fault in the N-boundary of the Muş basin. Dextral transtensional shear of S-margin boundary fault controls a wide range of the structures developed through it (see structural diversity in Fig. 3.39). Through S-margin boundary fault, dense intrusive and extrusive activity into the fault planes is clearly recognized (Figs. 3.13-3.16 and 3.18). Internal subbasin formations accompanied by intrusive and extrusive activity are also well seen (Figs. 3.13, 3.18-3.20 and 3.23). Horse-tail or imbricate fan-shaped termination of S-margin boundary fault results in an internal subbasin system (3.26-3.29 and 3.30 at the top).This subbasin system is controlled by dextral transtensional en echelon segments.

An axial elongation of S-margin boundary fault (PDZ) represents the N-end of BP-M along S-coastal sections and prominently characterizes W-E striking suture-parallel magmatic margin. S-margin boundary fault (PDZ) is almost parallel to trend of Cryptic suture zone and subparallel to that of Muş suture zone. In fact, this implies suture province character of this fault (see Cryptic suture zone from Keskin, 2005; 2007 and Muş suture zone from Şengör et al., 2008). Superimposed structure of S-margin boundary with suture complex represents a pre-existing weakness zone. Its W-segment is parallel to both Muş and Cryptic suture zones, while E-segment is only parallel to Cryptic suture zone. Muş suture zone curves around Deveboynu peninsula, continues to further S and extends into E. This implies that Muş suture follows the releasing bends in S-margin. These bends are the W-segment and and horse-tail termination of S-margin boundary fault in W-end of SE-delta offshore Deveboynu peninsula. This elongation of Muş suture shows a releasing boundary between EAAC in N (Lake Van and accretionary/ophiolitic complex) and BP-M (Paleozoic metamorphics) in S (see Şengör et al., 2008).

A complicated shear zone pattern of negative flower structure illustrated in Fig. 3.39 is an 3D analogue model of the S-margin boundary fault. Seismic structural interpretation as combined with the model structure implies that the discontinuous faulting activity through S-margin boundary is a surface expression of a pre-existing basement weakness and a reactivation product as kinematically recognized in N-margin boundary fault. This remarks that S-margin boundary fault follows the suture.

Suture-parallel elongation of the faulting implicates for the four structural provinces through S-margin. These provinces are W-E striking portions of negative flower structure, showing a kinematic link and transtensional strain transfer from Nemrut dome in W through Deveboynu peninsula and into SE-delta setting in E.

3.3.2.1 W-segment (Muş suture-parallel fault)

W-segment, Muş suture-parallel fault, is only partly imaged by the S-ends of seismic sections illustrated in Figs. 3.3, 3.5, 3.8 and 3.9, but it is completely shown from Fig. 3.13 (Ws-Tt_1) to Fig. 3.14 (Ws-Tt_2). Fig. 3.15 (Ws-Tt_3) only shows open vent, extension fracture or fissure-related nature of this segment. These seismic sections show that W-segment is entirely covered by a strong intrusive and extrusive activity and related vent, fissure or fracture systems, giving an evidence of transtensional activity and the subbasin formation (Figs. 3.13 and 3.14).

Structural interpretation from these seismic sections across W-segment shows that W-segment represents strain compatibility "holes and gaps", which are well reflected by collapsed parasitic cones, domes and intrusions, parallel to Muş suture zone. Intrusive and extrusive occurrences through this segment are described as passive (deactivated and collapsed fossil domes and strains) and active ones (presently active strains). This shows that both recently active and deactivated intrusions are present on this segment. The places, through which magma rises, are "holes or gaps" as termed by Dewey et al., (1986). These gaps or holes are filled by intrusive activity and they are the locus of intense volcanic activity. Complex faulting closes these gaps or holes, for example, the complex fault pattern seen in Figs. 3.13 and 3.14 may be due to such a complication. The position and shape of magmatic intrusions (for example in Figs. 3.14 and 3.15) are probably controlled by these compatibility holes and gaps caused by flaking of the elastic lid particularly beneath transtensional systems (Dewey et al., 1986). It is interpreted that from Nemrut volcanic dome complex area in W into offshore Deveboynu peninsula area in E, the rising magmatic material sequentially propagates toward W-segment and the further E, suggesting ductile strain transfer into the lake. Şengör et al., (1985) modeled a summary diagram of the overall deformational pattern in E-Anatolia (Fig. 3.40). The numbers (1-6) indicate the types of basins that form in this environment (see related paper for discussion). In this diagram illustrated in Fig. 3.40, number (1) typically illustrates formation structure of S-margin boundary fault (W-segment).

If extensional fissures in and around Nemrut volcanic dome complex originate independently of strike-slip systems (as seen number1 in Fig. 3.40), they may propagate into such systems (as indicated to S-margin boundary fault in this diagram) (Şengör et al., 1985).

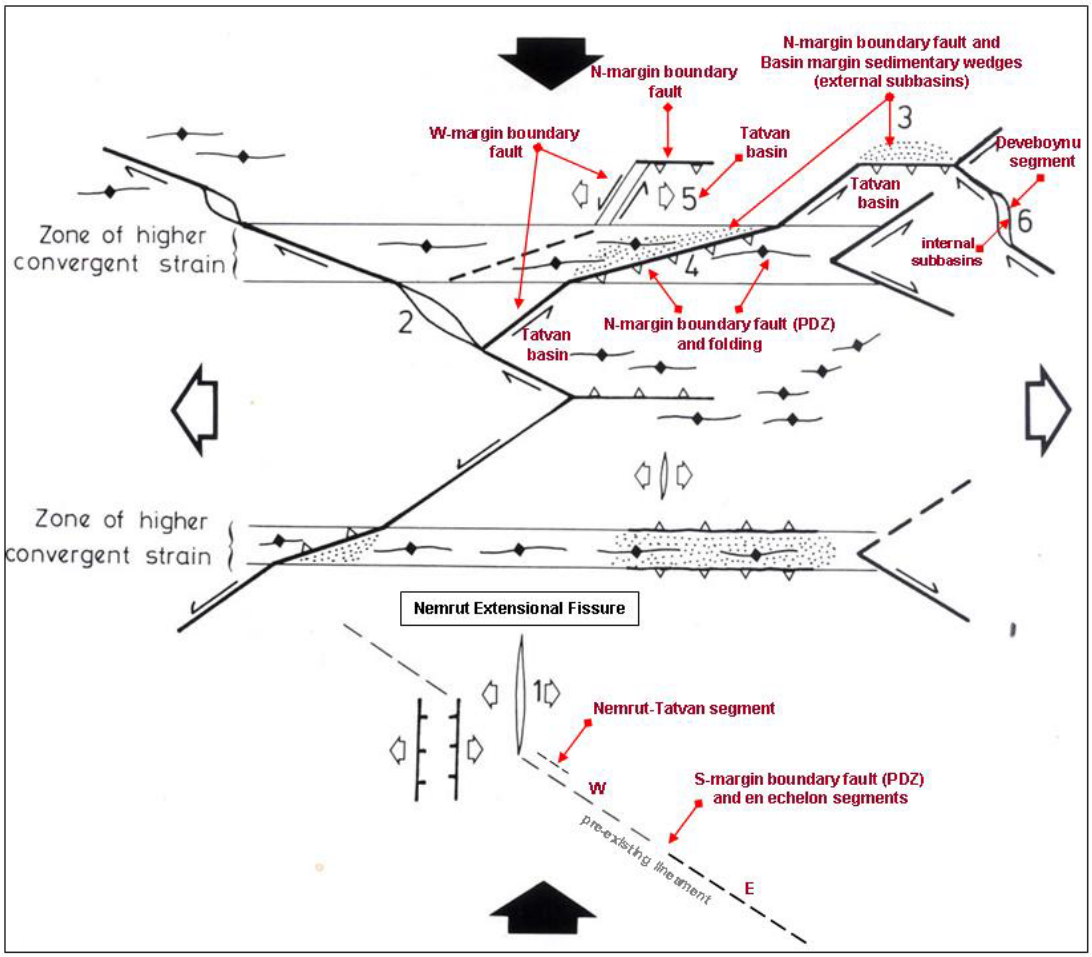

Figure 3.40 : Summary diagram of the overall deformational pattern in the East Anatolian contractional province. The numbers (1-6) indicate the types of basins that form in this environment (modified after Şengör et al., 1985). Note that the types of faulting, the subbasin and strike-/oblique-slip basin formation in the region (red arrows) are compatible with the deformation pattern in Lake Van basin (see text for discussion).

Structural relation seen in Fig. 3.40 between the extensional features of Nemrut volcanic dome complex and discontinuous en echelon faulting in S-margin boundary implies that W-segment, in fact, characterizes the en echelon fault-controlled emplacement mechanism of magmatic intrusions and/or volcanic domes through S-spur zone. Some of these occurrences are peripherally collapsed, parasitic concave cones, the one is Incekaya collapsed cone (Figs. 3.13 and 3.14) and the other is Reşadiye collapsed cone (Figs.3.3, 3.5, 3.8, 3.9, 3.15 and 3.16).

These seismic sections show the sublacustrine continuations of fissure and central vent volcanoes. Some of these seismic sections, due to the limited offset, only show the extrusive products of active and passive intrusive activity (Figs. 3.5 and 3.16) and some other sections well image a clear evidence of active or passive intrusive and extrusive activity (Figs. 3.3, 3.8 and 3.9). Strong coastal erosion, hole or gap-like irregular coastal morphology and very steep cone-like topography of S-coastal section suggest that there are, at least, two collapsed cones submerged into lake. Their pre-existing locations are morphologically well identified by bay formations (see geological map by MTA, 2001).

Small-scale W-E trending reverse faults are identified and mapped along N-portion of Deveboynu peninsula by MTA, (2001) (examine detailed geological structure of lake in MTA, 2001). W-segment, striking W-E, most probably merges with these faults in N-portion of Deveboynu peninsula. This suggests that these reverse faults might have been reactivated as transtensional faults during Quaternary (Koçyiğit et al., 2001). This also indicates that N-half of Deveboynu peninsula is highly deformed, this result is compatible with the present day oblique-slip activity of S-margin boundary fault. This N-portion of Deveboynu peninsula is the E-end of W-segment, while its W-end is at the location of Tatvan delta subbasin in SW-corner. Beyond SW-corner is an area of more complicated, irregular and discontinuous extensional and transtensional fault patterns, indicating an accommodation area of Nemrut volcanic dome complex (see and examine high-resolution morpho-tectonic map by Dhont and Chorowicz, 2006 for these fault patterns and faulting map of Nemrut volcanic area by Özdemir et al., 2006 for fault extensions).

3.3.2.2 E-segment (Cryptic suture-parallel fault)

E-segment, Cryptic suture-parallel fault, is imaged by seismic sections illustrated in Figs. 3.16-3.20, 3.23, 3.24 at the bottom, and 3.25. This segment is respectively ranged and shown from Fig. 3.16 (Es-Tt_1) to Fig. 3.20 (Es-Tt_5) and Fig. 3.23 (Es-Tt_6), Fig. 3.24 (Es-Tt_7) at the bottom and Fig. 3.25 (Es-Tt_8). These seismic sections show that E-segment is also entirely covered by a strong intrusive and extrusive activity and related vent, fissure or fracture systems, giving an evidence of transtensional activity and the subbasin formation (especially in Figs. 3.18 and 3.20). Structural interpretation from these seismic sections across E-segment shows that E-

segment represents strain compatibility “holes and gaps” as recognized W-segment and an echelon continuation of W-segment.

E-segment strikes W-E, obliquely cuts central Tatvan basin in W (Figs. 3.16 and 3.17) and results in Çarpanak block uplift and internal subbasins (Deveboynu and Varis spur zone subbasins) toward E. This segment is responsible for the formation of subbasins and Çarpanak uplift, while W-segment controls Tatvan delta subbasin in SSW-corner. These internal subbasins develop in W- and E-en echelon segments of S-margin boundary fault, indicating broadly widening shear zone of negative flower structure (see Figs. 3.39). This shows that en echelon nature of S-margin boundary fault has important structural implications for understanding transtensional system in S-margin.

Keskin, (2005 and 2007) postulated that Cryptic suture zone elongates all along the W-E cross sectional area of lake. E-extension of this suture zone possibly refers to some unmapped faults in E-part of SE-delta. Some dextral strike-/oblique-slip faults are reported by previous field and earthquake studies (pers. comm., Utkucu, 2004; Köse, 2006; Şaroğlu, 2007 and unpublished sketch maps by Utkucu, 2004). The possible existence of these unmapped faults is also expressed by seismotectonic studies from Türkelli et al., (2003). The prominent ones of these oblique faults are Gevaş/Gürpınar in S, Edremit in SE and Kalecik faults in E. Emplacement patterns of these dextral faults are compatible with fault-controlled coasts of SE-delta. It is interpreted that W-E striking Kalecik dextral strike-slip fault probably merges with E-segment in Çarpanak province (see and examine Figs. 3.24 at the bottom and 3.25). Figs. 3.24 at the bottom and 3.25 show that E-segment is overlain by a thin sedimentary section of Van delta, cuts the Çarpanak uplift, and extends into the further E, possibly an area of Kalecik. This implies that E-segment continues from Çarpanak province through N-part of SE-delta into merging of Kalecik fault in the furthest E and thus, it structurally divides delta setting into two subdeltas, NE- and SE-deltas. It also seems that Edremit and Gevaş/Gürpınar fault systems possibly extend into and deepen within SE-delta, controlling the basement structure of SE-delta (Figs. 3.20 and 3.41). Fig. 3.20 across Eastern delta between Gevaş in S and Çarpanak spur zone in NNE (also see detailed portions of this section seen in Figs. 3.21 and 3.22) and Fig. 3.41 across Van and Eastern deltas between Kalecik in NNE and Edremit in SSW show asymmetric structural geometry in SE-delta. Asymmetric

structural geometry seen in Figs. 3.20 and 3.41 is probably a tilted basement block structure recently controlling SE-delta. This, in fact, indicates extensional half-graben pattern of SE-delta setting between Edremit and Kalecik. This half-graben pattern is most probably resulted from lakeward extensions of Edremit and Gevaş faults, bounding traverten deposits. This implies that the basement of SE-delta is a reactivation product, recently controlled by dextral normal oblique faults. The evidence for this also comes from the recent studies.

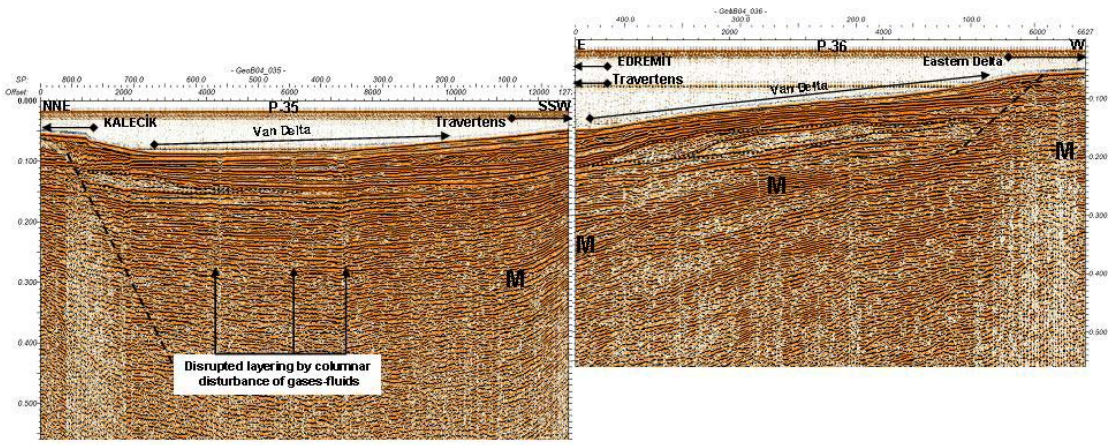

Figure 3.41 : NNE-W seismic section, a combination of NNE-SSW and E-W trending seismic profiles, from Van delta across a zone of Kalecik, Edremit, Eastern delta and traverten areas. Seismic profile numbers of this combined section are 35 and 36, (P-35 and P-36), as seen at the top center (see the location of this profile in Fig. 2.2). M: multiple. This seismic section clearly shows that the basement topography (probably tilted and fractured traverten deposits) underlying Van delta strongly controls possible half-graben structure, delta sedimentation and clinoform patterns. Note that sedimentation, due to rapid asymmetric subsidence, is faster than faulting. Dashed thin lines (black colour) indicate possible faults and dotted round thin lines (black colour) indicate slumped progradational wedges (max. sediment thickness: 190 m, min. sediment thickness: 115 m, max. water depth: 65 m-95 m, offset: 19 km, two-way travel time in sec).

Şengör et al., (2008) examined NE-, E- and SE-outcrops of Lake Van basin. Their geological sketch maps evident that some outcrops of accretionary-ophiolitic complex are controlled by dextral strike-slip faults. This suggests that E-part of lake is characterized by accretionary-ophiolitic outcrops and controlled by a zone of dextral fault systems (Şengör et al., 2008). Some of these dextral fault systems may have the continuations into the lake. If geological sketch maps of related areas are examined in the light of the present day seismic observations, it is seen that fault in ENE of lake (WNW of Erçek lake) probably extends toward the lake, to NE-Erek delta and into N-margin boundary fault (see Fig. 3.12).

In spite of having no any age data, it is speculated that dextral strike-slip fault systems located in E-part of lake might be a structural continuation of oblique-slip and extensional deformation of lake. As a result of this, SE-delta experiences normal oblique-slip deformation associated with dextral oblique faults in Gevaş/Gürpınar, Edremit and Kalecik and has extensionally-tilted basement block.

3.3.2.3 Deveboynu-segment (fault-stepover peninsula)

W-segment oversteps Deveboynu peninsula, beyond which E-segment initiates. Horse-tail or imbricate fan-shaped termination of S-margin boundary fault results in en echelon arrangement of transtensional Deveboynu and Varis spur zone subbasins offshore Deveboynu peninsula in the W-end of SE-delta setting (Figs. 3.26-3.29 and 3.30 at the top). Muş suture passes across Deveboynu segment, curves toward S and follows offshore Deveboynu peninsula. Hence, Deveboynu segment is an important structural factor controlling W- and E-en echelon segments of S-margin boundary fault and intrusive activity of rising magmas through Deveboynu and Varis spur zone subbasins.

Overall deformation pattern of these internal subbasins refers to number (6) seen in Fig. 3.40, reflecting a small-scale pull-apart boundary at the W-end of SE-delta. Their structural development and evolution around offshore Deveboynu segment is perfectly illustrated by structural pattern and geometry of Narman-Horasan earthquake as reported by Şengör et al., (1985) (see Fig. 3.42). Such an example is presented in Figs. 3.40 and 3.42 to emphasize the complexity of both local factors and the available physical mechanisms. These influence the formation of extensional and transtensional subbasins in regions of such complicated strike-slip fault development as recognized in S-margin boundary and Deveboynu segment. In Deveboynu segment, this is best illustrated by the population of faults, a number of which, located between Deveboynu peninsula and Çarpanak spur zone, are most probably reactivated by earthquakes (examine its best example “Narman-Horasan” earthquake in Fig. 3.42, as suggested by Şengör et al., 1985).

The most salient feature of Deveboynu segment is the abundance of NNW-SSE-striking en echelon arrangement of transtensional faults, forming Varis spur zone subbasin. These faults are clearly a part of S-margin boundary fault system and, subject to dextral oblique-slips. The discontinuous character of these faults and their

complex relationships with one another are clearly visible, as illustrated in Fig. 3.42 (compare them with Narman-Horasan earthquake area). They all work in such a way as to accomplish N-S shortening with corresponding transtensional subbasins. Hence, Deveboynu segment shows an active example of structure compatibility on a still smaller scale with an analogy to Narman-Horasan area. Both Deveboynu segment and Narman-Horasan area has extreme structural and faulting similarities in forming the subbasin at various scales.

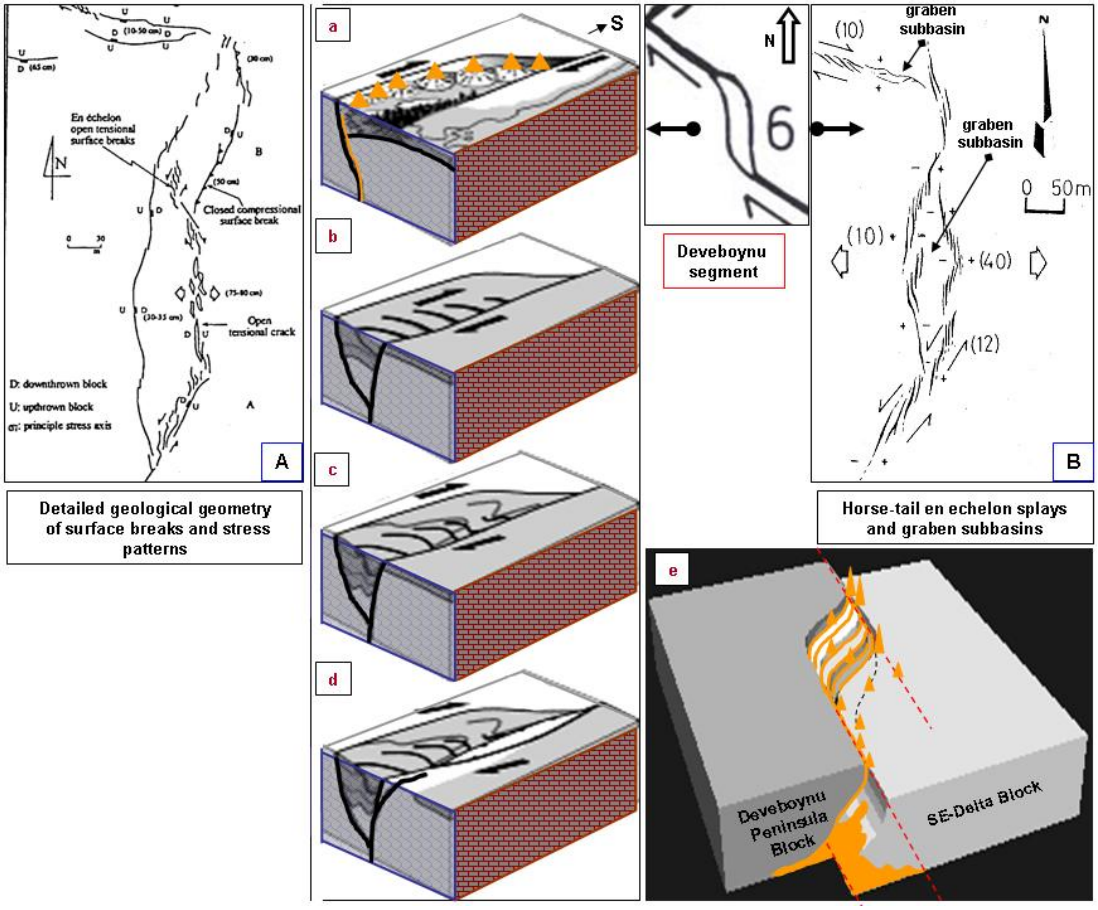

Figure 3.42 : A and B show active fault pattern and the surface breaks generated during Narman-Horasan earthquake (after Barka et al., 1983; Şengör et al., 1985 and Koçyiğit et al., 2001). Hybrid nature of surface breaks consists of a series of en echelon extensional shear fractures and extensional subbasins (the center) and dextral in N and sinistral strike-slip fault in S that formed during the same earthquake (A and B). Detailed geological geometry of surface breaks and stress patterns is also shown in A. 3D-tectonic block model of Deveboynu segment (number 6) is ranged in (a-e) that shows 3D-tectonic interpretation of the faulting pattern, pull-apart (sphenochasm) subbasin formation and extensional magmatism in W-margin of SE-delta setting. Notice active extensional magmatism within sphenochasm formation between SE-delta and Deveboynu peninsula blocks as seen in e).

Fig. 3.42 diagrammatically characterizes complex faulting geometry and related subbasin formation, similarly offshore Deveboynu segment. This diagram shows that the two sides of the surface break move away from one another, probably during the earthquakes as shown by the broad arrows. The motion is accommodated by a small graben or a subbasin in the central part of the break, which connects with strike-slip systems at both ends. The N-dextral system with W-E strike is characterized by predominantly by strike-slip with normal component, as suggested by the depression it encloses. This describes dextral transtensional formation of both Varis spur zone and Deveboynu subbasins, parallel offshore Deveboynu segment and toward the further S. The S-system with N-S strike exhibits a considerable component E-W extension (with a lesser strike-slip component) (examine similar structural and basinal models in Özgül et al., 1983 and Şengör et al., 1985). In fact, Fig. 3.42 is a detailed structural version of a small pull-apart basin, "sphenochasm" (pers. comm. Şengör, 2010) shown by number (6) in Fig. 3.40. Fig. 3.42 evident that the component of extension is indicated by the hybrid nature of surface breaks associated with the nearby earthquakes. Extensional component thus is responsible for the bifurcation and propagation of the fractures. This component produces the subbasin geometry, and the strike-slip component permits an extensional-transtensional basin to develop. This indicates that surface breaks such as secondary faults, splays or branches in and aroun Deveboynu segment consist of extensional and transtensional subbasins. Structural similarities between the faulting and subbasin geometry in Deveboynu segment and Narman-Horasan area suggest pull-apart type subbasin formation offshore Deveboynu peninsula that is the W-end of SE-delta.

3.3.2.4 Nemrut-Tatvan segment (en echelon faults-dome/cone complex)

Nemrut-Tatvan segment, located in SSW-corner of lake, has a complicated pattern of deformation characterized by en echelon nature of transtensional faults and intrusive-extrusive activity (Figs. 3.13 and 3.14). Splay faults-controlled Tatvan delta subbasin filled with rising intrusive activity is overlain by thin sedimentary section. The most prominent structural feature of Nemrut-Tatvan segment is a dense concentration and emplacement of intrusive-extrusive activity along and through a complex network of faults, vents, fractures or fissures (Figs. 3.13-3.15). This suggests a deformational relation of dome-cone complex in and around Nemrut volcano to Tatvan delta at SSW-corner. This situation relates an area of Tatvan delta to Nemrut complex,

namely “Nemrut-Tatvan segment”. This segment is entirely covered by a wide range of dome-cone complex and a transfer zone of ductile strains from Nemrut area to Tatvan delta and into W-segment. Overall deformation pattern of this segment refers to number (1) seen in Fig. 3.40, reflecting an internal subbasin developed in W-segment.

Nemrut volcano is located on a N-S orientated fissure that functioned as a magma conduit (Şengör et al., 1985). Morphology of the Nemrut volcano shows distribution of parasitic cones and small centres around it (see related map in Dewey et al., 1986).The linearity of parasitic cones extends through Tatvan delta into W-segment (see Şaroğlu and Yılmaz, 1986 and Yılmaz et al., 1987 for details). Some of these parasitic cones are prominently collapsed passive cones, “Incekaya Collapsed Cone”, and some is still active intrusions as imaged by seismic data (Figs. 3.13-3.15). In and around Nemrut-Tatvan segment, several dome-cone complexes and Quaternary volcanic spreads, especially immediately SW-corner of lake from the distribution of small conical volcanic centres are erupted from approximately N-S fissures. These N-S fissures are part of a widespread array of N-S fissures and fractures throughout Nemrut-Tatvan segment. They appear to be caused by extensional and transtensional processes. Dewey et al., (1986) stated, mainly on the basis of the distribution of the parasitic cones and using the principle outlined by Nakamura, (1977) that extensional fractures box the compass and many clearly rejuvenate older structures. However, there is a preponderance of N-S fractures, some of which control the positions of volcanoes (Nemrut) and parasitic cones associated with Nemrut-Tatvan segment show N-S (Nemrut) trends. Number (1) in the diagram seen in Fig. 3.40 implies structural relation between Nemrut extensional fissure and the faulting in Nemrut-Tatvan segment, indicating a kinematic link up with strike-/oblique-slip system in S-margin.

3.3.3 Overall deformational patterns and fault-margin basin types

The overall deformational patterns of margin-bounding faults and related basin types are illustrated in a schematic summary diagram (Fig. 3.40 from Şengör et al., 1985). This diagram shows the relationships of individual structures to one another and to the overall pattern of strain in the province.

This is best illustrated by the numbers (1-6) in the diagram (see text of Şengör et al., 1985 for discussion), indicating the various types of strike-slip basins that formed in the lake as the follows;

- Number 1; this indicates the relationship of Nemrut extensional fissure to en echelon oblique-slip system of S-margin boundary. This is originated by complex patterns of fracture and magma propagation along oblique-slip faults. This first forms in isolation to link up later with strike-slip systems. These may be zones of incipient strike-slip faulting (Şengör et al., 1985), as in the case of number (1).

Number 1 implies that S-margin boundary fault (PDZ) is an incipient faulting that forms en echelon nature of oblique-slip system trending from W to E. This faulting shows the transtensional segments in various scales and links up with W-segment.

- Number 3; this indicates the external subbasin with the coastal onlap-trough fill pattern in sublacustrine slope, which is basin margin sedimentary wedge, controlled by N-margin transpression system.

- Number 4; this indicates transpression system in N-margin with folding in central Tatvan basin and also the external subbasin, as in the case of number (3).

Numbers (3) and (4) form along restraining bend, which themselves may be primary or secondary features. It is to say that numbers 3 and 4 typically characterize general deformation pattern of N-margin of lake and external subbasin formation.

- Number 5; this indicates both N- and also W-margin boundaries, and central Tatvan basin, describing oblique-wedge block motion of central Tatvan basin.

According to this diagram, the margin-bounding faults are compatible with the rhombohedral block faulting (see number 5 and NE- and NW- conjugate wrench faulting and W-E escaping blocks).

- Number 6; this is oriented in NNW-SSE, indicating Varis spur zone and Deveboynu subbasins, and forming along releasing bend of strike-slip faults. Number 6 well reflects Deveboynu segment in the W-end of SE-delta.

Rhomb-shaped block faulting across N-, W-margin boundaries (number 5) and S-margin boundary (number 1) characterizes overall deformational pattern and related basin types (numbers 3, 4; 6) of the lake. Most seen in this diagram tend to maintain their orientation with respect to the regional orientation of the maximum N-S

shortening axis (numbers 1, 2, 3, 4) and some, however, must rotate around vertical axes (numbers 4, 5) (Şengör et al., 1985). Numbers 4 (N-margin and central Tatvan basin) and 5 (W- and N-margins and central Tatvan basin) in fact describe a kinematic pattern of central Tatvan basin block and also Lake Van. It is interpreted that numbers (4) and (5) are vertical axes-block rotational sections of Lake Van basin (see Dewey et al., 1986 for internal and external rigid body rotations of crustal flakes). Sinistral transpression in N-margin boundary has an external sense of rotation that is counterclockwise, whereas dextral transtension in S-margin boundary has clockwise external rotation. The effects of both the internal rotation due to wedging and the external rotation due to wrenching further distinguish synthetic and antithetic faults (Wilcox et al., 1973).

Overall deformational patterns and related basin types indicate a complex relationship between margin boundary faults and the N-S convergent regime. The evolutionary stages of oblique-slip deformation are developed throughout a W-E zone of higher convergent strain within the conjugate strike-slip fault systems (see Muş suture). These fault systems divide the area into rhombohedral blocks that move E or W, away from the zone of convergence. This is the most prominent feature of basin formation types seen in the lake (see Şengör et al., 1985 for a brief description of rhombohedral block tectonics). These basin types are compatible with strike-/oblique-slip basin formation seen in diagram (Fig. 3.40). Although strike-/oblique-slip influences the orientation of small, local features in a few cases, most large-scale structures are the products of the overall N-S convergence (Şengör et al., 1985). Margin-bounding faults and related basin types, all accommodate this N-S shortening, some by thickening the crust (local crustal thickening) and some others by elongating the crust perpendicular to N-S shortening (Şengör et al., 1985). This suggests that crustal structure of Lake Van is elongated, preferentially toward ENE. This also confirms that Muş and Lake Van basins are elongated and strike-slip/thrust-bounded basins (Dewey et al., 1986).

In Fig. 3.40, a zone of higher convergent strain is considered to be a W-E-striking Muş suture . W-E sideways of zone of higher convergent strain is represented by dextral and sinistral oblique-slip fault patterns, wedge-shaped escaping blocks, fold axes and pull-apart basins at various scales. Such a picture of the complex deformation describes overall deformational patterns and fault-margin basin types

recognized all over the lake. This picture also implies that Muş suture as zone of higher convergent strain may be a zone of the pre-existing linear weakness across S-margin boundary. The diagram clearly reveals the repeated cycles of basin formation and the overall deformational pattern at smaller scales, similarly in E-Anatolia. This indicates that all elongated basins in E-Anatolia overlie a strike-slip fault and that most of the elongate high areas are bounded by strike-slip faults (Dewey et al., 1986). The fault-bounded elongation of crustal structure of lake reveals that the lake is a crustal wedge-shaped piece of accreted continental material, squeezed out of the convergent area (also see Şengör et al., 1985; Dewey et al., 1986 and Şengör et al., 2008). Margin-bounding faults appear to be subordinate, shallow (thin-skinned or detached) features accommodating differential extension between hanging-wall block compartments that move on enormous low-angle normal faults (as proposed by Dewey et al., 1986). These faults generate a variety of basin types across marginal sections of the lake (Şengör et al., 1985).

An interesting point concerns the evidence indicating the wedge-block motion of Tatvan basin. Oblique wedge-block structure of central Tatvan basin is shown in numbers (4) and (5) and interpreted by a detailed analysis of the diagram in Fig. 3.40. This evidence speculates that initial wedge-block escape may have been accommodated by oblique-slip in S-margin and thus causing transpression in N-margin. This implies that a fault reactivated in S-margin and in places disrupting the suture and began to accommodate the ENE motion of central Tatvan basin. The disrupted suture youngs toward E due to recent activity of rising magmatic material, aligned from W to E, parallel to the suture. This situation suggests that the obvious places in the geological record to start searching for wedge-block escape regimes are where sutures progressively young in one direction (Şengör et al., 1985). If gravity potential-related elevation differences between N- and S-margins are taken into consideration, the wedge-block escape occurs from an area of high topography in S-margin towards a lowland in N-margin (an escape mechanism proposed by Şengör et al., 1985 in well-developed escape regimes). Tectonic interpretation of deformation patterns and margin-bounding faults suggests that inhomogeneous wedge constriction and segmentation trending normal to the N-S direction of convergence (Şengör et al., 1985) results in releasing and restraining bends along the strike-slip boundaries of the lake.

Inhomogeneous constriction of the escaping wedge block generates transtensional and transpressional structures such as push-up ridges along the strike-slip boundaries of the wedge. If the motion of the wedge away from the zone of constriction is checked by another continental object, the wedge tries the next easiest route to continue its escape. In this process, the wedge may disintegrate internally and experience oblique-slip deformation. As known, the accretionary basement complex of the lake is characterized by extensive terrains of high temperature/low pressure metamorphic rocks, extensive structural imbrication complicated by the presence of criss-crossing, steep, ductile shear zones (magma chambers and pointed stocks), and abundant alkalic intrusions (intrusive activity of rising magmas). As interpreted from seismic sections through S-margin boundary, these intrusions pass sideways, parallel with suture zones younging in same direction, towards E, into regions where the internal subbasins are nested on former zones of distributed extension, as well recognized in E-segment and Deveboynu segment. These observations are good candidates to be products of continental escape, as proposed by Şengör et al., (1985).

The remark is that the observed younger deformation across margin boundary faults has complex relationships with older, paleotectonic structures. Margin boundary faults seem to be "replacement structures" with respect to the penetrative and semi-penetrative paleotectonic structures of the basement (Şengör, 1982; Şengör et al., 1985). Many of the younger appear to have been controlled by the older ones. This proposes the pre-existing fabrics in crustal basement and replacement structures in fault margins. W-E striking Muş and Cryptic suture zones across the lake in S-margin are the penetrative pre-existing fabrics of the basement. Through these sutures, the PDZ of S-margin boundary fault develops. Its initial emplacement is most probably controlled by pre-existing thrust contacts or suture zones. The steep emplacement and structural development of N-margin boundary fault suggests that this fault is a pre-existing high-angle thrust (also see Şengör et al., 1985; Dewey et al., 1986 and Dhont and Chorowicz, 2006 for structural development of margin boundaries of Muş basin). It seems that N- and S-margin boundary faults are pre-existing thrusts and replacement structures bounding wedge-block structure of central Tatvan basin. This situation implicates for a recent reactivation of accretionary basement. Underlying accretionary complexes, adjacent ophiolitic or suture zones are usually steepened to overturned in late-stage crustal scale rotation.

Rétrocharriage zones (Roeder, 1979; Şengör and Yılmaz, 1981; Dewey et al., 1986) may also involve extensive backthrusting over adjacent plateaux or hinterlands. Seismic sections seen in Figs. 3.2-3.10 show the backthrusting in the sublacustrine basement block across N-margin boundary and related intrusive and extrusive activity across W-margin boundary. These younger structures coincide in space with paleotectonic structures, but do not perform the same function as the latter. The new structure replaces the old one. A high-angle thrust fault (N-margin boundary), for example, reactivates a former normal fault or a strike-/oblique-slip fault nucleating on a rotated suture. Highly penetrative pre-existing fabrics strongly control W-E striking basinal emplacement and structural development of lake, suggesting the development of mechanical anisotropy in the crustal basement of lake.

Seismic structural and tectonic interpretation through the summary diagram in Fig. 3.40 gives several clues to both deformation styles, basin types and basin history. Sinistral transpression in N and transtension in W and dextral transtensions in S and SE and a series of disconnected internal-external subbasins of similar age through the marginal sections may line up marking the course of former strike-slip faults (Şengör et al., 1985) or the course of former weaknesses or of pre-existing structural lineaments. This suggests that the subbasin formation with complex strain histories may mark places where strike-slip faults interfered in the past to generate incompatibility problems, as indicated by Şengör et al., (1985). Thus, incompatibility effects seem to dominate the causes of basin formation in complexly faulted areas, of the kind commonly generated in zones of wedge-block escape.

3.4 NE- and SE-Provinces of Delta Domain

NE- and SE-provinces of delta domain bounded by E-segment represent Erek delta in NE and Eastern and Van deltas in SE. E-segment in S-margin obliquely controls Çarpanak spur zone and thus, NE- and SE-delta settings shown in Figs. 3.16-3.25. Normal oblique-slip faulting results in Deveboynu and Varis spur subbasins (Figs. 3.26-3.30 at the top). These seismic sections show that sediment dynamics in delta settings is strongly effected by neotectonic deformation and related earthquakes. Given the difficulty in objectively defining the actual process or processes from seismic data and map views, sediment dynamics is adopted here because it encapsulates all modes of sediment failure, transport, and deposition in delta settings.

In sublacustrine slope and lacustrine shelf settings of lake, a continuum of gravity-driven re-sedimentation processes exists, ranging from rock falls to slumps, slides, glides of progradational wedges to viscous debris flows, and dilute turbidity currents to deep central basin (see and examine Figs. 3.16-3.20, 3.23, 3.25, 3.33 and 3.34). These seismic sections show that high magnitude sediment dynamics from NE-Erek delta to internal subbasins and into central Tatvan basin is mainly triggered by E-segment-controlled strong tectonic activity. E-segment across delta settings results in a sharp basement block uplift of Çarpanak spur zone (NE-Erek delta) and downlift of Eastern and Van deltas (SE-delta system) (see especially Figs. 3.20 and 3.41). A structural interpretation of these seismic sections considers that the shear strength of the slope sediment is a function of the cohesion between the grains and the intergranular friction (Stow, 1986), with failure occurring once the shear stress exceeds it. Sediment properties, such as chemical composition, cohesion, and angle of internal friction and the presence of free gas or gas hydrates also affect slope stability (Nigro and Renda, 2004 and Heiniö and Davies, 2006). Sublacustrine slope failures, as in submarine slopes, have common features that are independent of scale. Arcuate headwall scarps form at the upslope reach of the failure and commonly grade or transform abruptly into listric shear surfaces (Varnes, 1978; Prior and Coleman, 1982; Lastras et al., 2004 and Heiniö and Davies, 2006) (see progradational wedges in Figs. 3.23 and 3.25-3.27). These shear surfaces commonly have a lower dip than the lake floor and, therefore, intersect it (Mello and Pratson, 1999). A fault scar is left behind if the failed mass is mobilized post-failure and moved downslope (Figs. 3.16-3.21). The failed mass, if coherent, commonly exhibits evidence for extensional deformation near the scarp. In some cases as seen in Figs. 3.25, 3.33 and 3.34), progradational blocks of sediment become detached from the main mass of failed sediment and glide farther down the slope, forming out-runner clinoform blocks (Lastras et al., 2004). Failed sediment masses are identified from seismic data seen in Figs. 3.23, 3.25-3.28, 3.33 and 3.34 on the basis of their low-amplitude chaotic reflection pattern (Lastras et al., 2004; Frey Martinez et al., 2005 and Heiniö and Davies, 2006).

These seismic sections clearly indicate unstable delta dynamics and show that unstable dynamics of delta sedimentation characterizes a sedimentary development of the deformation-dominated delta and the physical character of subaqueous

sedimentary density flows and their depositional styles. Unstable sediment dynamics also provides seismic and structural information essential for understanding the stratigraphic, morpho-physiographic and topographic results of degradation of delta depositional sequences and *in situ* soft-sediment deformation structures. This identifies the role of deformation in controlling depositional patterns and depositional processes on the delta sedimentation and structural controls on the positioning of sublacustrine submerged channels on deltas. These seismic sections from delta settings well define, describe a range of features that form during delta degradation and show the variety of re-sedimentation styles, the function of pre-existing structure and slope morphology in degradation complex development. A seismic interpretation of the observed structural and sedimentary unstability products in delta settings can give a clue to both the transport mechanism on the basis of specific, objective observations (seismic geometry and a general knowledge of sediment properties) and a possible instability model for the evolution of shallow water delta degradation phenomena.

3.4.1 Morpho-physiographic and topographic structure

Morpho-physiographic and topographic structure, distributional patterns of delta progradational clinoforms, deeply incised submerged channels and *in situ* soft sediment deformation structures are summarized in the map shown in Fig. 3.43. This map reflects a complicated relation of soft sediment deformations to progradational clinoform patterns. In this map, Lake Van is divided into three morpho-physiographic provinces; (1) a lacustrine shelf, (2) a sublacustrine slope, and (3) a deep, relatively flat Tatvan basin province. The central Tatvan basin is quasi circular in shape and occupies an area of ~440 km^{2}. The most prominent features of the lacustrine shelf and sublacustrine slope are prograding delta sequences, submerged channels, as well as soft sediment deformation structures. Soft sediment deformation refers to strongly deformed and irregular karst-like topography, reflecting the variable history of the lake. The NE- and SE-delta provinces in Fig. 3.43 are divided into three structural domains: (1) a submerged river-channel domain, probably controlled by various-scales faults, (2) a progradational domain characterized by clinoform complexes and wedge-shaped sedimentary packages, and (3) a soft sediment deformation domain dominated by various sedimentary perturbations and internal sedimentary deformations.

Fig. 3.43 also implies mainly three depositional settings in the lake. These depositional settings are strongly controlled by near vertical motions rather than large-scale gravity tectonics within delta environment.

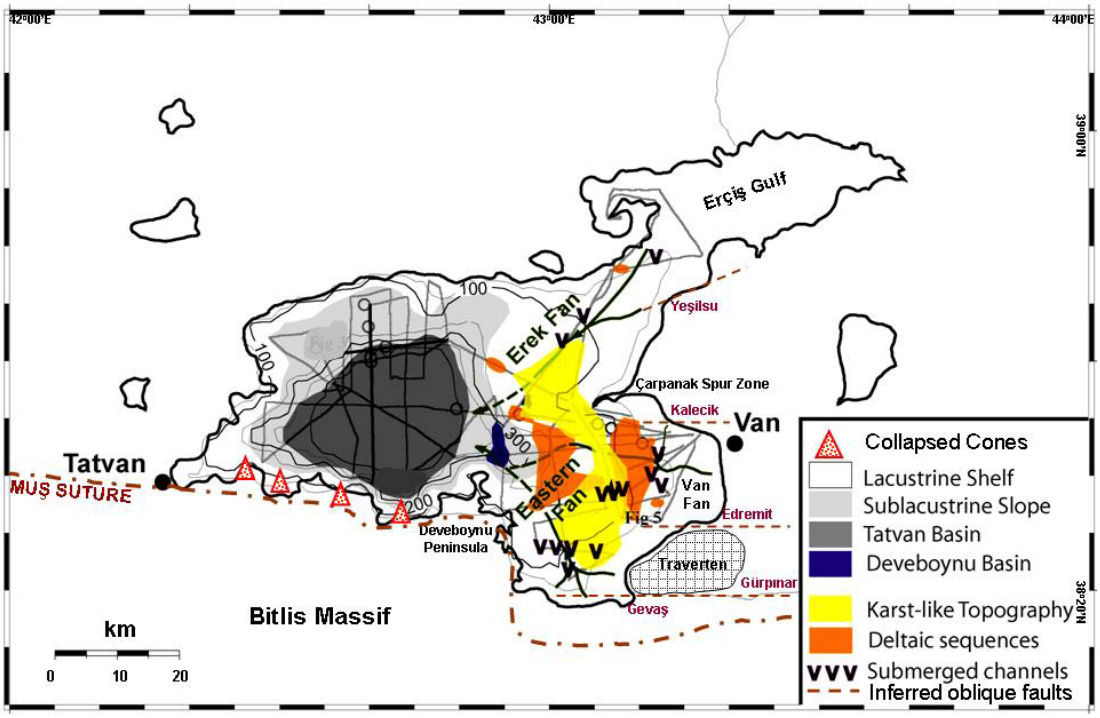

Figure 3.43 : General morpho-topographic map and physiographic provinces of Lake Van basin. NE-Erek and SE-delta settings are characterized by soft-sediment deformation structures (karst-like topography). Note that central Tatvan basin is rhomb-shaped and inferred oblique-slip faults around the delta settings are well compatible with the lakeward continuation of submerged river channel systems. In this map, Deveboynu subbasin is shown as a morphological feature.

a) central Tatvan basin, which is oblique-slip controlled wedge block, asymmetrically subsides.

b) NE-Erek delta lying on Çarpanak uplift is characterized by relatively low sediment and burial rates (Figs. 3.16-3.20, 3.24 at the top and 3.25). Its slope morphology is gently lowering and regularly smoothing toward central Tatvan basin, close to N-margin boundary (Fig. 3.25). However, its slope is sharply increasing towards Çarpanak spur zone in S, due to fault-controlled slope margin (E-segment) (Figs. 3.16-3.20). NE-Erek delta is characterized by submerged river channel complex seen in Figs. 3.24 at the top and 3.44-3.46 and there are only a few deltaic sequences recorded in seismic data shown in Figs. 3.19 and 3.25. These seismic sections with the map seen in Fig. 3.43 show that irregularly deformed soft sediment anomalies are locally distributed in and around Çarpanak spur zone, NE-Erek delta.

This implies that irregulary deformed morpho-topography, river-channel incisions and deltaic sequences show “zonal distribution”.

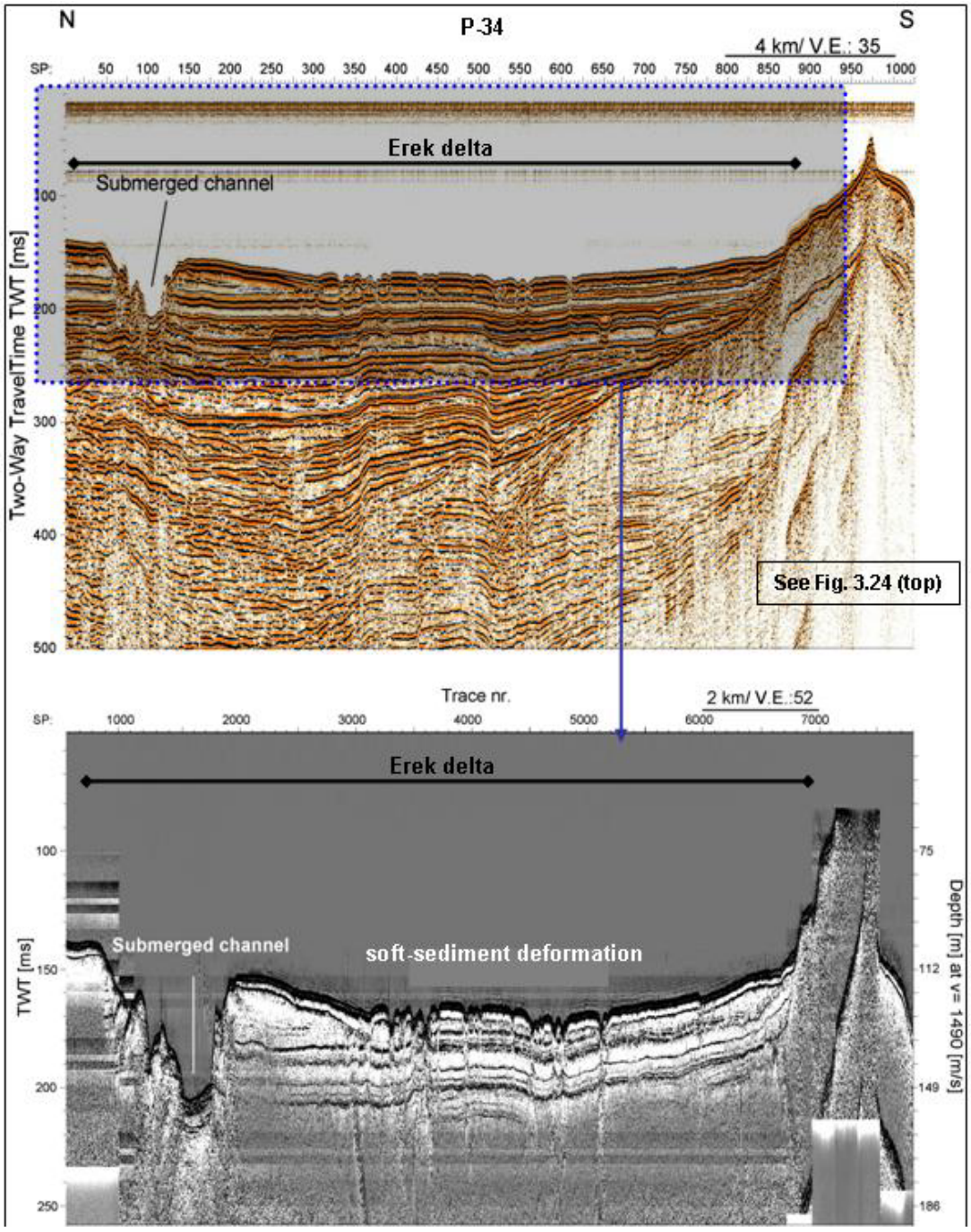

Figure 3.44 : Detailed seismic (upper) and high-resolution chirp (lower) image of N-S seismic section from Çarpanak spur zone and NE-Erek delta across deeply incised submerged channel and soft-sediment deformations (also see seismic section at the top in Fig. 3.24). Seismic profile number is 34 (P-34) as seen at top center (see Figs. 3.45 and 3.46 for detailed interpretation of these images). High-resolution chirp image (lower) shows strongly deformed bedding in time interval 0-260 (ms) of seismic section (dotted blue square in upper section).

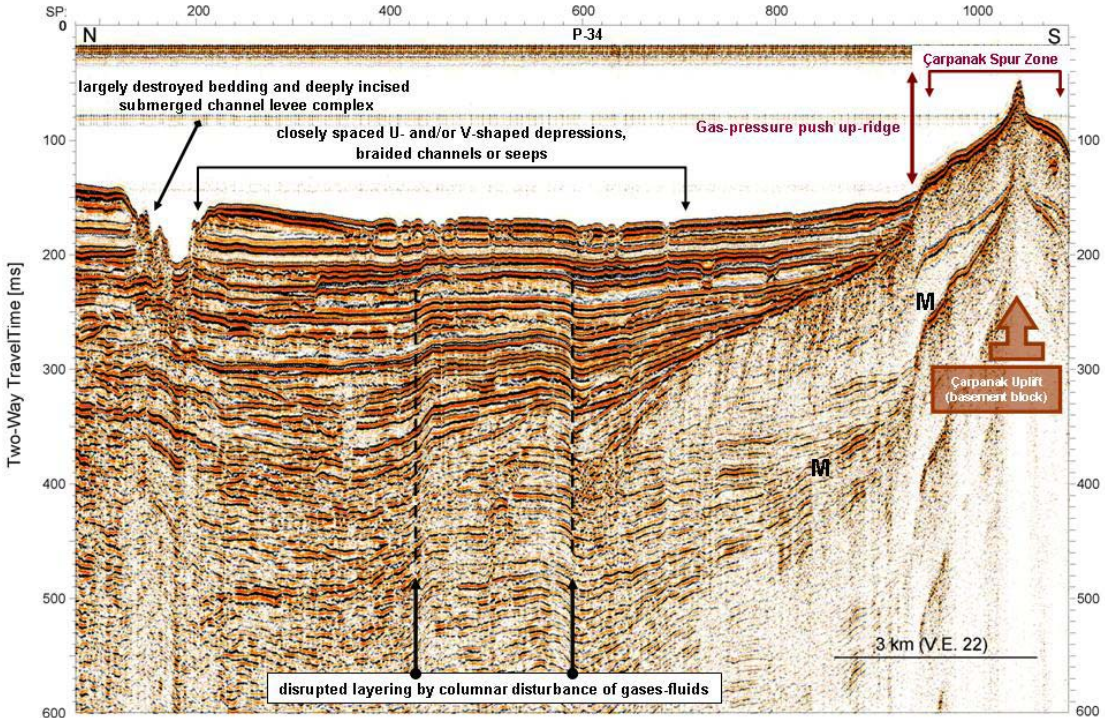

Figure 3.45 : Detailed seismic image of N-S seismic section from Çarpanak spur zone and NE-Erek delta across deeply incised submerged channel and soft-sediment deformation structures. Notice gas-pressure push up-ridge structure of Çarpanak spur zone and columnar disturbances of gases-fluids (see Fig. 3.46 for the high-resolution chirp image of this section).

c) SE-delta (Eastern and Van deltas) is asymmetrically subsiding block, characterized by relatively high sediment and burial rates (Figs. 3.20, 3.23, 3.24 at the bottom, 3.26-3.30 and 3.41). Its slope morphology is gently lowering and smoothing toward central Tatvan basin in NW, close to Deveboynu peninsula and characterized by Deveboynu and Varis spur zone subbasins (Figs. 3.18, 3.20, 3.23 and 3.26-3.30 at the top). But, its N-part is strongly controlled by E-segment across Çarpanak uplift (Figs. 3.16-3.20, 3.24 at the bottom and 3.25). SE-delta is also characterized by submerged river channel complex seen in Figs. 3.20, 3.22, 3.24 at the bottom, 3.29, 3.30 at the bottom, 3.47 and 3.48 and there are large amount of deltaic sequences recorded in seismic data shown in Figs. 3.26-3.29 and 3.30 at the top. These seismic sections with the map seen in Fig. 3.43 show irregularly deformed soft sediment anomalies are locally distributed in the central part of delta, extending toward Çarpanak spur zone in N. This implies that irregulary deformed morpho-topography, river-channel incisions and deltaic sequences show "non-zonal distribution".

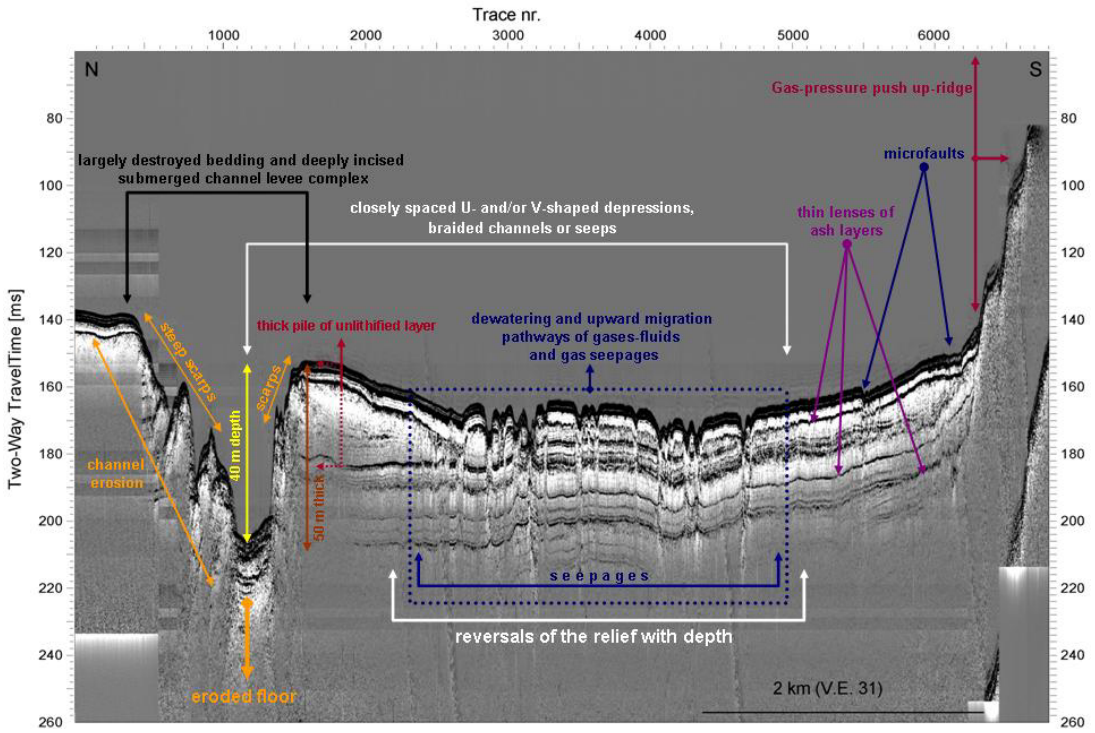

Figure 3.46 : High-resolution chirp image of N-S seismic section from Çarpanak spur zone and NE-Erek delta across deeply incised submerged channel and soft-sediment deformation structures. This chirp section well reflects the high-resolution image of depressurizing, dewatering, destabilization and degradation events in NE-Erek delta setting. Note that thin black lenses are ash layers faulted, unlithified, thick piles of soft sedimentary bedding are strongly dissected and eroded and reversals of the relief with depth also occurred (incised submerged channel depth: 40 m, max. thickness of sedimentary dissection: 50 m, max. water depth: 155 m, min. water depth: 105 m, two-way travel time in msec).

Morpho-physiographic and topographic view from the map shown in Fig. 3.43 is that soft sediment deformation structures are dissecting and disintegrating delta depositional setting and locally disturbing progradational clinoform stability. Internally deformed progradational sedimentary packages are well recognized in seismic sections as slumped, slided/glided, acoustically transparent and chaotically reflecting layers. Soft sediment deformation is also recorded in smoothed, plane-like surfaces in delta shelf settings (Figs. 3.17, 3.19, 3.24, 3.25, 3.28, 3.29, 3.30 at the top). This deformation event is locally covering delta settings, widely starting in SE-delta, locally trending N (Çarpanak spur zone) and partly extending further N (S-part of NE-delta). In map view, this is an “S-shaped zonal distribution”, finding a way between progradational sequences. Soft sediment deformations and progradational wedges are not broadly recorded in the further N of NE-Erek delta, towards Erçiş gulf. In SE-delta, soft sediment deformations and progradational wedges unevenly

end in W-limit of SE-delta, it is because of the presence of Deveboynu and Varis spur zone subbasins (Figs. 3.26-3.29 and 3.30 at the top).

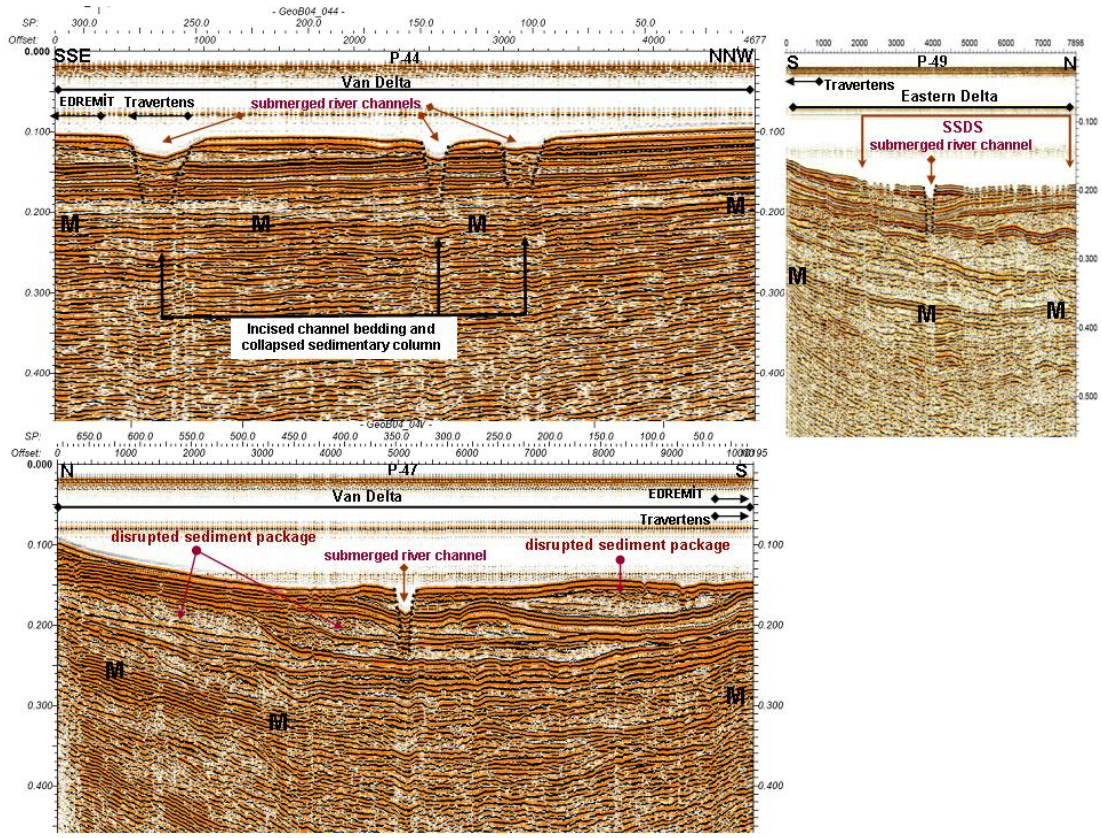

Figure 3.47 : SSE-NNW (top), N-S (bottom) and N-S (top right) seismic sections from SE-delta setting (Van and Eastern deltas) across Edremit and traverten areas through submerged river channel systems and soft-sediment deformation structures (SSDS). Seismic profile numbers of these sections are 44, 47 and 49 (P-44, P-47 and P-49) respectively, as seen at the top centers (see the locations of these profiles in Fig. 2.2). M: multiple. These seismic sections clearly show that the basement topography (probably tilted and fractured traverten deposits) underlying SE-delta strongly controls delta subsidence, sedimentation and river channel incision patterns. Note that depositional wedges and sediment packages are deeply incised and disrupted by submerged river channels (max. sediment thickness: 80-150 m, max. water depth: 70 m-150 m, offsets: 4.5 km (top), 10 km (bottom) and 8 km (top right), two-way travel time in sec).

Fig. 3.49 shows seven prograding sequences from SE-delta (also see same section in Fig. 3.28). These sequences are mapped, showing successions of overlapping clinoforms in SE-delta shown in Fig. 3.50. In this map, it is clearly seen that progradational wedges are strongly localized in the deeper sections of SE-delta. These wedges are sharply limited by lacustrine shelves in SE, Çarpanak spur zone in N and Varis spur zone, offshore Deveboynu peninsula in W. Morpho-topographic analysis, as combined with seismic and structural interpretations suggests that SE-delta environment has extensionally-faulted basement wedge (see Figs. 3.20, 3.41).

This indicates that SE-delta is a tilted wedge block, suggesting that it is most probably graben-like depression area. Hence, progradational wedges are prominently concentrated in the center of delta and probably tectonic-controlled.

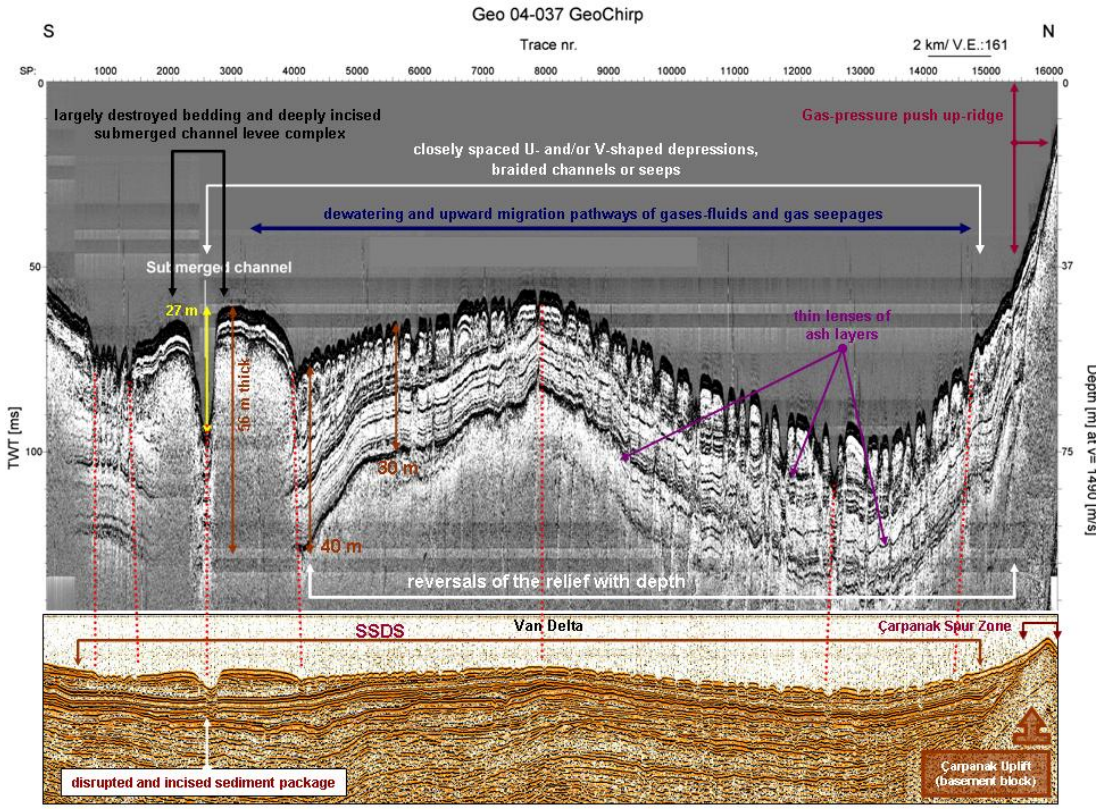

Figure 3.48 : High-resolution chirp image of N-S seismic section from Çarpanak spur zone and Van delta across deeply incised submerged channel and soft-sediment deformation structures. Seismic profile number is 37 (P-37) (also see and examine seismic section at the bottom in Fig. 3.24 for its detailed interpretation). In this figure, deformational correlation of seismic section (lower) with its chirp version (upper) is illustrated. This chirp section well reflects the high-resolution image of depressurizing, dewatering, destabilization and degradation events in Van delta setting. Note that thin black lenses are ash layers faulted, unlithified, thick piles of soft sedimentary bedding are strongly dissected and eroded and reversals of the relief with depth also occurred (incised submerged channel depth: 27 m, max. and min. thicknesses of sedimentary dissection: 30 m-60 m, max. water depth: 40-45 m, min. water depth: 35 m-40 m, two-way travel time in msec).

Seismic sections across delta settings and the maps seen in Figs. 3.43 and 3.50 reveal that relatively thicker sediments and large clinoform complexes characterize SE-delta. Submerged river-channel complex and soft-sediment deformation structures are broadly concentrated on this delta. Regular and relatively thinner sediments and a small amount of large clinoform complexes characterize NE-delta. Submerged river-channel complex and soft-sediment deformation structures are narrowly concentrated on this delta.

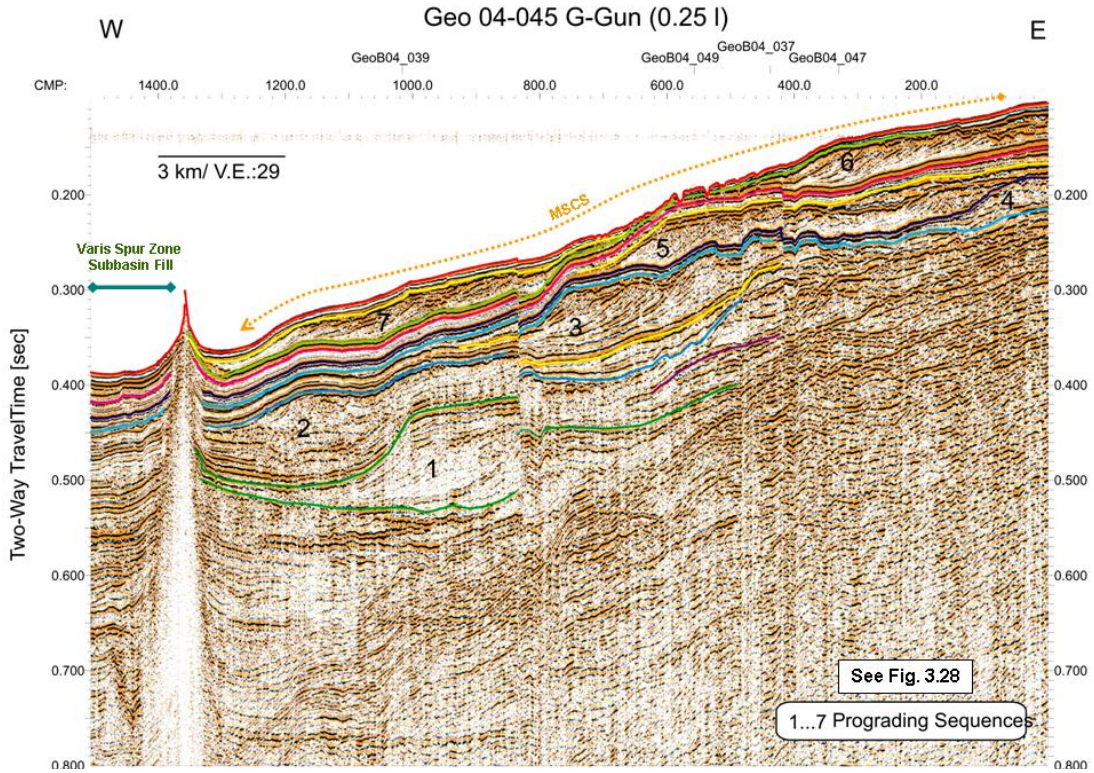

Figure 3.49 : W-E seismic section from SE-delta setting across multiple slumping of clinoform successions (MSCS) through Varis spur zone subbasin (also see Fig. 3.28 for a detailed interpretation). In this section, prograding sequences are highlighted and their sequential development is ranged in (1-7). This section well summarizes the progradational development and transgressive-regressive cycles of SE-delta setting. Note that the prograding sequences within Varis spur zone subbasin are not observed (examine Fig. 3.28).

Sedimentary structure of both NE-and SE-deltas is deformed by deeply incised and submerged river channel complex. NE-delta is an uplifted block, while SE-delta is an downlifted block. Tilted structural geometry of delta blocks is caused by E-segment. Thus, uplifting block geometry of Çarpanak spur zone produces the most distinct stratigraphic property. This is angular unconformity surface seen in Çarpanak uplifted block, covering all along NE-delta (Figs. 3.16-3.20, 3.24 and 3.25). It terminates against both SE-delta and central Tatvan basin. This implies that it is a local stratigraphic property in Çarpanak spur zone and NE-delta, indicating that NE-Erek delta is an uplifted block feature.

Fig. 3.43 shows that NE- and SE- deltas have submerged river-channel complexes, which have small-scale bifurcations, various branches and splays. These secondary, splayed features distinctly follow tectonic-controlled structures, which may be pre-existing weaknesses, faulted-block boundaries or presently identified faults (E-segment). Submerged river-channel complexes bound and control “S-shaped zonal

distribution" of soft-sediment deformation structures. These complexes extremely appear to have been at tightly narrowing and ending parts of this S-shaped distribution.

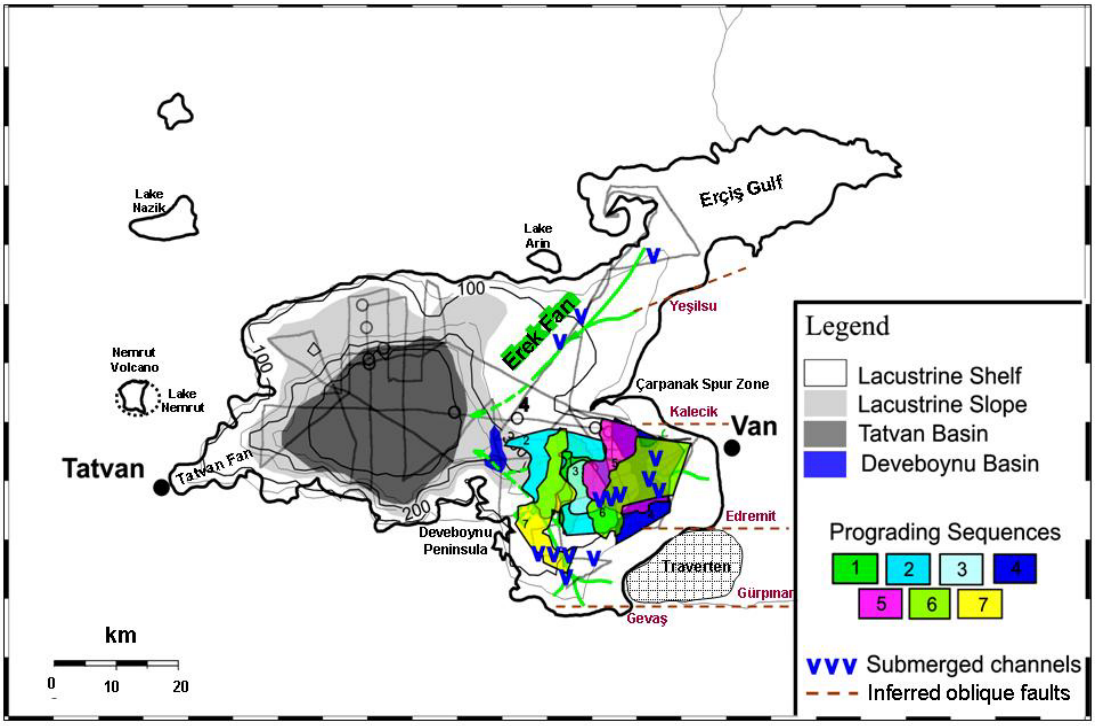

Figure 3.50 : Distribution of prograding sequences (1-7) in SE-delta setting is overlain with morpho-topographic and physiographic provinces of the lake. Note that overlapping clinoforms indicate constant lake levels (most likely low stand) only on the lacustrine slope and not in Varis spur zone and Deveboynu subbasins. Prograding sequences are only localized in rapidly subsiding SE-delta and controlled by oblique-slip faults (see and examine Fig. 3.49 for seismic architecture of prograding sequences).

Morpho-topographic map clearly shows that "S-shaped zonal distribution" of soft-sediment deformation structures indicates, indeed, a considerable tectonic control in delta settings (see Fig. 3.50). This tectonic control shows that NE-part of "S-shaped zonal distribution" in Erek delta is sharply limited by a faulted structure, which submerged river-channel follows. In and around Çarpanak spur zone toward SE-delta, tightly narrowing part of "S-shaped zonal distribution" is clearly controlled by a faulted structure, which is E-segment. In SE-delta, SE-part of "S-shaped zonal distribution" is also sharply ended by submerged river-channel complexes, probably controlled by faulted features (see and examine Fig. 3.50). Fault-controlled structure of NE- and SE-delta settings is also evident in Figs. 3.12, 3.20 and 3.41. The interpretation considers that NE- and SE-deltas of lake are tectonic-controlled.

This implies that these shallow water settings are sedimentologically unstable and hydrologically unmaturated, younger environments.

It is obvious from seismic sections that E-segment divides delta setting into two different areas in N and S of lake, implying active tectonic control. Seismically very active regions, such as Çarpanak spur zone, Deveboynu peninsula, Deveboynu and Varis spur zone subbasins, are unstable areas where earthquake activities are densely recorded as a result of active tectonic deformation. This is confirmed by a large amount of earthquake data set (Türkelli et al., 2003; Örgülü et al., 2003; Dhont and Chorowicz, 2006; Horasan and Boztepe-Güney, 2006, Pınar et al., 2007 and Toker et al., 2009 a, b). As far as concerned, overall structural and sedimentary configuration of NE- and SE-delta settings is mainly caused by E-segment of S-margin boundary fault and related en echelon faults in various scales. Structural interpretation from NE- and SE-deltas indicates that these deltas have different features of their structural and sedimentary history. Soft-sediment deformation is dominated in three important settings; slopes (inclinations), progradations (clinoform packages), and shelves (smooth planes). Therefore, it is not possible to suggest one or two reasons of how these sedimentary anomalies are generated.

3.4.2 Characteristic features and architectural elements of seismic sequences, progradational clinoforms and soft-sediment deformations

The diversity of progradational wedges is imaged by a wide range of seismic sections from the shallow water (Figs. 3.17, 3.19, 3.23, 3.25-3.29, 3.30 at the top and 3.41) and also deep water settings (Figs. 3.33 and 3.34). Their spatial distribution and morphology is well shown in Fig. 3.43. Typical architectural elements and seismic facies of these progradations are based on the recognition of seismic reflection character and geometry in the shallow-water domain. Based on seismic reflection patterns, the main seismic facies and architectural elements are ranged as the follows; low- to high amplitude, continuous reflections, which can have subparallel, hummocky, or divergent geometry and are interpreted as levee deposits and drapes. Low amplitude chaotic reflection packages, which are typical of mass transport complexes such as reflection configurations from sedimentary packages of progradational clinoforms and fault-controlled turbidities and debris flows. These are summarized in Figs. 3.16-3.20, 3.23, 3.25-3.28, 3.33 and 3.34. These seismic sections describe low amplitude-high frequency water level changes and high

magnitude instability of delta setting. High amplitude channel-fill elements are also very common (Figs. 3.6 and 3.7).

The most prominent features identified in water depths between 100 m and 200 m in the SE- and NE-deltas are submerged channel complexes and closely spaced U and/ or V-shaped depressions shown in Figs. 3.44-3.48, mapped based on the seismic data (Fig. 3.43). The closely spaced U- and/or V-shaped depressions are already described by Wong et al., (1978) and Wong and Finckh, (1978) as a karst-like topography, referred to soft-sediment deformation. Some of the depressions are associated with near vertical faults. Several of the structures show a reversal of the relief with depth (a depression at the lake floor) and upward bending reflectors in the subsurface. Seismic interpretation considers that this irregular morpho- topography is caused by erosion and channelized sediment-laden currents into horizontally bedded fan sediments. The re-suspension and dispersal of bottom sediments by the upward migration of gas and/or water as well as a true karst associated origin is also considered (Wong et al., 1978). Chirp profiles seen in Figs. 3.44, 3.46 and 3.48 show channel levee systems, which are clearly related to erosion and deposition by channelized, sediment-laden streams. These seismic sections show that depositional setting and clinoform complexes are strongly deformed by some distinct processes. The one of these is a distinct uplift of Çarpanak basement block and NE-Erek delta. This results in a sharp increase of deformation gradient and thus, an instability of shelf-margin prograding wedges, as illustrated in Fig. 3.25.

NE-Erek delta and Çarpanak spur zone is characterized by broadly widening angular unconformity surface (Figs. 3.16-3.21, 3.24 and 3.25). This unconformity surface identified in these seismic sections suggests that older underlying strata undergone uplift and erosion before the younger deposition. This block uplift of Çarpanak spur zone produces the wedge-shaped, slump-generated, thicker and chaotic turbidite packages towards central Tatvan basin and Deveboynu subbasin. Deep water transport and elongation of transparent clinoform patterns overlying the angular unconformity is also caused by this block uplift (Fig. 3.25). A peculiar topographic feature in Çarpanak uplift is described as intrusive gas-pressure ridge and/or pushed up-ridge zone. This ridge zone seismically appears to be a crestal topographic swell (Figs. 3.24, 3.25 and see 3.44-3.46 and 3.48 for details). Çarpanak uplift is widely surrounded by superimposed, large-scale progradational clinoform facies (Figs. 3.23

and 3.25), representing shelf-margin prograding wedges formed by shelf-margin system tract (SMST). Multiple slumping of clinoform successions are characterized by largely destroyed bedding and collapsed during slumping. Some clinoform packages are strongly deformed and cut by normal oblique slip faults in Eastern delta (Figs. 3.26-3.29 and 3.30 at the top). This case is very distinct across parallel seismic sections seen in Figs. 3.29 and 3.30 at the top. In these two sections, fault-controlled displacement of clinoform packages is clearly imaged. Chaotic, disturbed and slumped progradations suggest the intercalation of lower density and softer sedimentary packages. Such a seismic structural geometry assumes sedimentary ash or fine-grained flow, such as ash-cloud surge. This implies fluidized fine-grained (or ash) matrix downslope as a coherent flow and suggests that an expanded, turbulent, dilute flow of gas, pyroclasts and clastics are represented by hot-dry overriding gas and ash cloud above pyroclastic flows. Thus, the gas-fluid diluted clinoform packages are clearly slumped, slided-glided and radially dispersed towards central Tatvan basin from Çarpanak uplift and NE-delta. It is assumed that gases, fluids and possible volatile materials are mainly sourced from and fed back by intrusive-extrusive activity and pushed up, pressure ridge zone of Çarpanak high. Multiple slumped clinoforms are probably produced by simultaneous slumping at different sides of Çarpanak high. Overall disruption and deformation of progradational wedges implies a regional triggering mechanism such as an earthquake.

Seismic sections show that downslope slumps of progradations are superimposed with an effective erosion of river-channel margins in NE-Erek delta area, nearby around Çarpanak uplift. As mentioned above, clinoform packages are internally collapsed, forming depressions or troughs within packages (Fig. 3.25). These troughs are lately incised, indicating largely depressed and destroyed clinoform bedding. As these depressions initially reach smaller topographic lows, river-channel erosion begins, and this event incises depression more depthly (Figs. 3.28-3.30). This suggests that internally disturbed and collapsed clinoform packages increase channel incision gradient to a large degree. Thus, the submerged river-channels are the younger erosive factor in deltas (Figs. 3.44, 3.45 and 3.47). River-channel incision depth refers to bottom-floor depth of deeply incised submerged river-channel system from lake-floor. Incision depth is ranged from 25 to 45 m seen in Figs. 3.46 and 3.48. In these sections, total bedding thickness (or pre-incision thickness of bedding) of the

sedimentary packages is between 30-60 m. Maximum incision depths of small-scale depressions and highs around submerged river-channel are roughly ranged between 80-150 m from water surface. These sections show regular and systematic deformation of the softer sediments, showing the arrangement of sedimentary depressions and crestal highs at various erosive gradients. These patterns are ranged by narrower, higher and deeper and wider, lower and shallower. Figs. 3.44-3.48 indicate that bedding thicknesses are almost completely incised in relatively shallow depths, suggesting that there is one or more very weak, softer deposits, layering and bedding in shallower sections, such as tephra or ash layering. Weakness in layering probably causes an activation of soft sediment deformation, as clearly recognized in Figs. 3.17, 3.19, 3.20, 3.22, 3.24, 3.25 and 3.28-3.30. Fig. 3.51 summarizes a distinct variety of selected progradational wedges, indicating that a common feature of these deformed wedges is chaotic seismic facies of successions, transparent reflection patterns and acoustic voids. Some of these are internally collapsed and largely destroyed bedding pattern during slumping and some are slumped-glided and even cut by active faulting. Average thickness of these clinoform packages is ranged from 40-200 m. Sequence boundaries and terminations of clinoform successions are largely controlled by high-reflection coefficient and high-amplitude basal detachment-shear surfaces. These are probably listric planes within sediments. These planes suggest that they are rotational progradations by basal shear surface, having varying orientations. Their internal architecture is reflected by regularly accreted and/or imbricated sedimentary piles, but some by chaotic patterns and collapsed thin layers and some has preserved clinoform configuration.

Characteristic features and architectural elements of seismic sequences, progradational clinoforms and soft-sediment deformations in NE- and SE-delta settings show the high magnitude instability of sedimentation. An understanding of facies, depositional settings and sequential architecture of the delta-margin depositional systems of Lake Van provides a powerful tool in reconstructing low amplitude, high frequency lake level changes, lake margin hydrodynamics and the dominant soft-sediment deformation styles. The facies, sequences and depositional evolution of the sediments are closely related to lake level fluctuations resulting from long and short term hydroclimatic changes. Successive and rapid stages of lake level rises and large amounts of supply of coarse grained material imply a positive

hydrological balance and a relatively high rates of sediment discharge from the adjacent hillslopes. A prominent instability of clinoform beddings indicates that these beddings are transferred into the deep basin as recognized in Figs. 3.33 and 3.34 by slope failure and mass-wasting processes and thus, producing thick slump-generated turbidities. Such a picture of clinoform displacement and also soft sediment deformation products in delta settings provides an strong evidence of active tectonic control across Çarpanak uplift along E-segment .

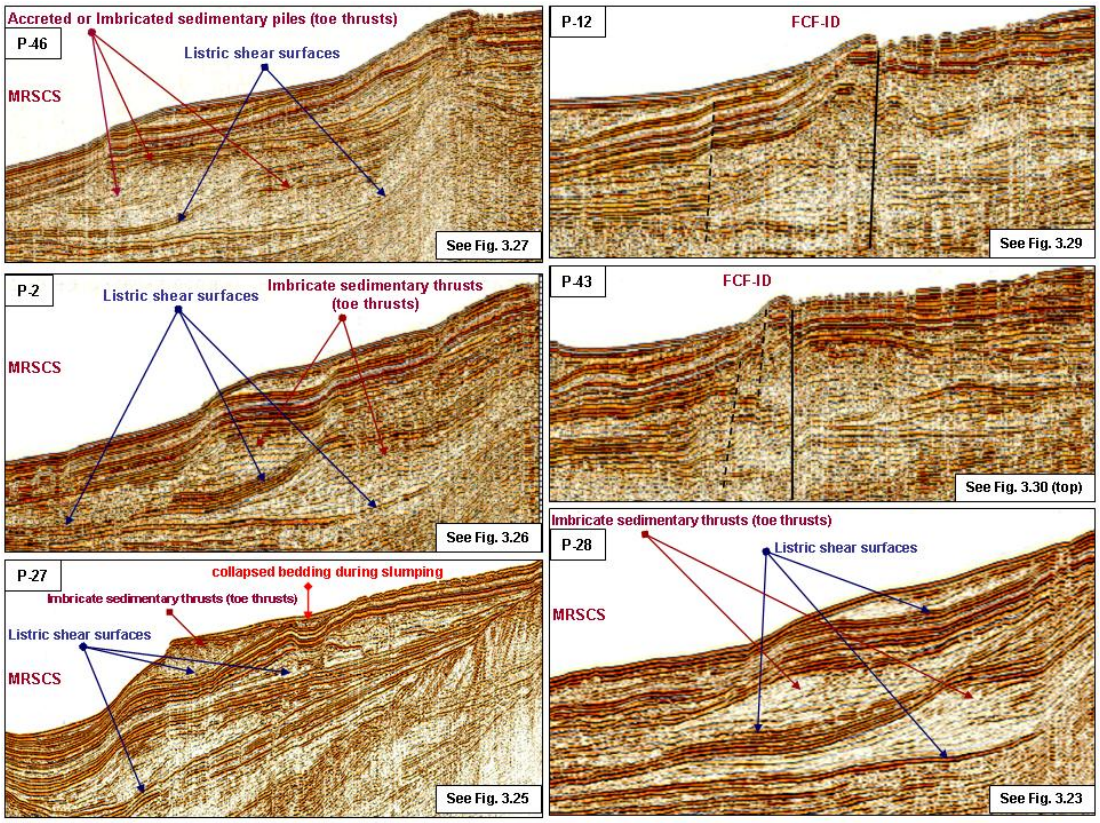

Figure 3.51 : Internal and external seismic architecture of rotational complex of slumped progradations in NE-Erek and SE-delta settings. Seismic profile and figure numbers of these images are shown at the top left corner and the bottom right corner respectively (see and examine given figure and profile numbers for detailed interpretation of related seismic sections). A series of these progradational wedges well illustrates faulted clinoform failures-internal destabilization (FCF-ID) and multiple rotational slumping of clinoform successions (MRSCS).

3.4.3 Soft sediment dynamics of NE and SE-delta settings

3.4.3.1 Degradation features

Evaluation of delta settings considering seismic reflection data from deformational products leads to the following concept, referring to soft sediment dynamics and overall delta degradation. Characteristic features and architectural elements of

seismic sequences, progradational clinoforms and overall patterns of soft-sediment deformations, which are diagnostic of delta degradation, are found both on the present-day lake floor and in the subsurface. Several styles of degradation are briefly described here, each with implications for slope failure mechanism and transport process. These are, (1) Failures linked to thin deposits, (2) Slumps-slides that show clear evidence for internal deformation and relatively short transport distances, (3) Failures associated with floor depressions and (4) degradation by shallow-water channel erosion and associated channel-margin collapse. The erosional truncation surfaces are also common to all these styles.

An examination of seismic data based on the above brief review of degradation features summarizes that some degradation complexes in NE-delta exhibit several typical characteristics of slope failures. As well summarized in Fig. 3.25, the failure deposits consist of low-amplitude, chaotic wedge-shaped seismic reflection packages. Most of progradational clinoform packages are slumped and transported products, particularly in NE-Erek delta. The wedge-shaped packages of progradational clinoforms, slumped-slided deposits and reworked products have distinctive, low-amplitude chaotic reflection characteristics and are readily traced over most of the seismic volume (see and examine Figs. 3.25, 3.33 and 3.34). The spatial extent is consistent with being a much more extensive mass transport complex that is deposited on the delta slope. These low-amplitude clinoform wedges are interpreted as deposits of mass failure or mass transport complexes. As clearly classified in Fig. 3.51, these wedges underwent slumping following deposition, with the possible detachment surface located at its base. Transparent internal reflections of sedimentary wedges are interpreted by Heiniö and Davies, (2006) as imbricate thrusts. This sedimentary imbrication or complex sedimentary pile and/or accretion formed as downslope movement of the sediment package on the detachment surface ceased.

Shallow-water sedimentary depressions-troughs and swells-highs are the most prominent sedimentary deformation groups (Figs. 3.44-3.48). The oval, closely spaced U- and/or V-shaped lake floor depressions are formed by some typical processes in the shallow-water environments. These distinct depressions are probably affected by rotational failures on a listric decollement (soft sediment-related listric control that is curved plane surface in Fig. 3.51) as a combination of pockmark

activity associated with escaping gas and processes of bottom-current activity (see Figs. 3.28-3.30). Seismic and high resolution chirp data from the further N of NE-Erek delta perfectly image a combination of these processes (see and examine Fig. 3.52 for degassing-dewatering processes and submerged channel levee and also see Fig. 3.53 for a high resolution, detailed view of degassing and its disturbance). The depth down to which reflections are cut by the depressions is, in all cases, max. 100-200 m. Thus, it is assumed that this is a critical depth for a failure. However, in Fig. 3.53, due to the shallower water depth with 30 m and thinner sediments ranged in 20-25 m, this depth across the chirp section gets shallower. Figs. 3.46 and 3.48 show that a weak layer intercalated with tephras, pyroclastics or softer sediments exists at that depth, probably because of dewatering and overpressure generation. Alternatively, it is proposed that these depressions are formed by lake-floor current activity, as illustrated in Fig. 3.52. This is supported by the roundedness of the depressions and highs and evidence of current activity in the form of sediment waves on the lake floor. In addition, as seen in Figs. 3.44-3.48 and 3.52, some depressions do not have any detectable deposits downdip from the scarp, suggesting that they formed as a result of current scouring. This situation is also imaged in Figs. 3.20, 3.22, 3.24, 3.29 and 3.30 at the bottom. Since, bottom currents are known to erode steep scarps on their path (for example in Judd Deeps in the Faeroe-Shetland Channel in Smallwood from Heiniö and Davies, 2006). The lake-floor highs, swells or crests can be such an obstacle that currents may accelerate locally and scour more effectively when they encounter an obstacle in their path or the slope flattens (Nemec, 1990 and Heiniö and Davies, 2006) (see the pathways of submerged channels through clionoform packages in Fig. 3.43).

During the fault growth (E-segment) along Çarpanak uplift, this faulting experiences tensional stresses that are clearly manifested by faulting and Çarpanak uplift has an upward-blocking geometry in cross section. Thus, the fault-controlled Çarpanak block can provide migration paths for gas and cause pockmark-like depressions on the lake floor (see Ingram et al., 2004 for this process) (see and examine Figs. 3.17, 3.19 and 3.23-3.25). A careful examination of chirp data seen in Figs. 3.44, 3.46, 3.48 and 3.53 suggests that these depressions can be attributed to upward migration of thermogenic gas or fluids (Demyttenaere et al., 2000 and Heiniö and Davies, 2006) (also examine seismic section in Fig. 3.52).

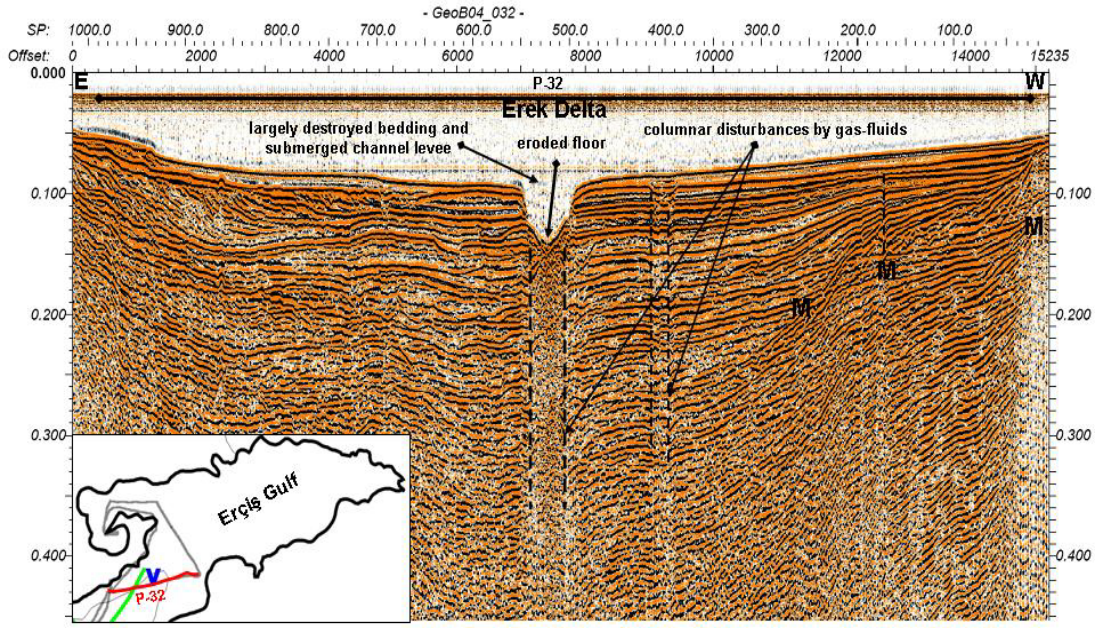

Figure 3.52 : W-E seismic section from NE-Erek delta across deeply incised submerged channel. Seismic profile number is 32 (P-32) and its location is shown in the location map at the bottom left corner. Notice columnar disturbances of gases-fluids (incised submerged channel depth: 30 m-35 m, sediment thickness: 80 m-90 m, max. water depth: 60-65 m, offset: 15 km, two-way travel time in sec).

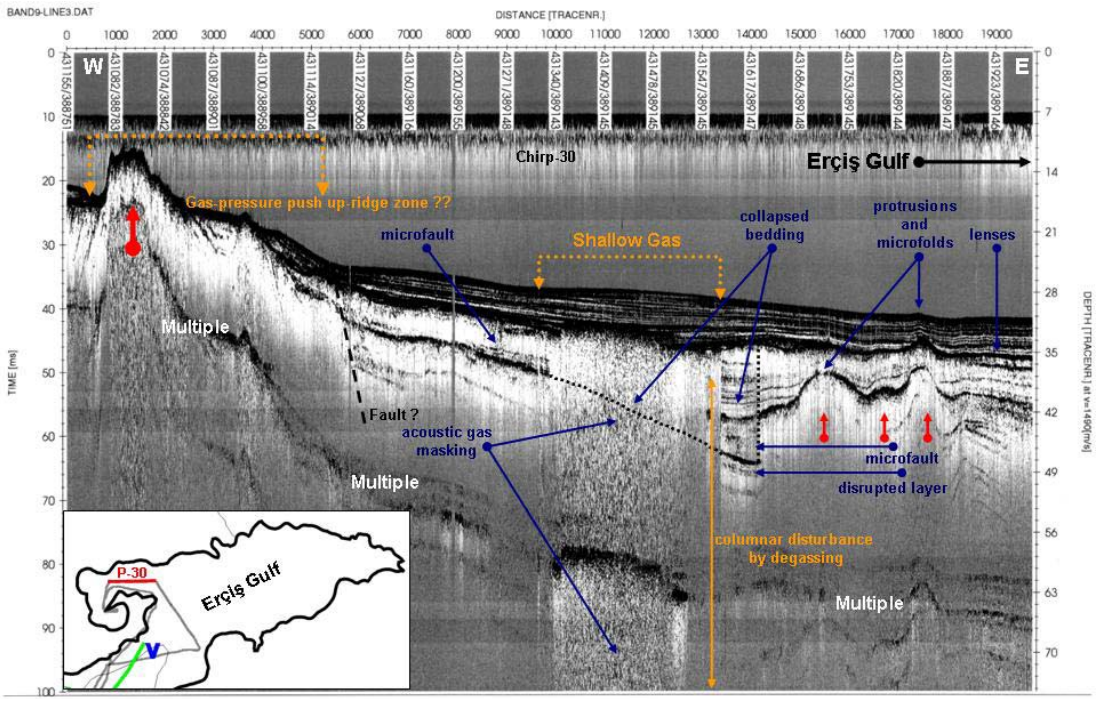

Figure 3.53 : W-E high resolution chirp image from Erçiş Gulf across gas-pressure push up-ridge and shallow gas zone. Seismic profile and chirp number is 30 (P-30) and its location is shown in the location map at the bottom left corner. Note that soft-sediment deformation is strongly dominated by the columnar disturbances of gases-fluids (max. sediment thickness: 20 m-25 m, max. water depth: 25-35 m, two-way travel time in msec).

Fig. 3.43 reveals that soft-sediment deformation area on map view shows a broadly widening distribution pattern trending towards NE-and SE-delta settings bounded by E-segment across Çarpanak spur zone. This pattern is probably due to dispersal patterns of fluid-gas related sedimentary perturbation, affected by tensional stresses of E-segment and associated tilted blocks. In this case, the seismic and structural geometries of soft-sediment deformations suggest that they are the result of a combination of mechanical failure and bottom-current activity. This notes that mechanical failures affect bottom-current activity and bottom-current activity affects mechanical failures. Both bottom-current activity and mechanical failure are strongly controlled by fault-related uplifts (Çarpanak high) and troughs (Deveboyun and Varis spur zone subbasins). This proposes tectonic-controlled sedimentation, deformation and delta instability in this case, prominently driven by transtensional activity.

3.4.3.2 Degradation processes

Evaluation of soft sediment dynamics of NE and SE-delta settings by both seismic and chirp data leads to a better analysis of degradation features. Specially designed and imaged versions of the high-resolution chirp data provide much detailed sections of these degradation features and related processes. A series of these chirp sections is ranged in Figs. 3.54-3.57. In these sections, the reflections from structures and sediments are particularly exaggerated to view details of degradations. Figs. 3.54, 3.55, 3.56 and 3.57 illustrate the high-resolution versions of seismic reflection data shown in Figs. 3.24, 3.29, 3.25 and 3.19 respectively. The figure numbers of these seismic sections are also written in their high-resolution versions.

Analysis of degradation features gives certain clues about deposition, erosion and tectonic intensity which control depositional characteristics and structural architecture of sequences. Consideration of degradation features along with the structural complexities can explain some processes resulting in degradation. The prominent one of the findings observed from degradation complexity is “the channel erosion”. The various views of the channel erosion process are recognized in seismic sections in Figs. 3.20, 3.22, 3.24, 3.29 and 3.30 at the bottom. Their high resolution images with seismic sections are seen in Figs. 3.44-3.48 and 3.52 and their more detailed expressions are shown in Figs. 3.54, 3.55 and 3.57.

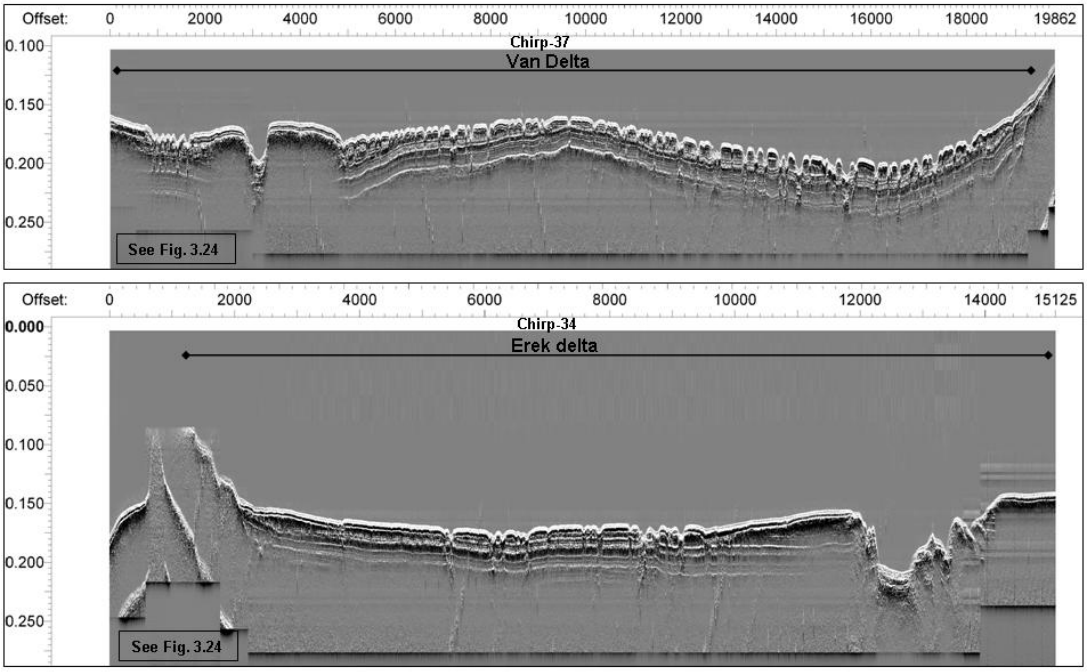

Figure 3.54 : High-resolution chirp sections from Van and NE-Erek delta settings show the exaggerated architecture of soft-sediment dissection, channel incision and the lake-floor deformation (two-way travel time in msec) (see Fig. 3.24 for seismic interpretation).

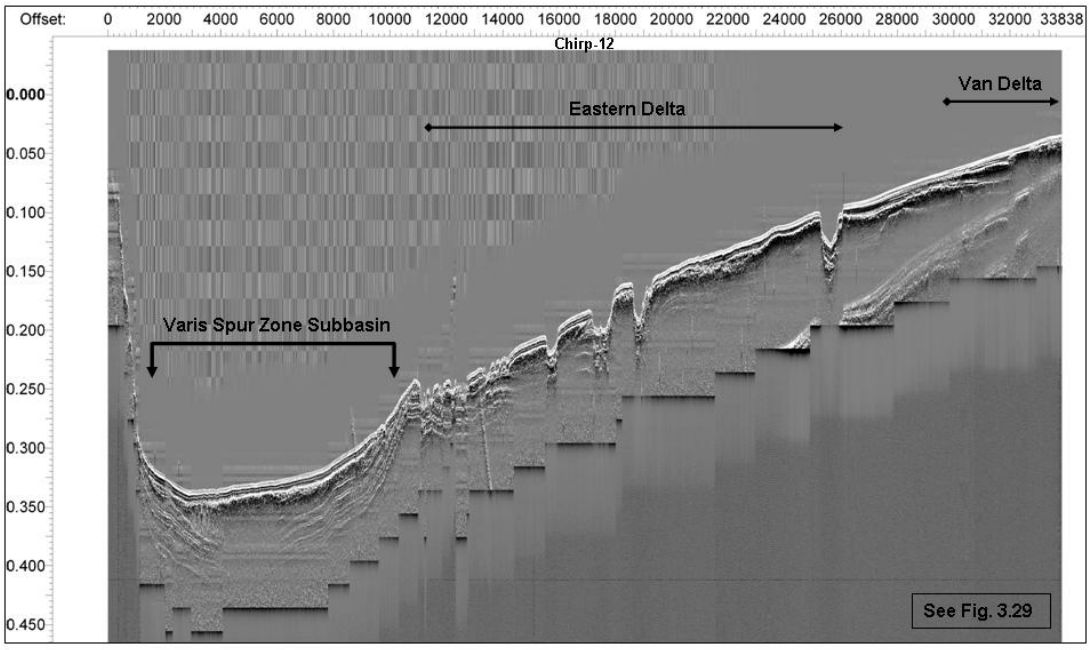

Figure 3.55 : High-resolution chirp section from Varis spur zone subbasin and SE-delta setting (Van and Eastern delta) show the exaggerated architecture of soft-sediment dissection, channel incision and the lake-floor deformation (two-way travel time in msec) (see Fig. 3.29 for seismic interpretation).

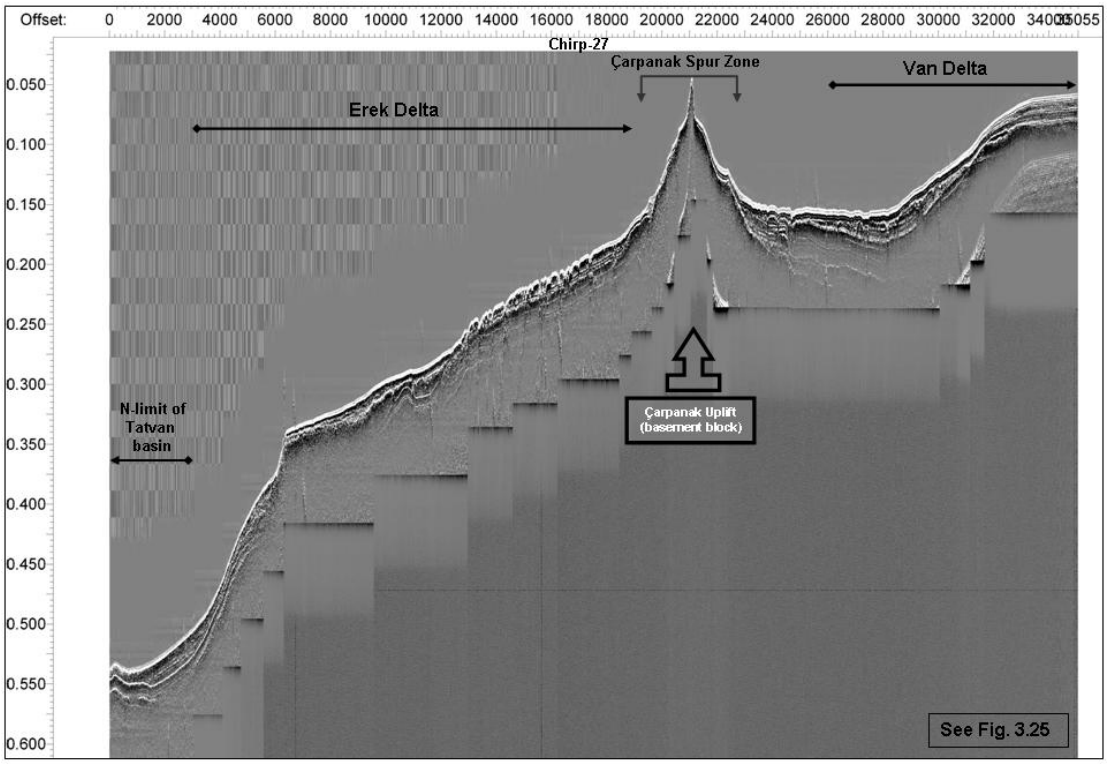

Figure 3.56 : High-resolution chirp section from Çarpanak spur zone, NE-Erek and Van delta settings show the exaggerated architecture of soft-sediment dissection, channel incision and the lake-floor deformation (two-way travel time in msec) (see Fig. 3.25 for seismic interpretation).

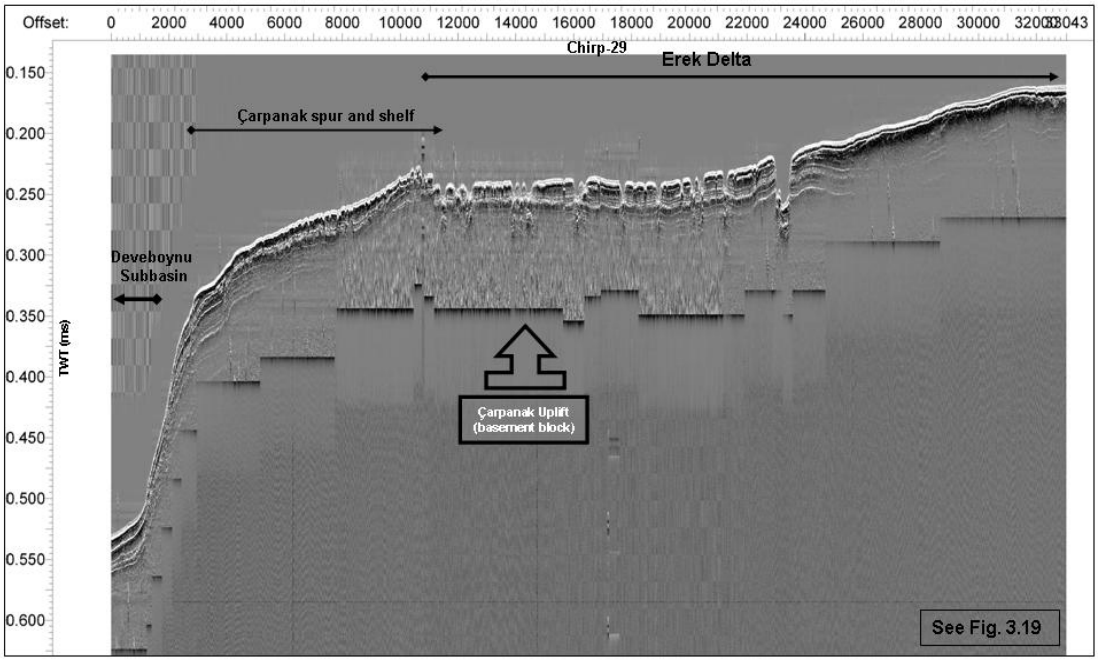

Figure 3.57 : High-resolution chirp section from Çarpanak spur zone, NE-Erek and Deveboynu subbasin show the exaggerated architecture of soft-sediment dissection, channel incision and the lake-floor deformation (two-way travel time in msec) (see Fig. 3.19 for seismic interpretation).

Morpho-physiographic and topographic analysis and the areal distribution of submerged river-channel systems in relation to soft sediment deformation zone shown in Fig. 3.43 show that "the channel erosion" is volumetrically the most important mechanism as one of the main styles of degradation. It is, since, obvious that the volume removed by channels is an order of magnitude greater than the volume removed by a single failure.

"Channel erosion" can be considered as a continuous process and thus differs from the other degradation mechanisms, which are considered as individual, repetitive failure events (Heiniö and Davies, 2006). The channel-margin failures, troughs and highs associated with thin, almost seismically indiscernible sedimentary deposits are the most common types of degradation in NE- and SE-deltas. Submerged river-channel related failures and erosive products are clearly identified within seismic data, as given above. They strongly affect morpho-physiographic framework of deltas and structural architectures of soft sediment deformations. Therefore, the main controls on the architecture of these types of failure are considered first in understanding a generic model for delta system degradation. The NE- and SE deltas are very unstable environments with higher soft-sediment deformation energy and hence, it is very important to distinguish primary depositional conditions from secondary ones. Since, as well known, morpho-physiographic, deltaic or structural differences in the pre-failure conditions or in the initial depositional settings can control the failure styles and the post-failure morphology. This implies that pre-failure, failure and post-failure cases may contribute to producing the different failure styles and depositional features. These can be ranged by (1) sediment physics and acoustic properties, (2) sediment anisotropy and orientation and (3) slope degradation.

1) sediment physics and acoustic properties; seismic and structural observations of depositional geometry and reflection characters allow for the consideration of the likely sediment properties prior to, during, and following the failure events. The formation of oval-shaped failures suggests that the sediment was coherent and most likely homogeneous at the time of the failure (Varnes, 1978 and Heiniö and Davies, 2006) (see detailed examples in Figs. 3.54-3.57). The highly dispersed and chaotic nature of the failed sediment wedges suggests that it was remobilized into a more

dilute, lower density flow, probably in the form of a debris flow, mud flow, or a turbidity current, as summarized in Fig. 3.51.

Soft clays and loose fine sands tend to flow great distances downslope as liquid material even on gentle slopes (Varnes, 1978 and Heiniö and Davies, 2006) and towards deep basin as seen in Fig. 3.25, 3.33 and 3.34. The resultant progradational sediment packages have strong chaotic reflection configurations. Moreover, distinct edges on the distal part of the lobes are typical of mud flow deposits, reported by Prior and Coleman, (1982). As illustrated in Fig. 3.51, the presence of slumps with internal slip planes indicates that movement could also occur as more coherent and viscous sediment bodies. The slump occurred because of the remobilization of a mass transport complex deposit. This more coherent style of sediment transport could be a coincidental relationship (Heiniö and Davies, 2006). But this may also suggest that the mass transport complexes had different sediment properties prior to failure than other kind of sediments, and this affected the type of failure that occurred.

2) sediment anisotropy and orientation; sediment anisotropy and orientation is common in NE- and SE-delta settings, caused by some certain factors. These factors are surficial expressions of structural and tectonic occurrences (for example Figs. 3.16-3.20 and 3.23-3.30), depositional beddings, internal layerings, rheological differences in sedimentary piles and possible groundwater flows. These seismic sections propose that the presence and orientation of seismic sequences and structural anisotropies can influence mass-wasting processes (Stewart and Reeds, 2003 and Heiniö and Davies, 2006) and also the areal distribution of submerged channels and soft-sediment deformations (see Fig. 3.43).

It is very clear in Fig. 3.43 that morpho-physiographic and topographic features, such as submerged-channel flow directions in NE-and SE-deltas, follow the distinct structural discontinuities of both NE- and SE-deltas. Depositional successions of wedge-shaped sedimentary packages and progradational clinoforms clearly show that planes of weakness reduce the shear strength of sediment and enable failure to occur with lower imposed shear stresses. This case is perfectly imaged in Figs. 3.25, 3.33 and 3.34 and a common case in the other progradational clinoforms briefly seen in Fig. 3.51. These seismic sections suggest that the main anisotropies in delta settings of lake are the bedding planes and the vertical faults associated with earthquake

growth. As an example, the vertical faults and related splays (E-segment), which are parallel to the Çarpanak spur zone, strongly affect sediment deformation (see the high resolution images in Figs. 3.56 and 3.57 and referred seismic data). The faults coincide with the lateral margins of the failure scarps and most likely control the width of the scarps (Heiniö and Davies, 2006) (Figs. 3.17 and 3.19).

3) slope degradation; the sediment physics, acoustic properties, anisotropies and orientations are typical parameters, controlling the unstability of shelf-margin delta environments where sedimentary deformations are initially triggered by well known sedimentary processes. These processes strongly effect slope gradients and can be well identified by internal sedimentary architectures and seismic reflection configurations of successions of progradational clinoforms. The seismic and high-resolution observations from delta settings can give certain clues to these processes, which are thought to have acted as effective processes. It is often interpreted that overpressure allows very low-angle activation of discontinuities. Elevated pore pressures are common in shallow sequences with relatively thin overburden. The presence of discontinuities (bedding planes or lithology contrasts) in combination with high pore pressure can allow the activation of discontinuities inclined at a very low angle to the maximum principal stress axis and the absorption of seismic energy (Figs. 3.23, 3.25-3.28 and briefly in 3.51). It is also possible that differential compaction allows the stepped and flat geometries. Since, differential compaction between materials can cause the fault plane to take on a stepped geometry, preserving steeper dips where it crosses sandstone or limestone layers and becoming more flat-lying in the shale (Jones and Addis, 1984). Additionally, flexuring of the cover sequence allows low fault-plane dips. Flexuring can lead to faulting with a low fault-plane dip, or elevated pore pressures can contribute to the low fault-plane dip (Mandl and Crans, 1981).

There are two distinct slope morphologies recognized in delta areas. The one is that the fault-controlled block in Çarpanak spur zone. This is the steeper block controlling sediment flows and re-sedimentation in the subbasins (Figs. 3.16-3.20). The other is the gentler slope gradient in NE-Erek delta, controlling long-distance sediment transport (Figs. 3.25, 3.33, 3.34 and see progradational wedges transported towards central Tatvan basin in Fig. 3.43). These seismic sections and the map view suggest that slope gradients determine the type of slope degradation. This occurs, because it

determines the failure plane geometry and affects the run-out distance (see Heiniö and Davies, 2006 for details). The fault-controlled steeper and the gentler slope morphologies, the instability of clinoform complexes and then deep-water transport of progradational wedges propose the slip planes, the stresses and the orientations on the slope settings. This means that the orientation of the slip plane is controlled by the distribution of principal stresses on the slope (Mello and Pratson, 1999). The mechanism proposed by Heiniö and Davies, (2006) is that the orientation of the stress field rotates within a slope because the upper part is under an extensional stress regime, whereas the lower part is in a compressional stress regime simply because of gravitational force (see and examine examples in Figs. 3.25-3.29, 3.30 at the top, 3.33, 3.34 and 3.51). This implies that the direction of the slip planes will rotate, producing listric surfaces in shallow slopes and more planar and slope parallel as the slope steepens. Mello and Pratson, (1999) predict that sediments fail when the slope inclination is greater than or equal to 2/3 of the friction angle (Heiniö and Davies, 2006). However, slope gradient is not always considered as an important factor in lacustrine slope instability (see Sultan et al., 2004). Some other factors are also ranged, such as rapid deposition, subsidence gradients, uneven overburdens and diagenetic factors. Particularly, abnormal pore water pressures will also contribute to the failure of shallower slopes.

In terms of the steeper slope gradients such as Çarpanak spur zone, the gravitational shear stress and the weight of the overlying sediment increase if a slope steepens. Thus, the steeper slope of Çarpanak spur zone is predicted to be higher transport velocities and more prone to failures (see and examine high-resolution data in Figs. 3.56 and 3.57). These failures are debris, turbidities or mud flows and re-sedimentation, which are recognized in Deveboynu and Varis spur zone subbasins (see Figs. 3.18-3.23). Because, an abrupt break caused by vertical fault in slope causes increased basal friction, deceleration, and deposition of the failed sediment mass, resulting in relatively thick deposits (Nemec, 1990 and Heiniö and Davies, 2006). In NE-Erek delta, on a longer, more uniform slope, towards central Tatvan basin nearby N-margin boundary fault, the failed sediment mass has more time and space to dilute by the entrainment of ambient water and, hence, disintegrate, as illustrated through seismic sections in Figs. 3.25, 3.33 and 3.34. This increases sediment transport distance and dispersal, leading to the formation of widespread,

acoustically transparent, progradational clinoform deposits. Because both basal and internal friction are reduced and shear strength decreases. The observations of the slope degradation structures and depositional anomalies in delta areas match perfectly with these interpretations. The most prominent and best one of these observations is illustrated by a seismic section seen in Fig. 3.58 and its high-resolution version seen in Fig. 3.59. A clinoform complex from NE-Erek delta is downslope transferred into central Tatvan basin by slope failure and mass-wasting processes. This clinoform wedge and sequence boundaries highlighted by various colors are strongly deformed by N-margin boundary fault and involved in rhomb-shaped push up horst in Fig. 3.58 (also examine cross sectional views in Figs. 3.25, 3.33 and 3.34).

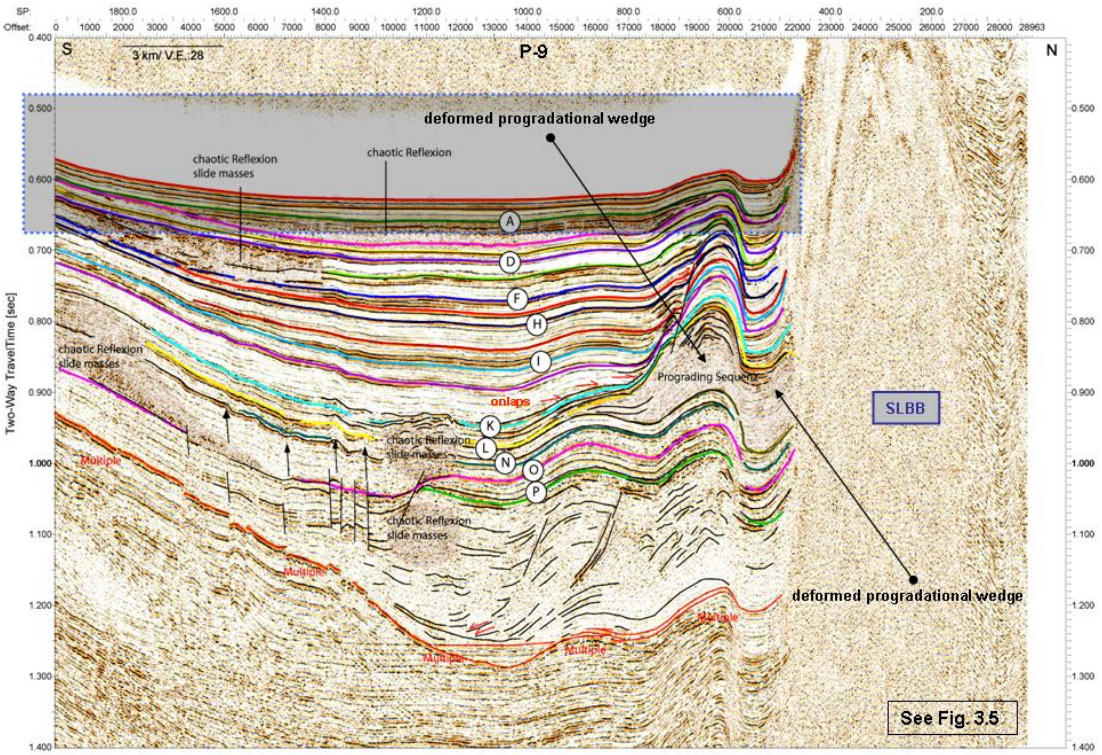

Figure 3.58 : N-S seismic section from central Tatvan basin (also see Fig. 3.5 for a detailed seismic interpretation). In this section, depositional sequences and facies are highlighted and the sequential development is ranged in (A-P). Note that chaotic reflection-slide masses indicate ridged sill and sill features intercalated with depositional layers and that the sequences ranged by B, C, E, G, J, M are not observed, indicating sill-ridged sill intrusions and onlapping onto the edge of deformed progradational wedge (examine Fig. 3.5). Dotted blue square indicates the time interval (0.480-0.680 sec) of the high-resolution chirp image (see Fig. 3.59 for the chirp image).

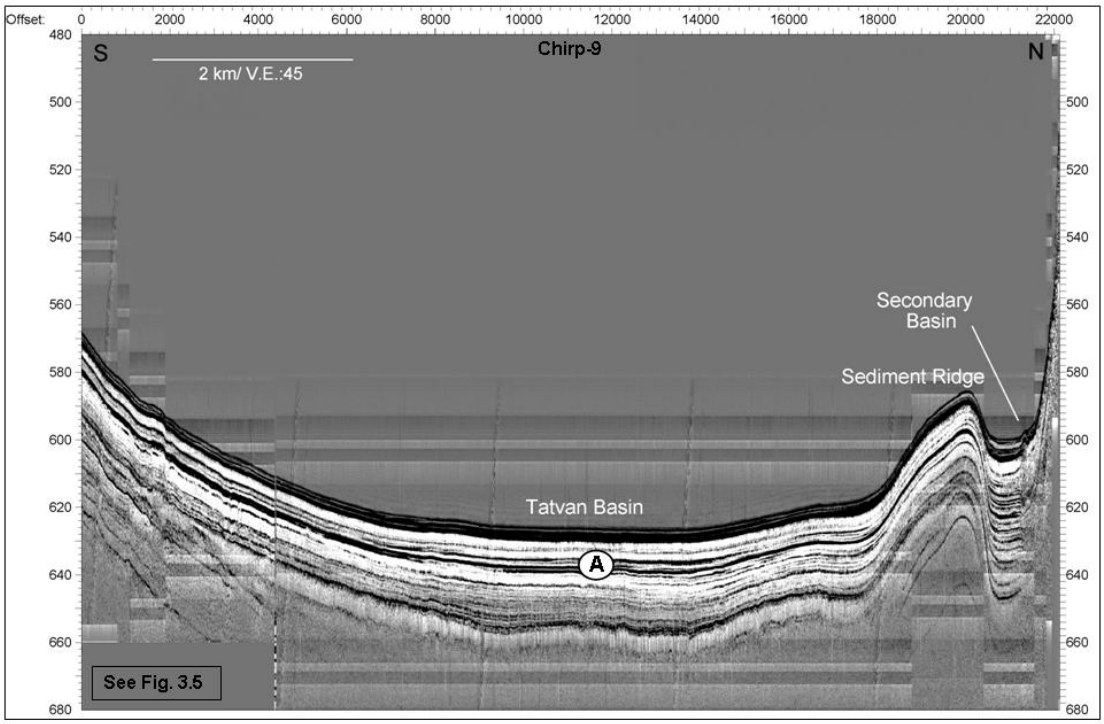

Figure 3.59 : High-resolution chirp image of seismic section shown in Fig. 3.58 (time interval is 480-680 msec) shows the bedding pattern (A) Note that thin black lenses are ash layers and that push up rhomb horst structure and fault-wedged subbasin is termed as sedimentary ridge and secondary basin in this image (see and examine Fig. 3.5 for seismic interpretation).

These seismic sections and high-resolution chirp data imply a strong evidence of slope degradation process. Slope degradation model briefly suggests that initial slope failure occurs, once the stresses become large enough for compressional failure on the lower part of the slope (Mello and Pratson, 1999 and Heiniö and Davies, 2006). This remarks the fault-controlled slope steepening and triggered earthquakes in and around the Çarpanak spur zone, resulting in an considerable instability of progradational clinoforms (see also Varnes, 1978; Mello and Pratson, 1999 and Heiniö and Davies, 2006 for triggering factors). Across the uplift of Çarpanak basement block along Çarpanak spur zone, the width of the fault scarp is most likely controlled by the pre-existing lineaments that act as planes of weakness. The E-segment-controlled steeper slope causes the slip plane to have an orientation parallel to the slope surface (see Mello and Pratson, 1999 for discussion). As a result, the sediment fails and it disintegrates after its failure during transport. Sediment is transported down the slope as a debris or mud flow or turbidity current as more ambient water is entrained by it and dilutes it. The transport distance is great enough that the failure scar is completely evacuated. The scarp retrogrades upslope as a

result of multiple small-volume failures. Subsequently, deposits onlap the empty failure scar, and bottom currents modify the stratal geometries.

3.4.3.3 Degradation mechanisms

Analysis of degradation processes leads to conclude that the products of delta instability prevailed on all scales. Surficially, the fault activity across Çarpanak spur zone is manifested by a series of rotational slump complex, slope failures and mass-wasting processes towards the deep basin. These failures are shown to be common to deformations taking place on all scales of delta environment. The study of degradation processes requires new parameters to be taken into account, such as possible mechanisms of degradation. The degradation mechanisms and the most important results obtained at each scale are briefly given below.

The fault-related activities, such as tilted blocks, can strongly disturb delta stability by triggering internal sedimentary processes. The previous studies reported that the most common trigger mechanisms for slope failure processes are earthquake shaking (Canals et al., 2004) and gas seepage (Lastras et al., 2004; Sultan et al., 2004 and Heiniö and Davies, 2006). This proposes that NE-and SE-delta settings are seismically most active regions of Lake Van and that destabilization process of these deltaic settings, degradation and deformation structures may be initiated by tectonic, seismologic, and sedimentary mechanisms as the most probable initiation mechanisms. Dynamic evolution of soft sediment deformation structures clearly imaged by seismic and high-resolution data shows that, in and around NE- and SE-delta areas, stress and strain gradients are considerably changed. Shear stresses are increased and shear strengths are decreased by some reasons. The view is that widespread earthquake shaking disturbs unconsolidated, water-saturated soft sediments and thus, affects dynamic evolution of these structures, termed as earthquake-related *in situ* soft-sediment deformation.

As often repeated, E-segment-controlled Çarpanak spur zone imposes a tilt. Rapid and high sedimentation rate due to a sharp uplift of Çarpanak basement block results in the uneven overburden of sediment progradation. This uplift disturbs overlying sedimentary cover and increases gradient of erosion and magnitude of deformations. Additionally, changes in stress-strain gradients in delta settings are resulted from removal of both underlying support (previous faults or failures) and lateral support

(sediment erosion by channels). The mobilization of residual stress causes changes in lateral pressure (Varnes, 1978; Hampton et al., 1996 and Heiniö and Davies, 2006). Presence of gas and its possible destabilization also contribute to gradient changes and thus, delta instability. On the other hand, dewatering and pore-fluid migration caused by faulting-fracturing and rapid sediment burial may contribute to the destabilization of sediments on slopes (Heiniö and Davies, 2006). Elevated pore-fluid pressures may create permeable extensional fracture networks (Ingram et al., 2004 and Heiniö and Davies, 2006). The extensional faults and fracture networks can act as pathways for pore-fluid migration. However, no pore pressure or sediment strength *in situ* information from the delta sediments is available. Therefore, it is difficult to be unequivocal about trigger mechanisms. The high-resolution chirp data indicate the presence of gas and gas-induced seismic noises, such as acoustic maskings, wipe-out reflections and acoustic voids and show also gas-induced sedimentary ridges, highs or crests. There are also some evidences for dissociation or seepage, suggesting that gas seepage may be an likely trigger of the failures (also see Figs. 3.44-3.46, 3.48, 3.52 and 3.53). As simply illustrated in Figs. 3.56 and 3.57, crestal unloading of the Çarpanak uplifted block can lead to relatively larger failures and to the depressurizing of gas. Gases and fluids derived from the gas reservoirs or pointed stocks, or from escaping free volcanic gas trapped beneath the magma chambers, can contribute to the destabilization of sediments and the degradation of the delta. Contributions of all these mechanisms to delta degradation events can be simplified in a context of dynamic evolution of soft sediment deformations.

Such a complicated picture of delta degradation events and related triggering mechanisms remark that delta environment of Lake Van is tectonically not quiescent, with small-moderate earthquakes recorded in historical times (Türkelli et al., 2003; Örgülü et al., 2003; Dhont and Chorowicz, 2006; Horasan and Boztepe-Güney, 2006 and Pınar et al., 2007). E-segment, perhaps seismically most active fault in the lake, has produced small-moderate earthquakes, which are capable of triggering sediment failures. Larger earthquakes, except Çaldıran-Muradiye earthquake, are less frequent and, thus, not recorded in lake.

3.4.3.4 Seismological and sedimentary factors

The interpretation from the map view seen in Fig. 3.43 with seismic and high-resolution sections shows that all the failures or deformation structures occur on both

slopes with various inclinations and also smoothed settings toward the shelves. A morpho-physiographic comparison of map views shown in Figs. 3.43 and 3.50 suggests that slope inclination is not only important factor contributing to failure generation, some other mechanism are also in action within non-inclined settings. These settings are recognized in Figs. 3.19, 3.24, 3.30, 3.44-3.48, 3.52-3.54 and 3.57, clearly indicating the presence of multi-component mechanisms as expressed above. Since, the sedimentation rate is considerably high, and overpressure is likely because of burial disequilibrium compaction. This suggests that effective stress is reduced sufficiently at approximately 100-150 m burial depth. High sedimentation rates also lead to thick piles of unlithified sediment, which failed more easily than thin piles or lithified rock (Schnellmann et al., 2005 and Heiniö and Davies, 2006). Some other failures are triggered by the removal of lateral support. New crown cracks develop as a result of the removal of lateral support and mark the location of subsequent failures. For example, channel erosion removes lateral support, and as a result, parts of the sediments fail into the channel. The same principle can be applied to the retrogradational failure process because each failure will result in the removal of lateral support (Heiniö and Davies, 2006). All these suggest that the main driven force may be something like a sequential development of micro-earthquake periods.

Morpho-physiographic map and overall topography (Fig. 3.43) showing distributional pattern of progradational clinoforms, submerged channels and soft sediment deformation is in a good agreement with earthquake distributions all over the deltas (see epicenters from Türkelli et al., 2003; Örgülü et al., 2003; Dhont and Chorowicz, 2006; Horasan and Boztepe-Güney, 2006 and Pınar et al., 2007). This means that overall deformational pattern of delta sedimentation is distributed where small-moderate sized earthquakes are recorded, indicating that seismically most active parts of the lake are the shallow water settings. Sedimentary instability of these settings can simply imply a regional triggering mechanism such as an earthquake. Earthquake studies previously reported by some authors clearly show very frequent 2-3 and rarely 4 magnitudes during the last 100 years. These records are considerably enough to motivate seismic and seismological factors effecting delta settings and to understand unstable sediment dynamics.

Earthquake-related instability of delta environments argues that sedimentary deformation features can be interpreted as “earthquake-induced *in situ* soft sediment

deformations", similarly those described by Marco et al., (1996) and Rodriguez Pascua et al., (2000) for well laminated lake sediments. *In situ* soft sediment deformation structures are also widely used to determine earthquake size (Ringrose, 1989, Obermeier, 1996, Rodriguez Pascua et al., 2000 and 2003). Obermeier, (1996) compiles liquefaction features of numerous earthquakes worldwide in different sedimentary environments and tectonic settings.

Internal and external structures of slumped and internally collapsed progradational wedges, particularly in SE-delta, are extremely similar to those identified and reported by Monecke et al., (2004) (see and examine Fig. 3.60). In Fig. 3.60, a seismic line through central basin of Lungerer See, Switzerland, shows that horizontally layered seismic facies represents regular sedimentation in the lake floor. The lake floor is almost undeformed. However, chaotic seismic facies indicate slump deposits, showing internally deformed clinoform wedge with 10 m thick. In this seismic section, white lines marking slump deposits are related to the 1601 Unterwalden earthquake(see Monecke et al., 2004 for the 1601 slumped deposits). Thickness distribution of the 1601 slump deposit in the northern and central basins of Lungerer See are also seen in Fig. 3.60, indicating that max. sediment thickness is less than 10 m. The slumped and internally deformed clinoform package seen in this seismic section is extremely similar to the clinoform packages in delta settings (also examine Fig. 3.51). This suggests the same genetic deformation style of these clinoform complexes and earthquake shaking, as indicated in Fig. 3.60. Correlation of earthquake-induced deformation structures to historically reported macroseismic intensities from Fah et al. (2003) and the dataset by Monecke et al., (2004) show that the threshold for sediment deformation during earthquake shaking lies at intensities VI to VII for delta settings of lake (see and examine Fig. 3.61).

Sedimentary factors; the threshold values for soft sediment deformation during earthquake shaking at intensities VI to VII for delta settings, as referred to the correlation card seen in Fig. 3.61, suggest that lithification properties of lacustrine sediments, sediment physics and their acoustic features are very important factors. This proposes that slump deposits, disturbed layering with microfolds-microfaults and liquefaction structures are most common deformational features recognized all over the delta environments.

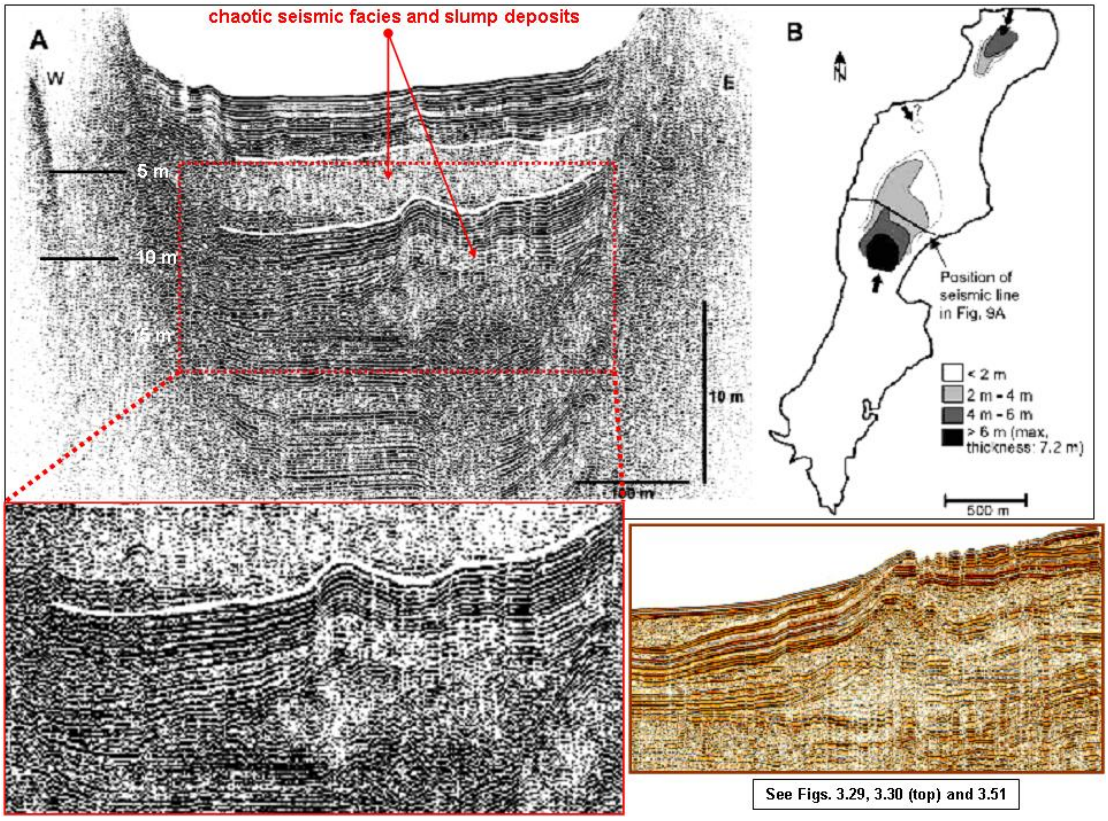

Figure 3.60 : (A) W-E Seismic line through central basin of Lungerer See (data from Monecke et al., 2004). Horizontally layered seismic facies represents regular sedimentation and chaotic seismic facies indicates slump deposits (red arrows). White lines mark slump deposit related to the 1601 Unterwalden earthquake. Seismic image at the bottom left is a detailed version of slump deposits (dotted red lines) with 10 m-15 m thick clinoform wedge. Notice the extreme similarity between deformed progradational wedges in Lungerer See and SE delta of Lake Van basin (bottom right), (see and examine Figs. 3.29, 3.30 (top) and 3.51 for an seismic interpretation of progradational wedge in SE-delta). (B) Thickness distribution of the 1601 slump deposit in the N and C-basins of Lungerer See is not more than 8 m.

It is assumed through a detailed examination of the high-resolution chirp and seismic sections shown in Figs. 3.44-3.48 and 3.51-3.57 that more brittle deformation with disturbed and disrupted layering by microfaults may occur within the already more lithified part in relatively greater depths below the clastic layer. Since, limnic mud has a high initial lithification rate and reaches a considerable strength and density shortly after deposition (Weaver and Jeffcoat, 1978). Thus, it may show brittle failure during earthquake shaking, leading to small microfaults and disrupted layers. In this case, limnic mud deposit is the main factor, controlling system (Monecke et al., 2004). This sedimentary process proposes that sandy to silty, clastic layers may be overlain by limnic mud. Then, the sand forms a mushroom-like structure protruding into the mud, while lenses of limnic mud are sunk into the clastic

material. Slight disturbances in the layering and disrupted layers occur below the clastic layer. The sandy silts are liquefied during earthquake shaking so that the denser and more cohesive limnic mud is sinking into the liquefied material while lighter, liquefied material is intruding into the overlying limnic mud (see Anketell et al., 1970 for this mechanism). Limnic mud is denser than turbiditic silts. The latter are liquefied during the earthquake, so that overlying heavier limnic mud sinks into the turbidite material (Anketell et al., 1970). Microfolds, which are another structural feature, are the result of shear stress applied to poorly lithified sediments, for instance during earthquake shaking. It is assumed that the sequence of these events is well reflected in Fig. 3.53. Because, this chirp section characterizes a more detailed image of events with a thinner layering (20-25 m).

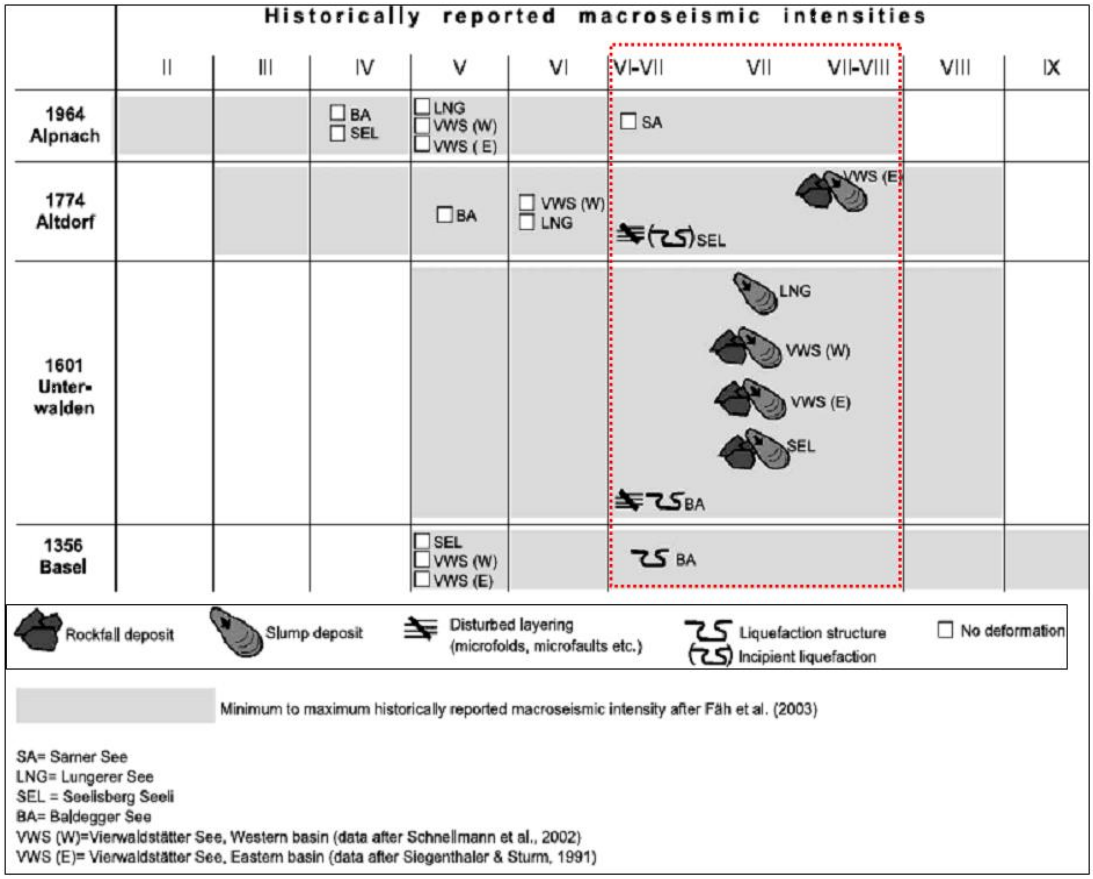

Figure 3.61 : Correlation chart of earthquake-induced deformation structures to historically reported macroseismic intensities from Fah et al. (2003) (Monecke et al., 2004). The dataset shows that the threshold for sediment deformation during earthquake shaking lies at intensities VI to VII (dotted red square). In these intensities, disturbed layering (microfolds, microfaults etc.), liquefaction structures, slumped and rockfall deposits are extensively observed, similarly in NE- and SE-delta settings of the lake.

It is clear that soft sediment deformations are mostly occurring in water-saturated, unconsolidated softer sections, close to the lake-floor. In NE- and SE-deltas, as deformation occurs only in water-saturated sediments, it takes place close to the water/sediment interface shortly after deposition of the clastic layer (see Sims, 1973; Sims, 1975 and Obermeier, 1996). This causes a wide range of structures, such as loading structures, mushroom-like intrusions and pseudo-nodules. These features are also supported by rapid sediment load and overburden.

Seismological factors; detailed structural analysis, origin and classification of deformational patterns of soft sediment anomalies are out of this scope. However, several numerous factors, such as seismological factors control the type, size, and extent of earthquake-induced deformation structures. These factors can be ranged by the duration of earthquake shaking, shaking amplitude, frequency, sediment type, structural geometry of delta settings, and amplification of shaking due to site effects. Therefore, sedimentary deformation features and their patterns can vary widely within a local area. This, to a certain degree, may explain some deformational differences between NE- and SE-deltas (see Fig. 3.43).

During field geology around the lake, some outcrops of soft sediment deformations in SE-delta are recognized within the exposed delta packages along the coasts of SE-corner of lake. These sedimentary outcrops excellently reflect hydro-plastic deformations. This suggests very fine-grained softer lacustrine materials and earthquake shaking-induced sedimentary patterns that are mainly seismites and flame structures. This implies that soft sediment deformation structures cover the past and present delta settings and that these deformation products continue towards the lake. Thus, it is clear that earthquakes, at least, during Holocene strongly affected lacustrine sedimentation in deltas (pers., comm. Karabıyıkoğlu, 2006 and 2007). It may be speculated that deformation structures may start to be formed during ground shaking of intensity VI to VII (Fig. 3.61). Since, small-scale structures, like disturbed and contorted lamination as well as liquefaction structures, dominate at lower intensities of VI to VII. Towards higher intensities, large-scale mass movements, like slumps and rockfalls, become more frequent and probably overprint small-scale structures. Galli and Ferelli, (1995) and Obermeier, (1996) reported that liquefaction structures become common at ground shaking of intensity VII. This is in agreement with experimental data indicating that the threshold for liquefaction lies at magnitude

5–5.5 by Moretti et al., (1999). Moreover, paleoseismic investigations in outcrops of lake deposits reveal threshold values of intensity VI for the formation of soft sediment deformation structures (Sims, 1973; 1975 and Hibsch et al., 1997). Rodriguez Pascua et al. (2000 and 2003) related soft sediment deformation structures within Miocene lake deposits to magnitudes even smaller than 4. These studies confirm earthquake shaking factor in deforming softer sediments of delta settings, even by smaller magnitudes than 4.

3.4.4 Implications for dynamic evolution of delta domain

Overall soft sediment dynamics of NE and SE-delta settings implicates that different styles of delta degradation complexes are the result of various failure and transport processes. These processes produce laterally discontinuous erosional surfaces and deposits that have impact on soft-sediment deformation.

An integrated interpretation of seismic and high-resolution chirp sections with morpho-physiographic and topographic map view suggests a synthesized delta degradation model. This model reveals a range of erosional, deformational and depositional clinoform features. These features are a prominent result of the delta degradation events. Degradation events include sedimentary and progradational failures, causing gravitational products, slumps, slides, debris flows and deposits no more than a few tens or hundreds of meters thick, as well as large progradational slumps with evidence for internal deformation and chaotic reflection patterns. Degradation model also proposes that different styles of degradation can occur along the same structures and implies that the submerged river-channel erosion is volumetrically the most important degradation mechanism. The most common style is that of multiple small-volume failures. These failures can have a common locus, if pre-existing planes of weakness are present. For example, a significant amount of sediment is removed from delta and thick deposits accumulated in the subbasins adjacent to E-segment fault. The degradation products described are closely spaced and relatively small, showing significant along-strike variability in the erosional and depositional features. This suggests that unconformities and individual seismic reflections can only be traced locally. Many of thinner debris flows or turbidites as dominant degradation products are not often seismically resolvable even close to the seabed. However, their function in filling subbasins is easily underestimated, particularly where seismic resolution is reduced.

The difference in the slope geometries is another fundamental control on the style of degradation and the run-out distance of such failures, particularly slumped progradational wedges. Fault-related abrupt break in slope of Çarpanak spur zone reduces the velocity of the failed sediment mass and causes deposition, resulting in relatively thick, short, and wide deposits. The longer and shallower slope of NE-Erek delta leads to the disintegration of failed sediment mass into debris flows or turbidity currents that produce widespread deposits with longer run-out distances. Sediments with higher internal shear strength form more coherent downslope mass movements on a basal detachment and shortening by internal imbricated sedimentary piles.

Strong dissection of the lake floor produces oval-shaped depressions and highs, clearly identified in seismic and chirp sections. These are formed as a result of slumping, bottom-current erosion and internal collapsing and disintegration of clinoform facies. This evident delta dissection and degradation by shallow-water submerged river-channel erosion and channel-margin slumping. Sedimentary reliefs such as crestal highs and swells on the lake-floor are at various stages of degradation and burial. The dominant style of degradation of deltas occurs as small-volume failures that form thin deposits at or below seismic data resolution. Oval-shaped depressions and highs are considered to represent small-scale slumping modified by bottom currents. In this case, differences in sediment reliefs are important. Erosion styles in relief patterns show that sediments having a minor and greater relief on the lake floor degrade differently through a combination of brittle failure and bottom-current erosion. The presence of anisotropies also affects the type of failure that occurs. A significant proportion of the sediment deposited in adjacent subbasins has been recycled from the faulted crests or highs. Given the variety and 3D-complexity of these degradations is essential to fully characterize degradation in collisional lacustrine environments.

NE and SE-provinces of delta domain are subjected to soft-sediment deformation processes. High amount of rapid sediment input, various burial rates, disequilibrium compaction, asymmetric subsidence gradients and catastrophic lake level fluctuations cause unstable shelf-margin delta environment. Both deltas are well represented by successions of progradational clinoform facies that are mainly disturbed by earthquake sequences, inducing small-scale soft sediment deformations. The occurrences and kinds of deformation depend on seismological factors, sediments.

It is also possible that traces of strong, historic earthquakes may be recorded in the sedimentary archive of recent lake deposits. The spatial distribution of deformation structures well reflects earthquake-controlled delta deformation dynamics, also providing additional data for historical earthquake dataset. Small-scale soft sediment deformation structures may have started to form at intensities of VI to VII. Large-scale slumps and turbities become more frequent at higher intensities. All these deformation structures can be used to estimate minimum values of earthquake size and also used to extend historic earthquake records further back into the Holocene. Earthquake-induced *in situ* soft sediment deformation structures are, in fact, a dynamic result of neotectonic factors, controlling the earthquake potential of delta and delta degradation.

Transgressive and regressive cycles; preliminary results by Kuzucuoğlu et al., (2007) regarding the lake terraces and sediment sequences on E-and S-coasts of Lake Van allow a confirmation of several transgression and regression cycles all possibly dated Upper Pleistocene. The interpretation of the terrace stratigraphy and past sedimentation environments is reconstructed from the depositional facies. These facies have an important significance with regard to the understanding of the climatic and tectonic meanings of this succession of very high-and-low stands of the lake level.

In principal, a cycle can be defined by central Tatvan basin. Deep lake sediments corresponding to a high lake level and associated formations such as shoreline alluvial fans, are followed by a regression generating the deep incision of the series by rivers. As the lake outlet is today positioned at *ca.* +101 m above lake level (Kuzucuoğlu et al., 2007), at N of Van and at Beyüzümü, E of Van appear to have been strongly uplifted during the Upper Pleistocene (> 40m at Beyüzümü). Tectonic activity is also recorded by syn-sedimentary faults, seismites, and post-depositional faults at Beyüzümü. The important regression before the Late Glacial, evidenced by Landman and Reimer, (1996), may correspond to the incisions (Kuzucuoğlu et al., 2007). Maximum water levels of lake (present water level is 1648 m) are ranged by a group of values, 10-15 m, 20-30 m, 55-60 m, 70-80 m ve 120-130 m, representing terraces and/or planes. These values confirm that the highest water level of lake was more than 100 m (Karabıyıkoğlu et al., 2007). Karabıyıkoğlu et al., (2007) reported

that these terraces interstratified with pyroclastics and tephra deposits are controlled by aluvial fans and/or lacustrine facies, fluvial deltas and Gilbert-type deltas.

It is possible that all these findings are combined with available seismic and high resolution data from lake. The integrated interpretation gives an synthesize of sublacustrine facies architectures of sequences, depositional settings and sequence stratigraphy. This indicates that paleo Lake-Van during late Quaternary is subjected to forced regression, transgression and normal regression cycles. These cycles are characterized by low to high amplitude and high frequency water level fluctuations. This suggests catastrophic lake level changes. All these evidences of high magnitude low and high stands of lake level contribute to identifying climate forcing, recent tectonic impact and relationships to volcanic activity during Upper Pleistocene. The remark is that the basic dynamic equation describing delta settings of lake is "*Sedimentation* > *Uplift* > *Subsidence*", if glacio-climatic factors fixed. The faster and higher sedimentation rates than the regional tectonic uplift rate resulted in regression (basinward migration of shore line), low stand system tract (LST), prograding wedge complexes (PWC) and overall sediment unstability. This lacustrine sedimentation and the resultant sediment dynamics during post-orogenic period can be termed as "strong orographically induced and concentrated precipitation" (as referred to a process by Weiland and Cloos, 1996 and Cloos et al., 2005). This precipitation is episodically disturbed by local earthquake sequences, meaning "lacustrine delta seismicity".

3.5 Tectono-sedimentary Development and Morpho-tectonic Structure

An examination and evaluation of active tectonic provinces considering seismic reflection and high-resolution chirp data is made of a detailed seismic structural analysis, structural description and interpretation of deformations along marginal, basinal, and delta domains. Consideration of these domains along with the structural complexities is shown to be common deformations taking place on the lake. These deformations reveal tectono-sedimentary interactions and their morpho-tectonic expressions, giving some certain clues about dynamic evolution of Lake Van on top of the underlying accretionary wedge.

Folding; the fold structures are clearly imaged through seismic sections shown in Figs. 3.3, 3.5, 3.8 and 3.9. In the N-limit of central Tatvan basin, close to the N-

margin boundary, the upper part of the sedimentary section has developed as positive flower structure, with reverse rather than normal sense of movement (Figs. 3.1-3.7). It forms fold structures, which increase in amplitude upwards through the section. Bedding dips steeply or vertically, with a strike parallel to the WSW-ENE trend of the N-margin. Obviously, these seismic sections are interpreted as showing that prior to the Plio-Quaternary the structure of the area was developed in a transtensional tectonic regime in S-margin, while the tectonic regime was transpressional in N-margin (see and examine Figs. 3.1-3.11). The depositional sequences in N-margin are seen to thin towards the flank of NE-Erek delta (Figs. 3.6 and 3.7). These sequences onlap the flanks of this extended delta (low-angle delta progradation in Figs. 3.33 and 3.34). This shows that NE-Erek delta is a growth structure during the deposition of all the sedimentary units in the basin.

Sedimentary cover of central Tatvan basin is, in fact folded in a simple fashion. These folds are interpreted as distinguished by being overlain by unfolded beds and underlain by folded beds, due to sedimentary slumping (Figs. 3.3, 3.5, 3.8 and 3.9). It is clear from these seismic sections that deeper sediments are more strongly folded than shallower sediments and magnitude of folding decreases upwards. These fold structures are formed of a series of arcuate, and asymmetrical folds with limbs. These become steeper and overturned towards N-margin boundary, and are broken by reverse oblique-slips in N. The N-margin boundary fault is vertical or steeply dipping and fall into two sets, one divergent strike-slip, and the other convergent strike-slip, trending E-W. Both sets of faults cut across dipping beds and are therefore probably later than the folding. Seismic structural interpretation also suggests that these folds can be considered to be disharmonic and harmonic folds, affecting deeper sedimentary units above a possible detachment in the underlying accretionary wedge. A gravitational origin, “gravity-driven instability process” is suggested for these folds, since they are formed by the slumping of the entire sedimentary column towards the N from the accretionary basement high in the S. Thus, the arcuate fold structures in central Tatvan basin are interpreted as due to gravitational sliding from the uplifted S-margin boundary on a probable detachment surface within the lake. The orientation of folds near N-margin boundary and the general trend of the fold axes is WSW-ENE, sub-parallel to the basin margin, and the vergence of the folds is to the ENE. The inference is that the present basin margin is parallel to the margin of

the basin during the deposition of the sediments. This also confirms that the sedimentary cover of central Tatvan basin has certainly undergone a great deal of syn-sedimentary deformation, with the formation of positive flower structure in N-margin. The syn-sedimentary deformation is accompanied by intrusive-extrusive activities, intercalated with depositional sequences from W- and S-margins (Figs. 3.3, 3.5 and 3.8-3.11).

The N-S cross-sectional views of central Tatvan basin shown in Figs. 3.3, 3.5, 3.8 and 3.9 are structurally similar to the map views from Barber and Crow, (2005), based on a seismic profile from the Ombilin Basin, Central Sumatra (also see related figures and references in Barber and Crow, 2005). These cross-sections well classify positive flower structure-related basin folding in central Tatvan basin. These seismic sections are also closely related to diagrammatic cross-section of the structure in the Simpang area to the N of Aru Bay, based on the interpretation of seismic profiles in Barber and Crow, (2005). By an analogy of this diagrammatic cross-section to central Tatvan basin, it can be seismically illustrated that diapiric anticline over positive flower structure (the term "diapiric anticline" by Barber and Crow, 2005 refers to "pushed-up rhomb horst structure" or "sedimentary ridge" as previously termed) and effect of faulting clearly increases up succession (Figs. 3.1-3.5). These anticlines or folds close to positive flower structure trend toward the basin centre and more flat anticlines or gentle folds far from positive flower structure are seen in the central basin. The gentler and smooth folds toward S-margin (for example, Figs. 3.3, 3.5, 3.8 and 3.9) suggests that effect of faulting clearly decreases up the succession (see also figure in Barber and Crow, 2005). This argues that normal or transtensional faults in the lower part of the succession are inverted as transpressional fault in N-margin during Quaternary or after the deposition of the Pliocene. The large amplitude of the anticline or folding at the N-margin is increased by the gravity-driven mass flowage of sedimentary block of central Tatvan basin into N-margin (see a process suggested by Barber and Crow, 2005). The interpretation above remarks that the fold structures developed across central Tatvan basin are clearly related to dextral in S and sinistral oblique motions in N and W. Overall structure and deformation pattern of these anticlines or folds clearly mark the inversion of the sediments deposited in central Tatvan basin.

Geological periods related to tectono-sedimentary events and stratigraphic relationships are based on Koçyiğit et al., (2001) and correlated with time-rock relationships of Şengör and Kidd, (1979); Şaroğlu and Güner, (1981); Şaroğlu and Yılmaz, (1986) and Yılmaz et al., (1987).

Subsidence; fault-controlled episodic sequences of turbiditic events and debris flows all along the margin boundaries of the lake suggest that subsidence is not uniform (at least partly) throughout the basin, with greater subsidence and thick sediments in the Deveboynu and Varis spur zone subbasins (see and examine turbitic sequences of events through Figs. 3.16-3.23, 3.25-3.29 and 3.30 at the top). Due to strong regional uplift in Çarpanak spur zone and NE-Erek delta, uneven asymmetric subsidence and rapid sedimentation is greatest in central Tatvan basin and the subbasins, so that the greatest thickness of sediments is found in the central part of Tatvan basin (approximately 600 m thick) and the sediments thin out over the S-margin (approximately 350 m thick).

With continuing subsidence, but a decrease in sediment supply, a major transgression might have occurred sometime in the Pleistocene, so that deposits were deposited across the delta surface, such as onlapping sequences in NE-Erek delta (Figs. 3.31-3.34). At the time of maximum transgression, sedimentation extended toward the E and NE to reach the delta well beyond the bounds of the Tatvan basin (NE-Erek delta). It is assumed that differential and asymmetric subsidence, with reactivation of the margin boundary faults continued during the deposition of the Plio-Quaternary sediments, which marks a transgressive phase. This is followed by the fully delta sediments (Quaternary), representing the period of maximum transgression.

Angular unconformity; particular attention is paid to this unconformity surface locally developed in the uplifted fault block of Çarpanak province. This surface of angular unconformity is clearly imaged through seismic sections shown in Figs. 3.16-3.21, 3.24 and 3.25. This surface entirely covers Çarpanak spur zone and NE-Erek delta, suggesting that delta sediments are eroded from developing uplifted structures (Deveboynu peninsula and Çarpanak spur zone) and deposited locally in subbasins. The younger, probably Quaternary-aged sediments rest on the older rocks with an angular unconformity, but towards central Tatvan basin, this unconformity disappears. This surface only locally extends all along the NE-Erek delta and is buried toward the gulf of Erçiş in the further N.

Angular unconformity between Quaternary and Pre-Quaternary rocks is considered to be a well-exposed surface for the early stages in development of internal subbasins (Deveboynu and Varis spur zone subbasins) of the lake. These subbasins are infilled by erosion products derived locally from the basement uplifts (Deveboynu peninsula and Çarpanak spur zone) in the extensional or transtensional phase. This case is well reflected in Deveboynu and Varis spur zone subbasins shown in Figs. 3.18-3.20, 3.23, 3.26-3.29 and 3.30 at the top. These seismic sections show that these internal depocentres during the deposition of the Quaternary sediments are situated in areas, which later became the sites of uplifted blocks. It is assumed that uplift and erosion of Çarpanak province probably in the latest Miocene-earliest Pliocene (Şengör and Kidd, 1979; Koçyiğit et al., 2001), provided a source of sediments for the subbasins. These deposits above angular unconformity are overlain by Pleistocene to Recent alluvial deposits.

Çarpanak spur zone is oblique slip fault-controlled area by E-segment and the angular unconformity characterizes the eroded upper surface of Çarpanak basement block, as mentioned above. This basement block structure may be interpreted as a large “homocline” or “monoclinal” flexure (Barber and Crow, 2005) between the faulted sediments of the Çarpanak uplift and the flat-lying sediments of the central Tatvan basin. If it is true, it may be suggested that this flexure is the surface expression of a pre-existed thrust at depth, on which the accretionary complex had been thrust over the basement. This basement had acted as a back stop during the development of the complex. This flexure zone can be recognised in seismic reflection profiles, and can be traced towards NE as a belt of structural disturbance (Figs. 3.16-3.20 and 3.23-3.25).

Evaluation of angular unconformity surface considering seismic reflection data from Çarpanak spur zone and NE-Erek delta proposes that the whole of the Çarpanak area (also with NE-Erek delta) is uplifted and exposed to subaerial erosion, probably with a landscape of significant relief. This supplied large quantities of terrigenous sediment to the extensional-transtensional subbasins. At the same time, the lake region itself underwent major subsidence. Prograding sediments overwhelmed the basement banks and, as sediment supply exceeded the rate of subsidence, built out to form a continental shelf and a continental slope towards the E and NE (see and examine Figs. 3.31-3.34). Further W, in the deeper part of the lake, deep water

turbidites of Quaternary age buried. Probably, this pattern of lacustrine sedimentation, with the progradation of the shelf and the deposition of turbidites in the deep Tatvan basin has continued through Late Pliocene times to the present day. The same broad sequence of events is thought to have affected all the deep lake setting.

Çarpanak basement block uplift, together with NE-Erek delta is the most prominent structural feature, affecting structural and sedimentary events in NE- and SE-delta settings. Probably, after the Miocene the great thickness of terrigenous sediments, which was scraped off the uplifts (Çarpanak province and Deveboynu peninsula), must have altered the dynamics of the accretionary complex underlying lake. This is based on the time periods of tectono-sedimentary events and stratigraphic relationships by Koçyiğit et al., (2001) and time-rock relationships of Şengör and Kidd, (1979); Şaroğlu and Güner, (1981); Şaroğlu and Yılmaz, (1986) and Yılmaz et al., (1987). When the accretionary wedge complex is composed largely of incompetent and relatively weak sedimentary materials, as proposed by Şengör and Yılmaz, (1981), later minor uplift and subsidence can be attributed to continual adjustments to the shape of the accretionary wedge or to the fluctuations in lake level during the Pleistocene. This may imply that the Çarpanak uplifted high is considered to have formed as a drape over an uplifted basement block, composed of Ophiolitic mélange complex or probably Cretaceous limestone which outcrops in land (see also Kurtman et al., 1978; Şengör et al., 2003; Şengör et al., 2008).

Asymmetric half graben; extensional-tilted geometry of central Tatvan basin is illustrated by seismic sections seen in Figs. 3.3, 3.5, 3.8-3.11 and 3.31. Figs. 3.58 and 3.59 also show depositional sequences and detailed surficial image of central Tatvan basin. Central Tatvan basin in the form of asymmetric half graben is bounded by oblique-slip faults across its margins. Transtensional margins of central Tatvan basin in W and S are densely covered by intrusive-extrusive activity, folding and faulting. Tatvan basin bathymetrically shows regular and straight lineaments at the accommodation zones, which are associated with N-, S- and W-margin boundary faults. This basin terminates at faults with the same orientation.

S-limit of central Tatvan basin is bounded by a broadly widening transtensional shear zone in S-margin, parallel to suture complex, as indicated by previous studies. Deveboynu and Varis spur zone subbasins in E and Tatvan delta subbasin in W

originated as a series of extensional-transtensional en echelon grabens through S-margin boundary fault (PDZ). W-segment of S-margin boundary fault as the S-end of central Tatvan basin is a complicated structural feature, characterized by active intrusions and passive collapsed dome-cone complex (Figs. 3.3, 3.5, 3.8, 3.9 and 3.13-3.15). It is assumed from overall asymmetric structure and depositional geometry of central Tatvan basin that the fault dip of W-segment considerably differs from that of E-segment. Relatively low-angle dip of W-segment suggests that this segment at the surface passes probably into listric fault, and an inferred flat-lying decollement surface in the basement at a upper crustal depth of 10 km (Şengör et al., 1985 and Dewey et al., 1986). Thus, the sedimentary cover of central Tatvan basin above flat-lying decollement experiences gravitational unstability from S to N. The folding of sedimentary cover is developed by the inversion of the thicker sediments, forming the half-graben fill, and strongly uplifted along the transpressional regime in N-margin.

Due to the subsidence of the accretionary wedge basement, the basement structure of central Tatvan basin is interpreted as rhomboidal block, termed by Şengör et al., (1985) between margin boundary faults as the result of local extension and transtension (see and examine diagram in Fig. 3.40). The sequence of events which can deduced from the relationships above is that the earliest stage was a period of reactivation-related extension and the formation of the half graben structure. Deformation with strike-slip faulting and oblique compression caused the reactivation and inversion of the normal faults and the formation of the fold structure in the basin, probably occurred during the Plio-Quaternary. Central Tatvan basin is, thus considered to have originated as a half-graben in the Late Pliocene, during the same phase of extension that formed the subbasins in the lake.

Reactivation; reactivation of margin boundary faults and basin inversion is, indeed, well characterized by seismic reflection images and their correlative structural interpretation**.** Margin boundary faults that bound Tatvan basin are considered to be the major bounding faults to the asymmetric half-graben. The sediments thicken towards the N-margin boundary fault, but this original normal fault is presently partially inverted as an oblique thrust (see and examine a structural trend and backthrusting through Figs. 3.2-3.10). The sediments thin towards the S-margin boundary fault. This fault is also inverted as an oblique extension. E-segment in S-

margin bounds Deveboynu and Varis spur zone subbasins, while W-segment bounds Tatvan delta subbasin. Such a structural picture of margin boundary faults in reactivation suggests that central Tatvan basin together with Çarpanak spur zone, is involved in the combined block-wedge system, obliquely moving towards the ENE trends. This implies that Çarpanak spur zone is a morpho-physiographic expression of the uplifted fault block caused by E-segment of S-margin boundary fault, while central Tatvan basin and SE-delta are downlifted blocks. This shows differential uplift and subsidence along the lake.

Seismic structural analysis, overall deformation patterns, and kinematic indicators show that a complex history of tectonic and sedimentary development with one dominant E-W structural trend is continually reactivated throughout its history. Pre-existing margin boundary faults behaved as dextral in S and sinistral oblique-slip faults in N and W, depending on the orientation of the stress system at different stages in the structural evolution of the basin. Based on time periods of regional tectonic relationships of Koçyiğit et al., (2001) and Şengör and Kidd, (1979), it should be briefly reported that the earliest phase (during Pliocene, just after Miocene compressional-contractional period) of deformation was extension and reactivated W-E trending basement fractures, such as Muş suture zone in S-margin, during Pliocene to Pleistocene time. A second phase of deformation with W-E transtensional regime in S during the Quaternary was associated with transpression in N and reactivated the W-E fault as dextral oblique-slip fault. These oblique-slip faults clearly follow the trace of initial normal faults, which bounded the margins of basin, filled with a thick sequence of the Plio-Quaternary. The change in the orientation is significant, as the normal faults have been reactivated as oblique faults.

Overall magmatic trend and lines of volcanoes (fissures, vents, intrusions); a group of structures characterizing W-E-striking S-margin boundary and NE-SW-striking W-margin boundary faults is reflected by seismic expressions of ductile events associated with intrusive-extrusive processes. These are extension fissures or fractures, open central vents, intrusions and regular lines of volcanoes along margin boundaries. These features are prominently localized through transtensional faults and related segments across W- and S-margins (see and examine these features shown in Figs. 3.3, 3.5, 3.8-3.11, 3.13-3.16, 3.18 and 3.26-3.29). Well-defined examples of the fissure and central vent volcanoes and collapsed parasitic cones are

seen at the summits of Nemrut volcanic dome complex area (Dewey et al., 1986). Along this area, less viscous magma has poured out and flowed down the steep slopes of volcanoes into the nearby Lake Van basin, its SSW-corner (also see Figs. 3.13-3.15).

Through S- and W-margin boundary faults, propagational trend of magmatic intrusions displays linear magmatic chains, consisting of numerous volcanic cones, fractures, fissure and central vent volcanoes. Fissures and vents (or local extensional normal faults) are well exposed at the summits of large isolated to composite volcanoes of probably Quaternary age in S-margin and SW-corner of lake, because these have not experienced yet enough long-lived erosion. All these isolated vent or fissure strato-type volcanoes occur inside the geometrical discontinuities, such as extensional bends, step-overs, bifurcations and tips, of faults (Koçyiğit et al., 2001 and Dhont and Chorowicz, 2006). This indicates that structural relationships of these products with the faulting show a complicated pattern of extensional strains. Along Muş suture-parallel structural trend, starting from SW-corner to W-segment and into E-segment towards Çarpanak spur zone and Deveboynu peninsula, a prominent linear trend of magmatic intrusions occurs as an isolated and W-E-trending single crack, or a zone of cracks or a fracture zone. This zone ranges from 2.5-3 km in width and 400 m to 60 km in length (see Koçyiğit et al., 2001 for a correction of these values). This suggests that line of volcanoes or linear volcanic chain occurs along the shoulders of fault-bounded margins of the lake.

As a similar example, it should be given that the Sevan Lake basin (with 1.5 km thick Plio-Quaternary basin fill) is a system of lake depression located in Ermenia. This lake is bounded by Lesser Caucasus suture zone in N, while Lake Van basin is bounded by Muş suture in S. This lake basin is well comparable example with Lake Van basin (see tectonic maps and cross-sections in Koçyiğit et al., 2001 for Sevan Lake basin). Margin fault of Sevan Lake basin, similar to S-margin boundary fault of lake, has numerous parallel to sub-parallel fault segments, en echelon faults, pressure ridges, tilted blocks, extensional structures, step-overs and bends. This margin fault bifurcates into numerous and S-concave splay faults in the pattern of extensional horse-tail structure, indicating the Sevan Lake fault wedge basin and the NNW-SSE-trending lines of Quaternary volcanoes (Koçyiğit et al., 2001). The W-E-trending fissures/fractures, vents and lines of Plio-Quaternary volcanoes have the same

orientation as the fissures and extensional normal faults are consistent with a local strain pattern of lake. Seismic structural analysis of intrusive-extrusive activities, their anomalous growth, relationships with local/regional faulting patterns suggest that overall magmatic trend, a line of fissures, vents and intrusions follow W- and S-margins and are related to active extensional and transtensional regime.

3.5.1 Implications for tectono-sedimentary development and morpho-tectonic structure

Tectono-sedimentary development and morpho-tectonic structure based on the above review of seismic structural interpretation from structural domains reveals the dynamic evolution of Lake Van basin, as summarized in morpho-tectonic, faulting and deformation map seen in Fig. 3.62. Tectonic and sedimentary development of Lake Van can be reviewed and interpreted in the light of not only seismic reflection data from structural domains, and but also a correlative examination of the map view in Fig. 3.62 to overall deformation pattern and basin types in Fig. 3.40.

Tectono-sedimentary development and morpho-tectonic structure of the lake clearly implicate for superimposed and successive deformational phases at various scales during Plio-Quaternary period (see and examine Figs. 3.40 and 3.62). It is interpreted from the most important findings obtained at each scale of marginal, basinal and delta domains that an initial phase of deformation was extension during which the asymmetric half-graben structure was formed (see also the Ombilin Basin as an example in Barber and Crow, 2005). Initial extensional deformation is perfectly reflected by asymmetric depositional geometry of central Tatvan basin. As indicated by the tilted structural geometry, half graben fill of central Tatvan basin, the extension has probably continued from the Pliocene, during the deposition of the deep lake sediments, until the Quaternary, during the deposition of the delta sediments. This extensional phase was followed by an asymmetric subsidence phase during the deposition of the Plio-Quaternary sediments. The evidence for the formation of the folds as growth folds and basin asymmetry indicates that there was some differential subsidence of the basement within the basin. Obviously, the extent to which extension was accompanied by a component of transcurrent fault movement resulting in a half graben basin is impossible to determine. A normal component of transtension in S-margin in the formation of the basin is important factor, as normal extension without some strike-slip component is exceedingly rare.

The N-margin boundary fault, which was inverted to form an oblique thrust. This transpression in N-margin caused the major folds in the central Tatvan basin, and intensified the folding near N-margin boundary. It was also responsible for the minor or flat folding seen in the S-marginal sections. The extent to which the compression was accompanied by a component of transpression is again impossible to determine, but some component of transpression is probable. The final event in the structural development of the lake was oblique-slip faulting, dextral in S and sinistral in N on the complementary W-E trends. Thus, oblique-slip deformation entirely controlled the present-day tectonic and depositional structure of the lake (see Fig. 3.62).

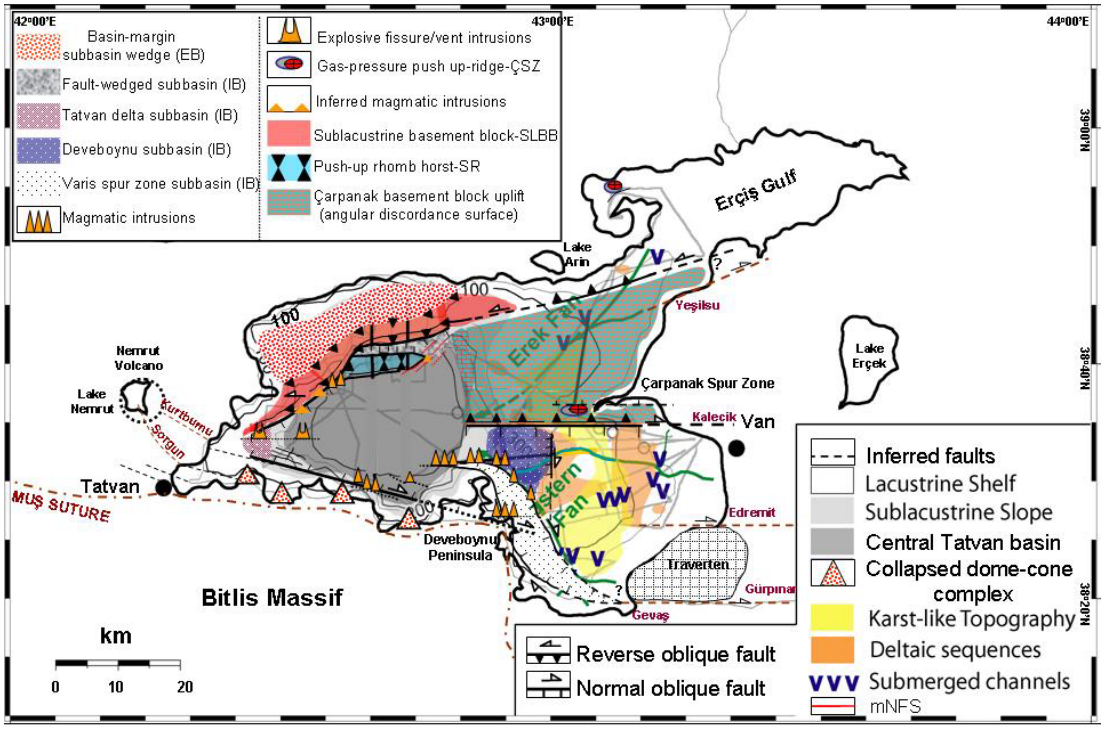

Figure 3.62 : Faulting and overall deformation map of rhomb-shaped Lake Van basin superimposed with morpho-topographic and physiographic structure of the lake. This map clearly shows the extensive distributional pattern of extensional magmatism through basin-margin sections and the complicated kinematics of strike-slip deformation, internal-external subbasin formation, associated with soft-sediment deformation, submerged channel incisions, and delta degradation in shallow water settings. Note that N-margin boundary is sinistral transpression (positive flower structure "palm-tree"), W-margin boundary is sinistral transtension and S-margin boundary is dextral transtension with W- and E-segments (negative flower structure "tulip"). Varis spur zone is pull-apart subbasin, termed as "sphenochasm". Also notice oblique block fragmentation and separation of the lake through S-margin boundary fault along Muş suture zone and lateral oblique-slip wedging toward ENE. EB: external basin, IB: internal basin; ÇSZ: Çarpanak spur zone, SLBB: sublacustrine basement block, SR: sedimentary ridge and mNFS: mini negative flower structure (see the legends for map descriptions).

From sedimentation style seen in seismic sections and also from Muş basin (data from Şengör et al., 1985; Dewey et al., 1986; Koçyiğit et al., 2001), it is estimated that large amount of the sedimentation has been eroded following Mio-Pliocene uplift of the Mountains around. Initial extensional sedimentation (half graben fill) in central Tatvan basin is imaged through seismic sections striking N-S. Strike-slip controlled sedimentation (thickening of deep lake sediments by onlapping) towards NE-Erek delta and Çarpanak spur zone in E is reflected through seismic sections striking W-E. This picture of sedimentation style implies that deposition in the basin was followed by oblique-slip deformation. This event caused inversion of the basin with reversal of the movement on the normal faults, including the N-margin boundary fault. Seismic data also indicate that the overlying sedimentary units in the central Tatvan basin did not fold as those underlying folded. This suggests that the younger sediments are not deformed by folding, probably due to strike or slip variations in fault activity along margin boundaries. It should be stated that wherever the relative age of strike-slip faults, normal faults and folds can be determined, strike-/oblique-slip faulting is always the youngest event (Barber and Crow, 2005). This confirms that the initial structural and sedimentary control in the basin is extensional deformation at varying magnitudes. Briefly, normal faulting in N- and S-margins resulted in rapid extensional sedimentation, due to strong orographic uplift, differential and episodic subsidence, and the resultant asymmetric pattern of half graben fill. Regime transition from extension to strike-slip processes was followed by strike-/oblique-slip sedimentation and then, recently pure oblique-slip events. These youngest events, as a whole, controlled Tatvan basin block and the lake. It is found from a correlative analysis of Fig. 3.40 with Fig. 3.62 that this major phase of strike-/oblique-slip faulting is most probably related to movements on the suture complex (Muş and Cryptic sutures). This suture complex lies to the S-margin boundary and on underlying accretionary wedges.

Morpho-tectonic and deformation map shown in Fig. 3.62 proposes that the present-day tectonic and sedimentary deformation and faulting style of Lake Van is a manifestation of deformation events in the accretionary basement structure. It is assumed that accretionary wedge complex beneath the lake is made of intra-lake wedges at various scales. It is also evident that these accretionary wedges are irresistant and unstable Mesozoic mélange materials. They seem to be squashed

crustal basement all along margin boundary faults (the term, “squashy zone” by Şengör and Yılmaz, 1981 and Şengör et al., 2008). This remarks that tectonic unstability of intra-lake accretionary wedges is probably represented by the recent deformation and faulting style of the lake. Movements on the accretionary wedges probably commenced in the Plio-Quaternary, after the deposition of all the sediments now preserved in the basin. Uplift of the Mountains around accompanied these movements. The subbasins then formed part of the source area for the Plio-Quaternary sediments of the lake. These subbasins are disturbed by magmatic intrusions and surrounded by up faulted blocks (Çarpanak spur zone), where the pre-Quaternary basement lies at a relatively shallow depth. E-segment of S-margin boundary fault represents an important structure in the pre-Quaternary basement. E-segment is reactivated as normal fault during extension to form the highs, the troughs, the grabens or the subbasins and then reactivated as oblique-slip fault, as in W-segment.

Through PDZ of S-margin boundary fault, W-segment controls Tatvan delta subbasin formation at SW-corner and peripherally collapsed passive and active dome-cone complex in and along the S-coasts, as E-segment controls the subbasin formations. The subbasin formations and complex activity of intrusive-extrusive events are the end-members of transtensional shear zone in S-margin. A dense concentration and localization of these active and passive ductile events through S- and W-margin boundary faults indicates that an active W-E magma propagation lies to the S-margin of the basin and thus, underneath central Tatvan basin. This significantly shows an evidence that delamination and break off of the lithospheric mantle is in progress at Quaternary time and probably commenced in Pliocene (see and examine Keskin, 2003; 2005; 2007 and Şengör et al., 2003; 2008 for a discussion of Cryptic and Muş suture zones trending all along the S-coasts of lake). Morpho-tectonic significance and deformation pattern of transtensional shear zone in S-margin and its relation to active magma intrusion and propagation confirm that the complex discontinuous faulting area in S-margin is broadly widening shear zone of a negative flower structure. Transtensional nature of this shear zone triggered upward ductile mass transport of rising magmas, resulted in the subbasin formations and thus, controlled S-oblique opening of lake along W-E trends, parallel to suture complex.

Although the lake was formed on top of the accretionary complex, it is clear from Figs. 3.40 and 3.62 that it developed during a phase of extensional deformation and is bounded to the major transtensional faults in W and S and transpressional fault in N. The asymmetric depositional geometry in thickness of the bedded succession towards N- and S-margins indicates that margin boundary faults are initially reactivated as active normal faults during the deposition of the sediments. The fault reactivation process is excellently recognized across N- and W-margins (see the sublacustrine basement block from Figs. 3.1 to 3.10). Sediments are eroded from basement uplifts, to be deposited in the lake developed on top of the accretionary complex. While more recent sediments in central Tatvan basin are sub-horizontal, older sediments are tilted basinwards, and increasingly folded. These sediments are highly deformed and disrupted by oblique-slips. This may imply that the accretionary complex underlying the lake is under transpression. This suggests that imbricate thrusts in the accretionary complex are continually reactivated to deform the sediments in the basin. This case reveals that in the accretionary complex, the original thrust surfaces bounding the lake were continually reactivated and thus, new fault planes developed. These faults disrupted the crustal basement and breaking it up into blocks. Seismic sections show that the N-margin of the basin is steep oblique-slip reverse fault along which the sublacustrine basement block has been uplifted, compressing and folding the bedded sediments in central Tatvan basin. Turbidities and debris flows are interpreted as rock falls, slumps, slides from active fault scarps, particularly along E-segment in S-margin. This probably indicates that slices of the accretionary basement within the accretionary complex were being uplifted and eroded along the basin margins during sedimentation. It is estimated that the chaotic and sheared nature of the mélange underlying the lake is considered to be due to the dynamic tectonic environment within the accretionary complex.

A seismic structural examination and interpretation of margin-bounding faults notes that fault reactivation and localized inversion took place and was followed by the infilling of the basin. This is indicated by the upward shallowing of the depositional environments in the lake. Following the deposition of the sediments during extensional period and half-graben formation, extensional normal faults of N- and S-margins are reactivated as strike-slip faults. Then, these strike-slip faults are reactivated and inverted in a transpressional tectonic regime in N-margin and a

transtensional regime in S-margin. This inversion process points out that the bounding faults have been continually reactivated as extensional and strike-/oblique-slip faults during the deposition of the sediments, so that older sedimentary units are more highly deformed. The alternations of extension and subsidence, compression and uplift in the lake can be attributed to variations in the rates of convergence at the delaminated zone and the effects of transpression and transtension. The remark is that Lake Van basin seems to have evoluted, at least, during two main periods; Pliocene and Quaternary. These periods attribute the tectonic inversion to the onset of extension and oblique-slip events in the lake, due to the doming of hot asthenosphere beneath lake. This suggests that asthenospheric doming has been responsible for the regional orographic uplift, subsidence and angular unconformity seen. As the slab delamination system became established, volcanicity and uplift of the basement around the basin led to a regression, with the deposition of Pliocene sediments. This deposition gradually extended eastwards (towards delta areas) to cover the whole of the lake basin by the Pleistocene and Quaternary. Perhaps commencing in the Late Pliocene, but completed during the Pleistocene, the lake became subject to oblique-slip deformation, reactivating basement faults, uplifting basement blocks and generating folds on WSW-ENE axes in the overlying sediments. Variations in the vergence of the fold structures are attributed to the movement of the developing folds in the central Tatvan basin away from the areas of basement uplift on decollement surfaces. Thus, both the basement and the overlying sediments have been completely affected by oblique-slip deformation as a result of movements along the accretionary wedges underlying lake (see and examine Şengör and Kidd, 1979 for full time periods and basement reactivation events, Şengör et al., 1985, Dewey et al., 1986 and Koçyiğit et al., 2001 for Quaternary events).

3.6 Tectono-stratigraphy, Basin Inversion and Tectonic Evolution

3.6.1 Stratigraphical outline and tectono-stratigraphy

Seismic reflection data show angular unconformity between Çarpanak basement block and overlying sediments, as detailed above. This unconformity separates pre-existing basement block from the younger sediments, indicating a period of tectonic reversals.

Based on the stratigraphic correlations of Koçyiğit et al., (2001), it is considered that Plio-Quaternary tectono-stratigraphy of the lake contains two sedimentary and/or volcano-sedimentary fills of dissimilar age, origin, lithofacies, internal structure and deformation pattern. The lower and older fill is Oligo-Miocene in age and inherited from the last compressional-contractional paleotectonic regime (Koçyiğit et al., 2001). The lower and older fill is highly deformed (folded and thrust to reverse-faulted structure). However, the upper fill is Plio-Quaternary-aged, almost flat-lying and extensionally deformed and rests with angular unconformity on the erosional surface of the lower fill. The great discrepancy in deformation pattern of the upper and lower fills and the angular unconformity separating them are remarkable records of an inversion of the tectonic regime and of basin type. A prominent angular unconformity within a columnar section in E-Turkey is also illustrated by Koçyiğit et al., (2001). This unconformity (elevation > 2000 m) appears to be on the uppermost surface of pre-Quaternary rocks. Rocks underlying this unconformity are controlled by thrust to reverse faulted. This unconformity represents a contact surface between Quaternary (upper fill) and Mio-Pliocene rocks (lower fill) for E-Turkey. The same unconformity surface (within a smaller scale) is also observed from stratigraphic correlation cards in the Muş-Van region (examine cross sections from Van and Ahlat-Adilcevaz vicinities from Kurtman et al., 1978). These stratigraphic correlations are also confirmed by the study of Şengör and Kidd, (1979) in E-Turkey.

Wong and Finckh, (1978) and Wong et al., (1978) obtained four unreversed seismic refraction profiles during the cruise by means of radio sonobuoys in Lake Van basin. The seismic velocities determined from these sonobuoy measurements are considered as approximate for several technical and methodological reasons (see Wong and Finckh, 1978). Therefore, these velocities are used to identify and illustrate a rough stratigraphic succession in the lake. All these velocity profiles obtained only show velocity-dependent stratigraphy and the presence of a thick section (up to 600 m) of unconsolidated sediments, consisting undoubtedly of alluvium and lacustrine deposits, immediately beneath the lake floor. Although not resolved on every profile, two characteristic layers with interval velocities of 1.5 km/s and 1.5-1.7 km/s respectively can be identified in these velocity sections. These overlie a 1.8-1.9 km/s material, which is in turn underlain by a 2.2-2.4 km/s layer. The former material is probably semi-consolidated or consolidated sediment, while

the latter may correspond to sedimentary rocks such as sandstone, silt stone and soft limestone (Pres, 1966; Grant and West, 1965). For profiles LV–2 and LV–3 located in central Tatvan basin and SE-delta respectively, the deepest layer penetrated has a refraction velocity of 4.0 and 4.8 km/s respectively. For profiles LV–2 and LV–4 located in central Tatvan basin and SE-delta respectively, these velocities are undetected, while values of 6.4 and 6.2 km/s are measured instead. The location of profile LV–1 in central Tatvan basin suggests that the 6.4 km/s material represents the faulted, crystalline Paleozoic metamorphic rocks forming a massif to the southwest of the lake. It is important to note that velocity-dependent stratigraphic result from LV-1 is at good agreement with a W-E elongation of S-margin boundary fault (PDZ), confirming metamorphic thrust contact of Muş suture zone. The proximity to profile LV–4 (from SE-delta towards Çarpanak spur zone) of the Upper Cretaceous limestone and dolomite, which outcrops on Çarpanak Island, dips sharply to W and SW beneath the lake floor. This strongly suggests that the highest velocity encountered here (6.2 km/s) originates from the top of this formation. It is conceivable that the acoustic basement here is also made up of partially hardened limestone and other calcareous rocks. The true identity of the 4.8 km/s layer of profile LV–3 (SE-delta) remains at present speculative. However, the magnetic data suggests that it may again represent Paleozoic metamorphics. If this is the case, its much lower refraction velocity here has to be explained in terms of layer slope and rock type.

Magnetic anomalies 100-200 γ in amplitude are invariably observed along profiles traversing faults bounding the lake basin province in the study of Wong and Finckh, (1978) and Wong et al., (1978). This suggests that the margin-bounding faults produce displacements in the magnetic basement as well as in the sedimentary cover. The most significant magnetic feature is an anomaly-pair situated in the SE-delta of the lake (LV-3 and LV-4). The maximum lying just offshore is much more pronounced than the minimum to its NW, indicating that the magnetic strike of the causative body must be low. A quantitative analysis based on two anomaly shape estimators (Heitzler et al., 1962) suggests that the anomaly could be due to an infinitely long tabular body with vertical sides, 5 km wide, lying 1.2 km below the lake surface, and striking N 35ºE. This body should possess a magnetic susceptibility of 0,005 emu, and should straddle roughly the location of sonobuoy profile LV–3.

The occurrence of a 4.8 km/s layer at approximately the same depth as the proposed body on profile LV–3 suggests that the magnetic body may be composed of Paleozoic metamorphic rocks. This reveals that metamorphic basement intercalated with this magnetic body underlies the SE-delta setting. The velocity results of seismic refraction studies and distinct magnetic anomalies summarize that the velocity values ranging from 1.5 to 2.4 km/s represent sediments and sedimentary rocks and those ranging from 4.0 to 6.4 km/s represent metamorphic basement intercalated with limestone rocks and magnetic bodies. This suggests that about 1 km of unconsolidated younger sediments underlie the lake bottom (Wong and Finckh, 1978) and accreted-ophiolitic basement complex at shallow depths.

In terms of angular unconformity surface observed all over the Çarpanak spur zone and NE-Erek delta, the stratigraphic correlation cards in the Muş-Van region give a possibility to examine the structure and distribution of unconformity in deep and shallow waters of the lake (examine cross sections from Van and Ahlat-Adilcevaz vicinities from Kurtman et al., 1978).

- *Angular unconformity between Late Miocene and Quaternary (shallow lake);* according to stratigraphic data from Van vicinity, almost 200-250 m thick Quaternary sediments (Pliocene is completely eroded or non-deposited) are unconformably overlying 980 m thick, shallow water limestone of Late Miocene.

- *Angular unconformity between Late Miocene and Plio-Quaternary (deep lake);* however, according to stratigraphic data from Ahlat-Adilcevaz vicinity, almost 700-800 m (or 900-1000 m, according to Wong and Finckh, 1978) thick Plio-Quaternary sediments (Pliocene is deposited) are unconformably overlying 800 m thick reefoidal shallow water limestone of Late Miocene.

- *Angular unconformity between Pliocene and Quaternary (deep lake);* in this vicinity, there is another unconformity recognized. 200-250 m thick Quaternary sediments are unconformably overlying 500-550 m thick Pliocene sediments. But, this surface is not clearly identified, it is probably due to thicker Quaternary sediments in central Tatvan basin

Miocene rocks recognized from stratigraphic correlation cards are underlying the lake, termed as accretion-ophiolitic complex (Kurtman et al., 1978 and Şengör et al., 2008). It is clear from stratigraphic correlation cards in the Muş-Van region by

Kurtman et al., (1978) for each case that Pliocene deposits are localized in deeper basin (deep lake environment) and terminated against the further E (Çarpanak spur zone). This shows that deep lake unconfirmities recognized in Ahlat-Adilcevaz vicinity are deeply buried in central Tatvan basin and terminating toward shallow water. Then, they become angular unconformity surface in Çarpanak uplifted block and NE-Erek delta (Van vicinity, shallow water). This stratigraphic geometry of unconformities suggests that angular unconformity surface is not clearly seen in seismic data across central Tatvan basin, due to thicker Plio-Quaternary sediments and rapid differential subsidence. However, deep water sediments onlap onto the foot of Çarpanak basement block seen in Fig. 3.31. This seismic section may imply, at least partly the deep water extension of angular unconformity surface from Çarpanak spur zone and NE-Erek delta. It is considered that Pliocene sequences in deep water terminate against shallow water, representing a localized sedimentation. The wedge-shaped termination of Pliocene sequences is followed by wedge-shaped pattern of rapidly deepening Quaternary sedimentation. This shows the high magnitude asymmetric subsidence of central Tatvan basin and strong uplift of Çarpanak spur zone and NE-Erek delta. Moreover, the margin boundary faults, the basin morphology, and the lower-lying basement suggest that the Tatvan basin is undergoing a gradual, continuous subsidence, at least 100 m in magnitude (Degens et al., 1978). In shallow water, the angular unconformity surface is distinctly seen in seismic sections (Pliocene is almost eroded or non-deposited), due to thinner Quaternary sediments (200-250 m) and uplifted block nature of Çarpanak spur zone and NE-Erek delta. Stratigraphic section from shallow water most probably implies that angular unconformity surface represents Late Miocene-Quaternary period.

Stratigraphic correlation cards well summarize that the wedge-shaped Plio-Quaternary sedimentation (max. 1 km thick) is unconformably overlying accretion-ophiolitic basement complex, intercalated with shallow water-reefoidal limestone (Late Miocene) and magnetic rocks. This finding also confirms ophiolitic and accretionary nature of basement beneath the lake (Şengör et al., 2008). Additionally, stratigraphic correlation of deep and shallow water environments suggests that the fault-controlled uplift of Çarpanak spur zone and NE-Erek delta represents an important structural and stratigraphic event. This event indicates a strong tectonic inversion and a change in stratigraphical development and thus, the formation of

angular unconformity. Stratigraphic and structural correlation of the unconformities identified by Wong and Finckh, (1978), Wong et al., (1978) and Kurtman et al., (1978) with the major tectonic events in E-Anatolia during Mio-Pliocene period (Şengör and Kidd, 1979 and Koçyiğit et al., 2001) gives an possibility of the strong tectono-stratigraphic anomaly in the lake. This stratigraphic anomaly is called "Late Miocene-Early Pliocene" and "Pliocene erosion and dissection" (Şengör and Kidd, 1979). In this manner, to understand the nature and time-rock correlation of the events in the lake, associated with similar events in E-Turkey is important, as given below.

- *Plio-Quaternary block uplift event and Late Miocene-Early Pliocene dissection;* angular unconformities identified from stratigraphic correlation cards of Kurtman et al., (1978) are also examined and discussed by a detailed study of Şengör and Kidd, (1979). Şengör and Kidd, (1979) stated Plio-Quaternary block uplift and Late Miocene-Early Pliocene dissection events in E-Turkey.

The Turkish-Iranian Plateau (E-Turkey), especially its central parts (thinned crustal sections), was significantly uplifted, probably as a block, by the beginning of the Pleistocene (Earlier Quaternary uplift) (Şengör and Kidd, 1979). The mountains on the site of the suture were uplifted only after the uplift of the Turkish-Iranian Plateau. In some places, they still lie lower than the plateau. In N of the suture, the uplifted and dissected "latest Miocene-early Pliocene" erosion surface still has a southerly dip (Erinç, 1953; Şengör and Kidd, 1979). As a result of the emergence, a latest Miocene-early Pliocene erosion surface was originated and interrupted by closed drainage basins (probably resembling the present Dasht-i Kavir Depression in Şengör and Kidd, 1979). The late Miocene-early Pliocene erosion surface, onto which the abundant andesitic-dacitic lavas of Pliocene age were erupted (Altınlı 1966a; Innocenti et al., 1976; Şengör and Kidd, 1979), was considerably uplifted in the central sections of the Turkish-Iranian Plateau, towards the end of the Pliocene (latest Pliocene). This uplift is documented by the deep dissection of the Miocene-Pliocene erosion surface and the infilling of the resulting valleys by Pleistocene lava flows (Erinç, 1953). The surprising uniformity of timing of uplift and of the elevations attained by the erosion surface is indicative of a block uplift of the entire region rather than of a progressive wave of uplift (Erinç, 1953). Şengör and Kidd, (1979) also noted that the fault-bounded depressions, such as Muş-Lake Van depression,

Erzurum-Pasinler and also Dasht-i Kavir depressions, may have originated or became isolated during this phase of uplift. This result may suggest that Lake Van basin must have experienced this isolated block uplift and subsidence. Angular unconformity recognized in the uplifted provinces of the lake (shallow water environment) is most probably a result of this block uplift event during Plio-Quaternary period. This remarks that uplifted block nature of Çarpanak spur zone and NE-Erek delta is responsible for the erosion (or non-deposition) and localization of Pliocene sediments toward deep water and the thinning Quaternary sediments in shallow water. The evidence for this also comes from a stratigraphic correlation by Koçyiğit et al., (2001) for E-Turkey. In this study, although thrust to reverse faulted-contact shown in stratigraphical column entirely represents E-Turkey, this contact may refer to the pre-existing thrust surface through S-margin boundary fault. This suggests that Çarpanak spur zone is a pre-existing basement thrust block and that E-segment is reactivated feature as oblique-slip normal fault. Since, E-segment resulted in the uplift of Çarpanak basement block and produced angular unconformity surface.

The integrated tectono-stratigraphic data from Kurtman et al., (1978), with tectonic events from Şengör and Kidd, (1979) and regional stratigraphy from Koçyiğit et al., (2001) conclude that angular unconformity surface is a contact between Late Miocene and Quaternary in shallow lake environment due to the strong uplift. However, this unconformity is a contact between Miocene and Plio-Quaternary in deep lake environment due to strong subsidence. This case shows that Pliocene sequences are partly or completely eroded, re-deposited and localized in deep water environment or non-deposited within shallow water environment. Such a picture confirms that an important tectonic event occurred in Lake Van basin. The present-day deformation style of Plio-Quaternary sediments by strike-/oblique-slip tectonics and the deformation style of pre-Pliocene sequences by folding and reverse-thrust faulting reveal an inversion in tectonic regime and a transition from paleotectonic to neotectonic regime in Lake Van basin. Since, when the pre-existing, thrust-controlled basement blocks (Çarpanak spur zone) emerged, neotectonic episode commenced in the lake (also see Şengör et al., 2003 for neotectonic episode in E-Anatolia).

3.6.2 Basin inversion and tectonic evolution

Seismic profiles from central Tatvan basin image that sedimentary sequences, close to lake bottom, are almost undeformed, while the deeper sequences are folded. It is strange that this folding suddenly ends upward and becomes the smoothed lake bottom. As these seismic sections indicate asymmetric half graben deposition, the W-E trending seismic profiles indicate not only asymmetrically tilted depositional geometry, but also strike-slip-controlled sedimentation. Strike- and dip-slip variations of margin-bounding faults and scale differences in magnitudes of fault offsets, such as asymmetric geometry, can be probably responsible for this depositional and folding geometry. It is considered from different depositional geometries and unfolded-folded sequences that there may be a transitional period of sedimentation and of deformation style. Episodic sequences of the events show that a complicated depositional pattern of central Tatvan basin is controlled by varying deformation modes, clearly indicating tectonic regime transition and structural inversion.

The previous studies in E-Turkey report that the pure strike-slip basins are Plio-Quaternary depressions originating from the geometrical complexities. Fig. 3.63 illustrates the one of these depression systems that is Muş-Lake Van depression, bounded by margin boundary faults. This depression system is considered to be extension-controlled in Fig. 3.63a by Şengör and Kidd, (1979) and thrust-controlled in Fig. 3.63b by Şengör et al., (1985). However, in Fig. 3.63c, it only appears as a fault-bounded depression system by Dewey et al., (1986). In each case, these map views shown in Fig. 3.63 confirm the morpho-tectonic structure and deformation style of the lake seen in Fig. 3.62. It is also reported that Plio-Quaternary depression systems have a single, nearly flat-lying and 5.3 km maximum thick basin fill resting with angular unconformity on the erosional surface of mostly pre-Oligocene basement rocks (see Şengör et al., 1985; Dewey et al., 1986 for sediment thickness in Muş basin, and Koçyiğit et al., 2001 for pure strike-slip basins). These studies suggest that Muş and Lake Van basins might be the recently formed pure strike-slip basins during sometime in Pliocene extensional period (or Latest Pliocene). These depressions may also be considered to be extensional basins with strike-slip component during Pliocene (see and examine Fig. 3.63). As seen in Fig. 3.62, the margin-bounding faults cut across and displace fold axes, steep faults (N-margin),

intrusions and sediments. This suggests that the oblique-slip faults are much younger than Miocene, most probably in Latest Pliocene-Early Pleistocene. This time relationship in basin formation indicates that the youngest oblique-slip deformation dominates during Quaternary. Outlines of the oblique-slip faults are very clearly recognized in seismic data and the map view in Fig. 3.62. Their margin-bounding characteristics are also well illustrated in Fig. 3.63 by the previous studies. The map views seen in Fig. 3.63 support the present-day deformation style of the lake in Fig. 3.62. These margin boundary faults display well-developed and preserved morpho-tectonic evidence indicating their oblique-slip nature and recent activity. N-margin boundary fault cuts fold axes in central Tatvan basin and displaces sedimentary column. As previously repeated, it seems to be a pre-existing steep thrust fault of Miocene age. S-margin boundary cuts and displaces sedimentary column. It seems to replace with a pre-existing thrust contact (Muş suture) in en echelon-like arrangement. It appears that these boundary faults are older compressional structures, reactivated as oblique-slip faults during the Plio-Quaternary neotectonic period (see and examine Figs. 3.62 and 3.63 for the locations of these faults).

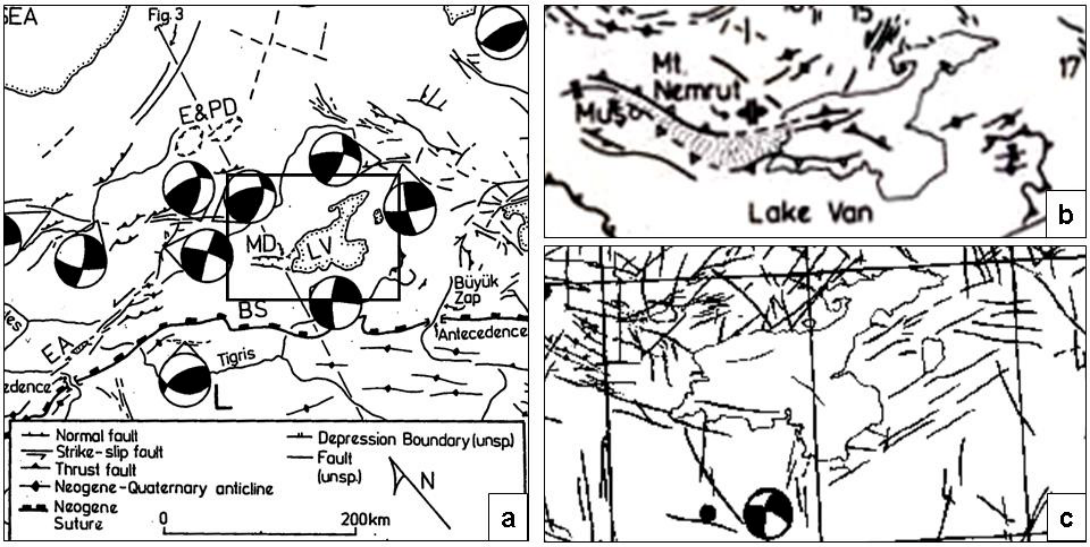

Figure 3.63 : Margin boundary faulting and overall deformation style of Muş-Lake Van (LV) basin system. a) Muş depression (MD) is extensional-faulted graben basin (Şengör and Kidd, 1979). b) Muş-Lake Van basin is compressional ramp-thrust basin system (Şengör et al., 1985). c) The faulting style of marginal sections of Lake Van and its surroundings (Dewey et al., 1986). Note that W-margin boundary fault is not observed and that W- and E-segments of S-margin boundary fault are not precisely positioned.

As recognized in Fig. 3.63b showing the faulting style and depositional continuation of Muş-Lake Van basin system, it is essential to say that Muş basin, as a W-continuation of the lake, is the largest inverted structure as proposed for Lake Van. Considered on digital morpho-tectonic studies of Dhont and Chorowicz, (2006), Muş basin is the deformed and dissected remnant of the WNW-ESE-trending Oligo-Miocene Muş-Van basin system, located at the N-foot of the Muş suture zone. Although Muş basin still seems to retain its earlier nature of compressional ramp basin (Şaroğlu and Güner, 1981 and Şaroğlu and Yılmaz, 1986), the margin-bounding reverse fault in its N-margin has a considerable dextral strike-/oblique-slip component (Koçyiğit et al., 2001, and Dhont and Chorowicz, 2006), rather than thrust to reverse faulted (as proposed by Şengör et al., 1985 and Dewey et al., 1986). Dhont and Chorowicz, (2006) reported that N-margin boundary fault of Muş basin is reactivated as dextral normal oblique-slip fault, namely "Otluk" fault. This fault also confirms an inversion in the nature of tectonic regime in Pliocene. Moreover, strong and widespread Plio-Quaternary alkaline volcanism and intrusive activity of basin-wide magmatism accompanied to the sedimentation in lake. This is the second stage of basin development, confirming strong evidence of inversion in both tectonic regime and basin type. A regional interpretation of Muş-Lake Van region in Fig. 3.63b proposes that compressional ramp basin structure of Muş-Lake Van, characterized by WNW-ESE-trending fold axes and margin-bounding thrust to reverse faults, was cut and dissected by extensional normal faults and controlled by differential uplifts during Pliocene (see related map in Fig. 3.63a by Şengör and Kidd, 1979). As seen in Fig. 3.62, the lake was displaced dextral and sinistral strike-slip faults and obliquely displaced by N- and S-margin boundary faults. As a result, the lake was overprinted by newly developing basin and their margin-bounding faults. A sequence of these events is simplified and given as the following. Extension-controlled half-graben sedimentation is localized in central Tatvan basin (pre-existing depression) and continued during Pliocene period (differential uplift, subsidence and tilting of marginal sections). Plio-Quaternary block uplifting event disturbed this period and resulted in erosion or non-deposition during the latest Pliocene (onset of Quaternary). This event also caused wedge-shape preservation and deepening of Pliocene sediments (sedimentary wedging towards E and NE) in central Tatvan basin. Then, wedge-shaped, strike-slip-controlled sedimentation (sub-parallel to underlying Pliocene deposits) began and extended to W-E trends during.

Thus, the entire Plio-Quaternary sedimentation is deformed by oblique-slip tectonics. Based on this simplification, tectonic and sedimentary events shaping the present day structure of lake seem to have dominated in Pliocene and Quaternary periods.

A stratigraphic examination of the previous studies, available seismic data and the map views clearly show that the earlier compressional-contractional regime (folds, thrust to reverse faults) and related structures (ramp to thrust-bounded basins) are replaced (see "replacement" structures in Şengör et al., 1985) and overprinted by the compressional-extensional tectonic regime (strike-slip-dominated tectonic regime) and related structures. Compressional nature of Miocene sequences (folded and high-angle thrust to reverse faulted margins) is reported by previous authors (references herein). However, the Plio-Quaternary volcano-sedimentary sequence in central Tatvan basin is almost undeformed (except for folded deeper sequences) and clearly represents basin fill of the compressional-extensional neotectonic period. This remarks that early formed Lake Van (also with Muş basin) is presently deformed and dissected into isolated smaller troughs (Muş and Lake Van, separately), rearranged obliquely, sub-parallel to the N- and S-margin-bounding faults. This shows an evolutionary stage of the present-day structural development of lake during neotectonic period, suggesting that Muş-Lake Van basin experienced a transitional period into neotectonic time. Probably, this period is responsible for the new structural development and replaced tectonic structure of lake.

A transitional tectonic period from paleotectonic to neotectonic times is reported by a large-scale field study of Koçyiğit et al., (2001). Koçyiğit et al., (2001) state that there is a relatively long-lived transitional period in Late Miocene-Early Pliocene (see Şengör and Kidd, 1979 for Plio-Quaternary block uplift). This transitional period reported is between the pre-late Serravalian compressional-contractional (paleotectonic) period and the Plio-Quaternary compressional-extensional (neotectonic) period. E-Turkey strongly experienced this transitional period in Late Miocene-Early Pliocene (see Şengör and Kidd, 1979) before the neotectonic period (this period is still continuing in Caucausus by Koçyiğit et al., 2001). The same kind of transitional tectonic periods has also been reported for various parts of Europe (Becker, 1993; Koçyiğit et al., 2001). It is assumed in the light of the previous studies and stratigraphic correlation that the transition into neotectonic period is when the basement terranes or accretionary contacts or sutures are reactivated.

As the process of crustal shortening and thickening has also been suggested to be responsible for the formation of wide terranes of "basement reactivation" (Şengör and Kidd, 1979; Şengör and Yılmaz, 1981) such as those of Grenville and Pan-African (Dewey and Burke, 1973; Şengör and Kidd, 1979). The tectonic and deformation history of the reactivated terranes and basement reactivation process in accretionary complexes (E-Anatolia) and related basin formations are often reported by Şengör and Kidd, (1979), Şengör and Yılmaz, (1981) and Şengör et al., (2008). The reactivated terranes and basement reactivation process of accretions simply suggest that accretionary complex beneath the Lake Van is reactivated, the blocks are uplifted and subdivided into a series of continental wedges and/or crustal blocks bounded by sinistral and dextral strike-/oblique-slip faults. This event is most probably from Pliocene time that is onset age of the strike-slip-dominated neotectonic regime (Koçyiğit et al., 2001).

3.6.3 Implications for basin inversion and tectonic evolution

Inversion process of Lake Van is mainly based on tectono-stratigraphic sequences and induced tectonic events around the region. These are regime transitions, fault reactivations, replacement structures and the resultant unconformities. As recognized in seismic sections across the lake and map views, the evolutionary stages of structural and sedimentary development of Lake Van have implications for basin inversion and tectonic evolution. Structural and sedimentary evolution of Lake Van is examined to identify the correlative deformation patterns, faulting styles and depositional geometries across Muş-Lake Van basin system and to understand basin inversion and overall tectonic evolution of the lake.

Structural inversion of the lake by its translation from a compressional ramp basin, through extensional, to a strike-/oblique-slip basin requires a more complicated deviation in regional stress directions. With these strike-/oblique-slip involved mechanisms operating, local basin inversion needs not involve regional adjustment of lithospheric stresses. This proposes that the alternate uplift and subsidence of the strike-slip controlled crustal blocks, known as "porpoising", irrespective of whether basin inversion occurs (see Crowell and Sylvester, 1979; Woodcock and Schubert, 1994 for this issue and Şengör et al., 1985 and Dewey et al., 1986 for upper crustal flakes/blocks). The term "porpoising" or "porpoising effect" can well describe the alternating motions of N-margin transpression, W-margin and S-margin transtensions

of the lake. This case clearly proposes that "inversion" process of extensional or compressional basins requires a major switch in regional stress directions, if both extensional and contractional processes are envisaged as primarily dip-slip (Woodcock and Schubert, 1994). In Lake Van basin, as recognized in strike-slip dominated systems, basin inversion arises under similarly oriented crustal stresses, by one of two processes, proposed by Woodcock and Schubert, (1994). The former of these is that a small rotation in regional stresses can put a previously transtensile zone into transpression (or compression into extension) and the latter is the heterogeneous flow within a strike-slip zone, indicating that at anytime some volumes are under contraction (transpression) and some under extension (transtension). As the zone evolves, one volume can be transferred from an extensional to a contractional zone, giving inversion.

Lake Van basin has experienced "local inversion" and complex alternating phases of extension and shortening at the margin boundaries, which are the margins of upper crustal rotational flakes (see Dewey et al., 1986 and Dewey, 1989 for oblique-/strike-slip zones in young collisions) during the neotectonic episode. "Local inversion", (as well recognized in strike-slip and rhombohedral pull-aparts in Dewey, 1989) can be considered as a natural consequence of alternating phases of transtension in S-margin and transpression in N-margin. Short extension-compression intervals, oblique-slip episodes and high extensional strain rates (flower structures in N- and S-margins) facilitate this basin inversion. Body force mechanisms proposed by Dewey, (1989) include salt-mud diapirism, salt-mud decollement tectonics, gravity spreading, sliding and consequent relaying of heel extension to toe thrusting. These body force mechanisms are also inversion elements. These mechanisms in the lake are represented by the intrusive activity of rising magmatic materials, gravitational sediment instability and ductile decollement tectonics. These seem to be essential contributions to the basin inversion process **(**see Dewey, 1989 for major causes of basin inversion in many cases and Dewey et al., 1986 for upper crustal detachment). In terms of magmatic intrusions imaged by seismic data in the lake, due to the non-elastic behavior for melts and a lack of yield behavior for crystal-bearing magmas (for magmas with such behavior), a driving force for intrusion besides buoyancy is the shear stress. This shear stress is induced by magma pressure differences or deformation of the country rock (see Dewey, 1989 for proposed ductile decollement).

Dewey, (1989) argued inversion of strong negative isostatic gravity anomalies in confined deep basins caused by upper crustal stretching. This argument implicates for basin inversion and tectonic evolution of the lake. Since, critical to whether a basin becomes inverted are, also, the timing of a compression phase relative to the initial basin-forming extensional event and the extensional strain rate. If the Muş-Lake Van basin in Fig. 3.63b is considered as a combined sedimentary system, controlled by upper crustal blocks (Şengör et al., 1985 and Dewey et al., 1986), upper crustal extensional basins lead to long distance compression relaying along mid-crustal detachments while preserving their negative gravity anomalies. Although this mechanism proposed by Dewey, (1989) is not clear for inversion period of the lake, due to the lack of high resolution gravity-bougger data, it can be considered that lithospheric delamination with substantial crustal thinning and Moho pull-up leads to mantle involvement in thrust complexes and positive gravity anomalies in inverted basins. Then, mantle involved in thrust complexes are released by extensional and transtensional reactivation of pre-existing thrust contacts. As a result of this, a prominent localization of dense intrusive-extrusive activity and a concentration of magma propagation are recognized through W- and S-margins of the lake and beneath the central Tatvan basin. This results in the shallow-seated ductile shear zone. Moreover, the retrocharriage development of margin boundary faults is thought to have acted as the most important parameter for inversion processes during the post-collisional neotectonic period. This implies that the pre-existing high-angle thrust faults are negatively reactivated, accompanied by extensional and strike-slip-controlled sedimentation. Magmatic propagation activity efficiently contributes to these inversion events.

Shortly, Lake Van basin is a large compressional ramp-depression system, filled by continental and shallow marine deposits of Oligo-Miocene age (Şaroğlu and Güner, 1981; Şaroğlu and Yılmaz, 1986; Yılmaz et al., 1987). This basin began to develop during the last stage of the subduction of the Bitlis Ocean and persisted until the end of Late Miocene or rarely Early Pliocene transitional period of intra-plate convergence (Koçyiğit et al., 2001). Pliocene and Quaternary tectonic evolution of Lake Van has experienced multi-stage deformation modes and basin inversion periods. These periods can be ranged by incipient negative inversion, and fault reactivation processes across the flake margins (see Dewey et al., 1986) and thus, an

extension of accretionary wedge blocks (upper crustal flakes in Dewey et al., 1986). Then, this is followed by the start of emplacement of magma. Magma emplacement leads to weakening and deformation under pure shear, the incorporation of melts and continuing deformation under simple shear. These stages of basin inversion and evolution show that deformation regime in Lake Van changed from thrust-bounded intermontane basin through extensional half graben and into strike-/oblique-slip basin. This shows obliquely escaping wedge-block structure toward ENE. The neotectonic regime of Lake Van is the strike-/oblique-slip-dominated compressional (N-margin)-extensional (W- and S-margins) regime, commenced in Pliocene period. Tectonic and depositional indications of this neotectonic event recognized in Lake Van are briefly given as the follows. 1- the clear regional inversions in the type of basin from WNW-ESE-trending compressional ramp basin to asymmetric half graben structure. 2- the style of deformation from folding-steep thrusting to extensional and oblique-slip faulting, such as en echelon arrangement of S-margin boundary fault. 3- the shape, structural geometry and marginal activity of rising magmatic materials, controlled by extensional and transtensional faults. 4- N-S trending, extension-controlled half-graben fill, and W-E trending, strike-slip-controlled depositional fill during Plio-Quaternary period. 5- the nature of volcanism from subduction-accretion related strong and regional calc-alkaline (subduction signature) to post-collisional, slab delamination related highly basaltic, alkaline volcanism (intra-plate signature) (Keskin, 2005, 2007; Şengör et al., 2008). 6- the epirogenetic elevation changes (regional plateau uplift, basin subsidence and orographically localized sedimentation)(also see Innocenti et al., 1982; Koçyiğit, 1985; Yılmaz et al., 1987; Rebai et al., 1993; Ambraseys and Finkel, 1995; Koçyiğit et al., 2001).

3.7 Neotectonic Deformation of Lake Van Basin

3.7.1 Tectonic structure of Tatvan half-graben basin

Tilted structural pattern of central Tatvan basin is the most prominent feature observed in the lake. However, only a few seismic reflection profiles show this distinct asymmetric geometry (Figs. 3.3, 3.5, 3.8-3.11 and 3.31). This can be also recognized in the map view shown in Fig. 3.62. Previous seismological studies are examined and their results are correlated with available seismic data and main

tectonic trends to understand overall tectonic structure of asymmetric half graben basin, structural origin and framework in the light of strike-/oblique-slip deformation in Lake Van. Moreover, some methodological informations needed to understand this type of basin structure are essentially given below.

Previous geophysical studies (seismic tomography by ETSE project, 2003, regional wave propagation by Gök et al., 2000 and attenuation models of seismic phases by Furumura and Kennett, 1997 on the nature and on the influence of structural barriers) are taken into account in understanding the tectonic structure of accretionary wedges or the crust and large/deep sedimentary basins on them. These studies can help in reconstructing tectonic models for deep sedimentary environments, such as the influence of sediments, crustal thickness and attenuation. Based on the nature of regional seismic phases and the influence of structural barriers, the amplitude of the Lg phase is very sensitive to variations in the crustal structure along the wave propagation path. Lg phase can provide an improved understanding of the nature of Lg-wave propagation in complex inelastic media and insight into the nature of the propagation process (Furumura and Kennett, 1997). The Lg phase propagating in the crustal waveguide is normally very prominent at regional distances, but is at the same time very sensitive to substantial lateral variations in crustal structure, especially at continental-oceanic margins (Furumura and Kennett, 1997). This remarks that the blockage of the Lg wave by crustal barriers such as continental margins and graben structures has long been recognized as providing a very useful tool for mapping large-scale lateral crustal variations along the propagation path

Several attempts to understand the seismic disturbances of the Lg wave in a graben zone have been made. Such studies display a clear outline of crustal heterogeneity by mapping the paths with poor Lg propagation across the region. Kennett et al., (1985) showed a clear outline of the graben structure in the centre of the North Sea basin in a detailed map of the apparent crustal heterogeneity derived from many different Lg propagation paths across the North Sea. Methodology of seismic Lg waves indicates that thick sedimentary basins covering an elongated graben structure, such as Muş-Lake Van basin, can have a major influence, since these large basins remove Lg energy by generating P conversion and scattering. This is the principal mechanism for strong Lg attenuation across a graben.

The reduction of the Lg energy is reinforced by inelastic attenuation in the sediments as well as the influence of the gradually thinning crustal waveguide associated with an elevated Moho.

Gök et al., (2000) successfully applied Lg-method to E-Turkey for understanding its crustal and sedimentary structure. In this manner, the integrated seismic reflection and seismological data from results of the Lg-wave propagation is combined with the observations from morphological and geographic data from Muş-Lake Van region. An examination and evaluation of seismic reflection profiles considering wave propagation coverage in E-Turkey and Muş-Lake Van basin leads to a better understanding tectonic structure of Tatvan half-graben basin and neotectonic deformation of Lake Van. A unique framework of thinner crustal and thicker sedimentary structure of Lake Van basin and widespread alkaline magmatism is detailed from attenuation properties of regional shear waves (Sn and Lg) for the crustal modeling of the basin. Consideration of wave propagation along with the structural complexities can well explain and support the seismic observations and the present-day tectonic and sedimentary structure of the lake. The findings lead to some critical conclusions in modeling crustal and sedimentary structure of the lake and give some certain clues about widespread sedimentation, accretionary basement and the main tectonic trends. Based on a single graben model with crustal thinning and a thick sedimentation in Lake Van basin, it is assumed that there will be severe attenuation for the Lg wave and the transmission of mantle Pn and Sn waves propagating in the uppermost mantle. As a result, a major contribution to the blockage of Lg waves will come from strong scattering, induced by the presence of thicker sedimentation in the lake. This event means that inelastic attenuation in the sediments helps suppress S-wave energy trapped in the sedimentary basin. Thus, the severe Lg attenuation can exist while crossing the graben zone. A number of studies have utilized this sensitivity of the Lg phase to map structural variations using anomalous propagation paths (see the numerical modeling used for the sedimentary basins by Furumura and Kennett, 1997).

3.7.1.1 Seismic configuration of structural and depositional framework

Morpho-tectonic and deformation map is seen in Fig. 3.62, showing fault-bounded and wedge-shaped central Tatvan basin. This basin includes a considerable amount of Plio-Quaternary sediments, more than 600 m thick. Plio-Quaternary sediment

thickness in Muş basin is almost 4-5 km, reported by Şengör et al., (1985) and Dewey et al., (1986). As previously stated, Lake Van basin is underlain by accretionary wedge complex and its basement consists of a thin crust squeezing (basement squash process in Şengör et al., 2008).

The nature of the crust beneath the Lake Van, its sedimentary structure and crust-basin interactions are, to a certain degree, accurately determined by a study of regional wave propagation from Gök et al., (2000). Kennett and Mykkeltveit, (1984), Kennett, (1986) and Bostock and Kennett, (1990) suggest that energy coupling between Lg modes and Sn modes associated with the elevation of the crust-mantle boundary beneath the graben zone is a major contributor to the attenuation of the Lg wave. Maupin, (1989), however, using a coupled local-mode method, claimed that the strong Lg attenuation across the graben zone can not be fully explained by the thinning of the crust. Furumura and Kennett, (1997) investigated the relative importance of different aspects of crustal structure across a graben-like feature for the blockage of the Lg wave, because a simple graben model can produce significant Lg attenuation. These studies also examined the relative importance of crustal variations, due to crustal thinning with elevation of the Moho and the presence of thick sediments, on the blockage of the Lg propagation. Methodology of these studies shows that Lg wave propagation is both affected by crustal structure variations, such as crustal roots, and sensitive to the surface topography, and thickness of sedimentary layers. These layers can disrupt Lg wave propagation (Furumura and Kennett, 1997). In terms of the results of these studies, geophysical and tectonic structure of crustal basement and depositional setting of Lake Van is examined, based on ray coverage for a detailed attenuation study of wave propagation (regional shear waves, Sn and Lg and also Pn) in E-Turkey. Gök et al., (2000) have included events with hypocentral depths smaller than 34 km in their analyses of Lg propagation and concluded that Lg is extremely attenuated. This indicates the presence of either strong scattering or crustal intrinsic attenuation. Lg wave attenuation or “intrinsic attenuation” in and around Lake Van is directly related to asthenospheric upwelling and magma intrusion through the crust as observed by Gök et al., (2000). Lateral and/or vertical heterogeneities in the crustal structure or the irregularities in crustal roots and morpho-topographical variations across the lake are also observed. These variations have strongly affected Lg wave propagation.

This study of Lg attenuation confirms that the crust under the lake is apparently thin and irregular enough to block Lg propagation. Since, Lg phase is obviously blocked for paths crossing the thinner crust of the lake. These paths are also characterized by thicker sedimentary basins across E-Turkey (see and examine maps in Gök et al., 2000). The most prominent result indicates that Lg phase propagates efficiently through the Arabian plate toward BP-M, except when it crosses the Bitlis-Zagros fold and thrust belt (BP-M). This implies a major change in crustal structure across BP-M due to "intrinsic attenuation or "scattering attenuation", caused by large lateral structural variations in the crust (Gök et al., 2000).

These attenuation events have very critical structural implications for interpreting tectonic and magmatic events in the lake, particular in S-margin boundary fault and Muş suture. It is mentioned beforehand that S-margin of the lake is densely covered by a complicated pattern of active and passive dome-cone complex, particularly through W-segment (Fig. 3.62). W-segment is parallel to Muş suture, which is the N-boundary of BP-M as an intraplate contact between the EAAC and BP-M. This contact from W to E is considerably weakened and irresistant. Muş Suture zone, as evident in S-margin, is completely covered by active magma propagation and migration. Crustal thickness in and around BP-M is almost 40-44 km, but 38 km in and around the lake (see also Zor et al., 2003 and Şengör et al., 2008). As known, BP-M is a metamorphic fragment with relatively thick root, but it is also a transitional zone into the lake with thin crust. A correlative analysis of the previous studies to Fig. 3.62 suggests that active magma migration and propagation from the further W (Solhan volcanics) through Nemrut volcanic dome complex and into S-margin boundary fault follows on the trend of Muş suture zone. Coastal sections of this suture trend (W- and E-segments and Deveboynu segments) are peculiarly dominated by peripheral collapsed parasitic dome-cone complex. These are preferably emplaced on S-marginal sections of the lake (Fig. 3.62). Passive, deactivated and active ones of these magmatic occurrences are lying on S-margin boundary fault, indicating extensional and transtensional activity of the faulting in S. All these observations across S-marginal section through S-margin boundary fault suggest that Lg-wave is blocked by crustal barriers (Muş suture and BP-M) and magma-related intrusive and extrusive events along Muş suture. The Lg-wave blocking confirms extensional and transtensional nature of S-margin boundary fault,

active magma propagation through it and an irregular character of the crust from BP-M to the lake.

Sedimentation and deformation patterns and faulting styles of Lake Van (Fig. 3.62) with an correlative interpretation of the maps from Gök et al., (2000) show that the interpreted zones of "efficient", "inefficient" and "not observed" Sn and Lg and correlation with major tectonic units in E-Turkey are very compatible with tectonic, magmatic and sedimentary structure in and around the lake. The influence of the lateral variations in irregular crustal structure in and around the lake significantly weakened the Lg phase. This implies very heterogeneous crust underlying the lake. However, the influence of crustal thinning alone cannot explain the severe Lg attenuation seen across graben structures and sedimentary basins in the region. The reduction in Lg amplitude for the sedimentary basin model is at most about 1/3. This is insufficient to explain the strong loss for the full graben model (to about 1/4 of the original amplitude in Furumura and Kennett, 1997). Since, the attenuation of the Lg phase is more pronounced for larger sedimentary basin structures. In these sedimentary basins, the basin contains thicker sediments (14.4 km of sediments) and the same thickness is sustained for a longer distance (160 km long basin). This proposes the significant weakening of the Lg phase after transmission through the models, containing these larger sedimentary basins (Furumura and Kennett, 1997). This result implies that Lake Van is a larger sedimentary basin as a structural continuation of Muş basin in W. In other words, Muş-Lake Van basin is overlying the heterogeneous accretionary crust and a larger and thicker (4 km thick) sedimentary system, rapidly subsiding. Such a picture of crustal and sedimentary structure well explains why significant energy loss for Lg is observed across the lake and Muş basin. For the lake, the Lg attenuation is produced by a larger sedimentary section, which includes thick sediments (more than 1 km) with a lower velocity (1.5 - 2.4 km s^{-1}) and higher attenuation than the crystalline crust. The strong influence of a very thick sedimentary layer is in good agreement with the observations of Baumgardt, (1990) of Lg blockage. (see and examine S-Barents Sea basin, sediment layer over 10 km thick with crustal thinning of nearly 10 km in Baumgardt, 1990 and Furumura and Kennett, 1997).

The considerations mentioned above indicate a complexity in understanding and interpreting Lg-waves in Muş-Lake Van region. This suggests that there is no single mechanism, which can provide a simple interpretation of the Lg-wave extinction at structures. Hence, the regional interpretation of Gök et al., (2000) is, in fact an oversimplification for the region. Structural and magmatic development of the lake is so complicated that the Lg blockage is not caused just by a thinning crust (Zhang and Lay, 1995). This blockage is also caused by strong topographical variations of the Moho and steep geography (Bouchon and Coutant, 1994), the presence of the overlying water, 451 m, (Cao and Muirhead, 1993) and strong intrinsic attenuation by scattering (Campillo et al., 1993; Gök et al., 2000). Faulting and deformation style, sedimentation and magmatic occurrence in and around the lake suggest that Lg attenuation is mainly due to the combination and interaction of a number of crustal, sedimentary and magmatic factors. The one of these factors is the influence of the geometry of the crustal thinning (Moho offset or not), crustal segmentation and detachment planes (ductile shear zone or not). The influence of attenuation in thicker sedimentation (thick and soft sediments or not) is also effective. These factors give a certain clue about heterogeneous and unstable accretionary basement of the lake, having thicker depositional section. Moreover, the partial melting and melting products, such as the intrusive-extrusive events of magmatism, and related tectono-magmatic complexities control the influence of strong lateral velocity gradients in the crust. This also gives a certain clue about magma contribution to unstable accretionary events beneath the lake. A regional combination of seismic reflection profiles with seismological attenuation studies and geomorphic evidences provide new additional constraints for tectonic structure of central Tatvan basin and thus, neotectonic deformation of Lake Van basin. These constraints give an evidence of thin-skinned tectonism and magmatism, the thicker and deeper sedimentary structure of the lake. Lg attenuation study confirms the strong heterogeneities of the crustal structure below the lake and irregularly distributed differential strains. This shows that the thinned, weakened and segmented crustal blocky structure is composed of squashed basement blocks (or accretionary wedge-blocks), accompanied by widespread active magmatism. As well recognized in Fig. 3.62, these fault-bounding blocks obliquely move above ductile shear zone and bear the half-graben basin geometry and thicker sedimentary pattern of the lake.

3.7.2 Strike- / oblique-slip deformation of Lake Van Basin

Fig. 3.62 clearly shows the strike-/oblique-slip deformation of Lake Van basin, the resultant morpho-tectonic expressions and related structural and deformational complexities. This map view mainly shows three important components of prevailing processes all over the lake. Initial extensional processes result in overall structure of asymmetyric half-graben basin formation, shaping central Tatvan basin. These processes are later followed by strike-/oblique-slip processes, causing complicated patterns of secondary structures and en echelon-like subbasins. This is accompanied by rotational processes at various scales. As emphasized above, these prevailing processes are significantly influenced and driven by heterogeneous structure of accretionary complex, forming basement mechanical anisotropy beneath the lake. In the light of Fig. 3.62, these processes are examined and evaluated below for understanding overall tectonic deformation of the lake, the formation of central half-graben basin, mechanism of oblique faulting and internal subbasins.

3.7.2.1 Extensional processes and half-graben basin formation

Deformation pattern and faulting styles in Fig. 3.62 show that Lake Van experiences considerable amount of extensional and transtensional strains. Seismic reflection profiles shown in Figs. 3.3, 3.5, 3.8-3.11 and 3.31 well evident a tilted geometry of central Tatvan basin in an asymmetric form of half graben structure. Figs. 3.58 and 3.59 illustrate depositional sequences, sedimentation patterns, and high-resolution chirp image of central Tatvan basin. Structural and depositional framework of central Tatvan basin clearly indicate that, as well known, essential features in extensional tectonics are graben-like structures. These structures develop perpendicular to the axis of maximal tension and parallel to the axis of maximal horizontal compression.

In terms of tectonic origin of central Tatvan basin by extensional or transtensional boundary faults seen in Fig. 3.62, early experiments show that grabens can either form in regions of crustal extension, or on the crests of broad anticlines related to contractional tectonism (crestal collapse graben). The simplest tectonic models relate extensional tectonics in pure shear to doming (asthenospheric) and subsequent rifting (continental break up). This set up corresponds to the classical Andersonian classification of planar non-rotational normal shear faults, the axis of maximum compression between which is vertical. This suggests that regional up-arching of the

rising asthenosphere and related flows produce tensional stresses in the thinned crust. However, the transition from compressional to tensional stress regimes in the crust is gradational and depends on a combination of factors, which are external to the stress system. These factors force the relative position and magnitude of the three principal stress directions to rotate gradually. This indicates that the originally vertical shear faults (pre-existing thrust faults) tend to rotate about a horizontal axis (tilt) during the horizontal extension. This case reveals accretionary wedge "thrust sheet" rotation and translation, showing the rigid body-block rotation of Lake Van (see Dewey et al., 1986 for strike-slip basins in E-Anatolia).

It is considered that the mantle upwelling and subsequent doming (Şengör et al., 2008) precedes graben formation for active extension along margin boundary faults of the lake (see and examine seismic sections through Figs. 3.2-3.11, 3.13-3.15 and the map view in Fig. 3.62). This event occurs trough (brittle) wedge subsidence of the upper crust above a weak, hot (visco-elastic) lower crust. However, horizontal tensile stresses of >200 MPa are required for a graben of several kilometers deep to develop (Dewey, 1988; Sylvester, 1988) and maximum sediment thickness in central Tatvan basin is not more than 1 km. Previous studies reported that Muş-Lake Van basin includes, at least, 5 km Plio-Quaternary sediment (Şengör et al., 1985; Şaroğlu and Yılmaz, 1986; Dewey et al., 1986). Therefore, it is important to note that bending stresses related to the up-arching alone are insufficient to provide this tension. Assuming a ductile lower crust, the existence of a (topographic) surface load together with a low density mantle wedge, however may provide the necessary tensile stress due to vertical buoyancy differences. These considerations complement the half-graben formation model of central Tatvan basin by some mechanisms. These mechanisms explain the modes of extension and evolution of sedimentary basin by generation of listric rotational and/or planar non-rotational faults, particularly in W- and S-margin (W-segment) boundaries of the lake (see seismic section shown in Fig. 3.11 and the map view in Fig. 3.62).

3D-block diagram of the map view in Fig. 3.62 is given in Fig. 3.64. Fig. 3.64 illustrates diagrammatic map showing progressive development of fault splays and wedges on a left-slip fault. The fault (or a weak structural lineament) gradually develops a bend through time and eventually forms a tilted geometry of a fault wedge basin. In this diagram, the fault splays represent marginal sections of the pre-

existing weaknesses (accretionary thrust contacts) and the developing wedge represents the differential subsidence of central Tatvan basin and basement block uplift of Çarpanak spur zone. Deformation, faulting and depositional geometry suggest the progressive transtensional development of the fault wedge basin on oblique-slip faults and thus, the development of asymmetric half-graben structure. In this case, the shear stresses, which necessarily follow any vertical displacement of a 3D-body, will dissipate by creating listric fault-bounded block with the geometry of major slumps, slides and turbidities (see Figs. 3.16-3.20, 3.25, 3.31, 3.33 and 3.34). As recognized in Fig. 3.64, the point of departure of this simple-shear scheme is crustal stretching along a low-angle detachment, confined between vertical weak zones (Dewey et al., 1986). This suggests that margin boundary faults are related to upper crustal deformation and extension.

Crustal-stretching faults accommodate the upper crustal part (seismogenic layer) of a whole crustal strain. Strain compatibility or space problems (Şengör et al., 1985) are probably solved by assuming plastic flow in the hot and weak lower crust accommodating the brittle extension within the upper crustal seismogenic layer. This argues that the margin boundary faults affect the upper crustal blocks and the faulting in W- and S-margins (W-segment) may seem to have a listric geometry and dip 30°-60°. Considered on half-graben structure of central Tatvan basin in Figs. 3.62 and 3.64, it should be pronounced that the asymmetric structures in ancient and modern extensional domains are generally attributed to simple shear deformation with fault rotation and detachment development. Therefore, this kind of asymmetric structures can be interpreted as remnants inherited from previous upper crustal deformation events, generally controlled by gravity-driven listric faults. This argues that the gravitational processes are of primary importance in W- and S-margin transtensional domains, as recognized in gravity-driven folding of the sedimentary cover of central Tatvan basin and in transpression of N-margin (see Figs. 3.10 and 3.11 in W-margin). Moreover, the existence of intracrustal detachment faults (Şengör et al., 1985; Dewey et al., 1986) is also explained by the mature evolution of a basic decollement (see the shear-wave splitting and anisotropy studies of ETSE project, 2003 and Sandvol et al., 2003 for decoupling zone between crust and mantle).

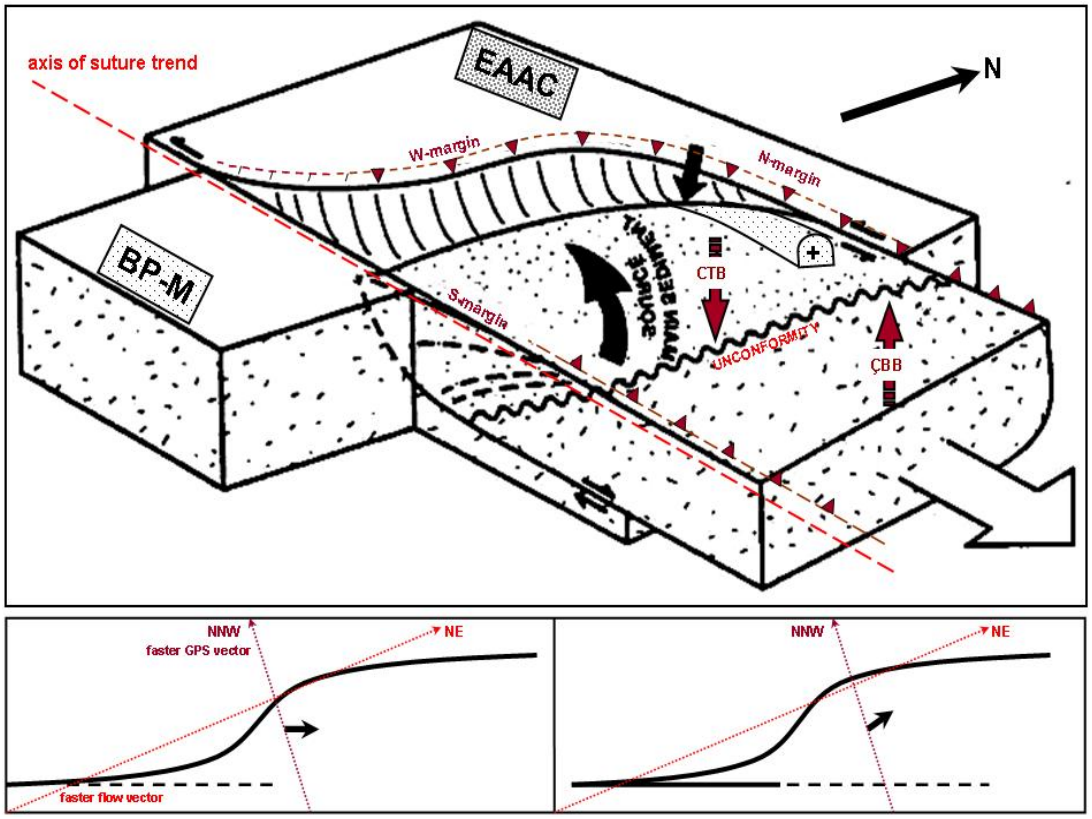

Figure 3.64 : 3D-block model diagram (looking toward NW) illustrating upper crustal tectonic and structural origin of Lake Van basin at a sigmoidal bend in W-margin boundary fault (see text for discussion). Tilted sedimentary section in subsiding central Tatvan basin (CTB-brown arrow), deltaic source of bulk of sediments (thick black arrow) overlying Çarpanak basement block uplift (ÇBB-brown arrow), unconformity surface and push-up rhomb horst structure (+) are also indicated on this model. Note that S-margin boundary fault, parallel to axis of suture trend (dashed red line), separates the basin into two structural blocks; Eastern Anatolia Accretionary Complex (EAAC) and Bitlis Pötürge-Massive (BP-M). Index maps at the bottom left and right show the relations of faster GPS vector (NNW) and faster asthenospheric flow vector (NE) to strike-/oblique-slip wedging pattern of Lake Van toward ENE. The progressive development of fault splays (W- and E-segments of S-margin boundary fault) results in basin-wedge on a dextral transtensional fault. The fault gradually develops a bend (W-margin boundary) through time and eventually forms a strike-/oblique-slip fault wedge basin by a low-angle detachment fault, (see and examine Fig. 3.62).

The critical question about graben symmetry related to crustal layering and variations in crustal strength profiles is investigated by previous studies (see references in Sylvester, 1988). These studies show that a three-layered system (upper crust-lower crust-mantle) with “a low coupling” between the ductile lower crust and the strong (and ductile) mantle produce narrow, symmetrical full graben, while “a strong coupling” induces wide deformation zones with half graben forming simple shear.

According to this result, asymmetric half graben structure of central Tatvan basin, however, proposes a strong coupling. As well known, there exists a very low coupling or uncoupling between the lower crust and upper mantle due to slab delamination event (Sandvol et al., 2003; Şengör et al., 2008) in the region. As referred to more recent conceptual models, structural interpretation of this asymmetric geometry relates the half graben asymmetry of the central Tatvan basin (as seen in most continental rift basins) to the locking of one of the initial normal faults in S- and N-margins. The faults in N- and S-margins form the subsiding wedge structure of central Tatvan basin. The other fault in N-margin becomes the leading border fault system of the developing half graben. This also proposes the initial extensional graben formation of the central basin and its differential asymmetric subsidence.

3.7.2.2 Oblique-slip processes and en echelon subbasin formation

The continuation of the border faults at depth, their relation with secondary fractures or splays and branches and the occurrence and architecture of accommodation zones (internal subbasin formations) or transfer zones are preferentially investigated by structural description and tectonic interpretation of seismic reflection profiles as summarized in Fig. 3.62. The occurrence of half-graben border fault segments is used as a distinctive criterion in the recognition of oblique tectonic setting of along axes segmented graben.

Strike/oblique-slip tectonics is the end-member of deformation system of Lake Van in which central Tatvan basin are transported between two confining surfaces of margin boundaries (Figs. 3.62 and 3.64). The sedimentary sequences are folded along vertical axes between vertical confining surfaces or zones of strike-slip faulting. As previously emphasized, the confining surfaces in this case are the floor and pre-existing thrusts. As evident by seismic sections through margin-bounding faults, oblique-slip deformation in marginal sections shows that the vertical and horizontal components of the faults combine. In the latter case, the deformation deviates from the simple shear and pure shear cases. Strike-slip and extension respect and contraction act simultaneously, causing transpression respect transtension. This shows that N-transpressional, W- and S-transtensional margins are strike-slip deformations that deviate from simple shear because of a component of, respectively, shortening or extension orthogonal to the deformation zone" (Dewey et al., 1998).

As seen in the map view in Fig. 3.62 and in 3D-block model section in Fig. 3.64, transpression or transtension occurs in undulating marginal strike-slip zones of the lake, which are the pre-existing thrust surfaces (also see Fig. 3.63). In N-, W- and S-margin boundaries, respectively shortening and extension (pure shear) and wrench deformation (simple shear) occur simultaneously at respectively N-restraining, W- and S-releasing bends.

Kinematic analysis and tectonic interpretation of seismic sections across basin-bounding faults from margin boundaries show transpression and transtension-induced secondary structures. Transpression occurs in N-margin boundary where the direction of the strike slip fault approaches that of the least compressive stress in the acting system and restraining bends (pushed up rhomb horst) are formed. N-transpression, W- and S-transtensions cause the long axis of the horizontal strain ellipse to develop at respectively lower and higher angles to the zone boundaries than in simple shear strike slip (Dewey et al., 1998). This causes in the case of transtension in S-margin boundary, Riedel shears and tensile fractures to develop at very low angles to the bounding zones (Dewey et al., 1998). Oblique arrangement of en echelon segments with respect to the shear zone in S-margin boundary, rotational subbasins (Tatvan delta subbasin, Deveboynu and Varis spur zone subbasins) and rhomb-shaped horst block uplifts in N-margin are bounded by strike-slip fault terminations. These are fundamental structural features of strike-/oblique-slip tectonics in the lake (Fig. 3.62). A combination of these structural observations determines the existence of a prevailing oblique-slip setting. Moreover, a distinct kind of extensional tectonics is typical in settings dominated by compressive oblique-slip, as in N-transpressional boundary (Dewey et al., 1998). This suggests that fault directions depart from the optimal shear directions in a stress system with vertical intermediate stress and approach the direction of highest compression. Thus, these faults might experience tensile stress (Sylvester, 1988; Dewey et al., 1998). This is the case well recognized along W- and S-margin boundary faults, through which en echelon-like transtensional fault segments and related subbasins developed. Through S-margin boundary fault, wide and deep subbasins with thick sedimentation (350-400 m) develop in the upper crust, since the underlying shear zone along S-margin is wide, and vice versa. The symmetry of these subbasins depends largely on the amount of overlap between the en echelon W- and E-segments in S-margin.

This suggest that overlap (small or large) between the en echelon border faults produces asymmetrical or symmetrical full or half grabens around the centre of the overlap, changing to asymmetric or symmetric half graben morphologies away from the centre (Woodcock and Schubert, 1994). Deveboynu and Varis spur zone subbasins develop almost around the centre of the overlap between W-and E-segments of S-margin boundary fault (Fig. 3.62).

Based on the subbasin formations along PDZ of S-margin boundary fault that is an axis of suture trend, some criteria concerning the geometry and morphology of graben axes and faults surge from the various proposed genetic models by previous rift and graben studies. Apart from the indentation of some marginal faults and the linearity of others, the sigmoid prolongation of the far ends of several rifts in down-faulted structures, which are oblique to the trend of the main longitudinal rift axis, seems a general characteristic of graben. For example, many of the E-African grabens, in fact, are successions of single depocentres disposed en echelon (Reeves, 2009). In S-margin of the lake, en echelon faults (W- and E-segments) are separated by the oblique cross-faults and accommodation zones, which are Deveboynu and Varis spur subbasins. It is assumed that these subbasins are typical examples of en echelons, juxtaposed to composite graben (see and examine the similar examples found on images of the Tanganyika and the Baikal rifts in Reeves, 2009). As an example, analogous modelling of rifting at a slow oceanic spreading ridge indicates that oblique extension (not perpendicular to the rift axis) in transtensional settings cause “en echelon half graben” separated by transfer zones (Casey and Dewey, 1984). This gives yet another possible way for the typical half-graben structures to develop. Thus, to a certain degree, it might be considered that internal subbasin formations through the S-margin boundary fault are “en echelon half grabens”. Another example from pull-apart basins indicates that the ratio length/width is mostly close to 3 or larger in mature pull-apart basins (this ratio for the lake is approximately 1/2). As in the lake (Fig. 3.62), their long axis is sub-parallel to the direction of the overstepping oblique-slip faults between which the subbasins develop. A marked off-centre position of the depocentres is a critical property in favour of rhombic strike-slip basins (Sylvester, 1988), implying rhomb-shaped strike-slip development of Lake Van basin (Fig. 3.64).

In the light of the analogous modeling studies given above, the complicated stress pattern related to these simple-shear settings and oblique-slip deformation in the lake results in variable deformation and complicated vertical and rotational movements by Woodcock and Schubert, (1994) (see Dewey et al., 1986 for the concept of rigid body-block rotation, internal viscous and external rotations). Tectonic interpretation of deformation styles in Lake Van shows that the vertical component of oblique-slip or the total component of the deformation is affected solely by strike-slip. Strike-/oblique-slip processes produce en echelon-like fault segments in S-margin, causing en echelon subbasins along PDZ of S-margin boundary fault. In principle, the image of the strike-slip corridors (or lineaments) between which faulting and folding are confined, is the rotated image of thrust duplexes (for example, rotational portions of Makran accretionary prism in Şengör and Yılmaz, 1981). This leads to two important views, one of which suggests that the half-graben structure of central Tatvan basin and folding of its sedimentary cover are confined between the strike-slip corridors in N and S. The other suggests that the structural image of the N- and S-margin boundaries is the rotated image of accretionary wedges beneath the lake (see Dewey et al., 1986 for a discussion of the flake margins and flake-block rotation of Muş-Lake Van).

3.7.2.3 Rotational processes and basement mechanical anisotropy

Tectonic interpretation of Figs. 3.62 and 3.64 shows that the half graben basin formation and differential subsidence are initially controlled by extensional processes. These processes are recently followed by strike/oblique-slip faulting, which is one of the most important deformation mechanisms in intraplate settings. Terminology of strike/oblique-slip deformation and classification is basically standardized and previously given in the review-article by Sylvester, (1988). Hence, the details are not given here, but only some specific mechanics of strike/oblique-slip deformation.

Margin boundary sections of the lake presently control central half graben structure and related deformations along the central Tatvan basin, which are typically related to strike/oblique-slip processes. It is considered that movements along these border faults are limited and remain relatively small, because of space problems at large displacements. Fault deformation analysis seen in Fig. 3.64 shows that central Tatvan basin, together with Çarpanak spur zone obliquely moves as accretionary wedge-

basin block and at least by one upper crustal block (Dewey et al., 1986). This block motion indicates that N-S convergence is accommodated by distributed simple shear deformation operating through block rotations (see Dhont and Chorowicz, 2006). The possibility of block rotations in strike/oblique-slip tectonics with continuous (distributed) deformation is of particular interest for the study area in terms of the pre-existing weaknesses.

The mechanical behaviour of pre-existing structural discontinuities (accreted high-angle thrust sheets) in the lake setting (together with Muş basin) is supposed to govern the orientation of the active shear zone. This shear zone adjusts itself to the movements on reactivated pre-existing fault orientations in order to take up the motion between the bounding (crustal) blocks (see McKenzie and Jackson, 1983). Then, extensional and contractional processes operate contemporaneously and continuing rotation inside the shear couple produces a complex basin morpho-tectonics and deformational history (Fig. 3.62). As a result, extreme development of basin partitioning thrusts one basin against the other. This indicates that tectonic deformation of Lake Van region is taken within a couple of strike/oblique-slip faults, producing transpression and transtension. Thus, simple (purely rotational) shear coupling basement (crustal) blocks deforms overlying sedimentary cover (half graben) in a very characteristic way and produces secondary structures. Secondary folds (gravity-driven folds) and faults (splays and branches of flower structures) have an oblique relationship with respect to the moving vertical master faults (PDZs) and related shear zones. These secondary structures also tend to rotate in the direction of the shear couple with ongoing deformation. As seen in Fig. 3.62, W- and E-segments have an oblique relationship with the PDZ of S-margin boundary fault that moves across a trend of structural weakness (Fig. 3.64) from W to E through the subbasins. As slip on the rotating faults is bounded by the regional stress orientation (N-S compression), rotation of the faults inside the shear couple is limited, as recognized in positive flower structure in N-margin. Folds are also seen to curve towards the vertical shear zones where they become folded along vertical axes toward N-margin (Fig. 3.62). Fig. 3.62 illustrates that along strike of the vertical margin-boundary structures, faulted and folded blocks are uplifted, such as pushed up rhomb horst (segments sub-parallel to the least compressive stress) and downlifted, such as subbasins (segments sub-parallel to the most compressive stress) from the basement.

In case of sedimentary cover, it follows the relative movement of the basement blocks by drape folding. En echelon occurrence of these structures such as push up uplifts, drag folds, fault splays and segments, can indicate the shear sense.

As these deformation patterns are compared with morphotectonic development of the lake (a correlative analysis of Fig. 3.62 to Fig. 3.63), tectonic interpretation suggests that somewhat different are the geomorphologic and tectonic consequences of transcurrent processes with simple shear strain in "an anisotropic basement", previously segmented by vertical discontinuities. As summarized in model section of Fig. 3.64, seismic structural and tectonic patterns of oblique-slip deformation indicate that upper crustal heterogeneity and basement mechanical anisotropy (also with decoupling of crust-mantle) basically control and drive the general tectonic and deformation structure of the lake. This implies that structural complication recognized in oblique-slip deformation is mainly induced by rock heterogeneity and basement anisotropy. As the simple-shear approach in basement terrains (especially for accretionary basement complexes) is used, structural complications should be also taken into account. In this point of view, it is noted that Muş-Lake Van basin, as a whole, is bounded by the shear zones of accreted thrusts (Fig. 3.63b). These shear zones are relatively longer intraplate and intralake shear zones, such as Muş and Cryptic sutures. A typical structural pattern in Lake Van, which prevalently underwent simple shear strike-slip tectonics is that of relatively long and straight shear zones (see an axis of suture trend in Fig. 3.64). In view of the general strike of faulting in the region, these shear zones delineate corridors in which sub-parallel tectonic elements are arranged in en echelon fashion (W- and E-segments of S-margin boundary fault). A volcanic chain of dome-cone complexes from Muş basin to Lake Van is located on a fracture zone having the same strike as the faulting in S-margin (also see number 1 in Fig. 3.40). This is also supported by studies of Kurtman et al., (1978) and Degens et al., (1978). Second-order faults and folds together with the inhomogeneous nature of the basement and the sedimentary cover complicate this simple image at a close view.

3.7.3 Implications for basement anisotropy and neotectonic deformation

S-margin boundary fault, parallel to axis of suture trend, is the major tectonic lineament passing through the lake. This fault transects the S-part of the lake and its adjacent shores. It is reported by Degens et al., (1978) that this fault represents a

continuation of the BP-M to the SE, along which the subduction and delamination is taking place (Şengör et al., 2008). As evident from Fig. 3.62, the sublacustrine slope is narrow and steep along the S-shores of the lake. This suggests that it can be the sub-lake portion of a large, E-W-trending fault scarp, implying W-segment of S-margin boundary fault.

The structural and geological appearance of S-margin boundary fault (PDZ) of the lake, parallel to both Muş suture (Şengör et al., 2008) and Cryptic suture (Keskin, 2005; Keskin, 2007; Şengör et al., 2008), reflects the N-end of BP-M (see Fig. 3.64). Indeed, the S-margin boundary fault (PDZ) represents the main weakness zone of accretionary complex underlying the lake. As previously described, the faulting in S-margin is en echelon in character and a typical negative flower structure, indicating the main extensional-transtensional axis of the lake through the suture complex in S. This implies that extensional-transtensional tectonics is localized along the mobile belts bordering continental regions (BP-M and EAAC or foreland-hinterland) and that the role of mantle anisotropy and crustal heterogeneity on the location and propagation of extensional strains is very effective through suture zones in accretions (see the shear wave splitting-anisotropy studies of Sandvol et al., 2003). This structural inheritance influences the propagation of extensional strains in many cases (see Şengör and Yılmaz, 1981 for a discussion of weaknesses of accreted terrains), as a well-known example, continental breakup mostly seems to occur along reactivated mobile belts between cratons. Based on the weakness and irresistance of accreted terrains and of suture complexes, models of vertical weak zones in elastic plates show that the deviatoric stress field in the weak zones can be higher than the one in the enclosed relatively strong blocks (the mechanism, although, should not be taken for granted). For example, many Cenozoic graben faults rejuvenated crustal structures whenever those were properly oriented with respect to the tensional stress (Reeves, 2009). Reeves, (2009) reported that such as, in the Malawi rift, Proterozoic basement structures belonging to the Ubende belt (separating the Tanzania and Zimbabwe cratons) represent the basic anisotropy along which active extension takes place. Also for the Baikal rift, the Proterozoic Primorski shear zone, delimiting the Angara craton, is reactivated as the main active border fault in the present-day rifting (Reeves, 2009).

Muş suture is an intraplate boundary between the EAAC and BP-M and anisotropic element, separating the region into two provinces; BP-M backstop and EAAC-Lake Van area (Şengör et al., 2008). This means that, in the lake, as seen in the Malawi rift, accretionary basement structures separate the EAAC and BP-M and represent the basic anisotropy along which active extension takes place. As recognized in the Baikal rift, the shear zone along Muş suture, delimiting the BP-M, is reactivated as the main active border fault (W-segment) in the present-day extension of S-margin. Margin boundary faults bounding the lake rejuvenated crustal structures, since these faults are properly oriented with respect to the tensional stress. The small discontinuous faults in and around SW-corner of the lake (around the Nemrut volcanic dome complex) and the occurrence of Muş suture zone are, in fact, transfer segments. These transfer segments, accommodating extension by oblique-slip along fault segments (W-and E-segments) oriented at various angles to the central graben trend (Tatvan basin) are strongly influenced by pre-existing basement anisotropy. Such transfer segments allow (or accommodate) the different slip rate on different normal fault segments (W-and E-segments) and allow the extension to transfer style and activity along the central graben.

Shear wave splitting and anisotropy studies of ETSE project, (2003) also contribute to understanding of mechanical relations between fast asthenospheric flow and surficial tectonic deformations. It is assumed from these tomographic studies that preferred orientations of olivine in upper mantle rocks are caused by continental assembly-related deformation during orogenesis. This entails a mechanical anisotropy in the deeper parts of the crust beneath the lake. This penetrative fabric reduces the crustal strength for extension normal to the foliation, favouring extension parallel to the existing fabric. This implies the orogen-parallel extension (axis of suture trend in Fig. 3.64) and graben formation. It should be stated that Lake Van region is domed by rising hot asthenosphere and subjected to intracrustal detachments (Şengör et al., 1985; Dewey et al., 1986; Şengör et al., 2003 and Şengör et al., 2008). Hence, it is noteworthy to mention the structural confirmation to the idea that the main controlling factor in half-graben geometry of central Tatvan basin is the strength ratio between the brittle upper and the weakened lower crust, highly depending on the extension rate. This argues that the crustal thinning, thermal weakening and upper crustal extension is a result of convective asthenospheric

upwelling (Şengör et al., 2003; Şengör et al., 2008). This implies that extensional processes and half-graben formation are not related to horizontal in-plate or far-field stresses generated by plate interactions. This means that the tensional stress fields responsible for upper crustal extension in Lake Van are caused by asthenospheric thermal doming, vertical topographic loading of the hinterland with elastic thinning of the foreland, crustal thinning and consequential gravity instabilities. Secondary tension along a load-free edge of a plate under compression is also thought to have acted through an axis of suture trend. These implications for basement anisotropy and neotectonic deformation indicate the importance of kinematic boundary conditions (versus stress), thin-skinned tectonism and related structural complications in Lake Van basin, showing intra-plate crustal deformation.

3.8 Tectonic Interpretation of Lake Van Block Fragmentation and Separation Events and Oblique Extensional Regime

Tectonic deformation and faulting styles in Lake Van and its deformation model cross section (see Figs. 3.62 and 3.64) from overall structural interpretation of seismic reflection profiles show that Lake Van is a rhomb-shaped basin block of oblique fragmentation and separation from a pre-existing weakness zone along S-margin (an axis of suture trend). An examination of seismic reflection data, tectonic evaluation of the lake and consideration of oblique extensional regime along with the structural complexities lead to a better interpretation of tectonic events affecting Lake Van basin. As interpreted from Figs. 3.62 and 3.64, a tectonic interpretation of block fragmentation and separation events in Lake Van reveals oblique extensional tectonics and magmatism.

Basin block fragmentation and separation relates to post-collisional opening of Muş and/or Cryptic suture zones, implying structural fragmentation, separation and differentiation of accretionary wedges underlying Lake Van. This remarks two structural divisions; the former is intra-lake “oblique” block fragmentation, separation and differentiation, resulting in the opening of internal subbasins through S-margin boundary fault. The latter is intra-plate suture zone separation from the BP-M, resulting in dextral transtensional faulting in S-margin. Both separation processes have geodynamic implications for understanding tectonic mechanisms of oblique extension in the Lake Van basin.

3.8.1 Tectonic origin and the opening of internal subbasins

Tatvan delta subbasin in SW-corner is controlled by W-segment, while Deveboynu and Varis spur zone subbasins are controlled by E-segment. These subbasins are internally originated and emplaced along S-margin boundary fault (Fig. 3.62). W-E elongation of PDZ of S-margin boundary fault, parallel to suture axis, is determined as reactivated product (negative flower structure). This shows that the pre-existing lineaments are important mechanical controls in sedimentary subbasin formation in the lake. Margin-bounding faults driving oblique motion towards ENE are mechanical discontinuities of the oblique faulting, while S-margin boundary fault is superimposed with Muş suture zone. In terms of internal subbasins along S-margin, sedimentation locally occurred in isolated depocenters. These are controlled by negative flower structure, which developed as a reactivation product within the basement and received sediments eroded from the uplifts. The formation of the subbasins and uplifts are also controlled by stratigraphic developments. This shows that the localized distribution of the subbasin sedimentation in the graben-extensional stage is reflected in a localized stratigraphic nomenclature, such as angular discordance. During the uplift and graben stage, deposition in Deveboynu and Varis spur zone subbasins is characterized by sediment transport over short distances, while subsidence in the subbasins is faster than sediment input. This leads to the accumulation of thick unconsolidated deposits with sedimentologically immaturated materials along shelf and slope regions. This is well recognized by acoustically transparent progradational clinoform facies in NE- and SE-deltas and soft-sediment deformation structures, particularly in SE-delta (Fig. 3.62).

The development of subbasins preceded the formation of the present basins at the SE-delta. These subbasins are controlled by Çarpanak uplifted province and Deveboynu peninsula high and extend toward the SE-delta (Fig. 3.62). These subbasins are also bounded and separated by intrusive magmatic activities. This indicates that these subbasins are subjected to underlying ductile shear zones and ductile activity, implying active magma propagation and upward low density mass transport through extensional fault planes. This is the case well recognized in Tatvan delta subbasin at SW-corner and W-margin boundary fault. Morpho-tectonic structure of SE-delta shows that Deveboynu and Varis spur zone subbasins are combined, forming a localized graben basin or trough channel system from SE-delta

into deep Tatvan basin (Fig. 3.62). Thus, these subbasins well represent the end-limit of progradational clinoform facies and delta sedimentation from SE-delta to Deveboynu peninsula, while they represent the beginning of graben depressions (Figs. 3.43, 3.50 and 3.62). This indicates that these subbasins form an elongated depression, trough-channel system or subbasinal gate-way between Deveboynu peninsula and Çarpanak highs, into deep Tatvan basin from SE-delta, while NE-Erek delta has a low-angle sloping and gentler elongation into Tatvan basin. The extensional-transtensional development of the subbasins is also evident throughout much of the lake with the development of asymmetric half-graben structure in central Tatvan basin and Tatvan delta subbasin in SW-corner of lake (Fig. 3.62). In SW-corner, Tatvan delta subbasin is the most prominent structural feature controlled by extensional and transtensional faulting. It is most probably an exposed and eroded structure due to having much less sediment thickness (< 200 m), strong intrusive activity and magmatic piles at its floor. In Tatvan delta subbasin, intruding and extruding magmas or growing magmatic piles are buried with much less sediment thickness. Magmatic materials are radially expanded, almost outcropped and intercalated with sedimentary sections.

It is identified from seismic structural and tectonic interpretation of Figs. 3.62 and 3.64 that extensional and transtensional movements coincided with the formation of these subbasins. These movements continued through the Plio-Quaternary, with the reactivation of pre-existing thrust faults, the folding of the sedimentary cover, the intrusive-extrusive activity along basin margins and the development of unconformities in the sequence (see Figs. 3.62 and 3.64). As illustrated in Fig. 3.64, it is clear that these movements are related to variations in the crust-seated processes. This implies that, due to the thin and weak crust, differential movements of underlying accretionary wedges lead to strike-slip, oblique extension and compression in the lake margins. These processes also coincide with the present day oblique activity of the Muş suture zone and Quaternary magmatism. As often mentioned, Muş suture zone extends all along the S-margin boundary of Muş-Lake Van basin system and the weakness boundary between the oldest BP-M and the younger EAAC. W-segment, parallel to the suture, controls active magmatic intrusions and collapsed parasitic dome-cone complex along S-coastal lines. These active and passive magmatic occurrences constructed S-coastal regions, which are

strongly irregular and eroded areas. As recognized in Fig. 3.62, these findings evident extensional and transtensional activity of Muş suture, magma-dominated faulting and suture-parallel magmatic margin in S. This shows that the oblique activity of Muş suture continued en echelon transtensional faulting along S-margin and caused transpressional movements in N-margin and active magmatism along W-E trends until the present day. The constraint on this interpretation is that Lake Van (also with Muş basin) is visualized as lying in an approximately W-E position along Muş suture zone with mantle lid being delaminated southwards and broken off beneath it (see related map views in Şengör et al., 2003; Keskin, 2005; 2007 and Şengör et al., 2008). This previews that slab is delaminated southwards and delamination is limited toward BP-M (back-stop) or somewhere beneath the lake. Then, slab is broken off beneath BP-M, close to lake. This points out that prevailing extensional-transtensional regime in lake coincided with the slab delamination and break off lithospheric mantle with the doming asthenosphere beneath the lake (Şengör et al., 2008). A sequential events of these processes has been attributed to the extrusion and rotation of Lake Van continental block to ENE of the site of collision (all along Muş suture zone) (Fig. 3.64). The extrusion and rotational motion of the lake can be interpreted as indicating the squashy feature of mélange wedges or the oblique flake-block motion of the upper crust, as referred to Şengör et al., (2008) and Dewey et al., (1986) respectively.

A reasonable model is that for the ENE extrusion of upper crustal blocks or flakes, delamination-induced thin crustal buoyancy, shear-wave and mechanical anisotropy lead to the Plio-Quaternary opening of Lake Van basin from W- and S-margin boundaries. During this extrusion event, numerous extensional-transtensional subbasins, (also including central Tatvan basin) are formed throughout S-margin by reactivated differential movements of underlying accretionary wedges. This process is almost similar to differential movement of small microplates as proposed by Barber et al., (2005) for Sumatran back arc region and good agreement in differential oblique movements of upper crustal flakes by Dewey et al., (1986) and strain incompatibilities in basin formation by Şengör et al., (1985). This implies that the subbasins originated as extensional and transtensional basins between major oblique-slip faults, one in the position of the N-margin boundary fault, and the other in the S-margin boundary fault. According to this model, strike-/oblique-slip deformation and

the development of internal subbasins with the opening of W- and S-margins from probably Late Pliocene to the present day caused further ENE-translation and rotation of lake. Moreover, transpressional faulting in N-margin and GPS higher velocity vectors from Şengör et al., (2008) well showed the NNW-motion of the lake. This motion is probably caused by dip-slip extensional component of S-margin boundary fault, while its right-lateral component strikes to E. This also evident the opening of Muş suture zone and its separation from BP-M, showing the oblique wedge motion of the lake as an upper crustal flake basin (Fig. 3.64). Thus, the prevailing N-S compression is gradually compensated by extensional and strike-/oblique-slip faults in the lake (see Koçyiğit et al., 2001 and Dhont and Chorowicz, 2006). Sequential development of these events caused a more oblique extension, a more magmatic activity, transpression in N, and reactivated oblique movement along Muş suture (see Dhont and Chorowicz, 2006 for a description of dextral oblique-slip fault of Muş basin in N). These events also initiated regressive rapid sedimentation in the lake during Quaternary, due to the strong orogenic uplift of the Mountains around.

Hypothesis that relates the formation of the internal subbasins to their relationship to the present slab delamination and accretionary system is that these subbasins form part of a network of extensional and transtensional basins. These originate in Plio-Quaternary and formed at about the same time throughout the whole Lake Van region. These basins are therefore the result of processes, which affected the whole of Lake Van. The precise age of formation of these subbasins is difficult to determine, due to the lack of age data. It appears that during the Plio-Quaternary, these subbasins were formed across a linear weakness zone from W to E, as referred to PDZ of S-margin boundary fault. However, the regional extent of strike-/oblique-slip basin formation in E-Turkey during the Plio-Quaternary (Şengör et al., 1985) has encouraged this hypothesis for a regional rather than a local explanation. The regional models proposed by Şengör et al., (1985) and Dewey et al., (1986) for E-Turkey seemed to provide such a solution. In their model, E-Turkey was extruded as a set of continental slivers separated by strike-slip faults, opening up pull-apart basins between the continental fragments as they moved away differentially from the site of the collision. This model is detailed in Fig. 3.40 for a region-scale and recognized in Fig. 3.64 for a basin-scale.

The consensus view is that the sedimentary basins developed initially as extensional basins, controlled by the orientation of pre-existing lineaments in the pre-Quaternary basement. As indicated by number (1) in Fig. 3.40, the orientation of pre-existing lineaments is consistent with that of the subbasins being W-E in the lake. This shows that the strike-/oblique-slip movement in the lake is superimposed on these earlier pre-existing trends and coincides with the uplifts of the Çarpanak spur zone, Deveboynu peninsula and Muş suture and movements along BP-M (Muş suture). S-margin boundary fault (PDZ) and internal subbasins are correctly oriented to have originated as extensional-transtensional basins. This shows that these subbasins are driven by en echelon movements on transtensional fault in S-margin. Hence, it is considered that there are no any problems in the application of the extrusion and strike-/oblique-slip model to sedimentary basins in E-Turkey and to Lake Van area as a whole. The impression given by the linear structural distribution of these subbasins is that there was overall expansion of Lake Van area (or probably the whole E-Turkey area) during Plio-Quaternary. This proposes that the opening of these internal subbasins is a result of upper mantle/lower crust shear-wave anisotropy beneath Lake Van region (see ETSE, 2003 for details) and thus, basement mechanical anisotropy, strongly affected by pre-existing lineaments (see Fig. 3.64). Hence, interactions of pre-existing lineaments with neotectonic structures in and around lake are essential mechanical parameters taken into account in understanding mechanical anisotropy. This clarifies extensional and transtensional processes responsible for the subbasin formation.

Tectonic interpretation from Figs. 3.62 and 3.64 suggests that, as Lake Van basin rotated, the original extensional faults initially defined the marginal uplifts and half-graben geometry of central Tatvan basin and reached their present W-E orientation. This orientation is almost similar to pre-existing thrust fault orientation (Fig. 3.63). The effect of oblique compression and extension in central Tatvan basin is to produce structural inversion and reactivate marginal faults as reverse/normal and strike-slip faults. Thus, positive flower structure in N-margin and folds throughout central Tatvan basin are generated, while negative flower structure in S-margin and internal subbasins throughout S-margin boundary fault are generated. Simplified tectonic interpretation of Lake Van block fragmentation and separation events is briefly given as the following manner;

1- thin crustal buoyancy is dynamically supported by doming hot asthenosphere due to slab delamination and break off. This results in buoyant crustal stresses and low shear strengths beneath the lake.

2- upper mantle anisotropy is driven by shear-wave splitting. This results in sub-crustal shears and ductile shearing stresses, transmitted through the crust. These are intra-plate asthenospheric flow stresses beneath the lake.

3- crustal mechanical anisotropy is caused by accretionary prism-suture complexes, concentrated on upper crustal sections and crustal discontinuities. This results in strain localization all along suture contacts. Structural mechanical anisotropy is related to basement reactivations, differential movements of accretionary wedge-blocks and oblique reactivation of basin margin faults.

4- kinematic boundary conditions finally govern strike-/oblique-slip deformation. This results in heterogeneous distribution of differential strains and their complex relationships, independently from plate motion vectors.

A wide range of crustal strength profiles is shown in Fig. 3.65 to give some certain clues about crustal shear strength beneath Lake Van region and extensional strains through an axis of suture trend. Dewey, (1988) illustrated shear strength envelopes in tension for lithospheric profiles with various combinations of dry and wet quartz and olivine, crustal thicknesses and geothermal gradient. In Fig. 3.65, percentages refer to strengths relative to B (100 per cent). Depth in km on vertical axes and shear strength in MPa on horizontal axes are also indicated. Based on the crustal and basinal models of Şengör et al., (1985), Dewey et al., (1986), Şengör et al., (2003) and Şengör et al., (2008) for accretionary complex of E-Turkey, strength profiles represented by *F* and *I* may represent the case expected for the crustal strengths of Lake Van, ranging between 25-32 %. This range particularly implies the thinned and weakened crust beneath the lake, namely “the squashy zone”. This strength range also indicates that shallow deviatoric tension can be developed in uplifts that are compensated in the crust, with a different stress regime in the upper mantle (Dewey, 1988). Similarly, flake rotation in shear zones (Dewey et al., 1986 and Karner and Dewey 1986) generates complex variation between shallow tension and compression. This emphasizes the role of compensated uplifts in generating horizontal tension and that stress regimes can vary vertically in the crust, particularly within highly anisotropic intra-plate regions.

According to *F* and *I*, the thinned crust beneath the lake is more likely subjected to extensional strains, since intra-plate crustal strength profile is much weaker and active brittle deformation is the shallow-seated. Intra-plate crust is seamed with zones of weakness and inhomogeneity, including weak orogenic zones (Şengör and Yılmaz, 1981 and Glazner and Bartley 1985) and recent zones of lithospheric stretching (Dewey, 1988). Intra-plate crust is the preferential site of tension-inducing uplift, and plateaux produced by lithospheric delamination and advective thinning of the lithosphere, and crustal underplating (McKenzie, 1984 and Şengör et al., 2008). Asthenosphere-related uplifts or volcanic edifices in intra-plate crust can generate deviatoric tension even against a background of deviatoric compression (Crough 1983 and Dewey, 1988).

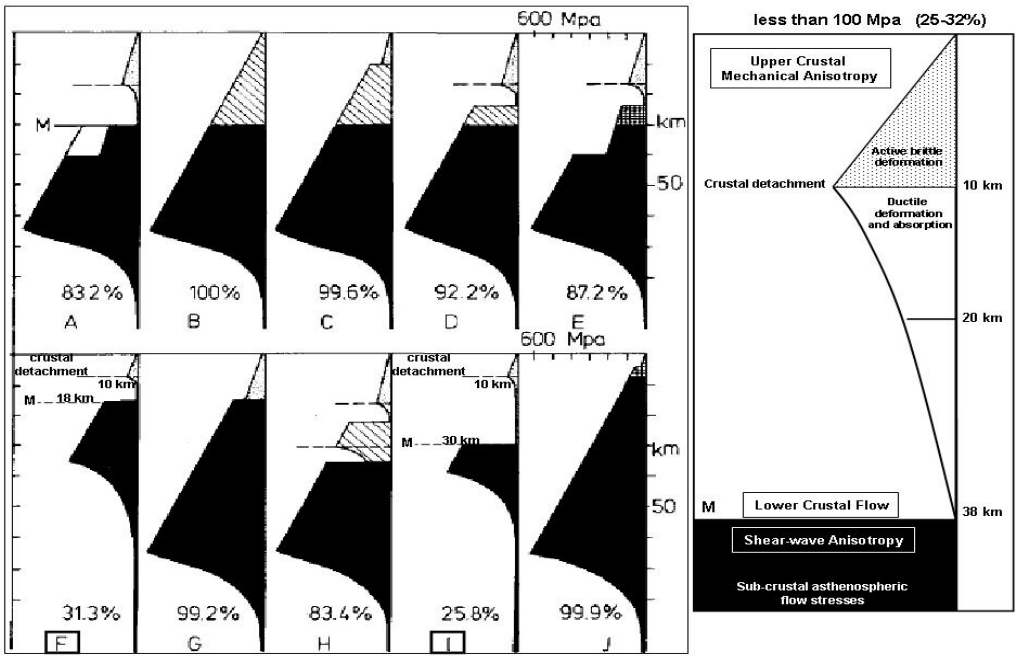

Figure 3.65 : Shear strength envelopes in tension for lithospheric profiles with various combinations of dry and wet quartz and olivine, crustal thicknesses and geothermal gradient (see Dewey, 1988 for details of this classification). Black: olivine, lines: dry quartz, dots: wet quartz, cross-hatching: mafic rocks. Percentages refer to strengths relative to B (100 per cent) and depths in km on vertical axes, shear strengths in MPa on horizontal axes. Note that shear strength, upper crustal detachment and moho in F envelope are 31.3%, 10 km, 18 km and these values for I envelope are 25.8%, 10 km and 30 km respectively. This parameterization in F and I envelopes is well compatible with that in crustal thickness profile of the lake that upper crustal detachment is 10 km and moho is 38 km . Shear strength envelopes in tension for thin crustal profile of Lake Van basin with F and I combinations of dry and wet quartz and olivine, crustal thicknesses and geothermal gradient are taken into account to obtain strength envelope (the right column). This envelope roughly estimates that the shear strength that upper crustal deformation requires is probably less than 100 Mpa with strengths 25-32%.

3.8.2 Tectonic instability of the upper crustal flakes and implications for oblique extensional regime

Tectonic instability of the upper crustal flakes and/or accretionary wedges is the important parameter to consider structural inequilibrium of the weak and thin crust and to examine the reasons-results of such a crustal inequilibrium and its tectonic impact on basin dynamics. Because, it seems that the extensional-transtensional events at the lake are originated and triggered by a crust-seated mechanism. This implies that crustal deformation processes have considerably contributed to the fragmentation of basin and separation at the marginal contacts. Tectonic instability of the upper crust briefly provides an insight into how different strain regimes can develop at different levels of the crust, in response to kinematic boundary conditions and rheological structure.

Pre-existing steep thrusts along the Muş-Lake Van basin highlight the profound effect that is syn-convergent, orogen parallel accretionary wedge structure (Fig. 3.63). This effect has an implication for transition to squashy basin structure, which is referred to the development of structures at different levels of the crust, particularly in the upper crustal levels (see Şengör et al., 1985 and Dewey et al., 1986). As previously mentioned, upper crustal deformation is characterized by the development of orogen- or suture-parallel and vertical curvilinear transpression and transtension zones in N- and S-margins. Their kinematics is probably governed by the polarity of lower crustal flow, rather than the tectonic boundary conditions such as the oblique convergence. This indicates that upper crustal deformation is decoupled from lower crustal strain, which may be characterized by vertical flattening and orogen-parallel stretching, as supported by Dewey et al., (1986). Theory suggests that the boundary between these deformation regimes is transitional and occurs below the brittle-ductile interface in the models. This means that different upper crustal deformation styles can be developed with non-buoyant versus buoyant lower crust. An examination of faster GPS vectors (Şengör et al., 2008) considering faster-slower asthenospheric flow vectors beneath Muş-Lake Van region (Sandvol et al., 2003) strongly imply the differential shearing movements at crustal depths, related to upper mantle and mechanical anisotropies. Vertical and lateral mechanical anisotropy is a direct result of very heterogeneous and weakened orogenic crust. This indicates that the accretionary wedge structure of the lake is weakened and disturbed

by the upper crustal deformation processes. As a result, the resulting strain in the basin is partitioned and localized. This shows that the upper crustal deformation is distinctly decoupled from the lower crust. This case accommodates the lake in the crust.

Two distinctive structural phenomena are well recorded in the seismic record; the former is the propagating magmatism, related intrusive activity in the lake, parallel to axis of the orogenic belt and profound changes in sedimentation patterns. The latter is extensional/oblique-slip deformation and related structural patterns. This shows that the lake is affected by major episodes of strike slip deformation with normal and reverse components. According to the basinal models by Dewey et al., (1986), the oblique-slip deformation of the lake is a distinct expression of upper crustal flakes, having an obliquity and significant deformation partitioning. This supports the idea that the upper crust is mechanically layered and obliquely separated (see Dewey et al., 1986). The upper crustal blocks are reactivated by post-collisional events, referring to slab delamination process. These events mainly resulted in basin block fragmentation and separation in Lake Van. Since, the rapid, late, morpho-tectonic uplifts of orogens with associated magmatism in high-level extensional environments are related to lithospheric delamination event (Bird 1978; Houseman et al., 1981 and Dewey 1988). These uplifts, and the weakened orogenic uplift zones, enhance tension and are the likely preferential sites of extensional tectonics, leading to lithospheric failure. Alkaline magmatism and intrusions are encouraged by deviatoric tension and are preferentially sited in plateau uplifts and rifts (Bedard 1985). As referred to Lake Van Dome, extension of some uplifts is buffered by crustal compensation and leads to “aborted rifts” (see Dewey, 1988 for tectonic nature of similarities between aborted rifts and the lake). Increasing deviatoric tension leads to accelerating continental extension accompanied by widespread magmatic swarms and the eruption of flood basalts (Cox 1978). This is immediately followed by splitting events, tension being enhanced by plateaux generated by basaltic underplating (McKenzie 1984 and Dewey 1988). The crust-seated effects of delamination event contribute to sedimentary basin formation (Massonne, 2005) and have important structural impacts. Because, it is believed that the delamination is the preferable descriptor of the slab break off process, for it implies that separation is strongly influenced by the mechanical anisotropies in the lithosphere. This indicates

that the mechanical layering of the sedimentary cover, of the crystalline crust (segmentation and flake formation), and the mantle each play a predictable role in controlling the structural evolution of the lake after collision, as summarized in the following;

After the slab break off process, asthenospheric material rose and spread laterally at the crust-mantle interface beneath the lake. Flow of upwelling asthenosphere is possibly channelized through BP-M and suture complexes (Muş and Cryptic sutures). A structural line of Muş and Cryptic sutures is called as "main fragmentation and separation zone" between the accretionary complex in N and the metamorphics in S (Fig. 3.64). The flow of the asthenosphere is believed to be under the influence of convection currents, which caused lateral spreading of the asthenosphere to only one side of the trough and dragged down the subcrustal lithosphere (see also shear-wave splitting, Pn/Sn tomography and anisotropy studies by ETSE-project, 2003). Within squashy zone where Lake Van is domed, a rheologically stratified (frictional/viscous) weak orogenic crust floats isostatically on a viscous asthenosphere and is squeezed between converging strong crustal blocks and thus, ductile lower crust and upper mantle is free to flow laterally (examine Fig. 3.65). This flow forms shear-wave anisotropy just beneath Muş-Lake Van region. The low density asthenosphere invasion caused plateau uplift, squashy zone and the rapid phase of orographic deposition of the continental sediments into the lake. This phase was followed by a massive intrusion of asthenosphere-derived mafic and ultramafic magmas into the thin crust. Their high density caused "tectonic instability" in the upper crustal flakes, also termed as "tectonic instability of accretionary wedges". Then, rapid subsidence of the lake as large quantities of basalts were intruded and erupted on to the lake floor. Break off and continued sinking of the subcrustal lithosphere is driven by asthenospheric convection currents, causing the final orogenic phase. This phase is induced by weakening and thinning of the crust by the slab break off and intrusive activity or changes in the velocity of the convection cells. Thus, the lake represents the end-member of the final orogenic phase. Finally, the production of basaltic magmas at the relatively shallow levels proposed for the basin requires that the melting temperature of the mantle be considerably lowered in someway. This is achieved by the derivation of water from hydrous phases in the crustal portion. In this way, the slab break off process has

strongly affected the high plateau dynamics and basin systems (see Şengör et al., 2003 and 2008 for a detailed explanation). All these steps briefly describe the delamination-dependent reactivations of accreted thrust blocks and alkaline magmatism during post-collisional period. Since, deformation is effectively decoupled from mantle dynamics and weakened by partial melting and intrusion of voluminous alkaline magmatism. As a result of this, tectonic development of the basins depends on the vertical and lateral rheological structure of the crust, the initial and final widths of the weak zone (see and examine numerical models from Pysklywec and Beaumont, 2004), erosion (Ellis et al., 2001) and 3D-effects such as lateral extrusion (Dewey et al., 1998).

Lake Van region is a product of accretionary prism system at various scales and levels, so it is an accretionary basin complex, having a wide range of weakness zones. As known, terrain blocks of the E-Anatolia are accreted directly to the continent as coherent masses of significant crustal thickness which did not, however, behave as rigid sub-plates and irresistant (Şengör and Yılmaz, 1981 and Şengör et al., 2008) and underwent strong internal deformation as discussed by Burchfiel, (1980) and Kearey and Vine, (1996). Further, it appears that terrain accretion is a viable mechanism of ophiolite emplacement, as ophiolites frequently occur at terrain margins (Kearey and Vine, 1996), as proposed by Şengör and Yılmaz, (1981) and Şengör et al., (2008). The lake is bounded by some forms of terrain margins such as suture complexes, which are presently reactivated as oblique slip flake margins along the Muş-Lake Van basin. In fact, this is well known process from previous studies. These studies state that oblique-/strike-slip faulting is common in many present-day orogenic belts and it would be expected that such faulting is a ubiquitous feature of ancient mountain belts and responsible for the fragmentation of accreted terrains. This statement reveals that Lake Van, as an accreted product, can be fragmented, suggesting post-collisional tectonic instability of the upper crustal flakes. This instability has initially resulted in extensional and oblique-slip fragmentation and separation along basin margins of the lake (Figs. 3.62 and 3.64). Marginal nature of transpressional and transtensional activities implies that a large amount of fragmentation and separation has occurred. The lake was subsequently fragmented and then translated to its present location by oblique slip faulting after the accretion

of the plateau. This event includes a reactivation of the pre-existing faults, inversion of the basin and the onset of magmatic intrusions on the lake bottom.

In terms of anisotropic effect on the dynamics of the crust-mantle system beneath Lake Van region, some important remarks are briefly given below. The view is that if the strong crust leads, whether the weak crust will follow, as questioned by Axen et al., (1998). Crustal strength profile seen at the right column in Fig. 3.65 is made of the results of the previous studies and a conceptual illustration of *F* and *I*. This profile indicates highly anisotropic, weak convergent crust from bottom to top. Differential shearing movements with various magnitudes at the contact interfaces of the upper mantle-the lower crust and of the upper crust-the lower crust are recognized in this profile. These shearing movements are principally caused by splitting shear waves and mechanical anisotropies within the crustal levels. The sense of shear of growing anisotropies in the region is the oblique, showing the differential movements of oblique ductile shearing between the layers. For example, the weak upper crust is heterogeneously deformed by brittle shears, while lower crust is highly deformed by very ductile shears due to delamination. This indicates that the crustal layers are decoupled and differentially deformed in various senses of the shear. According to this, the upper crustal vertical anisotropy strongly controls the margin boundaries of the lake, which are the pre-existing weakness zones and indeed, results in the tectonic instability of accretionary wedges. In fact, the entire crustal column underwent an instability process of crustal layering and thus, differential oblique movements. GPS and shear wave splitting data, and analysis of kinematic boundary conditions (versus stress) confirm these differential movements.

A correlative examination of the crustal strength profile in Fig. 3.65 with the model experiments of previous studies proposes that decoupling of lower- from upper-crustal deformation is more pronounced in models with non-buoyant lower crust. This is well evidenced by a lack of buckle folds at the brittle-ductile interface, and the confinement of shear zones to the upper crust (Fullsack, 1995; Ellis et al., 1998 and Bailey, 2001). In other words, the crustal decoupling results in the confinement of pre-existing shear zones, fault reactivation event and basin inversion process. Previous studies view that different upper crustal deformation styles are developed in models with non-buoyant versus buoyant lower crust (also see Fullsack, 1995; Ellis et al., 1998 and Bailey, 2001).

The differences in structural style compared to models with non-buoyant lower crust are attributed to the "water bed" effect of the buoyant, weak lower crust (Bailey, 2001). In these studies, surface deformation features developed in vise models with a non-buoyant weak lower crust and a buoyant weaker lower crust after the shortening. Oblique view of vise model with non-buoyant lower crust after the shortening shows that the brittle upper crust has been removed by vacuum on one half of the model, revealing the 3D structure of the brittle-ductile crust interface. This clearly remarks that the different structural characteristics developed in the upper and lower crust of the vise models. Thus, simple vise models provide insight into how different strain regimes can develop at different levels of the crust, in response to boundary conditions and rheological structure (also examine Fig. 3.65).

Consideration of all these model studies and evaluation of strength profiles in Fig. 3.65 indicate that deformation of the crustal column beneath the lake is extremely decoupled. This case leads to tectonic instability in the upper crust and active brittle deformation. Thus, the pre-existing boundary conditions are reactivated and reordered by oblique-slip conditions (Figs. 3.63 and 3.64). The resultant basin inversion best explains why the lake is a result of oblique movements of upper crustal flakes, as supported by Dewey et al., (1986) and thin-skinned tectonism. Thin-skinned tectonics proposes that the fragmentation and separation of terrains and/or of post-orogenic accreted basins (compressional ramp basins) is the most probable reason of extensional deformations in the plateau. As expressed above, because, upper crustal flakes (the vise model) with a buoyant weaker lower crust develop markedly different surface deformation fields and cross-sectional geometries in the plateau. Conjugate and discontinuous patterns of strike-/oblique-slip faults and rhombohedral block tectonics (Şengör et al., 1985) are clearly characterized by the styles of upper-crustal deformation (see also Dhont and Chorowicz, 2006). As well observed through suture-parallel magmatic margin in S (Fig. 3.62), en echelon crack and magma propagation through S-margin boundary is distinctly imaged by seismic data. This case across S-margin evident that strain localization in the frictional upper crust results in development of the curvilinear shear zones across margin boundaries. Kinematics of these shear zones change along strike as the flow direction in the ductile crust or in the asthenosphere reverses. This clearly points out the strong effect of anisotropy on the lake and strain localization in suture trend, resulting in the

curvilinear shear zones across basin margins. In nature, such zones would also contain structural characteristic of transpression, as seen in N-margin.

Implications for tectonic instability and oblique extensional regime in Lake Van basin point that instability event in the upper crustal section is a result of subsequence segmentation of the thinned and weakened crust and the dominant factor in present-day tectonic evolution of the lake. Since, tectonic instability implicates for oblique extensional regime in the lake. The oblique-slip mode of the instability of accretionary wedges (or upper crustal flakes) suggests a highly oblique slip setting and deformation partitioning in the lake. Oblique movements of upper crustal flakes are dominant mechanisms in the growth of the extensional/oblique slip deformations. This reveals that tectonic deformation is highly localized at the upper crustal levels and hence, thin-skinned. As referred to Barber, (1985) and Kearey and Vine, (1996), it is stated that the post-collisional fragmentation of terrains is probably a consequence of plates undergoing oblique convergence. This statement confirms that the fragmentation and separation of the lake, bounded by terrain margins or sutures complexes are a consequence of upper crustal blocks undergoing oblique convergence and extension. Oblique deformation shows complex alternating phases of shortening and extension at the margins of upper crustal rotational flakes within oblique-/strike-slip zones.

Shortly, Lake Van basin has undergone block fragmentation and separation process during the post-collisional episode. In fact, this process is the main result of delamination-dependent anisotropic events, resulting in differential movements of the crustal sections. While the flow direction in the ductile crust or in the asthenosphere reverses, kinematics of basin-bounding faults changes along strike, forming oblique deformation. The extensive magmatism localized in basin-bounding faults that are pre-existing discontinuities. One of the most prominent implications is that dextral transtensional faulting in S-margin represents the post-collisional opening of suture complex from BP-M. Suture zone opening implicates for understanding tectonic mechanisms of oblique extension in the lake (intra-lake) along S-margin and the plateau (intra-plate) along Muş suture and extensional alkaline magmatism. If lithospheric delamination (Bird 1978; Houseman et al., 1981) beneath an orogenic basin occurs, shallow tension may give way to lithosphere-penetrating tension in a rapidly uplifted region (squashy zone) and, hence, the

possibility of lithospheric splitting across a thinned and weaker lithosphere (Dewey 1988). This may be one reason why continental splitting is commonly roughly along the lines of earlier orogenic belts, such as the opening of the Central and North Atlantic along the Appalachian-Caledonian orogen (Wilson 1966) and the opening of intra-plate Muş suture zone along the Lake Van.

4. MAGMATISM OF LAKE VAN

4.1 Seismic Structural Characteristics of Basin-bounding Intrusive-Extrusive Magmatic Activity

Basin-wide intrusive activity and laterally extensive sheets (sills)of magmatism through margin boundary faults across central Tatvan basin are excellently illustrated by seismic reflection profiles. S-parts of seismic sections seen in Figs. 3.3, 3.5, 3.8 and 3.9 are entirely characterized by magmatic intrusions through W-segment and laterally extensive sheets (sills) across central Tatvan basin toward N-margin (Figs. 3.1-3.7) and W-margin boundaries (Figs. 3.8-3.11). Figs. 3.13-3.15 distinctly show that W-segment is deformed by fault-controlled intrusive-extrusive activity of magmatism. E-segment, Deveboynu and Varis spur zone subbasins are also densely covered by active magmatism shown in Figs. 3.16, 3.18 and 3.26-3.29. Laterally extensive sheets or sill products from active intrusions are well recognized all over the central Tatvan basin across inter-marginal sections. These products show multi-directional flows across central Tatvan basin.

Magmatic intrusive bodies generally produce seismically dead intervals. The intrusive nature of the body is evident from upturning of the adjacent sediments. These intrusives do not show the secondary rim syncline characteristic of salt or mud diapirs. As recognized in these seismic sections, the effects of the intrusions, rather than the intrusion itself, are the main features of the seismic sections. Lateral dispersal patterns and sedimentary disruption associated with the intrusions are evident up to 26-45 km away from margin boundaries across central Tatvan basin. Magmatic intrusions and their extensive products observed from seismic sections are the end-members of the rapid crack and magma propagation events through transtensional faults in W- (Figs. 3.8-3.11) and S-margins (Figs. 3.13-3.20, 3.23, 3.24 at the bottom, 3.25-3.29, and 3.30 at the top).

The complete seismic data set clearly illustrates the structural relationships between rising magmas and their extensive sills, evident that intrusions and sills occur,

frequently together (Figs. 3.1-3.11, 3.13-3.16, 3.18, 3.26-3.29, 3.31, and 3.33). A seismic structural interpretation of magmatic intrusions and related sills from these sections indicate that sills are magmatic bodies intruded laterally into sedimentary sequences and, hence are more easily identified, or at least produce a more pronounced effect in the seismic image. The observed sills across central Tatvan basin are very laterally extensive, covering hundreds of square kilometers. However, more commonly, individual sills are less extensive, with areas of a few tens of square kilometers. This shows that sills covering central Tatvan basin are not individual features and that they are interconnected with the feeder zones in and along transtensional faulting in S-margin (W-segment). This indicates that these sill features are prominently produced by intrusive activity of rising magmas in and along transtensional faults in W- and S-margins and they sequentially disperse into permeable sections of depositional sections in central Tatvan basin. The best criterion for the recognition of sills in seismic data is to observe discordant reflector relationships that demonstrate the intrusive nature of the sill. Seismic expressions of sills note the diagnostic discordant nature of the high-amplitude reflections. Moreover, sills can produce seismic expressions very similar to those of carbonate or evaporates and if thick enough, a sill can be also identified by high-interval velocities.

A series of seismic sections shown in Figs. 3.3, 3.5, 3.8-3.11, 3.13-3.16, 3.18, and 3.26-3.29 shows that the observed intrusive activity appears through opening vents, extension spaces, conduits or fracture-fissure systems and that the activity is continually fed back from feeder zones and/or point sources emplaced at the faults in basin margins. This clearly implies that transtensional faults from W- and S-margin boundaries are superimposed on the main fissure or a linear factures zone, suggesting a complex interconnected pattern of the faults-vents-fissures or fractures. This structural complexity is perfectly reflected by seismic sections seen in Figs. 3.13-3.15 from W-segment, indicating that active faulting is immediately accompanied by active magmatism. This forms a curve-linear pattern of central vent and fissure volcanic system in the lake. Magmatic intrusions show some clear relationship to a volcanic center or fissure system (Figs. 3.13-3.15). Figs 3.13 and 3.14 show seismic sections across PDZ of S-margin boundary fault and its-W-segment. The form of intrusions can be seen clearly in these sections, with reflections from the magma

flows dipping radially outwards, at up to a some degree, from a central volcanic vent (CVV) or fissure volcano (FV). The vents are roughly circular in plan, with a diameter of ranging about 2-4 km and a water depth of 300-400 m. The point from these sections is that the magmatic pile has been built up by the extrusion of thin magma flows, each in turn being weathered before burial by the next magma flow. It is essential to note that the clinoform prograding pattern of the radially outward-dipping magma flows could be mistaken for a prograding sedimentary sequence in situations where it was not possible to demonstrate the overall shape of the feature, for example, with a widely spaced seismic grid. Seismic sections give well-defined expressions of magmatic intrusions with branching sills and sill sequences into permeable depositional successions. It is seen in these seismic sections that magmatic intrusions with branching sills, sill sequences and water-laid volcanic clastics share external forms and internal structures in common with sedimentary deposits. Branching sills and sill sequences are intercalated with sedimentary sequences, characterizing a complex depositional setting of central Tatvan basin and complicated deformation processes in the lake (Figs. 3.3, 3.5, 3.8-3.10, 3.31, and 3.33).

Basin-bounding faults and deformation styles are given in Fig. 3.62, also associated with morpho-tectonic structure and rising magmatic activity all over the marginal sections of the lake. As referred to the map view shown in Fig. 3.62, seismic structural interpretation of basin-bounding intrusive and extrusive magma activity has already gained some insights into magmatism, magma propagation and magma pathways from seismic data. These data show that during the magmatism, magma branched from the main conduits emplaced at the faults, laterally dispersed and extensively formed lateral sheets or sills. Magma traveled several ten kilometers from W to E, to a depth of 300-450 meters below lake level. The intruded magmas then migrated horizontally to just beneath the summits and migrated upward to the surface, deformed overlying sediments and penetrated into the water column. In this way, active lacustrine magmatism entirely covered central Tatvan basin and strongly affected sedimentation pattern of the lake. Such data suggest that a complex network of intrusions and vents, supporting the younger activity of magmatism in the lake. As recognized in Fig. 3.62, the mean trend of the elongated intrusive activity is from W-margin to SW-corner, through S-margin boundary (W- and E-segments) into

Deveboynu and Varis spur zone subbasins in SE delta. This shows that transtensional margins of the lake are invaded and covered by upward magmatic mass transport, suggesting that magmatism has a close kinematic relation to Nemrut volcanic dome complex in the further W. In Fig. 3.62, interactions of the faulting and deformation styles with margin-bounding magmatism and intrusions are summarized, describing overall deformation pattern within the lake.

4.2 Extensional Magma Propagation

Magmatic intrusions are seismic examples of how distributional pattern of overall magmatism can give a clue to both basin type and basin deformation style (Fig. 3.62). Basin deformation and faulting analysis gives some certain clues about intrusion-extrusion periods and tectonic intensity, which control magma distribution and seismic structural architecture of intrusions. Consideration of magmatism along with the structural complexities, such as vents, fissures, fractures, clusters and conduits, explains the magma propagation into transtensional faults in S- and W-margins. Evaluation of magma system all over the lake considering faulting and deformation styles leads to a clear structural interpretation of extension-related magma propagation in explaining 3D-block model view of the lake (Fig. 3.64). A basinal examination of seismic structural characteristics of basin-bounding intrusive and extrusive activity and seismic structural interpretation of overall magmatism intrusions along with the faulted margins reveal that extensional and transtensional processes dominate in the lake. These processes shape deformational styles of rising magmas through margin boundary faults. Intrusive-extrusive activity of rising magma results in complex deformation patterns through sedimentary sequences.

Fig. 3.62 shows that, along PDZ of S-margin boundary fault from Tatvan delta subbasin in W to Deveboynu subbasin in E, transtensional activity in S-margin is more prominent and subjected to dense intrusive activity of magmas. S-margin boundary fault is accommodated by the subbasin formations and upward mass transport of magmas, as also seen in W-margin boundary fault. This suggests that magmatic potential energy and its subsequence dispersal are extensionally localized through S- and W-margin boundary faults of the lake. Deformation style and the characteristics of the faulted margins and seismic structural configurations of extensive magma distribution suggest the great amounts of vertical and lateral

separation in and along W- and S-margin boundaries, through which magma propagates across central Tatvan basin. This case also effects transpressional faulting in N-margin (Fig. 3.62). Such a picture of deformation along with the magma distribution pattern significantly considers that the geometry, shape, position and kinematics of magmatic intrusions are controlled by compatibility holes and gaps, caused by flaking of the elastic lid (see and examine Figs. 3.62 and 3.64). Since, these holes and gaps are characteristic features, particularly beneath extension-related basins (see Şengör et al., 1985 and Dewey et al., 1986).

Indeed, Fig. 3.62 well illustrates implication of tectonic and structural controls on magma movements and intrusion-eruption locations, indicating magma supply paths across margin boundary faults. It is very distinct that magmatic trend roughly follows the same structural trend of Nemrut volcanic complex, parallel to Muş and Cryptic suture zones from W to E. It seems that S-margin boundary fault, suture-parallel magmatic margin, is the main magma supply and dispersal path into central Tatvan basin. Structural relations between faulting and magmatism seen in Fig. 3.62 clearly provide certain evidences to thin-skinned extensional magma propagation and deformation, based on the relationship between the boundary faults and the Quaternary volcanics around the lake.

4.2.1 The relationship between the boundary faults and the Quaternary volcanics around the lake

Active and passive dome-cone complex is arranged in and along southern spur zone of the lake (Fig. 3.62). This complex is characterized by Reşadiye collapsed cone in Figs. 3.3, 3.8 and 3.15, Incekaya collapsed cone in Figs. 3.13 and 3.14 and some collapsed cones in Figs. 3.5, 3.9 and 3.16. It seems that active magmatic intrusions seen in these seismic sections are a secondary or parasitic continuation of these peripherally collapsed cones. This shows a close relationship to Quaternary volcanic centers (Nemrut volcanic dome complex) and to the traces of the margin boundary faults in W and S. Magmatic intrusion in Tatvan delta subbasin at SW-corner is the best example of this relation (Fig. 3.13). The present magmatic intrusions have given rise to trails of earlier volcanic edifices (collapsed dome-cone complex), which extend towards W-E on coastal line of W- and E-segments (Fig. 3.62). The W-E displacement of active and passive volcanic centers with time is attributed to dextral transtensional movement along S-margin, probably during the Quaternary.

In detail, as has been pointed out in the preceding account of local areas along this fault, volcanic centers are often located in step-overs and in releasing bends where they are associated with normal component of faulting and the formation of transtensional sedimentary basins (Tatvan delta subbasin, Deveboynu and Varis spur zone subbasins) (Fig. 3.62).

Along the coastal line of W-segment, collapsed parasitic cones with the steep walls due to strong erosion represent fossil eruptive vent systems (passive), enlarged by collapsing and erosion. Higher-angle dome/cone topography constitutes paleo-volcanic pile and extends into lake. Some of the fossil dome/cone complex submerges into the lake, resulting in the very irregular and eroded coastal patterns (see W-segment in Fig. 3.62). In W-segment, active and younger ones of these fossil intrusions are well imaged by seismic data (Figs. 3.13-3.15). Both passive and active magma intrusion complex seem to extend parallel to an axis of suture trend. Such a linear elongation of active and passive magmatism along S-marginal section of the lake suggests a complicated pattern of fracture-fissure system in and along Muş suture. As seen in Fig. 3.13, Tatvan delta subbasin at SW-corner is cut by oblique-slip en echelon faults, parallel to the Muş suture trend (also see Fig. 3.14). This indicates that the locations of these magmatic features are controlled by dextral transtensional movements in the basement. At this level, extensional normal faulting is probably dominant.

As seen in Fig. 3.62, the apparent close relationship between the traces of S- and W-margin boundary faults and the distribution of the volcanic centers has led to the suggestion that there is a genetic relationship between faulting and volcanicity (Barber and Crow, 2005). The suggestion is that the generation of basaltic magmas in the upper mantle and their intrusion into the upper crust has formed a weak zone of ductile material (ductile shear zone). This zone extends from the upper surface of the lower crust to the basin, along which the shear component of strain partitioning has been focused. In the upper crust, fractures and fissures related to the fault zone (volcanic vents and conduits) provide channels for the passage of magmas to the surface to construct volcanic edifices. This relationship is as close as first appears in the margin boundaries. Extensional volcanic fissures and strike-/oblique-slip faulting, volcanism does usually coincide with the active fault zones (Fig. 3.62). It should be pointed that the active volcanic centers are much younger than the

initiation of the active fault traces. It is conceded that the location of the fault zones may have been controlled by earlier Plio-Quaternary volcanism. It seems that the recent relationship between active faults and modern volcanoes is not co-genetic but coincidental and their relation to the faulting is given by the map view in Fig. 3.62. The relationship between the boundary faults and the magmatic intrusions also evident that magmatism is made of extensional intrusions, representing surface manifestation of underlying magma chambers. This suggests that active volcanic centers and intrusions are the loci of high magnetic anomalies and grouped around aeromagnetic anomalies that intersect the fault zones (see similar models developed for Sumatra active continental margin by Barber and Crow, 2005 and Keskin, 2007; Şengör et al., 2008).

A prominent linear elongation of magmatic intrusions along S-margin suggests that en echelon arrangement of transtensional faulting forms the loci of off-axial magmatic eruptions, parallel to an axis of suture trend (Fig. 3.62). This reveals that S-margin boundary fault is the site of massive outpourings of basalts (Şengör et al., 2008). The W-E trending axial zone (PDZ) along S-margin is presumed to be extensions of subaerial fissure-fracture or fault-controlled plateau basalts located on the margins of the lake. Quaternary centers of volcanic dome-cone complex and newly intruded magmas are aligned along the major extensional zones, which comprise the lake. It is considered that further injections occur along secondary faults, which trap rising magma at their points of intersection with the primary faults. Transtensional faults and extensional spaces (vents, fissures or fractures) along a broad zone of these intrusions suggest that magma can erupt rapidly to the surface along faults if they cut deeply enough through the crust. Block model seen in Fig. 3.64 illustrates such a structural case. In this manner, it is assumed that the pre-existing faults may completely or partially trap the propagating magmatism. Since, multiple zones of intrusions may be a common phenomena along newly inverted margins of the lake. Multiple zones of magma entrapment might occur within any number of pre-existing faults associated with compressional ramp basin formation of the lake. The net effect on the lake bottom would be the appearance of multiple parallel zones of magma intrusion creating a broad-diffuse margin boundary in S. This entrapment model is further complicated by changing stress fields and/or kinematic boundary conditions due to the reorientation of margin boundary faults.

A correlative interpretation of the map view in Fig. 3.62 and block model section in Fig. 3.64 clearly shows propagating magmatism and its interaction with pre-existing boundary faults and thus, implication of tectonic controls on magma movements and intrusion-eruption locations. This clarifies that S-margin boundary fault as a suture-parallel magmatic margin, is W-E trending magma supply path, through which magma propagates, disperses into the lake and localizes in the faulted margins.

4.2.2 Magma propagation dynamics into the S-shear zone

Seismic reflection profiles demonstrate that the younger magmatic intrusions onshore and offshore S-margin and associated collapsed parasitic dome-cone complex on S-shores are related to open tension fracture zones serving as conducts for the magma (Figs. 3.3, 3.5, 3.8, 3.9, 3.13-3.16, 3.18 and 3.26-3.29). These sections show that magma actively propagates and intrudes into transtensional shear zone in S-margin and related subbasins (Fig. 3.62). This argues that these isolated volcanoes or magmatic intrusions are rooted on geometrical discontinuities associated with strike-/oblique-slip faulting in S- and W-margins. Along these margins, extensional component of the oblique faulting simply provides fractures that enable magma to reach the surface or wherever the associated localized extension exists. It is considered that relatively low viscous magmatic activity densely generates ductile network system of underneath the SW-corner and S-margin of lake.

According to the map view of magma distribution pattern shown in Fig. 3.62, regional digital elevation maps are presented and compared with deformation styles, faulting pattern and magma distribution in the lake, as seen Figs. 4.1 and 4.2. These regional maps show a general pattern of faulting and magmatic relations of Muş-Lake Van basin in 2D- and 3D-morpho-tectonic views, compared to Fig. 3.62. Figs. 4.1 and 4.2 show regional distribution and localization of active and passive (collapsed) volcanic centers, fault and magma propagation from Muş basin in W to Lake Van in E. In these maps, consideration of the volcanic centers, fault and magma propagation along with the structural complexities well explains seismic structural observations, derived faults, and active magmatism in Fig. 3.62. It is clearly observed in these maps that extensive magmatism shows a localized feature in and along Muş-Lake Van basin and localized zones of magmatism and its propagation are controlled by margin-bounding faults. This shows a clear evidence of extensional-transtensional basin development associated with propagating magmatism such as central Tatvan

basin, Tatvan delta subbasin in W, Deveboynu and Varis spur zone subbasins in E (Fig. 3.62).

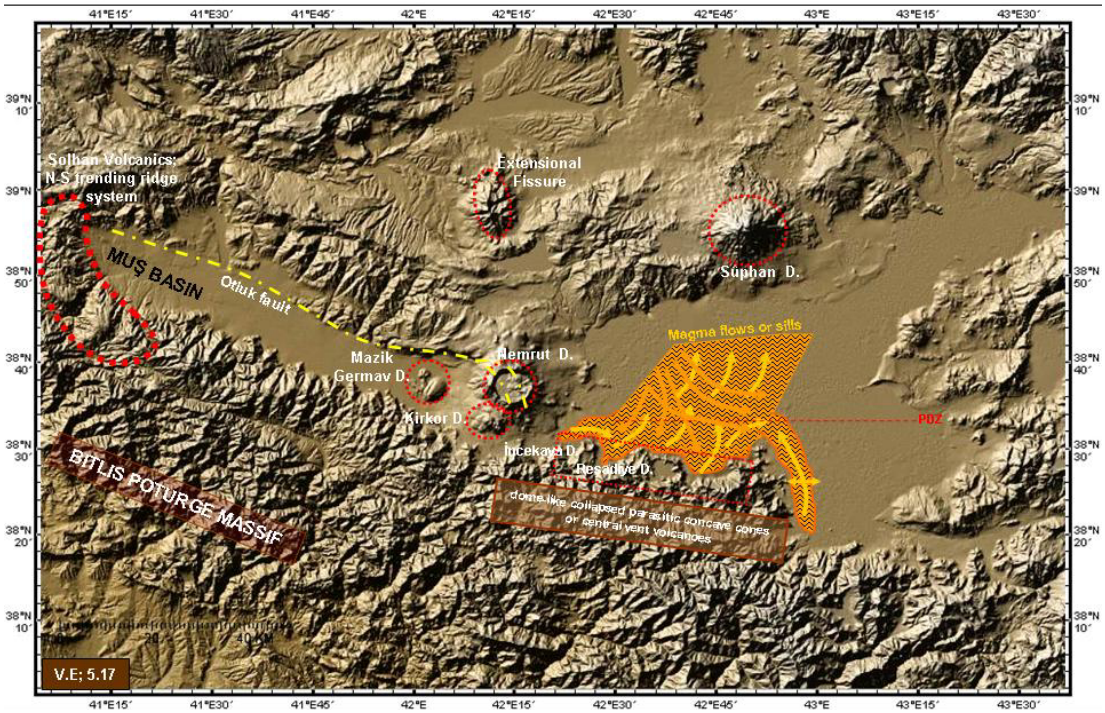

Figure 4.1 : Digital elevation map of Muş-Lake Van region shows the main volcanic provinces, active dome-cone complex around Nemrut volcano and collapsed parasitic cones in S-coast of the lake (W-segment). Rhomb-like area in center of the lake (orange) roughly indicates extensive lateral distribution of magmatic flows or sills in central Tatvan basin, Deveboynu and Varis spur zone subbasins. Orange arrows represent the flows from W-margin boundary and yellow arrows represent the flows from S-margin boundary (W-segment) and subbasins in SE-delta. N-S trending ridge system, Solhan volcanics, is shown in W-end of Muş basin (Şaroğlu and Yılmaz, 1986). Note that N-margin boundary fault of Muş basin is dextral normal oblique Otluk fault, accommodated in Nemrut province (see Dhont and Chorowicz, 2006). Red dashed line across the S-section of the lake is PDZ of S-margin boundary fault.

As clearly seen in active and passive volcanic dome-cone complex from Figs. 4.1 and 4.2, the low viscous magmatic flow seems to migrate from underneath the Nemrut-Krikor-Mazik Germav dome complex into the SW-corner of the Tatvan basin throughout S-margin boundary fault, parallel W-segment (Incekaya and Reşadiye collapsed cones). It continues to propagate, around offshore Deveboynu peninsula, toward the further S into SE-delta. A further evidence of the propagation is recognized along collapsed dome-cone complex in S-coasts. A correlative interpretation of the map views in Figs. 3.62, 4.1 and 4.2 shows that W-E trending magma propagation covers all along Muş-Lake Van basin.

This long-standing way of the propagation extends from Nemrut extensional fissure zone, even from the further W, area of Solhan volcanics (Şaroğlu and Yılmaz, 1987 and Yılmaz et al., 1987) along the S-portion of lake, parallel to Muş suture. This way characterizes the longer fracture-fissure zone of active magma propagation from the further W (Solhan volcanics) to the further E (Çarpanak spur zone). The fracture-fissure or fault system is accommodated in a more complicated way by horse-tail patterns at Nemrut-Krikor en echelon dome complex. This fault system continues to propagate, extends toward SW-corner of the lake, and accommodated by en echelon faulting in S-margin (W-segment). Then, probably it continues toward the further E. This fault system is interpreted as "Otluk fault" of Muş basin, which is dextral normal oblique-slip fault and consistent with S-margin boundary fault (examine maps from Dhont and Chorowicz, 2006). Otluk fault is, in some way, connected into a complex, discontinuous fault system in and around SW-corner of lake.

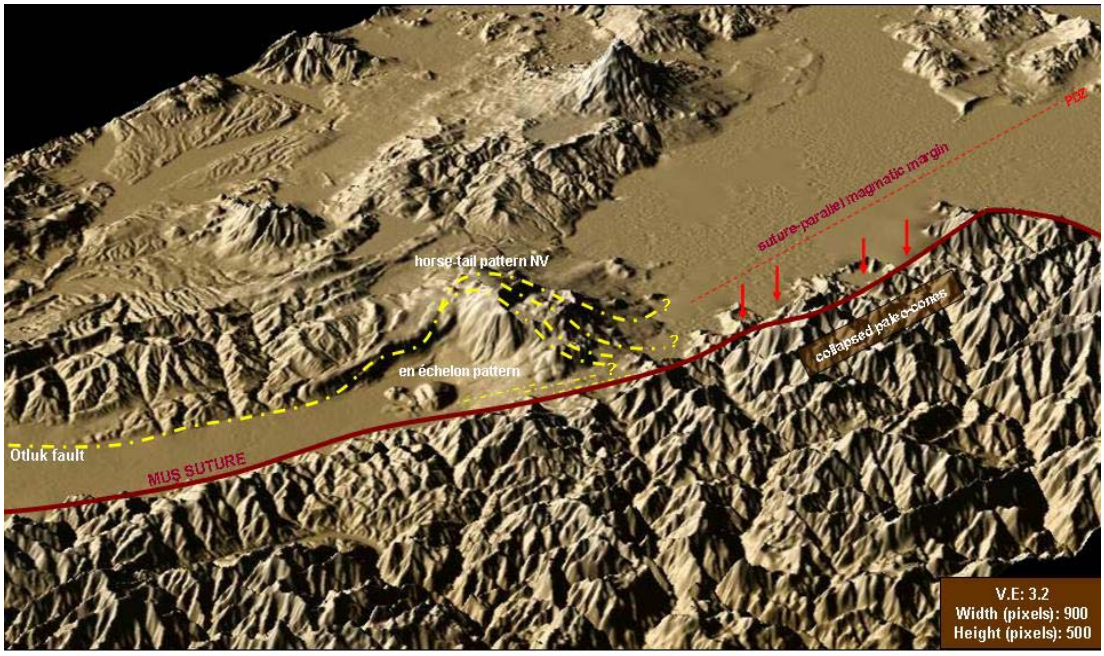

Figure 4.2 : Perspective view of the map seen in Fig. 4.1 shows morphological details of Nemrut volcanic province and collapsed dome-cone complex in S-coast of the lake (W-segment). En echelon faulting in Nemrut province is observed in the field study. Otluk fault is terminated as horse-tail pattern in Nemrut volcano. Red arrows show collapsed dome-cone complex in S-coast of the lake. Brown line represents Muş suture. Note that PDZ of S-margin boundary fault (red dashed line) seems to be an axis of suture-parallel magmatic margin.

It seems that the fault and magma propagation pattern from W (Muş) to E (Lake Van) through S-margin boundary represents a broadly widening, en echelon shear zone of transtensional system (see and examine negative flower structure in Figs. 3.39 and Number 1 in 3.40). This shear zone forms an excellent tectonic emplacement for suture-parallel magma propagation, initially through Muş suture and lately, into central Tatvan basin (Fig. 4.1) and controls tilted geometry of central Tatvan basin, active magmatism and also earthquake potential of lake. As also recognized in Fig. 3.62, magma propagation and intrusion activity along transtensional faults in W- and S-margins (W-segment) has a close relationship with tilted, asymmetric structure of central Tatvan basin. This indicates that strike-/oblique-slip faulting has played an important role in focusing magmas by generating localized extension and transtension beneath the lake (also see Dewey et al., 1986 and Pearce et al., 1990). Magmatism is shown to be common to this kind of deformations taking place on both regional and basinal scales. It is considered that magmatism prevails on all scales of extensional fault propagation in basin margins. As a result, magmatic intrusions are commonly developed in the faulted margins and magmatism is distributed widely in central Tatvan basin, especially in the subbasin formations in W- and E-ends of S-margin boundary fault (Fig. 4.1).

Overall distribution and deformation patterns of widespread magmatism show that magma initially propagates into the S-shear zone, from the further W and then, upward magmatic transport is densely localized in the faulted margins. Magma propagation is concentrated through the fault discontinuities and these discontinuities generate localized extension and transtension in margins, resulting in focusing magmas across zones of the faults. Then, fault-controlled flow of magmas is channelized in margins and dispersed into central Tatvan basin. S-margin boundary fault has a primary structural role controlling and localizing magmatic activity, rather than W-margin boundary, due to its being parallel to Muş suture. Because, propagating magma initially localizes in S-margin, then migrates from S toward NNW and lately localizes beneath central Tatvan basin. This reveals that the faulting characteristics of S-margin boundary (negative flower structure) form the compatible shear zone, implying the suture-parallel magma supply path and the main feeder zone of magmatism. Strike-/oblique-slip deformation pattern indicates some clear implications of structural controls on magma movements, eruption locations in basin

margins and focusing magma such as multi-directional mass transport and radial mass dispersion. Transtensional activity in S- and W-margins shows a critical role of strike-slip faulting in an oblique-slip basin in focusing magmas on the lake, as observed in similar focusing magmas on pull-apart basins, the Erzurum-Kars Plateau, the N of the Lake Van region by Keskin et al., (1998). Cooper et al., (2002) suggested a similar model for the origin of mafic magmas beneath the NW-Tibet and argued that magmas might have been created by mantle upwelling beneath the releasing bends of the strike-slip fault systems.

Seismic images of rising magma show the evolutionary stages of magma development across S-margin, indicating that some is at incipient stage and collapsed, while some is still intruding and dispersing (for example, Figs. 3.13-3.15). Hence, seismic structural configurations of magmatic intrusions, such as parasitic fissure volcano (PFV) and central vent volcano (CVV), are compared with 3D-morphological views of passive and active dome-cone complex in and around Nemrut volcano and on the S-shores of the lake (Figs. 4.1 and 4.2). This gives a clear image of structural relations between active and passive-collapsed domes.

Some topographic profiles over the dome-cone shaped landforms are obtained as shown in Fig. 4.3 (see the different views of their locations in Figs. 4.1 and 4.2). GeoMapApp Java script software program (SRTM data base management) is used in order to calculate the elevation (m), x- axis, and distance (km), y- axis, to plot the topographic profiles of these domal structures and to compare their structural styles with seismic similarities in reflection data. In Fig. 4.3, topographic profiles plotted extend from Mazik-Germav Dome (active dome, elevation 250 m) to Kirkor Dome (active dome, elevation 600 m) and Kirkor Dome to Incekaya Dome (peripheral collapsed cone, elevation 350 m) and their 3D-digital elevation model views are recognized. Based on lacustrine sediment velocity with 1700 m/sec, parasitic fissure volcano (PFV) is approx. 360 m in height and central vent volcano (CVV) is approx. 420 m in height. If these values are averaged in meters, due to seismic velocity effects, then the heights are, at least, more than 350 m. These values are in a good agreement with, for example, Incekaya Dome, peripheral collapsed cone (350 m), and Mazik-Germav Dome (250 m). This suggests that dome-cone complex in and around SSW-onshore and magmatic intrusions have the same genetic relationship and that they are originated by tectonic and magmatic processes, affecting the lake.

Seismic and morphological similarities between passive/active dome-cone complex and intrusions aligned in S-margin show that magma chamber-related pointed stocks or point sources are probably prograding into central Tatvan basin from S-margin (Fig. 4.1). Thus, they are continually feeding back magmatic activity.

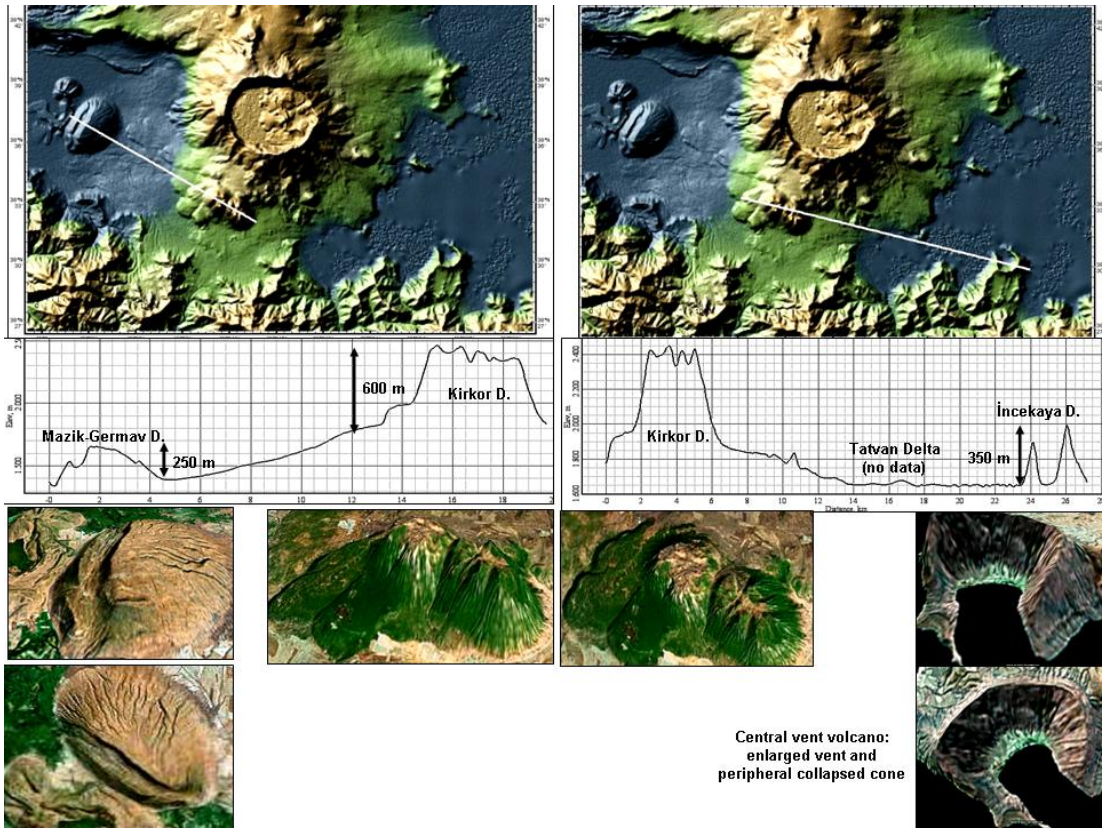

Figure 4.3 : Topographic profiles of dome-cone complex in and around Nemrut province and their 3D-morphological views shown from Mazik-Germav D. to Incekaya D. Vertical axis is elevation in m and lateral axis is distance in km. Note that Incekaya dome (350 m) is a peripheral collapsed cone and enlarged vent (bottom right corner).

Passive vents, Incekaya, Reşadiye domes and coastal landforms of collapsed ones, are often enlarged by the peripheral collapse of their walls and then, subside below lake level. This collapsing forms a peculiar coastal morphology of the deeply eroded dome-cone complex in S. The younger active ones, similar to magma intrusions in the lake, are Mazik-Germav, and Kirkor active domes. These are formed by the solidification of magma, resulting from repeating intrusions at the location. A prominent and linear elongation of active/passive dome-cone system suggests a complex relation between S-margin boundary and magmatic activity, implying that S-margin boundary fault (PDZ) is a dynamic feature, superimposed in Muş suture. This case is very distinct from coastal irregular and steeper morphology of W-

segment and S-coasts. As recognized in Figs. 4.1 and 4.2, W-segment represents the steeper coastal morphology caused by the fossil magmatic activity. This activity probably occurred somewhere in Quaternary, deactivated and some collapsed below the lake level. Then, new ones appeared in the lake (Figs. 3.13-3.15). Magmatic events, collapsing-deactivation and intruding-reactivation, are clearly observed along the S-ends of seismic sections across central Tatvan basin. Seismic images of this sequence of magmatic events significantly indicate that magmatism is continually fed back from point sources, preferentially aligned and emplaced at S-margin boundary. This shows that magmatism is younging toward N (Tatvan basin) from S (W-segment) and also toward the further E (E-segment) from the further W (Solhan volcanics) (Fig. 4.1). This finding points that suture-parallel marginal nature of S-margin boundary is, indeed, the main magma supply path and the feeder zone. As indicated in Figs. 4.1 and 4.2, the horse-tail termination of Otluk fault in and around Nemrut volcanic dome complex extends to SW-corner of the lake, Tatvan delta subbasin and into W-segment. Morphology and structural style of this fault pattern seems to be a continuation of S-margin boundary fault, toward the further E (E-segment).

In and around Nemrut volcanic complex and Lake Van basin, a number of parasitic collapsed cones, active domes and magma intrusions are indicators of the tectonic strain regime (Nakamura, 1977 and Dewey et al., 1986). The emplacement of these volcanoes and intrusions is related to local scale tectonic structures such as tension fractures (Chorowicz et al., 1997; Korme et al., 1997; Dhont et al., 1998b) or open faults (Cello et al., 1985; Chorowicz et al., 2001). The map views in Figs. 3.62, 4.1 and 4.2 indicate that the volcanic edifices form a pattern of elongate volcanoes or linear clusters of adjacent volcanoes. Such a structural continuity of the volcanoes implies that a curvilinear fracture zone through a main fissure line trends from Nemrut volcanic complex toward S-margin boundary and SE-delta. It is inferred from the geometry of these vents that they are ordinary vertical open fractures to deduce the local strain from their orientation. It is obvious that distributional pattern of magmatic intrusions within lake and an area of collapsed dome-cone complex in S-coasts are rooted on geometrical discontinuities associated with strike-slip faulting (see Fig. 3.62). Thus, passive and active intrusive-extrusive activity of magmatism is linked to transtensional regimes in S-and W-margins.

The evidence for this comes from the derived faults mapped by Adıyaman et al., (1998) in E-Turkey, indicating that the faults are only related with active volcanoes. As similar to faulting pattern and deformation style of the lake, volcanic edifices and related magmatic activity are also found in releasing-bends (Kandil volcano) and pull-apart (Süphan volcano) basins and at horse-tail terminations (Nemrut volcano) by Dhont and Chorowicz, (2006). Similarly, the observed magmatic intrusions are related to open tension fractures serving as conducts for the magma and the emplacement of the volcanic vents, fissures or fractures are related to faults, especially in extensional relay zones (Fig. 3.62). Passive-collapsed and active magmatic intrusions observed in and along W- and E-segments are rooted in a transtensional zone that opened in a right-stepping offset of the S-margin boundary fault. This is, for example, the case for the Süphan volcano. This volcano is also rooted in a transtensional zone that opened in a left-stepping offset of the Süphan fault. The Kandil volcano is another volcanic vent related to a tensional structure. Kandil volcano is located at the curvature between the E-trending Ağrı and NW-trending Hamur right-lateral faults. This volcano probably occupies a releasing bend opening. Some other edifices are elongate vents located in the plateau, reported by Dhont and Chorowicz, (2006). These are in a similar way to that described in Iceland (Chorowicz et al., 1997) or in Central Anatolia (Dhont et al., 1998b) (see Dhont and Chorowicz, 2006 for a wide-range morphological description of these structures).

The structural and morphological relationships between the boundary faults, magmatism and Quaternary volcanism in and around the lake suggest extensional magma propagation into the S-shear zone that is suture-parallel magmatic margin. The deformation activity of magma propagation is extended into central Tatvan basin. It is often found that a direct relationship between transtensional regime and younger magmatism in and around the lake appears to be a result of active tectonic and magmatic evolution of the lake, mostly during Quaternary. Seismic structural interpretation and morpho-tectonic structure of the lake and surrounding volcanic areas indicate that the observed magmatism is mainly triggered by deformational events at upper crustal depths and, hence driven by thin-skinned crustal magmatism and extensional magma propagation. Thin-skinned crustal events are thought to have acted as magma propagation channels and these events prevail on both regional and basinal scales, due to the strong differentiation of the anisotropic, thin and weak

convergent crust during Quaternary episode. For example, SSW-marginal section of the lake forms very critical weakness zone, where no mantle lid exists (Şengör et al., 2003) and moho thickness has a lowest value (Zor et al., 2003 and Şengör et al., 2008).

4.2.3 Magmatic implications for the elastic lid model

Seismic sections clearly show that magmatic intrusions are not formed by a group of single intrusions, rather, repeating intrusions occur in the faulted margins and magmas are solidified after repeated intrusions. This suggests that the magma pathway beneath S-margin (as a main source) has likely been the same during different intrusive-eruptive episodes. The rising magmas along S-margin are blocked by a cap of stiff rocks, but then find a way to reach the surface at the present location of the summits. Combining these results with locations of passive dome-cone complex and active intrusions in the map views through margin boundary faults (Figs. 3.62, 4.1 and 4.2) suggests that tectonic and structural controls implicate on magma movements, intrusion-eruption locations from the main magma supply path in S-margin. It is generally believed that the dome-cone complex in and around Nemrut area (Fig. 4.3) is extruded during Plio-Quaternary, ejected from Nemrut volcano (Kurtman et al., 1978). Then, magma is propagated into the lake, extended into central Tatvan basin and recently formed prominent magmatic intrusions. The dense concentration of younger volcanic domes, collapsed cones and active intrusions is a strong indicator of intensive tectonic movements, particularly in S-margin boundary. This suggests that tectonic and volcanic activities are abundant in Plio-Quaternary.

Regional and basinal interpretation of the map views shown in Figs. 3.62, 4.1 and 4.2 leads to a refined model of tectonic controls and magmatic events in the lake. This model is based on the elastic lid shown in Fig. 3.64 and hence, magmatism in the lake is considered within this context. The elastic lid model is superimposed on overall distributional pattern of magmatism shown in Fig. 4.4. The block model section in Fig. 4.4 provides a more clear illustration of superimposed tectonic and magmatic processes in the lake. In this model, both suture and magmatic trends along S-margin are parallel to each other, magma covers entirely central Tatvan basin and the fault discontinuities (see Dewey et al,. 1986 for the elastic lid model). Such a model section suggests that the factor of elastic lid controls magmatism and its

distribution in the lake. In other words, structural and marginal configurations of magmatic intrusions are strongly controlled by upper crustal block motion. This also evident that tectonic positions, structural configurations, morphological shapes of magmatic intrusions and their elongation along margin boundaries are controlled by flaking of the elastic lid (Dewey et al., 1986).

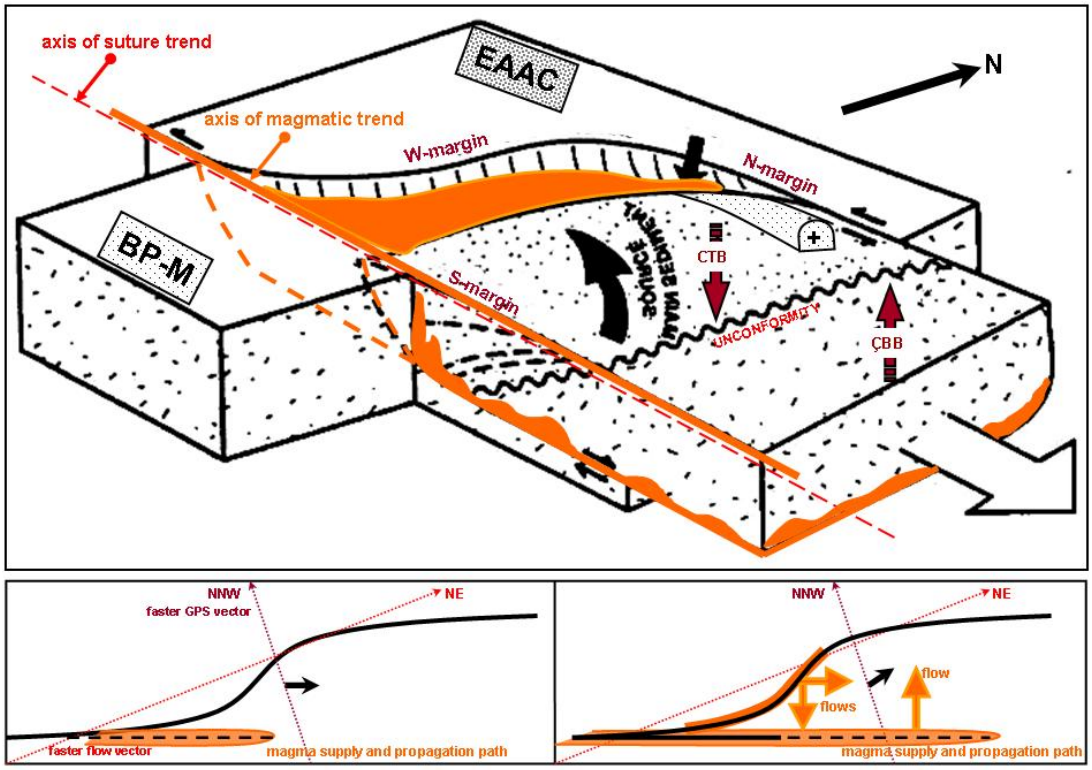

Figure 4.4 : 3D-block model section of magmatism (orange colour) in Lake Van shows the structural relations between fault-bounding margins and overall magma propagation. Note that axis of suture trend is parallel to that of magmatic trend across the PDZ of S-margin boundary fault. ÇBB: Çarpanak basement block (uplift) and CTB: central Tatvan basin (subsidence). Small inset diagrams illustrate simplified deformation geometry of the lake and show the vector relations of anisotropic effects in the lake; NNW-faster GPS vector, NE-faster flow vector of asthenosphere, magma supply and propagation path (thick orange line), parallel to suture trend and lateral wedging of the lake (black arrow) at the left. Then, magma supply and propagation entirely cover suture axis, PDZ of S-margin boundary fault and W-margin boundary (thick orange lines) and extensive magma begins to flow into the deep central basin (orange arrows) at the right. Note the vector relation between shear-wave anisotropy and dextral oblique motion of the lake (black arrow) (also see and examine Fig. 3.64).

As interpreted in Fig. 4.4, dense intrusive-extrusive activity of the rising magmas is more localized effect in margin boundaries than ever expected. This gives a possibility that rapid and localized stretching of the crust also affords an explanation for localized zones of magmatism and magma chambers beneath the lake.

The shallower and deeper sections of the magma chambers are also reported in a study of geochemistry and heavy mineral contents from tephra deposits of lake by Jung et al., (1978).

As illustrated in model section of Fig. 3.64, the segmentation of the thinned crust causes the upper crustal flakes that are upper high-strength layers or elastic lids (Dewey et al., 1986). A wide variety of detachment surfaces is also possible within these flakes (Dewey, 1982 and Dewey et al., 1986). Hence, these flakes are the surface expression of thin upper-crustal sheets above intracrustal décollements. As shown in the model section from Fig. 4.4, these detachment surfaces are, in fact, crustal magma traps, through which magma flows as lateral sheets and forms upper crustal magma chambers or point sources. Basin-bounding faults are boundaries of upper crustal flake moving over a detachment surface located at the shallow brittle-ductile boundary (10 km) supported by Dewey et al., (1986). Faulting and deformation style in Fig. 3.64 and distributional pattern of magmatism in Fig. 4.4 clearly show that the lake is a detached oblique flake basin or elastic lid, trending to rotate above ductile shear zone (see and examine similar flake basin model from Dewey et al., 1986). Elastic lid or flake detachment, especially where rotations about vertical axes occur, leads to complicated compatibility problems at flake margins (Şengör et al., 1985; Dewey et al., 1986) and thus strain compatibility holes and gaps. These holes and gaps are filled with rising magmas. In terms of magmatic potential energy beneath the lake and its squashy basement (Dewey, 1969b; Şengör and Yılmaz, 1981), the lake has a key role of the incoherent, rhomb-shaped basin bock tectonics proposed by Şengör et al., (1985) and the resultant extensional magmatism. This requires an oblique motion of the upper crustal flake basin above magma-genetic ductile shears (Fig. 4.4).

The critical one of magmatic implications for the elastic lid model is related to a prominent location of S-margin boundary fault that is superimposed feature on suture trend. En echelon pattern of discontinuous faulting in and around Nemrut area gives a clear evidence of horse-tail termination toward SW-corner of the lake (Figs. 4.1 and 4.2). There are indications from the field observations and also Wong and Finckh, (1978) that these smaller faults constitute a complex en echelon system into the lake and form a continuation of S-margin boundary fault, traced on land. Hence, it is considered that the curvilinear elongation of volcanic dome-cone centers from

Nemrut area into Deveboynu and Varis spur zone subbasins is due to either pre-existing weakness zone (Muş suture), or a through-going fracture zone in the delaminating plate along Muş suture such as Suture-Fracture zone (see model sections in Şengör et al., 2008). This weakness zone is probably responsible for the extent, the intensity and propagation of the rising magmatic materials along S-margin boundary fault and its segments. Since, it is stated that the subducted mantle lid is delaminating and breaking off into the mantle at a higher angle, so that the depth at which magmas are generated (38 km thin crust) is displaced towards the E of the lake (Şengör et al., 2003 and 2008). This shows that rapid lithospheric stretching and even small-scale delamination beneath the lake can easily generate decompressional partial melting in the upwelling mantle and thus, extensional alkaline magmatism along axes of suture and magmatic trends is extended into the further E of the lake (E-segment and SE-delta). Both tectonic and magmatic implications for the elastic lid model in Figs. 3.64 and 4.4 propose that magmatism and related products have been initiated by tectonic and thermal response of accretionary wedges beneath the lake to the doming hot asthenospheric front along basal detachment surface. This argues that the pre-existing basin-bounding thrust faults of Lake Van Dome are reactivated, kinematics of margin boundary conditions are changed and thus, basin is structurally inverted and adapted to a new stress regime at upper crustal levels during post-collisional period.

4.3 Basinal Dynamics of Hydrothermal Deformations

Extensional magmatism in Lake Van forms extensive magma-hydrothermal deformations, effects deformational pattern of lacustrine deposition and hence, deep basin sediment dynamics. This proposes dynamic interaction of magma-sediment mixture from basin-bounding faults across central Tatvan basin. Magma-related sedimentary deformation styles are the most prominent images in seismic data and different from soft sediment deformations recognized in NE- and SE-delta settings. Magma-induced sediment deformations are perfectly illustrated by a wide range of seismic images, showing hydrothermal alterations, alteration zones, related fluids and volatiles (Figs. 3.3, 3.5, 3.6, 3.8-3.11, 3.13-3.16, 3.18 and 3.26-3.29). The wide range of seismic images illustrates hydrothermal interaction of magma-sediment mixture and thus, evidences basinal dynamics of complex magma-sediment

deformations (see central Tatvan basin in Fig. 4.1). Based on this brief review of magmatism and its basinal distribution, evaluation of seismic reflection profiles considering the map views shown in Figs. 3.62, 4.1, 4.2 and 4.4 and hydrothermal deformations leads to the following interpretations.

Deep basin lacustrine sedimentation is sequentially interrupted by major hydrothermal phases (a series of sill events) of rising magmas through margin boundary faults. These phases are shown to be common to deformations taking place on each depositional scale. Consideration of hydrothermal mechanisms along with the structural and sedimentary complexities well explains basinal dynamics of hydrothermal deformations and related deformational styles across central Tatvan basin. Hydrothermal activity is manifested by a series of magmatic intrusions, prevailing on all marginal sections, directionally extended into deep central basin and deeply penetrated into depositional sequences and facies. It is often considered by examining seismic sections and interpreting the maps that magma bodies or magma chambers beneath the lake are dynamic systems, interacting with the unconsolidated lacustrine sediments. This argues that a magma body that resides at shallow levels beneath a volcanic complex is not static, it is in dynamic interaction with its surrounding sedimentary environment. This sedimentary interaction is the main source of hydrothermal deformations and basin dynamics. As a result of this, many fascinating phenomena, including volcanic gases, hydrothermal systems on coast and under the volcano-tectonic lakes, are observed (Delmelle and Stix, 2000 and Delmelle and Bernard, 2000). These interactions releasing gases and magmatic materials may be mostly seismic (Toker et al., 2007; Toker et al., 2009a, b).

The compositions of the gases are controlled by factors such as their solubilities in magma, the temperature and pressure at which they reside, the infiltration of surface waters (depositional pore water), and the geodynamic and tectonic setting of the volcanic environment (Delmelle and Stix, 2000). Sudden release of gases from rising magmas may cause rapid movements of the molten rock. When the magmatic gas traveling upward encounters water, lake water or groundwater (meteoric water) in an aquifier, it can be rapidly fragmented and steam is produced. Latent magmatic heat can also cause meteoric waters to ascent as a vapour phase. The rapid expansion of gases is the driving mechanism of most volcanic activity, debris flows and turbidities (Figs. 3.13 and 3.14). By analogy with shallow geothermal systems, volcanologists

have proposed a model for transferring heat and water from a degassing magma to a lake above it (Delmelle and Bernard, 2000). According to degassing magma and transport model, it is assumed that beneath the lake, a two-phase vapor-liquid zone is formed as high temperature magmatic gases condense into groundwater. Heat pipes or vapor-liquid counterflows may play an important role during heat transfer in the two-phase zone. Beyond this zone is a comparatively cool liquid envelope (Delmelle and Bernard, 2000). It is thought that the hot gas-water mixture is probably injected into the lake as a buoyant jet that powers wholesale convection of the water column, thus allowing for both thermal and chemical homogeneity. Seepage of the lake water through the lake floor and recirculation within the subsurface gas condensation zone probably complicate this picture and can be important components of the lake's hydrologic budget (Kempe et al., 1978; Delmelle and Bernard, 2000; Delmelle and Stix, 2000).

Based on active hydrological system of Lake Van basin (see hydrographic and isotopic data in Kempe et al., 1978; Kurtman and Başkan, 1978 and Faber, 1978), unconsolidated sediment thickness, sediment deformations and extensive magmatism, magma-hydrothermal system and related magma-sediment dynamics is well recognized across central Tatvan basin. Seismic structural picture of deep basin magma-hydrothermal system argues that, as ground waters percolate through a faulted, permeable volcanic edifice (Figs. 3.6, 3.11 and 3.13), they encounter a heat source, normally magma and hot rocks. The interaction of the water and the magma creates convection cells whereby hot water is circulated within a permeable zone (Delmelle and Stix, 2000). Hydrothermal system is created by interaction of waters with magmatic materials and hot rocks, forming impressive manifestations at the surface. These manifestations are clearly imaged by seismic reflection data (Fig. 3.9 as an example). Tectono-magmatic model proposed for the lake seen in Fig. 4.4 shows that the lake is an obliquely opening block system, followed by extensional magmatism from the main shear zone in S-margin, through which magma actively propagates into central Tatvan basin. The magma that is generated serves as a heat source. Lake and/or depositional pore water percolate into the faulted, fractured layers and is heated by the magmatic source, setting up hydrothermal convection cells.

As the heated water circulates, it dissolves rock and results in hydrothermal alteration zones in both sides of intruding magmas (Figs. 3.6, 3.8-3.11, 3.13-3.16, 3.18 and 3.26-3.28).

4.3.1 Magma-hydrothermal degassing system of Tatvan province

General seismic and structural picture of magma-hydrothermal system in central Tatvan basin is compared with the preliminary results of the previous hydrological analyses (see and examine hydrographic and isotopic data in Kempe et al., 1978; Kurtman and Başkan, 1978; Faber, 1978 and Degens and Kurtman, 1978 for full review of thermal and mineral waters). For this, model studies of isotope geochemistry (Kipfer et al., 1994; Keskin, 2003; 2005 and 2007) and extensional alkaline/ultra-alkaline magmatism (Şengör et al., 2008 for decompressional partial melts) are also taken into account. Helium isotope studies of Kipfer et al., (1994) in the lake and their postulation is not only supported by geochemical observations of Kempe, (1977) and Wong and Finckh, (1978), but also confirmed by Keskin., (2003 and 2005). These studies briefly state that Helium gas associated with the CO_2 has $^3He/^4He$ values (Kipfer et al., 1994), clearly showing the mantle-derived nature of the gas in the lake.

Magma-sediment mixture-related deformations in deep basin lead to a dynamic activity of the rising magmatic materials and its associated hydrothermal system. Since, as well known, certain constituents of volcanic gases may show very early signs of changing conditions at depth, making them a powerful tool to understand deformations. It is considered from the map view in Fig. 3.62 that the diffuse gas emissions are concentrated along the margin boundary faults associated with open vents, fissures, or extension fractures. Seismic sections well evidence that, along fault-bounded margins of the lake, there is a clear understanding of the complexity of the conduits, fractures, and other pathways such as fissures that channel gas to the surface. Some clear examples are given by seismic images seen in Figs. 3.8-3.11, 3.13-3.16, 3.18 and 3.26-3.28. These seismic sections indicate that the magmatic gas release (CO_2) is related to magmatic intrusions, to faulting of basin margins, to fracturing of conduits above an older or younger magma body (magma chambers). Gas release is also related to shaking and release of CO_2 bubbles from a magma chamber, triggered by seismicity (Delmelle and Stix, 2000 and examine seismogram data in Horasan and Boztepe-Güney, 2006). As expected, hydrothermal activity

regarding this style of degassing is mainly generated by extensional and transtensional strains and decompressional magmatism beneath the lake.

Magmatic degassing and fluids; margin boundary faults are zones, on which magmatic degassing and fluids prevail, even on nearby transpression of N-margin (Fig. 3.6). Degassing and fluid regime of rising magmas through boundary faults are extended into central Tatvan basin and intercalated with depositional sequences.

Dynamic interaction of magma-sediment mixture and its seismic expressions propose a reasonable lacustrine model of how diffuse gases are transported through the flanks of a magma and of how they laterally deform the sedimentary sections. Seismic results serve to constrain a model for the physical structure of magma-hydrothermal system in the lake. According to this model, upward, low density, magmatic mass transport strongly dominates in extensional and transtensional deformation zones of the lake (Fig. 3.62). A column of gases released by a rising magma body at depth is surrounded by an envelope of hydrothermal water and vapor in the sediments and thus, magmatic gas pressures build up in the conduit. Deep magmatic gases interact with shallow hydrothermal fluids surrounding the conduit of rising magmatic fluids. The lacustrine contaminant may be the lake water that directly enters the magma-hydrothermal system at shallow levels or pore water trapped in the sedimentary rocks (connate water) surrounding the magma that is heated and evaporated (Delmelle and Stix, 2000). This “connate water” entrapped in the interstices of pores of the unconsolidated soft sediment layers at the time of their deposition may also effect the quality of seismic reflection energy. As seen in seismic sections, this effect results in seismic attenuation and acoustically transparent reflections (acoustic voids) due to the low acoustic impedance contrast and reflection coefficient between water column and surficial sediments having high pore water rate. In addition to, local water supplies that seep and circulate within the host edifice, alter and dissolve the rock. This process may result in an increase in the permeability of flank aquifers over the lifetime of the hydrothermal system. In turn, this may weaken the volcano along preferential fluid pathways (faults and fractures) and eventually promote sector collapse of these volcanoes (Delmelle and Bernard, 2000) (Figs. 3.13, 3.14 and see Fig. 4.1 for collapse dome-cone complex). Infiltration through permeable stratigraphic units and/or flank fractures of the host edifice allows for prolonged water-sediment interactions and mixing with groundwater (Delmelle and Bernard,

2000). Debris flows and/or magma-genetic turbidities from flanks of intrusions along the fault planes toward the deep basin radially disperse. They contain mostly fragments of volcano-magmatic origin mixed with water, as proposed by Delmelle and Bernard, (2000). A seismic structural indication in transtensional margins in W and S that deep basin sediments (also sill features) are being remobilized by increasing water movements associated with enhanced vent activity. This water-sediment interaction reflects injection of rising fresh magma into the vent feeding the lake. As a result, local water supplies and water-sediment interactions can exhibit a dilute volcanic hydrothermal seismic signature (termed as small buoyant jets into the lake or diffuse emissions through the lake sediment pile) as reported by Delmelle and Bernard, (2000).

Seismic structural review of the proposed model above can be best illustrated by seismic sections across central Tatvan basin (Figs. 3.3, 3.5, 3.6, 3.8-3.11, and 3.16). These seismic images remark that magmatism along the fault-bounded margins and their sideway-deformation styles into the sedimentary sections along their flanks (lateral injection) highlight the interaction of magmatic gases with shallow hydrothermal systems and groundwaters. Importantly, the nature of this interaction depends on factors such as the state of activity and sediment permeability. The interaction of hot magmatic gases with a shallow groundwater or a hydrothermal lacustrine system results in a volcanic gas discharge characterized by relatively high CO_2 and low HCL contents (see related results in Degens and Kurtman, 1978). These contents selectively absorbe the more water-soluble gases (SO_2, H_2S, and HCL) into the liquid phase (Delmelle and Stix, 2000). Thus, continuous supply of magma from below results in relatively CO_2-rich gases being released at the summit. Seismic section in Fig. 3.9 shows best example of this process. In this section, magmatic-hydrothermal chimneys and/or hydrothermal vents are venting at the magmatic intrusion. As referred to model above, it is obvious in this section that the rising magma is subsequently transported laterally along the extensional zone, resulting in enhanced degassing and depletion of CO_2 (see Delmelle and Stix, 2000 for the rift zones). It is assumed that the hydrothermal steam component is produced as surface waters started to infiltrate the system and boiled, in response to progressive dilution of the magmatic gases by hydrothermal steam.

In parallel, the gas compositions became increasingly H_2O-rich with time because of the progressive infiltration of meteoric water into the intrusion, as proposed by Delmelle and Stix, (2000).

Sealing event; isolated and individual magmatic intrusions seem to be affected by sealing event and hence, they are interpreted as indicating overpressured conduits (also see Delmelle and Stix, 2000 for overpressured conduits) (examine Figs. 3.13 and 3.14). This argues that the failure of hot magmatic gases to escape the volcano appears to be related to the sealing of the gas conduits and that overpressure is developed in the cooling magma itself that filled the conduit system. The cause of the sealing and associated pressure buildups are active magma propagation and intrusion into the lake bottom. Therefore, magma-hydrothermal interaction is important for understanding the shallow-seated seismicity in the lake and related sediment deformations. Since, the sealing process is seismically important, both to the understanding of the shallow magma-hydrothermal lacustrine system and to the development of overpressure within the volcano as gas release is impeded.

The low-frequency-hybrid seismicity and tremor records are observed before the Lake Van earthquake (Horasan and Boztepe-Güney, 2006). These records are clear indications of the pressure buildup, which eventually results in the failure of the seal and sector collapse. The pressure buildups are well recognized along W-segment and S-coastal sections (see S-ends of seismic sections across central Tatvan basin in Figs. 3.3, 3.5, 3.8 and 3.13-3.16). Peripherally collapsed parasitic dome-cone complex aligned in and along W-segment is also shown in the map views (Figs. 4.1 and 4.2). These map views associated with seismic sections suggest that magma intrusion-related overpressure systems develop, particularly along W-segment in S-margin. These systems are, in fact, seismogenic sources for the magma-hyrothermal seismicity. It also seems that S-margin boundary fault, suture-parallel magmatic margin, is a zone, across which overpressured conduits and sector collapses are aligned. This implies that the higher pressure buildups are formed by a continuous feeding system emplaced at Muş suture trend (see and examine Figs. 4.1-4.3).

Seismic evidences of Diffuse Flank Degassing (DFD); a large amount of seismic reflection data set shows that magma-hydrothermal system of Tatvan basin province is entirely characterized by clear seismic evidences of “Diffuse Flank Degassing (DFD)”, trending from W- and S-margins towards deep basin.

In and along margin boundary faults, the gas release can occur by advection through fractures, or via diffuse degassing through large areas of permeable ground as "Diffuse Degassing Structures" (DDS), or "Diffuse Flank Degassing" (DFD), termed by Delmelle and Stix, (2000). The presence of DFD is acoustically understood by the complex interaction of magmatic intrusions with the permeable levels, fractures and faults. Such a complex interaction is illustrated by seismic sections shown in Figs. 3.3, 3.6, 3.8-3.11 and 3.13-3.16 and also imaged by seismic sections taken from Deveboynu and Varis spur zone subbasins in Figs. 3.18 and 3.26-3.29. These seismic sections imply that magmatic gases are clearly channeled through the central conduit or conduits (central vent volcano-CVV and fissure volcano-FV) (see the best examples in Figs. 3.13-3.15). Magmatic gases also may percolate through a volcano's porous flanks to the surface. As mentioned above, such gases include CO_2 and He emitted through the flanks. It is evident by previous studies that these gases are mantle-sourced components, derived from the magma or from shallow levels within the volcano (see data from Kipfer et al., 1994 and Delmelle and Stix, 2000 for magmatic gases). A seismic structural interpretation of magmatic intrusions from reflection data considers that faults and fractures play an important role in channeling the gases to the surfaces. This becomes increasingly obvious, since the presence or absence of faults having surface expression can be the principal control on whether a volcano is able to degas through its flanks.

Gases dissolved in magmas can be supplied at depth from various sources, including the mantle, during magma generation and magma ascent. These sources have distinct compositions and different types and amounts of volatiles are added to magmas depending on the tectonic and geologic setting of the volcano (Kipfer et al., 1994). According to geochemical data collected from the lake by Kipfer et al., (1994), for example, Helium is present in sediment gas, can be indicative of DFD, and is a good tracer of volcanic gas sources. The $^{3}He/^{4}He$ ratio is a very useful indicator of magmatic gas, reported by Kipfer et al., (1994) and a measure of the degree to which the mantle gases contribute to volcanic gas discharges from the lake bottom. Helium is also used as a reference to estimate various contributions to a volcanic gas. Hydrogen is another gas in zones of active faulting. H_2 is generated by the pulverization and fragmentation of rock during faulting. High concentrations of H_2 in sediment can indicate zones of active faulting, with gas generation at relatively deep

levels. H_2 is also a potentially useful gas for studying faulting and fracturing on volcanic complex. Geochemical studies from the lake by Kipfer et al., (1994) and from active volcanic domes around the lake by Keskin, (2005 and 2007) are integrated with geochemical results of Jung et al., (1978) and Khoo et al., (1978) from the lake bottom. The results of combined data set are compatible with a process of Diffuse Flank Degassing (DFD) in the lake.

The flanked degassing of magmatic intrusions and their diffusion through the permeable sedimentary layers into the deep basinal sections is a mechanism of DFD, imaged from seismic data. DFD, whereby changes in permeability-porosity in the sedimentary sections affect the DFD in more distant regions from source areas (from margins to deep basin). The association between faults and fractures and DFD seems clear from seismic data. However, a general model of DFD on volcanoes is not existed in related literature (Delmelle and Stix, 2000).

Implications for magma-hydrothermal degassing system; implications gain insight into a number of phenomena observed in and along margin boundaries, and across central Tatvan basin by studying magma-hydrothermal interaction and its seismic manifestations. It is assessed that whether there are magmas, pointed stocks pierce the sedimentary layers and/or subsurface chambers and present at shallow levels in a fault-controlled magmatic edifice. It is determined from seismic reflection configurations of sedimentary deformations by magma activity, if a magma is comparatively rich or poor in dissolved gas. The various sources of the gas, from the mantle, sediments or from fluids at shallow levels in the magma (hydrothermal system, groundwater, or even rainwater) are estimated by an integrated tectonic and geochemical data. The main controlling factors are, as expected, the tectonic and geological setting of the lake, the solubility of gases dissolved in magma (the magmatic volatiles), and the interaction with a hydrothermal system, groundwater, or rainwater at shallow levels within the magma.

The behavior of magmas that release large amounts of gas on a continuous basis is fundamentally different from that of magmas that store gas over long periods (Delmelle and Stix, 2000). This dichotomy between “open” and “closed” systems is fundamental (also see Degens and Kurtman, 1978; Delmelle and Stix, 2000). The implication is that Lake Van basin is an “open lacustrine system”. But, such a understanding is primitive and only based on seismic structural observations, faulting

and deformation styles from seismic data. It is re-emphasized that the lake is tectonically opened and detached oblique basin at upper crustal levels (Fig. 4.4). Volcano-magmatic events in and around the lake are mainly driven by decompressional alkaline magmatism during Quaternary. Thick depositional succession of central Tatvan basin is strongly deformed and interacted with rising magmatic activity. However, all evidences and implications are not enough to constraint volcano-magmatic and sedimentary interactions and thus, to generate a dynamic lacustrine model of magma-hydrothermal system in the lake. It is still needed that a reliable geochemical model, based on thermodynamic understanding and gas solubilities, to be able to confidently predict the temporal evolution of individual gas species.

4.3.2 Magma-hydrothermal sediment deformations in Tatvan province

4.3.2.1 Kinematics of shallow level magmatic intrusions and sediment dynamics

Magma hydrothermal-sediment deformations observed from seismic reflection and Geochirp data well evidence shallow level magma-sediment dynamics from basin-margins into deep Tatvan basin. Overall structure and internal dynamics of shallow level magmatic intrusions with lacustrine sedimentation are characterized by acoustically transparent magmatic flows, flow directions, feeder zones, sill sequences, chaotically ridged sill structures, and related sedimentary deformations (Figs. 3.1-3.11, 3.13-3.16, 3.18, 3.26-3.29 and 3.31). A complicated range of these deformational features is the end-members of the complex magma-sediment interactions and deformations recognized from available data. Shallow level magma-sediment dynamics is, as already emphasized primarily caused by extensional magmatism and intrusive-extrusive activity of rising magmas through margin boundaries of the lake. Extensional magmatism considerably results in hydrothermal sediment deformations and hydrothermal lacustrine environment. Hence, general structural pattern and overall kinematics of shallow level magmatic intrusions and sediment dynamics are acoustically analyzed and evaluated by a wide range of seismic reflection evidences. This contributes to understanding shallow level magma-sediment dynamics, its effect on sediment deformations and lacustrine sedimentation of Lake Van.

Seismic reflection profiles reveal the spectrum of deformational styles at the periphery of sills, both within the sill itself and within the surrounding sedimentary rocks (also see field-based investigations from Tweto 1951: Pollard et al. 1975; Brooks 1995 and Duffield et al. 1986). These deformational structures reported by these studies are generally small scale, ranging from micro to mesoscopic in size. From fault-bounding marginal sections into central Tatvan basin and also across Deveboynu and Varis spur zone subbasins, an important group of sill-related deformational features is acoustically observed, implying that sills intrude into soft sediments saturated with water (see and examine Figs. 3.1-3.11, 3.13-3.16, 3.18, 3.26-3.29 and 3.31). Indeed, these features are distributed widely in central Tatvan basin and the subbasins. These include features such as peperites and fluidization structures, which are documented by Schminke (1967), Kokelaar (1982), McPhie (1993) and Brooks (1995). It is considered that these structures can be genetically related to phreatic eruption and explosion breccias (Trude, 2004) due to heating and expansion of pore waters as observed by Grapes et al. (1972) in the Allen Hills region of Antarctica. It is interesting to note that seismic volcano-stratigraphy of large-volume basaltic extrusive complexes are reported in a relation to rifted margins by Planke et al., (2000). This implies an importance of extensional regime in understanding magma-sediment interactions in the lake.

For these reasons, the main interpretation from seismic structural observations offers a new look and consideration for the magma hydrothermal-sediment deformations and thus, brings a new perspective into the unique property of the plumbing of shallow intrusive systems within the lake. Seismic reflection and Geochirp data offer an ideal opportunity for seismo-acoustic observation and structural interpretation of magmatic sills emplaced into the lake. Thus, seismic data contribute to produce a new insight into extensional magmatism, magma transport and propagation, intrusion and extrusion and sediment deformation processes all over the lake.

General structural patterns; a wide range of seismic sections shown in Figs. 3.3, 3.5, 3.8-3.11, 3.13, 3.14, 3.16, 3.18, 3.26-3.29 and 3.31 evidences that, in central Tatvan basin, Tatvan delta, Deveboynu and Varis spur zone subbasins, magma flows are sourced by nearby magmatic intrusions or vents. These flows are directed toward the subsiding basin centers by intruding into the permeable zones of softer, unconsolidated sediments and deforming depositional facies. Magma flows-induced,

acoustically transparent and internally chaotic structures are sheet-like sills, distributing all over the basin centre. These flows are distinctly folded toward N-margin boundary and effected by transpressional deformation, as recognized in Figs. 3.1, 3.2, 3.4, 3.6 and 3.7. A rough distribution of these features is widely seen in central Tatvan basin and the subbasins (Fig. 4.1). In these seismic sections, some of these sills are fingered-like sheet intrusions with irregular bottom, intercalating with sediments (see Pollard et al., 1975 for the form and growth of fingered sheet intrusions). Some are laterally-sheeted sill wedges with flat bottom, compressing unconsolidated softer sediments. Such a case results in migration of heated pore fluids out of the intruded sediments, implying the importance of high water contents in the host sediments for sill emplacement (Einsele et al. 1980). Similarly, large decreases in porosity in soft-sediment-sill contact zones are found, for example, in the Guamas Basin, Gulf of California (see Trude, 2004 for details). In unconsolidated and softer depositional sections of the lake, the sediments intruded (poorly consolidated muds and sands) can contain a significant proportion of water (estimated at approximately 50%, based on Einsele 1992 and Trude, 2004). This supports substantial migration of heated pore fluids out of the intruded sediments. This style of interaction between hot magma and fluid-saturated sediments is perfectly imaged from available seismic data. Similar styles of interaction are also recorded associated with lava flows (Trude, 2004).

The most characteristic features of the magmatic sills identified on the seismic data are their discordant, chaotic and transparent reflection geometry with respect to the encompassing sedimentary reflections and the extremely high-amplitude reflections from sill-sediment contacts. The sills seen in the upper depositional sections across central Tatvan basin have folding-like surface undulations and structural irregularities related to styles of their flow regimes (Figs. 3.1-3.6, 3.8-3.10, 3.13, 3.14, and 3.16). These features are very similar to highly concentrated turbulent flows (also see seismic and petrophysical analysis of these characteristic features by Planke et al. 1999 and the ridge-like features by Trude, 2004). Some distinct seismic images across central Tatvan basin shown in Fig. 4.5 give highly chaotic and disordered internal structure of these features, trending NNW and also SSE (also see and examine Figs. 3.3, 3.5, 3.8 and 3.9 for correlation and basinal view). These detailed images of seismic sections seen in Fig. 4.5 are best reflection examples of

how ridged sills across central Tatvan basin can give some certain clues to both the intrusion type (active-passive), history and basinal development of magmatism and related products. These sill-related ridges themselves can be distinguished from side effects and coherent seismic noise. The upper surfaces of these sills are characterized by radiating concentric ridges that are well aligned with the lobate outer periphery (Trude, 2004) (examine Fig. 4.5). In terms of a detailed stratal, depositional, geometrical and reflection configuration analysis, it is considered that these novel features are related to the viscosity of the magma, depth of emplacement and the nature of the sediment into which the sill intruded (Trude, 2004). As illustrated in different seismic details of Fig. 4.5, the presence of a series of concentric ridges that track parallel to the lobate protrubances, such as in an arcuate nature is the most striking feature of the top surfaces of the sills in central Tatvan basin (see Figs. 3.3, 3.5, 3.8 and 3.9 for general structural view).

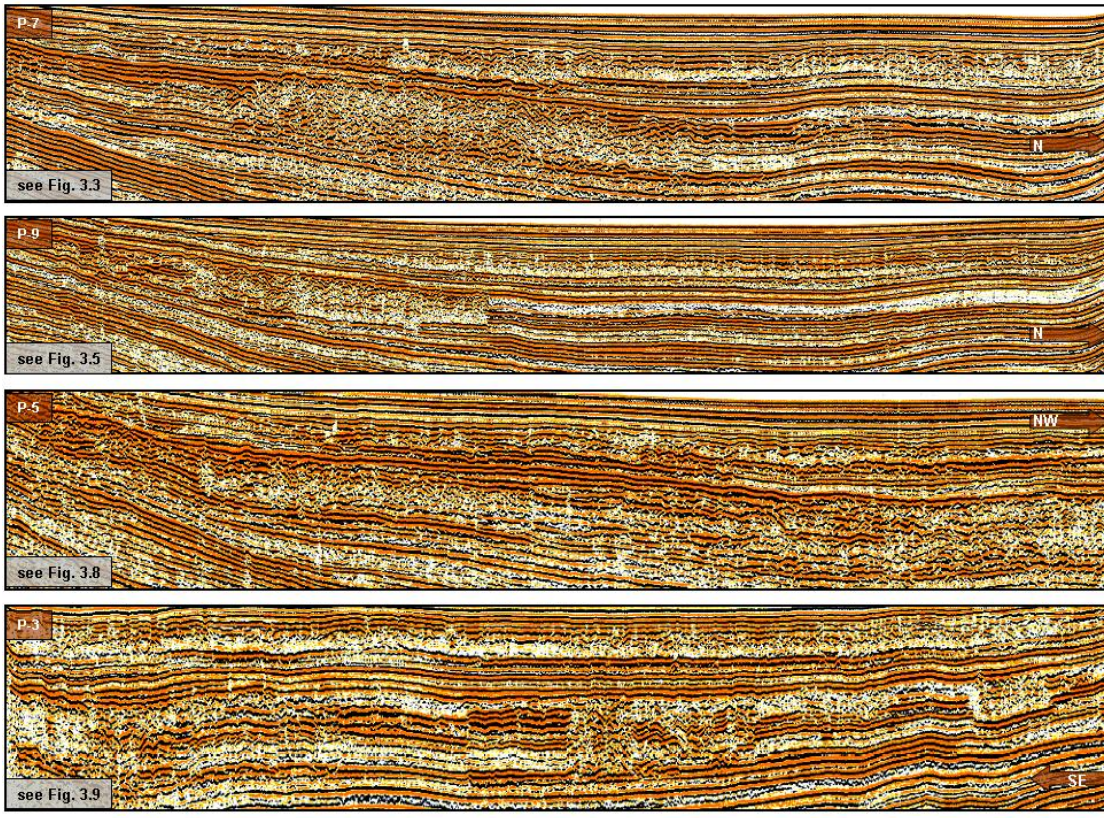

Figure 4.5 : Detailed seismic expressions of ridged sills and their flow directions across central Tatvan basin (brown arrows). Profile numbers of these sections are shown at the top left corner. Figure numbers seen at the bottom left corner refer to interpreted seismic profiles, from which these sections are taken. Note the branching pattern of these ridged sills, the diagnostic discordant nature of the high amplitude reflections and chaotic reflection configurations (also see interpreted version of seismic reflection profiles by using figure numbers).

Simplified 2D-seismic interpretation of the ridge features with observed magma flow directions and magma feeder zones from available data suggests that magma directionally flows from feeder zones, vents or pointed stocks and magma flow or sill itself produces ridge-like features. However, it is difficult to determine the actual geometry of the contact between the sill and the surrounding sediments, although it is tentatively suggested by Trude, (2004), the lower surface of the sill may be relatively flat (Fig. 4.5). Since, the depth of intrusion and composition of strata intruded may have important effects on the overall geometry and nature of sill-sediment contacts (see Trude, 2004).

Selected seismic sections in Fig. 4.5 show that the sills observed across central Tatvan basin have the lobate-shape geometry. Lobate geometries are exhibited by the peripheries of the sills, similarly, some shapes adopted by basaltic lava flows, extruding onto the Earth's surface or the lake floor (Trude, 2004). This indicates that the rounded nature of the flow front is caused by the tendency of the lava to “spread laterally under the influence of gravity” (Griffiths and Fink 1992). This shows that the development of lobes may be caused by slight variations in topography and hence division of the flow (Trude, 2004). As expected from the observed sills, these features in Fig. 4.5 reflect almost similar geometry attained. The propagation of a sill front moves through highly porous, poorly consolidated sediments at relatively shallow depths. This shows that the sill spreads laterally under the influence of the driving pressure of the magma entering the sill body. Perturbations in the advancing front cause formation of lobes in a similar way to slight topography on the land surface. The similar observations to attribute the initiation of finger formation at the periphery of sills to instability of the advancing interface between magma and host rock are documented by Pollard et al. (1975) and Trude, (2004).

Seismic structural observations from reflection data all over central Tatvan basin clearly evidence that sills are continually sourced from fault-bounding margins through which magmas intrude (Figs. 3.62 and 4.1). Magmas flow from high into low topographic regions as observed in N-S striking seismic profiles. Acoustically transparent, highly disordered and chaotic reflection configurations of these flows indicate that these flows are radially dispersed, even nearby N-margin. Fault-bounding nature of central Tatvan basin, flow directions of magma and related sills from faulted margins suggest possible linear structure of the sill margin.

The linear nature of the sill margin is well associated with the presence of a block-bounding fault system (see a structural comparison with the observations by Tweto, 1951 and Trude, 2004). Hence, the observed sills may have a straight edge due to faulted nature of basin margins. This makes the sills more likely that a fault acted as a barrier along their W- and S-margin boundaries. This suggests that W- and S-margin boundary faults acted as feeders for the observed sills and also for the large magmatic intrusions. This confirms a structural relation between extensional magma propagation, magmatism and active tectonics of the lake (also see Fig. 4.4). Moreover, various intrusion depths, such as small and large-scale intrusions, are observed, not necessarily at the same depth. Seismic data show that depositional sequences are locally uplifted by the intrusion of an underlying sill and the resultant topography at the sediment-water interface in-filled by onlapping sediments (Figs. 3.6, 3.14 and 3.27). The amount of topography created, the close proximity of the sill to the deformed horizon and the correlation between the uplifted region and the shape of the underlying sill makes it unlikely that this structure is due to differential compaction (Trude, 2004). This process clearly results in the confinement by onlap of a package of sediment.

Flow morphology, folding and fluidization; highly undulated ridge patterns or sedimentary irregularities on the surfaces of sills seem to have been the result of some external process shaping the sill by local tectonics and/or by local adjustments to differential loading of the sill mass on the underlying strata. However, Trude, (2004) proposes that the contribution from such an external process seems a lesser possibility. Since, the alignment of the ridges with the sill margin strongly suggests that there is a genetic link between the propagation of the sill and the growth of the ridges (see Trude, 2004). Seismic sections across central Tatvan basin seen in Figs. 3.3, 3.5, 3.8-3.10 and 4.5 clearly show this genetic relation. These seismic sections well evidence the interactions between hot magma and water-saturated sediments during the emplacement of the intrusion. These interactions are acoustically represented by transparent, reflection-free and chaotic reflection configurations of sill and ridged sill features all over the lake (Figs. 3.1-3.11, 3.13, 3.14, 3.16, 3.18, 3.26-3.29, 3.31 and 3.33). These reflection patterns and reflection effects are also summarized in Fig. 4.5. It is obvious from seismic sections that these interactions are most probably connected to both magma intrusions with high volatile content and

unconsolidated, softer sediments with high pore water content. These factors imply magma hydrothermal sediment deformations. The hot magma-soft sediment interactions (peperites) and related deformational features during this interaction result in distinct flow morphology, folding and fluidization structures (see Kokelaar 1982; Hanson and Schweikert 1982; McPhie 1993, Brooks 1995 for a detailed description of these features).

Magma hydrothermal-sediment deformations observed from seismic data are such distinct, peculiar and widespread features produced that these deformations continually vary in character, magnitude and configuration. This deformational instability depends on some parameters as identified by Trude, (2004). For Lake Van case, particularly central Tatvan basin, these parameters are more refined by observations from seismic images as followed; a) sedimentation-related parameters that are the intruded depositional pattern, the depositional consolidation-compaction state and depositional pore water content. b) magmatism-related parameters that are the magma viscosity-rheology, the magma volatile content and temperature, the magma intrusion depth, the confining pressure at intrusion. One of the more important controls is confining pressure vs. temperature. Since, this governs the possibility of boiling, fluidization and steam explosions (Kokelaar 1982 and Trude, 2004). To illustrate, boiling and loss of volatiles is suppressed, as confining pressure is relatively high. This produces brecciation of the magma with little intermixing of magma and sediments (Hanson and Schweikert 1982). The degree of sediment-magma mixing and fluidization structures increases, as confining pressure is relatively low, decreasing relative to temperature. Seismic sections seen in Figs. 3.3, 3.5, 3.6, 3.8-3.11, 3.13, 3.14, 3.16, 3.18, 3.26, 3.27 and 3.31 show folding and fold structures in sediments above shallow intrusions. These sections clearly evidence that these structures are caused by fluidization (see Brooks 1995 for modeling of some fold structures and their illustration). These folds trend roughly parallel to bedding and they are relatively small in meters and discontinuous. Therefore, they are discounted as a possible genetic analogue for the ridged sill. According to the model proposed by Trude, (2004), it is interpreted that the magma intruded into unconsolidated water saturated ash flow tufts. N-S striking seismic section and its high-resolution chirp image seen in Figs. 4.6 and 4.7 show the ridged sill and soft sediment interactions (also see Fig. 3.3).

In the high-resolution chirp image of Fig. 4.8, the depositional complexity of this interaction is detailed by showing bedding package of ash-tufts layers in central Tatvan basin (also see Fig. 3.5). Bedding thickness is approximately 25-30 m max. These seismic and chirp sections indicate that, in and along central Tatvan basin, ash flow-tufts layers are intercalated with unconsolidated, softer sediments. Sedimentation rates of Tatvan basin and of push up rhomb horst structure are calculated as 75 cm/1000a and 50 cm/1000a, respectively. In such a depositional case, invasion of fractures on the top of the intrusions is by fluidized ash. This is best illustrated by seismic image shown in Fig. 4.9 (also see Fig. 3.26). Then, subsequent expansion of pore water results in the upward movement of detached magmatic materials into the overlying tuff. An elongate dome shaped forced fold is formed where an intrusion invaded the tuff. Some secondary products such as fault splays or fractures form as an explosive fissure growing from the extension space (opening vent) in front of the sill or magmatic pile as it propagates forward (see Grapes et al. 1972 for the dykes and Trude, 2004). The only means of preservation of the fissure is by venting to the surface causing the intrusion to cease (see Figs. 3.3, 3.5, 3.6, 3.8-3.11, 3.13-3.16, 3.18, 3.26-3.29, and 3.31 for a complex sequence of all these events).

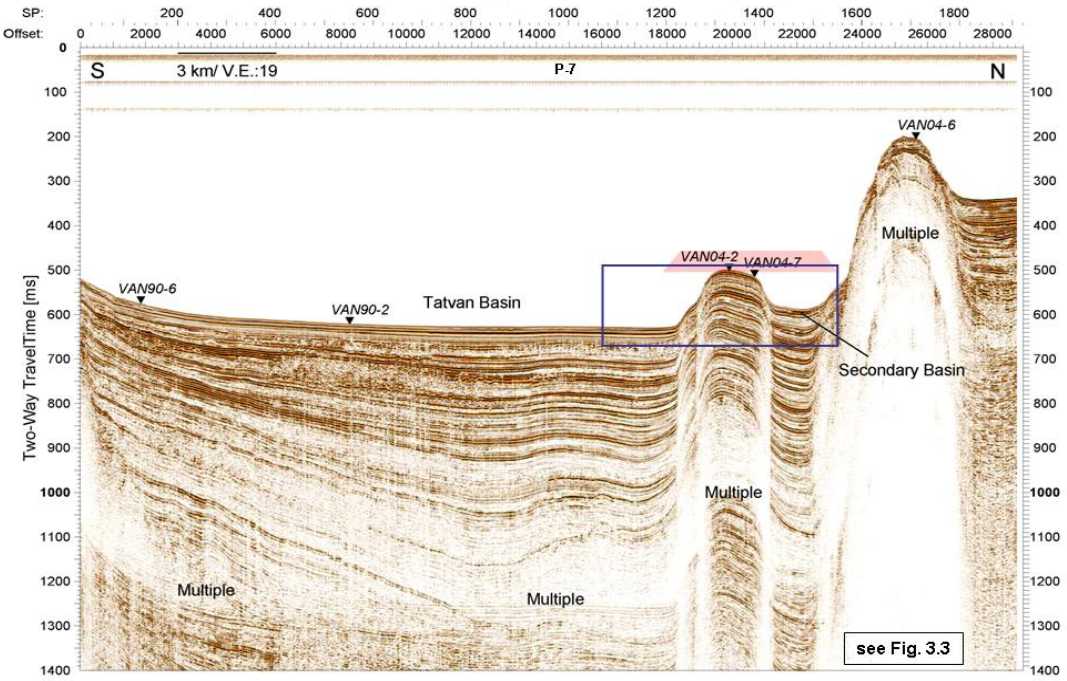

Figure 4.6 : N-S trending seismic section across central Tatvan basin. Seismic profile number (P-7) is shown at the top center. See Fig. 3.3 for a detailed structural interpretation of this seismic section and Fig. 4.7 for the high resolution-chirp image of section indicated by blue square (V.E: vertical exaggeration).

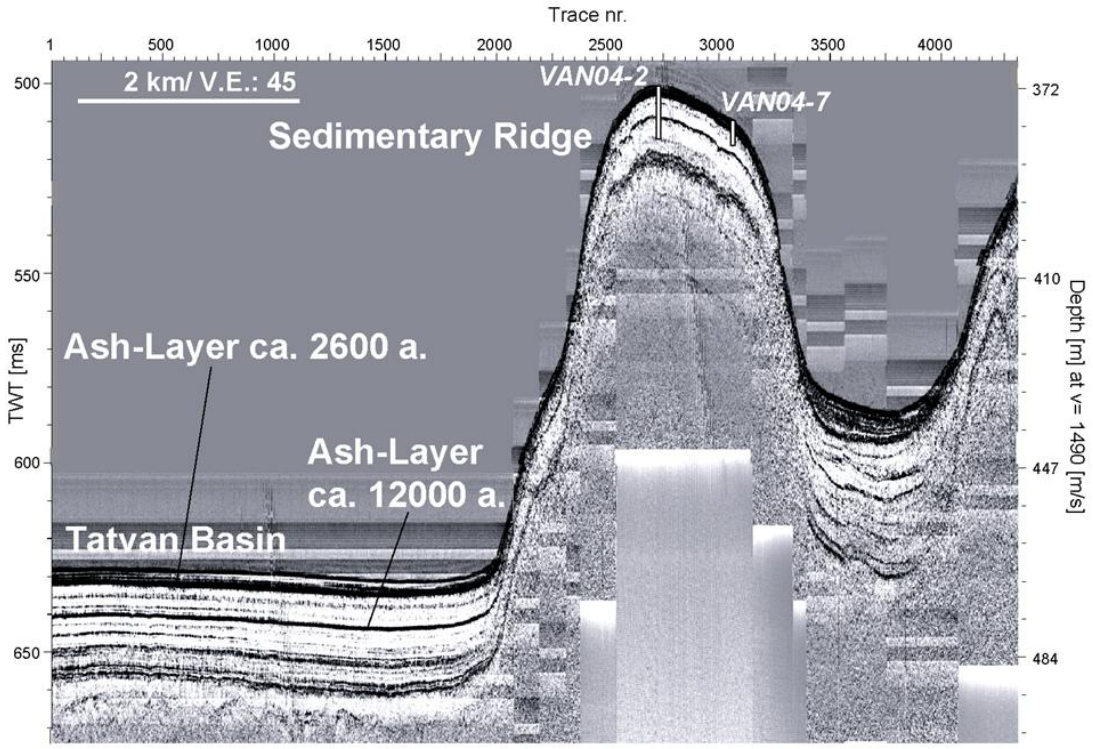

Figure 4.7 : The high resolution-chirp image of the small section shown Fig. 4.6 shows the core locations in sedimentary ridge (VAN04 stations) and ash layers in Tatvan basin (TWT: Two-Way Travel Time, V.E: vertical exaggeration).

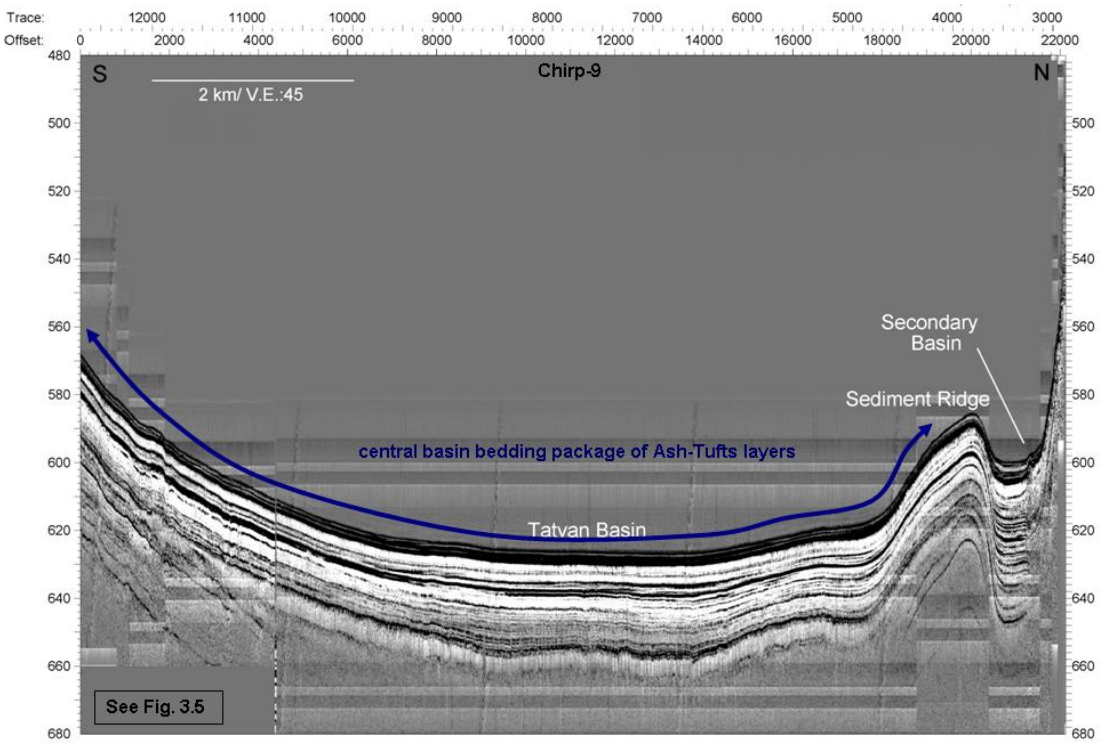

Figure 4.8 : N-S trending high resolution-chirp image of central Tatvan basin (Chirp-9) shows bedding package of ash-tufts layers (curved blue arrow). See Fig. 3.5 for seismic structural interpretation of this chirp image (V.E: vertical exaggeration).

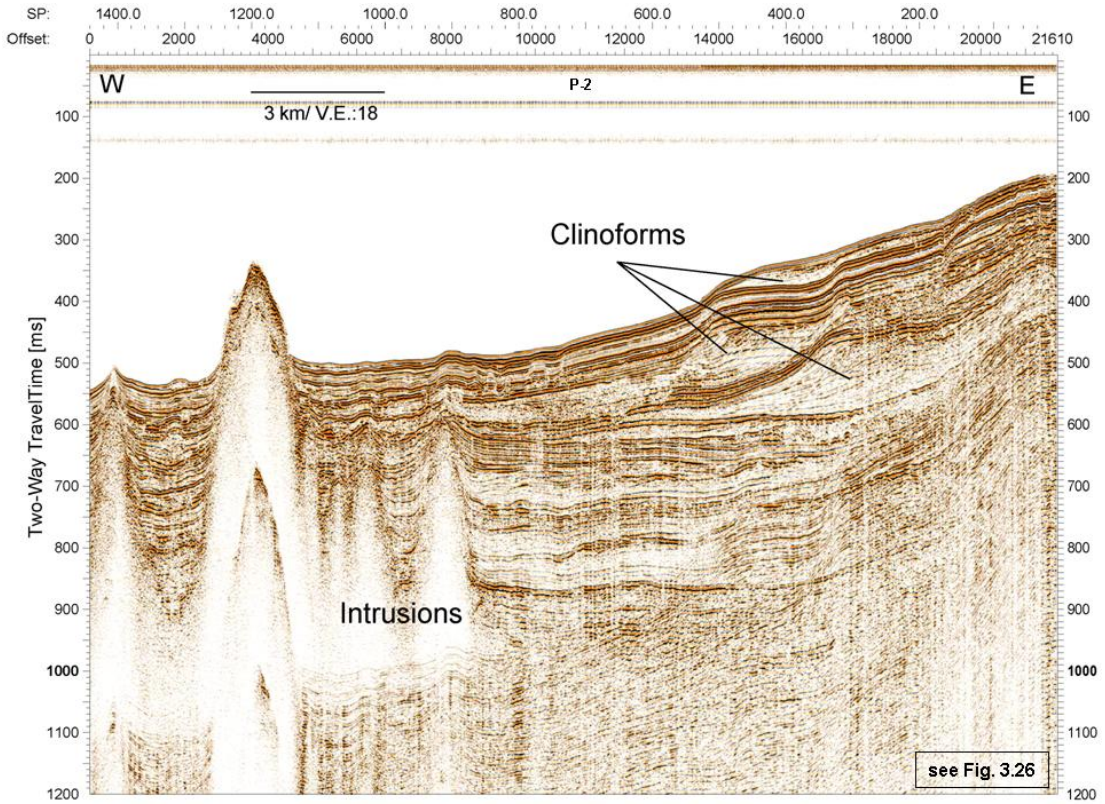

Figure 4.9 : W-E trending seismic section across Deveboynu subbasin and SE-delta shows magmatic intrusions and clinoform packages. Seismic profile number (P-2) is shown at the top center. See Fig. 3.26 for a detailed structural interpretation of this seismic section (V.E: vertical exaggeration).

Some similarities between the processes for ridge sill development and the surface morphologies of lava flows can be considered by an interpretation of seismic reflection images. Central basin sill and ridged sill development is derived from consideration of the lava flow morphology (Trude, 2004). This similarity seems an unlikely due to the presence of overburden above sills when they intrude and obvious lack of overburden above lavas during eruption, such as Nemrut volcano. However, as followed through seismic sections, highly water saturated lacustrine sediments can provide such a low shear resistance to the intruding magma and it could act like and exhibit some of the properties of surface flows (see Trude, 2004 for discussion). As recognized in Figs. 4.6-4.9, for example, a very fine-grained water-rich ash at the top of an intrusion is fluidized by expanding steam and shows no resistance to the intruding magma (Brooks 1995). It is observed by Guest and Sanchez (1970) that the top surfaces of the lava flows are characterized by broad arcuate ridges, and these ridges are very similar to those seen in Fig. 4.5. The shape of these ridges reflects the movement of the flow and in part corresponds to the lobate front of the main flow. As similarly recognized in Fig. 4.5, the ridges on the observed lava flows radiate

from the eruption cone. These ridges are best kinematic indicators for the feeder zones and indicate the direction of magma flow (Guest and Sanchez 1970 and Trude, 2004). In fact, this similarity describes the case for the ridged sill. This case suggests that there are grounds for considering the analogy between lava surface flow morphology and sill surface morphology a stage further (Trude, 2004). It is to note from the similarities mentioned above that sill surface morphology observed from seismic data is prominently the same with lava surface flow morphology. Structural similarity between surface flow morphologies suggests that sill and ridged sill features in central Tatvan basin are originated from upward mass transport of rising magmas and that they are lava products as well. This means that a high viscosity magma intruded into soft, water-logged sediment may act in a similar way to a lava extruded onto a free surface under conditions. In these conditions, the strength of the intruded sediments is very low or reduced to near zero (Trude, 2004). This evidences that there is considerable similarity of form between the ridged sills and those expected on the surface of an intermediate lava flow. Such a similar morphological picture is often found in and around Nemrut volcanic dome-cone complex (see and examine Fig. 4.3).

Fink and Fletcher (1978) and Fink (1980) suggest that, due to the compression of a fluid whose viscosity decreases with depth, regularly spaced surface folds in lava flows may be modeled as folds forming. This implies that surface folds can develop in lavas with various compositions. As mentioned above, the morphological similarities between the flows suggest that the ridge-like structures form by a similar mechanism, although the ridges on various flow regimes are an order of magnitude larger or smaller (Fink 1980). As known, the folding pattern and the amplitude of folds is dependent on the temperature gradient, the viscosity contrast (between interior and exterior viscosities) and the stress ratio (between the compressive stress due to flow and the gravitational stress due to the weight of the lava) (Fink 1980). It is proposed here, as referred to Trude, (2004) that a similar mechanism acted in the formation of the pressure ridges that cover the surface of the sills (Fig. 4.5). This mechanism suggests that the drag of advancing internal magma against a more viscous outer layer and retardation of flow by the material at the nose of the sill cause subsequent compression and ridges to form (also see Fink 1980). This remarks that the sill injections (basaltic) preferentially occur in unconsolidated softer

sediments some hundred meters below the lake floor, even less than 100 m (see Figs. 4.6 and 4.7). Deep-water lacustrine sediments at depths shallower than 100 m are highly softer and porous (Fig. 4.8).

A sequential succession of the sheeted sills (transparent/reflection-free patterns) and ridged sills (chaotic-disordered patterns) are shown in Figs. 3.1-3.11, 3.16, 3.18, 3.26-3.29, 3.31 and 3.33 and deep-water depositional stratigraphy, together with these sill sequences are also colored in Fig. 3.58. These seismic sections show that the surrounding sediments become indurated, consequently new sills tend to intrude above older ones, due to the sill intrusion (Einsele et al. 1980; Einsele 1986 and Trude, 2004). Very simplified 3D-stratigraphic block diagram of laterally extensive, sheeted and ridged sill complex and its sequential development in central Tatvan basin is recognized in Fig. 4.10. This stratigraphic block diagram shows deep-basin flow directions of these sill features, indicating that sill formation is mainly effected by extensional and transtensional strains in W- and S-margins, but no sill formation in N-margin. Based on sill stratigraphy in central Tatvan basin, the ridged sills (RS_1 and RS_2) are observed to be the highest sills stratigraphically in the surrounding depositional complex. This suggests that the sediments intruded by the sill, at the time of its intrusion are unlikely to suffer induration, as expected in the underlying sediments surrounding the lower sheeted sills (S_3, S_2 and S_1) (see Trude, 2004 for this example). Simplified rough estimations for central Tatvan basin are that the overburden pressure due to the overlying 400 m of sediment at the time of magma intrusion is calculated as 7.8 MPa assuming a density of 2.0 Mgm^{-3}, according to estimations by Trude, (2004). However, the depth of lake water above the intrusion at the time of emplacement is less constrained. On the other hand, Kokelaar (1982) noted that boiling and steam explosions are suppressed during magma eruption in lake water or unconsolidated wet sediment at pressures above 31.2 MPa (Trude, 2004). This case indicates that there will need to be about 2.4 km of water above the sill at the time of intrusion to prevent boiling occurring. But, the depth of water in the lake at this time was probably less, 300-400 m, as inferred from clinoform geometry of progradations in NE- and SE-delta settings. Hence, it is likely assumed that boiling and fluidization related features have been able to develop in the lake, as proposed by Trude, (2004). These simple estimations confirm seismic structural observations and conclude that the fluidization factor is responsible for the

mobilization or replacement of large amounts of sediment and magma-sediment dynamics in the lake (see Kokelaar 1982). The fluidization reduces the effective strength of the intruded sediments significantly, allowing the sill to invade or replace the surrounding sediment (Trude, 2004).

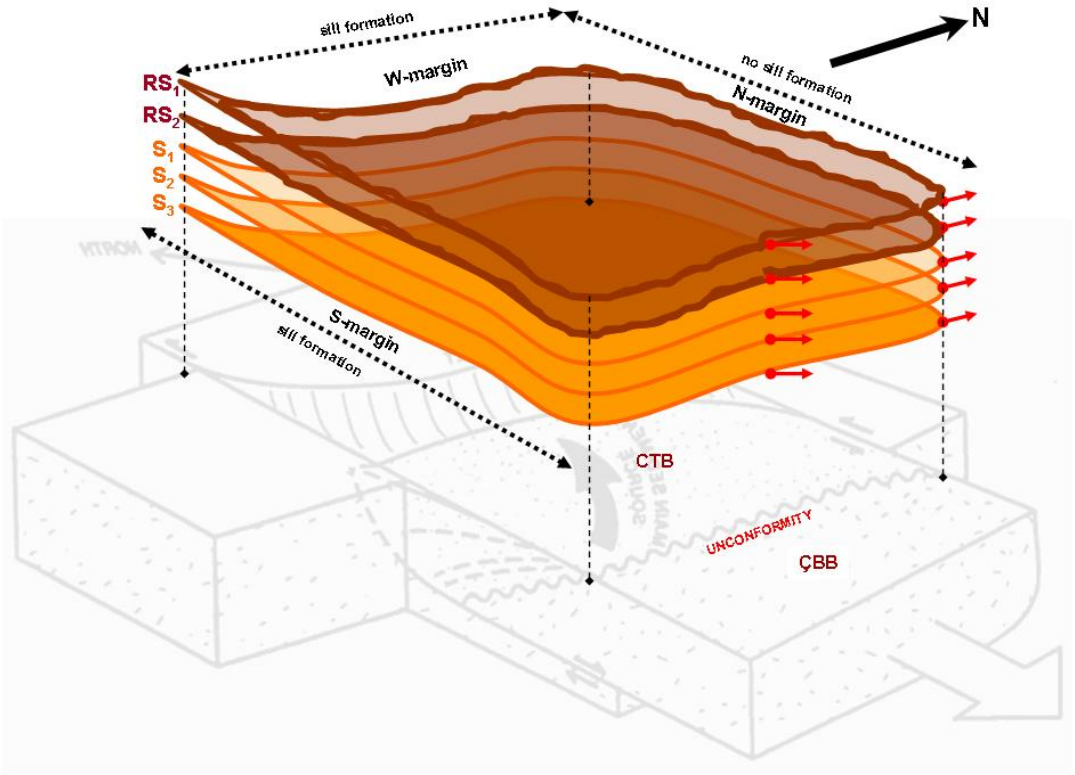

Figure 4.10 : 3D-block model section of laterally extensive sheets, the sill (S, orange) and ridged sill (RS, brown) structures illustrates the sill stratigraphy in central Tatvan basin (S_3: the oldest sill sheet and RS_1: the youngest ridged sill sheet). Note that the sill sheets are formed in W- and S-margins (sill formation), but not in N-margin (no sill formation). Red arrows indicate the flow directions. ÇBB: Çarpanak basement block and CTB: central Tatvan basin (also see lateral sheet model in Fig. 4.1 and block model in Fig. 4.4).

Model proposal for the ridged sills; the schematic cross sectional model through the ridged sill at the time of intrusion is proposed by Trude, (2004). This model is well consistent and compatible with the sill development observed in the lake. According to this model, the sill initiates intrusion with arbitrary surface irregularities. The sill intrusion continues with surface irregularities growing into folds and shortening distance between folds and then, the distance between folds decreasing and causing folds to grow further. This model is well represented by a series of selected ridged sill sequences in central Tatvan basin (Fig. 4.5). This model section is extended into central Tatvan basin, as recognized in Figs. 3.3, 3.5, 3.8 and 3.9 and, evaluated for

the ridged sills and magma hydrothermal-sediment dynamics in the lake. It is often found that a surface layer of more viscous magma with numerous low-amplitude irregularities develops at the contact with the overlying sediment, as the magma radiates out. Viscous drag is caused by forward movement of the sill interior. This forces the more viscous layer towards the solidifying nose of the sill and thus, causing amplification of irregularities, as the intrusion continues. Further forward movement of magma causes greater compression of folds and draws out the arcuate nature of the ridges in the direction of flow, thus indicating the direction of flow and the feeder zones. The base of the sill is interpreted as relatively flat. The weight of the overlying magma, coupled with sediment compaction below may prevent ridges forming (Trude, 2004). It is recognized from this model and detailed seismic sections in Fig. 4.5 that magmatic pressure drove the lateral intrusion in the areas where the sill has flowed upwards. High magma viscosity caused drag on the more solidified outer magma layer. The forward drag from the movement of the magma is coupled with the resistance, caused by the solidifying frontal carapace. This caused the formation of ridges. These stages can be also reconciled with the observations of Tweto (1951) and Trude, (2004).

In central Tatvan basin, maximum sill and ridged sill thicknesses roughly yield values, ranging from 30-75 m with a mean value, less than 100 m, using a sediment velocity of 1.7 km s^{-1} (see sill thickness values ranging from 64-88 m with a mean of approximately 75 m using a P-wave velocity of 6 km s^{-1} by Trude, 2004). Seismic reflection data, particularly in Fig. 3.58, show that the spaces in the depositional sequences are created for the formation of ridges (see Fig. 3.5). This implicates that total water loss in sediments is caused from the uppermost sill in a complex intruded into soft-sediment. This water loss is of the same order of magnitude as the thickness of the sill (Trude, 2004), ranging from 30-75 m. This suggests that water removal from sediments creates space for the sill and also causes an extensive activity of fluidization, as summarized in Fig. 4.5. As reported by Brooks (1995), thermal fracturing and invasion of the sill top by fluidized sediments can create further space for ridge formation. This event is obvious from most of seismic sections shown in Figs. 3.3, 3.5, 3.6, 3.8, 3.9, 3.13, 3.14, 3.16, 3.18, 3.26-3.29 and 3.31 and very distinctly recognized in Figs. 4.5, 4.6 and 4.9. For example, 30-40 m ridges should easily be accounted for by thermally induced differential compaction between and

above ridges (Trude, 2004). The creation of space in the sediment for the formation of ridges is well consistent with observations made by Einsele et al. (1980) and supported by Trude, (2004). However, it is not possible to calculate the viscosity of the magma as the driving pressure of the magma from seismic data. It is very difficult to calculate meaningful flow or deformation rates for ridge-fold formation (Trude, 2004). Fink (1980) suggested that the magma must have been quite viscous. Since, in terrestrial flows, there does seem to be some correlation between fold size and magma viscosity. As referred to Trude, (2004), if it is assumed that the size of the folds on the surface is due to high-viscosity lava, this either indicates that the magma was of a basic type but relatively cool or that it may have been more acidic in composition.

Implications for magma-hydrothermal sediment dynamics; magma hydrothermal-sediment deformations as a component of hydrothermal lacustrine system are well identified by seismic reflection data. Seismic structural interpretation provides significant potential to further understanding of magma transport, propagation and intrusive processes in the basin fill of the lake.

Overall structure and kinematics of magma hydrothermal-sediment deformations evidence the effect of shallow level magma-sediment dynamics on sediment deformations and lacustrine sedimentation of Lake Van. Magma-sediment dynamics entirely covers central Tatvan basin, from faulted basin-margins into the deep-water settings. Sediment deformations, ridged sill features or turbulent architecture-shaped sills all over central Tatvan basin are intercalated with depositional sequences and emplaced at less than hundreds meters below the lake floor in to poorly consolidated, softer sediments. The surfaces of these sills are covered in complex arcuate ridges, dispersing and extending into the deep basin, even towards N-margin transpression zone. Such a widespread sill coverage is resulted from a mixture of low viscous magma and high pore water content of surrounding sediments, something like highly fluidized and lubricant mass-flow transport all over the lake.

The prominent stratigraphy of sill sequences prevails on central Tatvan basin and also the subbasins, revealing dynamic sequential nature of extensional magmatism in Lake Van. Surface morphology of lava flows and ridged sills is reconciled with previous field studies and 3D-seismic observations and combined with available reflection data. Comparison with analogue model studies of previous works indicates

that the ridges of sills are likely to have formed as a direct result of shallow intrusion of a viscous magma into soft sediment. Seismic sections evidence that intrusion of the sills into highly porous sediments results in hydrothermal activity (Einsele et al., 1980). Then, poorly consolidated, softer lacustrine sediments are strongly deformed during shallow emplacement of the sills (see Dufeield et al., 1986). This shows that softer and wet sediments are fluidized during the emplacement and cooling of various magmatic bodies (Kokelaar, 1982). Surface of a sill-like, viscous magmatic fluid is effectively folded (Fink and Fletcher, 1978). This shows that, during intrusion, compression of a more rigid outer layer is retarded by the solidifying sill front. This causes amplification of irregularities between the sediment and the outer cooler layer of the sill. Forward movement of the surface layer is likely to be caused by viscous drag from within the sill. As interpreted from seismic sections, kinematics of the sills and the ridges on the sill surfaces indicate the flow directions of the magma, feeder zones and confirm shallow-seated magmatic intrusions through basin-bounding faults. This enables identification of the feeder zones and the evidence of flow direction, which display a clear link to the sills and evidence that Lake Van is magma hydrothermal-dominated lacustrine system.

4.3.3 Travertine-hydrothermal sediment deformations in SE-delta province

Seismic data evidence that soft-sediment deformation structures in SE-delta are most probably effected by the factor of underlying travertine mass. This mass has, at least a thickness of 20-50 m and forms a big plate, which dips towards the lake 7^{o} at a strike of 201^{o} (WNW) (Valeton, 1978 and Wong and Finckh, 1978). It is prominently located in the S-end of SE-delta and bounded by dextral oblique-slip fault systems such as Gevaş, Gürpınar and Edremit. This mass dips with the low angle toward SE-delta and probably extends into the deeper levels (see sketch cross sections in Şengör et al., 2008). Seismic sections seen in Figs. 3.20, 3.22, 3.24 at the bottom, 3.30 at the bottom, 3.41 and 3.47 show soft sediment deformation structures in SE-delta, which are probably effected by underlying travertine deposits. The map views in Figs. 3.43 and 3.50 show fault-controlled distribution of delta progradations and soft sediment deformations in SE-delta. It is interpreted from seismic data and map views that SE-delta is subject to hydrothermal effects of travertine deposits, suggesting that travertines have hydrothermal relations to soft sedimentary deformations in the SE-delta.

Seismic sections in Figs. 3.20, 3.22 and 3.41 show the tilted half-graben geometry of SE-delta, indicating that the basement structure of SE-delta is controlled by faulted travertine mass. Structural interpretation of these seismic sections shows that the dip of the travertine deposits may be caused by precipitation on a bed inclined towards SE-delta, implying an evidence of post-depositional tectonic tilt or post-travertine tectonic movement (Valeton, 1978 and Wong and Finckh, 1978). Wong and Finckh, (1978) reported that the surface exposure of the travertine is limited to Edremit in E and Gevaş-Gürpınar faults in SSE. The tectonic movements responsible for tilted geometry are dated as post-travertine, but before the accumulation of the lake terraces (Wong and Finckh, 1978). Delta degradation mechanisms, distribution of soft sediment deformation styles and the presence of active and/or inactive travertine deposits in the vicinity of SE-delta suggest more complicated faulting pattern in the basement of SE-delta. This gives some certain clues about hydrothermal activity-dependent deposition, erosion periods and tectonic intensity, which controls deformational characteristics and structural architecture of sequences during Quaternary. Consideration of soft sediment deformations along with the basement complexity explains travertine-induced hydrothermal effects in SE-delta. This suggests the Quaternary evolution of travertine mass and its relationships to structural deformation of SE-delta. Areal distribution of soft sediment deformation in SE-delta is broadly widening, nearby travertine area, in which progradational clinoforms are almost deformed, particularly by deeply incised, submerged river-channel systems (Figs. 3.43 and 3.50). Buried faults, sediment deformations and underlying higher magnetic anomaly in SE-delta (Degens and Kurtman, 1978) indicate that the travertine mass is probably originated as fissure-ridge travertine and it is thought to have resulted from active faulting. Faulting originated in extensional-transtensional regime in this area. Since, the coastal emplacement of this fissure-ridge travertine and its relation to areal faulting link the formation of the travertine to the regional tectonic regime.

Tectonic discontinuities in SE-delta, such as faults and major joints, cause hydrothermal fluids to rise to the surface and thus, hot water rises to the surface and precipitates travertine. Fissure-ridge travertine beneath SE-delta, which possesses open fissures, is subject to extensional tectonics. Since, these deposits form, when calcium bicarbonate-rich hot water rises up from a crack or fissure and precipitates

travertine, both in the crack and when it spills out on the surface. As the crack continues to expand during regional extension, travertine is precipitated progressively on the crack walls. At the surface, due to changing physical conditions, porous and bedded travertines are formed as dipping layers perpendicular to fissure axis. When the hydrothermal activity ceases, fissures may continue to expand due to the regional extension and an open cavity can form along the central axis of the main fissure ridge. This evidences that the fissures in the fissure-ridge travertines are products of an extensional regime in and around SE-delta (Figs. 3.20, 3.22 and 3.41). They provide concrete information about the direction and rate of regional extension. However, there is no any structural data related to the fissures in travertine mass. Geological sketch maps related to this area in Şengör et al., (2008) indicate that structural location of the travertine mass and its inclination towards SE-delta is strongly controlled by areal (dextral) shear systems.

Seismic sections from SE-delta show that sedimentation and subsidence rates are much faster than extensional fault activity in the basement. This is the reason of why the fault offsets are not clearly identified in the lake floor. Extensional deformation in SE-delta causes hot waters to rise to the surface and forms travertines that define when the normal fault movements occur (Çakır, 1999). This highlights the tectonic significance of travertine deposits (Scholl, 1960; Martelli et al. 1989) underlying SE-delta. Structural relationship of travertine mass with sedimentary deformations in SE-delta indicates that tectonic factors led to the hydrothermal activity and caused the deposition of travertine. Post-travertine hydrothermal activity probably continued to affect the deformational patterns of delta sediments. When the structural and geological emplacement of the travertine mass is investigated, it seems that travertine may have had open structures formed in dextral shear-zones, which would produce the fissure-ridge travertine. The soft sediment deformation styles in SE-delta are conformable with the possible fissure systems in the travertine. This shows that hydrothermal solutions have been transported to the surface by the open and en echelon fissure systems and small faults located in the SE-delta. The evidence shows that these fissures may have formed due to transtensional and extensional activity and the travertine mass is classified as fissure-ridge travertine. Faults and fissures developing in this type of travertine are linked to one another. It is considered that the patterns of soft sediment deformations in SE-delta are partly dominated by

hydrothermal effects of travertine mass. This implies the contribution of travertine-hydrothermal sediment deformations in SE-delta, which is also important travertine field with active hot springs.

4.4 Thin-skinned Crustal Emplacement of Extensional Lake Magmatism

Seismic structural interpretation of intrusive-extrusive activity of magmatism, extensional magma propagation and basinal dynamics of hydrothermal deformations propose that Lake Van basin constitutes an "open window" into the conduits and underlying feeding system (magma chambers or pointed stocks) and offers a rare opportunity to observe a shallow convecting magmatic system. Seismic data, the map views and 3D-block model sections greatly assist a crustal-scale interpretation of extensional magmatism in its understanding of the dimensions, positions, and complexity of the conduits and magmatic system. Further, seismic structural knowledge of the physical makeup of edifices of magmatic intrusions helps to generate a unified model of magmatism and to solve questions about the emplacement mechanism, location, and generation of magmatism, magma convection and crustal factors.

Seismic structural expressions of magmatism evidence the complexity of the magmatic evolution of the lake. Seismic reflection data is well analysed and interpreted to build a lake model of magma emplacement mechanism. Previous multidisciplinary seismic and seismological studies suggest that the slab is delaminated and the upper mantle beneath the lake is hotter than its surroundings, showing the existence of an extreme thermal anomaly under the region (Şengör et al., 2003 and 2008). The surface expression of this thermal anomaly is a magma-hydrothermal lake, termed as "Lake Van Dome" (Şengör et al., 2008). This dome is located at the center of squashy zone, entirely covered by decompressional melting magmatism. This means that the magma feeding Lake Van Dome is alkaline/ultra-alkaline rich, a factor indicative of intraplate extensional magmatism. Highly anisotropic, thin and weak convergent crust beneath the lake is thought to have acted as magma transport, propagation and migration channels through weakness zones, such as Muş or Cryptic sutures.

Crustal emplacement model requires upper crustal reconstruction of tectono-magmatic and tectono-thermal structure of the lake and thus, it is related to the active

Quaternary magmatism and its basinal products. Crustal emplacement of magmatism focuses on searching for the origin and rise of magmatic intrusions, diapiric ascent of magmas through power-law crust and mantle and emplacement mechanics of magmatic products in the lake. This leads to a better and common understanding of tectonic and magmatic events in the lake. Extensional magmatism and its emplacement provide some certain evidences in understanding the regional intraplate magmatism and its local tectonic and volcanic implications for lake magmatism at upper crustal levels. As previously mentioned, the upper crustal flake tectonics, delamination event and decompressional magmatism have played active roles in driving magmatic and tectonic processes in and around the lake as this process previously described by Weinberg and Podladchikov, (1995). As recognized in seismic sections, these roles evidence that the extensive magmatism observed in the lake provides some important insights from integrated tectonic and magmatic interpretations of seismic data into the emplacement mechanism of magmatism.

Emplacement model describes the mechanisms of magma ascent and emplacement in the crust, widely debated in the literature (Brown, 1994; Weinberg, 1994; Weinberg and Podladchikov, 1994; Weinberg, 1997). Several studies seemed interpreting whether the softening of the wall rocks by heat released by the magma diapir would enhance the diapir's ability to penetrate the crust (Emerman and Turcotte, 1984; Daly and Raefsky, 1985; Mahon et al., 1988; Miller et al., 1988; Weinberg, 1997). These studies concluded that the heat content of single magma diapir is insufficient to considerably enhance diapirism, because faster ascent rates are accompanied by faster cooling rates leading to early freezing of the diapir. Marsh, (1982) suggested that if several diapirs followed the same path (lateral magma propagation), they could form a hot pathway allowing younger diapirs to rise increasingly higher before freezing such as the nesting of diapirs into each other (Holder, 1979; Bouchez and Diot, 1990; Allen, 1992; Paterson and Vernon, 1995; Weinberg, 1997). Tackley and Stevenson, (1993) proposed a novel “self-perpetuating” (SP) mechanism of magma production by decompression melting in the asthenosphere. This well indicates the case seen beneath the lake. These authors noted that if an element of rock, partially molten or at the onset of melting, are given an infinitesimal velocity upward, it will undergo decompression melting and density decrease, increasing the upward velocity. The system is thus unstable and upward movement will feed itself and lead

to large-scale melting. Tackley and Stevenson, (1993) in fact, describe a well-known situation, implying decompressional magmatism and melting volcanism in and around the lake. Based on these studies, the interaction of the rising magmas with the upper crustal levels and renewal of the magma source in the crust along with the decompressional melting are considered as a reference for the lake. This provides an evidence for the evolution of sequential intrusions originating at a partially molten layer at the base of a power-law crust, suggesting a crustal emplacement model of sequential magmatism.

4.4.1 Upper crustal emplacement mechanism of sequential magmatic intrusions

Vertical and lateral mass transport of magma movement through margin boundary faults of the lake evidences the upper crustal magma activity into the basin and extensive magma propagation covering Muş-Lake Van basin system (see and examine Figs. 3.64, 4.4 and 4.10). Upper crustal magmatic activity is modelled by Dewey et al., (1986), supported by Şengör et al., (2008). This magma activity apparently deforms the depositional sequences, and gravitationally flows into the permeable sedimentary layers toward the deep basin center (Fig. 4.10). As already pointed, margin-bounding magmatic activity is spreading laterally and continuously sourced from depths. It is already evidenced that delamination-dependent decompressional magmatism and melting volcanism are primary factors, triggering upward low density mass transport of basaltic magmas through accretionary wedge blocks beneath the lake (Şengör et al., 2008).

The marginal distribution and fault-controlled propagation of the magmatic intrusions show that these intrusions appear to have only dominated along the basin margin boundaries, suggesting localized subbasinal magma chambers in various scales. Because, partially melted products are restricted to the magmatic intrusions observed in the lake and probably sourced by considerable reservoirs of magmatic potential energy beneath the lake. As known, where decompression melting can occur (hot lower crust, low solidus temperature, high intrusive buoyancy), the initial intrusive activity might also cause the partial melting of wall rocks. In this way, the thermal and mechanical energy spent by the intrusion during its ascent (by heating and dragging the wall rock) is partly recovered. The upward magmatic mass transport leads to strongest decompression melting directly beneath the intrusion. When the intrusion rises through a crust too cold to melt, the intrusion cools and

gradually loses its buoyancy and velocity. However, in a warm, thin and wet crust beneath the lake, decompression melting of the surrounding rocks adds buoyancy to the intrusion allowing faster and higher rise into the upper crust. The high level potential energy of magma chambers sequentially and rapidly transfers the magmatic material into the low energy environment through the sediments to the lake bottom. This event causes highly squashy environment and domed-like formation of the lake in the highest center of the plateau (see related discussion in Şengör et al., 2008).

These considerations well explain the basics of a model mechanism proposed by Weinberg, (1997). This mechanism postulates that the ascent of magma intrusions may impose a convective flow pattern concentrated mostly in the low-viscosity lower crust. In lower crust, the rocks immediately surrounding the diapir are dragged upwards and rocks a few radii to the sides of the intrusion are pushed downwards to fill the gap left by the rising mass. This suggests that very warm and water-saturated rocks may undergo decompression melting when dragged upwards. This is to enhance the ability of an intrusion to intrude the crust, because the partially molten wall rocks gain buoyancy and add to the total buoyancy of the diapir, which regains part of the energy it spent on heating and dragging the surroundings (Weinberg, (1997). The downward flow of rocks renews the magma source with potentially fertile rocks, which may undergo melting and give rise to a new intrusion. This new one will follow the same path as the first one and repeat the process, giving rise to a sequence of intrusions. According to this model, magma intrusions impose a convective movement in the crust by dragging surrounding rocks upwards and causing rocks further away to flow downwards to replace the ascending mass. This convection has two important implications stated by Weinberg, (1997). The one is that it may lead to decompression melting of the ascending rocks, and the other is that it feeds the magma source with fresh, potentially fertile material that may re-melt and originate a new diapir. Based on these results of model study of Weinberg, (1997), it is thought that an extensional regime of magmatism in the lake, indeed, reveals the nature of intrusion-driven crustal convection, decompression melting, renewal of the magma source and the origin of nested magmas. Moreover, structural interpretation of seismic sections provides detailed examples and evidences of how and why several magmatic intrusions follow the same path, how nested intrusions

could result from this process, and how sequential magmatism is propagated through margin boundary faults (see Figs. 3.62 and 4.4).

Sequential intrusions and/or diapirs, particularly those with sharp internal contacts, have been interpreted as resulting from the nesting of sequential diapirs (Bouchez and Diot, 1990; Allen, 1992; Weinberg, 1997). The interpretation of sequential magmatism of the lake considers that a direct consequence of sequential intrusions/diapirism is the nesting of diapirs as they become trapped in the upper, stiffer upper crust. However, for magmas to pierce the crust and nest directly into each other, it is necessary to appeal to other mechanisms such as a thermal disturbance. As known, a thermal disturbance is created by hot asthenospheric contact at the base of thin convergent crust (Şengör et al., 2008). Then, thermal disturbance is introduced to trigger the first intrusion. This process results in a series of intrusions, each rises and melts the surroundings similarly to the isolated blobs by Weinberg, (1997). The first one of the series is larger than the others due to probably unstable initial emplacement. Subsequent ones are smaller but increase in size with time as the crust becomes warmer due to heat, advected by earlier intrusions. There is a fast increase in volume (due to decompression melting) followed by a sharp decrease corresponding to the rapid freezing of the intrusion at upper crustal levels. It can follow a period of quiescence where the base of the crust slowly warms up and melts until the buoyancy becomes sufficiently high, decreasing the effective viscosity of the power-law crust and allowing another intrusion to leave the source. This cyclic development of sequential intrusions is strongly evidenced by seismic data through margin boundary faults, particularly Deveboynu and Varis spur zone subbasins. This intrusive cycle strongly proposes intracrustal thermal perturbation to feed back upward mass transport, sill production and maintains the continuous intrusive activity in basin margins and subbasins of the lake. It can be assumed that the initial state geothermal gradient of the upper crust is perturbed by a large amount of intrusive activity beneath the lake. Since, given a long-lasting heat supply to the base of the thin and weak crust, such as hot asthenosphere, the intrusive ascent of crustal magmas or asthenospheric heat transfer causes renewal of the source, renewed melting and repetition of the process. This suggests that a long-lasting heat supply to the base of the crust results in a series of intrusive activity, following the same path and nesting into each other in the upper crust. Asthenosphere-induced thermal

perturbation beneath the lake lasts long enough to cause more voluminous melting under the path of previous intrusions and to control the site of renewed magma ascent (see Şengör et al., 2008). Considered on active magma chambers or pointed stocks at the upper crustal depths, it is also possible to consider that once the melt becomes interconnected, it starts to segregate and migrate into the intrusion. If the intrusion rises rapidly as compared to typical segregation time scales, very little melt is added to the intrusion (Weinberg, 1997). As the intrusion slows in colder upper crust levels, more melt may migrate into and inflate this intrusion.

Indeed, this model implies a feed back mechanism for decompressional melting magmatism (see Şengör et al., 2008 for details), its crustal emplacement and extensional propagation across the lake. It seems that decompressional magmatism enhances the penetration ability of intrusions, triggers melting and leads to sequential magma intrusion in the lake. The asthenosphere-induced thermal disturbance (c. 1330 ^{o}C) of the thin crust allows the magmatic intrusions to rise faster through the thin and warm crust, and to solidify at slightly shallow sedimentary levels. This sequential ascent of intrusions might also explain the pulsating or even the periodic character of magmatic activity. However, it is to note that the renewal of the source caused by the intrusive rise of magmas contrasts with the increasingly refractory nature of the source resulting from the removal of melt by an interconnected network of veins and dykes. Dyking is, for example, unable to renew the source. In such a case, the melting will rapidly stop unless the source is renewed by other external processes (Weinberg, 1997). The model simply reveals that magma intrusion is an efficient mechanism of magma transport through the viscous crust beneath the lake. The combination of magmatic intrusion with decompression melting is an efficient way of melting partially large volumes in a few million years (see Şengör et al., 2008 for volume estimations). These conditions are often found in a domed squashy zone where the orogenic thermal profile is strongly disturbed by mantle-derived basaltic magmas (Keskin, 2003; 2005 and 2007). A combination of previous studies with available seismic data confirms that an external heat source mainly triggers upward low-density mass transport of the mantle-derived alkaline magmatism across zones of extensional and transtensional margins of the lake (Kipfer et al., 1994 and Şengör et al., 2008). This means that an external heat source ultimately drives partial melting and magma intrusion. Since, the volume of partially molten rock is not simply linked

with the amount of heat flow into the crust. This clearly suggests that the amount of magmatic potential energy and melt depend on dynamical processes and on the renewal of the source by the crustal motion and tectonic deformation imposed by intrusions. Given a relatively long-lasting heat source at the base of the thin crust, in the direct contact to asthenosphere, 1330 ^{0}C, the ability of one intrusion to renew the magma source with fertile rocks to originate a new intrusion leads to sequential intrusions that nest into each other in the upper crust. This sequential pattern of magmatic intrusions densely follows the basin margins (see Dewey et al., 1986 for the flake margins). The temperature disturbance caused by previous intrusions controls the position of ascent of new intrusions. This enhances their ability to penetrate the crust and even the sedimentary sections. It is possible that time interval of magmatic pulses may be relatively short. Each magma pulse, for example, lasts 10^4-10^5 years, and the time in between pulses lasts 10^5-10^6 years (Weinberg, 1997). This well explains rapid intrusive activity of Quaternary magmatism in the lake. For example, some of magmatic intrusions intrude the water column into the shallower levels. As noted above, this process contrasts with magma ascent through dykes. In this case, the source rapidly becomes refractory, and a new melt pulse requires either a renewal of the source through tectonic activity or an increase in temperature or water influx (Weinberg, 1997).

This model well describes the sequential nature of extensional magma propagation and intrusive-extrusive events through basin-bounding faults of the lake. Moreover, this model clarifies how decompression melting enhances intrusive magma activity and explains how the thermal and mechanical energy spent by the intrusions may be partly regained in the form of increased buoyancy. Magma intrusion and decompression melting may interact to create favourable conditions for production, transport and emplacement in the upper crust of large volumes of magmas underlying the lake. Thus, basin-bounding intrusive activity of rising magmas is sequentially emplaced at upper crustal depths. Crustal emplacement mechanism of sequential magmatism is irrespective of which started first, asthenospheric doming and decompressional magmatism and/or melting volcanism, these processes reinforce each other. If the thin crust domes due to asthenospheric upwelling, its warmer parts in the lower crust may melt causing faster doming; conversely, if melting starts, buoyancy-driven doming may cause further melting. Thus, both cases

support the proposed model above. The field descriptions and crustal sections presented by Talbot, (1979) and models proposed by Weinberg, (1997) closely correspond to these approaches, and ascribe to some form of crustal convection (pers. comm. with Şengör, 2006). Moreover, detailed study of the upper crust flakes and strike-slip basin interactions (determination of pressure-temperature-time paths) by Şengör et al., (1985) and Dewey et al., (1986) also provide comprehensive field support to the ideas put forward here. Sequential magmatism of the lake shows that upward low density mass and heat transport is sequentially emplaced at upper crustal depths. Magma laterally propagates through margin boundary faults in S and W and vertically intrudes through a complex network of extension fracture-fissure-vent system into the sediments. As combined available seismic data with previous works, this model confirms thin-skinned crustal emplacement of extensional magmatism, magma propagation and deformation dynamics.

4.4.2 Magmatic implications for heterogeneous crust and mechanical anisotropy

Based on the above review of upper crustal emplacement mechanism and formation of sequential magmatic intrusions, extensional magmatism in the lake is shown to be common to deformations taking place on crustal scales. Lake magmatism is interpreted as indicating an effect of heterogeneous crust in the deformation mechanisms in the lake, since heterogeneous crust is thought to have acted as magma migration and propagation channels or pathways and thus, it is interpreted in terms of the mechanical anisotropy. Consideration of magmatism along with the crustal complexities well explains the seismic structural observations, kinematics of the basin-bounding faults and overall deformation styles (see Dewey et al., 1986). Hence, the study of crustal complexities requires new parameters to be taken into account, such as the anisotropic effect of underlying accretionary complex on extensional magmatism of the lake. This leads to an understanding of thin-skinned crustal magmatism, since extensional magma propagation offers thin-skin mechanism of underlying accretionary wedge blocks, by which magma laterally propagates from the further W, through S-margin, into the further E. This weakness zone is characterized by an axis of PDZ of S-margin boundary fault, parallel to both Muş and Cryptic sutures.

Extensional magma propagation through the accretionary basement structure of the lake implicates for heterogeneous crust and mechanical anisotropy. Therefore, the relationship between magma driving pressure, level of emplacement, and final form of intrusions in an extensional tectonic setting of the lake is given below using the margin boundary faults and magmatic intrusions observed from the lake and also the Nemrut volcanic province. In terms of the relationships between crustal magma traps and driving pressure, the excellent study of Hogan et al., (1998) reports some critical consequences for intrusion shape and emplacement in an extensional regime by modelling calculations of magmastatic analysis. The similarities reported in this study of Hogan et al., (1998) are interpreted as indicating similarities in the magma deformation mechanism and the anisotropic crustal basement of the lake. Their study documents two types of magma transport, greatly facilitated by a complex network of fracture-fissure-vent system (see Clemens and Mawer, 1992; Nakashima, 1993 and Hogan et al., 1998) and hence, this study is referred to isolated (individual intrusions) and non-isolated (grouped intrusions) magma transport, propagation and deformation mechanisms observed in the lake, as given below:

“Isolated transport” within fractures without the magma reservoir suggests that the ascent of isolated liquid-filled cracks is driven by the buoyancy of the liquid with respect to its immediate surroundings. Such magma-filled cracks may rise to the level of neutral buoyancy, or alternatively, terminate against a subhorizontal mechanical anisotropy (Weertman, 1971; 1980 and Hogan et al., 1998). This remarks that in a heterogeneous crust, large-scale horizontal anisotropies (the brittle-ductile transition) can trap rising magma at deeper crustal levels under the conditions and thus, the magma driving pressure exceeds the lithostatic load at the depth of the anisotropy (Hogan and Gilbert, 1995; Hogan et al., 1998).

“Non-isolated transport” within fractures with the magma reservoir suggests the magma ascent within a fracture that remains connected to a magma reservoir, is driven by the magma driving pressure (Baer and Reches, 1991 and Hogan et al., 1998). This remarks that in a homogeneous crust, magma within fractures that remain connected to the reservoir has the potential to ascend to the level in the crust where the magma driving pressure becomes negligible. These magmas rose through the continental crust despite their “negative buoyancy” (Hogan et al., 1998). This implies that large volumes of magma are transported within dikes that maintain

connectivity with the underlying magma reservoir. Based on this mode for magma transport, then the level at which rising magma stops (the emplacement level) and acquires its final shape, is to an extent determined by the magma driving pressure (Hogan et al., 1998).

Both transport mechanisms briefly suggest that magma rising within a fracture that remains connected to the magma reservoir has the potential to ascend to the level at which the driving pressure becomes negligible. Magma with a positive driving pressure at the surface possesses the potential to erupt. However, rising magma may be trapped at deeper crustal levels by subhorizontal anisotropies present within the crustal column if the driving pressure is greater than or equal to the lithostatic load at the depth of the anisotropy (crustal magma traps). Subhorizontal sheet-like intrusions form along these crustal magma traps when the driving pressure greatly exceeds the lithostatic load at the depth of the trap (Hogan et al., 1998). This means that the magma has sufficient driving pressure to lift the overburden and allow the magma to spread laterally along the crustal magma trap prior to solidification. If the driving pressure is approximately equivalent to the lithostatic load at the depth of the intrusion, magma ascent may be arrested, but the driving pressure will be insufficient to lift the overburden. This implies that the necessary space for the intrusion must be created by other processes (Cruden, 1998). The resulting intrusions can have the form of a relatively thick, steep-sided stock. Then, magma that solidifies at a depth where the driving pressure is less than lithostatic load will have the form of subvertical sheets oriented perpendicular to the direction of the least principal stress (Hogan et al., 1998). All these considerations as combined with magmastatic calculations by Hogan et al., (1998) draw the following conclusions of extensional magmatism in the lake. These concern the level of emplacement and the shape of magmatic intrusions observed from the lake.

Magma can rise to a crustal or basinal depth (the magma driving pressure is negligible). Magma maintaining a positive driving pressure at the surface has the potential to erupt and to spread laterally. Magma ascent can be arrested at intracrustal depths by subhorizontal strength anisotropy that is the form of crustal magma traps (magma driving pressure ≥ lithostatic load at the depth of the subhorizontal strength anisotropy). This would occur due to the upper crustal discontinuity at 10 km (Dewey et al., 1986 and Angus et al., 2006) and highly anisotropic convergent crust.

Then, sheet-intrusions (almost horizontal) form at and along crustal magma traps (magma driving pressure >> lithostatic load). This suggests that magma is trapped by the upper crustal discontinuities and/or detachment planes, but this case also allows the magma driving pressure to lift the overburden so as to create the available space for the intrusion. This well explains how the magma driving pressure lifts the sedimentary overburden and creates the available spaces (compatibility holes or gaps) for the magmatic activity along the margin boundaries of the lake. It is possible that thicker steep-sided stocks form at crustal magma traps (magma driving pressure = lithostatic load). This case allows the available space for the intrusion to be created by other mechanisms (stoping). For example, in the central Tatvan basin, no apparent intrusive activity observed, this may be resulted from the trapped magmas or magma stocks at upper crustal depths and the formation of ductile shear surfaces beneath the basin. This implies that subvertical sheets form at the level of emplacement (magma driving pressure < lithostatic load).

All these steps suggest that magma driving pressure beneath the lake is much larger than lithostatic load in the lake at the depth of the upper crustal strength anisotropy. A large volume of the rising magmatic materials is efficiently localized at detachment levels and densely channelized through margin boundary faults. This means that the crustal level to which magma may rise and the final shape it assumes is to a large degree, predetermined by the magnitude of the pressure driving force relative to the lithostatic stress, and by the presence of large-scale subhorizontal strength anisotropies (Hogan et al., 1998). Strength anisotropies can act as crustal magma traps (not discounting many other factors, such as thermal history and feeder conduit shape). Such a complicated crustal structure of emplacement and entrapment model of extensional magmatism is, in fact, an expected result of decompressional magmatism and melting volcanism in and around the lake (see Şengör et al., 2008). It is obvious that transtensional faults in W- and S-margins in a heterogeneous structure of convergent crust are simply acting as zones of weakness (the actual means by which magmas ascend and displace host rock being left). This shows that transtensional fault movements are somehow assisting magma ascent, or that magma ascent is occurring by flow into localized extensional regions, which then migrate along the faults. The appropriate locations, seismic structural and morphological geometries, reflection configurations of magmatic intrusions and kinematics of the

faulting require the fault-controlled magma propagation in the lake. As previously mentioned, S-margin boundary fault, suture-parallel magmatic margin, is the main structural weakness zone, through which magma trends an axis of the suture direction, propagates into the faulted margins and distributes widely in central Tatvan basin. The sheeted magmatic bodies are emplaced at ductile decollement surface beneath the lake, most probably bounded by margin boundary faults and the most likely outcome at mid- to shallow crustal levels as noted by Paterson and Fowler, (1993) (see Dewey et al., 1986 for granitic melts at the upper crust). Much attention focuses on the ascent of magmas along faults (D'Lemos et al., 1992; Berger et al., 1996) and/or emplacement in local extensional zones in margin boundary faults (Hutton, 1988). Therefore, the fault model has also the increasing popularity, ascent of magma along faults, even though it is a poorly defined process by Paterson and Miller, (1998).

Paterson and Miller, (1998) studied mid-crustal magmatic sheets in the Cascades Mountains, Washington and reported some critical implications for magma ascent. To some degree, these implications are referred to the possible existence of upper crustal magmatic sheets extending from Muş region to Lake Van basin. Because, diking, diapirism, ascent along faults, and ascent during heterogeneous deformation are championed as "the ascent mechanism" for magmatism in the crust, however, it is believed that these ascent mechanisms form end-members in a continuum (Paterson and Miller, 1998).

Paterson and Miller, (1998) noted the fluid dynamics modeling, showing that flow instabilities result in finger-like, rather than sheet-like protrusions (Talbot et al., 1991; Whitehead and Helfrich, 1991). These flow instabilities occur, however, except in three cases. These exceptional cases are both recognized from available data and also previously reported, as the follows; **(a)** the existence of pre-existing rigid boundaries (Talbot, 1977; Rönnlund, 1987; Talbot et al., 1991) is already known, such as the Muş suture contact between EAAC and BP-M. **(b)** the existence of faults, facies changes, topography, or other lateral changes (Talbot, 1977; Rönnlund, 1987; Talbot et al., 1991) in the lake is known and, **(c)** regional active deformation occurring during rise of magmatic materials (Koyi, 1988; Talbot et al., 1991) is also known. These three cases are applicable to the magmatism in the lake and, therefore, the magmatic intrusions may not represent diapiric instabilities in

which ascent is not controlled by growth along extensional fractures (Paterson and Miller, 1998). However, some factors can be considered as combined effects, based on both diapiric instabilities and also anisotropies at crustal depths. Therefore, several controls on the shapes and orientations of such magma bodies formed in contractional orogens (Paterson and Miller, 1998) are briefly given below.

While flow instabilities form protrusions above elongate diapirs, the existence of rigid boundaries and other crustal heterogeneities along with contracting host rock preserve existing sheet-like shapes or force new protrusions into sheet-like shapes (Talbot et al., 1991; Paterson and Miller, 1998). This suggests that early formed sheets form vertical walls that potentially focus later rise of magma. The focusing magma well explains how magma concentrates and propagates through suture-parallel magmatic margin between EAAC and BPM, suggesting that plastic yield strength anisotropy of the host rock may play an important role in controlling intrusion shapes and orientations (Kirby, 1985). This implies that a heterogeneous convergent crust has lower crustal sections with compositionally or thermally controlled lower yield strengths (Kirby, 1985; Paterson and Miller, 1998). Magma bodies rising by any mechanism involving flow of host rock (Weinberg and Podladchikov, 1994) change shape in response to their ability to rise faster and farther in these weak units in preference to adjacent stronger units. As these weak lithological units (EAAC) strike parallel to the suture zone (Muş suture), then rising magma bodies tend to become elongate parallel to the suture (Muş suture). The heterogeneous crust beneath the lake and overall trend of lithological units (EAAC and BP-M) parallel to the suture complexes are consistent with this hypothesis. Furthermore, the common flat-lying geometry of crustal layering is also an important effect for the earliest magmatic sheets. All these consider that the propagating magma intrusions displace host rock and include ductile flow. Lateral and downward flow of the ductile deformation is along W- and S- margins, into central Tatvan basin.

One of the most convincing implications is that elongate, internally sheeted magmas all along Muş-Lake Van region form during suture-perpendicular contraction without forming in local zones of extension (Hutton, 1988) or during regional suture-perpendicular extension (Paterson and Miller, 1998). Along Muş-Lake Van region, the consistent orientation of magmatic sheets parallel to the axial planes of active

folds/thrusts and perpendicular to the regional contraction direction implies that sheet-like magmatic bodies may form perpendicular to $б_1$ rather than $б_3$ as is typically assumed for dikes by Paterson and Miller, (1998). This ascent model suggests that at least one mechanism of magma ascent at mid-crustal levels may be the diapiric rise of large sheets during active deformation of region. Magma hydrothermal and thermal considerations requiring warm host rocks and slow cooling of sheets clearly imply that such a mechanism is unlikely at rigid and brittle upper crustal levels. Therefore, sheeted bodies may be emplaced at depths greater than 10 km (Dewey et al., 1986 and see Paterson and Miller, 1998 for the depth ranges). Magmas emplaced at shallower sedimentary levels (less than 10 km) tend to be more elliptical and much less sheeted. This ascent model suggests that intracrustal sheeted zones may represent "the advancing front of a magma chamber", rather than the trailing feeder zone, as proposed by Paterson and Miller, (1998). The advancing front of a magma chamber beneath the lake is most probably responsible for the observed magmatism in the lake. This possibility is readily tested by crustal cross section geometries of detailed geochemical studies from Keskin, (2005; 2007) and Şengör et al., (2008) along the Muş suture-parallel zone and BP-M.

Magmatic implications for heterogeneous convergent crust show that magmatic intrusions, diapirism, diking, ascent along margin boundary faults or during heterogeneous ductile flow, all these mechanisms of magma ascent in the crust are the end-member products in a complexity of ascent processes. The magmatic sheets having high length/width ratios can be associated with suture zones, faults or fracture zones extending from their tips from W (Muş) to E (Lake Van). This indicates that sheet walls are oriented parallel to the axial planes of upright folds and thrusts. The sheets are emplaced at high angles to $б_1$, not $б_3$ as proposed in elastic dike models, and are always associated with complex, viscoelastic flow of host rock. These results do not rule out elastic faulting models, as mentioned above, but also favor diapiric rise of magma sheets during viscoelastic behavior of host rock. A complex combination of ascent processes may form sheet-like bodies in the mid-crustal levels (deeper than 10km) beneath the lake. This implies, at least, the possibility of diapiric rise of upper crustal magmatic sheets through suture-parallel magmatic margin of the lake. Many model studies for magma propagation and transport consider the crust to be a homogeneous body free of any zones of weakness. However, such is certainly

not the case, particularly for the accretionary complex underlying the lake. Magmatic implications for mechanical anisotropy show that the transport of melts away from their source regions is strongly controlled by the presence of faults and zones of weakness which provide natural pathways for melt migration. Magma ascent, propagation, transport and emplacement mechanisms suggest that a complex accretionary geology and extensional-transtensional deformation of the lake control the transport of magmas from source regions at depths to their final destinations in the basin. The some general implications from the interpretation of the model studies are that only large multiple intrusions produce enough heat to allow transport of magmas (see Baker, 1998 for the melt viscosity and formation). This suggests that the easiest magmas to transport are high-temperature ones, confirming upper crustal emplacement of the sequential magmatic intrusions and magma hydrothermal deformations in the lake. These implications for heterogeneous convergent crust and mechanical anisotropy clearly evidence that extensional magmatism in the lake is thin-skinned and emplaced at upper crustal depths, mechanically controlled by basement anisotropy.

These results are compared with detailed model studies and interpretations on the dynamics of the crust-mantle system in and around the squashy environment at the centre of the plateau. These results are well consistent with geochemical studies, slab delamination and break off models, decompressional alkaline magmatism and oblique flake-wedge basin structure, supporting thin-skinned emplacement of extensional magmatism in the lake. Şengör et al., (2008) state that highly buoyant, water-saturated accretionary wedge-block structure of Muş-Lake Van basin is certainly unrooted, floating mass over doming hot asthenosphere, indicating the possibility of thermal convection and thin-skinned processes. Basin-scale seismic structural manifestation of decompressional alkaline magmatism provides excellent tectonic and magmatic constraints on the crust-mantle system dynamics beneath Muş-Lake Van region.

5. DISCUSSION

5.1 Strike-slip Tectonics of Lake Van: Deformation, Sedimentation and Basin Formation

5.1.1 General framework of strike-slip Lake Van basin

The Lake Van basin underwent stages of growth and development as recognized in many strike-slip basins. However, this lake can fit into any of strike-slip basin types, based on the classification by Nilsen and Sylvester, (1995). This classification permits easy recognition of strike-slip basins in their initial stages of formation. Changes in the plate-tectonic framework such as the slab delamination and break off events, even minor changes in direction and rate of plate motion may radically affect basin structure and history (Nilsen and Sylvester, 1995). As strike-slip basins evolve through time and space, they may undergo significant translation along principal strike-slip zones. As the basins are laterally being translated, referring to "the porpoising effect, they are commonly subjected to multiple cycles of subsidence and uplift (in general, partly to wholly uplifted) (Nilsen and Sylvester, 1995).

Seismic data, faulting and deformation maps showed that the Lake Van seems to be a "fault-bend basin". Since, the fault-bend basins generally develop at releasing bends along strike-slip faults as in S-margin boundary fault. Extension results as one fault block slides past and away from the other. At larger and longer scales, the sliding block may sag into the extended zone. More commonly, parts of both blocks sag toward the fault to form an elongate zone of subsidence along the fault bend. However, how the walls of a fault-bend basin converge at depth and merge with the master fault is largely unknown (Nilsen and Sylvester, 1995). Fault-bend basins may also form near restraining bends as in N-margin boundary fault, where one of the fault blocks extends differentially as it slides around the bend, out of the zone of restraint. Fault-bend basins are strongly asymmetric as in half-graben filling of central Tatvan basin. These basins have prominent coarse-grained aprons along their principal displacement zones (PDZs). These aprons are commonly lens-shaped in

map view, and generally develop in transtensional settings, subsequently undergoing inversion in transpressional settings as well recognized in and along N-margin transpressional boundary in which progradations are inverted and strongly transpressed. It is essential to emphasize that these kinds of the basins may resemble the rift basins, especially in 2D-seismic reflection profiles (Nilsen and Sylvester, 1995). It is to say that continued transtensional-extensional activity of S- and W-margin boundary faults probably extend and rupture the thin crust, and thus, producing extensional magmatic activity and the high heat flow. This has an important structural and geometric implication. Since, with continued elongation, intraplate convergent crust thins and extends sufficiently to rupture, yielding mantle-originated basaltic magmas (and possibly generation of an oceanic spreading ridge) (Nilsen and Sylvester, 1995). In this type of basin, the length is commonly more than three times greater than width (1/3) (Nilsen and Sylvester, 1995). A good measure for the steepness of the Lake Van basin is the ratio of area against volume. For Lake Van, this ratio is 5.3 (graphically deduced). Typical rift lakes like Lake Tanganyika and Lake Kivu (Hecky et al., 1973) have ratios of 1.5 and 3.0 respectively. This is in the same range as Lake Van. Lakes in tectonically stable regions are characterized by shallow depth and relatively large area. Their area to volume ratio is one or two orders of magnitudes greater than those of the rift lakes. This indicates that Lake Van belongs morphologically to the group of the rift lakes which are situated at the margins of crustal plates (Degens and Kurtman, 1978 and Kurtman et al., 1978).

Detachment faults within the upper crust (Dewey et al., 1986) floor the lake and separate upper rotated blocks from underlying unrotated blocks. The upper crustal flake or block undergoes inversion, rotation and strike-slip deformation during and following deposition. Since, as proposed by Nilsen and Sylvester, (1995), in convergent settings, strike-slip faults and strike-slip basins can be confined to the upper plate of allochthonous thrust sheets, yielding a type of piggyback basin and major amounts of slip along basin-bounding faults are not necessary, as reported by Nilsen and Sylvester, (1995). Many strike-slip basins pass through multiple phases of subsidence and uplift during the complex evolution of the basin. Different parts of the same basin may undergo rapid uplift and rapid subsidence at the same time. In the lake, S-margin transtension during formation of subbasins yields extraordinarily

high rates of subsidence and sedimentation. Equally high rates of uplift and erosion occur during N-margin transpression.

The remark is that the Lake Van basin has the evolutional cycles of the structural development through its whole tectonic history during Neogene-Quaternary time episode (Koçyiğit et al., 2001). The episodes of pure extensional rifting or pure compressional thrusting alternate with episodes of strike-slip and thus, generating complex and commonly "multicyclic" or "polyhistory" basin (Nilsen and Sylvester, 1995). This type of the complex basin commonly occurs in complex orogenic belts, preferentially, in intraplate accretionary orogens or in areas of germanotype deformation (Şengör and Natal'in, 2007) and characterizing "successor basins", as termed by Nilsen and Sylvester, (1995). These basins are long-lasting, having multi-episodic histories of uplift and subsidence, due to shifting tectonic settings. Major deviations in tectonic regimes of the plate boundary conditions such as from collision-compression to strike-slip/extension produce these basin types. Because of their varying tectonic framework, these basins tend to be even more complicated. These polyhistorical strike-slip basins have almost similar characteristics of the other types of strike-slip basins (see the basin classification of Nilsen and Sylvester, 1995).

5.1.1.1 Structural framework and deformation patterns

The complicated structural and deformational patterns (transpression and transtension) developing along strike-slip fault systems depend on four principal factors (Christie-Blick and Biddle, 1985 and Nilsen and Sylvester, 1995), as referred to deformation style of the Lake Van basin; a) the configuration of pre-existing structures or weak zones, implying the structural and geometric importance of pre-existing thrust contacts; b) the kinematics of the fault system, indicating structural complexity of margin boundary faults; c) the magnitude of the displacement and d) the material properties, indicating rheological structure of basin filling and also crustal basement. These factors efficiently yield the curve-planar PDZ with subsidiary faults having widely divergent and changing strikes in margin boundaries of the lake. The subsiding fault-wedge basin and uplifted horst block in N-margin are produced by the curve-planar fault as well as overstepping faults (subbasins) in S-margin. Since, extension occurs at releasing bends and shortening takes place at restraining bends (Nilsen and Sylvester, 1995). Because the basins along and adjacent to strike-slip fault systems may change both gradually and abruptly through

time and space from divergence (transtension) to convergence (tranpression) and hence, their tectonic and sedimentary histories may be extraordinarily complex (Nilsen and Sylvester, 1995).

The upward branching "flower structures", characteristic in seismic cross sections of strike-slip faults, range from simple, single-strand features with uniform dips toward the PDZ to complex, upward convex, multi-strand faults that dip in variable directions (Harding et al., 1983; Harding, 1985 and Nilsen and Sylvester, 1995). In N-margin transpressional zone, convergent strike-slip faults that make up "positive flower structure" have the cross-sectional appearance of reversed oblique-slip faults. Positive flower structures have an overall antiformal character with abundant folds as a result of net shortening. In S-margin transtensional zone, divergent strike-slip faults that make up "negative flower structures" appear to be normal oblique-slip faults. The development of basins along releasing bend of S-margin boundary fault yields subbasins that, with continued displacement, may form rhomb-shaped basins, locally referred to as "rhombochasms" (Mann et al., 1983 and Nilsen and Sylvester, 1995). Negative flower structures have an overall synformal character with folds that result from net extension. These marginal flower structures indicate that the overall strike-slip displacements include regional to local oblique as well as dip-slip displacements. Useful criteria for the correct interpretation of positive and negative flower structures are also described and discussed by Harding (1985 and 1990) (also see Nilsen and Sylvester, 1995).

As Dewey et al., (1986 and 1998) proposed, rotation of blocks about vertical to subvertical axes within strike-slip fault zones may also produce areas of shortening and extension (see Luyendyk and Hornafius, 1987). Rotation of large blocks or flakes may result in formation of sedimentary basins of regional extent (Dewey et al., 1986). Dewey et al., (1986) stated the presence of the upper crustal oblique flakes and their effect on strike-slip basin formation in E-Turkey (Fig. 5.1). This flake model is used for understanding tectonic development of the lake and also Muş basin (Fig. 5.1c). Since, flake-wedge tectonics assumes that some strike-slip basins have subhorizontal detachment surfaces. These detachments separate structurally higher, rotated crustal fragments (oblique flakes) characterized by brittle deformation from structurally lower crustal units characterized by more ductile deformation.

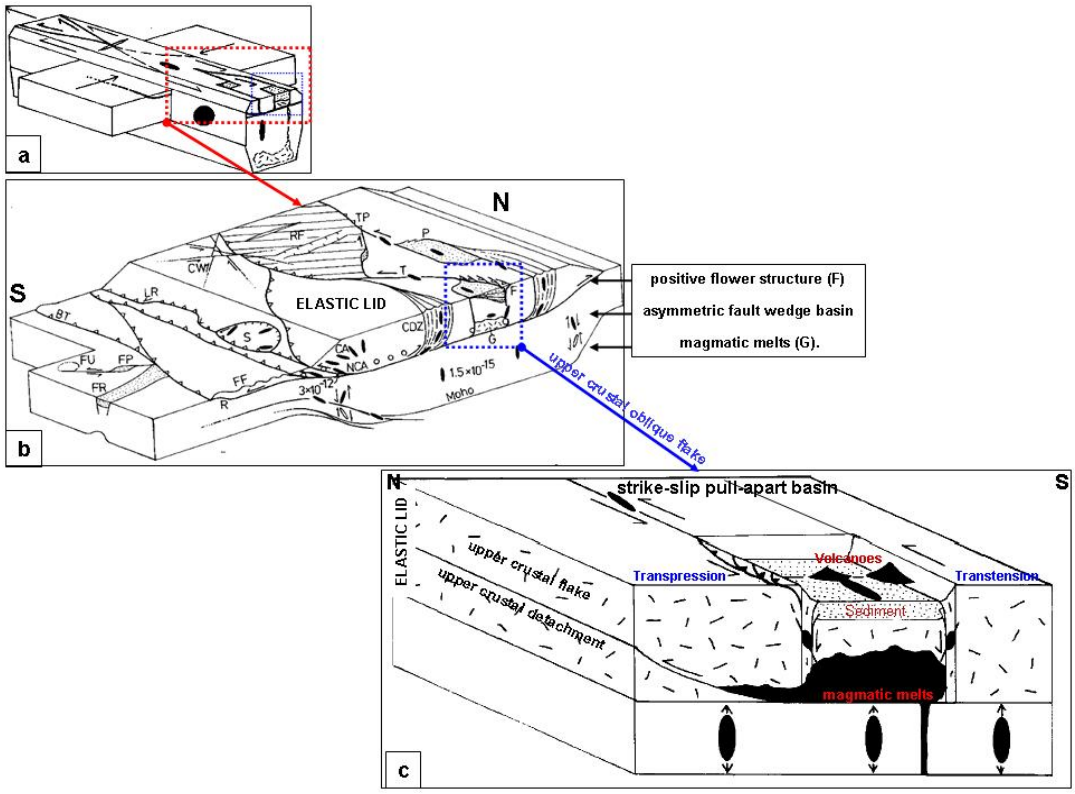

Figure 5.1 : The flake-wedge tectonics (elastic lid model), tectonic origin of upper crustal oblique flakes and strike-slip deformation in E-Anatolia (Dewey et al., 1986). a) lateral extrusion model of the thin convergent crust shows that a crust originally 31 km thick shortened by vertical plane strain and thickened to 80 km is followed by horizontal plane strain by lateral extrusion (see Dewey et al., 1986 for log deformation plot with shortening-elongation lines and theoretical strain path for a thin crust). Dots: strain states (replotted from Pfiffner and Ramsay, 1982). b) schematic illustration of the strains and displacements in the collisional zone of E-Anatolia represents deformation patterns in elastic lid model and modes of detachment termination referred to the flake-wedge tectonics in Dewey et al., (1986). BT: basement thrust; CW: conjugate wrenching; F: flower structure; G: granite; LR: lateral ramp; P: pull-apart; R: ramp; RF: rigid flake; S: surge zone; T: transform; TP: transpression; small circles: hypocentre of large earthquakes. Ellipses indicate finite elongation/shortening directions. c) schematic strike-slip pull-apart basin involves only the elastic lid (basement symbol). Note that the similarity in faulting style of basin margins, basin subsidence and magmatism seems to represent strike-/oblique-slip deformation in Lake Van basin. Black: granitic melts; fine stipple: sediment; fine random ornament: mafic igneous rocks of upper mantle origin (see Şengör et al., 1985 and Dewey et al., 1986 for details of the flake-wedge tectonics).

On the basis of mantle involvement (Allen and Allen, 1990), two major strike-slip basin types may be distinguished by Nilsen and Sylvester, (1995). “Hot basins” involve the mantle. In these basins, uniform-extension models with modifications for lateral loss of heat have been applied with some success. This proposes that the Lake Van is a hot basin due to its warm and weak crustal basement and also its structural geometry.

Because narrow and elongate basins like this lake cool rapidly by lateral heat conduction. These basins appear to undergo rapid early subsidence to form deep basins with associated sediment starvation during early stages of development (Allen and Allen, 1990 and Nilsen and Sylvester, 1995). As a result of greater lateral heat loss, however, narrower basins subside at faster rates and to greater depths than do wider basins. However, "Cold basins" do not involve the mantle and these basins are thus, generally thin-skinned (Nilsen and Sylvester, 1995).

5.1.1.2 Depositional framework and sedimentary patterns

Depositional histories, sedimentary patterns and basin development of the strike-slip regions are difficult to summarize in simple terms or to model effectively their depositional framework. Since, source areas and depocenters migrate laterally through time. This is "migration phenomena of depocenters" in strike-slip basins. Hence, depositional framework and sedimentary patterns of three strike-slip basins are correlated with those of Lake Van basin and discussed in terms of tectonic and sedimentary comparison as the follows.

Nilsen and McLaughlin, (1985) summarized the stratigraphic and sedimentological aspects of threes well exposed strike-slip basins and later reviewed by Nilsen and Sylvester, (1995) (Fig. 5.2). These basins are the Little Sulphur Creek (McLaughlin and Nilsen, 1982), the Ridge (Link, 1982) as basins of California and the Hornelen Basin (Steel and Gloppen, 1980) of W-Norway (Fig. 5.2). These basins are principally of nonmarine origin and of varying size and character, having unconformity surfaces. Especially, the depositional and structural setting of the Hornelen basin is almost similar to that of the Lake Van basin. Common and prominent depositional and sedimentary features of three basins, associated with the lake are as summarized below.

These basins are extremely asymmetric, with their structurally deepest parts close to and subparallel to the syndepositionally most active strike-slip margins. These basins are also characterized by diverse depositional facies. These facies include alluvial fan, braided- and meandering-fluvial, deltaic, fan-delta, shoreline, shallow- and deep-lacustrine, and turbidite deposits. Their basin fill is characterized dominantly by axial infilling, subparallel to the PDZs. Moreover, the basin-margin deposits are so distinctive that small-large debris flow-dominated alluvial fans contain coarse

sedimentary breccia and conglomerate, formed along the syndepositionally active (PDZs). These basins contain very thick sedimentary sections compared to their areas and the basin fill is characterized by high rates of sedimentation (2.5-3.0 mm/y). The reason is that the basin fill is derived from multiple basin-margin sources that changed through time as a result of continued lateral movement along basin-margin faults. This argues that these basins are characterized by depocenters that migrated in the same directions as source terranes along the PDZs. The migration direction is generally opposite to the directions of axial sediment transport. Hence, the basin fill may be petrographically diverse and complex and is characterized by abrupt facies changes as a result of the multiple sources that changed through time and space. The basin fill is commonly characterized by abundant synsedimentary slumping and deformation, possibly in response to basinwide shaking from earthquakes along basin-margin faults. This is evident by the earthquake-induced soft-sediment deformations in NE- and SE-delta settings of the lake (see data from Horasan and Boztepe-Güney, 2006 and Pınar et al., 2007). Particularly, NE-delta, the fault-controlled uplift (E-segment), is characterized by angular discordance and slumping-sliding progradations toward the deep basin.

The remark is that these depositional features are also characteristic of other generally elongate and restricted types of basins, especially rift basins, foreland basins and trench-slope basins (Nilsen and Sylvester, 1995). This may significantly imply rift-related tectonic origin of elongate and restricted Lake Van basin, confirming extensional-transtensional events in the lake (also see Şengör and Yılmaz, 1981 for accretionary structure of E-Turkey and Makran; Şengör et al., 1985 for strike-slip basin formation and basin types in E-Turkey and Dhont and Chorowicz, 2006 for restricted geography of the lake in the confined high plateau of E-Turkey).

5.1.2 Tectono-sedimentary controls on lake sedimentation: upward coarsening sequences and depocenter migration

Recognition of strike-slip basins is probably a more straightforward process on the basis of structural development and margin-bounding faults than is their recognition on the basis of stratigraphic and sedimentologic development (Nilsen and Sylvester, 1995). The PDZs of margin-bounding faults and lateral/oblique-wedge motion provide the most useful structural evidences.

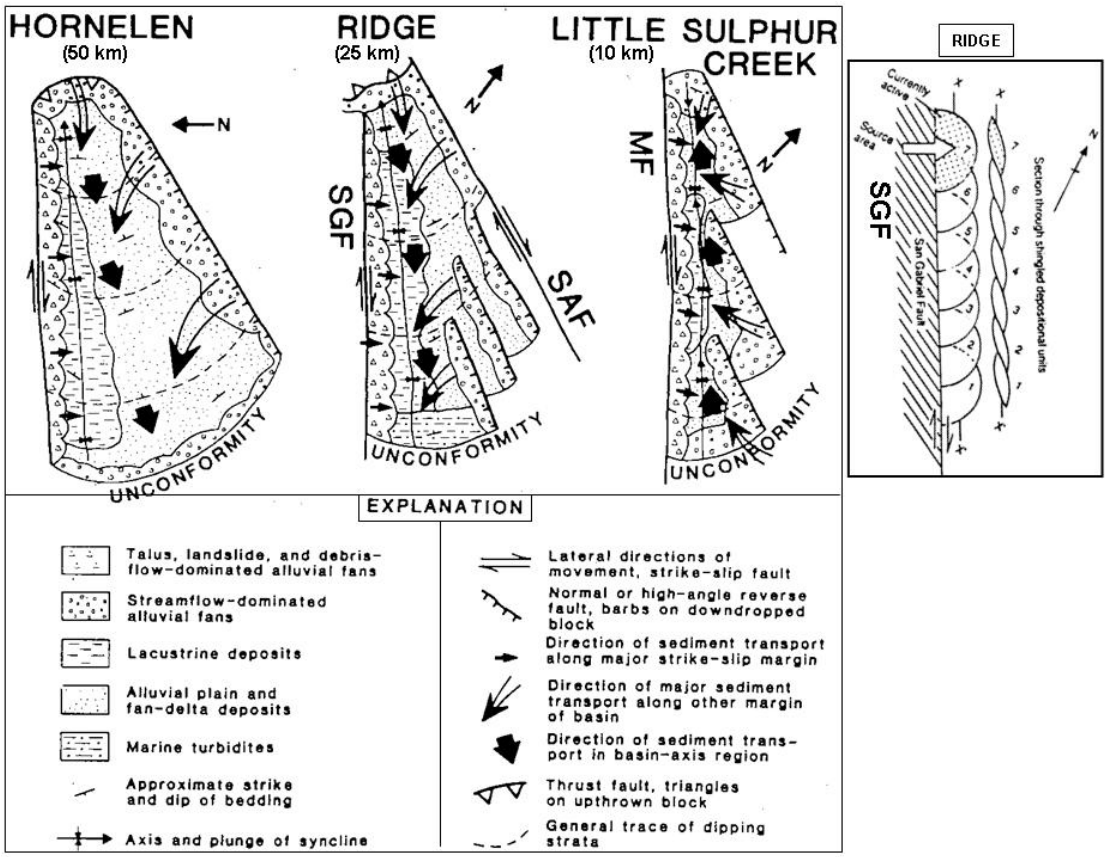

Figure 5.2 : Comparative diagram of strike-slip deformation and sedimentation in different sedimentary basins shows Hornelen basin, Norway, Ridge basin, S-California, and Little Sulphur Creek basin, N-California (from Nilsen and McLaughlin, 1985). Orientations and scales of basins vary considerably but are shown here at the same orientation and size for comparison. Length of each basin is also indicated in km. MF: Maacama fault; SAF: San Andreas fault; SGF: San Gabriel fault (Nilsen and Sylvester, 1995). At the right, small diagrammatic sketch of Ridge basin shows sedimentation model that gives rise to shingled arrangement of basin margin strata (Violin Breccia) (Crowell, 1982b and Nilsen and Sylvester, 1995). Note that extreme similarities in strike-slip deformation and sedimentation pattern between Hornelen, Ridge and Lake Van basins are supported by unconformity surface (uplifted basement block), oblique-slip faults in basin margins, asymmetric half graben geometry of central basin and direction of sediment transport in basin-axis region (depocenter migration towards ESE in Ridge basin).

Since, it is recognized that the sedimentary source areas are laterally displaced from sedimentary successions, containing unique detritus, especially if coarse-grained. Therefore, as well recognized from depositional successions, N-S asymmetric half graben and W-E strike-slip basin fill of the Lake Van, the sedimentary fill of many strike-slip basins is, in general, dominated by repetitive, basinwide, upward coarsening sequences that cut across all facies boundaries, as supported by Nilsen and Sylvester, (1995). It seems that these sequences are tectonically controlled by basin-wide changes in base level.

This results in progradation of marginal and axial coarse-grained facies over axial finer-grained lacustrine and related facies, particularly in NE-delta setting toward the deep basin, characterized by large amount of slumped-slided progradational clinoforms. As mentioned above, for example, upward coarsening sequences are well developed in these basins; the Little Sulphur Creek basins, Hornelen basin and Ridge basin (Steel et al., 1977; Steel and Gloppen, 1980; Nilsen and McLaughlin, 1985 and Nilsen and Sylvester, 1995) (Fig. 5.2). These coarsening sequences are resulted from episodic major tectonic subsidences and uplifts of the basin and basin-margins, lowering of lake level, and climatic changes or combinations of all these factors (Nilsen and Sylvester, 1995). For example, asymmetric differential uplift (basin-margins and deltas) and subsidence (central Tatvan basin) in the lake show that, as seen in NE- and SE-delta settings, while the initial subsidence rate decreases, the pathways are established for sediment to enter the basin. As a result of this, sedimentation rates ultimately exceed subsidence rates, leading to basin filling toward the deep basin.

Some structural and sedimentary factors, however, reported by Nilsen and Sylvester, (1995) make tectonic and depositional recognition of the strike-slip basins and their interpretation difficult and complex. This complexity is well evident in the Lake Van basin. Since, margin boundary strike-slip faults are commonly reactivated as normal, reverse, oblique or thrust in more complex collisional zones of faulting. Regime changes in tectonic framework of the region may yield preservation of only parts of the original strike-slip basins. Lateral movements along PDZs of margin-bounding faults commonly detach, rotate and translate basins or parts of basins from their places of origin, and thus, making paleogeographic reconstructions tenuous. Multicyclic strike-slip development or polycyclic episodes of subsidence and uplift commonly remove major parts of the stratigraphic and structural record and thus, inducing unconformity surfaces as well recognized in NE-delta setting of the lake and Çarpanak uplifted zone. This makes their depositional and structural histories more complex. Interestingly, many features of strike-slip basins resemble those of rift basins and forelands (N-S cross-sectional seismic profiles and plan-view of the lake). This makes their recognition problematic. For example, the reliance upon these 2D-seismic reflection lines is commonly misleading. Based on the recognition problems by Nilsen and Sylvester, (1995) mentioned above, more reliable tool to

recognize the strike-slip basins is generally developed from the sedimentation styles and patterns, stratal successions and basin filling mechanisms. This is lateral migration of depocenters parallel to PDZs, appearing to be the most useful (the depositional criteria outlined by Nilsen and McLaughlin, 1985 and Nilsen and Sylvester, 1995). This means that, in strike-slip basins, depocenters migrate laterally, parallel to the principal bounding faults. This tectonic-controlled depositional event is excellently observed all along the sedimentary strata and basin filling style of the lake. By this process, the lake basin lengthens through time without excessive widening, accumulate extraordinary thicknesses of fill, and contain abrupt facies changes and petrographic variations throughout its history (Nilsen and Sylvester, 1995). As different from the other basins, however, depocenters in most other basins tend to migrate either transversely away from or toward the principal bounding faults, or to remain in more or less the same location through time (Nilsen and Sylvester, 1995).

Structural, sedimentologic and stratigraphic evidences for tectono-sedimentary controls and sedimentary evolution of the Lake Van strike-slip basin include the following important implications. One of these is that tectono-sedimentary controls dominating all over the lake results in two prominent components; upward coarsening sequences and depocenter migration. The strike-/oblique slip faults on N- and S-sides of the basin result in lateral displacement of related depocenter and lateral offset of matched source areas and deposits. During active tectono-sedimentary control, localized subsidence/uplift and erosion, results in unconformities of the same age as thick nearby sedimentary fill. Very high sedimentation rates characterize laterally restricted, but thick sedimentary sequences. These depocenters, upward coarsening sequences, coarse-grained alluvial-fan, fan-delta, sublacustrine-fan aprons, and related sediments along the flanks of margin bounding faults (PDZs), typically alternate along strike in extensional basins (as recognized from rift basins by Nilsen and Sylvester, (1995) from one flank to the other, and thus reflecting activity of border faults and abrupt lateral facies variations. Particularly, basinwide upward coarsening sequences develop in response to tectonically induced basin deepening. It should be stated that intraplate, nonmarine and strike-slip-controlled lacustrine environments result in poor intra-basinal and inter-basinal age control and stratigraphic correlations (also see nonmarine settings

of late Cenozoic strike-slip basins in Nilsen and Sylvester, 1995). Hence, a detailed study of seismic sequence stratigraphy and facies analysis in delta-margin sections of the lake seems problematic.

5.1.3 Dynamic and comparative analysis of strike-slip basin systems

The strike-slip basins, their deformation styles, sedimentary patterns are extensively analyzed and discussed below, in terms of their similarities and differences with the Lake Van basin. Since, dynamic and comparative analysis of some strike-slip basin systems and their correlative synthesis may provide several critical implications for understanding tectonic, structural and sedimentary development of the lake within its neotectonic history during Plio-Quaternary period.

Ridge basin, S-California, is the best studied fault-bend basin in the world, as reported by Nilsen and Sylvester, (1995) (Fig. 5.2). This basin developed as a stretched and sagged crustal wedge NE-of the San Gabriel fault in the area where the fault had a curvilinear trace (Nilsen and Sylvester, 1995). In this basin, the fan-delta and alluvial-fan deposits interfinger basinward with fluvial and lacustrine strata that record longitudinal basin filling. It is important to say that, as well recognized in the half-graben basin fill of central Tatvan basin in the lake, the total stratigraphic thickness is much greater than the accumulated thickness at any particular locality in the basin. Moreover, abundant synsedimentary deformational structures in the basin fill may record penecontemporaneous seismicity.

Ridge basin is extensionally formed at dextral releasing bend of San Gabriel fault on the low-angle detachment surface. This basin is clearly controlled by upper crustal flakes or wedges. Its central area is asymmetrically tilted half-graben basin structure in NE-SW cross section (see diagrammatic sketches of Ridge basin showing its tectonic origin, after May et al., 1993 and Nilsen and Sylvester, 1995). This cross-section is very similar to N-E seismic profiles of the lake. Sedimentation model of Ridge basin gives rise to shingled arrangement of basin-margin strata (Crowell, 1982b and Nilsen and Sylvester, 1995) (Fig. 5.2). This model shows, during section through shingled depositional units, the migration of source area, controlled by dextral San Gabriel fault. This is arrangement of basin axial strata, parallel to depositional trough. Depocenter remained fixed relative to source areas across from San Gabriel fault as previously deposited strata are rotated and carried relatively S.

As expected, total stratigraphic thickness is much greater than maximum thickness in any single well (from Crowell, 1982a and Nilsen and Sylvester, 1995). The stratigraphic and sedimentologic cross-sections by Nilsen and Sylvester, 1995 well reflects the W-E trending sedimentary section of the lake and also erosional surface of uplifted delta setting as a source area. All these indicate that tectonic, structural and sedimentary development of Ridge basin has very close similarities with the lake, at least, based on upper crustal wedge pattern, fault-bend/wedge basin geometry and strike-slip sedimentation styles.

Dextral normal oblique and stepover system of S-margin boundary fault has W- and E- en echelon fault segments. As known, the geometric patterns, structural axes, and depocenters of stepover basins depend on the spacing between overstepping or en-echelon strike-slip faults, the amount of overlap between the faults and the depth to basement (Rodgers, 1980 and Nilsen and Sylvester, 1995). Varis spur zone and Deveboynu subbasins are developed by such a system of en echelon faulting. This shows where basement is shallow and where the overlap is from slight to the increasing overlap, two or more small subbasins may develop. A single, central basin may form, where basement is deep. However, several individual basins between overstepping strike-slip faults may coalesce into a single, larger basin, such as Binchuan basin in Yunnan province of S-China (Deng et al., 1986 and Nilsen and Sylvester, 1995). On the other hand, along the central Tatvan basin and within subbasins of the lake, the intervening of sedimentary strata is relatively undeformed, except for ductile-related folding. Because, the presence of a magmatic layer beneath much of the basin partly decouples the sedimentary fill from the basement (see Dead Sea Basin example by TenBrink and Ben-Avraham, 1989 and Nilsen and Sylvester, 1995). Strike-slip-controlled depocenter has migrated from W to E, accompanied by intrusions of magmas through margin boundary faults. This generates an asymmetric basin with extraordinarily abrupt facies changes (see Dead Sea Basin example by TenBrink and Ben-Avraham, 1989 for the role of diapiric intrusions of evaporites and underlying salt layer). The best example, evident for this event, comes from Los Angeles Basin, S-California. Miocene volcanic rocks are present at depth nearly everywhere in the central part of the Los Angeles Basin, but crop out only locally along its edges. This implies that magma intruded in response to cracking of the crust and opening of the basin (Nilsen and Sylvester, 1995).

Magma rose nearly hydrostatically to a compensating level within the sedimentary fill (Wright, 1991 and Nilsen and Sylvester, 1995). This extensional magmatic event at crustal depths strongly confirms the oblique opening of the lake and its upper crustal flake origin (Dewey et al., 1986). Now the Los Angeles Basin is filled so that alluvial fans stretch from the N-bounding mountains across the basin almost to the sea, and surface streams carry sedimentary debris to offshore basins (Nilsen and Sylvester, 1995). In NE-delta of the lake, larger alluvial fans and progradations stretch from the delta across the basin, almost to the N-margin boundary fault. Submerged channels and surface streams carry sedimentary debris and turbidities to deeper basin.

Although the recent evolution of the Lake Van basin is extensional-transtensional or transrotational, its later history (latest Quaternary) is dominated by transpression in N-margin boundary. Narrow transpressional basin observed in seismic data is marginal to N-margin transpressional boundary (PDZ and/or positive flower structure). This basin is characterized by coastal-onlap trough fill pattern on sublacustrine slope of the lake. This fault-controlled, sublacustrine marginal depression is resulted from flexural subsidence induced by loading from branching reverse faults (reversed oblique-slip faults). This margin-bounding transpressional basin is also known as “fault-angle depression” that is topographic depression by (Balance, 1980) and as “fault-margin sag” that is special type of this depression by (Crowell, 1976). This marginal strike-slip basin seems to be, in fact, “miniforeland basin”. This type of transpressional basins has more complex patterns of sedimentation and structural evolution (Nilsen and Sylvester, 1995). Rapid sedimentation in this transpressional basin induces additional subsidence by sediment loading. This transpressional basin is probably originated from synclinal downfolding or fault-dominated subsidence marginal to reverse faults (Nilsen and Sylvester, 1995). Since, N-margin boundary is characterized by a more complex transpressional regime, marked by multiple faults, fault strands and interfault basins, such as “fault-wedge basin”. As the lake province underwent wedge-block rotation, in the N-margin boundary, extensive sinistral faults sliced the block into a series of sub-blocks, some of which underwent uplift (pushed up rhomb-horst block), and others of which underwent subsidence (fault-wedge basin and fault-margin sag) in response to rotation-induced shear.

The best example of this later transpressional development is well seen in Ventura Basin, S-California. Similar to the lake, early evolution of this basin was transtensional and transrotational, but, its later history has been dominated by transpression (Crowell, 1976 and Nilsen and Sylvester, 1995). The sinistral faults sliced the block into a series of sub-blocks, while the Ventura Basin was undergoing rotation. In response to rotation-induced shear, some blocks underwent uplift and subsidence (Crowell, 1976 and Nilsen and Sylvester, 1995). In the Ventura Basin, the basin inversion has locally occurred during the past one-half million years. Sandy siliciclastic turbidities transported axially down the basin from basement source areas more than 50 km to the E (Hsü, 1977; Hsü et al., 1980). Coarser-grained submarine debris flows were shed into the basin from the subparallel N and S-flanks of the basin. Basin inversion also caused uplift of older rocks along basinward directed reverse faults along both flanks of this basin. The Ventura basin formed within such a zone as a complex transpressional basin during the Plio-Quaternary period and characterized by rapid subsidence and high rates of sedimentation typical of strike-slip basins by Nilsen and Sylvester, (1995). Sedimentary and structural development of the Lake Van basin seems to reflect that of the Ventura Basin. Along margin boundary sections of the lake, basin inversion has only locally occurred during probably Pliocene period. Debris flows and highly concentrated turbiditic deposits transported axially down the deep Tatvan basin from deltas and source areas in response to strong uplift and fault activity in NE-delta. Coarser-grained sublacustrine debris and magmatic flows were shed into the deep Tatvan basin, particularly from the subparallel W- and S-flanks of the lake. Local inversion of the basin caused the block uplifts and subsidences along the marginal flanks of the lake. Transpressional subbasins in N-margin boundary very recently formed within such suture-bounded compressional-ramp region as complex transpressional subbasin systems along N-margin. These subbasins are considered to be the lacustrine transpressional basins, forming mini-foreland basins, which are depressed by structural loading and resultant flexural bending as a consequence of partitioned convergent/divergent strike-slip in N-transpressional setting. Thus, they are characterized by rapid subsidence, uplift and high rates of sedimentation typical of strike-slip basins. As the last example, it is given that the S- and SW-flanks of the San Joaquin basin, C-California, are bounded by transpressonal regions of the San Andreas fault (Wilcox et al., 1973 and Harding, 1976 and Nilsen and Sylvester, 1995).

Marginal to the thrusts is a series of recent lacustrine transpressional basins, including, from SE to NW, Kern, Buena Vista, and Tulare lakes (Nilsen and Sylvester, 1995). Structural and sedimentary interactions between NE-delta setting and central Tatvan basin are perfectly seen in these lacustrine basins. As well recognized in Çarpanak uplifted zone, the block SW of the San Andreas fault was uplifted and provided detritus to fan deltas and turbidite systems into the deep basin (Ryder and Thomson, 1989 and Nilsen and Sylvester, 1995). At the same time, as observed in Tatvan basin, en-echelon folds were growing and forming submarine hills along the W-edge of the basin, partly as a result of shear along the San Andreas fault (Nilsen and Sylvester, 1995). The growing folds focused turbidity currents along synclinal valleys and through saddles to basin plains (Nilsen and Sylvester, 1995).

5.1.3.1 Thermal polygenetic/polyhistoric structural evolution and tectonic mobility

The Lake Van basin, during paleotectonic period, formed as Oligo-Miocene compressional ramp basin, bounded by high-angle thrust contact in N- and S-flanks of the basin. In Pliocene, the lake experienced fault reactivation and structural inversion. During Plio-Quaternary, tectonic and structural development is characterized by strike-/oblique-slip margin boundary faults, W-E trending strike-slip and N-S trending asymmetric half-graben sedimentation. So, the lake is a polyhistoric basin, having complex structural patterns that result from alternating episodes of strike-slip, compressional and extensional faulting. This confirms that the lake has a multi-component dynamic evolution and evolutional periods of structural development during its whole history. Polycyclic evolutional development or multi-component basin history, changing structural settings, and repeated episodes of rapid subsidence/uplift characterize rapid structural development or relatively long-lived strike-slip zones, such as many of those along the San Andreas fault (Crowell, 1974a,b and Nilsen and Sylvester, 1995), even though these basins themselves are commonly short-lived. Such a kind of polyhistoric basins commonly forms in areas of changing plate-tectonic framework by Nilsen and Sylvester, (1995), such as the slab delamination and break off processes. Since, these processes can easily trigger tectonic unstability of accretionary wedges. During collision, Lake Van developed as a polygenetic basin along accretionary thrust-sheet boundaries in intraplate collision.

Due to delamination and break off events, post-collisional extensional faults lately modified thrust-sheet boundaries (see Nilsen and Sylvester, 1995 for fault reactivations). In this type of accretionary setting, strike-slip basins along margin boundary faults confined to the upper plate of thrust sheets (at upper crustal depths) underwent reversal of movement along marginal faults during subsequent extensional faulting, revealing a dominant effect of germanotype deformation (Şengör and Natal'in, 2007). Some collapse basins, such as the strike-slip-bounded, Devonian Hornelen Basin of W-Norway (Steel and Gloppen, 1980), may have resulted from this process (Nilsen and Sylvester, 1995) (Fig. 5.2).

As referred to upper crustal oblique flakes and flake-wedge tectonics proposed by Dewey et al., (1986) (Fig. 5.1), at releasing bends in divergent settings, the strike-slip basins can develop along transfer or accommodation zones that link major loci of normal faults. They can also form along the flanks of individual detached crustal segments, especially in horseshoe faults, where low-angle strike-slip faults mark the margins of detached segments (Nilsen and Sylvester, 1995). On the other hand, at restraining bends in convergent settings, the strike-slip basins develop along transfer zones that link intact individual segments of larger thrust or underthrust crustal segments (Nilsen and Sylvester, 1995). This convergent/divergent strike-slip development in basin margins confirms that Lake Van, as a polyhistoric and/or polygenetic basin, is confined in upper crustal sections, driven by flake-wedge tectonics. This means that the lake is interpreted as asymmetric half-graben structure, which locally developed in a regionally extended crustal slab, flake or wedge. One of well-known half-graben basins, very similar to the lake, is Death Valley basin, E-California. This basin is an N-trending, asymmetric half-graben that has formed as a result of regional extension (Nilsen and Sylvester, 1995). Sediments are derived from the bounding mountains and transported into the half graben as debris-flow-dominated alluvial fans. Alluvial fans are small and steep on the E-side, and by larger, gentler-sloping and regionally extensive stream-flow-dominated fans on the W-side (Nilsen and Sylvester, 1995). In addition to being a pull-apart between two fault systems, as proposed originally by Burchfiel and Stewart, (1966), Death Valley has been interpreted as one of several asymmetric half-grabens that developed locally in a regionally extended crustal slab (Wernicke, 1985; Wernicke et al., 1988; Hodges et al., 1989 and Nilsen and Sylvester, 1995).

The most prominent and famous example of the upper crust-driven block tectonism is rhombohedral Vienna Basin, Austria, extremely similar to the lake (see Şengör et al., 1985 for strike-slip basin formation and rhombohedral block tectonics, in E-Turkey). Vienna basin is a well-developed rhombohedral basin along an active left-stepping, left-lateral tear fault between two thrust blocks of the Carpathian thrust belt (Nilsen and Sylvester, 1995). Sinistral oblique-slip and rhombic opening of Vienna basin occurred in the strike-slip fault-bend of thrust contacts (active and inactive thrusting). These faults are roughly parallel to structural trends in the underlying nappes. Thus, this basin is opened as a fault-bend basin at a left step in a left-slip tear fault within an allochthon thrust NE-ward onto the European platform (see Royden, 1985 and Nilsen and Sylvester, 1995 for schematic diagrams of this basin). Sinistral faults developed contemporaneously with thin-skinned thrusts (Royden, 1985) that are also active and inactive. Both the Lake Van and the Vienna basins are confined entirely to the allochthon and formed along a releasing bend. In this type of polygenetic Vienna basin, mantle was not involved and a thermal anomaly is not present beneath the basin (Nilsen and Sylvester, 1995), indicating "cool polygenetic basin". However, in Lake Van, upper mantle-generated alkaline magmas are strongly involved and a thermal anomaly is present beneath the lake, indicating "hot polygenetic basin".

Some prominent accretionary basins, the Tyaughton-Methow, Bowser and Gravina-Nutzotin basins are "complex successor basins" (Nilsen and Sylvester, 1995). These successor basins developed along the continental margin in response to accretionary events in the NW-part of the N-American Cordillera (Nilsen and Sylvester, 1995). Therefore, they have some genetic and structural similarities to the Lake Van. For example, the Bowser basin is bounded by Teslin suture in NE and Shakwak suture in SW, while the lake is bounded by Muş suture in S and pre-existing thrust in N. So, both basins are suture-bounded troughs. Particularly, the E-Bowser basin and the Lake Van were also tectonically reactivated basins. In the E-Bowser, generally coarse-grained fluvial and lacustrine strata were deposited unconformably on the older marine fill. Dextral slip and uplift along the Shakwak suture on the W-flank of the basin resulted in E-transport of nonmarine, lacustrine clastic detritus into the basin (Nilsen and Sylvester, 1995). Similarly, dextral oblique-slip, subsidence of Tatvan basin and uplift along the Muş suture on the W-margin of the lake resulted in

strike-slip transport of lacustrine clastic detritus to E into the delta settings, as typical of strike-slip sedimentation. The framework established by Eisbacher, (1981 and 1985), including the outboard Queen Charlotte basin, reflects the shifting influences of convergent and strike-slip tectonics on depositional systems and basin morphology (Nilsen and Sylvester, 1995). This framework significantly implies that tectonic regime changes in intraplate accretionary setting, fault reactivation processes and structural inversions from thrust/ramp-bounded to extension/strike-slip-bounded basin, strongly affect on depositional systems, sedimentation styles, patterns and basin morpho-physiography. These entirely reflect the shifting influences of collisional/compressional and extensional/strike-slip tectonics on the Lake Van basin.

The last example, Salton Trough, S-California, is an active strike-slip basin system. The initial formation of this basin during Middle Miocene time appears to have been the result of extensional tectonics related to formation of the Gulf of California and the Basin and Range (Crowell, 1987 and Nilsen and Sylvester, 1995). The recent history of the basin reflected dextral along the San Andreas fault and related transform faults to the S. The initial record of extensional opening is well preserved in outcrops along the W-margin of the trough, where pre-rift, braided-stream deposits are overlain in angular unconformity by syn-rift alluvial-fan, landslide-breccia, lacustrine, fluvio-deltaic and evaporitic deposits (Nilsen and Sylvester, 1995). The basin in this area appears to have been a half-graben, with its principal N-striking border fault to the W (Nilsen and Sylvester, 1995). The later history of the basin has been dominated by strike-slip tectonism associated with several dextral faults of the San Andreas system, including various faults. As well seen in many strike-slip basins discussed above, coarse-grained and very thick alluvial-fan deposits grade axially into lacustrine mud, similar to the modern setting surrounding the Salton Sea. Faults and deformation patterns outline uplifted blocks and subbasins nested within the Salton Trough (Nilsen and Sylvester, 1995). These patterns show very close similarity to Çarpanak uplifted block and Deveboynu and Varis spur zone subbasins. These subbasins nested between Deveboynu peninsula and Çarpanak spur zone. The subbasins are similar to those strike-slip basins in the Gulf of California that have not filled with sediments. Orientation of these subbasins relative to the PDZ-strike of the S-margin boundary fault and the Muş suture (or Cryptic suture) suggests that their

direction of stretching corresponds to the direction of extension in dextral simple shear in S (also see Crowell, 1985 and Nilsen and Sylvester, 1995).

The Salton Trough reflects the complex evolution of a polyhistory basin with an initial rift origin, an irregularly stretched floor, strike-slip, development of en-echelon subbasins, and rerouting of a major fluvial-dominated delta into the widening trough. Modern strike-slip faulting is superposed on Miocene detachment faults which were superposed on Mesozoic and early Tertiary thrusts (Nilsen and Sylvester, 1995). Similarly, the Lake Van basin also has the complex evolution of a polyhistory basin with initial compression-ramp origin, fault reactivation and extension, an stretching floor, the strike-/oblique-slip deformation, development of en-echelon faults and subbasins, rerouting of the fluvial-dominated delta into the subsiding and laterally migrating deep Tatvan trough and a late transpression and transpressed progradations in NNE-marginal section. Tectonic mobility of the Lake Van basin probably began about Late Miocene-Early Pliocene (Mio-Pliocene transitional period) and has intensified during the Plio-Quaternary periods. The strike-slip faulting is presently superposed on the low-angle detachment faults which were superposed on early thrusts. This confirms that the lake is bounded by crustal-flake margins, indicating oblique flake origin of the lake at upper crustal depths.

Finally, an understanding of the strike-slip Lake Van basin is mostly enhanced by a thorough understanding of how other types of strike-slip basins develop. These basins, Ridge, Los Angeles, Ventura, San Joaquin (Kern, Buena Vista and Tulare lakes), Hornelen, Death Valley, Vienna, Bowser Basins and Salton trough, are the most famous examples of crust-seated deformation at upper crustal scales. Each strike-slip basin is carefully considered, separately evaluated and interpreted in a comparison with Lake Van.

5.2 Flake-block Nature of The Lake Basement and Kinematic Implications for Block Rotation and Lake Seismicity

If all these results and related implications have applications elsewhere in the high plateau of E-Turkey, they highlight some new concepts for understanding the tectonic behavior of flake-block nature of the thinned crust, kinematic constraints of block rotation and thus, oblique-slip tectonics of the Lake Van basin in E of Karlıova. ETSE project, (2003), particularly Türkelli et al., (2003) and Örgülü et al.,

(2003) reported that dextral wrench system E of Karliova is an continuation of the N-Anatolian Transform Fault towards Zagros fault belt. However, strike-/oblique-slip faults E of Karliova are elements of the intra-plate convergent regime (Şengör and Kidd, 1979) and these faults are not continuations of the N-Anatolian Transform Fault (Dewey et al., 1986). The most important thing is that strike-slip motion on these faults is due to their oblique orientation with respect to the Arabia/Eurasia convergence.

In the Lake Van basin, the position and orientation of associated en echelon folds, local domains of extension and shortening, and related vents, fractures and faults depend on the bending or stepping geometry of the strike-slip faults or fault zones, and thus the degree of convergent or divergent strike-slip faults in N- and S-margin boundaries. Subbasins such as Tatvan delta graben basin, Deveboynu and Varis spur zone subbasins, formed as result of crustal extension in domains of divergent strike-slip such as releasing bends or negative flower structure of S-margin boundary. Deveboynu and Varis spur zone subbasins evolve between overstepping oblique-slip faults (W- and E-segments). The arrangement of these segments which bound basins is tulip-shaped. Elongate block uplifts, ranging from pushed up rhomb-shaped horst (pressure sedimentary ridge) to low hills or small ranges (gas pressure ridge) in Çarpanak spur zone, formed as a result of crustal shortening in domains of convergent strike-slip such as restraining bends or positive flower structure of N-margin boundary. These are bounded by an arrangement of strike-slip faults having the profile of a palm tree. It is essential to point out that N- and S-margin boundary faults are in intraplate setting and hence, are forced by intraplate stresses, reactivating pre-existing thrust faults and propagating them laterally and vertically into unfaulted rock. Reactivation in strike-slip mode is favoured in a regional conjugate wrench regime on faults which have moderate to steep dips (Şengör et al., 1985; Dewey et al., 1986 and Şengör et al., 2008). Although displacements of these faults are small, they may produce faulted blocks and fault-surface features which obliterate earlier movement indicators (Woodcock and Schubert, 1994). Seismic reflection data lacks sufficient information about the 3D-geometry of strike-/oblique-slip faults, but it can still provide valuable information about the mechanism of translation and rotation of faulted sedimentary blocks around strike-/oblique-slip fault bends, or about the sequential development of structures in the complex zone of

heterogeneous strain. However, the kinematic theory of strains (except for block rotations and fault displacements) in complex continental convergent plate boundary zones reported by McKenzie and Jackson, (1983) are not discussed here.

5.2.1 Nature of the blocky structure

Morpho-tectonic and structural interpretation from available data and previous studies has identified relations between oblique-slip faults and crustal segmentation (see Dewey et al., 1986 for crustal flakes) at or near the seismogenic upper crust (Türkelli et al., 2003 and Örgülü et al., 2003). This gives a mechanism for block rotation and translation of crustal flakes (or slabs) (Fig. 5.1). How widespread is this phenomena, and how the mechanisms operate that drive this detachment tectonics is well discussed by Şengör et al., (1985) and Dewey et al., (1986) for Muş-Lake Van region. In continental convergence zones, fault-bounded blocks or flakes can be mostly observed and the basic problem is how relative plate displacement directions and rates are converted in strains and strain rates within the convergent plate boundary zone and to what extent are flakes internally rigid with strain confined to narrow slip zones at their boundaries.

Neotectonic deformation with the oblique-slip boundary faults of the lake has reviewed the notion of "flake tectonics" (Oxburg, 1972), that is, of "thin-skinned tectonics" (Yeats, 1981), where much or most of the accretionary wedge basement of the lake is detached on S-dipping low-angle thrust faults (Dewey et al., 1986). Above these low-angle faults, high-strength, flake-like slabs up to 10 km thick have detached from the lower crust to offset strike-slip faults at depth (Dewey et al., 1986 and Lemiszki and Brown, 1988) (see Fig. 5.1). In this model, the slabs may slide away from one another and are free to rotate externally about a vertical axis in the prevailing regime of simple shear (Dewey et al., 1986 and Sylvester, 1988). These rotated blocks are, in fact, flakes (Oxburg, 1972), slabs or crustal panels (Dickinson, 1983; Sylvester, 1988), which detach on a shallow horizontal shear surface as Brown, (1928) observed in model studies. In these studies, the rotation of upper layers occurred where horizontal shear took place in a weak, underlying layer (Sylvester, 1988). Thin-skinned neotectonic deformation of the lake showed that flake-block geometry of the lake appears to have been governed by pre-existing fault discontinuity. In other words, the Lake Van flake-block had detached at a mechanical anisotropy (10 km) to rotate, as referred to Dewey et al., (1986).

Such a flake structure of the lake is the surface expression of thin upper-crustal sheets above intracrustal *decollements* rather than small "platelets" (Fig. 5.1b, c). Oblique-slip deformation can, thus accommodate shear-induced rotation, suggested by the presence of alternating transtensional and transpressional features in N- and S-margin boundaries. This argues that block rotation by strike-/oblique-slip faulting is responsible for a number of structural relationships and small-scale tectonic features observed along margin boundary faults (Garfunkel and Ron, 1985). Thus, in the lake where shear is distributed, deformation is likely to be inhomogeneous (Şengör et al., 1985) and largely controlled by block geometry and the kinematics of block interaction (Garfunkel and Ron, 1985). The elastic (rigid upper section) and non-elastic behavior (very ductile lower section) of the thin and warm crust will strongly depend on the nature of any pre-existing fabric and the depth to either a decollement or ductile shear zone, as proposed by Şengör et al., (1985) and Dewey et al., (1986). Since, as known, strike-slip faults in general need not be vertical. They may form parallel to a pre-existing bedding or fabric anisotropy, or may reactivate dipping faults formed in thrust or gravity dynamic regimes (Woodcock and Schubert, 1994) such as pre-existing thrust contacts of the lake.

In the Lake Van, structural conditions favoring block rotation over translation by simple shear are overall distribution of shear, the strength of the deforming basin relative to the zone of low shear resistance at depth, the orientation of the regional stress field and the pre-existing faults situated relative to margin boundary faults that define the zone of shear (Walcott et al., 1981; Ron et al., 1984; Seeber and Nicholson, 1986). Furthermore, it is clear that low-angle structures like detachments at upper crustal levels (Dewey et al., 1986) are involved in contemporary strike-/oblique-slip deformation and, in the analysis of regional GPS-strain data, block rotations must be considered. However, classical interpretations of small-scale tectonic features (subbasins) along major wrench faults that assume irrotational models (Aydın and Page, 1984) should need to be modified to allow for various degrees of block rotation, particularly between fault zones or fault systems of finite width (Nicholson et al., 1986). Most major intra-plate strike-slip zones occur in domains of crustal-scale simple shear rather than pure shear, because they are related to transpression or transtension at basin margin boundaries as recognized in the Lake

Van basin (see Woodcock and Schubert, 1994 for oblique convergence or divergence at plate boundaries).

S-margin boundary fault is a zone of pre-existing weakness in which basin block fragmentation and separation takes place and thus, is the prominent structural feature characterized by extension fractures, fault segments or Reidel shears, splays, subbasins and rising magmas. These structures, during prolonged shear across the lake, twisted and extended in response to rigid body rotation of the flake (see the same example of rotating ice slabs in Wilson, 1960 from Sylvester, 1988). Moreover, its-W-segment, parallel to Muş suture, and E-segment, parallel to Cryptic suture, are ideal strike-/oblique-slip fault boundaries to accommodate much of the horizontal plate motion, as proposed for the Arabia-Eurasia collision. Since, suture complexes make perfect strike-slip boundaries to accommodate the horizontal plate motion (see Karig, 1980; Tapponier et al., 1986 for the Indo-Eurasia collision). Strike-slip faults, particularly with small displacements occur both in deformation belts bordering plate boundaries, particularly as elements of linked fault systems and in intra-plate settings (Woodcock and Schubert, 1994). Therefore, S-margin boundary fault perfectly characterizes the oblique opening of Muş suture zone (also Cryptic suture) or intra-lake suture fragmentation and separation during post-collisional period. In terms of mechanics of the accretionary complex, this structural case has a close similarity to the tectonics of a block mosaic. An interesting evidence of the tectonics of a block mosaic (Hill, 1982; Sylvester, 1988) comes from S-China. In S-China, N-S shortening and E-W elongation of a tectonic domain composed of a number of blocks cause horizontal slip of several blocks relative to one another, thus opening large basins between blocks that are wedged away from one another along strike-slip faults (also examine the wedge-shaped Mojave Desert in S-California on intra-plate smaller scale in response to the localized upper crustal shortening in Cummings, 1976; Wu and Wang, 1988; Sylvester, 1988).

5.2.2 Block rotation and seismicity

Strike-/oblique-slip faulting along S-margin boundary is a ubiquitous process, particularly in volcanic provinces. Nemrut volcanic dome-cone complex is located in horse tail-shaped extensile zones above a crustal shear zone which itself is preferentially oriented to accommodate horizontal strike-/oblique-slip within the volcanic province (see Weaver et al., 1987 for details). It is also noteworthy that the

majority of volcanic eruptions or rising magmatic materials are preceded by upper crustal earthquakes having strike-/oblique-slip focal mechanisms and long-term periods (Weaver et al., 1981 and see seismogram data from Örgülü et al., 2003; Horasan and Boztepe-Güney, 2006; Pınar et al., 2007). Moreover, S-margin boundary fault is segmented feature and responsible for the small and moderate-sized earthquakes in delta setting of the lake. The segments of S-margin boundary fault behave differently in terms of the maximum magnitude of earthquakes they have generated or are capable of generating, the maximum amount of surface displacement they display with those earthquakes, the return frequency of earthquakes and the rate of aseismic fault creep (Allen, 1968; Wallace, 1970; Sylvester, 1988). Çarpanak spur zone (and NE-Erek delta) controlled by E-segment is a uplifting bend and a center of moderate earthquakes where the fault is considered to be locked (Allen, 1968) relative to the straight, very similar to the creeping segment of the fault in central California which is typified by rather frequent minor to major earthquakes (Brown and Wallace, 1968; Wallace, 1970; Sylvester, 1988). Therefore, presently defined segment lengths are determined by the depth to the upper crustal seismogenic zone, by the presence and position of releasing or restraining bends, by fault bends, and by "asperities" (Tang et al., 1984; Barka and Kadinsky-Cade, 1988).

W- and E-segments of S-margin boundary fault are secondary en echelon features, termed R shears, these en echelon segments are found to rotate above basal master fault (PDZ) as slip continues and deformation increases (see Hempton and Neher, 1985 for details). Since, seismicity related to S-margin boundary fault presently exhibits an unusual pattern of seismic deformation in and around E-segment. The distributional pattern of overall seismicity (Türkeli et al., 2003; Örgülü et al., 2003; Dhont and Chorowicz, 2006; Horasan and Boztepe-Güney, 2006; Toker et al., 2007; Pınar et al., 2007 and Toker et al., 2009a, b) is densely concentrated on Deveboynu peninsula and Çarpanak spur zone and localized within Deveboynu and Varis spur zone subbasins near around the SE- delta. Only few moderate-sized earthquakes are directly related to dextral transpression along faulted structures (see focal mechanisms from Örgülü et al., 2003; Dhont and Chorowicz, 2006; and Pınar et al., 2007). Instead, earthquakes tend to cluster in areas where major faults splay, or define short linear segments (E-segment and subbasins). Slip and motion along these

secondary features is predominantly normal oblique dextral and is consistent with the reactivation of pre-existing fault in S by the current regional stress field and also with a set of small subbasin blocks rotating as a result of oblique dextral shear of S-margin boundary. This indicates that much of the seismic activity is presently occurring on secondary structures, particularly in and along E-segment. This confirms that much of the present seismic activity on secondary features accommodates dextral oblique motion as a result of block rotation. Since, block rotation appears most prevalent in areas where major faults splay, overlap, diverge or converge (Nicholson et al., 1986). Zones of dense earthquake activity along the Deveboynu peninsula and Çarpanak spur zone may thus reflect areas of abundant secondary cross faults within small-scale fault-bounded domains such as subbasin formations. Thus, faults and fault slip respond to local kinematic constraints, once finite rotations have occurred, N-S directions of regional compressional stress will no longer be simply related to existing fault orientations (Nicholson et al., 1986 and Dewey et al., 1998). However, not all dextral oblique motion on secondary cross faults signifies block rotation. Such displacements may simply be the response of pre-existing fault structures to the present regional stress field (see Zoback and Zoback, 1980) that currently has a maximum horizontal compressive stress axis that strikes N. Although fault displacements along secondary structures associated with block rotations remain small (Nicholson et al., 1986), these displacements can strongly influence the nucleation and the characteristic rupture length of earthquakes (Horasan and Boztepe-Güney, 2006 and Pınar et al., 2007) in and along Deveboynu peninsula and Çarpanak spur zone, bounded by W- and E-segments. It is obvious that various scales of the smaller normal oblique-slip faults controlling Deveboynu and Varis spur zone subbasins and also magmatic intrusions interact to each other. Thus, these smaller scale faults contribute to earthquake activity. A more complete kinematic description of how these secondary structures interact is very similar to structural style and deformation pattern of Narman-Horasan earthquake (Şengör et al., 1985 and Koçyiğit et al., 2001). This can prove critical to any fundamental understanding of the earthquake process and any realistic assessment of the seismic hazard in lake.

The presence of rhomb-shaped and fault-bounded wedge-block structure of the lake does imply that the upper crust is more likely to exhibit oblique block tectonic

behavior (Hill, 1982; Şengör et al., 1985 and Dewey et al., 1986) and is more likely to experience finite rotations once shear becomes distributed. However, how much strain, in fact, accounted for by shear rotation is not certain. It is probable that the partition between simple translation and block rotation varies considerably in both space and time. This means that block rotations produced by tectonic shear are likely to be non-uniform in both space and time. This suggests that block rotations are likely to be concentrated in areas where shear is distributed between fault zones or fault systems of finite width, in the vicinity of major fault bends, or in areas experiencing fault-parallel extension (Nicholson et al., 1986). In Lake Van region, it is well evident that the block rotation model accounts for a number of small-scale structural styles and features (pushed up rhomb-shaped horst, fault wedge basin, divergent/convergent strike-slip faults, en echelon folds and subbasin formations) observed along margin boundary faults, characteristics of strike-/oblique-slip deformation in lake. This style of deformation pattern indicates that the rotation includes variable slip rates and alternating transtensional and transpressional features observed along strike of boundary faults (see Fig. 5.1c). Block rotation about a vertical axis requires a decoupling surface (detachment) at depth to permit rotational movement (Dewey et al., 1986), and thus, low-angle structures or detachments of either local or regional extent are involved in the contemporary strike-/oblique-slip deformation of the lake.

A flake-block nature of the thin crust significantly implies that strain patterns in the lake are inhomogeneous and likely concentrated along edge-bounding faults (Fig. 5.1c). This indicates that local stress orientations largely respond to local kinematic constraints of block rotation and fault interaction, as proposed by Dewey et al., (1998). Therefore, a rotating flake structure of the lake is very useful block model in terms of identifying the local kinematic constraints of oblique-slip fault interaction and of block rotation. For example, the marginal sections of the lake where the major deflections in the geometry of boundary faults are likely to occur, such as positive-negative flower structure (restraining-releasing bends), fault offsets, oversteps, en echelon segments, subbasins. Some of these places (E-segment) are sites where small-moderate seismicity often nucleate, and so would offer some of the best locations for further seismological study and instrumentation, if a better understanding of the processes leading to lake seismicity is to be achieved. The

evidence from the analysis of structural and tectonic elements along margin boundary faults suggests that at least, a component of the oblique-slip deformation is accomplished by block rotation of the lake. On the other hand, evidence from GPS data (Şengör et al., 2008) and active seismicity indicates that shear rotations also accommodate current accumulations of regional shear during the seismic period. This implies that not all seismic deformation reflects stored elastic strain energy that is eventually released as slip during small or moderate earthquakes, and some strains are permanent and eventually accumulate to produce the tectonic block rotations.

5.2.3 Seismogram data and deformations

Öncel and Wilson, (2002) computed the magnitude frequency relations and seismotectonic parameters for the North Anatolian Transform Fault and E-Anatolia seismic provinces and found high seismic b-values (0.95-1, low magnitude) for E-Anatolia. Horasan and Boztepe-Güney, (2006) additionally computed the magnitude frequency relations and epicenter-hypocenter distributions of the lake and they found relatively high seismic b-values for the lake (low magnitude) and low b-values for Çaldıran-Muradiye fault zone (high magnitude). Pınar et al., (2007) recently computed, using earthquake data, fault focal mechanisms in the lake and found dextral transpressions both in Çarpanak spur zone and Deveboynu peninsula. Toker, (2007), Toker et al., (2007; 2009a, b) analyzed all earthquake data and documented a seismogenic zone and thin crust-oblique faulting model of the lake. Toker et al., (2009a, b) firstly postulated the shallow-seated volcano-seismic activity and tectono-magmatic relations at upper crustal levels, extracted from seismic b-values and earthquake waveforms (Long-Period, Hybrid-Period and Tremor data) of Horasan and Boztepe-Güney, (2006). Toker et al., (2009a, b) also modeled the upper crustal discontinuity as combined with accretionary contact surfaces and reviewed intra-crustal earthquakes along hypocenter and epicenter profiles. Toker et al., (2009a, b) concluded the relatively low b-values found as an indication of high strain accumulation for Çaldıran-Muradiye fault zone, in contrast with the lake having the higher b value. This indicates the low magnitude seismic activity and strain releasing for the lake. These results remark that the process of basin block fragmentation and separation is accompanied by highly ductile magma chamber events at upper crustal depths. The best evidence for this comes from central Tatvan basin where no any earthquake recorded, but only at fault terminations (W- and E-segments) and faulted

uplifts (Çarpanak spur zone and Deveboynu peninsula). Even though a few magma intrusions are recognized in seismic data, these uplifted areas are relatively rigid zones where strains are continually accumulated and locally condensed. In these uplifted areas, fault focal mechanisms of Örgülü et al., (2003), Dhont and Chorowicz, (2006) and Pınar et al., (2007) showed dextral transpressive character of intra-crustal seismicity, particularly at upper crustal depths. This is in a good agreement with the structural pattern of S-margin boundary fault.

Earthquake data analysis combined with deformation patterns and structural styles in and along the E-segment of S-margin boundary fault concludes that dextral transtensional shear zone of S-margin boundary fault (negative flower structure) completely controls internal subbasins and thus, earthquake activity in and around its E-segment. This clarifies that the oblique opening of subbasins (Deveboynu and Varis spur zone subbasins) is a clear structural response to block rotation and overall seismicity in Deveboynu peninsula, Çarpanak spur zone and SE-delta. These areas are seismically very critical places, characterized by dextral transpressional focal mechanisms (Pınar et al., 2007). All along the NE- and SE-delta settings, delta progradations, clinoform wedges and unconsolidated softer sediments are extremely deformed, representing a deltaic deformation pattern of magmatic gas-pore water-sediment mixture (soft sediment deformations). Particularly, Çarpanak block uplift in the NE-Erek delta controlled by E-segment is clearly characterized by faulting and seismicity-related gravitational instabilities. These instability products are turbidities or debris flows and slumped-slided cliniform packages, having very high hydro-plasticity and hence, acoustically chaotic and transparent reflection configurations. Uplifted delta sediments containing deformed horizons are possibly characterized by seismites triggered by seismic activity (see Hempton and Dewey, 1983; Hempton et al., 1983 and Dewey et al., 1986 for Lake Hazar).

Block rotation and deformation complexity of the lake is the most prominent feature and the characteristics of earthquake distribution in the lake. Because, intra-plate convergent plate boundaries are wide, diffuse and complicated zones where relative plate displacements are converted into complex and variable strains and smaller block-bounding displacements. This contrasts with oceanic plate boundaries, which are generally narrow, relatively simple zones in which only a small portion of relative plate motion is converted into strain and smaller displacements (McKenzie,

1972 and Dewey et al., 1986). The great inhomogeneity and anisotropy of the continental crust, riddled with zones of low strength is generated and modified by many varied mechanisms (Dewey, 1982; Dewey et al., 1986). Upper-crustal strains appear to be discontinuous in space and time, with zones of strong shortening representing shoaling of crustal detachment zones flattening between 5 and 10 km. In Lake Van, dextral in S and sinistral in N trending lineaments bound less deformed wedge (low relief seismically "dead" area such as central Tatvan basin) and vary from simple strike-slip faults to complicated braided transform-flake boundaries with extensional and compressional segments (Dewey et al., 1986). This indicates that elastic lid or flake detachment occurs where rotations about vertical axes and leads to complicated compatibility problems at flake margins. This is well seen in and along the flake boundaries of lake where divergent/convergent strike-slip zones, localized subbasins and faulted block uplifts occur on a restricted geographic scale at these flake boundaries. Since, local termination of basal flake detachments offers a possible explanation for a wide variety of localized crustal structures, which may be arranged in various of geometrical combinations. These may comprise listric extensional detachments passing laterally into zones of lower-crustal stretching with resulting pop-ups, batholiths with mid-crustal flat bases (Lynn et al., 1981) passing laterally into thrust zones, and rotated flakes with marginal flower structures above detachments that relay transform motion laterally into wide lower-crustal and mantle shear zones (Dewey et al., 1986).

The range of crustal structures characterizing collisional orogens and their forelands, most of which occur in E-Anatolia, is schematically summarized by Dewey et al., (1986) and applied to Lake Van basin (Fig. 5.1). Structural, tectonic and seismic evidence appears to suggest that most of these upper crustal flakes have undergone rigid body rotation, (external rotation rather than internal viscous rotations). For example, as discussed earlier, rotation of crustal flakes up to 90° (Luyendyk et al., 1980) has occurred at the edges of which upper-crustal basins, such as the Ridge Basin, have opened (Dewey et al., 1986). The flake-block model proposed for the Lake Van has the particular merit of explaining E-W lateral wedging and extension as a late stage consequence of collision such as delamination and thus, the present-day localized seismicity in and around E-segment. This model predicts that lateral oblique wedging along margin boundary faults with their associated secondary

products is superimposed on the orogen at a late stage. This model also accounts well for the younger extensional deformation and the oblique opening of subbasins accompanied by smaller and moderate-sized earthquakes.

5.3 Deformation Modes and Tectonic Evolution of The Convergent Crust beneath Lake Van: Accretionary Generation, Extensional Modification and Differentiation of The Crust

Delamination event is shown to produce common crustal deformations taking place on both regional and local scale and thus, effects accretion rheology of orogenic structure and deformation modes and tectonic evolution of the convergent crust beneath Lake Van. Strike-slip deformation and extensional magma propagation reveal that tectonic nature of the convergent crust beneath Lake Van seems to have three distinct evolutional elements. These are accretionary generation, extensional modification and differentiation of the crust. These elements are related to collision (subduction-accretion), post-collisional modification (delamination and denudation), differentiation of the convergent crust and formation of squashy zone beneath Lake Van region. Post-collisional modification of the convergent crust implicates for basin block fragmentation, separation and differentiation and thus, the oblique opening of Muş suture and extensional magmatism. This modification also contributes to crustal consolidation and crust-forming process as indicated by Şengör et al., (2008). Therefore, based on crustal model structure and strike-slip deformation of Lake Van discussed above, it is essential to underline accretionary wedge dynamics during collisional and post-collisional period and to discuss which deformation modes control generation, modification and differentiation of the convergent crust and contribute to extensional and transtensional processes in Lake Van basin.

5.3.1 Accretionary generation

Accretionary crustal generation in intra-plate collisional setting occurs, most interestingly, in subduction-accretion prisms. Since, subduction-accretion prisms can involve the structural accumulation of a 30 km silicic sedimentary upper and middle crust or greenschist and sub-greenschist facies above a lower crustal mafic foundation of subcreted remnant oceanic crust (Şengör and Yılmaz, 1981 and Dewey, 1986). Moreover, water is present to lower crustal depths and the lower part

of the silicic crust is likely to be characterized by sub-horizontal structure and fabrics (Dewey, 1986). More complicated blob geometries with a large mafic component typifies the lower parts of accretionary prisms where substantial volumes of seamounts and oceanic plateaux are accreted (Şengör and Yılmaz, 1981 and Dewey, 1986). Complex sub-crustal process (delamination) or ridge/trench interaction (Dewey, 1986) beneath accretionary prisms results in mafic injection into and partial melting of the accretionary prism and a consequent trend towards lower crustal dehydration and the upward movement of volatiles and minimum melting silicic magmas (Dewey, 1986). A similar trend also occurs where an arc environment is superposed on an accretionary prism (Hudson and Plafker, 1982 and Dewey, 1986). E-Turkey has such an orogenic anatomy of accretionary crustal generation and hence, it is essential to discuss post-collisional sedimentary basins in intra-plate settings.

Şengör et al., (2008) questioned and discussed what a continent is and how to make continents from squashed subduction-accretion complexes and arc roots?. This study has given an actualistic example of crustal consolidation in accretionary wedges in E-Turkey. It is noticed that the critical structural anomaly of accretionary wedges that is the inconsistency of the vergence in E-Turkey. It is clear that terrain accretion was a dominant mechanism in the growth of the continents during Precambrian times (Kearey and Vine, 1996). Windley, (1984) has argued that some form of plate tectonics is the only mechanism capable of continuously replenishing, over hundreds of millions of years, the mantle-derived material which enabled a large proportion of the present continental crust to have been created during Archaean times. This is very important aspect of E-Turkey. Since, it represents a “continental hole”, created as a result of the collision of four continental objects that did not have perfectly matching margins and filled with oceanic island arcs and mélange complexes (Şengör and Yılmaz, 1981).

The final collision of E-Turkey with Arabia further deformed it internally and “consolidated” it by magmatic intrusions (see Şengör and Kidd, 1979). Similarly, the Sungpan-Kantze system is the “continental hole” that resulted from the imperfect closure of Palaeo-Tethys among four continental objects (Şengör et al., 2008). Its fill and overall geometry have an amazing resemblance to E-Turkey. Such “deer’s head”-shaped accretionary complexes, caught up in the suture knots where continents

can not fill holes that result from irregular margin collision. These accretionary complexes may be more widespread than previously recognized and may contribute substantially to the areal growth of continents as has obviously been the case in Turkey and China (Şengör and Yılmaz, 1981). As the N-S shortening across E-Turkey continued between the converging jaws of Eurasia and Arabia, the relatively soft and irresistant accretionary complex took up much of the initial post-collision convergence by shortening and thickening (Şengör and Yılmaz, 1981). However, the rapidly rising elevations made it eventually more economic to wedge out of the way a considerable piece of Turkey, roughly coincident, particularly in E. Thus, the N- and E-Anatolian transform faults, and with them the Anatolian Plate (ova regime), originated (Şengör, 1979b; Şengör and Yılmaz, 1981).

Based on the accretionary generation of the crust, types of continental crust can be classified according to tectonic environment and process and be considered as model cross-sections of the lake basement and they give collisional and post-collisional characteristics and deformation modes of the convergent crust (Fig. 5.3). In this model study of Dewey, (1986), subduction-accretion related continental crust is well shown. Subduction-accretion prism (6) with clipped-off seamounts and oceanic crustal slivers (7) or with trench-ridge interaction (8) is overprinted by volcanic arc (9). These types well show that accretionary crustal basement beneath Lake Van has a complicated combination of one or two of these crustal types (see Şengör and Yılmaz, 1981 for accretionary generation of collisional crust in E-Turkey). This accretionary crust underplated by mafic igneous rocks (12) is deformed by crustal extension to $\beta > 2$ (13) or crustal extension to $\beta < 2$ (14). Before the extensional deformation (β), it is important to emphasize that accretionary crustal structure of the lake is a type of thrust stacked crust with high level ophiolite nappe (16) and can be thickened by vertical stretching (17-19) or thickened by thrust stacking (21-22). This type of generation also evidenced upper crustal low-angle detachment surfaces and oblique flakes (Şengör et al., 1985 and Dewey et al., 1986). Then, due to the higher elevation, this accretionary crust is denuded back to normal thickness (17 and 21) or denuded and delaminated back to normal thickness (18) or delaminated back to normal thickness (19 and 22) and stretched back to normal thickness (20). These evolutional types and stages of accretionary crust modified according to intra-plate collisional tectonic environment and delamination process indicate that the

accretionary convergent crust is denuded and delaminated back to normal thickness (18) and stretched back to normal thickness (20). Thinned crustal types, particularly (13, 14 and 20) showed that extensionally tilted sedimentary basin blocks with thin (20) and thick sediments (13 and 14) occurred in upper crustal detachment surfaces. These sedimentary basins, as for Lake Van basin, are controlled by oblique-slip deformation and subjected to granitic melts or melted products through detachment planes (13 and 20). These sedimentary basins also have lower/mid-crustal horizontal stretching fabrics (13, 14 and 20). Crustal type of delamination and denudation (18) and of extension (13, 14 and 20) well characterizes how accretionary convergent crust is extensionally modified beneath the lake.

It should be pointed that since Arni, (1939) it has been known that the structure of E-Anatolia consists of stacked, steepened, imbricate thrust sheets of coloured mélange (Şengör and Yılmaz, 1981). Intensity of deformation in these sequences decreases with decreasing age. They are often infolded or imbricated into the underlying mélange slices which have generally steep contacts. It is interpreted that the entire basement of E-Anatolia is an accretionary wedge with at least one ensimatic island arc complex caught up within it (Şengör and Yılmaz, 1981 and Şengör et al., 2008). Therefore, in terms of crustal model classification of Dewey, (1986), the sediments above the accretionary wedge such as Muş-Lake Van region are essentially arc-trench gap and upper-slope basin deposits recording the progressive thickening and progradation of the wedge, similar to the Aleutian accretionary prism with its multiple arc-trench gap basins (Dickinson and Seely, 1979) or the largely subaerial Makran accretionary wedge with its large, subaerial forearc basin, the Jaz Murian depression, and the multiple, steep-sided upper-slope basins (Farhoudi and Karig, 1977; Şengör and Yılmaz, 1981). It is interesting to note that Arni, (1939) had already pointed out the great similarity between the lithologic associations and tectonic style of E-Anatolia and those of Makran and included both of these areas into his Iranides. Arni's (1939) cross sections have an amazing similarity to those of the rotated portions of modern large accretionary complexes (Karig, 1974; Mascle et al., 1977; Şengör and Yılmaz, 1981). This highlights a point that E-Turkey accretionary complex has the rotated portions of upper crustal detached blocks related to extensional modification (examine and compare 13, 14, 20 to 16, 21, 22 in Fig. 5.3) as proposed by Dewey et al., (1986).

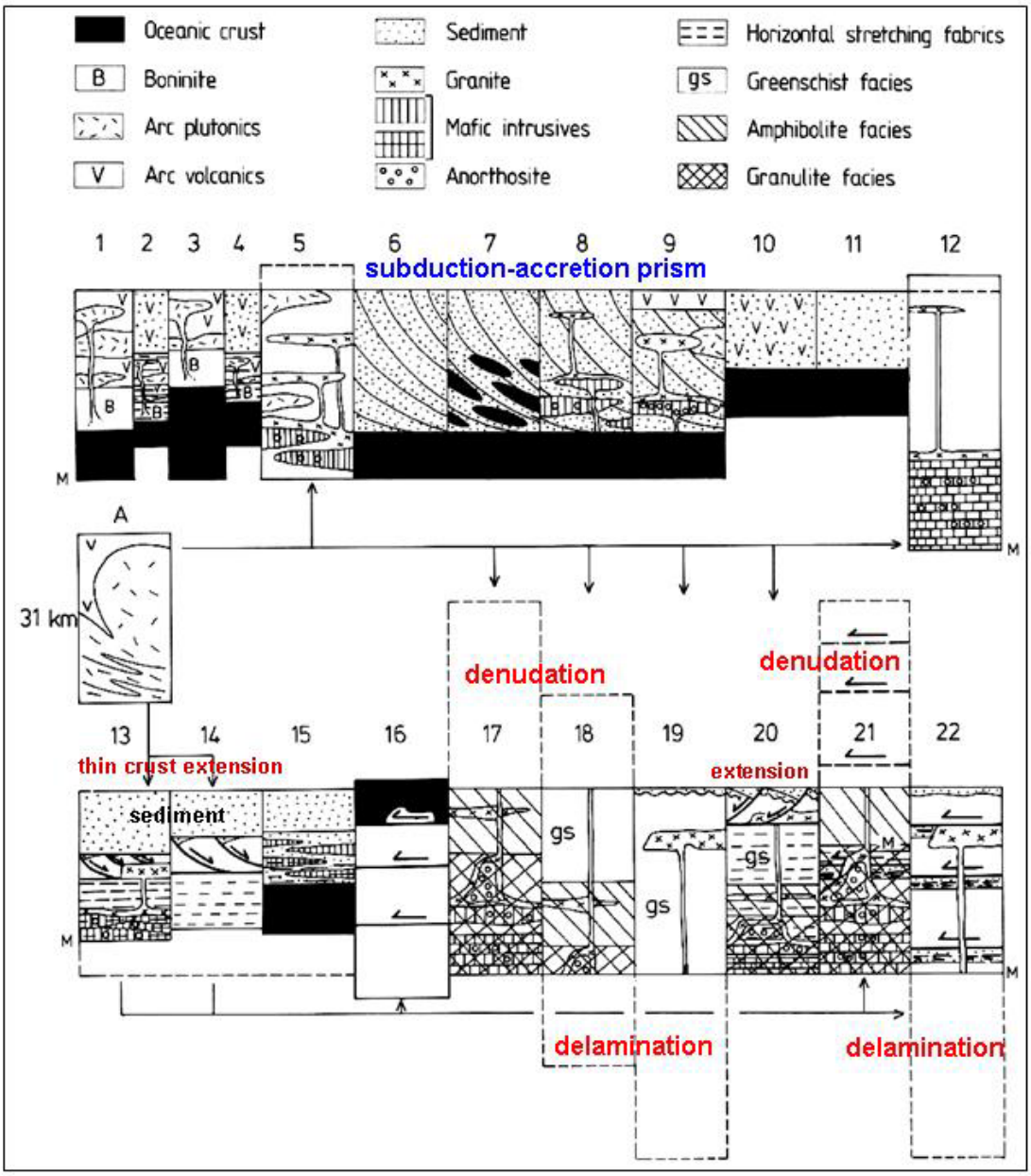

Figure 5.3 : Types of continental crust are classified according to tectonic environment and process (Dewey, 1986). A-Archaean protolith. 1-Volcanic arc nucleated on oceanic crust; 2-intra-arc pull-apart in 1; 3-volcanic arc nucleated on oceanic plateau; 4-intra-arc pull-apart in 3; 5-continental margin arc; 6-subduction-accretion prism; 7-subduction accretion prism with clipped-off seamounts and oceanic crustal slivers; 8-subductionaccretion prism with trench-ridge interaction: 9-subduction accretion prism overprinted by volcanic arc; 10-back-arc basin; 11-oceanic delta; 12-crust underplated by mafic igneous rocks; 13-crustal extension to $\beta > 2$; 14-crustal extension to $\beta < 2$; 15-ridge blanketed by sediment; 16-thrust stacked crust with highlevel ophiolite nappe; 17-19-crusts thickened by vertical stretching; 21 and 22-thickened by thrust stacking; 17 and 21-denuded back to normal thickness; 18-denuded and delaminated back to normal thickness; 19 and 22-delaminated back to normal thickness; 20-stretched back to normal thickness. Note dynamic evolution of thick convergent crust from subduction-accretion through delamination-denudation into thin crustal extension and sedimentary basin formation (also see and examine Fig. 5.2).

5.3.2 Extensional modification

Lake Van basin is the one of the rotated portions of E-Turkey, therefore it has considerable structural complexities. These complexities are well characterized by a process of structural inversions from ramp/thrust to transpression/transtension-bounded basin with extensional subbasins. The active deformation of Lake Van is a kinematic proxy of extensional modification, indicating crustal deformation and strike-slip basin formation in E-Turkey (Şengör et al., 1985).

Upper crustal extensional models (13, 14 and 20) and low angle detachments (16, 21 and 22) clarified that structural evolution of Lake Van basin is mainly controlled by localized effects of accretionary wedge dynamics at upper crustal levels (Fig. 5.3). These localized effects are related to the effect of kinematic boundary conditions versus stress, concentrated along the W-E striking basin margins. Thick depositional sections (Tatvan basin) remained almost undeformed. Strong structural inversion of the basin margins from thrust to oblique slip presently controls the Lake Van basin. This means that the lake is laterally wedged under the control of accretionary complex. Therefore, it is necessary to discuss the characteristics of accretionary wedge dynamics, to understand squashed portions of accretionary wedges (Şengör et al., 2008) and how it contributes to the structural inversion and tectonic evolution of Lake Van.

As well seen in Fig. 5.3, modification of continental crust occurs in two principal tectonic environments; post-collisional extension (13 and 14) and syn-collisional shortening (16-22). As just mentioned above, extended crust is characterized by thick sediments overlying a faulted layer beneath which ductile extension occurs (13 and 14). The amount of stretching (β) determines the role of syn-extensional magmatism. Where β is sufficiently large to allow fertile mantle at the peridotite solidus to rise to partial melting depths, basaltic volcanism (Şengör et al., 2008) is accompanied by basaltic underplating with partial melting of the extended lower crust and the rise of silicic minimum melting liquids to freeze in upper crustal flat-based batholiths (Lynn et al., 1981; Verma et al., 1984; Dewey, 1986 and Dewey et al., 1986).

The shortening causes crustal warming and softening of accreted terrains and prograde metamorphism (see Şengör and Yılmaz, 1981 for irresistant accretionary complex of E-Turkey and Dewey, 1986). This shortening is accomplished by thrust stacking (16, 21 and 22) or, possibly, by vertical stretching (Dewey and Burke, 1973;

Dewey, 1986; Dewey et al., 1986). Thrust stacking enables sediments and water to reach lower crustal depths and is likely to generate subhorizontal shortening structures and fabrics in the lower crust. Crustal thickening, by either mechanism, accompanies lithospheric thickening and either progessive heating as the lithospheric root is converted into peridotite at its solidus or rapid heating if the lithospheric root is delaminated (that is detached as a slab from the overlying crust). Delamination to the base of a thickened crust (Bird, 1978) is a mechanism by which fertile mantle at 1330^0C would cause rapid heating (Şengör et al., 2008), the injection of mafic magmas into the lower crust and very rapid uplift and denudation.

The interpretation shows that accretionary basement complex beneath the Lake Van, as in most orogenic settings, shows a regional late kinematic phase of rapid heating, uplift and denudation and magma injection, which can only be accounted for by some form of delamination (Dewey, 1986). At squashy zone, lower crustal rapid heating by delamination leads to the upward flux of volatile, lithophile and radiogenic elements with minimum melting granites and thus crustal differentiation into a dry, refractory, granulitic, anorthosite-rich lower crust and a wet upper amphibolitic/greenschist upper crust (Dewey and Burke, 1973 and Dewey, 1986). It is clear that the eventual nature of the crust in such a zone of shortening depends not only upon the shortening mechanism but also upon the mechanism(s) by which the thickened crust is returned to normal thickness. As given above, this may be by denudation (17 and 21) and delamination (19 and 22). Between the end members of denudation and delamination, transitional combinations are also possible (18) that is accompanied by crustal extension (20). Crustal extension and magmatic activity appear to correlate in time with the onset of strike-/oblique-slip movements. This is the case postulated for Lake Van as in the Basin and Range, the Aegean, the Pannonian Basin and the Tyrrhenian (Şengör et al., 1985; Dewey et al., 1986 and Dewey, 1986). The injection of large volumes of magmas into the lower crust of such provinces provides a heat source for lower crustal melting and the rise of minimum melting liquids. It is important to note that random magmatic injections into the lower crust are an effective way of generating plateaux with upper crustal granites, such as the Jos Plateau in Nigeria (Dewey, 1986). However, this mechanism encounters some difficulties as a general one for plateau uplift in that some plateaux,

such as the Colorado, do not have the expected higher heat flow and do not appear to be characterized by upper crustal silicic magmatism (Dewey, 1986).

5.3.3 Crustal differentiation

Accretionary crustal generation and extensional modification modes outlined above can be superposed to give complicated tectonic pathways and sequence linkages (Dewey, 1986). This, in turn, means that the convergent crust must be laterally and vertically heterogeneous and highly anisotropic. A further degree of complex lateral inhomogeneity is induced by accretion, terrain transfer and assembly (Coney et al., 1980; Şengör and Yılmaz, 1981 and Dewey, 1986). Since, terrain accretion at the margins of large long-lived oceans will generate an exceedingly complicated and rapid lateral variation in crustal types bounded by steep transform and more gently-dipping thrust boundaries (Şengör and Yılmaz, 1981 and Dewey, 1986). However, as Dewey, (1986) stated, a general temporal trend will exist from simpler undifferentiated crusts with wet low grade lower crusts to highly differentiated crusts with drier higher-grade lower crusts.

E-Turkey is dominated by steeply to moderately dipping thrusts and numerous ophiolitic sutures. Continuous suturing of micro-continents (see crustal digitations in Şengör et al., 2008) has created there a series of moderately to steeply dipping suture zones with abundant ophiolites. The limiting case of the latter tectonic style is “to squash a mélange wedge” between two continents (see Dewey, 1969b for an excellent example of such a situation), which has been the case for the E-Turkey still farther E, at which the tectonic emplacement of Lake Van region is “a squashed mélange wedge” between Bitlis-Pötürge Massif (BPM) and EAAC. Current surface motions with respect to Eurasia showed the narrow boundary of abrupt velocity reduction in E-Turkey, N of the squashy zone (Şengör et al., 2008). Rapid movement of points within the area of thin crust corresponds with the squashy zone (Şengör et al., 2008).

At squashy zone, crustal differentiation by upward flow of volatiles, radiogenic nuclides and silicic liquids is accomplished by crustal warming, which occurs where mafic magmas intrude the lower crust and in regions of crustal shortening, especially where enhanced by delamination process. This is confirmed by Magnetotellüric studies in E-Anatolia (Türkoğlu et al., 2008). The lower crustal electrical resistivity

and the higher electrical conductivity suggest fluid-filled cracks, of some lower crusts with a complicated upper crustal history that is somewhat enigmatic in that a system of cracks interconnected to the surface for a long time would lead to rapid fluid loss by upward flow. These fluids may weaken the crust and mantle sufficiently to permit lateral flow, and may also allow a decoupling of the upper and lower portions of the crust. This weakened crustal structure with zones of elevated fluid content and low resistivity is found in isolated pockets, rather than the widespread regions (see and examine the electrical data in Türkoğlu et al., 2008). A possible explanation from Dewey, (1986) is that mid-crustal ductile strain forms an effective seal zone between upper and lower crustal brittle zones (Dewey et al., 1986) so that fluids could be trapped at pressures approaching lithostatic for long periods of time. Fluid recharging of the lower crust can occur only in convergent tectonic regimes by subduction or the thrust stacking of thinned continental crust. The latter has affected much of the continental crust and is, therefore, an important mechanism for recycling large amounts of water through the crust. Furthermore, thrust stacking is an effective way of enabling sediment to reach lower crust depths (Dewey, 1986). Underplating, that is the injection of mafic magmas into the lower crust (8, 9, 12, 13, 15, 17, 21), gives a lower crust younger than the upper crust and generates silicic minimum melts (Patchett, 1980), which rise into the upper crust with volatiles (Dewey, 1986) (Fig. 5.3).

Accretionary generation and extensional modification of the crust beneath Lake Van lead to a layered lower crust and an upper crust with a blob geometry (Dewey, 1986). Lower crustal layering probably results especially from basaltic underplating and ductile fabric development. However, upper crustal amorphous and blob geometries with scattered reflecting surfaces below layered stratigraphical sequences result from discontinuous brittle deformation and magma intrusion (Rickard and Ward, 1981; Rickard, 1984; and Dewey, 1986). This shows that all large-scale deformation styles, except transcurrent, yield horizontal to sub-horizontal lower crustal structures and fabrics (Dewey, 1986). The origin of upper crustal detachments and oblique flake basins (see Dewey et al., 1986 for crustal segmentation) and/or a mid-crustal Conrad discontinuity between a lower layered and an upper unlayered crust (Dewey, 1986) is the logical consequence of multiple tectonic modification in a mature crust.

This highlights a clear evidence of extensional modification of accretionary generated crust, crustal differentiation and anisotropic crust beneath the Lake Van.

5.3.4 Anisotropic crust

The problem of nature of the convergent crust in squashy zone of E-Turkey is approached from a tectonic standpoint in the light of oblique-slip deformation of Lake Van basin above. Tectonic arguments, collision-accretion, post-collision-extension and differentiation, suggest that the structural evolution of the convergent crust is in good agreement with, at least, several models of twenty-three types of the crust (Dewey, 1986), with an associated great variation in the structure and composition of the lower crust.

The evidence now available suggests that the convergent crust is vertically and laterally inhomogeneous on the scale of at least tens and probably hundreds of kilometers (Dewey, 1986). The interpretation shows the upper crust to be exceedingly inhomogeneous at all scales (Şengör et al., 1985 and Dewey et al., 1986). Upper crustal structure and composition is, to a large extent, typical of and dependent upon the tectonic environment in, and processes by, which the crust was made and modified (Dewey and Windley 1981; Dewey, 1986 and Şengör et al., 2008). The consequent lateral variation is likely to be reflected also in the lower crust. Crustal rheology and structural mechanics of accretionary complex is not isotropic, particularly in a tectonic case of delamination and denudation. This means that rheological change in the convergent crust is not continuous nor uniform such as suture boundary between BP-M and EAAC. For example, in and around the Lake Van region, the thickness of an upper crustal seismogenic layer (Türkelli et al., 2003 and Örgülü et al., 2003) in which brittle discontinuous strains and strain compatibility problems occur (Şengör et al., 1985), is controlled by the intersection of fracture and creep envelopes for quartz which, in turn, are controlled by strain rate, geothermal gradient and the presence or absence of water (Meissner and Strehlau, 1982; Dewey, 1986 and Dewey et al., 1986). Below the seismogenic layer, the hot and weak middle and lower crust deforms by creep except at very high strain rates in dry cold lithologies (Dewey, 1986). For a range of likely geological strain rates and geothermal gradients, ductile deformation will begin below depths from about 5 to 20 km (this is 5-10 km for the lake from Horasan and Boztepe-Güney, 2006), assuming that quartz is the dominant mineral phase (Dewey, 1986).

In E-Turkey, the hot and thin convergent crust composed of crustal slivers that are in relative motion to one another (Dewey et al., 1986). Therefore, E-Turkey is similar to the crustal mosaic of central Iran to a certain degree (Şengör and Kidd, 1979). It is recognized from Muş-Lake Van region that, unlike Iran, there is no well-developed fold and thrust belt in front of the Bitlis suture similar to the Zagros. This shows lateral variations in the structure and rheology of the leading edge of the Arabian plate and their ability to partially escape from the advancing Arabia. This suggests that E-Turkey is a mélange of several lithospheric fragments (Şengör and Yılmaz, 1981). Angus et al., (2006) did not observe whether the convergent crust also shows similar fragmentation, since the spatial resolution of the *S*-wave receiver function is on the order of 10 km and due to the large station spacing (Angus et al., 2006). Therefore, these authors did not determine whether the faults extend deep into the lower crust, as would be expected for a region composed of several crustal blocks, or whether deformation is distributed throughout the crust with no Moho offset (Wilson et al., 2004 and Angus et al., 2006). However, Şengör et al., (1985), Dewey et al., (1986), Şengör et al., (2008) and deformation style of the lake showed upper crustal blocks, their oblique motion and strike-slip basin formation in E-Turkey.

In E-Turkey, Sandvol et al., (2003b) correlate large shear-wave splitting delay times with regions of low Pn velocity and find that the fast symmetry axes are not consistent with surface or crustal deformation, indicating upper mantle anisotropy, where the fast axis is related to the vector difference between the lithospheric and mantle flow velocity vectors (also see ETSE project, 2003). In addition to, an upper-crustal discontinuity (UCD) is well observed by Angus et al., (2006) at roughly 10 km depth. Along the N-S and E-W cross sectional profiles of Angus et al., (2006) in squashy zone, the fluctuation of the UCD depth appears to be independent of the Moho depth. This suggests that the UCD represents a boundary between differing deformation styles in the crust. Active deformation and faulting is occurring in the upper crustal sections and ductile flow in the lower crust. Thus, it is interpreted that the UCD is a boundary with differing crustal velocities of crystalline basement below and thick volcano-sedimentary successions above (see data from Angus et al., 2006). This confirms flake-block nature and block rotation of the upper crust and related seismicity. Moreover, the thick crust beneath the E-Turkey (Angus et al., 2006) suggests that the upper crust is being thickened by extensive magma generation

(Keskin, 2005) as well as thrust and strike-slip faulting, where as the lower crust thickened by crustal flow processes. This confirms crustal accretion or basaltic underplating (see Şengör et al., 2008). The one evidence comes from crustal low velocity zone (CLVZ). Crustal low velocity zone (CLVZ) at 25 km is observed below Quaternary volcanic centres near the city of Van (Angus et al., 2006). This suggests that the CLVZ mostly represents a pocket of partial melt in the middle crust, which is related to the magmatic ascension process for these volcanoes (Keskin et al., 1998 and Zor et al., 2003). This is also in good agreement with the results of electrical resistivity studies at shallower depths (lower resistivity at 10 km) by Türkoğlu et al., (2008).

A schematic representation of the crust and mantle for N-S profile (see data in Angus et al., 2006) bisecting the Bitlis suture zone and BP-M shows that due to the tectonically complex geometry of this region, the 2- and 3-D structure of the lithosphere below the Bitlis–Zagros suture (e.g. truncation and inter-fingering of delaminated lithospheres) introduced wave-front diffractive and scattering effects. Also, below the Bitlis suture in the S-W, Rayleigh wave tomography has imaged an extensive zone of low shear wave velocity (Sandvol, in prep. and Angus et al., 2006). These observations in and around BP-M indicate that this region of partially melted mantle is acting as lens by focusing or de-focusing upcoming teleseismic energy (Angus et al., 2006). This not only confirms the squashy nature of BP-M, but also of Lake Van region (see and examine earthquake waveforms of Horasan and Boztepe-Güney, 2006 and cross sectional models of Şengör et al., 2008).

Crustal seismic observations from N-S and E-W cross sectional profiles of Angus et al., (2006) all along the squashy environment around the Muş-Lake Van region confirm the arguments related to tectonic nature of the convergent crust mentioned above and also postulations of Şengör et al., (1985), Dewey et al., (1986) and Dewey, (1986). Muş-Lake Van region is characterized by CLVZ and UCD at 25 and 10 km, lower values of electrical resistivity at same depth and upper crustal seismicity (Pınar et al., 2007; Toker et al., 2009a, b). The UCD at 10 km depth is likely associated with volcano-magmatic and sedimentary successions and the crustal low velocity zones at depths of 25 km are consistent with the location of geothermal and Quaternary volcanic centres. The observation that the asthenosphere is at direct contact to the crust supports the idea that the tectonically deformed domal structure

of region is supported by an asthenospheric upwelling. Thus the fact that the crust is hot and weak below the lake is not plausible. Furthermore, geophysical studies of Angus et al., (2006) showed that the Lithosphere-Asthenosphere Boundary (LAB) of the Arabian shield does not appear to underthrust E-Turkey. This is consistent with the oceanic slab break-off model of Keskin, (2003) and also model studies of Şengör et al., (2008). Upper mantle anisotropy complicates the style of crustal deformation at the squashy zone and results in differential deformation types in the crust. Then, highly anisotropic convergent crust underlying the Lake Van region complicates the deformation patterns and structural evolution of the lake at upper crustal levels.

5.4 Intraplate Magmatism of Muş-Lake Van Region

It is noticeable that concomitant occurrence of both subduction-related and within-plate magmas in the same tectonic environment dominated by collision processes is not a unique feature of E-Turkey (Bonin, 2004 and Macera et al., 2008), but represents a widespread phenomenon in the whole Mediterranean area during Tertiary-Quaternary time.

Collisions create major magmatism that spreads across vast areas on both sides of terminal sutures such as Pontide and BP-M welding the apposed continents (see Dewey and Burke, 1973 on collision-related basement reactivation and related magmatism, Şengör et al., 1991, 1993). Collisional magmatism differentiates the continental crust and intensive reheating of the lower crust during collision leads to high grade metamorphism under dehydrating conditions (Şengör et al., 2008). Collisional reactivation of the continental crust in the model of Dewey and Burke (1973) involves generation of Tibet-type high plateaux with considerable crustal thickening (Dewey et al., 1988), loss of lithospheric mantle (Bird, 1978; Houseman et al., 1981; Molnar et al., 1993) and/or eclogite to granulite transformation of the lower crust (Le Pichon et al., 1997) and consequent crustal melting (e.g. Nelson et al., 1996). The resulting magmatism is dominantly of alkaline type. For example, the vast vitrophyric rhyolite eruptions of Mt. Nemrut in the form of pyroclastic falls and flows (Notsu et al., 1995; see the stratigraphy in Özdemir et al., 2006) are triggered by decompressing the magma chambers below Lake Van when the lake evaporated (Şengör et al., 2008).

A progressive transition with time from calc-alkaline to alkaline products has been noticed in many European and N-Africa centres, such as E- and S-Spain, Sardinia, S-Italy, Romania, Pannonian Basin, Morocco, Tunisia (Szabo et al., 1992; Downes et al., 1995a,b; Dobosi et al., 1995; Cebria and Lopez-Ruiz, 1995; Rosembaum et al., 1997; El Bakkali et al., 1998; Wilson and Bianchini, 1999; Cebria et al., 2000; Harangi, 2001; Coulon et al., 2002; Gasperini et al., 2002; Duggen et al., 2005), where compressive phases alternated with tensional phases (Macera et al., 2008). The latter were responsible for the Cenozoic rift system of E- and C-Europe (Ziegler, 1992), as well as for the formation of new oceanic basins, such as the Alboran Sea, the Valencia Trough, the Algero-Liguro-Provencal and the Tyrrhenian basin, from early Eocene to late Miocene (see Docherty and Banda, 1995; Faccenna et al., 1997 and Macera et al., 2008). The development of alkaline basalts in most of these mentioned areas often affected by previous subduction episodes has been interpreted in different ways. The one of these is upwelling of enriched asthenospheric mantle after the detachment of the subducted slab (Harangi, 2004) or upwelling of a deep mantle component through a plate window generated after a slab breakoff (Albar`ede et al., 2000; Gasperini et al., 2002; Macera et al., 2003a) and then, intrusion of hot mantle fingers beneath the rift areas (Granet et al., 1995;Wilson and Patterson, 2002). Similarly, in Lake Van basin, extensional magmatism and magma propagation activity through margin boundaries is interpreted as indicating intrusion activity of hot mantle fingers beneath the rift area. For example, in the Veneto Volcanic Province, the occurrence of within-plate basalts of Tertiary age has been ascribed to upwelling of plume-like mantle diapirs taking place before the subducting slab crossed the upflow of plume material or, later on, through a plate window generated after Alpine slab breakoff (Macera et al., 2003a; Ranalli et al., 2004 and Macera et al., 2008).

Some studies (Gülen, 1984; Tokel, 1984; Şaroğlu and Yılmaz, 1986; Yılmaz et al., 1987; Pearce et al., 1990; Yılmaz, 1990; Notsu et al., 1995; Yılmaz et al., 1998; Buket and Temel, 1998) have given results related to convergence between the Arabian and Eurasian Plates. Pearce et al., (1990) assumed that the collision-related magmas all originate in variably enriched mantle lithosphere. Although these studies gave some general information about the E-Anatolian volcanism, there is no detailed geochemical data from the Lake Van basin. This lake remained as an important area

of investigation to further understanding of the geochemical characteristics of magmatism related to intraplate tectonics and evolution of the volcanic provinces in E-Turkey. Lake Van region is in need of detailed and careful identification of volcanism, magmatism, crustal assimilation-fractional crystallization, related to intraplate tectonics. Major and trace elements concentrations, isotopic data and principal geochemical results for the volcanic provinces around the lake are examined and discussed below.

Intraplate magmatism, the alkaline suite, in and around Lake Van region shows geochemical patterns typical of ocean island basalts (OIB). Interestingly, these features are comparable to those of Tertiary-Quaternary OIB basalts from the W-Mediterranean area (Gasperini et al., 2003; Macera et al., 2004 and 2008). The Lake Van basin represents an ideal study site to observe the He flux from the lithosphere to the atmosphere, due to tectonically active location of this lake, the presence of many fault zones and the fact that a caldera probably lies at the origin of this lake supposed by Kipfer et al., (1994). Related hypothesis argues that He degassing from solid Earth occurs very heterogeneous in the spatial domain and is focused on particular geological structures in the Earth crust (fault zones, calderas, volcanoes, and volcano-tectonic lakes as for Lake Van basin). For example, lacustrine sediments in lakes represent an ideal frame to assess the He emanation on relative small but defined spatial scales (Kipfer et al., 1994). From the spatial distribution of the He concentrations measured by Kipfer et al., (1994) in six sediment cores from Lake Van in a preliminary phase, one can presume that the main He emanation occurs in the deepest region of the lake. Mantle He in the basin of Lake Van and also the mantle He gradient is visible in the lake sediments (Kipfer et al., 1994). Their observations near the deepest point of the basin show a clear increase of the He concentration with increasing depth within the sediment. Their results add direct experimental evidence to the hypothesis that He emanation is restricted on specific geological spots (in this case most likely a caldera) and does not occur homogeneous over the crust. Therefore, these results are examined below and compared with studies of Pearce et al., (1990), Yılmaz et al., (1998) and Buket and Temel, (1998).

Based on the origin of extensive magmatism all over the marginal sections of Lake Van basin, an interpretation of geochemical data by Şengör et al., (2008) indicates that the volcanoes within E-Turkey are fed by an enriched asthenosphere. Güleç et al.

(2002) found, in the water samples from the Nemrut caldera lake and Lake Van, the highest R/RA values in Nemrut and Van, clearly indicate more than 75% mantle He (Şengör et al., 2008). The Lake Van Dome is, as known, on the thinnest part of the crust where the observations on He isotopes in the volcanic rocks indicate the highest mantle contribution (Güleç et al., 2002). It is clear that this is expected in an extensional region as stated by Şengör et al., (2008). Although Lake Van lies mainly in a major shortening structure, a sort of "ramp valley" (Şengör et al., 1985), it has significant strike-/oblique-slip faulting along its N- and S-margins with some amount of extension and the resultant subbasins. Interestingly, this indicates that such a thing occurs in an extensional and transtensional regime of the lake in a shortening region. In addition to transtensional and extensional normal faults in the Lake Van, some oblique-slip and normal fault-plane solutions (Örgülü et al., 2003 and Türkelli et al., 2003) all along BP-M and Bitlis suture zone are on the highest ground of E-Turkey. Much of the volcanic cover in and around Nemrut volcanic dome complex blankets the region and they are fed by fissures as recognized in the lake (fissure and central vent volcanoes). As evidenced from the lake, they are related to strike-/oblique-slip faults as so illustrated by the case of Mt. Ağrı (Karakhanian et al., 2002 and Şengör et al., 2008). In addition to fissure eruptions (fissure volcanoes) dominated the volcanic activity, there are also major volcanic centres (Mt. Bingöl, Mt. Nemrut, Mt. Süphan, Mt. Ağrı, Mt. Tendürek) and numerous smaller ones in E-Anatolia, corresponding to central eruption sites (central vent volcanoes) (Şengör et al., 2008). It is essential to note that the erupted volume represents only a small fraction of the melt generated beneath the region (Şengör et al., 2008). This suggests that a greater proportion presumably is emplaced deeper in the crust in the form of plutons.

5.4.1 Upper crustal extensional magmatism

The mafic alkaline lavas of the Muş–Nemrut–Tendürek volcanoes show a progressive shift from the mantle metasomatism array with increasing SiO_2 (Şengör et al., 2008). These lavas derived from an enriched source with or without a slight subduction signature evolved through combined assimilation-fractional crystallization that is very important process for the Muş–Nemrut–Tendürek lavas (Pearce et al. 1990 and Şengör et al., 2008). Assimilation-fractional crystallisation modelling results presented by Şengör et al., (2008) support intra-crustal magmatism in the Muş–Nemrut–Lake Van region and corroborate that the degree of magma-

crust interaction is larger in the S (Muş-Nemrut-Tendürek-Lake Van) than in the N, corroborated by eruption histories as stated by Şengör et al., (2008).

From Yılmaz et al.'s (1998b) mapping of the four great young and partly active volcanoes of E-Turkey, the dominant material erupted by Mt. Nemrut consists of eruptions of much basalt indicating decrease of SiO_2 with time (Şengör et al., 2008). This means that basaltic melts gradually make their way to the surface by heating and assimilating their way through the lithosphere along a "preheated" path (Turcotte, 1981, 1982 and Şengör et al., 2008). This also confirms that the repeated injections of basalt into the crust and consequent crustal melting. As simple examples given by Şengör et al., (2008), Mt. Tendürek is with first trachytes then basalts, indicating basalt reached the surface through the lithosphere. Mt. Ağrı has basalt/andesite alternation throughout its history, indicating repeated basalt injections into the crust. It is clear that all these processes are the same in the magma-crust interaction in Lake Van region. Since, these processes suggest the existence of naturally varying degrees of fractional crystallisation in magma chambers greatly complicating upper crustal sections. These observations imply the N-S variation in mantle source composition with a southward increase in "intraplate" signature (Keskin, 2007). This variation is linked to interactions between magmas derived from two contrasting mantle domains via mixing (Şengör et al., 2008). In other words, the absence of lithospheric mantle lid beneath a squashy zone (Şengör et al., 2008) suggests that these two mantle domains are asthenospheric. The end-member with a distinct within-plate component corresponds to an undepleted asthenosphere beneath the slab (beneath the Arabian continent) (also see Keskin, 2007). The main cause of this mixing event between two contrasting mantle domains is a slab window that opened up beneath the region as a result of slab breakoff (Şengör et al., 2008). More interestingly, the removal of the slab between these mantle domains created flows in the uppermost asthenosphere, while decompression resulted in extensive magma generation beneath the squashy region (see upper mantle anisotropy in ETSE project, 2003 and Şengör et al., 2008). Mantle upwelling (Şengör et al., 2003 and Macera et al., 2003a) scenario is only a working hypothesis for within-plate volcanic centres showing small eruption volumes, discontinuous magma production, and lack of well-defined hotspot tracks. Nevertheless, the possibility of occurrence of several weaker and smaller plumes, in addition to major hotspot centres, lately has gained

increasing consensus (Dalrymple et al., 1987; Malamud and Turcotte, 1999; Davis et al., 2002). Several studies based on tomographic images and geochemical data proposed the existence of small intra-continental magmatic fields fed by mantle upwelling (Macera et al., 2008). An interesting example is given by the numerous Cenozoic volcanic centres of C-Europe for which an origin from a series of individual diapir-like mantle upwelling has been suggested, rising either from the top of a continuous layer (fossil plume-head?) within the upper mantle (Wilson and Downes, 1991; Granet et al., 1995; Hoernle et al., 1995; Vaselli et al., 1995; Rosembaum et al., 1997; Jung and Hoernes, 2000) or from a deeper mantle reservoir (Goes et al., 1999; Ritter et al., 2001). In this context, the intraplate alkaline suite could represent the shallow expression of mantle upflow. A detailed discussion on a possible plume-related origin for the upper mantle low-velocity anomaly under the alkaline suite is given in Keskin, (2003; 2005 and 2007) and Angus et al., (2006).

In the alkaline suite, asthenospheric flow and flow directions have important tectonic implications for both understanding active deformation of the upper crust, ductile deformation of the lower crust and also extensional magmatism in Lake Van region. On the basis of the geochemical data presented by Şengör et al., (2008), the basalts of the Muş–Nemrut–Tendürek area, data points of which align towards the upper crustal composition have assimilated variable amounts of crustal material. Based on geochemical tracing of mantle domains beneath the region by Şengör et al., (2008), it is interesting to note that the contours of wedge-type mantle form a broad lobe-like shape extending from Erzurum in the NW to Lake Van, to Mt. Süphan, in the SE. However, undepleted asthenosphere beneath the Arabian continent seems to form two flow fronts extending from Diyarbakır in W to Muş in E and from Iran in E to Tendürek in W respectively (examine and correlate slab window block models of Faccenna et al., 2006 with Şengör et al., 2008). It is well evidenced from the correlative analysis of models of Faccenna et al., (2006) with Şengör et al., (2008) and magmatic intrusions through the S-margin boundary fault of the lake, W-E flows are probably channelized by the suture complex (Muş suture and Bitlis-Zagros sutures). More interestingly, the tip of the asthenospheric lobe with a subduction component is located right beneath Lake Van, at the culmination of the domal structure of E-Anatolia. Moreover, undepleted mantle seems to have underplated the thinnest portion of the crust (Şengör et al., 2008). This confirms basaltic underplating

and crustal accretion and shows that the origin of magmatism consequent to slab fallout is a situation identical to extensional magmatism in Lake Van basin. This is, in fact, the most unusual aspect of the magmatism in Lake Van dome on the high plateau of E-Anatolia. This has occurred in an intra-plate orogenic setting, particularly in Lake Van region, where extensional and transtensional faults mapped produced crustal earthquakes at upper crustal depths (see data Türkelli et al., 2003; Horasan and Boztepe-Güney, 2006 and Pınar et al., 2007). Based on recent studies on alkaline basalts, the studies on Tertiary-Quaternary alkaline basalts from E-Atlantic, N-Africa, and C-Europe seem to indicate a common mantle reservoir with a typical geochemical signature beneath the entire area (Hoernle et al., 1995; Gasperini et al., 2003; Macera et al., 2004 and Macera et al., 2008). Such a reservoir has been interpreted as the head of a mantle plume whose tail may be located in correspondence of the Cape Verde-Madeira-Canary Islands region (Gasperini et al., 2003; Macera et al., 2004). Based on geochemical, geological and geophysical data, Gasperini et al., (2003); Macera et al. (2004) suggested that the large-scale swell of the plume was frayed by the Eurasian plate while the latter was moving towards the NE, and that plume material has been trapped in the sublithospheric mantle by flat-lying detached slabs above the transition zone (Macera et al., 2008). As a result, at different points in time, local extensional tectonics and slab detachment may favor plume-related volcanism, even in areas dominated by plate convergence and subduction (Macera et al., 2008).

E-Turkey as a Turkic-type collisional environment with abundant structures showing shortening and associated strike-slip faulting, covered and intruded by a thick blanket of volcanic and intrusive rocks indicates an entirely “extensional” character. This is a confirmation of the oblique-slip deformation and extensional magmatism in Lake Van Dome, as recognized from seismic reflection data. These volcanic and intrusive rocks have both “intraplate” and “subduction” signatures, both mantle and crustal origins (Şengör et al., 2008). In the light of geochemical and geophysical results, the following scenario proposed serves as a working hypothesis for further more detailed work. This remarks that the intraplate magmatism (OIB) is able to manifest itself, as the upflow from the mantle encountered no obstacle. This highlights the compositional variations of various magmatic units across the region and the relationship between inferred mantle source regions. This means lavas in N with a

distinct subduction component and those in S with a distinct within plate component. Intra-plate component distinctly characterizes Muş-Nemrut-Tendürek-Lake Van setting, the larger degree of magma-crust interaction in the S (Şengör et al., 2008) and upper crustal extensional magmatism in Lake Van. Since, the generated melts pooled under the accretionary complex (its bottom exposure), penetrated it through suture contacts (Muş suture) into the upper crustal depths and began melting it.

The wedge-type asthenosphere with a subduction component had originally flowed from the N through Muş-Lake Van region into BP-M backstop in the S, forming a lobe-like flow engulfed in hot and undepleted asthenospheric material, invading from the slab window (Şengör et al., 2008). This flow also penetrated into the upper crust of the Arabian foreland, beneath northernmost Arabia. Since, its lithosphere is also already greatly thinned (Gök et al., 2003 and Şengör et al., 2008). Mixing between these two distinct sources combined with crustal assimilation and crystallisation is responsible for generating the great variety of the volcanic material around the Muş–Nemrut–Tendürek volcanoes. The process here envisaged suggests its general applicability to asymmetric collisional belts (Şengör, 1990b). The presumed presence of such slab-driven asthenospheric flows provides an answer to the question of why the volcanic activity initiated much earlier in the N and migrated to the S in time (Şengör et al., 2008). This also explains why calc-alkalic with a distinct subduction signature in the N while alkalic with a distinct within-plate signature in the S (Keskin, 2003, 2007 and Şengör et al., 2008). Lake Van Dome at squashy zone of E-Turkey is presently probably rising above a doming hot asthenosphere. This dome is an extraordinary place, in which a thin and warm crust underlies this shortening zone, covered by volcanic dome-cone complexes and active magmatic intrusions typical of extensional regime in Lake Van region. Upwelling of mantle diapirs through a plate window generated by slab detachment also provides a petrogenetic model for the presence of mantle plume material in convergent settings, which are compatible with geochemical evidence and first-order geodynamic modeling. These considerations provide a framework for the occurrence of plume-related and calc-alkaline magmatism in the SE-Alps and probably in other similar tectonic settings, such as the Central Europe Magmatic Province (CEMP) (Macera et al., 2008). The similar processes also dominated the post-collisional tectonics of such orogenic systems as the Pan-African collage of NE-Afro-Arabia and all other Turkic-Type

orogens (Şengör et al., 2008). For example, Archaean collisions are dominated by Turkic-type post-collisional events rather than Tibetan ones (Şengör and Natal'in, 1996a, 2004). Hence, E-Anatolia and Lake Van constitute a marvelous region to study how continental crust is generated and consolidated in Turkic-type orogens.

5.4.2 Alkaline dome-cone series in Muş suture trend

Intraplate alkaline dome-cone series seem to represent the morphological expressions of the primitive mantle invasion into the crust and extensional magmatism in the Muş-Solhan-Lake Van region. Spatial distribution of the alkaline dome-cone series is roughly aligned in W-E Muş suture trend along the S-margin boundary of Muş-Lake Van region. Geochemical composition of these dome and cones, Solhan volcanics, Kirkor Mt., Mazik-Germav Mt., Nemrut Mt, also together with Süphan Mt., Tendürek Mt., and Ağrı Mt., are strongly alkaline. Parasitic collapsed cones (passive) and magmatic intrusions (active) from the lake are most probably generated by the same alkaline origin and strongly controlled by the fault activity in S-margin boundary of the lake. The core of parasitic dome-like broad concave cones consists of autoclastic breccias and scoria breccias (Yılmaz et al., 1987). Some of the northernmost volcanic ridges are situated within the E-Anatolian fault zone. An intensive active tectonism along the branches of the main fault zone destroyed most of the primary volcanic features of the rocks in this area (Yılmaz et al., 1987). Similarly, peripherally collapsed parasitic cones in and along W-segment of S-margin boundary fault in the lake are caused by strong Quaternary activity of transtension (W-segment). Extensional nature of these dome-cone series is clearly indicated in places where the volcanic centres and the parasitic cones are located (Yılmaz et al., 1987 and Şaroğlu and Yılmaz, 1987). This suggests a close relation of alkaline magmatism to extensional processes in and around the lake. It is to say that magmatic intrusions along the S-marginal section of the lake as a part of Muş suture trend are the sub-lake continuation of this alkaline dome-cone complex. This alkaline complex strongly confirms intraplate signature of magmatism younging towards Muş suture and BP-M backstop (Keskin, 2005 and 2007). This means that Nemrut volcanic dome complex, together with collapsed parasitic cones and magmatic occurrences in and around the Lake Van basin is a clear expression of intraplate signature of extensional alkaline magmatism at crustal depths as detailed from the previous studies below.

Yılmaz et al., (1998) is the first comprehensive description of the major Quaternary volcanoes of the E-Anatolia (Ağrı, Süphan, Tendürek and Nemrut). The trace and isotope evidence from this study indicates that the young volcanism of E-Anatolia was not temporally associated with any subduction system and generated from variably enriched mantle. This suggests that the geochemical differences among the volcanoes appear to be related to the inherited lithospheric characteristics of the region. A logical conclusion of this is that the magmas were derived from a permanently enriched source in the uppermost mantle. For this reason, the E-Anatolian volcanic domain may be analogous to a Tibetan type tectono-magmatic environment. The magmatic evolution of the two regions, which have experienced N-S compressional deformation since the Middle Eocene, also show close similarities (Pearce and Houjun, 1988; Pearce et al., 1989, 1990; Şengör and Kidd, 1979; Yılmaz et al., 1993). These results are confirmed by an important study of Buket and Temel, (1998) from Varto (Muş) volcanic rocks in E-Turkey. Buket and Temel, (1998) analyzed the major-element/trace-element geochemistry and genesis of Varto (Muş) volcanic rocks. These authors argued that generation of the magmas from a depleted mantle source and/or their emplacement within the continental crust with variable degrees of contamination and fractional crystallization has been related to a detached sinking slab following Miocene continental collision along the Bitlis Suture Zone. All geochemical data presented in their study indicate that the Varto volcanics are products of mantle partial melting that have been subjected to AFC (DePaolo, 1981) processes during ascent of the magmas through the crust. This significantly suggests that these volcanic rocks are thought to have ascended from the mantle using the deep fractures of the fault segments and that alkaline and calc-alkaline Varto volcanic rocks have formed from magmas that originated in the mantle. This also argues that these fault segments at crustal depths are the suture complexes of the highly anisotropic convergent crust such as Muş and Bitlis sutures. Products of these volcanic suites were formed by partial melting of mantle sources and emplaced during continental rifting and/or extensional processes. This strongly remarks extensional alkaline origin of magmatic occurrences observed all over the lake, (see and examine spider diagrams, these diagrams normalized to MORB are not related to subduction processes in Buket and Temel, 1998. Interestingly, these spider diagrams are also in accordance with Red Sea in Altherr et al., 1988 and Rio Grande Rift in Gibson et al., 1992 patterns).

More interesting evidence from Kipfer et al., (1994) confirms the MORB-type mantle component of overall magmatism within the lake and clarifies what the MORB-type mantle component means for the lake setting. Based on the measurement of the helium isotopes (^{3}He and ^{4}He) and Ne by Kipfer et al., (1994), it was found that, in the area of Lake Van, helium from a depleted mantle source is rising to the surface. The fact that the concentration of ^{4}He also increases with depth gave a first indication for the probable existence of an additional source of helium in the lake. Furthermore, the most important clue was found by Kipfer et al., (1994) when new samples from Lake Van were measured along with samples from the volcanic crater lake of Nemrut Mt. extensional system, in which a large input of mantle helium was detected. These samples from crater lake Nemrut, even in the springs seem to originate from the same mantle source that is a neon free, helium rich MORB type mantle component (Kipfer et al., 1994). This concludes that in the bottom water of the Lake Van, the mean excess ^{3}He/^{4}He ratio is slightly higher than the MORB ratio found in Lake Nemrut (see data in Kipfer et al., 1994). Moreover, Pearce et al., (1990) plotted the diagram showing basalts on the mantle trend, and confirming that the enriched mantle source had no subduction component. It can, hence be inferred that a small proportion of lavas from volcanoes around the lake and magmatism within the lake reached the surface with neither extensive assimilation and with nor the extensive mixing in crustal magma chambers. These magma chambers might have homogenized their isotopic and trace element variations as stated by Pearce et al., (1990). Since, there is no evidence for pure crustal melting both in the E-Anatolia (Pearce et al., 1990) and in and around the Lake Van basin. As an example, the geochemical variations of the Solhan volcanics in the W-end of Muş basin are explained with reference to fractional crystallization under low to moderate pressure conditions (Yılmaz et al., 1987). The scarcity of typical basaltic rocks leads that the parental magma commenced close to an alkali-olivine basalt composition (Yılmaz et al., 1987). This indicates no any clear geochemical and petrographical evidence of crustal contamination. Moreover, as compared generalized stratigraphical section of the Solhan-Muş district by Yılmaz et al., (1987) with seismic sections of the Lake Van, it is commonly recognized that dark flows dominate the sequence (the hawaiite the Solhan volcanics). These flows display well-developed flow structures and consolidation cracks (Yılmaz et al., 1987). In both Solhan and Lake Van areas, the attitude of vesicles in the flow surfaces together with

flow structures and associated sedimentary horizons indicate that the lavas commonly flowed over subhorizontal surfaces (Yılmaz et al., 1987). Lavas and pyroclastic rocks intercalate with sedimentary beds and several extrusion phases in sequences are also recognized.

Geochemical studies by Keskin, (2005; 2007), model cross sections by Şengör et al., (2008) and MORB-type mantle component evidenced by Kipfer et al., (1994) as associated with a study of genesis of collision volcanism by Pearce et al., (1990) have significantly directed a way of the interpretation to crustal-scale tectonic events. The results of Kipfer et al., (1994) clearly revealed that lake bottom sediments and lake water contain excessive amount of helium derived from a depleted mantle source. The results of previous studies and available seismic reflection data indicate that extensional magma propagation and intrusion is still in progress in the weak and irresistant marginal sections of Lake Van. Along the marginal sections, the magmatic activity is considerably driven by tectonic and magmatic events at upper crustal depths. It is recognized that the extensive He injection associated with magmatic intrusions is locally related to extensional magmatic activity in the lake. This is also discussed by Kempe, (1977) and Wong and Finckh, (1978) and supported by geochemical observations of Kipfer et al., (1994). Hence, Isotope concentrations measured in Lake Van focus upon the importance of an integral interpretation of such data by taking into account the simultaneous influence of tectonic events in the lake. Geochemical processes mentioned above are mixing and decay of tritium and the external addition of helium either from the crust or the mantle and thus, they represent active tectonic and magmatic interactions in the lake. This supports that the Lake Van depression is linked to extensional tectono-magmatic activities during the Quaternary episode. Also, alkaline cycle largely developed during this time (Yılmaz et al., 1987 and Şaroğlu and Yılmaz, 1987). Alkaline dome-cone series along Muş suture were formed during this cycle. This period also postdated the formation of the two transform faults. Since, the beginning of the westward escape tectonism (Şengör et al., 1985) is characterized mainly by rocks with a strong alkaline affinity (Yılmaz et al., 1987).

Alkaline dome-cone series in suture trend extend in W-E, through Muş-Lake Van and localize into margin boundary faults of the lake. The extensive intrusive activity of the rising magmas through the lake seems to have been, such likely “the surface

expression of the primitive mantle invasion" within the Lake Van. This concludes "extensional alkaline magmatism" originating in variably enriched mantle lithosphere and the oblique opening of Lake Van basin in S. More recent investigations in other lakes located in volcanic or tectonically active zones show that the input of mantle helium found in E-Turkey is not unique in continental regions. Similar results have been also observed in crater Lake (Oregon) by Collier et al., (1991) and in Lake Laacher (Germany) by Kipfer et al., (1993).

5.5 An Insight into The Processes of Crustal Differentiation beneath Lake Van

Extensional magmatism is a manifestation of extensional tectonism, indicating that magmatic regimes originate and evolve under the control of prevailing tectonic regimes. The Lake Van basin is imbricated by accreted thrust slices, through which one or more active magma chambers exist and these chambers have prominent morphological expressions. As recognized from a linear morphological distribution of alkaline dome-cone series all along the Muş suture trend, a number of pointed stocks into the upper crust, piercing the sedimentary layers appear to be volcano-magmatic similar to those in the circum-Muş Basin. The vast amount of the surface volcanic cover suggests a corresponding abundance of magma that injected into the accretionary wedge complex and to the lake and there became solidified as tower-like intrusive patterns. As emphasized by Şengör et al., (2008), the erupted volumes on the surface may represent only a small fraction of the melt generated beneath the region, because a greater proportion presumably was emplaced deeper in the crust as intrusions. These intrusions have strongly deformed deep basin sediments such as lateral flows into depositional sequences and effectively controlled morpho-tectonic development of the lake and dispersal system of delta sedimentation.

A perspective from partial melting and migration through the crustal structure of lake suggests that the Muş-Lake Van basin system is particularly interesting from the view point of tectonic and magmatic development, because despite the sharp distinction that exists between the paleo and neotectonic regimes in the E-Turkey (Şengör et al., 1985), there seems to be an continuity in its magmatic evolution. Since, when extension set in, the rising mantle material began injecting into the crust and the lake. Therefore, an understanding the rheology and verifying flow laws of partially molten systems are important in basin formation, such as the dynamic

conditions for melt generation, ascent and emplacement for the crust. The importance of the interplay between the perturbations to initiate crustal melting and the tectonic setting, or "plumbing," in dictating the style of melt movement is necessary conditions for crustal differentiation. Internal differentiation of the crust by upwelling mantle is a localized phenomenon and it is clear that crustal evolution is dominated by the fractionation of hydrous mantle magmas in the region (Şengör et al., 2008). This process is driven either by crustal thickening (but, this is not the case for the region), or by invasion of mantle-derived magmas into the crust, or by lithospheric delamination and asthenospheric replacement. Processes involved in the evolution of slices of differentiated crust include underplating or intraplating, particularly through the involvement of basaltic melts, magma extraction and intrusion, which relates to upper crustal heterogeneities, involving both tectonic pumping of intrusive melts and opportunities for mixing between melts from different sources.

Comparison of a number of basalt patterns by Pearce et al., (1990) from E-Turkey suggested that melting of "plume" asthenosphere, or lithosphere enriched by small volume melts from the asthenosphere, produces "humped" patterns. This can be interpreted in terms of a mantle source with significant enrichment of a small volume asthenospheric melt and an insignificant subduction or crustal assimilation component (Pearce et al., 1990). Alkaline magmatism from Muş-Solhan area, Nemrut-Krikor domes and Tendürek volcano show "humped" patterns. Active and passive (collapsed cones) magmatism also show the same "humped" patterns, which are parasitic end-products of the humped volcanic chain surrounding the lake. The data from the alkaline volcanoes (where the isotopic and trace element contrast between magma and crust is largest) do indicate that extensive combined assimilation and fractional crystallization of crust is taking place at depth beneath E-Turkey (Şengör et al., 2008). This shows that only a small volume of basic magmas has avoided these magma reservoirs and reached the surface in an uncontaminated state (Pearce et al., 1990), confirming that magmatism and volcanism invades the former mélange-accretion wedges shortly after the cessation of subduction (Şengör et al., 2003). This "post-orogenic magmatism" is structurally an important step in converting mélange-accretion wedges into continental crust and is thus critical for

our understanding of the evolution of the crustal growth (Şengör et al., 2003) and also accretionary wedge deformation by processes of crustal differentiation.

The temporal changes in volcanic activity over the last 6 Ma show a trend from more regional-scale activity (the early creation of the Kars Plateau in the N and the Muş-Solhan volcano-sedimentary units in the S) to localized activity in an aligned set of central vent volcanoes (Pearce et al., 1990). This is the reverse of that observed in the early stages of plume-related volcanic activity. The systematic changes in lava chemistry across the collision zone indicate a number of spatially-distinct magma sources, inconsistent with a plume being a source of magma (though not of heat) (Pearce et al., 1990). This trend from more regional-scale to localized activity in aligned central vent volcanoes is well concentrated in and around the Muş-Lake Van basin, striking the W-E trends. This trend is, as mentioned above, covered by alkaline dome-cone series in Muş suture zone. This basin-margin concentration of the alkaline magmatic activity proposes a number of the systematic changes across the Muş suture zone. These are the concentration of alkaline magmatic trend, localized extension and focusing of magmatic products through the marginal faults. These changes indicate a number of spatially-distinct magma sources controlled by an aligned set of linear fracture network system. Network system of extensional strains is characterized by complex kinematic patterns as recognized in subbasins pierced by magmatic intrusions.

The suture-margin distribution of the youngest alkaline magmatism in space and time in and around the Muş-Lake Van has also implications for the scale and timing of delamination of thickened mantle lithosphere. Because there is systematic linear progression of magmatic patterns across or along the thinned crustal zone north of the Bitlis thrust. As mentioned above, the only source of magmatism and associated intrusions in the Lake Van is the marginal expression of a domal asthenosphere. This alkaline magmatism can be explained by some other type of thermal perturbation of the asthenosphere, because, only little perturbation is necessary to initiate partial melting. A perturbation of the lithosphere geotherm is the basic requirement due to upwelling of hot asthenosphere either by stretching of lithosphere (Dixon et al., 1981) or an increase of asthenosphere temperature which then brings the metasomatized “layer” above it solidus (Pearce et al., 1990). Convectively replacement of the colder and denser mantle lithosphere by asthenosphere

(Houseman et al., 1981; England and Houseman, 1988) causes asthenosphere to be brought into very close contact with the thinned crust (Şengör et al., 2003). The close contact between the thinned crust and the uppermost asthenosphere has an important structural implication on the appearance of a basal detachment of the crust and flake-wedge tectonics of the lake. Dewey, (1982) and Dewey et al., (1986) stated that the asthenosphere is brought near the surface and is more likely to be involved in subsequent flake detachment. The width over which stretching occurred may vary from very narrow, as for the sharply defined Red Sea margins, to over 100 km and as for the more diffuse Bay of Biscay margin (Dewey, 1982 and Dewey et al., 1986). On the other hand, the fact that delamination is a catastrophic rather than continuous event results in a rapid increase in surface elevation (England and Houseman, 1988; Pearce et al., 1990) which would be about 2 km for the E-Turkey (Şengör et al., 2003). Such an internal process can be accompanied by the other mechanisms of stretching that characterize thinned crust, notably the creation of pull-apart basins (Süphan and Ağrı volcanoes), extensional and oblique-slip basins (Lake Van basin) associated with continental escape strike-slip faults (N-and E-Anatolian transform faults), discontinuous and conjugate strike-slip fault segments (Şengör et al., 1985; Dewey et al., 1986 and Dhont and Chorowicz, 2006). These fault segments control small sedimentary basin blocks and their escaping routes (Şengör et al., 1985). The linear W-E trend of much of the youngest magmatism from the S-marginal portions of the lake to Muş-Solhan volcanics suggests a response to "localized stretching", due to the lateral stress release associated with the escape of the Anatolian to W and Iranian microplates to ENE, reducing the angularity of the Eurasian margin into which the Arabian plate is being indented (Şengör, 1976; Pearce et al., 1990). This also supports that a delamination event starting at about 6 Ma with the initiation of magmatism and uplift could then result from "subsequent localized extension" associated with continental escape (Pearce et al., 1990).

Neogene episode of E-Turkey affected a previously thickened crust and resulted in widespread magmatism. The continuity in the character of magmatism and the gradual transition from a dominantly calc-alkaline to a dominantly alkaline magmatism, therefore reflect a gradual transition in the nature of tectonic processes, and also expresses the "residual" effects of the last paleo-tectonic processes during the neo-tectonic regime. It is speculated that the tectonic transition in the E-Turkey

was transitional, the magmatic one was gradual. The Plio-Quaternary evolution of Lake Van is controlled by the crustal structure, when extensional tectonics began in the lake and it affected continental crust. The morpho-tectonic expression of crustal imbrication of accretionary basement of the lake is oblique slip fault-controlled depression, whereas its depth extension is accomplished mainly by ductile flow or by ductile shear zone. This shows that the structure of accretionary wedge controls the present-day tectonics of the lake. Accretionary wedge deformation is a process of the post-collisional basin fragmentation and separation. This deformation process resulted in considerable degrees of stretching which must have created extensional/transtensional magmatism in the lake. Tectono-thermal constraints in melting the upper mantle beneath the lake and tectono-magmatic occurrences in deforming the lake, overall basin geometry and the style of tectonism can be inferred to be caused by thermal perturbation of the accretionary wedge system underlying the lake. The likely mechanisms causing the accretionary wedge deformation and thus, shaping the lake are the slab delamination process and localized extension. The style of deformation and the faulting patterns suggests that the Lake Van is characterized by a set of mantle domains running parallel to the Muş suture zone. Each of which has yielded magmas of a particular composition since the start of magmatism in the region.

6. CONCLUSIONS AND RECOMMENDATIONS

Tectono-magmatic framework, deformation style and faulting characteristics of the Lake Van basin and its present-day crustal deformation and dynamic evolution, as well as its sedimentary structure have been investigated by means of seismic reflection profiles and high-resolution GeoChirp data. For that purpose, the entire Lake Van region has been mapped at a basinal scale using available seismic and GeoChirp data, field observation, digital elevation model and seismic mapping softwares. Tectonic, magmatic and sedimentary structure have been mapped and superimposed with morpho-physiographic/topographic maps for a correlative analysis of overall deformation dynamics of the lake. In addition, the deformation patterns and styles related to instrumental recordings of the earthquake sequences are analysed and classified in order to extract deformation characteristics of the strike-/oblique-slip tectonics and crustal magmatism. Several model approaches related to strike-slip tectonism and extensional magmatism at upper crustal depths, particularly in young and hot intraplate collisional settings have been applied in order to document the type of crustal deformation and lake seismicity and prior upper crustal events along the basin-bounding faults. Here, some critical results of the related chapters are summarized and an overall conclusion on tectono-magmatic evolution, the present-day structural development, and sedimentary characteristics of the Lake Van region is shortly provided. These results bring new insights from diverse styles of upper crustal deformation beneath the lake and thus catalyze more comprehensive interdisciplinary research between thin-skinned crustal deformation and extensional magmatism towards a better understanding of the structural complexity of the Lake Van basin and accretionary system of E-Turkey.

1- Seismic reflection profiles show a late stage of extension-transtension of W- and S-margins of Lake Van, implying that there is a growing appreciation of the role of extensional/strike-slip tectonics in accretionary orogen. This gives an important view that local or large-scale tectonic contacts such as suture complex in orogenic belt have changed.

2- Basin-bounding strike-/oblique-slip faults of Lake Van are the reactivated features, implying basin inversion. The lake is also characterized by various types and geometric combinations of external and internal subbasin systems, driven by strike-/oblique-slip tectonics.

3- Asymmetric half-graben basin fill patterns in N-S and strike-slip basin fill patterns in W-E cross-sections are well recognized in seismic data. Wedge-shaped central depocenter migrates parallel to the active strike-slip margins. This migration results in accumulation of extraordinarily thick sedimentary sections in the lake and in subbasins. Since, marginal activity of the strike-slip faulting results in lateral displacement of the source areas, sedimentary facies, and depositional centers, typical of strike-slip sedimentation. Since, larger, longer and slumped-slided delta progradations into the deep central basin, thick onlap sequences of basin fill and complicated abrupt facies changes within narrow and elongate depositional framework of the lake are typical of the fill of strike-slip basins.

4- Strike-slip basin fill represents very high sedimentation rates, very thick stratigraphic successions, and abundant evidence of paleoseismic activity, as observed in soft-sediment deformations in delta settings. Strike-slip fault-controlled margins are, principally represented by coarse-grained debris-flow-dominated aprons, as well seen in NNE-marginal section of the lake. Since, upward coarsening sequences record progradational sedimentary systems.

5- These progradations are resulted from forced regressions. These regressions are caused by episodic lowering of base level, induced by active tectonism, catastrophic, abrupt and sharp changes of lake level and climatic factors as well. On the other hand, fluvio-deltaic facies represent the opposite margins and sublacustrine turbidites, debris flows and fluvio-deltai facies typify axial deposystems.

6- Dynamic and comparative analysis of the strike-slip basins with strike-slip deformation and sedimentation in Lake Van indicates “crustal deformation”, concentrated at upper crustal sections. These strike-slip basins have common and almost similar deformation styles and sedimentation patterns, although they seem to be different in diverse tectonic settings, triggered by various kinds of stresses. Hence, these basins well represent structural and sedimentary evolution of the lake, external and internal subbasins in various scales, indicating that the strike-slip deformation

and basin formation is mainly driven by crustal tectonics, particularly at upper crustal levels.

7- Lake Van is the one of mostly long-lived strike-slip and “polycyclic” basins. These kinds of basins undergo repeated episodes of generally transtensive and transpressive subsidence and uplift within continuing strike-slip settings. Hence, the lake may be a prototype of complex basin types and considered as a prototypical sediment-rich accretionary wedge-basin complex. Strike-/oblique-slip faulting, periodic fault displacement, polycyclic episodes of sedimentation, continuing and episodic subsidence and uplift yield complex basin types and place many long-lived strike-slip basins in the “complex basins”. Therefore, it is too difficult to model accurately these kinds of basins, especially by 2D-seismic reflection data. To understand and reconstruct initial paleotectonic framework of these basins is also difficult, especially in accretionary orogens.

8- In Lake Van, upper crustal tectonic mobility and strike-slip sedimentation went on together across the whole basin, but, in areas where, for a time, either deformation or sedimentation dominated. Seismic reflection profiles are more complicated at depth, inasmuch as older beds are subjected to more deformation than younger beds.

9- Lake Van is a “hot and complex polycyclic and/or polygenetic strike-slip basin”, driven by upper crustal deformation within younger and hot accretionary orogen. This gives a strong evidence of germanotype deformation in a small Turkic-type orogeny.

10- Reflection data also illustrate seismic pattern, external geometry and basinal emplacement of shallow level magmatic intrusions and their cryptoexplosions and reveal clear evidences of dynamics of crustal magma transfer, storage and differentiation.

11- Strike-/oblique-slip deformation in Lake Van has been taking place along a broad zone of magmatic intrusions, suggesting that magma can erupt rapidly to the surface along margin boundary faults if they cut deeply enough through the crust. This implies pre-existing faults may completely or partially trap the propagating magmatism, implying extensional magma propagation through flake margins of the lake at upper crustal depths. This shows that multiple zones of magmatic intrusions

through margin boundary faults should be a common phenomena along newly inverted basin margins of the lake.

12- The net effect of extensional magma propagation on the lake bottom would be the appearance of multiple parallel zones of intrusions showing a broad-diffuse plate and/or suture boundary. This effect is further complicated by changing stress fields and/or kinematic boundary conditions due to the reorientation of the basin boundary faults

13- Extensional magmatism is subject to a series of processes that lead to its differentiation during transfer through and storage within the convergent crust beneath the lake. This provides new insights to the subject of magmatic processes operating within the crust, and remarks important links between subsurface processes and magmatism.

14- Extensional magmatism includes volcanic eruptions, crypto-explosions, explosive fissure and central vent volcanoes, intrusions-extrusions, sealing conduits-pressure buildups, CO_2 diffuse flank degassing, extensive hydrothermal chimneys, larger sheeted sill products, peripherally collapsed dome-cone complexes, post-magmatic hydrothermal alteration zones and volatile-boiling deformations.

15- Extensional magmatism and propagation has been most probably initiated by the tectono-thermal response of underlying accretionary wedge complex to decompressional melting magmatism and hence, to doming hot asthenospheric front along basal detachment surface of the highly fractured upper crustal flake. This shows that kinematics of marginal conditions is changed, the pre-existing boundary faults are reactivated as strike-/oblique-slip faults, and the lake experiences the basin inversion, followed by extensional magmatism.

16- The vast amount of extensional magmatic cover in the lake suggests a corresponding abundance of alkaline melting materials. These materials inject into the accretionary complex and there become solidified. The generated partial melts by adiabatic decompression pool under the accretionary structure, penetrate it and begin melting it. This is the first-order mechanism of upper crustal emplacement of rising magmas, concluding extensive marginal distribution of extensional magmatism in the lake.

17- The first order mechanism builds the crust and drives hydrothermal circulation and consequent melting of the wet accretionary complex rocks, implying basalt-hosted hydrothermal system in Lake Van. This evident the transport of extensional alkaline magmas from the uppermost mantle through the basin-bounding fault zones/suture trends and its cooling and crystallization. Decompressional melting magmatism is correlated with alkaline magmatic surges around Lake Van and clearly appears associated to the present-day area of the crustal thinning defined by the previous studies. The timing of these magmatic surges is related to upwelling pulses from the uppermost mantle, dependent of the extensional and strike-slip tectonic setting of Lake Van.

18- Seismic data evidences reveal that , to some extent, Lake Van can be viewed as volcano-tectonic lake and the uppermost lacustrine manifestation of a hydrothermal reservoir between the surface and an underlying magma. Seismic reflection data, regional interpretation of seismogram waveforms and basinal distribution of earthquake locations confirm seismic structural evidence of the role of magmas and volatiles from extension inceptions, along-axis variations of strain related to upper crustal structure, crustal heterogeneity, and rates of faulting and magma production.

19- It is recognized that 3-D field, analytical, and tomography modelling tools are necessary to address these issues and to improve well-identified seismological evidences of magmatic activity in such a complicated volcanic area. Ideally, it is needed to infer and validate a lacustrine model of heat and mass transport from magmatic intrusions to the lake bottom, taking gas-sediment, gas-water, water-sediment interactions, and detailed magma hydrothermal deformations into account. These play an important role in determining the dynamic state of the lake and its earthquake potential.

20-Available seismic and high-resolution data showcase reflection evidences of tectonic, volcanic and magmatic deformations to provide satisfactory explanations of the earthquake waveform patterns, even in highly anisotropic hot orogenic systems. The results strongly point to an underlying crustal heterogeneity and crustal differentiation process, with respect to roles of decompressional melting magmatism that brings about this apparent difficulty. How this happens and the possible existence of underlying organizing principles are puzzles that need to be pursued in future research. This gives an opportunity to lead to a better tectono-magmatic and

volcano-seismological modelling of hotter, smaller and younger accretionary orogens in understanding post-collisional, intraplate volcanic seismicity as in E-Turkey.

REFERENCES

Addicott, W. O., 1968. Mid-Tertiary zoogeographic and paleogeographic discontinuities across the San Andreas Fault, California, in Dickinson, W. R., and Grantz, A., eds., Proceedings of Conference on Geologic Problems of the San Andreas Fault System: Stanford University Publications in *the Geological Sciences*, **v. 11.** 144-165 pp.

Adiyaman, Ö , Chorowicz, J, and Köse, O., 1998. Relationships between volcanic patterns and neotectonics in Eastern Anatolia from analysis of satellite images and DEM. *J. Volcanol Geotherm Res.* **85**:17–32 pp.

Akçar, N., Schlüchter, C., 2005. Paleo-glaciations in Anatolia: a schematic review and first results. Eiszeitalter und Gegenwart-*Quaternary Science Journal* **55**, p. 102–121 pp.

Albarede, F., Gasperini, D., Blichert-Toft, J., Bosch, D., Del Moro, A., Macera, P., 2000. OIB-type magmas in subduction zones: mantle counterflow above detaching plates. *EOS* **81**, 1271.

Aldanmaz, E., Pearce, J.A., Thirwall, M.F., Mitchell, J.G., 2000. Petrogenetic evolution of late Cenozoic, post-collision volcanism in western Anatolia, Turkey. *J. Volcanol. Geother. Res.* **102**, 67–95 pp.

Al-Lazki AI, Seber, D, Sandvol, E., Turkelli, N., Mohamad, R., and Barazangi, M., 2003. Tomographic *Pn* velocity and anisotropy structure beneath the Anatolian plateau (Eastern Turkey) and the surrounding regions. *Geophys Res Lett* **30**(24):8043 doi:10.1029/2003GL017391

Allen, C. M., 1992. A nested diapir model for the reversely zoned Turtle Pluton, southeastern California. *Trans. R. Soc. Edinburgh, Earth Sci.,* **83**: 179-190.

Allen, C. R., 1965. Transcurrent faults in continental areas. *Phil. Trans. R. Soc.* London, A258, 82-9.

Allen, C.R., 1968. The tectonic environments of seismically active and inactive areas along the San Andreas fault system, in Dickinson, W.R., and Grantz, A., eds., Proceedings of Conference on Geologic Problems of the San Andreas fault system: Stanford University Publications in the *Geological Sciences,* **v.11,** p. 70-82.

Allen, M.B., Şengör, A.M.C., Natal'in, B., 1995. Junggar, Turfan, and Alakol basins as Late Permian to Early Triassic sinistral shear structures in the Altaid orogenic collage, Central Asia. *Journal of the Geological Society* London **152**, 327–338.

Allen, P.A., and Allen, J.R., 1990. *Basin analysis principles and applications:* Blackwell Scientific, London, 451 p.

Altherr, R., Henjes-Kunst, F., Puchelt, H., Baumann, A., 1988. Volcanic activity in the Red Sea axial trough-evidence for a large mantle diapir. *Tectonophysics* **150**, 121-133.

Altınlı, E., 1966a. Doğu ve Güneydoğu Anadolu'nun jeolojisi. Kısım I: *MTA Enstitüsü Dergisi,* v. **66**. p. 35-74.

Ambraseys, N.N., and Finkel, C.F., 1995. The seismicity of Turkey and adjacent areas, a historical review, *Eren yayıncılık ve Kitapçılık Ltd. Şti.,* Istanbul, p. 1500-1800.

Angus, D. A., Wilson, D.C., Sandvol, E., and Ni, J. F., 2006. Lithospheric structure of the Arabian and Eurasian collision zone in eastern Turkey from S-wave receiver functions. *Geophys. J. Int.* v. **166**, no.3, p. 1335–1346.

Anketell, J. M., Cegla, J., and Dzulynski, S., 1970. On the deformational structures in systems with reversed density gradients. *Ann. Soc. Geol. Pol. XL*, 3– 30.

Argand, E., 1916. Sur l'arc des Alpes occidentales. *Eclogæ Geologicæ Helvetiæ* **14**, 145–191.

Arni, P., 1939. *Tektonische Grundzüge Ostanatoliens und benachbarter Gebiete. Veröffentlichungen des Institutes für Lagerstättenforschung der Türkei, Serie A: Abhandlungen* **4**, 89 pp. + 5 foldout plates.

Arni, P., 1939a. *Tektonische Grundzüge Ostanatoliens und benachbarter Gebiete. Veröffentlichungen des Institutes für Lagerstättenforschung der Türkei, Serie B: Abhandlungen* **4**, 89 pp. + 5 foldout plates.

Arni, P., 1939b. Relations entre la structure régionale et les gisements mineraux et pétrolifères de l'Anatolie. *Maden Tetkik ve Arama Enstitüsü Dergisi* **4/2**, 29–36.

Arni, P., 1942. Materialien zur Altersfrage der Ophiolithe Anatoliens. *Maden Tetkik ve Arama Enstitüsü Dergisi* **7/3**, 481–488.

Avouac, J. P., and Tapponnier, P., 1993. Kinematic model of active deformation in central Asia. *Geophysical Research Letters* **20**, 895–898.

Axen, G. J., Selverstone, J., Byrne, T., and Fletcher, J. M., 1998. If the strong crust leads, will the weak crust follow? *GSA Today*, **8**, 1-8.

Aydın, A., and Nur, A., 1982. Evolution of pull-apart basins and their scale independence: *Tectonics,* v. **1**, 91-105 pp.

Aydın, A., and Page, B.M., 1984. Diverse Plio-Quaternary tectonics in a transform environment, San Francisco Bay region, California: *Geological Society of America Bulletin*, v. **95**, p. 1303-1317.

Babcock, E. A., 1974. Geology of the NE-margin of the Salton trough, Salton Sea, California: *Geological Society of America Bulletin,* v. **85**, 321-332 pp.

Baer, G. and Reches, Z., 1991. Mechanics of emplacement and tectonic implications of the Ramon dike systems, Israel. *Journal of Geophysical Research* **96**, 11,895±11,910.

Bailey, R. C., 2001. Dynamical analysis of continental overflow. *Journal of Geodynamics*, vol.**31**, 293-310.

Balance, P. F., 1980. Models of sediment distribution in non-marine and shallow marine environments in oblique-slip fault zones. In: *Sedimentation in Oblique-slip Mobile Zones* (edited by Ballance, P. F., and Reading, H. G.,). Spec. Publs. Int. Ass. Sediment. **4,** p. 229-236.

Balance, P. F., and Reading, H.G., 1980. Sedimentation in oblique-slip mobile zones: *International Association of Sedimentologists Special Publication* **4**, 265p.

Bally, A. W., 1983. Seismic Expression of Structural Styles; *American Association of Petroleum Geologists Studies in Geology*, ser. **15**. 3 volumes.

Barber, A. J., and Crow, M. J., 2005. Structure and structural history of Sumatra, SE-Asia in Chapter 13. doi:10.1144/GSL.MEM.2005.031.01.02. *Geological Society, London, Memoirs* 2005; v. **31**; p. 175-233.

Barber, A. J., Crow, M. J., and De Smet, M. E. M., 2005. Tectonic Evolution of Sumatra, SE-Asia in Chapter 14. doi:10.1144/GSL.MEM.2005.031.01.02. *Geological Society, London, Memoirs* 2005; v. **31**; p.234-259

Barka, A.A., and Kadinsky-Cade, K., 1988. Strike-slip fault geometry in Turkey and its influence on earthquake activity: *Tectonics*, v. **7**, p. 663-684.

Baumgardt, D. R., 1990. Investigation of teleseismic Lg blockage and scattering using regional arrays, *Bull. seism. Soc. Am.,* **80**, 2261-2281.

Beaumont, C., and and Pedreira, D., (in progress). Accordion Tectonics, Postdoctoral project, the Geodynamics Group at Dalhouise, Canada.

Beaumont, C., Jamieson, R.A., Nguyen, M.H., and Lee, B., 2001. Mid-crustal channel flow in large hot orogens: Results from coupled thermal-mechanical models, in: *Slave-Northern Cordillera Lithospheric Evolution (SNORCLE) and Cordilleran Tectonics Workshop, Lithoprobe Report* **79**, 112-170.

Beaumont, C., Kamp, P.J.J., Hamilton, J., and Fullsack, P., 1996. The continental collision zone, South Island, New Zealand: Comparison of geodynamical models and observations, *Jour. Geophysical Res.*, **101**, 3333-3359.

Beaumont, C., Munoz, J.A., Hamilton, J., and Fullsack, P., 2000. Factors controlling the Alpine evolution of the central Pyrenees inferred from a comparison of observations and geodynamical models, *Jour. Geophys. Res.*, **105**, 8121-8145.

Becker, A., 1993. An attempt to define a neotectonic period for central and northern *Europe, Geol. Rundsch.,* **82**, p. 67-83.

Bedard, J. H., 1985. The opening of the Atlantic, the Mesozoic New England Igneous Province and mechanisms of continental breakup. *Tectonophys.* **113**, 209-32.

Berger, A., Rosenberg, C. and Schmidt, S. M., 1996. Ascent, emplacement, and exhumation of the Bergell pluton within the southern steep belt of the central Alps. *Schweizerische Mineralogisch Petrographische Mitteilungen* **76**, 357±382.

Bird, P., 1978. Initiation of intracontinental subduction in the Himalaya. *Journal of Geophysical Research* **83**, 4975–4987.

Bökh, H., Lees, G.M., Richardson, F.D.S., 1929. Contribution to the stratigraphy and tectonics of the Iranian ranges. In: Gregory, J.W. (Ed.), *The Structure of Asia. Methuen & Co*., London, pp. 58–176. + 23 plates.

Bonin, B., 2004. Docoeval mafic and felsic magmas in post-collisional to within-plate regimes necessarly imply two contrasting, mantle and crustal, sources? A review. *Lithos* **78**, 1–24.

Bos, B., 2001. Faults, Fluids and Friction, *Ph.D Thesis*, Universiteit Utrecht, Netherlands, 157 pp.

Bostock, M. G. and Kennett, B. L. N., 1990. The effect of 3-D structure on Lg propagation patterns, *Geophys. J. ht.,* **101**, 355-365.

Bouchez, J. L. and Diot, H., 1990. Nested granites in question: contrasted emplacement kinematics of independent magmas in the Zaer pluton, Morocco. *Geology,* **18**: 966-969.

Bouchon, M., and Coutant, O., 1994. Calculation of synthetic seismograms in a laterally varying medium by the Boundary Element-Discrete Wavenumber Method, *Bull. seism. Soc. Am.*, **84**, 1869-1881.

Braun, J., Chery, J., Poliakov, A., Mainprice, D., Vauchez, A., Tomassi, A., and Daigniéres, M., 1999. A simple parameterization of strain localization in the ductile regime due to grain size reduction: A case study for olivine, *Jour. Geophys. Res.,* **104**, 25167-25181.

Brooks, E. R. 1995. Paleozoic fluidization, folding and peperite formation, northern Sierra Nevada, California. *Canadian Journal of Earth Science,* **32**, 314-324,

Brown, G.L., Schmidt, D.L., Huffman Jr., A.C., 1989. Geology of the Arabian Peninsula-Shield Area ofWestern Saudi Arabia.U. S. *Geological Survey Professional Paper* 560-AX+ 188 pp.

Brown, M., 1994. The generation, segregation, ascent and emplacement of granite magma: the migmatite-to-crustally derived granite connection in thickened orogens. *Earth Sci. Rev.,* **36**: 83-130.

Brown, R.W., 1928. Experiments relating to the results of horizontal shearings: *American Association of Petroleum Geologists Bulletin,* v. **12**, p. 715-720.

Buiter, S.H.J., Govers, R., and Wortel, M.J.R., 2002. "Two-Dimensional Simulations of Surface Deformation Caused by Slab Detachment", *Tectonophysics*, **354**, 195-210.

Buket, E., and Görmüş, S., 1986. Varto_Mus¸.havzasındaki Tersiyer yaslı istifin stratigrafisi. *Yerbilimleri* **13**, 17–29, in Turkish with English abstract.

Buket, E., and Temel, A., 1998. Major-element, trace-element, and Sr-Nd isotopic geochemistry/and genesis of Varto Muş volcanic rocks, Eastern Turkey. *Journal of Volcanology Geothermal Research* **85**, 405-422.

Campbell, J. D., 1958. En Echelon Folding: *Economic Geology,* v. **53**, 448-472 pp.

Campillo, M., Feignier, B., Bouchon, M. and Bethoux, N., 1993. Attenuation of crustal waves across the Alpine range, *J. geophys. Res.,* **98**, 1987-1996.

Canals, M. G., Lastras, R. Urgeles, J. L. Casamor, J. Mienert, A. Cattaneo, M. De Batist, H. Haflidason, Y. Imbo, and Laberg, J. S., 2004. Slope failure dynamics and impacts from seafloor and shallow sub-seafloor geophysical data: Case studies from the COSTA project: *Marine Geology,* v. **213**, p. 9–72.

Cao, S., and Muirhead, K. J., 1993. Finite difference modelling of Lg blockage, *Geophys. J. Int.,* **115**, 85-96.

Casey, J. F., and Dewey, J. F., 1984. Initiation of subduction zones along transform and accreting plate boundaries, triple junction evolution and fore-arc spreading centres--implications for ophiolitic geology and obduction. *In:* Gass, I.G., Lippard, S.J. and Shelton, A.W. (eds) *Ophiolites and Oceanic lithosphere, Geol. Soc. Lond. Spec. Publ.* p. 269-290.

Castro, A., 1985. The Central Extremadua Batholith: Geotectonic implications (European Hercynian Belt): *Tectonophysics,* v. **120**, 57-68 pp.

Cebria, J.M., and Lopez-Ruiz, J., 1995. Alkali basalts and leucitites in an extensional intracontinental plate setting: the late Cenozoic Calatrava Volcanic Province (Central Spain). *Lithos* **35**, 27–46.

Cebria, J.M., Lopez-Ruiz, J., Doblas, M., Oyarzun, R., Hertogen, J., Benito, R., 2000. Geochemistry of the quaternary alkali basalts of Garrotxa (NE-Volcanic Province, Spain): a case of double enrichment of the mantle lithosphere. *J. Volcanol. Geotherm. Res.* **102**, 217–235.

Cello, G, Crisci, G., M, Marabini, S, and Tortorici, L., 1985. Transtensive tectonics in the strait of Sicily: structural and volcanological evidence from the osland of Pantelleria. *Tectonics* **4**; 311–322.

Chorowicz, J, Emran, A, and Alem, E. M., 2001. Tectonique et venues volcaniques en contexte de collision, exemple du massif neogene du Siroua (Atlas marocain) : effets combine´ s d'une transformante et de la suture panafricaine. Can *J. Earth Sci* **38**: 411–425.

Chorowicz, J., Bardintzeff, J. M., Rasamimanana, G., Chotin, P., Thouin, C., Rudant, J. P., 1997. An approach using SAR ERS images to relate extension fractures to volcanic vents: examples from Iceland and Madagascar. *Tectonophysics* **271**, 263–283.

Christie-Blick, N., and Biddle, K. T., 1985. Deformation and basin formation along strike-slip faults. In: Biddle, K. T., Christie-Blick, N. (Eds.), *Strike-slip Deformation, Basin Formation and Sedimentation.* Special Publication of the Society of Economic Paleontologists and Mineralogists **37**, pp. 1–34.

Clemens, J. D. and Mawer, C. K., 1992. Granitic magma transport by fracture propagation. *Tectonophysics* **204**, 339±360.

Cloos, M., Sapiie, B., van Ufford, A.Q., Weiland, R.J., Warren, P.Q., and McMahon, T.P., 2005. Collisional delamination in New Guinea: the geotectonics of subducting slab breakoff. *The Geological Society of America. Special Paper*, vol. **400**. iv + 51 pp.

Collier, R.W., Dymond, J., and McManus, J., 1991. Studies of Hydrothermal Processes in Crater Lake, OR, 201 pp., College of Oceanography, Oregon State Univ.

Coney, P.J., 1992. The Lachlan belt of eastern Australia and Circum-Pacific tectonic evolution. *Tectonophysics* **214**, 1–25.

Coney, P.J., Jones, D.L., and Monger, J.W.N., 1980. Cordilleran suspect terranes. *Nature*, **288**, 329-33.

Cooper, K. M., Reid, M. R., Dunbar, N. W., and McIntosh, W. C., 2002. Origin of mafic magmas beneath northwestern Tibet: Constraints from ^{230}Th-^{238}U Disequilibria, *Geochem. Geophys. Geosys.,* 3/1, art. no. 1065.

Coulon, C., Megartsi, M., Fourcade, S., Maury, R.C., Bellon, Louni-Hacini, A., Cotton, J., Coutelle, A., Hermitte, D., 2002. Post-collisional transition from calc alkaline to alkaline volcanism during the Neogene in Oranie (Algeria): magmatic expression of a slab breakoff. *Lithos* **62**, 87–110.

Cox, K. G., 1978. Flood basalts, subduction and the breakup of Gondwanaland. *Nature* **274**, 47-9.

Craddock, C., Hauser, E. C., Maher, H. D., Sun, A.Y., and Zhu, G. Q., 1985. Tectonic evolution of the W Spitsbergen fold belt: *Tectonophysics,* v. **114**, 193-211 pp.

Crough, S. T., 1983. Hotspot swells. *Ann. Rev. Earth Planet. Sci.* **11**,165-93.

Crowell, J. C., 1962. Displacement along the San Andreas Fault, California: *Geological Society of America Special Paper* **71**, 61 pp.

Crowell, J. C., 1974a. Sedimentation along the San Andreas Fault, California, in Dott, R. H. Jr., and Shaves, R. H., (eds.), *Modern and ancient geosynclinal sedimentation:* Society of Economic Paleontologists and Mineralogists Special Publication No. **19**, 292-303 pp.

Crowell, J. C., 1974b. Origin of Late Cenozoic Basins in S-California, in Dickinson, W. R., eds., *Tectonics and Sedimentation:* Society of Economic Paleontologists and Mineralogists Special Publication No. **22**, 190-204 pp.

Crowell, J. C., 1976. Implications of crustal stretching and shortening of coastal Ventura basin, California, in Howell, D.G., eds., Aspects of the geologic history of the California continental borderland: *American Association of Petroleum Geologists, Pacific Section, Miscellaneous Publication* **24**, 561 pp.

Crowell, J. C., 1979. The San Andreas fault through time. *Journal of the Geological Society of London* **136**, 293±302 pp.

Crowell, J. C., and Link, M. H., 1982. Geologic history of Ridge basin, S-California: *Society of Economic Palaeontologists and Mineralogists, Pacific section, Guidebook,* 304 pp.

Crowell, J. C., and Sylvester, A. G., 1979. Introduction to the San Andreas-Salton Trough juncture, in Crowell, J. C., and Sylvester, A. G., (eds.), *Tectonics of the juncture between the San Andreas fault system and the Salton Trough, SE-California-A Guidebook:* Department of Geological Sciences, Universiyt of California, 1-14 pp.

Crowell, J.C., 1982a. The tectonics of Ridge basin, southern California, in Crowell J.C., Link M.H., (eds.), *Geological history of Ridge basin southern California (Book 22):* Pacific Section, Society of Economic Paleontologists and Mineralogists, Los Angeles, p. 25-41

Crowell, J.C., 1982b. The Violin Breccia, Ridge basin, southern California, in Crowell J.C., Link M.H., (eds.), *Geological history of Ridge basin southern California (Book 22):* Pacific Section, Society of Economic Paleontologists and Mineralogists, Los Angeles, p. 89-97.

Crowell, J.C., 1985. The recognition of transform terrane dispersion within mobile belts: *Circum-Pacific Council for Energy and Mineral Resources Earth Science Series,* v. **1**, p. 51-62.

Crowell, J.C., 1987. Late Cenozoic basins of onshore southern California: complexity is the hallmark of their tectonic history, in Ingersoll R.V., Ernst W.G., (eds.), *Cenozoic basin development of coastal California* (Rubey Volume **VI**): Prentice-Hall, Englewood Cliffs, p. 207-241.

Cruden, A. R., 1998. On the emplacement of tabular granites. *Journal of the Geological Society of London* **155**, 852±862.

Cummings, D., 1976. Theory of plasticity applied to faulting. Mojave Desert, southern California: *Geological Society of America Bulletin,* v. **87**, p. 720-724.

Dalrymple, G.B., Clague, A.C., Tracy, L.V., 1987. 40Ar/39Ar age, petrology, and tectonic significance of some seamounts in the Gulf of Alaska. In: Keating, B.H., Fryer, P., Batiza, R., Boehlert, G.W. (Eds.), Seamounts, Islands, and Atolls, *American Geophysics Union Monograph,* vol. **43**. AGU, Washington, DC, pp. 297–315.

Daly, S. E and Raefsky, A., 1985. On the penetration of a hot diapir through a strongly temperature-dependent viscosity medium. *Geophys. J.R. Astron. Soc.,* **83**: 657-681.

Davies, J. H., and von Blanckenburg, F., 1995. Slab break off: A model of lithospheric detachment and its test in the magmatism and deformation of collisional orogens: *Earth and Planetary Science Letters,* v. **129**, p. 85–102.

Davis, A.S., Clague, D.A., Gray, L.B., Hein, J.R., 2002. The Line Islands revised: new 40Ar/39Ar geochronologic evidence for episodes of volcanism due to lithospheric extension. *Geochem. Geophys. Geosyst.* **3**, doi:10.1029/2001GC000190.

Degens, E. T., and Kurtman, F., 1978. The geology of Lake Van. *MTA Press*. Ankara, **169**, 158 pp.

Degens, E.T., Wong, H.K., Kempe, S., Kurtman, F., 1984. A geological study of Lake Van, Eastern Turkey. *Geologische Rundschau* **73**, 701–734.

Delmelle, P., and Bernard, A., 2000. Volcanic lakes. Volcanic Interactions Part VI, In: *Encylopedia of Volcanoes,* vol: **2**, Academic Press. p. 877-895.

Delmelle, P., and Stix, J., 2000. Volcanic gases. Volcanic Interactions Part VI, In: *Encylopedia of Volcanoes,* vol: **2**, Academic Press. p. 803-815.

Demirel-Schlueter F, Krastel S, Niessen F, Demirbag E, Imren, C, Toker, M, Litt T, and Sturm, M., 2005. Seismic pre-site survey for a potential new ICDP site – PaleoVan – at Lake Van, Turkey. *EGU Geophys Res Abstr* **7**:07997

Demyttenaere, R., Tromp, J. P., Ibrahim, A., Allman-Ward, P., and Meckel, T., 2000. Brunei deep-water exploration: From sea floor images and shallow seismic analogues to depositional models in a slope turbidite setting: Gulf Coast Section SEPM Foundation *20th Annual Research Conference Deep-Water Reservoirs of the World,* December 3–6, p. 304–317.

Deng, Q., Wu, D., Zhang, P., Chen, S., 1986. Structure and deformation character of strike-slip fault zones: *Pure and Applied Geophysics,* v. **124,** p. 204-223.

DePaolo, D.J., 1981. Trace element and isotopic effects of combined wall-rock assimilation and fractional crystallization. *Earth Planet. Sci. Lett.* **53**, 189–202.

Dewey J., F, Hempton M., R, Kidd, W. S. F, Saroglu, F., and Sengör, A. M. C., 1986. Shortening of continental lithosphere; the neotectonics of eastern Anatolia, a young collision zone. In: Coward MP, Ries AC (eds) Collision tectonics. *Geol. Soc. Lond. Spec. Publ.* **19**: 3–36.

Dewey, J. F. Holdsworth, R. E., and Strachan R. A., 1998. Transpression and transtension zones. doi:10.1144/GSL.SP.1998.135.01.01. *In:* Holdsworth, R. E., Strachan, R. A. and Dewey, J. E (eds) 1998. *Continental Transpressional and Transtensional Tectonics.* Geological Society, London, Special Publications, **135**, 1-14.

Dewey, J. F., 1969b. Structure and sequence in the paratectonic Caledonides. *Amr. Ass. petrol. geol. Mem.* **12**. 309-35.

Dewey, J. F., 1977. Suture zone complexities: a review. *Tectonophysics,* **40**, 53-67.

Dewey, J. F., 1982. Plate tectonics and the evolution of the British Isles. *Journal of the Geological Society, London,* **132**, 371-412.

Dewey, J. F., 1988. Lithospheric stress, deformation, and tectonic cycles: the disruption of Pangea and the closure of Tethys. Geological Society, London, Special Publications; doi:10.1144/GSL.SP.1988.037.01.03. In: Audley-Charles, M. G. and Hallam, A. (eds) *Gondwana and Tethys Geological Society Special Publication* No. **37**, pp. 23-40.

Dewey, J. F., 1989. Kinematics and dynamics of basin inversion. doi:10.1144/GSL.SP.1989.044.01.20. *Geological Society, London, Special Publications* 1989; v. **44**; p. 352.

Dewey, J. F., Holdsworth, R. E., and Strachan, R. A., 1998. Transpression and transtension zones. In: Dewey, J. F., Holdsworth, R. E., Strachan, R. A. (Eds.), *Continental Transpressional and Transtensional Tectonics.* Special Publication Geological Society of London **135**, pp. 1–14.

Dewey, J.F., 1986. Diversity in the lower continental crust. Geological Society, London, Special Publications 1986; v. 24; p. 71-78 From: Dawson, J.B., Carswell, D.A., Hall, J. and Wedepohl, K.H. (eds) 1986, *The Nature of the Lower Continental Crust,* Geological Society Special Publication No. **24**, pp. 71-78.

Dewey, J.F., and Burke, K.C.A., 1973. Tibetan, Variscan and Precambrian basement reactivation: products of continental collision. *Journal of Geology* **81**, 683-692.

Dewey, J.F., and Windley, B.F., 1981. Growth and differentiation of the continental crust. *Phil. Trans. Roy. Soc.* London, **301**, 189-206.

Dewey, J.F., Shackleton, R.M., Chang, C.F., Sun, Y.Y., 1988. The tectonic evolution of the Tibetan Plateau. P*hilosophical Transactions of the Royal Society of London* A **327**, 379-413.

Dhont, D, Chorowicz, J, Yürür, T, Froger, J-L, Küse, O, and Gündogdu, N., 1998b. Emplacement of volcanic vents and geodynamics of Central Anatolia, Turkey. *J Volcanol Geotherm Res* **85**:33–55

Dhont, D., and Chorowicz, J., 2006. Review of the neotectonics of the Eastern Turkish–Armenian Plateau by geomorphic analysis of digital elevation model imagery. *Int., J Earth Sci., Geol Rundsch,* **95**: 34–49 doi 10.1007/s00531-005-0020-3.

Dickinson, W. R., and Seely, D. R., 1979. Structure and stratigraphy of forearc regions. *Am. Assoc. Pet. Geol. Bull.,* **63**: p. 2-31.

Dickinson, W.R., 1983. Cretaceous sinistral strike-slip along Nacimiento fault in central California: *American Association of Petroleum Geologists Bulletin,* v. **67**, p. 624-645.

Dixon, J. E., Fitton, J. G., and Frost, R. T. C., 1981. The tectonic significance of post-Carboniferous igneous activity in the North Sea basin. In: L.V. Illing and G.D. Hobson (Editors), *Petroleum Geology of the Continental Shelf of North West Europe.* Blackwell, London, pp. 29-52.

D'Lemos, R. S., Brown, M. and Strachan, R. A., 1992. The relation-ship between granite and shear zones: magma generation, ascent, and emplacement in a transpressional orogen. *Journal Geological Society* London **149**, 487±490 pp.

Dobosi, G., Fodor, R.V., Goldberg, S.A., 1995. Late-Cenozoic alkalic basalt magmatism in northern Hungary and Slovakia: petrology, source compositions and relationship to tectonics. *Acta Vulcanol.,* 7 (**2**), 199–207.

Docherty, C., Banda, E., 1995. Evidence for the eastward migration of the Alboran sea based on regional subsidence analyses: a case for basin formation by delamination of the subcrustal lithosphere? *Tectonics* **14**, 804–818.

Downes, H., Panto, G., Poka, T., Mattey, D.P., Greenwood, P.B., 1995a. Calc-alkaline volcanics of the inner Carpathian arc, Northern Hungary: new geochemical and oxygen isotopic results. *Acta Vulcanol.* 7 (**2**), 29–41.

Downes, H., Vaselli, O., Seghedi, I., Ingram, G., Rex, D., Coradossi, N., Pecskay, Z., Pinarelli, L., 1995b. Geochemistry of late Cretaceous-early Tertiary magmatism in Poiana Rusca (Romania). *Acta Vulcanol.* 7 (**2**), 209–217.

Dubey, A.K., 1980. Model experiments showing simultaneous development of folds and transcurrent faults: *Tectonophysics,* v. **65**, p. 69-84.

Dufeield, W. A., Bacon, C. R. and Delaney, P. T. 1986. Deformation of poorly consolidated sediment during shallow emplacement of a basalt sill, Coso Range, California. *Bulletin of Volcanology,* **48**, 97-107.

Duggen, S., Hoernle, K.,Van den Bogaard, P., Garbe-Schönberg, D., 2005. Postcollisional transition from subduction-to intraplate-type magmatism in the westernmost Mediterranean: evidence for continental-edge delamination of subcontinental lithosphere. *J. Petrol.* 46 (**6**), 1155–1201.

Dunne, L. A., and Hempton, M. R., 1984. Strike slip basin sedimentation at Lake Hazar (eastern Taurus Mountains): *International Symposium of the Geology of the Taurus Belt,* MTA, Ankara, Turkey, p. 229-235.

Einsele, G. 1986. Interaction between sediments and basalt injections in young Gulf of California-type spreading centres. *Geologische Rundschau,* **75**, 197-208.

Einsele, G. 1992. *Sedimentary Basins; Evolution, Facies, and Sediment Budget.* Springer, Berlin.

Einsele, G., Gieskes, J. M. et al. 1980. Intrusion of basaltic sills into highly porous sediments, and resulting hydrothernaal activity. *Nature,* **283**, 414-445.

Eisbacher, G.H., 1981. Late Mesozoic-Paleogene Bowser basin molasse and Cordilleran tectonics, western Canada: *Geological Association of Canada Special Paper* **23**, p. 125-151.

Eisbacher, G.H., 1985. Pericollisional strike-slip faults and synorogenic basins, Canadian Cordillera: *Society of Economic Paleontologists and Mineralogists Special Publication* **37**, p. 265-282.

El Bakkali, S., Gourgaud, A., Bourdier, J.L., Bellon, H., Gundogdu, N., 1998. Post -collision neogene volcanism of the Eastern Rift (Morocco): magmatic evolution through time. *Lithos* **45**, 523–543.

Ellis, S., Beaumont, C., Jamieson, R. A., and Quinlan, G., 1998. Continental collision including a weak zone: The vise model and its application to the Newfoundland Appalachians. *Canadian-Journal-of-Earth-Sciences,* **5,** 1323-1346.

Emerman, S. H. and Turcotte, D.T., 1984. Diapiric penetration with melting. *Phys. Earth Planet. Inter.,* **36**: 276-284.

England, P.C., and Houseman, G.A., 1988. The mechanics of the Tibetan Plateau: *Philosophical Transactions of the Royal Society,* London, v. **A 326**, p. 301–320.

Erdlac, R.J., Jr., and Anderson, T.H., 1982. The Chixoy-Polochic fault and its associated fractures in western Guatemala: *Geological Society of America Bulletin,* v. **93**, p. 57-67.

Erinç, S., 1953. Doğu Anadolu Coğrafyası: İstanbul Üniversitesi yayınları No. 572, *İstanbul Üniversitesi, Edebiyat Fakültesi, Coğrafya Enstitüsü Yayınları* No. **15**, İstanbul, [IV] + 124 pp.

ETSE-project, 2003. The Eastern Turkey Seismic Experiment-project: The study of a young continent-continent collision, edited by Sandvol, E., Turkelli, N., and Barazangi, M., *Geophysical Research Letters,* Vol. **30**, No. 24, 8038, doi:10.1029/2003GL018912, 2003.

Faccenna, C., Bellier, O., Martinod, J., Piromallo, C., Regard, V., 2006. Slab detachment beneath eastern Anatolia: A possible cause for the formation of the North Anatolian fault. *Earth and Planetary Science Letters* **242**, p. 85– 97.

Faccenna, C., Mattei, M., Funiciello, R., Jolivet, L., 1997. Styles of back-arc extension in the central Mediterranean. *Terra Nova* **9**, 126–130.

Fah, D., Giardini, D., Bay, F., Bernardi, F., Braunmiller, J., Deichmann, N., Furrer, M., Gantner, L., Gisler, M., Isenegger, D., Jiminez, M.J., Kastli, P., Koglin, R., Masciardi, V., Rutz, M., Scheidegger, C., Schibler, R., Schorlemmer, D., Schwarz-Zanetti, G., Steimen, S., Sellami, S., Wiemer, S., and Wissner, J., 2003. Earthquake Catalogue of Switzerland (ECOS) and the related macroseismic database. *Eclogae Geol. Helv.* 96 (**2**), 219– 236.

Farhoudi, G., Karig, D.E., 1977. Makran of Iran and Pakistan as an active arc system. *Geology* **5**, 1089–1114.

Fink, J. H. 1980. Surface folding and viscosity of rhyolite flows. *Geology,* **8**, 250-254.

Fink, J. H. and Fletcher, R. C. 1978. Ropy pahoehoe: Surface folding of a viscous fluid. *Journal of Volcanology and Geothermal Research.* **4**, 151-170.

Fitch, T. J., 1972. Plate convergence, transcurrent faults and internal deformation adjacent to Southeast Asia and the Western Pacific. *Journal of Geophysical Research* **77**, 4432–4460 pp.

Frey Martinez, J., Cartwright, J., and Hall, B., 2005. 3D seismic interpretation of slump complexes: Examples from the continental margin of Israel: *Basin Research,* v. **71**, p. 83–108.

Fullsack, P., 1995. An arbitrary Lagrangian-Eulerian formulation for creeping flows and applications in tectonic models. *Geophys. J. Int.* **120**:1-23.

Furumura, T., and Kennett, B. L. N., 1997. On the nature of regional seismic phases-11. On the influence of structural barriers, *Geophys. J. Int.* **129**, 221-234.

Gabrielse, H., 1985. Major dextral transcurrent displacements along the northern Rock Mountain Trench and related lineaments in north-central British Columbia: *Geological Society of America Bulletin,* v. **96**, p. 1-14.

Galli, P., and Ferelli, L., 1995. A methodological approach for historical liquefaction research. In: Serva, L., Slemmons, D.B. (Eds.), *Perspectives in Paleoseismology,* Assoc. Eng. Geol., Spec. Publ., vol. **6**, pp. 35–48.

Gamond, J.F., and Odonne, F., 1984. Critéres d'identification des plis induits par un décroachment profond: modélisation analogique et données de terrain: *Bulletin de la Société Géologique de France,* v. **7,** p. 115-128.

Gapais, D., and Barbarin, B., 1986. Quartz fabric transition in a cooling syntectonic granite (Hermitage Massif, France): *Tectonophysics,* v. **125**, p. 357-370.

Garfunkel, Z., and Ron, H., 1985. Block rotation and deformation by strike-slip faults, 2: The properties of a type of macroscopic discontinuous deformation, *J. Geophys. Res.,* **90**, p. 8589-8602.

Gasperini, D., Blichert-Toft, J., Bosch, D., Del Moro, A., Macera, P., Albarede, F., 2002. Upwelling of deep mantle material through a plate window: evidence from the geochemistry of Italian basaltic volcanics. *J. Geophys Res.* **107** (B12), 2367, doi:10.1029/2001JB000418.

Gasperini, D., Maffei, K., Piromallo, C., Macera, P., Faccenna, C., Martin, S., Ranalli, G., 2003. Where is the tail of the European plume volcanism? In: *EGS-AGU-EUG Joint Assembly,* Nice, France, 6–11 April.

Gibson, S.A., Thompson, R.N., Leat, P.T., Dickin, A.P., Morrison, M.A., Hendry, G.L., Mitchell, J.G., 1992. Asthenosphere-derived magmatism in the Rio Grande rift, western USA: implications for continental break-up. In: Storey, B.C., Alabaster, T., Pankhurst, R.J. Eds., Magmatism and Causes of Continental Break-Up. *Geol. Soc. Spec. Publ.,* **68**, 61–89.

Glazner, A. F., and Bartley, J. M., 1985. Evolution of lithospheric strength after thrusting. *Geology* **13**, 42-5.

Goes, S., Spakman, W., Bijwaard, H., 1999. A lower mantle source for central European volcanism. *Science* **286**, 1928–1931.

Gök, R., Sandvol, E., Türkelli, N., Seber, D., and Barazangi, M., 2003. Sn attenuation in the Anatolian and Iranian plateau and surrounding regions. *Geophys. Res. Lett.* 30(**24**):8042. doi: 10.1029/ 2003GL018020

Gök, R., Türkelli, N., Sandvol E., Seber, D., and Barazangi, M., 2000. Regional wave propagation in Turkey and surrounding regions. *Geophys. Res. Lett.* **27**: 429–432.

Granet, M., Wilson, M., Achauer, U., 1995. Imaging a mantle plume beneath the Massif Central (France). *Earth Planet. Sci. Lett.* **136**, 281–296.

Grapes, R. H., Reid, D. L. and McPherson, J. 1972. Shallow dolerite intrusion and phreatic eruption in the Allen Hills region, Antarctica. *New Zealand Journal of Geology and Geophysics,* **17**, 563-577.

Griffiths, R. W. and Fink, J. H. 1992. Solidification and morphology of submarine lavas: A dependence on extrusion rate. *Journal of Geophysical Research,* **79**, 19 729-19 737.

Guest. J. E. and Sanchez, R. J. 1970. A large Dacitic Lava Flow in Northern Chile. *Bulletin of Volcanology,* 33(**3**), 778-790.

Guineberteau, B., Bouchez, J. L., and Vigneresse, J. L., 1987. The Mortagne granite pluton (France) emplaced by pull-apart along a shear zone: Structural and gravimetric arguments and regional implication: *Geological Society of America Bulletin,* v. **99**, p. 763-770.

Güleç, N., Hilton, D.R., Mutlu, H., 2002. Helium isotope variations in Turkey: relationship to tectonics, volcanism and recent seismic activities. *Chemical Geology* **187**, 129–142.

Gülen, L., 1984. Sr, Nd, Pb, isotope and trace element geochemistry of calc-alkaline and alkaline volcanics, eastern Turkey, *PhD Thesis.* Massachusetts Institute of Technology, USA, 232 pp., unpublished.

Hall, R., 1976. Ophiolite emplacement and the evolution of the Taurus suture zone, south-eastern Turkey. *Bull. Geol. Soc. Am.* **87**, 1078–1088.

Hampton, M. A., Lee, H. J., and Locat, J., 1996. Submarine landslides: *Reviews of Geophysics,* v. **34**, p. 33– 59.

Handy, M.R., 1989. Deformation regimes and the rheological evolution of fault zones in the lithosphere: the effects of pressure, temperature, grain size and time, *Tectonophysics*, **163**, 119-152.

Hanson. R. E. and Schweikert, R. A. 1982. Chilling and brecciation of a Devonian rhyolite sill intruded into wet sediments, Northern Sierra Nevada, California. *Journal of Geology,* **90**, 717-724.

Harangi, S., 2001. Neogene to Quaternary volcanism of the Carpathian-Pannonian Region-a review. *Acta Geologica Hungarica* 44 (**2–3**), 223–258.

Harangi, S., 2004. Origin of the common enriched mantle component in the Neogene volcanic rocks of the Mediterranean and the Carpathian-Pannonian region. In: *32nd International Geological Congress,* Florence, Italy, 20–28 August.

Harangi, S., Tonarini, S., Vaselli, O., Manetti, P., 2003. Geochemistry and petrogenesis of Early Cretaceous alkaline igneous rocks in Central Europe: implications for a long-lived EAR-type mantle component beneath Europe. *Acta Geologica Hungarica* **46**, 77–94.

Harding, T. P., 1974. Petroleum traps associated with wrench faults. *American Association of Petroleum Geologists Bulletin* **58**, 1290±1304 pp.

Harding, T. P., 1985. Seismic characteristics and identification of negative flower structures, positive flower structures and positive structural inversion. *American Association Petroleum Geology Bulletin* **69**, 582–600 pp.

Harding, T. P., 1988. Criteria and pitfalls in the identification of wrench faults with exploration data (abs.): *American Association of Petroleum Geologists Bulletin,* v. **72**, p. 193.

Harding, T. P., Vierbuchen, R .C., Christie-Blick, N., 1985. Structural styles, paleotectonic settings, and hydrocarbon traps of divergent (transtensional) wrench faults, in Biddle, K. T., and Christie-Blick, N., (eds.), Strike-slip deformation, basin formation, and sedimentation: *Society of Economic Paelontologists and Mineralogists Special Publication,* **37**, p. 51-77.

Harding, T.P., 1976. Tectonic significance and hydrocarbon trapping consequences of sequential folding synchronous with San Andreas faulting, San Joaquin Valley, California: *American Association of Petroleum Geologists Bulletin,* v. **60**, p. 356-378.

Harding, T.P., 1990. Identification of wrench faults using subsurface structural data: criteria and pitfalls: *American Association of Petroleum Geologists Bulletin*, v. **74**, p.1590-1609.

Harding, T.P., and Lowell, J.D., 1979. Structural styles, their plate tectonic habitats and hydrocarbon traps in petroleum provinces, *Bull. Am. Ass. Petrol. Geol.,* **69**, 582-600.

Harding, T.P., Gregory, R.F., Stephens, L.H., 1983. Convergent wrench fault and positive flower structure, Ardmore basin, Oklahoma: *American Association of Petroleum Geologists Studies in Geology series* 15, v. **3**., p. 4.2-13-4.2-17.

Harland, W. B., 1971. Tectonic transpression in Caledonian Spitzbergen. *Geological Magazine*, **108**, 27-42 pp.

Heiniö, P., and Davies, R. J., 2006. Degradation of Compressional Fold Belts: Deep-Water Niger Delta. doi:10.1306/11210505090. *AAPG Bulletin*, v. **90,** no. 5, pp. 753–770.

Hempton, M. R., Dunne, L.A., and Dewey, J. F., 1983. Sedimentation in a modern strike-slip basin, southeastern Turkey. *J. Geol.* **91**, p. 401-12.

Hempton, M.R., and Dewey, J.F., 1983. Earthquake-induced deformational structures in young lacustrine sediments, East Anatolian Fault, southeast Turkey. *Tectonophysics,* **98**, p. 7-14.

Hempton, M.R., and Dunne, L.A., 1984. Sedimentation of pull-apart basins: Active examples in eastern Turkey: *Journal of Geology,* v. **92**, p. 513-530.

Hempton, M.R., and Neher, K., 1985. Experimental fracture, strain and subsidence patterns over en echelon strike-slip faults: Implications for the structural evolution of pull-apart basins: *Journal of Structural Geology,* v. **8**, p. 597-605.

Hibsch, C., Alvarado, A., Yepes, H., Perez, V.H., and Sebrier, M., 1997. Holocene liquefaction and soft-sediment deformation in Quito (Ecuador): a paleoseismic history recorded in lacustrine sediments. *J. Geodyn.* **24**, 259– 280.

Hill, D.P., 1982. Contemporary block tectonics, California and Nevada: *Journal of Geophysical Research,* v. **87**, B7, p. 5433-5450.

Hodges, K.V., Wernicke, B.P., Walker, J.D., 1989. Middle Miocene (?) through Quaternary extension, northern Panamint Mountains area, California, in Wernicke, B.P.,Extensional tectonics in the Basin and Range province between the southern Sierra Nevada and the Colorado Plateau (28th IGCGuidebook T138): *American Geophysical Union,* Washington, p. 45-55.

Hoernle, K., Zhang, Y.S., Graham, D., 1995. Seismic and geochemical evidence for large-scale mantle upwelling beneath the eastern Atlantic and western and central Europe. *Nature* **374**, 34–39.

Hogan, J. P. and Gilbert, M. C., 1995. The A-type Mount Scott Granite Sheet: importance of crustal magma traps. *Journal of Geophysical Research* **100**, 15,779±15,793.

Hogan, J. P., Price J. D., and Gilbert M. C., 1998. Magma traps and driving pressure: consequences for pluton shape and emplacement in an extensional regime. *Journal of Structural Geology,* Vol. **20**, No. 9/10, pp. 1155-1168.

Holder, M. T., 1979. An emplacement mechanism for post-tectonic granites and its implications for their geochemical features. In: M.P. Atherton and J. Tarney (Editors), Origin of Granite Batholiths, *Geochemical Evidence.* Shiva, Orpington, Kent, pp. 116-128.

Holdsworth, R.E., Butler, C.A., and Roberts, A.M., 1997. The recognition of reactivation during continental deformation, *Jour. Geol. Soc.* London, **154**, p. 73-78.

Holdsworth, R.E., Strachan, R.A., Magloughlin, J., and Knipe, R.J., (eds.) 2001. The Nature and Significance of Fault Zone Weakening, *Geol. Soc. London Spec. Publ.,* **186**, 328 pp.

Horasan, G., and Boztepe-Güney, A., 2006. Observation and analysis of low-frequency crustal earthquakes in Lake Van and its vicinity, eastern Turkey. *J Seismol.* doi 10.1007/s10950-006-9022-2.

Houseman, G.A., McKenzie, D.P., Molnar, P., 1981. Convective instability of a thickened boundary layer and its relevance for the thermal evolution of continental convergent belts. *Journal of Geophysical Research,* v. **86**, 6115-6132.

Hsü, K.J., 1977. Studies of Ventura field, California, I: facies geometry and genesis of lower Pliocene turbidities: *American Association of Petroleum Geologists Bulletin,* v. **61**, p. 137-168.

Hsü, K.J., Kelts, K., Valentine, J.W., 1980. Resedimented facies in Ventura basin, California, and model of longitudinal transport of turbidity currents: *American Association of Petroleum Geologists Bulletin,* v. **64,** p. 1034-1051.

Hudson, T., and Plafker, G., 1982. Palaeogene metamorphism of an accretionary flysch terrane, eastern Gulf of Alaska. *Bull. Geol. Soc. Am.,* **93**, 1280-1290.

Huismans and Boutilier (in prep.). Active/Passive Rifting Gravitational Instabilities, Phd. project.

Huismans, R.S., and Beaumont, C., (in prep.). Asymmetric lithospheric extension: the role of frictional-plastic strain softening inferred from numerical experiments, *Geology* **3**.

Hutton, D. H. W., 1988. Granite emplacement mechanisms and tectonic controls: inferences from deformation studies. Transactions of the Royal Society of Edinburgh: *Earth Sciences* **79**, 245±255.

Ingram, G. M., Chisholm, T.J., Grant, C.J., Hedlund, C.A., Stuart- Smith, P., and Teasdale, J., 2004. Deepwater north west Borneo: Hydrocarbon accumulation in an active fold and thrust belt: *Marine and Petroleum Geology,* v. **21**, p. 879– 887.

Innocenti, F., Mazzuoli, R., Pasquare, G., Radicati di Brozolo, F., Villari, L., 1976. Evolution of volcanism in the area of interaction between the Arabian, Anatolian and Iranian plates-Lake Van, Eastern Turkey., *J., Volcanol. Geotherm. Res.* **1**, p. 103–112.

Innocenti, F., Mazzuoli, R., Pasquaré, G., Radicati di Brozolo, F., and Villari, L., 1982. Tertiary and Quaternary volcanism of the Erzurum-Kars area (Eastern Turkey): geochronological data and geodynamic evolution, *J. Volc. Geotherm. Res*., **13**, 223-240.

Jackson, N.J., 1986. Petrogenesis and evolution of Arabian felsic plutonic rocks. *Journal of African Earth Sciences* **4**, 47–59.

Jahn, B.M., Wu, F.Y., Chen, B., 2000a. Granitoids of the Central Asian Orogenic Belt and continental growth in the Phanerozoic. Transactions of the Royal Society of Ediburgh: *Earth Sciences* **91**, 181–193.

Jahn, B.M., Wu, F.Y., Chen, B., 2000b. Massive granitoid generation in Central Asia: Hd isotope evidence and implication for continental growth in the Phanerozoic. *Episodes* **23**, 82–92.

Jones, R. R., and Tanner, P. W. G., 1995. Strain partitioning in transpression zones. *Journal of Structural Geology* **17**, 793–802 pp.

Jung, S., and Hoernes, S., 2000. The major-and trace-element and isotope (Sr, Nd, O) geochemistry of Cenozoic alkaline rift-type volcanic rocks from the Rhon area (Central Germany): petrology, mantle source characteristics and implications for asthenosphere-lithosphere interactions. *J. Volcanol. Geotherm. Res.* **99**, 27–53.

Kadioglu, M., Sen, Z., Batur, E., 1997. The greatest soda-water lake in the world and how it is influenced by climatic change. *Annales Geophysicae* **15**, 1489–1497.

Karabıyıkoğlu, M., Litt, T., Örçen, S., Krastel, S., Kipper, R., 2007. Van Gölü Havzasının Geç Kuvaterner Çökelme Ortamları, Göl Seviyesi Oynamaları ve İklim Değişiklikleri. *TURQUA-Türkiye Kuvaterner Sempozyumu VI, 16-18 Mayıs 2007.*

Karakhanian, A., Djrbashian, R., Trifonov, V., Philip, H., Arakelian, S., Avagian, A., 2002. Holocene-historical volcanism and active faults as natural risk factors for Armenia and adjacent countries. *Journal of Volcanology and Geothermal Research* **113**, 319–344.

Karig, D. E., 1974. Evolution of arc systems in the western Pacific. *Annu. Rev. Earth Planet. Sci.,* **2**: 51-75.

Karig, D.E., 1980. Material transport within accretionary prisms and the "knocker" problem: *Journal of Geology,* v. **88**, p. 27-39.

Karner, G. D., and Dewey, J. F., 1986. Rifting: lithospheric versus crustal extension as applied to the Ridge Basin of Southern California. *Am. Mem. Assoc. Petrol. Geol.* **40**,317-38.

Kelts, K., Briegel, U., Ghilardi, K., Hsu, K., 1986. The limnogeology-ETH coring system. *Aquatic Sciences – Research Across Boundaries* **48**, 104–115.

Kempe, S., 1977. *Hydrographie, Warven-Chronologie und Organische Geochemie des Van Sees, Ost-Türkei. Mitteilungen* aus dem Geologisch-Paläontologischen Institut der Universität Hamburg, Heft **47**, 125–228.

Kempe, S., and Degens, E. T., 1978. Lake Van varve record: the past 10,420 years. In: Degens, E.T., Kurtman, F. (Eds.), Geology of Lake Van. *MTA Press,* Ankara, pp.56–63.

Kempe, S., Kazimierczak, J., Landmann, G., Konuk, T., Reimer, A., Lipp, A., 1991. Largest known microbialites discovered in Lake Van, Turkey. *Nature* **349**, 605–608.

Kennett, B. L. N. and Mykkeltveit, S., 1984. Guided wave propagation in laterally varying media-11. Lg-wave in north western Europe, *Geophys. J. R. Astr. Soc.,* **79**, 257-261.

Kennett, B. L. N., 1986. Lg waves and structural boundaries, *Bull. seism. Soc. Am.,* **76**, 1133-1141.

Kennett, B. L. N., Gregersen, S., Mykkeltveit, S. and Newmark, R., 1985. Mapping of crustal heterogeneity in the North Sea basin via the propagation of Lg-waves, *Geophys. J. R. Astr. Soc.,* **83**, 299-306.

Keskin, M., 2003. Magma generation by slab steepening and breakoff beneath a subduction–accretion complex: an alternative model for collision-related volcanism in Eastern Anatolia, Turkey. *Geophys Res Lett* 30 (**24**):8046 doi:10.1029/2003GL018019

Keskin, M., 2007. Eastern Anatolia: a hotspot in a collision zone without a mantle plume. *Geological Society of America Special Paper* **430**, 693–722.

Keskin, M., Pearce, J. A., Mitchell, J. G., 1998. Volcano-stratigraphy and geochemistry of collision-related volcanism on the Erzurum–Kars Plateau, North Eastern Turkey. *Journal of Volcanology and Geothermal Research* **85**, 355–404.

Keskin, M., Pearce, J.A., Kempton, P.D., Greenwood, P., 2006. Magma–crust interactions and magma plumbing in a post-collision setting: geochemical evidence from the Erzurum–Kars Volcanic Plateau, Eastern Turkey. In: Dilek, Y., Pavlides, S. (Eds.), *Postcollisional Tectonics and Magmatism in the Mediterranean Region and Asia.* Geological Society of America Special Paper, vol. **409,** pp. 475–505.

Kipfer, R., Aeschbach-Hertig, W., Baur, H., Hofer, M., Imboden, D. M., Signer, P., 1994. Injection of mantle type Helium into Lake Van (Turkey). The clue for quantifying deep water renewal. *Earth and Planetary Science Letters* **125**, 357–370.

Kipfer, R., Aeschbach-Hertig, W., Hofer, M., Imboden, D. M., and Baur, H., 1993. Helium and CO_2 fluxes from the Earth mantle in Laacher See, Germany, *Annal. Geophys.* **11**, C 236.

Kirby, S. H., 1985. Rock mechanics observations pertinent to the rheology of the continental lithosphere and to the localization of strain along shear zones. *Tectonophysics* **119**, 1±27.

Koçyiğit, A., 1985. Muratbağı–Balabantaş (Horasan) arasında Çobandede fay kuşağının jeo-tektonik özellikleri ve Horasan-Narman depremi yüzeykırıkları. Cumhuriyet Üniversitesi Mühendislik Fakültesi *Yer Bilimleri Dergisi* **2**, 17–33.

Koçyiğit, A., Yılmaz, A., Adamia, S., and Kuloshvili, S., 2001. Neotectonics of East Anatolian Plateau (Turkey) and lesser Caucasus: implications for transition from thrusting to strike-slip faulting. *Geodinamica Acta* **14**, 177–195.

Kokelaar, B. P. 1982. Fluidization of wet sediments during the emplacement and cooling of various igneous bodies. *Journal of the Geological Society of London,* **139**, 21-33.

Korme, T, Chorowicz, J, Collet, B, and Bonavia, F. F., 1997. Volcanic vents rooted on extension fractures and their geodynamic implications in the Ethiopian Rift. *J. Volcanol. Geotherm. Res.* **79**: 205–222.

Köse, O., 2006. Personal Communication.

Koyi, H., 1988. Experimental modeling of role of gravity and lateral shortening in Zagros mountain belt. *Bulletin of the American Association of Petroleum Geologists* **72**, 1381±1394.

Krohe, A., 1996. Variscan tectonics of central Europe: Postaccretionary intraplate deformation of weak continental lithosphere: *Tectonics,* v. **15**, p. 1364-1388.

Kurchavov, A.M., 1983. An analysis of the magmatism of the Central Kazakhstan Fault System. *Geotectonics* **17**, 62–69.

Kurchavov, A.M., Yarmolyuk, V.V., 1984. Distribution of Permian continental volcanics in Central Asia and its tectonic interpretation. *Geotectonics* **18**, 344–354.

Kurtman, F., and Baskan, E., 1978. Mineral and thermal waters in the vicinity of Lake Van. In: Degens ET, Kurtman F (eds) The geology of the Lake *Van. Miner. Res. Explor. Inst.* (Ankara) **169**:50–55

Kusznir, N. J., and Bott, M. H. P., 1977. Stress concentration in the upper lithosphere caused by underlying visco-elastic creep. *Tectonophys.* **43**, 247-56 pp.

Kuzucuoğlu, C., Karabiyikoglu, M., Dogu, A. F., Christol, A., Fort, M., Akköprü, E., Mouralis, D., Brunstein, D., Zorer, H., and Fontugne, M., 2007. Evidences of High Magnitude Low and High Stands of Van Lake Level. A contribution to identifying climate forcing, recent tectonic impact and relationships to volcanic activity during Upper Pleistocene. *TURQUA-Türkiye Kuvaterner Sempozyumu VI,* 16-18 Mayıs 2007.

La Fontaine, C.V., Bryson, R.A., Wendland, W.M., 1990. Airstream regions of North Africa and the Mediterranean. *Journal of Climate* **3**, 366–372.

Lamy, F., Arz, H.W., Bond, G.C., Bahr, A., Patzold, J., 2006. Multi centennial-scale hydrological changes in the Black Sea and northern Red Sea during the Holocene and the Arctic/North Atlantic Oscillation. *Paleooceanography* **21**, 1008–1019.

Landmann, G., and Reimer, A., 1996. Climatically induced lake level changes at Lake Van, Turkey during the Pleistocene/Holocene transition. *Global Biochemical Cycles* **10**, 797–808.

Landmann, G., Reimer, A., Kempe, S., 1996a. Climatically induced lake level changes at Lake Van, Turkey, during the Pleistocene/Holocene transition. *Global Biochemical Cycles* **10**, 797–808.

Landmann, G., Reimer, A., Lemcke, G., Kempe, S., 1996b. Dating Late Glacial abrupt climate changes in the 14,570 yr long continuous varve record of Lake Van, Turkey. *Palaeogeography, Palaeoclimatology, Palaeoecology* **122**, 107–118.

Lastras, G., Canals, M., Urgeles, R., Hughes-Clarke, J. E., and Acosta, J., 2004. Shallow slides and pockmark swarms in the Eivissa Channel, western Mediterranean Sea: *Sedimentology,* v. **51**, p. 837– 850.

Le Pichon, X., Henry, P., Goffé, B., 1997. Uplift of Tibet: from eclogites to granulites-implications for the Andean Plateau and the Variscan belt. *Tectonophysics* **273**, 57-76.

Lemcke, G., 1996. *Palaoklimarekonstruktion am Van See (Ostanatolien, Türkei)*. Diss. ETH Zurich, Nr. **11786**, 182 pp.

Lemcke, G., Sturm, M., 1997. $d^{18}O$ and trace element measurements as proxy for the reconstruction of climate changes at Lake Van (Turkey): preliminary results. *NATO ASI Series* **149**, 653–678.

Lemiszki, P.J., and Brown, L.D., 1988. Variable crustal structure of strike-slip fault zones as observed on deep seismic reflection profiles: *Geological Society of America Bulletin,* v. **100**, p. 665-676.

Link, M.H., 1982. Provenance, paleocurrents, and paleogeography of Ridge basin, southern California, in Crowell, J.C., Link, M.H., (eds.), Geologic history of Ridge basin, southern California: Pacific Section, *Society of Economic Paleontologists and Mineralogists,* Los Angeles, p. 265-276.

Litt, T., Krastel, S., Sturm, M., Kipfer, R., Örcen, S., Heumann, G., Franz, S. O., Ülgen, U.B., and Niessen, F., 2009. 'PALEOVAN', International Continental Scientific Drilling Program (ICDP): site survey results and perspectives. *Quaternary Science Reviews* **28**, 1555–1567.

Luyendyk, B.P., and Hornafius, J.S., 1987. Neogene crustal rotations, fault slip, and basin development in southern California, in Ingersoll R.V., Ernst, W.G., (eds.), *Cenozoic basin development of coastal California (Rubey Volume VI)*: Prentice-Hall, Englewood Cliffs, p. 259-283.

Luyendyk, B.P., Kamerling, M. J., and Terres, R., 1980. Geometrical model for Neogene crustal reactions in southern California. *Bull. geol. Soc. Am.* **91**, p. 211-8.

Lynn, H.B., Hale, L.D., and Thompson, G.A., 1981. Seismic reflections from the basal contacts of batholiths. *J. geophys. Res*. **86**, p. 10633-8.

Macera, P., Gasperini, D., Piromallo, C., Blichert-Toft, J., Bosch, D., Del Moro, A., Martin, S., 2003a. Geodynamic implications of deep mantle upwelling in the source of Tertiary volcanics from the Veneto region (South-Eastern Alps). *J. Geodyn.* **36**, 563–590.

Macera, P., Gasperini, D., Piromallo, C., Funiciello, F., Faccenna, C., Ranalli, G., 2004. Recent hot spot volcanism in the European and Mediterranean area. In: *32nd International Geological Congress,* Florence, Italy, 20–28 August.

Macera, P., Gasperini, D., Ranalli, G., and Mahatsente, R., 2008. Slab detachment and mantle plume upwelling in subduction zones: An example from the Italian South-Eastern Alps. *Journal of Geodynamics* **45**, p. 32–48.

Maggi, A., and Priestley, K., 2005. Surface waveform tomography of the Turkish-Iranian plateau: *Geophysical Journal International,* v. **160,** no. 3, p. 1068–1080.

Mahon, K. I., Harrison, T. M. and Drew, D. A., 1988. Ascent of a granitoid diapir in a temperature varying medium. *J. Geophys. Res.*, **93**: 1174-1188.

Malamud, B.D., Turcotte, D.L., 1999. How many plumes are there? *Earth Planet. Sci. Lett.* **174**, 113–124.

Mann, P., Draper, G., and Burke, K., 1985. Neotectonics of a strike-slip restraining bend system, Jamaica. In: Biddle, K. T., Christie-Blick, N. (Eds.). *Strike-slip Deformation, Basin Formation, and Sedimentation,* 37. Society of Economic Paleontologists and Mineralogists Special Publication, pp. 211±226.

Mann, P., Hempton, M.R., Bradley, D.C., Burke, K., 1983. Development of pull-apart basins*: Journal of Geology,* v. **91,** p. 529-554.

Marco, S., Stein, M., and Agnon, A., 1996. Long term earthquake clustering: a 50,000-year paleoseismic record in the Dead Sea Graben. *J. Geophys. Res.* **101**, 6179– 6191.

Marsh, B. D., 1982. On the mechanics of igneous diapirism, stoping, and zone melting. *Am. J. Sci.,* **282**: 808-855.

Mascle, A., Biju-Duval, B., Letouzey, J., Montadert, L., and Ralenne, C., 1977. Sediments and their deformations in active margins of different geologic settings. In: *Geodynamics in southwest Pacific, Editions Technip, Paris,* pp. 327-344.

Massonne, H, J., 2005. Involvement of Crustal Material in Delamination of the Lithosphere after Continent-Continent Collision, *International Geology Review*, Vol. **47**, 2005, p. 792–804.

Matte, P., and Burg, J. P., 1981. Sutures, thrusts and nappes in the Variscan Arc of western Europe: Plate tectonic implications, *in* McClay, K. R., and Price, N. J., eds., Thrust and nappe tectonics: *Geological Society of London Special Publications,* v. **9**, p. 353-358.

Maupin, V., 1989. Numerical modelling of Lg wave propagation across the North Sea Central Graben, *Geophys. J. Int.,* **99**, 273-283.

May, S.R., Ehman, K.D., Gray, G.G., and Crowell, J.C., 1993. A new angle on the tectonic evolution of the Ridge basin, a "strike-slip" basin in southern California: *Geological Society of America Bulletin,* v. **105**, p.1357-1372.

McKenna, L.W., Walker, J.D., 1990. Geochemistry of crustally derived leucocratic igneous rocks from the Ulugh Muztagh area, northern Tibet and their implications for the formation of the Tibetan Plateau. *Journal of Geophysical Research* **95**, 21,483–21,502.

McKenzie, D. P., and Jackson, J. A., 1983. The relationship between strain rates, crustal thickening, palaeomagnetism, finite strain and fault movements within a deforming zone. *Earth planet. Sci. Lett.* **65**, 182-202.

McKenzie, D.P., 1972. Active tectonics of the Mediterranean region: *Geophys. J.R. Asr., Soc.,* **30**, 109-185.

McKenzie, D.P., 1984. A possible mechanism for epeirogenic uplift. *Nature,* **307**, 616-618.

McLaughlin, R.J., and Nilsen, T.H., 1982. Neogene non-marine sedimentation and tectonics in small pull-apart basins of the San Andreas fault system, Sonoma County, California: *Sedimentology,* v. **29**, p. 865-876.

McPhie, J., 1993. The Tennant Creek porphyry revisited: a synsedimentary sill with peperite margins, Early Proterozoic, North Territory. *Australian Journal of Earth Sciences,* **40**, 545-558.

Meissner, R., and Strehlau, J., 1982. Limits of stresses in continental crusts and their relation to the depth frequency distribution of shallow earthquakes. *Tectonics,* **1**, 73-89.

Mello, U. T., and Pratson, L. F., 1999. Regional slope stability and slope-failure mechanics from the two-dimensional state of stress in an infinite slope: *Marine Geology,* v. **154,** p. 339– 356.

Michael, A. J., 1990. Energy constraints on kinematic models of oblique faulting: Loma Prieta versus Parkfield-Coalinga. *Geophysical Research Letters* **17**, 1453–1456 pp.

Michard-Vitrac, A., Albarede, F., Dupuis, C., and Taylor, H. P., 1980. The genesis of Variscan plutonic rocks-Inferences from Sr, Pb and U studies on the Maladeta Igneous Complex, central Pyrenees, Spain: *Contributions in Mineralogy and Petrology,* v. **72**, p. 57-72.

Miller, C. E, Watson, M. E. and Harrison, T. M., 1988. Perspectives on the source, segregation and transport of granitoid magmas. *Trans. R. Soc. Edinburgh, Earth Sci*., **79**: 135-156.

Molnar, P., 1992. Brace-Goetze strength profiles, the partitioning of strike-slip and thrust faulting at zones of oblique convergence, and the stressheat flow paradox of the San Andreas Fault. In: Evans, B., Wong, T.-F. (Eds.), *Fault Mechanics and Transport Properties of Rocks,* Academic Press, London, pp. 435–459.

Molnar, P., England, P., Martinod, J., 1993. Mantle dynamics, uplift of the Tibetan Plateau, and the Indian monsoon. *Reviews of Geophysics* **31**, 357-396.

Monecke, K., Anselmetti, F.S., Becker, A., Sturm, M., and Giardini, D., 2004. The record of historic earthquakes in lake sediments of Central Switzerland. *Tectonophysics* **394**, 21–40.

Moody, J.D., 1973. Petroleum exploration aspects of wrench-fault tectonics: *American Association of Petroleum Geologists Bulletin,* v. **57**, p. 449-476.

Moretti, M., Alfaro, P., Caselles, O., and Canas, J. A., 1999. Modelling seismites with a digital shaking table. *Tectonophysics* **304**, 369– 383.

Mount, V.S., and Suppe, J., 1987. State of stress near the San Andreas fault: implications for wrench tectonics. *Geology* **15**, 1143-1146.

MTA., General Directorate of Mineral Research and Exploration-GDMRE., 1999. Geophysics studies has been done by the Aerial Geophysics Unit and prepared for publishing by the management of Geophysics department's Gravity and Magnetic Unit of General Directorate of Mineral Research and Exploration, *MTA press,* Ankara-Turkey.

Nakamura, K., 1977. Volcanoes as possible indicators of tectonic stress orientation-principle and proposal. *J. Volcanol. Geotherm. Res.* **2**, 1–16.

Nakashima, Y., 1993. Static stability and propagation of a fluid-filled edge crack in rock; implication for fluid transport in magmatism and metamorphism. *Journal of Physics of the Earth* **41,** 189±202.

Naylor, M. A., Mandl, G., and Sijpesteijn, C. H. K., 1986. Fault geometries in basement-induced wrench faulting under different initial stress states. *Journal of Structural Geology* **8**, 737–752 pp.

Nelson, K.D., Zhao, W.J., Brown, L.D., Kuo, J., Che, J.K., Liu, X.W., Klemperer, S.L.,Makovsky, Y., Meissner, R., Mechie, J., Kind, R.,Wenzel, F., Ni, J., Nabelek, J., Chen, L.H., Tan, H.D., Wei, W.B., Jones, A.G., Booker, J., Unsworth, M., Kidd, W.S.F., Hauck, M., Alsdorf, D., Ross, A., Cogan, M., Wu, C.D., Sandvol, E., Edwards, M., 1996. Partially molten middle crust beneath southern Tibet: synthesis of project INDEPTH results. *Science* **274,**1684-1688.

Nelson, M. R., 1988. Constraints on the seismic velocity structure of the crust and upper mantle beneath the eastern Tien Shan, Central Asia, *PhD Thesis,* MIT, Cambridge, MA.

Nemec, W., 1990. Aspect of sediment movement on steep delta slopes, in A. Colella and D. B. Prior, eds., Coarse-grained deltas: *International Association of Sedimentologists Special Publication* **10**, p. 29–73.

Nicholson, C., Seeber, L., Williams, P., and Sykes, L.R., 1986. Seismic evidence for conjugate slip and block rotation within the San Andreas fault system, southern California: *Tectonics,* v. **5**, p. 629-648.

Nigro, F., and Renda, P., 2004. Growth pattern of underlithified strata during thrust-related folding: *Journal of Structural Geology,* v. **26**, p. 1913–1930.

Nilsen, T. H., and Sylvester, A.G., 1995. Strike- slip basins. In: *Tectonics of Sedimentary Basins* (Ed. by C.J. Busby and R.V. Ingersoll), pp. 425-457. Blackwell Scientific Publications, Oxford.

Nilsen, T.H., and McLaughlin, R.J., 1985. Comparison of tectonic framework and depositional patterns of the Hornelen strike-slip basin of Norway and the Ridge and Little Sulphur Creek strike-slip basins of California: *Society of Economic Paleontologists and Mineralogists Special Publication* **37**, p. 79-103.

Notsu, K., Fujitoni, T., Ui, T., Matsuda, J., Ercan, T., 1995. Geochemical features of collision related volcanic rocks in central and Eastern Anatolia, Turkey. *Journal of Volcanology and Geothermal Research* **64**, 171-192.

Obermeier, S. F., 1996. Use of liquefaction-induced features for paleoseismic analysis—an overview of how seismic liquefaction features can be distinguished from other features and how their regional distribution and properties of source sediment can be used to infer the location and strength of Holocene paleoearthquakes. *Eng. Geol.* **44**, 1 – 76.

Oxburg, E.R., 1972. Flake tectonics and continental collision: *Nature,* v. **239**, p. 202-204.

Örgülü, G., Aktar, M., Türkelli, N., Sandvol, E., and Barazangi, M., 2003. Contribution to the seismotectonic of eastern Turkey from moderate and small size events. *Geophys Res Lett* 30(**24**):8040 doi:10.1029/2003GL018258

Özdemir, Y., Karoğlu, Ö., Tolluoğlu, A.Ü., Güleç, N., 2006. Volcanostratigraphy and petrogenesis of the Nemrut stratovolcano (East Anatolian High Plateau): The most recent post-collisional volcanism in Turkey. *Chemical Geology* **226**, 189-211.

Özgül, N., Seymen, İ., and Arpat, E., 1983. 30 Ekim 1983 Horasan-Narman Depreminin makrosismik ve tektonik özellikleri: *Yeryuvari ve İnsan,* v. **8**, p. 21-25.

Patchett, P.J., 1980. Thermal effect of basalt on continental crust and crustal contamination of magmas. *Nature,* **283,** 559-561.

Paterson, S, R., and Miller, R.B., 1998. Mid-crustal magmatic sheets in the Cascades Mountains, Washington: implications for magma ascent. *Journal of Structural Geology,* Vol. **20**, No. 9/10, pp. 1345 to 1363, 1998.

Paterson, S. R. and Fowler, K., Jr 1993 Extensional pluton emplacement models: Do they work for the large plutonic complexes?. *Geology* **21**, 781±784.

Paterson, S. R. and Vernon, R. H., 1995. Bursting the bubble of ballooning plutons: a return to nested diapirs emplaced by multiple processes. *Geol. Soc. Am. Bull.,* **107**: 1356-1380.

Pavoni, N., 1961b. Faltung durch Horizontalverschiebung. *Eclog. geol. Helv.* **54**, 515-34.

Pearce, J. A., Bender, J. F., De Long, S. E., Kidd, W. S. F., Low, P. J., Güner, Y., Saroglu, F., Yilmaz, Y., Moorbath, S., Mitchell, J. G., 1990. Genesis of collision volcanism in Eastern Anatolia, Turkey. *Journal of Volcanology and Geothermal Research* **44**, 189–229.

Pearce, J.A., Houjun, M., 1988. Volcanic rocks. Tibet Geotraverse, Lhasa to Golmud. *Philos. Trans. R. Soc. London* **327**, 165–168.

Pearce, J.A., Mei, H.J., 1988. Volcanic rocks of the 1985 Tibet Geotraverse: Lhasa to Golmud. P*hilosophical Transactions of the Royal Society of London* A **327**, 169–201.

Pearce, J.A., Wanming, D., Oliver, R.A., Coulon, C., Kyser, K., 1989. Geochemistry and tectonic significance of post-collision volcanism in Tibet. *Terra Abstracts* 1r1:**175**.

Pınar, A., Honkura, Y., Kuge, K., Matsushima, M., Sezgin, N., Yılmazer, M., and Öğütçü, Z., 2007. Source mechanism of the 2000 November 15 Lake Van earthquake (*Mw = 5.6*) in eastern Turkey and its seismotectonic implications. *Geophys. J. Int.,* v. **170**, 749–763.

Piromallo, C., Morelli, A., 2003. P wave tomography of the mantle under the Alpine-Mediterranean area. *Journal of Geophysical Research* **108** (B2), 2065. doi:10.1029/ 2002JB001757.

Planke, S., Alvestad, E. and Eldholm, O. 1999. Seismic characteristics of basaltic extrusive and intrusive rocks. *The Leading Edge,* March, 342-348.

Planke, S., Symonds, P. A., Alvestad, E. and Skogseid, J., 2000. Seismic volcanostratigraphy of large-volume basaltic extrusive omplexes on rifted margins. *Journal of Geophysical research-Solid Earth,* **105** (B8), 19 335-19 35.

Platt, J. P., and England, P., 1994. Convective removal of lithosphere beneath mountain belts: thermal and mechanical consequences: *American Journal of Science,* v. **294,** p. 307-336.

Pollard, D.D., and Aydin, A., 1984. Propagation and linkage of oceanic ridge segments. *J. Geophys. Res.* **89**, 10017-10028.

Pollard, O. D., Müller, O. H. and Dockstader, O. R., 1975. The form and growth of fingered sheet intrusions. *Geological Society of America, Bulletin,* **86**, 351-363.

Prior, D. B., and Coleman, J. M., 1982. Active slides and flows in underconsolidated marine sediments on the slopes of the Mississippi delta, in S. Saxov and J. K. Nieuwenhuis, eds., *Marine slides and other mass movements:* New York, Plenum Press, p. 21–49.

Pysklywec, R. N., and Beaumont, C., 2004. Intraplate tectonics: feedback between radioactive thermal weakening and crustal deformation driven by mantle lithosphere instabilities. *Earth and Planetary Science Letters* **221,** p. 275-292.

Rajlich, P., 1990. Variscan shearing tectonics in the Bohemian massif: *Mineralia Slovaka,* v. **22**, p. 33-40.

Reading, H.G., 1980. Characteristics and recognition of strike-slip fault systems. In: *Sedimentation in Oblique-slip Mobile Zones* (edited by Balance, P.F., and Reading, H.G.). Spec. Publs. Int. Ass. Sediment. **4**, 7-26.

Rebai, S., Philip, H., Dorbath, L., Borisseff, B., Hacissler, H., Cisternas, A., 1993. Active tectonics in the Lesser Caucasus: coexistence of compressive and extensional structures, *Tectonics* **12**, p. 1089-1114.

Regard, V., Bellier, O., Martinod, J., Faccenna, C., 2005. Analogue Experiments of Subduction vs. Collision Processes: Insight for the Iranian Tectonics, *JSEE:* Fall, vol. **7**, No. 3.

Regard, V., Bellier, O., Thomas, J.C., Abbassi, M.R., Mercier, J., Shabanian, E., Fegghi, K., and Soleymani, S., 2004. "The Accommodation of Arabia-Eurasia Convergence in the Zagros-Makran Transfer Zone, SE Iran: A Transition between Collision and Subduction through a Young Deforming System", *Tectonics*, **23**, p. TC4007, doi:10.1029/2003TC001599.

Regard, V., Faccenna, C., Martinod, J., Bellier, O., and Thomas, J. C., 2003. "From Subduction to Collision: Control of Deep Processes on the Evolution of Convergent Plate Boundary", *J. Geophys. Res.,* **108**, 2208, doi:10.1029/2002JB001943.

Rickard, M.J., 1984. Pluton spacing and the thickness of crustal layers in Baja California. *Tectonophysics,* **101**, 167-172.

Rickard, M.J., and Ward, P., 1981. Palaeozoic crustal thickness in the southern part of the Lachlan orogen deduced from volcano and pluton-spacing geometry. *J. Geol. Soc. Aust.,* **28**, 19-32.

Ringrose, P. S., 1989. Paleoseismic (?) liquefaction event in late Quaternary lake sediment at Glen Roy, Scotland. *Terra Nova* **1**, 57– 62.

Ritter, J.R.R., Jordan, M., Christensen, U.R., Achauer, U., 2001. A mantle plume below the Eifel volcanic fields, Germany. *Earth Planet. Sci. Lett.* **186**, 7–14.

Roberts, N., and Wright, H.E., 1993. Vegetational, lake-level, and climatic history of the Near East and Southwest Asia. In: Wright, H.E., Kutzbach, J.E., Webb III, T., Ruddiman,W.F., Street-Perrot, F.A., Bartlein, P.J. (Eds.), *Global Climates Since the Last Glacial Maximum,* pp. 194–220.

Roberts, S., and Jackson, J. A., 1991. Active normal faulting in central Greece: An overview, in *The Geometry of Normal Faults,* Spec. Publ. Geol. Soc. Lond., **56,** p. 125-142, Eds. Roberts, A.M., Yielding, G. and Freeman, B., Blackwell Scientific Publications,Oxford.

Rodgers, D.A., 1980. Analysis of pull-apart basin development produced by en echelon strike-slip faults: *International Association of Sedimentology Special Publication* **4**, p. 27-41.

Rodriguez Pascua, M. A., Calvo, J. P., De Vicente, G., and Gomez-Gras, D., 2000. Soft-sediment deformation structures interpreted as seismites in lacustrine sediments of the Prebetic Zone, SE Spain, and their potential use as indicators of earthquake magnitudes during the late Miocene. *Sediment. Geol.* **135**, 117–135.

Rodriguez Pascua, M. A., De Vicente, G., Calvo, J. P., and Perez-Lopez, R., 2003. Similarities between recent seismic activity and paleoseismites during the Late Miocene in the external Betic Chain (Spain): relationship by dbT value and the fractal dimension. *J. Struct. Geol.* **25,** 749– 763.

Roeder, D., 1979. Continental collisions. *Rev. Geophys. Space Phys.* **17**, 1098-109.

Ron, H., Freund, R., Garfunkel, Z., and Nur, A., 1984. Block rotation by strike-slip faulting: structural and paleomagnetic evidence. *J. Geophys. Res.* **89**, p. 6256-6270.

Rönnlund P., 1987. Diapiric Walls, Initial Edge E.ects and Lateral Boundaries. *UUDNMP Research Report* **45**.

Rosembaum, J.M., Wilson, M., Downes, H., 1997. Multiple enrichment of the Carpathian-Pannonian mantle: Pb–Sr–Nd isotope and trace element constraints. *J. Geophys. Res.* **102**, 14947–14961.

Royden, L.H., 1985. The Vienna basin: a thin-skinned pull-apart basin: *Society of Economic Paleontologists and Mineralogists Special Publication* **37**, p. 319-338.

Ryder, R.T., and Thomson, A., 1989. Tectonically controlled fan delta and submarine fan sedimentation of late Miocene age, southern Temblor Range, California: *United States Geological Survey Professional Paper* **1442**, 59 p.

Sandford, A.R., 1959. Analytical and experimental study of simple geologic structures: *Geological Society of America Bulletin,* v. **70**, p. 19-62.

Sandvol, E., Türkelli, N., Zor, E., Gök, R., Bekler, T., Gürbüz, C., Seber, D., and Barazangi, M., 2003. Shear wave splitting in a young continent–continent collision: an example from Eastern Turkey. *Geophys Res Lett* 30(**24**):8041 doi:10.1029/2003GL017390.

Sandvol, R., (in prep). Rayleigh wave tomography of Eastern Turkey. *Geophys Res Lett* 35 (**29**).

Şaroğlu, F., 1985, Doğu Anadolu'nun Neotektonik Dönemde Jeolojik ve Yapısal Evrimi: *Unpublished Doctoral Dissertation,* İstanbul Üniversitesi, Fen Bilimleri Enstitüsü, Jeoloji Mühendisliği Ana Bilim Dalı, 240 pp. + 7 folded plates in back pocket.

Şaroğlu, F., 2007. Personal Communication.

Şaroğlu, F., and Güner, Y., 1981. Doğu Anadolu'nun jeomorfolojik gelişimine etki eden öğeler: jeomorfoloji, tektonik, volkanizma ilişkileri. *Türkiye Jeoloji Kurumu bülteni* **24,** 39–50.

Şaroğlu, F., and Yılmaz, Y., 1986. Geological evolution and basinmodels during neotectonic episode in the eastern Anatolia. *Bulletin of the Mineral Research and Exploration* **107**, 61–83.

Şaroğlu, F., and Yılmaz, Y., 1987. Geological evolution in neotectonic episode in the eastern Anatolia. *Bulletin of the Mineral Research and Exploration* **107**, 84–90.

Şaroğlu, F., Yılmaz, Y., Güner, Y., 1984. Nemrut yanardağının jeolojisi, jeomorfolojisi ve volkanizmasının evrimi: *Jeomorfoloji Bull.,* **12,** 23-65.

Schandelmeier, H., Reynolds, P.O., Semtner, A.K. (Eds.), 1997. Palaeogeographic-Palaeotectonic *Atlas of North-Eastern Africa, Arabia, and Adjacent Areas–Late Proterozoic to Holocene,* Explanatory Notes (XIX + 160 pp.) + 17 + 1 plates in a separate volume.

Schminke, H. W. 1967. Fused tuff and peperites in South-Central Washington. *Bulletin of the Geological Society of America,* **78**, 319-330.

Schnellmann, M., F. S. Anselmetti, D. Giardini, and McKenzie, J. A., 2005. Mass movement-induced fold-and-thrust belt structures in unconsolidated sediments in Lake Lucerne (Switzerland): *Sedimentology,* v. **52**, p. 271–289.

Scholz, C.H., 2000. Evidence for a strong San Andreas fault, *Geology*, **28**, 163-166.

Schulmann, K., Ledru, P., Autran, A., Melka, R., Lardeaux, J. M., Urban, M., and Lobkowicz, M., 1991. Evolution of nappes in the eastern margin of the Bohemian Massif: A kinematic interpretation: *Geologische Rundschau,* v. **80**, p. 73-92.

Schweizer, G., 1975. Untersuchungen zur Physiogeographie von Ostanatolien und Nordwestiran. Geomorphologische, klima- und hydrogeographische Studien im Van See-und Rezaiyehsee-Gebiet. *Tübinger Geographische Studien* 60 (**9**).

Seeber, L., and Nicholson, C., 1986. Block/fault rotation in geologic and interseismic deformation, *in Natural Earthquake Prediction Council Special Report 1:* Workshop on Special Study Areas in Southern California, edited by Shearer, C., U.S. Geol. Surv. Open File Rep.

Sengör, A. M. C, Özeren, S, Genç¸ T, and Zor, E., 2003. East Anatolian high plateau as a mantle-supported, north-south shortened domal structure. *Geophys Res Lett* 30(**24**):8045 doi:10.1029/2003GL017858

Sengör, A. M. C., 1976. Collision of irregular continental margins: implications for foreland deformation of Alpine-type orogens. *Geology,* **4**, 779-82.

Sengör, A. M. C., 1979. North Anatolian Fault: its age offset and tectonic significance. *J. geol. Soc. London,* **136**, 269-282.

Şengör, A. M. C., 1982. Outlines of Tethyan evolution in the Tibetan/Himalayan segment of the Eurasiatic Alpides. *Abstr. of the Symp. on Qinhai-Xizang (Tibet) Plateau, Beijing,*

Sengör, A. M. C., 1984. The Cimmeride Orogenic System and the tectonics of Eurasia. *Geol. Soc. Amer. Spec. Pap.* **195**, 82 pp.

Şengör, A. M. C., 2010. Personal Communication.

Şengör, A. M. C., and Kidd, W. S. F., 1979. The post-collisional tectonics of the Turkish-Iranian Plateau and a comparison with Tibet. *Tectonophysics* **55**, 361–376.

Sengör, A. M. C., and Yılmaz, Y., 1981. Tethyan evolution of Turkey: a plate tectonic approach. *Tectonophysics* **75**: 181–241 pp.

Sengör, A. M. C., Görür N, and Saroğlu F., 1985. Strike-slip faulting and related basin formation in zones of tectonic escape: Turkey as a case study. In: Biddle K T, Christie-BlickN (eds) Strike-slip deformation, basin formation and sedimentation. *Soc Econ Paleont Min Spec Publ* **37**: 227–264 (in honor of Crowell JC).

Şengör, A. M. C., Özeren, M. S., Keskin, M., Sakınç, M., Özbakır, A. D., and Kayan, İ, 2008. Eastern Turkish high plateau as a small Turkic-type orogen: Implications for post-collisional crust-forming processes in Turkic-type orogens. *Earth-Science Reviews,* Earth-01531; No of Pages **48.** journal homepage: www.elsevier.com/ locate/earscirev.

Şengör, A.M.C., 1980. Türkiye'nin neotektoniğinin esasları: *TJK Pub.*

Şengör, A.M.C., 1990b. Plate tectonics and orogenic research after 25 years: a Tethyan perspective. *Earth Science Reviews* **27**, 1–201.

Sengör, A.M.C., 2006. Tectonics of the Turkish-Iranian High Plateau: Lake Van Drilling Project (ICDP), *PaleoVan Workshop in Van*, Turkey, June 6–9.

Sengör, A.M.C., and Natalin, B.A., 1996. Turkic-type orogeny and its role in the making of the continental crust, *Ann. Rev. Earth Plan. Sci.,* **24,** 263–337.

Şengör, A.M.C., Cin, A., Rowley, D.B., Nie, S.Y., 1991. Magmatic evolution of the Tethysides: a guide to reconstruction of collage history. *Palaeogeography, Palaeoclimatology, Palaeoecology* **87**, 411-440.

Şengör, A.M.C., Cin, A., Rowley, D.B., Nie, S.Y., 1993. Space-time patterns of magmatism along the Tethysides: a preliminary study. *Journal of Geology* **101**, 51-84.

Şengör, A.M.C., Natal'in, B.A., 1996a. Palaeotectonics of Asia: fragments of a synthesis. In: Yin, A., Harrison, M. (Eds.), *Tectonic Evolution of Asia,* Rubey Colloquium. Cambridge University Press, Cambridge, pp. 486–640.

Şengör, A.M.C., Natal'in, B.A., 1996b. Turkic-type orogeny and its role in the making of the continental crust. *Annual Review of Earth and Planetary Sciences,* v. **24**, p. 263–337.

Şengör, A.M.C., Natal'in, B.A., 2004. Phanerozoic analogues of Archaean oceanic basement fragments: Altaid ophiolites and ophirags. In: Kusky, T.M. (Ed.), *Precambrian Ophiolites and Related Rocks.* Developments in Precambrian Geology, vol. **13**. Elsevier, Amsterdam, pp. 675–726.

Sibson, R.H., 1977. Fault rocks and fault mechanisms, *Jour. Geol. Soc. London*, **133,** 191-213.

Sims, J. D., 1973. Earthquake-induced structures in sediments of Van Norman Lake, San Fernando, California. *Science* **182**, 161– 163.

Sims, J. D., 1975. Determining earthquake recurrence intervals from deformational structures in young lacustrine sediments. *Tectonophysics* **29**, 141–152.

Slyvester, A.G., (ed.)., 1984. Wrench fault tectonics. *Am. Ass. Petrol. Geol. Reprint Ser.* **28**, 1-374.

Soesoo, A., Bons, P.D., Gray, D., Foster, D., 1997. Divergent double subduction: tectonic and petrologic consequences. *Geology* **25**, 755–758.

Speight, J. M., and Mitchell, J. G., 1979. The Permo-Carboniferous dyke-swarm of northern Argyll and its bearing on dextral displacement on the Great Glen fault: *Geological Society of London Journal,* v. **136,** p. 3-11.

Steel, R. J., Maehle, S., Nilsen, T.H., Roe, S.L., Spinangr, A., 1977. Coarsening-upward cycles in the alluvium of Hornelen basin (Devonian), Norway: sedimentary response to tectonic events: *Geological Society of America Bulletin,* v. **88**, p. 1124-1134.

Steel, R., and Gloppen, T.G., 1980. Late Caledonian (Devonian) basin formation, western Norway: signs of strike-slip tectonics during infilling: *International Association of Sedimentology Special Publication* **4**, p. 79-103.

Steel, R.J., Gjelberg, J., Helland-Hansen, W., Kleinspehn, K., Nootvedt, A., and Rye-Larsen, M., 1985. The Tertiary strike-slip basins and orogenic belt of Spitsbergen, in Biddle, K.T., and Christie-Blick, N., (eds.), Strike-slip deformation, basin formation and sedimentation: *Society of Economic Paleontologists and Mineralogists Special Publication* **37**, 386 p.

Stewart, S. A., and Reeds, A., 2003. Geomorphology of kilometerscale extensional fault scarps; factors that impact seismic interpretation: *AAPG Bulletin*, v. **87**, p. 251– 272.

Stoeser, D.B., 1986. Distribution and tectonic setting of plutonic rocks of the Arabian Shield. *Journal of African Earth Sciences* **4**, 21–46.

Stow, D. A., 1986. Deep clastic seas, in H. G. Reading, eds., *Sedimentary environments and facies*: Oxford, Blackwell Scientific Publications, p. 399–444.

Sultan, N. P., Cochonat, F., Cayocca, J., Bourillet, F., and Colliat, J. L., 2004. Analysis of submarine slumping in the Gabon continental slope: *AAPG Bulletin,* v. **88**, p. 781– 799.

Sylvester, A. G., and Smith, R. R., 1976. Tectonic transpression and basement controlled deformation in the San Andreas fault zone, Salton Trough, California. *American Association of Petroleum Geologists Bulletin* **60**, 2081±2102 pp.

Sylvester, A.G., 1988. Strike-slip faults: *Geological Society of American Bulletin,* v. **180**, p. 1666-1703.

Szabo, C., Harangi, S., Csontos, L., 1992. Review of Neogene and quaternary volcanism of the Carpathian-Pannonian region. *Tectonophysics* **208**, 243–256.

Tackley, P. J., and Stevenson, D. J., 1993. A mechanism for spontaneous self-perpetuating volcanism on the terrestrial planets. In: D.B. Stone and S.K. Runcorn (Editors), *Flow and Creep in the Solar System: Observations, Modeling and Theory.* Kluwer, Dordrecht, pp. 307-321.

Talbot, C. J., 1977. Inclined and asymmetric upward-moving gravity structures. *Tectonophysics* **42**, 159±181.

Talbot, C. J., 1979. Infrastructural migmatitic upwelling in east Greenland interpreted as thermal convective structures. *Precambrian Res.,* **8**: 77-93.

Talbot, C. J., Rönnlund, P., Schmeling, H., Koyi, H. and Jackson, M. P. A., 1991. Diapiric spoke patterns. *Tectonophysics* **188**, 187±201.

Tang, R., and others, 1984. On the recent tectonic activity and earthquake of the Xianshuihe fault zone, in A collection of papers of *International Symposium on Continental Seismicity and Earthquake Prediction (ISCSEP):* Beijing, China, Seismological Press, p. 347-363.

Tapponier, P., Peltzer, G., and Armijo, R., 1986. On the mechanics of the collision between India and Asia, in Coward, M.P., and Reis, A.C., eds., *Collision tectonics:* Geological Society of London Special Publication v. **19**, p. 115-157.

Tchalenko, J. S., and Ambraseys, N. N., 1970. Structural analysis of the Dasht-e-Bayaz (Iran) earthquake fractures. *Geological Society of America Bulletin* **81**, 41–60 pp.

Tchalenko, J.S., 1970. Similarities between shear zones of different magnitudes. *Bull. Geol. Soc. Am.* **81**, 1625-1640.

TenBrink, U.S., and Ben-Avraham, Z., 1989. The anatomy of a pull-apart basin: seismic reflection observations of the Dead Sea Basin: *Tectonics,* v.**8**, p. 333-350.

Tobisch, O.T., Saleehy, J.B., and Fiske, R.S., 1986. Structural history of continental volcanic arc rocks, eastern Sierra Nevada, California: A case for extensional tectonics: *Tectonics,* v. **5**, p. 65-94.

Tokel, S., 1984. Doğu Anadolu'da kabuk deformasyonu mekanizmasi ve genç, volkanitlerin petrojenezi. *Ketin Symposium Proceeding,* in Turkish with English abstract, pp. 121–130.

Toker, M., 2006. Van segmenti mikrodeprem potansiyelini kontrol eden neotektonik unsurlar. *ATAG-10, Aktif Tektonik Araştırma Grubu 10. Toplantısı,* Dokuz Eylül Üniversitesi, Jeoloji Mühendisliği Bölümü, abstract kitabı 91-92 pp.

Toker, M., 2007. Muş-Van Havzası ve Doğu Van segmenti sığ derinlikli ($\leq$ *10 km)*, uzun peryotlu deprem aktivitelerine *(2* $\leq$ *Md* $\leq$ *4)* volkano-sismojenik bir yaklaşım, *İTÜ Avrasya Yer Bilimleri Enstitüsü. Türkiye Kuvaterner Sempozyumu VI Bildiriler ve Makaleler* (CD-room).

Toker, M., Krastel, S., Demirel-Schlueter, F., Demirbağ, E., İmren, C., 2007. Volcano-Seismicity of Lake Van (Eastern Turkey): A comparative analysis of seismic reflection and three component velocity seismogram data and new insights into volcanic lake seismicity. *In Proceedings Book of International Earthquake Symposium*, 22-26 October, Kocaeli, pp. 103-109.

Toker, M., Krastel, S., Demirel-Schlueter, F., Demirbağ, E., İmren, C., 2009a. Thinned crust-oblique slip faults and mechanism of intraplate volcanic lake seismicity: The Lake Van basin, Eastern Anatolia Accretionary Complex (EAAC), E-Turkey. *In Abstract book and CD of International Association of Seismology and Physics of the Earth's Interior-IASPEI General Assembly,* 10-16 January, Cape Town, S-Africa.

Toker, M., Krastel, S., Demirel-Schlueter, F., Demirbağ, E., İmren, C., 2009b. Seismic effect of magmatic and tectonic events on the static and dynamic stress triggering processes driving intra-lake seismicity: The Lake Van basin, Eastern Anatolia Accretionary Complex (EAAC), E-Turkey. *In Abstract book and CD of International Association of Seismology and Physics of the Earth's Interior-IASPEI General Assembly,* 10-16 January, Cape Town, S-Africa.

Towmend, J., and Zoback, M.D., 2000. How faulting keeps the crust strong, *Geology*, **28**, 399-402.

Trude, K. J., 2004. Kinematic indicators for shallow level igneous intrusions from 3D seismic data: evidence of flow direction and feeder location in Davies, R. J., Cartwright, J. A., Stewart, S. A., Lappin, M. and Underhill, J. R. (eds) 2004. 3D *Seismic Technology: Application to the Exploration of Sedimentary, Basins.* Geological Society, London, Memoirs, **29**, 209-217. 0435-4052/04/ The Geological Society of London 2004.

Turcotte, D.L., 1981. Some thermal problems associated with magma migration. *Journal of Volcanology and Geothermal Research* **10**, 267–268.

Turcotte, D.L., 1982. Magma migration. *Annual Review of Earth and Planetary Sciences* **10**, 397-408.

Türkelli, N., Sandvol, E., Zor, E., Gök, R., Bekler, T., Al-Lazki, A., Karabulut, H., Kuleli, S., Eken, T., Gürbüz, C., Bayraktutan, S., Seber, D., and Barazangi, M., 2003. Seismogenic zones in eastern Turkey. *Geophys Res Lett* 30(**24**):8039 doi:10.1029/2003GL018023

Türkoğlu, E., Unsworth, M., Çağlar, I., Tuncer, V., Avşar, U., and Tank, B., 2008. Magnetotelluric imaging of the Eurasian-Arabian collision in Eastern Anatolia: *International Association of Geomagnetism and Aeronomy Working Group 1.2 on Electromagnetic Induction in the Earth,* Extended Abstract 18, Workshop, El Vendrell, Spain, September, 17–23.

Tweto, O., 1951. Form and structure of sills near Pando, Colorado. *Geological Society of America Bulletin,* **62***,* 507-532.

Utkucu, M., 2004. Personal Communication.

Vandenberg, A.H.M., 1978. The Tasman Fold Belt in Victoria. *Tectonophysics* **48**, 267-297.

Varnes, D. J., 1978. Slope movement types and processes, in R. L. Schuster and R. J. Krizek, eds., *Landslides; analysis and control:* Special report—Transportation Research Board, National Research Council: Washington, D.C., United States, Transportation Research Board, National Research Council, v. **176**, p. 11–33.

Vaselli, O., Downes, H., Thirlwall, M., Dobosi, G., Coradossi, N., Seghedi, I., Szakacs, A., Vannucci, R., 1995. Ultramafic xenoliths in Plio-Pleistocene alkali basalts from the Eastern Transylvanian Basin: depleted mantle enriched by vein metasomatism. *J. Petrol.* **36**, 23–53.

Verma, R.K., Sarma, A.U.S., and Mukhopadhyay, M., 1984. Gravity field over Singhbhum, its relationship to geology and tectonic history. *Tectonophysics,* **106**, 87-107.

Vinogradov, A.P., 1969. Glavniy Redaktor Devonskii, Kammenougolnii i Permskii Periodi: Ministerstvo Geologii SSSR, Akademiya nauk SSSR, Vsesoyuznii Aerogeograficheskii Trest. *Atlas Litologo-Paleogegraficheskikh Kart SSSR,* vol. **II**. Ministerstvo Geologii SSSR, Moskva. 65 sheets.

Walcott, R. I., Christoffel, D. A., and Mumme, T.C., 1981. Bending within the axial tectonic belt of New Zealand in the last 9 my from paleomagnetic data, *Earth Planet. Sci. Lett.,* **52**, p. 427-434.

Walker, R., and Jackson, J., 2002. Offset and Evolution of the Gowk Fault, SE Iran; A Major Intra-continental Strike-Slip System, *J. Struct. Geol.*, **24**, 1677-1698.

Wallace, R.E., 1968. Notes on stream channels offset by the San Andreas fault, southern Coast Ranges, California, in Dickinson, W.R., and Grantz, A., (eds.), *Proceedings of Conference on Geological Problems of San Andreas fault system:* Stanford University Publications in the Geological Sciences, v. **11**, p. 374.

Wallace, R.E., 1970. Earthquake recurrence intervals on the San Andreas fault: *Geological Society of America Bulletin,* v. **81**, p. 2875-2890.

Wang, H.Z., 1985. Chief compiler Atlas of the Paleogeography of China. *Cartographic Publishing House,* Beijing. XV +143 + 85 + 28 + 25 pp.

Wartes, M.A., Carroll, A.R., Greene, T.J., 2002. Permian sedimentary record of the Turpan-Hami basin and adjacent regions, northwest China: Constraints on post-amalgamation tectonic evolution. *Geological society of America Bulletin* **114**, 131–152.

Wartes, M.A., Carroll, A.R., Greene, T.J., Cheng, K.M., Ting, H., 2000. Permian lacustrine deposits of northwest China. In: Gierlowski-Kordesh, K.R., Kelts (Eds.), Lake basins Through Space and Time. *American Association of Petoleum Geologists Studies in Geology,* vol. **46**, pp. 123–132.

Weaver, C.S., Grant, W.C., and Shemeta, J.F., 1987. Local crustal extension at Mount St. Helens, Washington: *Journal of Geophysical Research,* v. **92** (B10), p. 10.170-10.178.

Weaver, C.S., Grant, W.C., Malone, S.D., and Endo, E.T., 1981. Post May 18 seismicity: Volcanic and tectonic implications, in Lipman, P.W., and Mullineaux, D.R., eds., The 1980 eruptions of Mount St. Helens, Washington: *U.S. Geological Survey Professional Paper* **1250**, p. 109-121.

Weaver, J. D., and Jeffcoat, R. E., 1978. Carbonate ball and pillow structures. *Geol. Mag.* **115**, 245– 253.

Weertman, J., 1971. Theory of water-filled crevasses in glaciers applied to vertical magma transport beneath oceanic ridges. *Journal of Geophysical Research* **76**, 1171±1183.

Weertman, J., 1980. The stopping of a rising liquid-filled crack in the Earth's crust by a freely slipping horizontal joint. *Journal of Geophysical Research* **85**, 967±976.

Weinberg, R, F., 1997. Diapir-driven crustal convection: decompression melting, renewal of the magma source and the origin of nested plutons. *Tectonophysics* **271**, 217-229

Weinberg, R. E and Podladchikov, Y., 1994. Diapiric ascent of magmas through power-law crust and mantle. *J. Geophys. Res.,* **99**: 9543-9559.

Weinberg, R. E, 1992. Internal circulation in a buoyant twofluid Newtonian sphere: implications for composed magmatic diapirs. *Earth Planet. Sci. Lett.,* **110**: 77-94.

Weinberg, R. E, 1994. Re-examining pluton emplacement processes: discussion. *J. Struct. Geol.,* **16**: 743-746.

Weinberg, R. F. and Podladchikov, Y.Y., 1995. The rise of solidstate diapirs. *J. Struct. Geol.,* **17**:1183-1195.

Weinberg, R. F. and Schmeling, H., 1992. Polydiapirs: multiwavelength gravity structures. *J. Struct. Geol.,* **14**: 425-436.

Weinberg, R. F., 1996. Ascent mechanism of felsic magmas: news and views. Transactions of the Royal Society Edinburgh: *Earth Sciences* **87**, 93±104.

Wellman, H.W., 1955. The geology between Bruce Bay and Haast river, South Westland: *New Zealand Geological Survey Bulletin 48, (2nd edition)*, p. 46.

Wernicke, B.P., 1985. Uniform-sense normal simple shear of the continental lithosphere: *Canadian Journal of Earth Sciences,* v. **22**, p. 108-125.

Wernicke, B.P., Axen, G.J., Snow, J.K., 1988. Basin and Range extensional tectonics at the latitude of Las Vegas, Nevada: *Geological Society of America Bulletin,* v. **100**, p.1738-1757.

Whitehead, J. A. and Helfrich, K. R., 1991. Instability of flow with temperature-dependent viscosity: a model of magma dynamics. *Journal of Geophysical Research* **96**, 4145±4155

Wick, L., Lemcke, G., Sturm, M., 2003. Evidence of Late glacial and Holocene climatic change and human impact in eastern Anatolia: high-resolution pollen, charcoal, isotopic and geochemical records from the laminated sediments of Lake Van, Turkey. *The Holocene* **13**, 665–675.

Wilcox, R. E., Harding, T. P., and Seely, D. R., 1973. Basic wrench tectonics. *American Association of Petroleum Geologists Bulletin* **57**, 74–96 pp.

Willis, B., 1938a. San Andreas Rift, California: *Journal of Geology,* v. **46**, p. 793-827.

Willis, B., 1938b. Wellings' observations of Dead Sea structure: *Geological Society of America Bulletin,* v. **49**, p. 659-668.

Wilson, C.K., Jones, C.H., Molnar, P., Sheehan, A.F., and Boyd, O.S., 2004. Distributed deformation in the lower crust and upper mantle beneath a continental strike-slip fault zone: Marlborough fault system, South Island, *New Zealand, Geology,* 32(**10**), 837–840.

Wilson, G., 1960. The tectonics of the "Great Ice Chasm" Filchner Ice Shelf, Antarctica: *Geologists Association Proceedings,* v. **71**, p. 130-138.

Wilson, J. T., 1966. Did the Atlantic close and then reopen? *Nature* **211**, 676-81.

Wilson, M., Bianchini, G., 1999. Tertiary–quaternary magmatism within the Mediterranean and surrounding regions. In: Durand, Jolivet, Horvath, Seranne (Eds.). The Mediterranean Basins: Tertiary extension within the Alpine orogen. *Geol. Soc. London, Special Publication,* vol. **156**, pp.141–168.

Wilson, M., Downes, H., 1991. Tertiary-Quaternary extension-related alkaline magmatism in western and central Europe. *J. Petrol.* **32**, 811–849.

Wilson, M., Patterson, R., 2002. Intraplate magmatism related to short-wavelenght convective instabilities in the upper mantle: evidence from the Tertiary-Quaternary volcanic province of western and central Europe. *Geological Society of America,* vol. **352**, pp. 37–58 (special papers).

Wong, H. K., and Degens, E. T., 1978. The bathymetry of Lake Van; a preliminary report. In: Degens, E.T., Kurtman, F. (Eds.), *Geology of Lake Van.* MTA Press, Ankara, pp. 6–10

Wong, H. K., and Finckh, P., 1978. Shallow structures in Lake Van. In: Degens, E.T., Kurtman, F. (Eds.), *Geology of Lake Van.* MTA Press, Ankara, pp. 20–28.

Woodcock, N. H., and Fischer, M., 1986. Strike-slip duplexes. *Journal of Structural Geology* **8**, 725–735 pp.

Woodcock, N. H., and Rickards, R. B., 2003. Transpressive duplex and flower structure: Dent Fault System, NW England. *Journal of Structural Geology* **25**, 1981–1992 pp.

Woodcock, N. H., and Schubert, C., 1994. Continental strike-slip tectonics. In: Hancock, P.L., (Ed.), *Continental Tectonics,* Pergamon, Oxford, pp. 251–263.

Wright, T.L., 1991. Structural geology and tectonic evolution of the Los Angeles basin, California: *American Association of Petroleum Geologists Memoir* **52**, p. 35-134.

Wu, F.T., and Wang, P., 1988. Tectonics of western Yunnan Province, China: *Geology,* v. 16 (**2**), p. 153-157.

Yeats, R.S., 1981. Quaternary flake tectonics of the California Transverse Ranges: *Geology,* v. **9**, p. 16-20.

Yılmaz, Y., 1984. Türkiye'nin jeolojik tarihinde magmatik etkinlik ve tektonik evrimle ilişkisi: *TJK Ketin simpozyumu bildirileri,* 63-81.

Yılmaz, Y., 1987. Initiation of the neomagmatism in East Anatolia. *Tectonophysics* **134**: 177–199.

Yılmaz, Y., 1990. Comparison of young volcanic associations of western and eastern Anatolia formed under a compressional regime: a review. *J. Volcanol. Geotherm. Res.* **44**, 69–87.

Yılmaz, Y., 1993. New evidence and model on the evolution of the Southeast Anatolia Orogen. *Geol. Soc. Am. Bull.* **105**: 251–271.

Yılmaz, Y., 2005. Morphotectonic development of Eastern Anatolia. *Tutorial lecture series on the geodynamic evolution of Eastern Mediterranean.* ITU, Faculty of Mines, Istanbul, Turkey, 28 February 2005

Yılmaz, Y., Dilek, Y., and Işık, H., 1981. Gevaş (Van) ofiyolitinin jeolojisi ve sinkinematik bir makaslama zonu: *TJK Bull.,* **24/1**, 37-44.

Yılmaz, Y., Güner, Y., and Saroglu, F., 1998. Geology of the quaternary volcanic centers of the east Anatolia: *Journal of Volcanology and Geothermal Research,* v. **85**, nos. 1–4, p. 173–210.

Yılmaz, Y., Şaroğlu, F., and Güner, Y., 1986. Initiation of neomagmatism in the Eastern Anatolia.

Yılmaz, Y., Şaroğlu, F., and Güner, Y., 1987. Doğu Anadolu'da Solhan (Muş) volkanitlerinin petrojenetik incelenmesi. *Yerbilimleri* **14**, 133–163.

Yılmaz, Y., Tüysüz, O., Yigitbas, E., Genç, S.C., and Sengör, A.M.C., 1997. Geology and tectonic evolution of the Pontides, *in* Robinson, A.G., ed., Regional and petroleum geology of the Black Sea and surrounding region: Tulsa, Oklahoma, *American Association of Petroleum Geologists Memoir* **68**, p. 183–226.

Yılmaz, Y., Yiğitbaş, E., Genç, S.C., 1993. Ophiolitic and metamorphic assemblages of southeast Anatolia and their significance in the geological evolution of the orogenic belt. *Tectonics* **12**, 1280–1297.

Zeck, H. P., 1996. Betic-Rif orogeny: Subduction of Mesozoic Tethys lithosphere under E-ward drifting Iberia, slab detachment shortly before 22 Ma, and subsequent uplift and extensional tectonics: *Tectonophysics*, v. **254**, p. 1-16.

Zhang, T., R., and Lay, T., 1995. Why the Lg phase does not traverse oceanic crust, *Bull. Seism. Soc. Am.,* **85**, 1665-1678.

Ziegler, P.A., 1992. European Cenozoic rift system. In: Ziegler, P.A. (Ed.) Geodynamics of Rifting, vol. 1, *Tectonophysics,* **208**, 91–111.

Zoback, M. D., Zoback, M. L., Mount, V. S., Suppe, J. P., Healy, J. H., Oppenheimer, D. H., Reasenberg, P. A., Jones, L. M., Raleigh, C. B., Wong, I. G., Scott, Oona, and Wentworth, C. M., 1987. New evidence on the state of stress of San Andreas fault system. *Science* **238,** 1105±1111 pp.

Zoback, M.L., and Zoback, M., 1980. State of stress in the conterminous United States, *J. Geophys. Res.,* **85**, p. 6113-6156.

Zor, E., Gürbüz, C., Türkelli N, Sandvol E, Seber D, and Barazangi, M., 2003. The crustal structure of the East Anatolian Plateau from receiver functions. *Geophys Res Lett* 30(**24**):8044, doi:10.1029/2003GL018192

CURRICULUM VITAE

Candidate's Full Name: Mustafa TOKER

Place and date of birth: Kırşehir –25.08.1975

Permanent Address: İTÜ residences, D: 2, No: 42, Maslak – Istanbul

Universities and
Colleges attended:

- Middle East Technical University, Institute of Marine Sciences – M.Sc.

Marine Geology and Geophysics Department / Program of Marine Geophysics (2001– 2003)
Thesis: Salt Tectonics, Plio–Quaternary sediments and Paleo–topography of Messinian Evaporties, Cilicia–Adana Basin, NE–Mediterranean Basin, Mersin–Turkey
Advisor: Assoct. Prof. Vedat EDIGER

- Yıldız Technical University – B.Sc.

Geophysical Engineering Department, (1988– 1992)
Thesis: Analysis of Reservoir Parameters in Well–Logging, Batman–Turkey
Advisor: Prof. Dr. Uğur KAYNAK

Publications:

- **Toker, M.,** and Ediger, V., 2005a. The Orientation of The Nonlinear Stress-Strain Relations to Acoustic Parameters and Elastic Modulus for Irreversible Plastic Strain Field in the Cilicia-Adana Basin, NE-Mediterranean Sea. In SEISMIC MODELLING & INTERPRETATION. Journal of the Balkan Geophysical Society, Vol. 8, 2005, Suppl. 1. 4th Congress of the Balkan Geophysical Society, 9-12 October 2005, Bucharest, Romania.

- **Toker, M.**, and Ediger, V., 2005b. Incoherent Acoustic Response of Viscous-Plastic Salt Intrusions as being diagnostic for Abnormal Fluid Pressure Regimes in the Cilicia-Adana Basin, NE- Mediterranean Sea In SEISMIC MODELLING & INTERPRETATION. Journal of the Balkan Geophysical Society, Vol. 8, 2005, Suppl. 1. 4th Congress of the Balkan Geophysical Society, 9-12 October 2005, Bucharest, Romania.

- **Toker, M.,** Ediger, V. and Evans, G. 2006. Mechanism of Delta Overburden Deformation above Viscous Creep of Messinian Substratum of the Cilicia-Adana Basin, the NE-Mediterranean Sea. 17th International Geophysical Congress and Exhibition by UCTEA , November 14-17, 2006.

▪ **Toker, M.,** and Ediger, V., 2005. Incoherent Acoustic Response of Visco-Plastic Salt Intrusions as being diagnostic for Abnormal Fluid Pressure Regimes in the Cilicia-Adana Basin, NE-Mediterranean Sea. International Earth Sciences Colloquium on the Aegean Regions (IESCA-2005), Dokuz Eylül University, 4-7 October, Izmir-Turkey.

▪ **Toker, M.,** and Ediger, V., 2005. The Orientation of The Nonlinear Stress-Strain Relations to Acoustic Parameters and Elastic Modulus for Irreversible Plastic Strain Field in the Cilicia-Adana Basin, NE-Mediterranean Sea. International Earth Sciences Colloquium on the Aegean Regions (IESCA-2005), Dokuz Eylül University, 4-7 October, Izmir-Turkey.

▪ **Toker, M.,** and Ediger, V., 2005. Lower Amplitude Energy and Seismic Reflection Loss from Non-Lithologic Acoustic Impedance Changes at a Elastic to Pressurised Viscous-Plastic Fluid Interface in the Cilicia-Adana Basin, NE-Mediterranean. *In Nonlinear Processes in Geophysics of Geophysical Research Abstracts*, Vol. 7, EGU 05-A-00412. European Geosciences Union (EGU) General Assembly in Vienna, 24-29 April 2005, Austria.

▪ **Toker, M.,** and Ediger, V., 2005. Formation Mechanisms of Acoustic Mirror Images as a Proxy of Abnormal Pressure Regimes in the Cilicia-Adana Basin, NE-Mediterranean Sea. Türkiye Kuvaterner Sempozyumu (TURQUA-V, 2-5 June 2005). İTÜ Avrasya Yer Bilimleri Enstitüsü.

▪ Ediger, V., Evans, G., and **Toker, M.,** 2005. The Ridge between the Adana and Cilicia Basins and Halokinesis, NE-Mediterranean. The 2nd International Conference of Applied Geophysics on 12-13 March-2005 by Egyptian Society of Applied Petrophysics (ESAP) Abstract book, Egypt.

▪ Demirel-Schlueter, F., S. Krastel, F. Niessen, E. Demirbag, C. Imren, **M. Toker,** T. Litt, M. Sturm. 2005. Seismic Pre-Site Survey for a potential new ICDP site – PaleoVan - at Lake Van, Turkey. in Sedimentology, Stratigraphy and Paleontology of Geophysical Research Abstracts, Vol. 7, EGU 05-A-07997. European Geosciences Union (EGU) General Assembly in Vienna, 24-29 April 2005, Austria.

▪ Demirel-Schlüter, F., Krastel, S., Niessen, F., Demirbag, E., Imren, C., **Toker, M**. 2006. Reflexionseismische Untersuchungen am Van See, Türkei, als Beitrag zur Bestimmung einer potentiellen ICDP-Lokation und Rekonstruktion von Seespiegelschwangungen. DGG Bremen (Deutshce Geophysik Congress).

▪ Demirel-Schlueter, F., S. Krastel, E. Demirbag, C. Imren, **M. Toker,** F. Niessen, T. Litt, M. Sturm. 2006. Determination of potential ICDP Sites and Reconstruction of Lake Level Changes at Lake Van, Turkey, based on high resolution seismic Surveying. European Geosciences Union (EGU) General Assembly in Vienna, 24-29 April 2006, Vienna, Austria.

▪ **Toker, M.** 2006. Van segmenti mikrodeprem potansiyelini kontrol eden neotektonik unsurlar. ATAG-10, Aktif Tektonik Araştırma Grubu 10. Toplantısı, abstract kitabı 91-92 pp. 2–4 Kasım 2006, Dokuz Eylül Üniversitesi, Jeoloji Mühendisliği Bölümü, İzmir.

▪ **Toker, M.,** Ediger, V., and Evans, G., 2007a. Physiographic, Morpho-tectonic provinces and Sedimentary patterns of the Cilicia-Adana basin, the NE-Mediterranean. European Geosciences Union 2007, Geophysical Research Abstracts, Vol. 9, 00287, 2007 S Ref-ID: 1607-7962/gra/EGU2007-A-00287.

▪ **Toker, M.,** Ediger, V., and Evans, G., 2007b. Intra-basin salt regime and its thin-skinned tectonism into delta sedimentation of the Cilicia-Adana Basin, The NE-Mediterranean. European Geosciences Union 2007, Geophysical Research Abstracts, Vol. 9, 00290, 2007**,** SRef-ID: 1607-7962/gra/EGU2007-A-00290

▪ **Toker, M.,** Ediger, V., and Evans, G., 2007c. Critical Research Parameters among Halokinetic processes organizing the Cilician Salt-Sediment System, The Northeastern Mediterranean. Rapp. Comm. Int. Mer Médit., 38th CIESM Congress, 9-13 April CIESM-2007, International Mediterranean Science Comission, Istanbul.

▪ **Toker, M.,** 2007. Muş-Van Havzası ve Doğu Van segmenti sığ derinlikli (≤ *10 km)*, uzun peryotlu deprem aktivitelerine *(2 ≤ Md ≤ 4)* volkano-sismojenik bir yaklaşım, İTÜ Avrasya Yer Bilimleri Enstitüsü. Türkiye Kuvaterner Sempozyumu VI Bildiriler ve Makaleler (CD), 16-18 Mayıs 2007.

▪ **Toker, M.,** Ediger, V., and Evans, G., 2007. Formation Mechanisms of Salt Withdrawal Minibasins in the NE-Corner of Mediterranean. *In the EAGE proceeding book (F006) on CD,* 11 - 14 June 2007, European Associaton of Geoscientists and Engineers 69th Conference and Exhibition, London, UK.

▪ **Toker, M.,** Ediger, V., and Evans, G. 2007. Salt deformation and pore fluid related hydraulics-induced overburden unstability and overpressure regime in the Cilicia-Adana Basin, the NE-Mediterranean Sea. *In the UAM proceeding book*, *Regular Session II: Seafloor Characterization.* Underwater Acoustic Measurements Technologies and Results 2nd International Conference and Exhibition, 25-29 June 2007, Crete.

▪ **Toker, M.,** Ediger, V., and Evans, G. 2007. Distortion of the salt-cored fold system and its effects upon abyssal plain sedimentary processes in the Cilicia-Adana evaporitic basin, the NE-Mediterranean. *In Theme I: Geographic, topic selection: O1: New and Emerging Plays from the Circum Mediterranean Region on CD.*. The AAPG European Region International Energy Conference & Exhibition (November 17-20, 2007). Megaron, Athens International Conference Center, Greece.

▪ **Toker, M.,** 2006. Van segmenti mikrodeprem potansiyelini kontrol eden neotektonik unsurlar. ATAG-10, Aktif Tektonik Araştırma Grubu 10. Toplantısı, Dokuz Eylül Üniversitesi, Jeoloji Mühendisliği Bölümü, abstract kitabı 91-92 pp.

▪ **Toker, M.,** 2007. Muş-Van Havzası ve Doğu Van segmenti sığ derinlikli (≤ *10 km)*, uzun peryotlu deprem aktivitelerine *(2 ≤ Md ≤ 4)* volkano-sismojenik bir yaklaşım, İTÜ Avrasya Yer Bilimleri Enstitüsü. Türkiye Kuvaterner Sempozyumu VI Bildiriler ve Makaleler (CD-room).

▪ **Toker, M.,** Krastel, S., Demirel-Schlueter, F., Demirbağ, E., İmren, C., 2007. Volcano-Seismicity of Lake Van (Eastern Turkey): A comparative analysis of seismic reflection and three component velocity seismogram data and new insights into volcanic lake seismicity. In Proceedings Book of International Earthquake Symposium, 22-26 October, Kocaeli, pp. 103 109.

▪ **Toker, M.,** Krastel, S., Demirel-Schlueter, F., Demirbağ, E., İmren, C., 2009a. Thinned crust-oblique slip faults and mechanism of intraplate volcanic lake seismicity: The Lake Van basin, Eastern Anatolia Accretionary Complex (EAAC), E-Turkey. In Abstract book and CD of International Association of Seismology and Physics of the Earth's Interior-IASPEI General Assembly, 10-16 January, Cape Town, S-Africa.

▪ **Toker, M.,** Krastel, S., Demirel-Schlueter, F., Demirbağ, E., İmren, C., 2009b. Seismic effect of magmatic and tectonic events on the static and dynamic stress triggering processes driving intra-lake seismicity: The Lake Van basin, Eastern Anatolia Accretionary Complex (EAAC), E-Turkey. In Abstract book and CD of International Association of Seismology and Physics of the Earth's Interior-IASPEI General Assembly, 10-16 January, Cape Town, S-Africa.

▪ Demirel-Schlueter F, Krastel S, Niessen F, Demirbag E, Imren, C, **Toker, M,** Litt T, and Sturm, M., 2005. Seismic pre-site survey for a potential new ICDP site – PaleoVan – at Lake Van, Turkey. EGU Geophys Res Abstr 7:07997.

▪ Bialas, J., Klauke, I., **Toker, M.,** and Scientific crew of R/V METEOR cruise, 2009. Scientific observations and the work reports from R/V METEOR (IFM-GEOMAR) Expedition in the Black Sea Cruise M72/4-2007. 2nd International Symposium on the Geology of the Black Sea Region, ISGB-2009, October 5-9, 2009, Ankara-Turkey.

▪ **Toker, M.,** Bialas, J., Klauke, I., and Scientific crew of R/V METEOR cruise, 2010. Implications for formation mechanisms of methane hydrates and recommendations for the future researches in correlative anoxic basins: observations from R/V METEOR (IFM-GEOMAR) expedition in the Black Sea Cruise M72/4-2007. Abstract volume of AAPG European Region Annual Conference, October 17-19, 2010 Kiev, Ukraine. AAPG Search and Discovery Article #90109©2010.

▪ **Toker M.,** Krastel S., Demirel-Schlueter F., and Demirbag E., 2010. Seismic evidences of magma-hydrothermal deformations and Implications for intraplate volcanic seismology: The Lake Van basin, Eastern Anatolia Accretionary Complex (EAAC), E-Turkey, 12th Symposium of Study of Earth's Deep Interior-SEDI 2010 Conference, July 18–23, Santa Barbara, California-USA, in Book of Poster Abstracts, pp.105-107; 25340685 Toker and abstract book of Cooperative Institute for Dynamic Earth Research-CIDER 2010, pp. 28-30.

▪ **Toker M.,** Krastel S., Demirel-Schlueter F., and Demirbag E., 2010. Extensional magma propagation, magmatic interactions with pre-existing boundary faults and implications for post-collisional crust-forming process in a small Turkic-type orogen: Lake Van region, Eastern Anatolia Accretionary Complex (E-Turkey). XIX Congress of the Carpathian- Balkan Geological Association Thessaloniki, Greece, 23-26 September 2010. Abstracts Volume of Geologica Balcanica, an Official Journal of the Carpathian-Balkan Geological Association ISSN 0324-0894. Addendum to the CBGA 2010 Abstracts Volume.

▪ **Toker, M.,** Krastel, S., Demirel-Schlueter, F., and Demirbag, E., 2010. Seismic and Crustal Implications for evolving accretionary wedge-basin: Lake Van, Eastern Anatolia Accretionary Complex (E-Turkey). Abstract volume of Tectonic Crossroads: Evolving Orogens of Eurasia-Africa-Arabia, Middle East Technical University, 4-8 October 2010, Ankara-Turkey.

▪ **Toker, M.,** Krastel, S., Demirel-Schlueter, F., Demirbağ, E., Imren, C., 2008. Basin inversion and extensional magmatism by accretionary wedge deformation in Lake Van basin, Eastern Anatolia High Plateau (E-Turkey), In session of STT-03 Accretionary orogens: Character and processes, Abstract volume CD-ROM of 33rd International Geological Congress, Oslo, Norway, 6 – 14 August 2008.

▪ **Toker, M.,** Krastel, S., Demirel-Schlueter, F., Demirbağ, E., Imren, C., 2008. Thermal cooling of Lake Van basin deep structure and crustal consolidation, Eastern Anatolia Accretionary Complex, (E-Turkey), In session of STT-03 Accretionary orogens: Character and processes, Abstract volume CD-ROM of 33rd International Geological Congress, Oslo, Norway, 6 – 14 August 2008.

▪ **Toker, M.,** Ediger, V., and Evans, G., 2008. Halotectonic unstability and gravity potential-enhanced deformation in the NE-corner of Mediterranean, In session of EUR-18 Palaeogeographic and palaeotectonic development of the Mediterranean and Middle East regions, Abstract volume CD-ROM of 33rd International Geological Congress, Oslo, Norway, 6 – 14 August 2008.

▪ **Toker, M.,** Ediger, V., and Evans, G., 2004. The Dome-Shaped Acoustic Voids of Homogeneous Salt Zone in the Cilicia-Adana Basin (NE-Mediterranean Sea), In Proceedings (v:1) of the 7th European Conference on Underwater Acoustics (ECUA 2004, edited by Dick G. Simons), 5-8 July 2004, Delft, the Netherlands.

▪ **Toker, M.,** Ediger, V., and Evans, G., 2006. Mechanism of Delta Overburden Deformation above Viscous Creep of Messinian Substratum of the Cilicia-Adana Basin, the NE-Mediterranean Sea. In CD-ROM Abstract of 17th International Geophysical Congress and Exhibition by Union of Chambers of Turkish Engineers and Architectures (UCTEA), November 14-17 2006, Ankara, Turkey.

▪ **Toker, M.,** Ediger, V., and Evans, G., 2008a. Tectonics and kinematics of prevailing salt regime in an incompatibility oblique rift structure; an updated case study on The Cilicia-Adana Basin, NE-Mediterranean. In CD-ROM Abstract of the 18th International Geophysical Congress and Exhibition by Union of Chambers of Turkish Engineers and Architectures (UCTEA), October 14-17, 2008, Ankara, Turkey.

▪ **Toker, M.,** Ediger, V., and Evans, G., 2008b. Salt-related unstability and gravity Potential-enhanced deformation in the NE-corner of Mediterranean. In CD-ROM Abstract of the 18th International Geophysical Congress and Exhibition by Union of Chambers of Turkish Engineers and Architectures (UCTEA), October 14-17, 2008, Ankara, Turkey.

▪ **Toker, M.,** 2011. Tectonic and Magmatic Structure of Lake Van Basin and its Structural Evolution, Eastern Anatolia Accretionary Complex (EAAC), E-Turkey. Phd. Thesis, In Mustafa Inan Library of Istanbul Technical University, Istanbul, Turkey.

▪ **Toker, M.,** and Şengör, A. M. C., (In Press). Van Gölü havzasının temel yapısal unsurları, tektonik ve sedimanter evrimi, Doğu Türkiye, (Basic structural elements of Lake Van Basin, its tectonic and sedimentary evolution, Eastern Turkey). İstanbul Teknik Üniversitesi Dergisi (Journal of Istanbul Technical University), Mühendislik (d), itüdergisi/d mühendislik (Engineering Journal d). "Van Gölü havzasının tektonik ve magmatik yapısı ve yapısal evrimi, Doğu Anadolu Yığışım Karmaşığı (DAYK), Doğu Türkiye" adlı doktora tezinden hazırlanmıştır.

▪ **Toker, M.,** Ediger, V., and Evans, G., (In Press). Extensional tectonic control upon Neogene sedimentation and sediment termination and its implications for tectonic evolution, The Morphou Sub-Basin, NW-active seismic margin of Cyprus Arc. In Abstract Book of GeoSynthesis 2011, The International Conference and Exhibition of "Integrating the Earth Sciences", 28 August-2 September 2011, Cape Town, South Africa.

▪ **Toker, M.,** Krastel, S., Demirel-Schlueter, F., and Demirbağ, E., (In Press). The Highlands Rifting Phenomena in Lake Van Dome as a morphological paradigm and Model Synthesis, Eastern Anatolia Accretionary Complex (EAAC), E-Turkey, In Extended Abstract Book of Scientific Conference of Geological Processes in the Lithospheric Plates Subduction, Collision, and Slide Environments. The Far East Geological Institute, Far Eastern Branch, Russian Academy of Sciences, 20-26 September, 2011, in Vladivostok, Russia.

▪ **Toker, M.,** Krastel, S., Demirel-Schlueter, F., and Demirbağ, E., (In Press). Tectonic and Magmatic Structure of Lake Van Basin and its Structural Evolution, Eastern Anatolia Accretionary Complex (EAAC), E-Turkey, In Extended Abstract Book of 6th Congress and Technical Exhibition of Balkan Geophysical Society (BGS 2011), 3-7 October 2011, in Budapest, Hungary.

▪ **Toker, M.,** Ediger, V., and Evans, G., (In Press). Unstable Shelf-Margin Tectonics of NE-corner of Mediterranean Region, the Cilicia-Adana Basin. In Abstract Book of The International Conference on Geology, Geotechnology, and Mineral Resources of INDOCHINA, GEOINDO 2011, December 1-8, 2011, Khon Kaen, Thailand.

Books:

▪ **Toker, M.** (Author), 2011, The Highlands Tectonics and Magmatism of Lake Van Volcanic Basin, its Accretionary Dynamics and Plio–Quaternary Structural Evolution, Eastern Anatolia Accretionary Complex (E Turkey) (in preparation for MTA and Chamber of Turkish Geological Engineers).